申报	系列：教师系列教学科研并重型
	专业：中药资源与开发
	职称：副教授

业绩成果材料

（申报人的业绩成果材料包括论文、科研项目、获奖以及其他成果等）

单　位（二级单位）　林学与风景园林学院

姓　名　　张 旭

材料核对人：　　单位盖章：

核对时间：

华南农业大学制

目　录

一、教学研究业绩

1.教改论文：茶学专业实践教育改革研究..... 4

2.编写教材：十四五规划教材《药理学与临床药物应用》 13

二、科研项目

1.主持：关于广东省林业局中央财政林业草原生态保护恢复资金项目的立项通知（合同）及有关佐证材料..... 18

2.主持：关于云浮市创新创业团队项目的立项通知（合同）及有关佐证材料 58

3.主持：关于广东省科技创新支撑“百千万工程”项目的立项通知（合同）及有关佐证材料 80

4.主持：关于广东省公益研究与能力建设项目的立项通知（合同）及有关佐证材料 100

5.主持：关于广州市农村科技特派员专题项目的立项通知（合同）及有关佐证材料 113

6.主持：关于广东省林业局生态林业建设及自然保护地体系建设项目的立项通知（合同）及有关佐证材料..... 128

7.主参：关于国家自然科学基金项目的立项通知（合同）及有关佐证材料 133

8.主参：关于广东省自然科学基金项目的立项通知（合同）及有关佐证材料 144

9.主参：关于广东省自然科学基金项目的立项通知（合同）及有关佐证材料 155

三、论文、著作等

1.检索证明 166

2.以第一作者发表本专业论文情况
2.1. Advance in Anti-tumor Mechanisms of Shikonin, Alkannin and their Derivatives 171
2.2. An Approach for Searching Bioactive Compounds from Traditional Chinese Plant Food and Herb Medicines by Investigating Spectrum–Effect Relationships 187
3.以通讯作者发表本专业论文情况
3.1. Short-term steaming during processing impacts the quality of Citri Reticulatae 'Chachi' peel 204
3.2. Differences in the components of *Neolamarckia cadamba* from different provenance and the drug resistance reversal activity of characteristic alkaloid . 229
3.3. Design and synthesis of epigallocatechin (EGC) analogs selective to inhibit α-amylase over α-glucosidases via the incorporation of caffeine acid and its derivatives 252
3.4. Flavor Characteristics of Ganpu Tea Formed During the Sun-Drying Processing and Its Antidepressant-Like Effects 288
3.5. A treasure reservoir of genetic resource of tea plant (*Camellia sinensis*) in Dayao Mountain 302
3.6. Chemical compositions of Pu'er tea fermented by Eurotium Cristatum and their lipid-lowering activity 320
3.7. Quality components and antidepressant-like effects of GABA green tea . 344
3.8. Study on the Anti-Tumor Ability of Niaowangzhong Green Tea 366
3.9.柑普提取物对 HepG2 和 SGC-7901 肿瘤细胞系的抗增殖作用 390

四、科研成果

1.知识产权
1.1.专利授权证书：一种发酵陈皮的制备方法,产品及应用405
1.2.专利授权证书：一种微生物发酵制作 GABA 茶的方法 406

2.地方标准：全生晒柑普茶生产技术规程..... 407

五、其他业绩

1.指导学生学科竞赛

1.1.第八届全国医药院校药学/中药学专业大学生实验技能竞赛二等奖 416

1.2.2024 年华南农业大学“创客杯”大学生创新大赛铜奖“可茶——高 GABA 低咖啡因茶产品开拓者” 417

福建茶叶

8

2016年8月
总第176期

国际标准刊号：ISSN 1005-2291　国内统一刊号：CN35-1111/S

■全国中文核心期刊　■全国优秀农业期刊　■福建省优秀科技期刊



ISSN 1005-2291

福建省茶叶学会　主办

福建茶叶 TEA IN FUJIAN

刊名题写：张家坤



白茶系列摄影 / 茶园小憩（陈兴华）

主管单位：福建省科学技术协会
主办单位：福建省茶叶学会
编辑/出版：《福建茶叶》编辑部

福建省茶叶学会期刊编委会
主　任：冯廷佺
副主任：汤鸣绍　杨　磊
委　员：冯廷佺、杨江帆、余文权、苏　峰、汤鸣绍、郭吉春
吴光远、郑廼辉、张文锦、林金科、叶乃兴、郭雅玲
金心怡、李远华、潘玉华、姚信恩、周玉璠、杨　磊
汤荣辉、唐　辉、赖笔进
主　编：冯廷佺（兼）
执行主编：汤鸣绍
副主编：唐　辉、姚信恩
编辑部主任：姚信恩（兼）
责任编辑：林春莲、王　欢、赖笔进
运营中心主任：唐　辉（兼）

编辑部地址：福建省福州市湖东路189号凯捷大厦6层西侧
编辑部电话：0591-38704750
办公室电话：0591-87601225
传　真：0591-87609027
投稿邮箱：fjtea@vip.163.com
订阅邮箱：fjtea@163.com
新浪博客：blog.sina.com.cn/fjtealeaf
国际标准刊号：ISSN1005—2291
国内统一刊号：CN35—1111/S
广告经营许可证号：3500004000353
法律顾问：福建宽达律师事务所　张圣林
印刷单位：彩星印刷有限公司
总期数：176期
出版日期：2016年8月25日
定　价：人民币30元/期，一年360.00元

本刊公告

1. 本刊自2000年起就先后加入“万方数据——数字化期刊群”全文上网、“中国学术期刊综合评价数据库（CAJCED）统计源期刊”、被《中国核心期刊（遴选）数据库》、《中国期刊全文数据库（CJFD）全文收录期刊》、《中文科技期刊数据库》、超星“域出版”收录期刊、华艺CRPS中文电子期刊等收录。凡被本刊录用学术论文稿件将统一纳入上述期刊网，本刊所付稿酬已包含上述网络版报酬。

2. 本刊如有引用的部分文章及图片，涉及到版权人情况不明晰的，请原作者主动与本刊联系，按规定支付相应稿酬。

3. 本刊迄今为止，从未发出过任何纸质或电子形式的所谓录稿通知书。如有作者收到以本刊名义发放的任何形式的录稿通知书，均系假冒。请第一时间报警，或者联系本刊提供相应证据，本刊将介入调查。

福建茶叶 TEA IN FUJIAN

2016 年第 38 卷第 8 期(总第 176 期) Contents 目录

法规·政策

1 茶文化视角下现代企业制度建设的思考 …… 汤迪操
2 明代茶法的建立、变革与监察研究 …… 卢 珺
4 茶文化保护与发展的法律问题研究 …… 申技红
5 我国茶叶地理标志的法律保护策略研究 …… 田妍妍

实验方法

7 普洱茶自动化生产线的检测设备及技术特点 …… 贾媛媛

生产技术

8 蕉城区茶叶质量安全可追溯体系建设 …… 宋岸伟
10 计算机在茶叶生产中的应用 …… 张 霞

综合开发

11 谈茶叶产品开发对经济发展的促进作用 …… 郑英美

品质鉴测

13 基于人工神经网络的茶叶鉴定专家系统设计与研究 …… 刘 洋，郑 华，李筱楠

人才培养

15 从茶产业就业创业培训视角谈大学生就业创业教育培养模式创新 …… 周海英
16 浅析茶文化的高职院校人力资源管理策略 …… 薛 铨

茶与健康

18 茶叶碱对运动员竞技能力与成绩的活态影响分析 …… 罗 军，赵 凯
19 红茶配合运动改善心血管功能的作用分析研究 …… 柴娜娜
21 论茶饮料对体育运动员运动功能的影响研究 …… 尹志琼
22 基于运动员饮茶对于体质改变的研究 …… 傅 云，郭晓琴
24 茶氨酸延缓运动性疲劳的作用研究 …… 杨建丰，杨 光等
25 茶多酚对体育运动能力的影响 …… 郭素艳
27 茶酚酸抗运动性疲劳机制的应用 …… 李 丹

茶叶贸易

28 英语在茶叶贸易中的影响研究 …… 唐 慧
30 茶企广告中模糊语言的语用功能及翻译 …… 李 燕
31 我国茶企出口商务英语的跨文化交际 …… 郑坤丹
33 论中国茶叶的国际竞争力 …… 贾孝魁
35 接受理论与茶叶商标翻译研究 …… 徐媛媛
37 基于国际标准差距视角下绿色壁垒对我国当前茶叶出口贸易的影响 …… 李武歌
38 转型经济条件下的茶企国际贸易问题研究 …… 安伟洁，王依然
40 关联——顺应翻译模式指导下的茶企外宣翻译研究 …… 艾 玉
41 美国技术性壁垒对中美茶叶贸易的影响 …… 陈薇薇

市场营销

43 中国茶企业微博营销策略分析与研究 …… 谢 萌
44 四川茶企业如何做好品牌营销 …… 张 焱
46 影响我国茶叶消费因素与发展对策研究 …… 徐 振
47 茶叶互联网销售背景下完善纠纷解决体系的内容与策略分析 …… 马 亮
49 浅析推动中国茶产业电子商务化的进程 …… 翁文娟
50 茶业电子商务的现状与对策分析 …… 闫 寒，纪亚楠
52 电子商务模式下的茶叶物流配送 …… 任友德
53 社会营销视角的中小型茶叶企业市场品牌塑造 …… 杨曼琳
55 茶马古道品牌的文化特征与商业运作模式研究 …… 王嘉惠，吴 莎等
56 茶叶企业市场营销的创新策略分析 …… 董水生
58 探析互联网营销模式下的茶叶经营管理 …… 李文贵

经济管理

59 茶叶企业财务审计的若干问题探讨 …… 招 燕
61 茶企业税务筹划优化策略研究 …… 张金媛
63 茶企业财务会计信息化管理研究 …… 朱文杰
65 金融会计理论在茶叶经济中的应用 …… 聂瑞芳
66 茶企财务内控管理绩效的策略研究 …… 李 涛
68 安溪县茶叶产业链的整合管理研究 …… 贺 杰
69 内部控制视角的茶企会计信息质量研究 …… 张鹏凯，李建光
71 茶叶企业财务成本精细化管理途径探析 …… 潘宗玲
72 茶叶生产企业的成本核算研究 …… 吴让军
74 以金融会计服务促进区域茶产业发展模式研究 …… 张源曲
75 新常态下茶叶家族企业财务信息质量的优化 …… 陆 晶
77 古代法家经管思想对现代江西茶叶市场管理的借鉴意义 …… 徐慧茗，张爱云
78 目标成本管理在茶企经济管理中的应用 …… 杨小彬
80 试论茶叶企业的经营现状及财务分析 …… 李爱香

茶馆设计

81 浅析茶艺会所室内空间设计 …… 潘 源

83 谈现代茶馆设计中传统元素的运用 …… 陈 明
85 中国庭院元素在现代茶馆室内设计中的运用探讨 …… 王玮璐
86 室内外景观元素融合在仰山禅茶体验区设计中的应用 …… 闫晓从
88 自然景观元素在茶饮空间设计中的应用 …… 杨正中
89 茶馆室内空间设计中对传统装饰元素的运用 …… 杜丽娜
91 谈仰山禅茶体验设计中室内外景观元素的多元化融合 …… 龙 洋
92 传统茶文化在现代环境艺术设计中运用研究 …… 曾 强
94 现代综合式茶楼建筑装饰特点研究——以昆明茶馆为例 …… 叶砚葳
95 茶馆环境设计的视觉影响 …… 崔营营
97 茶文化在现代茶馆环境设计中的渗透与应用研究 …… 盛 丽

茶艺创作

98 民乐艺术在茶艺文化中的体现研究 …… 陶曙光
100 论茶文化对茶艺人才培养的影响 …… 汪 建
101 公共管理专业茶艺课程的教学实践研究 …… 袁 媛，谢明荣
103 论音乐在茶艺表演中的重要性 …… 李云翔

生态旅游

104 茶文化旅游推进茶叶经济发展研究 …… 龚 娜
106 茶文化旅游与茶叶经济发展策略分析 …… 范 晔
108 黄山茶产地构建深度休闲旅游的实证研究 …… 杨征权
109 我国茶文化旅游资源开发思路 …… 易红燕
111 茶文化旅游经济发展策略探讨 …… 张 慧
112 探究茶文化旅游与茶业经济发展 …… 朱琳琳
114 浅析观光茶园的具体设计思路 …… 郑 昱
115 浅析观光茶园的具体设计思路 …… 窦 炎
117 茶文化产业园景观设计策略研究 …… 史俊巧
118 基于SWOT方法的温州茶文化旅游环境分析 …… 陈 超
120 浅析普洱茶文化旅游产品组合性开发构想和模式 …… 张博雅
121 生态观光茶园的规划设计 …… 席 晖
123 信阳毛尖茶叶文化旅游生态开发探究 …… 赵 华
124 环太湖地区茶文化旅游资源研究 …… 戴欣佚
126 论茶文化旅游区的可持续发展 …… 李 霞
127 茶资源的旅游模式开发研究 …… 范晓梅，李 艳等
129 现代茶树景观在园林中的应用 …… 王 伟，王兆卓
130 探析我国茶文化旅游深度开发的措施 …… 李 智
132 新时期背景下的中国茶旅一体化发展研究 …… 梅 华
133 新媒体背景下的茶文化旅游经济发展研究 …… 赵 艳
135 四川茶文化旅游资源特色及开发策略研究 …… 张 娟
136 茶园生态旅游项目的开发策略 …… 任媛媛
138 旅游经济与茶文化融合下的发展模式探讨 …… 李 红

机具·包装

139 茶叶揉捻自动化控制设备的技术分析 …… 任晓娜
141 茶叶抖筛筛分过程数学模型的建立 …… 杨 凯，高俊明等
142 基于PLC的茶叶装箱机组控制系统改造 …… 杨 征
144 现代茶具的设计理念走向与发展趋势 …… 况 敏
145 浅析现代紫砂茶具设计工艺 …… 李书志
147 瓷器茶壶传统造型对现代产品设计的启示 …… 郑 昊，张 彭
148 液压式茶饼紧压机械的单片机控制设计研究 …… 刘 峥
150 茶叶包装设计中水墨元素的应用分析 …… 阎 飞
152 茶叶包装设计的构成美学分析 …… 杨程中
154 茶叶包装的视觉传播特点分析 …… 张洪梅
156 水墨艺术元素在茶叶包装设计中的应用 …… 周 升
157 中国茶叶包装设计的审美体现与追求 …… 李 正
159 云纹在信阳茶叶包装设计中的运用与审美体现 …… 胡国锋
160 茶叶包装设计中民间美术造型的艺术表现 …… 牛东辉
162 视觉元素在普洱茶品牌包装设计中的应用 …… 宋 夏
163 我国传统文化元素在茶包装中的应用研究 …… 易雪峰
165 从禅意美学看茶叶包装中的文化延伸 …… 曹小兵，张文松
166 茶产品包装设计中的审美心理分析 …… 罗 京
168 浅析茶叶包装工艺中设计的重要性 …… 傅小芳
169 复古怀旧风格设计在茶叶包装上的应用 …… 李淑琴
171 茶叶包装设计中文字和色彩的审美体现与运用 …… 张 武，闫 力等
172 传统文化理念下茶的器具审美设计研究 …… 郑铭磊
174 浅析茶叶包装袋上的平面设计 …… 包 琳
175 论数字技术在黑茶包装设计中的应用 …… 宋馥利
177 茶叶品牌设计中"诗画"元素的应用与体现 …… 吴星辉
178 平面艺术在茶品中的应用分析 …… 连晓君
180 中国当前茶具设计的继承与创新研究 …… 徐 慧
181 花草茶包装设计的要素和新理念 …… 程甘霖
183 中国书法字体在茶叶包装设计中的运用 …… 陆 琦
184 平面视觉设计效应在茶叶包装过程中的应用分析 …… 张荟惠
186 茶产品包装中的摄影技巧分析与研究 …… 李恒全

187 油画静物教学中茶具的表现 …… 徐少华，高艳慧
189 茶叶包装设计中的传统文化元素分析与应用 …… 赵新伟

思考·探索

190 关联翻译理论在茶企简介翻译中的实用性 …… 邹艳芳，史慧娇
192 茶学专业实践教育改革研究 …… 张 旭，曾 贞等
193 提高职校机械制图教学策略探究 …… 陈加友
194 奥运商圈视阈下大型体育赛事对茶企发展的影响分析 …… 程 锋，易招华
196 茶叶品牌的商业会展设计研究 …… 袁雪雯
198 茶文化与当代大学生的素质培养研究 …… 张俊丽
200 基于茶文化角度的我国传统文化与平面设计关联性分析 …… 李 丹
201 谈茶道精神在中国式摔跤训练中的融入 …… 赵 蓉
203 在我国高校中开展采茶健身操的可行性及实践浅析 …… 尤海平
204 如何有效结合休闲农业环境与茶耕文化 …… 程 巍
206 基于生态足迹理论的茶文化探究 …… 张兴梅
207 基于微信的碎片化移动学习资源设计研究——以《茶文化产业实务》课程为例 …… 朱 楠，李明睿
209 茶学科技论文英译原则及其策略研究 …… 史云燕
210 在体育教学中融入民族传统体育运动项目的研究——以采茶操为例 …… 解 皓
212 传统与现代相结合的茶叶产品 LOGO 设计 …… 高 英
213 从茶文化看大学生人文修养 …… 陈 争
215 基于茶道精神的图书馆人文环境建设研究 …… 刁 歆
216 多维空间技术在《茶博会》动画广告中的应用探析 …… 索玉婵
218 现代家居纺织品设计中对中国茶染艺术的应用 …… 杨 尧
219 平面设计与茶文化关联性研究 …… 李晓丹
221 茶领域中计算机视觉图像处理技术应用方法研究 …… 刘宗平
222 探究奥运精神中的茶文化 …… 向玉山
224 采茶健身操在高校公共体育教学中的应用研究 …… 田造轩
225 采茶健身操实践与锻炼效果研究 …… 崔芮铭
227 基于茶道的中国传统武术研究 …… 王焱源
228 论茶文化在大学英语文化教学中的实施 …… 谭 鑫
230 从中西茶文化的差异看高校英语教学中的文化教学 …… 杨 椰
231 茶产业人力资源培训需求研究 …… 伍贤达
233 采茶健身操在高校公共体育课中的应用 …… 徐 鹏
234 大数据视角下茶叶智能技术应用的几点分析 …… 田 勇
236 探析茶文化对体育精神的塑造 …… 唐 溢
237 计算机技术在茶叶试验数据处理中的应用 …… 黄元力
239 中西茶文化差异视角下的英语学习与教学研究 …… 李 娜
240 基于茶文化理念的景观设计 …… 曾 艳
242 新课改形势下茶学专业英语课程的创新研究 …… 王 臻
243 传统茶文化与高校品德教育相融合的研究 …… 李 旭
245 从茶文化视角浅谈高校英语教学工作 …… 刘瞳菲，王 慧等
246 茶文化生态视角下关于湖南古丈茶歌进课堂的思考 …… 匡泓锦
248 如何在大学校园里面设置茶吧进行二次课堂教育 …… 张 桐
249 浅谈茶叶品牌建设中的知识产权保护思路分析——以安化黑茶为例 …… 张卫国
251 以 99°茶吧独立运行为例探讨河南省高职生就业创业教育培养模式创新 …… 关 霞
252 民族传统体育中采茶舞引入高校的"文化植入式"教学模式探析 …… 付文灿
254 城镇化建设背景下传统茶文化的传承与发展 …… 王淑兰，谭品峰
255 高校英语文化教学中开展茶文化教学的思考和建议 …… 闫 静
257 高职特色资源库建设现状分析——以茶文化数据库为例 …… 胡海东
258 茶文化引领学生感悟数学思想 …… 张新爱
260 提高云南茶叶产业精准扶贫绩效的对策 …… 陈惠敏
261 传统优势茶产业发展的思考与建议 …… 陈义吉
263 语言交际在茶事活动中的体现和重要性分析 …… 季彦君
264 茶文化对体育学生心理健康的影响 …… 涂爱云，孙镇雷
266 以茶文化教育为导向的体育教学设计与实践 …… 雷先龙
267 浅析茶文化对大学生传统文化教育的影响 …… 梁晓明
269 论茶文化与高校学生人文素质的培养 …… 梁 富，李玉清
270 茶企的人力资源管理模式创新与决策优化 …… 王文贤，霍 岩
272 茶理论在体育人文教育中的运用 …… 吕 辉
273 茶文化在高校对外交流中的作用 …… 赵 厦
275 茶艺教学在大学生素质教育中的作用 …… 潘运华，欧阳群
276 传统茶文化对高校管理思维的影响分析 …… 邹满丽
278 功能翻译理论下的茶艺解说词翻译初探 …… 宋丽萍
279 中华茶道与大学生传统文化教育结合初探 …… 张力派
281 论茶文化在大学英语文化教学中的实施 …… 孙用常
282 传统茶文化与高校英语教学相融合的研究 …… 向莎莉
284 我国茶文化的德育功能探求 …… 唐益政
285 茶叶储存网络监控系统平台的设计研究 …… 杨令省
287 茶道融入武术教育的研究 …… 吴金涛
288 茶文化对体育礼仪文化的倡导与发展模式研究 …… 臧海波

290 茶文化对提升体育修养的影响 …… 杨志伟
291 低碳经济背景下茶业发展的思路与对策研究 …… 张岩峰，王翔宇

历史·文化

293 儒家思想与茶文化内在关联性的研究 …… 陈 琳，赵崇俊
295 从茶文化解读中英价值观异同 …… 郭巧棉
297 论赣南采茶歌舞戏中的音乐特色 …… 黄海燕，梁 婧
299 普洱市城市景观与茶文化的关联性研究 …… 解 俊
301 浅谈《茶经》的美学意蕴及英译再现 …… 刘云霞，董国栋
303 古诗词曲中的茶文化英译之我见 …… 吴亚萍
305 茶文化在杨宪益英译本《红楼梦》中的处理 …… 肖 健
307 从中西茶文化的差异看高校英语教学中的文化教学 …… 闫 虹
309 茶道文化中民族音乐的变异及发展 …… 杨桂兰，王立宁
311 论赣南采茶戏与当地民歌艺术之间的相互借鉴 …… 张 坚
313 略论茶典籍的对外翻译与文化传播 …… 赵素娟，董国栋
315 中国茶文化在西方英语国家的传播研究 …… 朱计峰
317 论《红楼梦》中的茶文化内涵 …… 朱一华
319 从茶文化看英国文化向上的价值取向 …… 尹 鑫，何志静
320 英国文学作品中的"下午茶"研究 …… 黄 娟，肖 玲
322 浅谈茶文化的特色及其在古籍中的翻译研究 …… 邹园艳
323 浅谈中日茶文化异同及展望 …… 姜力维
325 从中国茶文化看传统道德修养的现实意义 …… 张 丹，张小明 等
326 跨文化视野下的中英茶文化比较分析 …… 全 涛
328 茶道文化的历史书写与权力语境 …… 尹巧瑞
329 论音乐教育在茶文化中的运用 …… 钟莉萍
331 云南"茶马古道"民歌音乐文化研究 …… 宗莉加
332 中英茶文化对比研究 …… 杨春冉
334 浅析赣南采茶舞蹈服装的设计和艺术表现形式 …… 吴 茜
335 浅谈茶与儒道佛思想文化 …… 韩 竹
337 官营茶马贸易的历史若干问题研究 …… 赵宏欣
338 从明清茶文化看才子佳人小说中的茶道文化 …… 周 燕
340 中日茶文化不同发展方向探究 …… 吕美佳
341 赣南地区茶篮灯设计艺术研究 …… 王志强
343 中西方"茶"文化的内涵及翻译理论实践研究 …… 何志静，叶 娜
344 茶文化在和谐社会建设中的作用研究 …… 李 林
346《红楼梦》中"茶"文化符号探析 …… 余高峰
347 大学英语翻转课堂评价在中西方茶文化传播中的应用 …… 孔 维
349 英国诗歌中的茶文化研究 …… 王 萍
350 中国茶文化英文翻译过程中技巧的应用 …… 张 丹
352 英语文学作品中的红茶文化研究 …… 蒋丽琴
353 茶道精神的"中庸"与马克思理论探讨 …… 张 元，杨 航
355 英国茶文化在西方文学作品中的体现 …… 魏 芳
356 江西茶歌的分类及其艺术特征分析 …… 韩 晶
358 中日茶文化精神及审美意识对比分析 …… 燕 青
359 顺应论视角下看《红楼梦》茶文化翻译 …… 李林蔚
361 广东客家茶文化及采茶舞的研究 …… 郭晓芳
362 简析红茶文化对英美文学的影响 …… 邹 灿，向 敏
364 由《傲慢与偏见》看英国文学作品中的茶文化 …… 季佩璇
365 赣南茶文化与茶俗对当地采茶歌舞的助推作用 …… 韩立民，杜 鹃
367 寻找茶文化的诗意——以纪录片《茶，一片树叶的故事》为例 …… 毛小芬
368 英语翻译教学中的中西茶文化比较 …… 陈 敏
370 宋代茶文化与建盏的相互作用关系研究 …… 牛丽彦
371 初探先秦时期的古代茶文化 …… 侯力丹，刘习宁
373 安溪茶文化与安溪茶歌的发展与传承 …… 任红星
374 跨文化视阈下《红楼梦》饮茶对白英译策略 …… 郭冬会
376 茶文化语境下之采茶音乐研究 …… 汪珂成
377 探究日本文化中的茶道文化 …… 图 雅
379 我国茶文化道德价值作用体现与分析 …… 王 辉，王嘉惠 等
380 从中英茶文化差异看茶语的翻译缺失 …… 魏慕连
382 中西茶文化的内涵分析与茶语交流 …… 吴贤雯
383 茶文化与体育文化之融合研究 …… 陈爱国
385 英国茶文化及其影响分析 …… 苏花青
386 探析采茶音乐的文化涵韵 …… 杨 杰，李 超
388 简·奥斯汀小说作品中的茶文化研究 …… 杨 梅
389《茶经》英译中茶文化的遗失与嬗变 …… 杨公建
391 音乐教育融入茶艺及茶文化学习中的作用 …… 刘凤桐
392 中国书画在茶文化中的探索 …… 王 雁
394 中英茶文化对比及对中国茶文化传播的影响 …… 张 楠
395 有关茶的诗词文学作品里的文学性和实用性探析 …… 张英沛
397 会计学在茶企业资产管理中的应用研究 …… 武美云
398 茶文化在大学英语角活动中的应用研究 …… 王秋云
399 中国茶道文化对小学教师专业发展的可借鉴性探索 …… 袁 霞

茶学专业实践教育改革研究

张 旭[1]，曾 贞[2]，肖 遂[1*]

（1. 华南农业大学，林学与风景园林学院；2. 华南农业大学，园艺学院，广东 广州 510642）

摘 要：茶学专业的实践教育目前存在着实验部分创新性不够，学生缺乏主动性，实习部分与社会接轨不足，基地建设和管理不完善等问题。应当通过增强实验部分的创新性和前沿性，引导学生主动学习，完善校内外实习基地的建设和管理，为学生今后踏入社会，更好地融入社会和服务社会打下坚实的基础。

关键词：茶学；实践教育；创新性；实习基地

实践是检验真理的唯一标准，茶学专业做为农学类专业之一，对于实践性有着极高的要求。理论与实践的统一是教师在教学过程中一直追求的目标，同样也是大学生在校学习期间努力的方向。各门理论课基础知识的学习是为了能在理论层面上对指导实践，而实践教育的开展是对理论知识的检验与补充。茶学专业要求学生掌握茶园生产管理技术、茶叶加工技术、茶饮料、茶叶深加工与综合利用、茶艺表演、茶叶评审与质量检验和营销方面的基本技能，因此，对于实践教育有着更高的要求。本文将对目前实践教育存在的问题以及实践教育的改革思路进行阐述和分析，期望能引发茶学教育工作者进一步的思考和完善。

1 目前实践教育存在的不足和改革的必要性

1.1 实验部分创新性不够，学生缺乏主动性

当前的实践教育包括两方面，即实验部分和实习部分。在试验部分的课程设置中首先是基础实验课，然后按专业方向不同开设不同的专业实验课。基础实验课的开设按基础课程需要设置，目的是让学生掌握基本的实验操作技能，而专业实验课由本专业负责设计开展，目的是让已学会基本实验操作技能的学生能将所学操作技能用于本专业的具体实验操作中。然而由于基础实验和专业实验的脱节，往往导致学生在学习基础实验课程时缺乏目的性，只是单纯和机械地按照学习大纲进行实验操作，并不知道该实验操作在今后本专业实验中的作用，从而也进一步导致在专业实验课过程中，无法有效运用基本的实验操作进行整体的实验设计，只能由专业课老师负责实验的整体设计，以至学生在学习专业实验课时缺乏主动性，最终导致学生在试验课程中只是接受了操作上的训练，无法培养学生的创新性思维和科研能力。

传统实验课程的教学模式是按照教材让学生课前预习，上课时先由实验课老师介绍实验目的讲解实验原理，在示范操作之后由实验员带领学生按实验内容进行操作，课程结束后写实验报告并上交。且实验课所用教材内容更新慢，实验室设备陈旧，实验手段落后，学生所学的实验手段可能现在早已不在实际中使用。这种传统的模式缺乏创新性，不利于激发学生的学习兴趣，也无法适应研究生阶段以及社会对人才的需求。

1.2 实习部分与社会接轨不足，实习基地建设存在问题

茶叶行业是一个非常专业的行业，茶学专业毕业的学生大多是在本行业工作，因此，我们的教育方式必须主动去适应社会，培养学生毕业后能尽快走上工作岗位，适应社会的需要，而实习教育是学生在校学习阶段最能接近社会的时期。现阶段我们的实习教育，由于实践教育经费不足，校内实习基地建设和管理往往达不到实际的需求，存在着实习基地面积不够、专业设备陈旧落后、管理方式松散等问题，导致在校内实习基地开展的实习教育与社会接轨不足，不能学习和实践到目前社会上的先进理念和先进技术。校外的实习基地则缺乏长期的合作关系，以至于出现需要带领实习的老师动用私人关系自己找地方给学生实习，所以导致每一届学生校外实习地点都不一致，前后没有延续性，无法系统地为学生设计实习内容，达不到理想的目的，同时，由于校外实习基地的不固定，学生实习住宿生活条件差，因此，学生和老师都对于实习教育兴趣不高。

2 茶学专业实践教育改革思路

2.1 增强实验部分的创新性和前沿性，引导学生主动学习

在基础实验教学部分，可以由茶学专业的老师为学生量身定制实验内容，设计完整的实验来串联起基础实验原本分散的实验内容，如茶叶内在成分的分析，能将滴定、比色、蒸馏、旋干等操作步骤系统地进行学习，而普洱茶中菌落的分析又能学习到微生物中的无菌操作、种属鉴定等内容。这样的实验设计既能和传统的基础实验教学一样，学习到基础的实验操作，还能让学生对实验设计有了直观和整体的感受，让他们了解到做一个完整的实验需要哪些实验步骤，而只有认真完成这些实验步骤里面所涉及的每一项操作内容，整个实验才可能成功。学生在基础实验课的学习当中，目的性会更强，更有助于消化学习内容，为下一步的专业实验课打下良好的基础。

在专业实验的教学中，可以让学生更多地参与到实验的设计当中，改变原有的由老师设计实验学生操作的模式。专业实验课的老师可以设计一些实际课题，让学生分组设计实验，用于解决该问题，先由学生查阅文献设计实验方案并上交，老师根据实验室的现有条件给他们分析设计的可行性，辅导学生确定最终实验方案，在试验完成后，由老师指导学生对实验数据进行整理分析，最终以科技论文的形式提交作业。这些课题既有经典的实验，又有老师目前的在研课题中的分支方向，经典的课题能用于给学生建立良好的科研思路，在研的课题有利于增加实验内容的前沿性。在实验设计和开展的过程中，可以鼓励学生将有潜力的课题申报大学生创新项目等实验相关的项目，增强学习的主动性。改革以后的专业实验课能在文献查阅、试验设计、项目申请书的撰写、实验操作、数据整理和分析、科技论文写作等方面全面培养学生的科研能力。实验部分创新性和前沿性的加入，有助于提高学生学习的兴趣，在实验过程中更好地发挥他们的主观能动性。

2.2 完善实习基地的建设和管理

实习基地的建设直接关系到实习教育开展的质量，好的实习基地能将学生的实践能力和创新能力落到实处。对于校内实习基地已经落后的实验设备应予以淘汰，购买先进的实验设备以及生产线等，建设新的温室和加工室，根据设备的更新换代，改进目前的实习内容。不再由课程老师兼职管理基地，设置专门的实习基地管理人员团队，规范化管理校内实习基地，在实习课程开展期间定期邀请企业的专业技术人员过来进行交流和指导，加强学校基地与社会的沟通，多了解目前茶叶行业的先进技术和生产理念，以及各岗位对人才的需求状况，对学生将来的就业起到一定的指导作用。

由于茶学专业方向跨度较大，如茶叶加工与贸易方向、茶艺与品牌营销方向以及茶学方向，在校外实习基地选择时将要考虑到工业、贸易、农业等不同方向的需求，因此，需要根据专业的特点，有目的有计划的选择校外实习单位。建立学校或学院的实习基地，双方签订长期有效合同，对实习基地进行挂牌，保障实习基地的稳定性，有利于实习教育开展的延续性。要求校外实习基地要利用已有的生产技术和管理模式满足实习教育任务的有效完成，定期接收一定量学生参加实习教育，提供必要的住宿、生活、工作条件，按学校规定收取一定费用；学院方面在实习期间应选派具有丰富实践教学能力的老师随实习学生一同前往，指导学生实习，并且给予实习基地提供技术指导，做到双方互惠互利，义务和责任共同分担。

实践教育是我们为培养“产学研”三位一体的创新性人才而实施的教育方式，只有当我们的实践教育的形式和内容更具创新性和前沿性，管理方式更加规范，所学知识与社会接轨而更有实用性，才能充分调动学生的积极性，发挥他们的主观能动性，让理论教育不会仅限于纸上谈兵，为学生今后踏入社会，更好地融入社会和服务社会打下坚实的基础。

参考文献

[1] 郭风法，宁堂原，王守义等.农学专业实验教学改革与实践[J].实验科学与技术，2006（2）：88-91.

[2] 刘向东，郭海滨.现代农学专业实验课整合改革研究[J].中国农业教育，2013(5)：60-63.

[3] 杨晓萍.茶学专业实践教学改革与创新[J].实验室科学，2010（13）：9-12.

[4] 林宏政，郝志龙，金心怡等.茶学专业实践教学现状及创新发展思路[J].福建茶叶，2016（1）:170-171.

(C)1994-2024 China Academic Journal Electronic Publishing House. All rights reserved. http://www.cnki.net

SCAULIB202518653

检索证明

根据委托人提供的论文材料，委托人**华南农业大学 张旭** 15 篇论文收录情况如下表。

序号	论文名称	发表刊物及发表的年月卷期/页码等	作者排名	论文等级	作者文中单位	收录情况	影响因子	中科院大类分区
1	Short-term steaming during processing impacts the quality of Citri Reticulatae 'Chachi' peel	FOOD CHEMISTRY 出版年：2024 出版日期：JUL 30 卷期：447 页码：- 文献号：138964 文献类型：Article	共同通讯作者（排名最后）	T2 类	华南农业大学林学与风景园林学院	SCI	IF2-year=9.8 IF5-year=9.7 （2024）	农林科学 1 区 Top 期刊：是 （2025）
2	CKLF instigates a "cold" microenvironment to promote MYCN-mediated tumor aggressiveness	SCIENCE ADVANCES 出版年：2024 出版日期：MAR 15 卷期：10 11 页码：- 文献号：eadh9547 文献类型：Article	并列第一作者	T2 类	华南农业大学林学与风景园林学院	SCI	IF2-year=12.5 IF5-year=14.1 （2024）	综合性期刊 1 区 Top 期刊：是 （2025）
3	Differences in the components of Neolamarckia cadamba from different provenance and the drug resistance reversal activity of characteristic alkaloid	INDUSTRIAL CROPS AND PRODUCTS 出版年：2022 出版日期：OCT 15 卷期：186 页码：- 文献号：115145	共同通讯作者	T2 类	华南农业大学林学与风景园林学院	SCI	IF2-year=5.9 IF5-year=6.0 （2022）	农林科学 1 区 Top 期刊：是 （2022）

华南农业大学图书馆SCAULIB202518653 查询检索专用章

11	STUDY ON THE ANTI-TUMOR ABILITY OF NIAOWANGZHONG GREEN TEA	JOURNAL OF FOOD BIOCHEMISTRY 出版年：2017 出版日期：FEB 卷期：41 1 页码：- 文献号：e12305 文献类型：Article	共同通讯作者（排名最后）	B 类	华南农业大学林学与风景园林学院	SCI	IF2-year=1.552 IF5-year=1.328 （2017）	生物 4 区 Top 期刊：否 （2017）
12	An Approach for Searching Bioactive Compounds from Traditional Chinese Plant Food and Herb Medicines by Investigating Spectrum-Effect Relationships	CURRENT PHARMACEUTICAL ANALYSIS 出版年：2017 卷期：13 5 页码：417-426 文献类型：Article	第一作者	B 类	华南农业大学林学与风景园林学院	SCI	IF2-year=0.859 IF5-year=0.756 （2017）	医学 4 区 Top 期刊：否 （2017）
13	柑普提取物对 HepG2 和 SGC-7901 肿瘤细胞系的抗增殖作用	现代食品科技 出版年：2020 卷期： 页码：- 文献号： 文献类型：	通讯作者	C 类	华南农业大学林学与风景园林学院	北大核心	无	无
14	茶学专业实践教育改革研究	福建茶叶 出版年：2016 卷期： 页码：- 文献号： 文献类型：	第一作者	C 类	华南农业大学林学与风景园林学院	CNKI	无	无

华南农业大学图书馆SCAULIB20251206153
华南农业大学图书馆 版权所有 禁止商业用途

普通高等教育“十四五”规划教材

药理学与临床药物应用

石雪梅 等主编



黑龙江科学技术出版社
HEILONGJIANG SCIENCE AND TECHNOLOGY PRESS

图书在版编目（CIP）数据

药理学与临床药物应用 / 石雪梅等主编. — 哈尔滨：黑龙江科学技术出版社，2021.4
ISBN 978-7-5719-0915-4

Ⅰ. ①药… Ⅱ. ①石… Ⅲ. ①药理学②临床药学 Ⅳ. ①R96②R97

中国版本图书馆 CIP 数据核字(2021)第 060754 号

药理学与临床药物应用

责任编辑 焦 艳
封面设计 麻 凯
制 版 哈尔滨博宇印务有限公司
开 本 710mm×1000mm 1/16
字 数 600 千字
印 张 25.25
印 数 1-500 册
版 次 2023 年 4 月第 1 版
印 次 2023 年 4 月第 1 次印刷

出 版 黑龙江科学技术出版社
发 行 黑龙江科学技术出版社
地 址 哈尔滨市南岗区公安街 70-2 号
邮 编 130021
印 刷 哈尔滨博宇印务有限公司

书 号 ISBN 978-7-5719-0915-4
定 价 88.00 元
版权所有 翻印必究

《药理学与临床药物应用》

编委会

主　编：

石雪梅　武汉大学人民医院

鉴红霞　温州市人民医院

郑媛媛　铜陵市人民医院

张红静　杭州医学院

张友志　赣南医学院第一附属医院

副主编：

张　旭　华南农业大学林学与风景园林学院

前　言

本书系统介绍了药理学总论、作用于传出神经系统的药物、中枢神经系统药理学、心血管系统药理学、血液及内脏系统药理学、内分泌系统药理学、化学治疗药物等内容。其内容的深度、广度、新度适宜，尽可能的做到深入浅出，简明精炼，力求达到科学性、先进性、系统性思想性和实用性的原则，对各个章节进行了有效融合。可作为临床医师、药学专业技术人员参考使用。

本书具体编写分工如下：石雪梅编写了第四篇、第六篇的内容（共计11.4万字）；鉴红霞编写了第一篇、第七篇（第四十四章、第四十五章）的内容（共计10.7万字）；郑媛媛编写了第三篇的内容（共计9.6万字）；张红静编写了第二篇的内容（共计8.8万字）；张友志编写了第五篇的内容（共计8.6万字）；张旭编写了第七篇（第三十五章至第四十三章）的内容（共计10.9万字）。全书由石雪梅负责统稿完成。

由于学识水平有限，书中难免有疏漏甚至谬误，期望广大专家学者给予批评指正。

ISBN 978-7-5719-0915-4

定 价：88.00元

广东省财政厅文件

粤财资环〔2024〕84号

广东省财政厅关于下达2024年中央财政林业草原生态保护恢复资金（第二批）的通知

省直有关单位，有关地级以上市财政局，有关财政省直管县（市）财政局：

根据《财政部关于下达2024年林业草原生态保护恢复资金预算（第二批）的通知》（财资环〔2024〕30号）和《广东省林业局关于报送2024年中央财政林业草原生态保护恢复资金（第二批）分配方案和绩效目标的函》（粤林函〔2024〕110号），现下达2024年中央财政林业草原生态保护恢复资金（具体项目、金额见附件1）。该项资金收入列一般公共预算收入科目“1100250 节能环保共同财政事权转移支付收入”，涉及自然保

护地、野生动植物相关支出列“2110406 自然保护地”，其余方向支出列“2110499 其他自然生态保护支出”。有关事项通知如下:

一、请认真落实《财政部 国家林草局关于印发〈林业草原生态保护恢复资金管理办法〉的通知》（财资环〔2022〕170 号）等文件要求，切实管好用好林业草原生态保护恢复资金。各地、各单位应抓紧将资金安排到具体项目，加快资金拨付使用进度，充分发挥资金使用效益。切实加强资金监管，不得挤占、截留或挪用，确保专款专用。

二、请严格落实全面实施预算绩效管理的要求，在预算执行过程中，对照本次下达的绩效目标做好绩效运行监控，确保年度绩效目标如期实现，财政资金发挥预期效益。年度终了，请按规定编列决算，并于 2025 年 1 月底前将项目绩效自评报告报送省林业局、省财政厅。

附件：1. 2024 年第二批中央财政林业草原生态保护恢复资金安排表

2. 野生动植物保护补助情况表

3. 野生动植物保护补助项目绩效目标表

4. 国家级保护区补助情况表

5. 国家级保护区补助项目绩效目标表

6. 湿地保护修复补助情况表

7. 湿地保护修复补助项目绩效目标表

8. 古树名木保护补助情况表

9. 古树名木保护补助项目绩效目标表

广东省财政厅

2024 年 7 月 31 日

附件1

2024年第二批中央财政林业草原生态保护恢复资金安排表

单位：元

单位名称	单位编码	项目名称	分配单位	三保目录	是否直接“三保”专户	功能分类科目	部门经济分类科目	政府经济分类科目	金额	备注
合计									39180000.00	
一、各省直部门合计									31180000.00	
省教育厅小计	156								1300000.00	
华南农业大学	156003	2024年中央财政林业草原生态保护恢复资金（第二批）-大叶茶、华南锥等国家重点保护野生植物的综合保护		无	否	2110406 自然保护地			1000000.00	
							30299 其他商品和服务支出	50502 商品和服务支出	1000000.00	
广东海洋大学	156007	2024年中央财政林业草原生态保护恢复资金（第二批）-广东省候鸟重要病毒的病毒数据库建立及风险评估		无	否	2110406 自然保护地			300000.00	
							30299 其他商品和服务支出	50502 商品和服务支出	300000.00	
省林业局小计	199								28180000.00	
广东省林业局	199001	2024年中央财政林业草原生态保护恢复资金（第二批）-广东省一级古树和名木抢救复壮（第二批）		无	否	2110499 其他自然生态保护支出			600000.00	
							30299 其他商品和服务支出	50299 其他商品和服务支出	600000.00	
广东省林业局	199001	2024年中央财政林业草原生态保护恢复资金（第二批）-华南国家植物园建设-4种国家重点保护红豆属植物的多维多样性智慧化监测与迁地保护（中国科学院华南植物园）		无	否	2110406 自然保护地			2500000.00	
							30299 其他商品和服务支出	50299 其他商品和服务支出	2500000.00	
广东省林业局	199001	2024年中央财政林业草原生态保护恢复资金（第二批）-古树名木监测救护		无	否	2110499 其他自然生态保护支出			500000.00	
							30299 其他商品和服务支出	50299 其他商品和服务支出	500000.00	
广东省林业局	199001	2024年中央财政林业草原生态保护恢复资金（第二批）-广东省越冬水鸟种群监测（粤西片区）（中山大学）		无	否	2110406 自然保护地			300000.00	
							30299 其他商品和服务支出	50299 其他商品和服务支出	300000.00	

单位名称	单位编码	项目名称	分配单位	三保目录	是否直拨“三保”专户	功能分类科目	部门经济分类科目	政府经济分类科目	金额	备注
广东省林业局	199001	2024年中央财政林业草原生态保护恢复资金（第二批）-厚叶木莲种质资源收集保存和丹霞栲铜野外回归示范（中国林业科学研究院热带林业研究所）		无	否	2110406 自然保护地			1500000.00	
							30299 其他商品和服务支出	50299 其他商品和服务支出	1500000.00	
广东省林业调查规划院	199004	2024年中央财政林业草原生态保护恢复资金（第二批）-广东省越冬水鸟和国家重点物种种群专项监测		无	否	2110406 自然保护地			800000.00	
							30299 其他商品和服务支出	50502 商品和服务支出	800000.00	
广东车八岭国家级自然保护区管理局	199024	2024年中央财政林业草原生态保护恢复资金（第二批）-车八岭保护区松材线虫病防治		无	否	2110406 自然保护地			500000.00	
							30299 其他商品和服务支出	50502 商品和服务支出	500000.00	
广东内伶仃福田国家级自然保护区管理局	199027	2024年中央财政林业草原生态保护恢复资金（第二批）-内伶仃鸟猕猴种群资源监测及人为干扰评估		无	否	2110406 自然保护地			350000.00	
							30299 其他商品和服务支出	50502 商品和服务支出	350000.00	
广东内伶仃福田国家级自然保护区管理局	199027	2024年中央财政林业草原生态保护恢复资金（第二批）-广东内伶仃福田国家级自然保护区趣味故事编制		无	否	2110406 自然保护地			950000.00	
							30299 其他商品和服务支出	50502 商品和服务支出	950000.00	
广东内伶仃福田国家级自然保护区管理局	199027	2024年中央财政林业草原生态保护恢复资金（第二批）-中华穿山甲野外科学观测研究站建设		无	否	2110406 自然保护地			3100000.00	
							30299 其他商品和服务支出	50502 商品和服务支出	3100000.00	
广东湛江红树林国家级自然保护区管理局	199030	2024年中央财政林业草原生态保护恢复资金（第二批）-基于无人机遥感的红树林资源监测系统建设		无	否	2110406 自然保护地			760000.00	
							30299 其他商品和服务支出	50502 商品和服务支出	760000.00	
广东湛江红树林国家级自然保护区管理局	199030	2024年中央财政林业草原生态保护恢复资金（第二批）-湛江红树林国际重要湿地宣教与动态监测能力提升		无	否	2110499 其他自然生态保护支出			4800000.00	
							30299 其他商品和服务支出	50502 商品和服务支出	4800000.00	
广东鹤江罗坑鳄蜥省级自然保护区管理处	199043	2024年中央财政林业草原生态保护恢复资金（第二批）-2024年广东罗坑鳄蜥国家级自然保护区松材线虫病防治项目		无	否	2110406 自然保护地			760000.00	
							30299 其他商品和服务支出	50502 商品和服务支出	760000.00	

单位名称	单位编码	项目名称	分配单位	三保目录	是否直拨“三保”专户	功能分类科目	部门经济分类科目	政府经济分类科目	金额	备注
广东省野生动物救护中心	199057	2024年中央财政林业草原生态保护恢复资金（第二批）-野生动物收容救护及野化训练能力提升		无	否	2110406 自然保护地			300000.00	
							30299 其他商品和服务支出	50502 商品和服务支出	300000.00	
广东省野生动物救护中心	199057	2024年中央财政林业草原生态保护恢复资金（第二批）-穿山甲等珍稀濒危物种野外监测、收容救护和疫源疫病监测能力提升		无	否	2110406 自然保护地			3210000.00	
							30299 其他商品和服务支出	50502 商品和服务支出	3210000.00	
广东省德庆林场	199092	2024年中央财政林业草原生态保护恢复资金（第二批）-红豆属植物繁育回归示范项目		无	否	2110406 自然保护地			1000000.00	
							30299 其他商品和服务支出	50502 商品和服务支出	1000000.00	
广东珠江口中华白海豚国家级自然保护区管理局	199095	2024年中央财政林业草原生态保护恢复资金（第二批）-中华白海豚宣传能力提升项目		无	否	2110406 自然保护地			750000.00	
							30299 其他商品和服务支出	50502 商品和服务支出	750000.00	
广东徐闻珊瑚礁国家级自然保护区管理局	199098	2024年中央财政林业草原生态保护恢复资金（第二批）-广东徐闻珊瑚礁国家级自然保护区珊瑚礁生态系统修复		无	否	2110406 自然保护地			3000000.00	
							30299 其他商品和服务支出	50502 商品和服务支出	3000000.00	
广东徐闻珊瑚礁国家级自然保护区管理局	199098	2024年中央财政林业草原生态保护恢复资金（第二批）-广东徐闻珊瑚礁国家级自然保护区调查监测与环境治理项目		无	否	2110406 自然保护地			1300000.00	
							30299 其他商品和服务支出	50502 商品和服务支出	1300000.00	
广东南澎列岛海洋生态国家级自然保护区管理局	199099	2024年中央财政林业草原生态保护恢复资金（第二批）-广东南澎列岛国际重要湿地海洋垃圾清理项目		无	否	2110499 其他自然生态保护支出			1200000.00	
							30299 其他商品和服务支出	50502 商品和服务支出	1200000.00	
省农科院小计	403								300000.00	
广东省农业科学院动物卫生研究所	403013	2024年中央财政林业草原生态保护恢复资金（第二批）-广东省人工繁育野生动物病毒学本底数据库及预警平台建设		无	否	2110406 自然保护地			300000.00	
							30299 其他商品和服务支出	50502 商品和服务支出	300000.00	
广东省科学院小计	405								1400000.00	

单位名称	单位编码	项目名称	分配单位	三保目录	是否直拨“三保”专户	功能分类科目	部门经济分类科目	政府经济分类科目	金额	备注
广东省科学院动物研究所	405003	2024年中央财政林业草原生态保护恢复资金（第二批）-黑脸琵鹭等珍稀鸟类、越冬水鸟种群和肇事野生动物专项监测		无	否	2110406 自然保护地			1400000.00	
							30299 其他商品和服务支出	50502 商品和服务支出	1400000.00	
二、各市合计									6000000.00	
广州市小计	440199000								5500000.00	
广州市本级	440100000	2024年中央财政林业草原生态保护恢复资金（第二批）-虎保护及救护能力提升	440100000广州市本级	无	否	2300250 节能环保共同财政事权转移支付支出			1500000.00	
								51301 上下级政府间转移性支出	1500000.00	
广州市本级	440100000	2024年中央财政林业草原生态保护恢复资金（第二批）-2024年广东广州海珠国际重要湿地生态巡护管理及生物多样性科研宣教项目	440100000广州市本级	无	否	2300250 节能环保共同财政事权转移支付支出			4000000.00	
								51301 上下级政府间转移性支出	4000000.00	
肇庆市（不含省直管县）小计	441299000								500000.00	
肇庆市本级	441200000	2024年中央财政林业草原生态保护恢复资金（第二批）-肇庆市濒危野生动物救护中心收容救护能力提升	441200000肇庆市本级	无	否	2300250 节能环保共同财政事权转移支付支出			500000.00	
								51301 上下级政府间转移性支出	500000.00	
三、各直管县合计									2000000.00	
韶关市小计	440299000								2000000.00	
南雄市	440282000	2024年中央财政林业草原生态保护恢复资金（第二批）-广东省南雄市乳江国家重要湿地2024年湿地保护能力提升项目	440282000南雄市	无	否	2300250 节能环保共同财政事权转移支付支出			2000000.00	
								51301 上下级政府间转移性支出	2000000.00	

附件2

野生动植物保护补助情况表

序号	项目单位	项目名称	金额（万元）
合　　计			1461
省级及中央驻穗单位			1261
1	广东省野生动物监测救护中心	2024年穿山甲野外监测、收容救护、疫源疫病监测能力提升项目	321
2	广州市野生动物救护中心	广州市野生动物救护中心动物救护笼舍及野化训练区提升改造项目	30
3	广东省林业调查规划院	广东省越冬水鸟和国家重点物种种群监测	80
4	广东省德庆林场	红豆属植物繁育回归示范项目	100
5	中国科学院华南植物园	华南国家植物园建设-4种国家重点保护红豆属植物的多维多样性智慧化监测与迁地保护	250
6	中国林业科学研究院热带林业研究所	厚叶木莲种质资源收集保存和丹霞梧桐野外回归示范	150
7	广东省农业科学院动物卫生研究所	广东省人工繁育野生动物病毒学本底数据库及预警平台建设	30
8	广东省科学院动物研究所	黑脸琵鹭等珍稀鸟类、越冬水鸟种群和肇事野生动物专项监测	140
9	中山大学	广东省越冬水鸟种群监测（粤西片区）	30
10	广东海洋大学	广东省候鸟重要病毒的病毒数据库建立及风险评估	30
11	华南农业大学	国家二级保护植物大叶茶、华南锥的综合保护	100
市县单位			200
12	广州动物园	虎保护及救护能力提升	150
13	肇庆市林业局	肇庆市濒危野生动物救护中心收容救护能力提升	50

附件3

野生动植物保护补助项目绩效目标表

项目名称	穿山甲等珍稀濒危物种野外监测、收容救护和疫源疫病监测能力提升						
主管部门	广东省林业局				用款单位	广东省野生动物监测救护中心	
实施期限	起始年度	2024			终止年度	2024	
预算金额（万元）	立项总金额	321			当年度金额	321	
项目概述	本项目主要内容穿山甲野外监测、收容救护、疫源疫病监测能力，预算321万元，由广东省野生动物监测救护中心承担。具体内容为： 一、开展2个我国南方重要穿山甲分布省份（江西、福建）的野外监测工作； 二、采购分发应急处置物资一批（防护服、医用口罩、护目镜、消毒液和高筒雨鞋等），以提升我省24个国家级监测站应急处置能力； 三、开展穿山甲救护设备的购置，穿山甲个体识别技术的研究； 四、开展穿山甲保护工作，组织编写《穿山甲保护行动方案》，印刷制作穿山甲保护宣传材料。						
实施周期总目标	进一步推动我省穿山甲保护工作，通过开展穿山甲巡护看守、调查监测、收容救护、繁育放归等工作，为穿山甲的保护研究提供技术支撑。开展广东省陆生野生疫源疫病监测体系维护与预警及相关数据分析工作，提高我省野生动物疫源疫病应急处置能力。						
当年度目标	进一步推动我省穿山甲保护工作，通过开展穿山甲巡护看守、调查监测、收容救护、繁育放归等工作，为穿山甲的保护研究提供技术支撑。开展广东省陆生野生疫源疫病监测体系维护与预警及相关数据分析工作，提高我省野生动物疫源疫病应急处置能力。						
绩效指标	一级指标	二级指标	三级指标	指标解释	实施周期指标值		当年度指标值	
	产出指标	数量指标	完成穿山甲重点监测单元监测	开展穿山甲监测	≥6个		≥6个	
			国家级监测站应急值守率	节假日国家级监测站应急值守在岗率	100%		100%	
			完成穿山甲等野生动物救护批次	中心完成穿山甲等野生动物救护	≥20批次		≥20批次	
		质量指标	成果验收合格率	项目成果验收的合格率	100%		100%	
		时效指标	应急储备物资采购完成时间	应急储备物资采购的完成时间	2024年12月前		2024年12月前	
	效益指标	生态效益指标	是否完善广东省陆生野生疫源疫病监测体系	项目完成后，广东省陆生野生疫源疫病监测体系是否得到完善提升	是		是	
	满意度指标	服务对象满意度指标	服务对象满意度	服务对象满意程度	≥95%		≥95%	

野生动植物保护补助项目绩效目标表

项目名称	广东省越冬水鸟和国家重点物种种群专项监测				
主管部门	广东省林业局			用款单位	广东省林业调查规划院
实施期限	起始年度	2024年		终止年度	2024年
预算金额（万元）	立项总金额	80		当年度金额	80
项目概述	根据《2024年度全国越冬水鸟同步监测工作方案》、《全国越冬水鸟同步监测技术方案》、《关于印发<陆生野生动物监测技术指南（试行）>和规范开展陆生野生动物监测有关事项的通知》和《关于开展全国珍稀濒危野生动植物监测工作的函》的要求，组织开展我省越冬水鸟同步监测工作和莽山烙铁头蛇、黑脸琵鹭、中华秋沙鸭、中华凤头燕鸥等珍稀濒危物种监测体系建设工作，并收集整理我省分布国家重点物种情况。				
实施周期总目标	明确我省越冬水鸟组成及其种群状况；推进我省珍稀濒危鸟类监测体系建设；掌握莽山烙铁头蛇在我省的具体分布情况，及其种群动态变化；分析掌握广东省国家重点保护动物情况。				
当年度目标	明确我省越冬水鸟组成及其种群状况；推进我省珍稀濒危鸟类监测体系建设；掌握莽山烙铁头蛇在我省的具体分布情况，及其种群动态变化；分析掌握广东省国家重点保护动物情况。				

	一级指标	二级指标	三级指标	指标解释	实施周期指标值	当年度指标值
绩效指标	产出指标	数量指标	野生动物监测设备	反应野生动物监测设备的布设数量。	10套	10套
			设置围栏陷阱	反应围栏陷阱的设置数量。	5处	5处
			撰写项目内容相关报告	反应完成相关内容的报告数量。	2份	2份
	效益指标	可持续影响	资源监测能力	反映项目实施对资源监测能力的影响情况。	明显提高	明显提高
	满意度指标	服务对象满意度指标	服务对象满意度	反映受益对象对工作开展的满意度情况。	≥95%	≥95%

野生动植物保护补助项目绩效目标表

项目名称	红豆属植物繁育回归示范项目				
主管部门	广东省林业局		用款单位	广东省德庆林场	
实施期限	起始年度	2024	终止年度	2024	
预算金额（万元）	立项总金额	100	当年度金额	100	
项目概述	本项目拟在广东省德庆林场范围内地势平坦，水热条件好的芒坑工区、林场森林生态综合示范园及苗圃等区域进行8种广东红豆属植物种子育苗、扦插扩繁培育种苗5000株，为后续德庆林场的林分改造，国家重点保护极小种群植物的保育、回归、复壮提供理论和实践依据，为绿美广东生态建设提供珍稀特有红豆属种苗保障。种苗繁育成功后，在广东省德庆林场范围内选择合适的地段，进行回归种植示范20亩，完善红豆属育苗回归示范点的科普步道、引水喷水设施、科普节点设计及相关科普牌制作安装，展示红豆属特级用材树种材性、优良品种选育、保育回归等方面信息，将其打造成华南特色红豆中心基地，成为集展示红豆属植物保育、回归，科普教育、绿美广东生态建设成果的综合窗口。				
总体绩效目标	实施周期总目标			当年度目标	
	在广东省德庆林场范围内地势平坦，水热条件好的芒坑工区、林场森林生态综合示范园及苗圃等区域进行8种广东红豆属植物种子育苗、扦插扩繁培育种苗5000株，种苗繁育成功后，在广东省德庆林场范围内选择合适的地段，进行回归种植示范20亩，完善红豆属育苗回归示范点的科普步道、引水喷水设施、科普节点设计及相关科普牌制作安装，展示红豆属特级用材树种材性、优良品种选育、保育回归等方面信息，将其打造成华南特色红豆中心基地，成为集展示红豆属植物保育、回归，科普教育、绿美广东生态建设成果的综合窗口。			8种广东红豆属植物种子育苗、扦插扩繁培育种苗5000株，回归种植示范20亩，完善红豆属育苗回归示范点的科普步道、引水喷水设施、科普节点设计及相关科普牌制作安装，展示红豆属特级用材树种材性、优良品种选育、保育回归等方面信息，将其打造成华南特色红豆中心基地，成为集展示红豆属植物保育、回归，科普教育、绿美广东生态建设成果的综合窗口。	
绩效指标	一级指标	二级指标	三级指标	实施周期指标值	当年度指标值
	产出指标	数量指标	繁育红豆属植物	8种	8种
			苗木繁育数量	5000株	5000株
		质量指标	成果验收合格率	≥95%	≥95%
	效益指标	经济效益指标	带来间接的经济效益（是/否）	是	是
		社会效益指标	加强生态保护意识（是/否）	是	是
		生态效益指标	加强重点保护物种的保育（是/否）	是	是
		可持续影响指标	对地方经济发展、促进就业的影响	良好	良好
		服务对象满意度指标	服务对象满意度指标	≥95%	≥95%

野生动植物保护补助项目绩效目标表

项目名称	华南国家植物园建设-4种国家重点保护红豆属植物的多维多样性智慧化监测与迁地保护			
主管部门	广东省林业局		用款单位	中国科学院华南植物园
实施期限	起始年度	2024	终止年度	2024
预算金额（万元）	立项总金额	250	当年度金额	250
项目概述	本项目针对鼎湖山自然分布的红豆属植物均面临生存面积狭小、更新困难等问题，将通过科学监测和创新技术，对鼎湖山自然保护区内的4种红豆属植物开展长期群落监测；在华南植物园、广东鹤山和德庆林场建立迁地栽培种质资源圃；利用遗传多样性、繁殖生态学、生理生态学和群落生态学的综合研究方法，开展迁地保护；利用科学数据智慧化采集、监测与迁地保护应用系统，构建高效的生物多样性监测网络，实现数据的精准管理和智能化应用。项目结果将有利于加强红豆属植物的高效保护管理，提出全面合理的保护复壮方法与措施，确保珍稀植物资源的长期可持续性，为推动生态文明建设贡献科技力量。			
实施周期总目标	本项目聚焦鼎湖山自然保护区自然分布的4种国家重点保护红豆属植物（肥荚红豆、茸荚红豆、软荚红豆和光叶红豆），以群落监测为基础，结合鼎湖山20公顷固定大样地20年的植物群落动态监测数据，从“分类-谱系-功能”多样性等维度，在全球变化背景下开展多层次多维度多样性珍稀濒危野生植物监测。进一步以华南植物园、广东鹤山和德庆林场为基地，拟收集上述4种红豆属植物的种质资源，每种5-50份，利用高效繁育技术培育优质苗木1000株，开展“个体-种群-群落”可持续的迁地保护，建设迁地保育示范地100亩，并集成智慧化采集、监测与可视化应用子系统1套，为红豆属植物的种群保护与生态恢复提供种质材料和繁育技术支撑。			
当年度目标	本项目聚焦鼎湖山自然保护区自然分布的4种国家重点保护红豆属植物（肥荚红豆、茸荚红豆、软荚红豆和光叶红豆），以群落监测为基础，结合鼎湖山20公顷固定大样地20年的植物群落动态监测数据，从“分类-谱系-功能”多样性等维度，在全球变化背景下开展多层次多维度多样性珍稀濒危野生植物监测。进一步以华南植物园、广东鹤山和德庆林场为基地，拟收集上述4种红豆属植物的种质资源，每种5-50份，利用高效繁育技术培育优质苗木1000株，开展“个体-种群-群落”可持续的迁地保护，建设迁地保育示范地100亩，并集成智慧化采集、监测与可视化应用子系统1套，为红豆属植物的种群保护与生态恢复提供种质材料和繁育技术支撑。			

	一级指标	二级指标	三级指标	指标解释	实施周期指标值	当年度指标值
绩效指标	产出指标	数量指标	群落调查	调查红豆属群落多样性	20公顷	20公顷
			迁地保护资源圃面积	建设的红豆属迁地保护资源圃的面积	100亩	5亩
			智慧化采集、监测与可视化应用子系统	集成数据的实时感知与交互	1套	1套
		质量指标	育苗成活率	繁育出的苗木的成活率	≥80%	≥80%
			苗木生长状况	繁育出的苗木的生长状况	健康	健康
		时效指标	年度任务完成率	本年度任务的完成效率	100%	100%
	满意度指标	服务对象满意度指标	服务对象满意度	相关人员对本项目实施和苗木等的满意程度	≥95%	≥95%

野生动植物保护补助项目绩效目标表

项目名称	厚叶木莲种质资源收集保存和丹霞梧桐野外回归示范				
主管部门	广东省林业局		用款单位	中国林业科学研究院热带林业研究所	
实施期限	起始年度	2024	终止年度	2024	
预算金额（万元）	立项总金额	150	当年度金额	150	
项目概述	选择国家二级重点保护野生植物厚叶木莲（Manglietia pachyphylla ）和丹霞梧桐（Firmiana danxiaensis H. H. Hsue & H. S. Kiu）为研究对象，通过在主要分布区开展野生种群调查，掌握其分布生境和种群结构特征。厚叶木莲通过开花结实物候监测，确定种实采集的候选单株和最适时间，开展人工扩繁技术研究，培育厚叶木莲苗木，并总结繁育关键技术。同时，研发高效的丹霞梧桐野外定居技术体系，提高其在野外的定居率，并在石漠化地区、省属林场建立回归示范林。通过两种重点保护野生植物的种质资源收集与保存，加强其人工扩繁技术和野外定居回归，其成果为加强我省野生植物保护和促进遗传资源的利用提供支撑。				
总体绩效目标	实施周期总目标			当年度目标	
	摸清厚叶木莲、丹霞梧桐的分布区域和种群大小，掌握野生种质遗传性多样性水平，收集保存一批野生种质资源。建设厚叶木莲种质繁育基地并开展人工扩繁，为后期回归种植和野生种群恢复提供材料与技术保障。在丹霞梧桐相近生境的石漠化地区、省属林场营造回归保护示范林；促进丹霞梧桐种群的多样性、稳定性和持续性，为我省重点保护野生植物保护和遗传资源利用提供科技支撑。			（1）繁育丹霞梧桐3000株，保育种质资源100份；在石漠化生境、省属林场中营造丹霞梧桐回归示范造林50亩，回归保存率超过80%；研究丹霞梧桐野外回归定居技术1套。 （2）收集野生种质20份以上和DNA样品50份，繁育厚叶木莲实生苗10000株，优良种质发芽率达60%；建立厚叶木莲种苗繁育基地600m^2；提交厚叶木莲分布生境和种群结构的分析报告1 份； （3）提交项目总结报告1份，撰写学术论文3篇。 （4）项目建设周期为1年，项目确保如期、高质量完成，严格按照经费预算控制成本开支。	

	一级指标	二级指标	三级指标	实施周期指标值	当年度指标值
绩效指标	产出指标	数量指标	收集野生种质（份）	120	120
			提取DNA样品（份）	50	50
			营建种苗繁育基地（㎡）	600	600
			繁育苗木（株）	13000	13000
			回归示范林（亩）	50	50
			提交分布生境与种群结构的分析报告（份）	1	1
		质量指标	优良种质发芽率（%）	≥60%	≥60%
			造林保存率	≥80%	≥80%
		时效指标	指标完成率	≥90%	≥90%
	效益指标	社会效益指标	提高公众对野生植物保护的认识	有效提高	有效提高
		生态效益指标	促进濒危植物的拯救保护	是	是
	满意度指标	服务对象满意度指标	服务对象满意度（%）	≥95%	≥95%

野生动植物保护补助项目绩效目标表

项目名称	广东省人工繁育野生动物病毒学本底数据库及预警平台建设			
主管部门	广东省林业局		用款单位	广东省农业科学院动物卫生研究所
实施期限	起始年度	2024	终止年度	2024
预算金额（万元）	立项总金额	30	当年度金额	30
项目概述	本项目将对我省境内各种野生动物进行样本采集，开展重点疫病检测、病毒本底摸排和分子流行病学调查等相关工作，有效掌握重要疫病在我省野生动物中的流行情况，明确病毒的遗传变异情况和跨物种传播能力，及早发现未知病毒，建立预警平台。			
实施周期总目标	开展广东省人工繁育野生动物疫源疫病监测及预警工作，提高我省野生动物疫源疫病应急处置能力。 （1）收集各类样本数量不少于1000份，对重点样品进行病毒宏基因组测定，获得不少于4个病毒病原种/株的全基因组序列，对全部获得的病毒序列进行生物信息学分析和变异、重组、跨种间传播和人兽共患风险进行预测，建立我省人工繁育野生动物携带病毒谱数据库。 （2）完成项目研究报告1份。 （3）建立疫病监测队伍1个，发表论文1-2篇，培养研究生1-2名。 （4）建立1种重要病毒快速检测方法并申请专利。			
当年度目标	（1）收集人工繁育野生动物样品1000份，对重点样品进行病毒宏基因组测定，获得不少于4个病毒病原种/株的全基因组序列，对全部获得的病毒序列进行生物信息学分析和变异、重组、跨种间传播和人兽共患风险进行预测，建立我省人工繁育野生动物携带病毒谱数据库。 （2）完成项目研究报告1份。 （3）建立队伍1个，发表学术论文1-2篇，培养研究生1-2名。 （4）建立1种重要病毒快速检测方法并申请专利。			

	一级指标	二级指标	三级指标	实施周期指标值	当年度指标值
绩效指标	产出指标	数量指标	采集样品数	1000份	1000份
			保存样品数	1000份	1000份
			完成报告数量	1份	1份
			申请专利	1件	1件
		质量指标	检测数据有效率	≥95%	≥95%
		时效指标	任务按时完成率	≥95%	≥95%
	效益指标	生态效益指标	保持人工繁育野生动物种群数量稳定（是/否）	是	是
		可持续影响指标	人工繁育野生动物救护能力	显著提高	显著提高
			为人工繁育野生动物疫病防治提供数据支撑（是/否）	是	是
	满意度指标	服务对象满意度指标	服务对象满意度	≥95%	≥95%

野生动植物保护补助项目绩效目标表

项目名称	黑脸琵鹭等珍稀鸟类、越冬水鸟种群和肇事野生动物专项监测			
主管部门	广东省林业局		用款单位	广东省科学院动物研究所
实施期限	起始年度	2024	终止年度	2024
预算金额（万元）	立项总金额	140	当年度金额	140
项目概述	本项目计划开展三部分的内容： （1）全省越冬水鸟同步监测 在全省41个越冬水鸟同步监测地点，采用样线法、样点法和直接计数法等越冬水鸟常规调查方法，在国家林草局规定的同步监测时间内，开展越冬水鸟种类、数量、行为等进行观测调查，评估重点候鸟的种群状况、栖息地现状、干扰与受胁因素，以此推断东亚一澳大利西亚迁徙路线候鸟生态安全及发展趋势。 （2）重点野生鸟类监测 在全省10个重点野生鸟类监测单元内，采用样线法、样点法和直接计数法等鸟类调查方法，开展针对主要监测对象及伴生鸟类的调查监测工作。在2024年11-12月及翌年1-2月各开展一次实地调查监测。 （3）肇事野生动物专项监测 以野猪为代表的典型肇事野生动物为调查对象，通过搜集历史数据、文献资料、实地走访等方式获取的信息确定出野猪致害频繁县市作为监测示范单元，根据分层抽样原则布设固定样线与			
实施周期总目标	掌握广东省重要水鸟越冬地的越冬水鸟种群、栖息地状况；确定广东省林业局重点鸟类监测单元内主要监测对象及伴生鸟类的监测样地位置，完成年度越冬水鸟同步监测和重点鸟类监测任务，为广东省越冬水鸟保护与监测提供科学依据；掌握以野猪为代表的广东省典型肇事野生动物种群状况及分布规律，在野猪致害频繁的监测示范单元开展种群调查监测，评估野猪种群数量和发展动态，为广东省肇事野生动物监测和防控管理提供数据基础及理论依据，以达到维护国家生态安全、保护野生动物资源的最终目标。			
当年度目标	掌握广东省重要水鸟越冬地的越冬水鸟种群、栖息地状况；确定广东省林业局重点鸟类监测单元内主要监测对象及伴生鸟类的监测样地位置，完成年度越冬水鸟同步监测和重点鸟类监测任务，为广东省越冬水鸟保护与监测提供科学依据；掌握以野猪为代表的广东省典型肇事野生动物种群状况及分布规律，在野猪致害频繁的监测示范单元开展种群调查监测，评估野猪种群数量和发展动态，为广东省肇事野生动物监测和防控管理提供数据基础及理论依据，以达到维护国家生态安全、保护野生动物资源的最终目标。			

	一级指标	二级指标	三级指标	实施周期指标值	当年度指标值
绩效指标	产出指标	数量指标	完成野猪监测样区	≥30个	≥30个
			完成《广东省重点鸟类监测单元监测报告》	1份	1份
			完成《广东省越冬水鸟同步监测报告》	1份	1份
			提交肇事野生动物年度监测报告及相关数据、图件	1份	1份
		质量指标	成果验收合格率	100%	100%
		时效指标	任务按时完成率（%）	100%	100%
	效益指标	生态效益指标	掌握广东省越冬水鸟种群状况	≥90%	≥90%
			掌握广东省重点监测鸟类种群状况	≥90%	≥90%
	满意度指标	服务对象满意度指标	服务对象满意度	≥95%	≥95%

野生动植物保护补助项目绩效目标表

项目名称	广东省越冬水鸟种群监测（粤西片区）			
主管部门	广东省林业局		用款单位	中山大学
实施期限	起始年度	2024	终止年度	2024
预算金额（万元）	立项总金额	30	当年度金额	30
项目概述	在雷州半岛重要水鸟繁殖地点进行水鸟监测，开展繁殖水鸟的生活史研究。同时调查水鸟与沿海滩涂水产养殖的关系，评估水鸟的捕食是否影响养殖户的经济效益。通过预调查与实地调查的方式，于2025年1月对湛江、阳江共14个调查单元湿地进行实地水鸟监测，监测内容为越冬水鸟的分布现状、栖息地现状、种群数量、干扰因素、受胁因素、保护现状等。2024年11月至翌年2月，对湛江红树林、九龙山红树林、电白红树林三个监测单元的黑脸琵鹭、中华凤头燕鸥进行每月一次的固定监测。			
实施周期总目标	获取广东省西南部水鸟的种类、种群数量、栖息地状况、保护现状、人鸟冲突的基础数据，为准确评估我国的候鸟迁徙道鸟类的资源动态提供第一手数据，为未来水鸟及其栖息地保护管理提供科学支撑。			
当年度目标	2024-2025年度按方案完成雷州半岛、湛江市与阳江市共14个调查单元湿地的实地水鸟监测，人鸟冲突现状，整理并存档原始数据，分析监测数据并撰写报告。项目经费也服务于2024年湛江水鸟重要繁殖地点的监测工作，按计划落实资金支出。			
绩效指标	一级指标	二级指标	三级指标	当年度指标值
	产出指标	数量指标	调查水鸟重要越冬地数量	14个
			水鸟的照片或视频文件	≥100个
			原始监测记录表存档	1份
			科学论文	1篇
			撰写项目报告	1份
		质量指标	监测成果验收合格率	1份
	满意度指标	服务对象满意度指标	服务对象满意度	≥95%

野生动植物保护补助项目绩效目标表

项目名称	广东省候鸟重要病毒的病毒数据库建立及风险评估					
主管部门	广东省林业局			用款单位	广东海洋大学	
实施期限	起始年度	2024		终止年度	2024	
预算金额（万元）	立项总金额	30		当年度金额	30	
项目概述	本项目结合前期研究结果，整合测序技术和系统发育地理学的方法，在对该生境的候鸟和留鸟展开流行病学调查及病毒溯源的基础上，以保护生物学的角度揭示鸟类携带流感病毒和副粘病毒的遗传多样性，解析广东省跨地域不同湿地间流感病毒传播的时空特征。通过本研究，建立野生鸟类重要病毒的数据库，阐明野鸟迁徙活动在病毒传播中的生态学价值，对维持鸟类的种群数量，维护生态平衡具有重要的意义。					
实施周期总目标	（1）明确流感病毒在不同宿主内的遗传多样性和分布以及禽流感病毒基因片段与全球禽流感病毒基因片段的关系；解析野鸟禽流感病毒的病原生态学； （2）以流感病毒为主，同时揭示候鸟迁徙在副粘病毒的传播、重组中的生态学价值； （3）了解候鸟在到达迁徙地时所携带的病原种类以及离开迁徙地前携带病原种类的变化数据。					
当年度目标	完成广东省鸟类集中地的冬候鸟、夏候鸟以及留鸟的样品采集、病原的分离鉴定和序列分析工作。					
绩效指标	一级指标	二级指标	三级指标	指标解释	实施周期指标值	当年度指标值
	产出指标	数量指标	采集样品数	样品采集数量	5000份	5000份
			检测样品数	样品分离鉴定数量	5000份	5000份
		质量指标	检测数据有效率	样品检测数据的有效率	≥95%	≥95%
		时效指标	任务完成时间	所有工作完成时间	2024年12月前	2024年12月前
	效益指标	生态效益指标	是否完善广东省鸟类迁徙过程病原携带情况本底数据库	项目完成后，广东省鸟类迁徙过程病原携带情况本底数据库是否得到完善提升	是	是
	满意度指标	服务对象满意度指标	服务对象满意度	服务对象的满意程度	≥95%	≥95%

野生动植物保护补助项目绩效目标表

项目名称	大叶茶、华南锥等国家重点保护野生植物的综合保护			
主管部门	广东省林业局		用款单位	华南农业大学
实施期限	起始年度	2024	终止年度	2024
预算金额（万元）	立项总金额	100	当年度金额	100
项目概述	对广东省连南、英德等地大叶种茶树资源进行科学考察，研究其特征特性、制定就地保护措施；收集茶树果实、种子等有性繁殖材料，开展有性繁殖技术研究。依据野生植物迁地保护原则，将繁殖的野生大叶茶种质材料集中种植于华南农业大学增城宁西教学科研基地，建立迁地保护园。调查华南锥的本底资源。对华南锥实施就地保护、迁地保护、遗传保护、回归保护等综合保护行动。			
实施周期总目标	调查广东连南、英德野生大叶种茶树资源，撰写研究报告1份，制定大叶茶就地保护措施1套，采用有性繁殖方法扩繁，建立其迁地保护园5亩，保存野生资源500余份。开展华南锥本底资源调查、种子收集；开展种苗繁育为迁地保护作好准备。			

	一级指标	二级指标	三级指标	当年度指标值
绩效指标	产出指标	数量指标	迁地保护园数量	1座
			资源收集率	≥90%
		质量指标	种群净度	≥90%
		时效指标	成果产出率	≥90%
	效益指标	生态效益指标	大叶茶、华南锥物种多样性的保护率	≥90%
	满意度指标	服务对象满意度指标	服务对象满意度	≥95%

野生动植物保护补助项目绩效目标表

项目名称	虎保护及救护能力提升			
主管部门	广东省林业局		用款单位	广州动物园
实施期限	起始年度	2024	终止年度	2024
预算金额（万元）	立项总金额	150	当年度金额	150
项目概述	本项目拟对广东省内虎以及全国20只以上的虎（含已收集在资源库内样本）进行遗传疾病风险基因筛查，对患有常见虎高发遗传病的个体或者家系进行全基因组水平的遗传数据建档建库，提交20只以上虎遗传疾病发生风险评估报告；对广东省以及国内主要饲养机构的虎个体进行疫源疫病监测，对潜在的病原微生物进行风险评估，提交虎疫源疫病监测评估报告，保障虎的健康；对虎的日粮进行关键营养成份检测和评估，提供优化的虎营养日粮谱，开展动物丰容、繁育笼舍改造与科普教育设施建设，提高圈养虎的营养、繁育水平与动物福利。通过对虎个体AI智能识别和健康评估系统建设，提升虎的饲养管理水平，更好地对促进圈养虎的繁育工作，扩大种群规模，为虎的野化训练、野外重引入提供优质种源。以期唤起民众对保护的热情和认识，对我省经济社会协调发展和生态文明建设起到积极的促进作用。			
实施周期总目标	1.提交20只以上虎遗传疾病发生风险评估报告1份；2.提交虎疫源疫病监测评估报告1份；3.对虎的日粮进行关键营养成份检测和评估，提供优化的虎营养日粮谱，提交虎健康食谱1种；4.开展动物丰容、繁育笼舍改造与科普教育设施建设；5.建立虎AI智能个体识别和健康评估系统建设，提高圈养虎的营养水平与动物福利；6.对虎生殖激素进行监测。			
当年度目标	1.提交20只以上虎遗传疾病发生风险评估报告1份；2.提交虎疫源疫病监测评估报告1份；3.对虎的日粮进行关键营养成份检测和评估，提供优化的虎营养日粮谱，提交虎健康食谱1种；4.开展动物丰容、繁育笼舍改造与科普教育设施建设；5.建立虎AI智能个体识别和健康评估系统建设，提高圈养虎的营养水平与动物福利；6.对虎生殖激素进行监测。			

	一级指标	二级指标	三级指标	指标解释	实施周期指标值	当年度指标值
绩效指标	产出指标	数量指标	遗传学研究生物样本	收集用于虎遗传学研究的生物样品	20只	20只
			遗传疾病发生风险评估报告	虎遗传疾病发生风险评估报告	1份	1份
			疫病监测评估报告	虎疫源疫病监测及评估报告	1份	1份
			生殖激素监测	虎尿液和粪便生殖激素检测	30份	30份
		成本指标	项目经费使用率	项目经费使用效率	≥95%	≥95%
	效益指标	社会效益指标	保护科普活动	开展虎保护科普教育专题活动	2次	2次
			科普教育设施	增设虎科普教育设施	2套	2套
	满意度指标	服务对象满意度指标	科普教育活动满意度	参与科普教育活动的游客的满意度	≥90%	≥90%

野生动植物保护补助项目绩效目标表

项目名称		肇庆市濒危野生动物救护中心收容救护能力提升			
主管部门		广东省林业局		用款单位	肇庆市林业局
实施期限		起始年度	2024	终止年度	2024
预算金额（万元）		立项总金额	50	当年度金额	50
项目概述		通过健全完善野生动物收容救护设施，进一步提升肇庆野生动物收容救护能力，进一步做好野生动植物保护工作，有效地维护生物多样性，促进生态文明建设。			
实施周期总目标		完善野生动物救护基础建设，进一步提升肇庆野生动物收容救护能力，有效地维护野生动物种群资源生态安全。			
当年度目标		一是利用现有池塘，因地制宜，增加水禽类、龟类等动物饲养区，其中水禽区300平方米、龟类200平方米；二是建设200平方米野生动物野化区。			
绩效指标	一级指标	二级指标	三级指标	实施周期指标值	当年度指标值
	产出指标	数量指标	改造水禽饲养区面积	300平方米	300平方米
			改造龟类饲养区面积	200平方米	200平方米
			改造野化区面积	200平方米	200平方米
	效益指标	生态效益指标	是否有利于肇庆市生态平衡，保护生物多样性	是	是
		可持续影响指标	是否提升辖区内野生动物资源保护水平	是	是
	满意度指标	服务对象满意度指标	服务对象满意度	≥95%	≥95%

野生动植物保护补助项目绩效目标表

项目名称		野生动物收容救护及野化训练能力提升			
主管部门		广东省林业局		用款单位	广州市野生动植物保护管理办公室
实施期限		起始年度	2024	终止年度	2024
预算金额（万元）		立项总金额	30	当年度金额	30
项目概述		为提升广州市野生动物救护中心动物救护能力，为救护的野生动物提供更适宜的救护环境，拟申请资金用于对广州市野生动物救护中心老化破损的面积约300平方动物笼舍进行维修改造。			
实施周期总目标		提升广州市野生动物救护中心动物救护能力，为救护的野生动物提供更适宜的救护环境。			
当年度目标		提升广州市野生动物救护中心动物救护能力，为救护的野生动物提供更适宜的救护环境。			
绩效指标	一级指标	二级指标	三级指标	实施周期指标值	当年度指标值
	产出指标	数量指标	提升改造300㎡动物笼舍	300㎡	300㎡
		质量指标	项目安全事故发生率	0	0
	效益指标	社会效益指标	提升全市执法罚没、受困野生动物接收能力	有效提升	有效提升
	满意度指标	服务对象满意度指标	服务对象满意度	≥95%	≥95%

附件4

国家级保护区补助情况表

序号	项目单位	项目名称	金额（万元）
合　　计			1147
1	广东内伶仃福田国家级自然保护区管理局	内伶仃岛猕猴种群资源监测及人为干扰评估	35
2	广东内伶仃福田国家级自然保护区管理局	中华穿山甲野外科学观测研究站建设	310
3	广东内伶仃福田国家级自然保护区管理局	广东内伶仃福田国家级自然保护区趣味故事编制	95
4	广东徐闻珊瑚礁国家级自然保护区管理局	广东徐闻珊瑚礁国家级自然保护区珊瑚礁生态系统修复	300
5	广东徐闻珊瑚礁国家级自然保护区管理局	广东徐闻珊瑚礁国家级自然保护区调查监测与环境治理	130
6	广东湛江红树林国家级自然保护区管理局	基于无人机遥感的红树林资源监测系统建设	76
7	广东曲江罗坑鳄蜥省级自然保护区管理处	2024年广东罗坑鳄蜥国家级自然保护区松材线虫病防治项目	76
8	广东车八岭国家级自然保护区管理局	松材线虫病防治	50
9	广东珠江口中华白海豚国家级自然保护区管理局	中华白海豚宣传能力提升项目	75

附件5

国家级保护区补助项目绩效目标表

项目名称	内伶仃岛猕猴种群资源监测及人为干扰评估				
主管部门	广东省林业局		用款单位	广东内伶仃福田国家级自然保护区管理局	
实施期限	起始年度	2023年1月	终止年度	2025年12月	
预算金额（万元）	立项总金额	120万元	当年度金额	35万元	
项目概述	本项目基于GPS追踪技术与DNA微卫星技术进行内伶仃岛猕猴种群数量、分布及遗传多样性监测，并结合前期工作基础，评估人为干扰对内伶仃岛猕猴种群影响。				
当年度目标	对广东省内伶仃岛猕猴种群数量进行调查，产生一套完整的项圈佩戴方案及种群数量调查数据分析及可视化流程并为海岛猕猴的保护和管理提供参考。				
绩效指标	一级指标	二级指标	三级指标	实施周期指标值	当年度指标值
			空间位点数据(条)	≥250000	≥100000
			猕猴DNA样品（份）	≥40	≥40
			项目报告(份)	≥1	≥1
	效益指标	社会效益指标	是否为保护区科研工作和有效管理提供支持（是/否）	是	是
		生态效益指标	是否为内伶仃岛猕猴的保护管理提供科学依据（是/否）	是	是
		可持续影响指标	是否为内伶仃岛猕猴保护提供长期技术支持（是/否）	是	是
	满意度指标	群众满意度	群众满意度	≥95%	≥95%

国家级保护区补助项目绩效目标表

<table>
<tr><td colspan="2">项目名称</td><td colspan="5">2024年广东罗坑鳄蜥国家级自然保护区松材线虫病防治项目</td></tr>
<tr><td colspan="2">主管部门</td><td colspan="2">广东省林业局</td><td>用款单位</td><td colspan="2">广东曲江罗坑鳄蜥省级自然保护区管理处</td></tr>
<tr><td colspan="2">实施期限</td><td>起始年度</td><td>2022</td><td>终止年度</td><td colspan="2">2024</td></tr>
<tr><td colspan="2">预算金额（万元）</td><td>立项总金额</td><td>366</td><td>当年度金额</td><td colspan="2">76</td></tr>
<tr><td colspan="2">项目概述</td><td colspan="5">继续开展保护区范围内松材线虫病除治及打针注药防治，保护松林及广东松</td></tr>
<tr><td colspan="2" rowspan="2">总体绩效目标</td><td colspan="3">实施周期总目标</td><td colspan="2">当年度目标</td></tr>
<tr><td colspan="3">1、作业设计及防治规划，3年2次
2、疫木除治，20000亩
3、日常监测，3年30次
4、专项监测，3年6次
5、注射树体免疫剂，3年3次
6、松材线虫病防治区划一张图</td><td colspan="2">1、编制2025年防治规划
2、完成2024年度疫木除治
3、完成2024年度日常监测
4、完成2024年度秋季专项调查
5、完成6000剂注射树体免疫剂注射</td></tr>
<tr><td rowspan="7">绩
效
指
标</td><td>一级指标</td><td>二级指标</td><td>三级指标</td><td>实施周期指标值</td><td colspan="2">当年度指标值</td></tr>
<tr><td rowspan="4">产出指标</td><td rowspan="3">数量指标</td><td>疫木清除率</td><td>≥90%</td><td colspan="2">≥90%</td></tr>
<tr><td>日常监测</td><td>≥10次</td><td colspan="2">≥10次</td></tr>
<tr><td>专项监测</td><td>≥1次</td><td colspan="2">≥1次</td></tr>
<tr><td>质量指标</td><td>验收合格率</td><td>100%</td><td colspan="2">100%</td></tr>
<tr><td>时效指标</td><td>任务按时完成率</td><td>100%</td><td colspan="2">100%</td></tr>
<tr><td>效益指标</td><td>生态效益指标</td><td>广东松松材线虫感染率</td><td>≤5%</td><td colspan="2">≤5%</td></tr>
<tr><td>满意度指标</td><td>群众满意度</td><td>群众满意度</td><td>≥95%</td><td colspan="2">≥95%</td></tr>
</table>

国家级保护区补助项目绩效目标表

项目名称		车八岭保护区松材线虫病防治			
主管部门		广东省林业局		用款单位	广东车八岭国家级自然保护区管理局
实施期限		起始年度	2024	终止年度	2024
预算金额（万元）		立项总金额	50	当年度金额	50
项目概述		项目主要对车八岭保护区的松材线虫病死树进行检测、紧急处置和消杀，保障自然资源和自然环境的安全，提高保护区管理水平，维护国家生物安全和生态安全。			
当年度目标		全面砍伐和清理病死树，预防再次发病高峰，遏制松材线虫病扩散蔓延势头，保障新的小班维持健康状态。			
绩效指标	一级指标	二级指标	三级指标	实施周期指标值	当年度指标值
	产出指标	数量指标	疫木清除率	≥90%	≥90%
			日常监测	≥10次	≥10次
			专项监测	≥1次	≥1次
		质量指标	验收合格率	100%	100%
		时效指标	任务按时完成率	100%	100%
	效益指标	生态效益指标	广东松松材线虫感染率	≤5%	≤5%
	满意度指标	群众满意度	群众满意度	≥95%	≥95%

国家级保护区补助项目绩效目标表

项目名称	广东徐闻珊瑚礁国家级自然保护区珊瑚礁生态系统修复			
主管部门	广东省林业局		用款单位	广东徐闻珊瑚礁国家级自然保护区管理局
实施期限	起始年度	2023年	终止年度	2025年
预算金额（万元）	立项总金额	900	当年度金额	300
项目概述	本项目通过人工干预方式恢复广东徐闻珊瑚礁国家级自然保护区海域内受损的珊瑚礁生态系统，提升珊瑚礁生态系统服务，并对生态修复效果进行评估，提高保护区珊瑚覆盖率、海底生物多样性，改善海洋生态环境，恢复受损的珊瑚礁生态系统。			
实施周期总目标	本项目拟通过在保护区海域内采用珊瑚断肢培育、人工生态礁投放、珊瑚移植、原位增殖，功能生物放流等综合措施提高保护区珊瑚覆盖率、海底生物多样性，改善海洋生态环境，恢复受损的珊瑚礁生态系统。修复珊瑚礁面积6 ha，其中培育珊瑚苗20000株，种植珊瑚面积6 ha，珊瑚苗圃区6 ha。投放人工珊瑚礁500座、育苗架500个。放流徐闻保护区功能生物5种，总计投放数量5万尾（头），并进行修复后效果评估1次。			
当年度目标	1.完成珊瑚苗培育12000株；2.种植珊瑚面积2 ha；3.制作投放育苗架250个，投放人工珊瑚礁150座；4.放流徐闻保护区功能生物2万尾（头）。			

	一级指标	二级指标	三级指标	实施周期指标值	当年度指标值
绩效指标	产出指标	数量指标	修复珊瑚礁面积	≥6公顷	≥2公顷
			培育珊瑚苗	≥20000株	≥12000株
			种植珊瑚面积	≥6公顷	≥2公顷
		时效指标	任务按时完成率	100%	100%
		生态效益指标	提高公众的海洋保护意识，有助于渔业资源的恢复（是/否）	是	是
		可持续影响指标	项目长期持续产生效益	≥3年	≥3年
	满意度指标	群众满意度	群众满意度	≥95%	≥95%

国家级保护区补助项目绩效目标表

项目名称	基于无人机遥感的红树林资源监测系统建设			
主管部门	广东省林业局		用款单位	广东湛江红树林国家级自然保护区管理局
实施期限	起始年度	2024	终止年度	2024
预算金额（万元）	立项总金额	411	当年度金额	76（第一批已下达335）
项目概述	为进一步提高广东湛江红树林国家级自然保护区的科研监测水平，拓展红树林资源监测方法，加强保护区巡护能力，更好的保护好保护区内自然资源，建设完成无人机遥感巡护监测系统1套、架设热红外相机1批、野外高清摄像头1批。			
实施周期总目标	强化资源监测手段，及时掌握红树林资源变化情况和人类活动情况，通过无人机智能巡护提高巡护效率，提高巡护准确效率和效果，确保巡护无死角，结合无人机和感像等科技手段提高资源管理水平，提高保护区资源销细化、科学化管理水平，并易于基层管理人员操作，操作简易。1、人机遥巡护监测系统1套:2、架设热红外相机1批:3、野外高清摄像头1批。			
当年度目标	强化资源监测手段，及时掌握红树林资源变化情况和人类活动情况，通过无人机智能巡护提高巡护效率，提高巡护准确效率和效果，确保巡护无死角，结合无人机和感像等科技手段提高资源管理水平，提高保护区资源销细化、科学化管理水平，并易于基层管理人员操作，操作简易。1、人机遥巡护监测系统1套:2、架设热红外相机1批:3、野外高清摄像头1批。			

绩效指标	一级指标	二级指标	三级指标	实施周期指标值	当年度指标值
		质量指标	基地硬件设施达标率	100%	100%
			设备设施完好率	100%	100%
		时效指标	任务按时完成率	100%	100%
		社会效益指标	提升保护区社会影响力、加强生态保护意识（是/否）	是	是
		生态效益指标	湿地生态系统生态效益发挥明显（是/否）	是	是
		可持续影响指标	保持红树林生态系统功能稳定（是/否）	是	是
			维护生物多样性（是/否）	是	是
	满意度指标	群众满意度	群众满意度	≥95%	≥95%

国家级保护区补助项目绩效目标表

项目名称	广东徐闻珊瑚礁国家级自然保护区调查监测与环境治理项目			
主管部门	广东省林业局		用款单位	广东徐闻珊瑚礁国家级自然保护区管理局
实施期限	起始年度	2024年	终止年度	2025年
预算金额（万元）	立项总金额	130	当年度金额	130
项目概述	本项目对广东徐闻珊瑚礁国家级自然保护区开展珊瑚资源与水质环境状况监测调查，摸清保护区生态系统环境指标及资源变化，积累基础观测数据，为珊瑚礁管理和保护提供指导意见和决策思路。			
总体绩效目标	实施周期总目标		当年度目标	
	本项目对广东徐闻珊瑚礁国家级自然保护区开展珊瑚资源与水质环境状况监测调查，摸清保护区生态系统环境指标及资源变化，积累基础观测数据，为珊瑚礁管理和保护提供指导意见和决策思路。同时，开展保护区环境治理，为清理保护区内非法养殖捕捞等设施提供后勤保障，确保清退工作顺利推进。		完成2024年度保护区海水水质环境调查（包括生物残毒五项指标）及珊瑚群落资源调查，以及开展保护区环境治理，统环境指标及资源变化，积累基础观测数据，为珊瑚礁管理和保护提供指导意见和决策思路。开展清理整治在徐闻珊瑚礁国家级自然保护区内的非法养殖捕捞设施，出动巡护船艇及车辆，做好后勤保障工作，确保清理整治工作顺利开展，清理整治保护区海域面积10000亩等。	

	一级指标	二级指标	三级指标	实施周期指标值	当年度指标值
绩效指标	产出指标	数量指标	珊瑚资源调查站次	≥13站次	≥13站次
			水质调查站次	≥13站次	≥13站次
			清理海域面积	≥10000亩	≥10000亩
		质量指标	项目按照规定及国家标准建设	合格	合格
			项目设备质量符合国家及相关行业标准	合格	合格
		时效指标	任务按时完成率	100%	100%
	效益指标	社会效益指标	是否有利于促进人与自然和谐发展	是	是
		生态效益指标	是否有利于加强珊瑚资源保护	是	是
		可持续影响指标	是否有利于海洋生态系统可持续发展	是	是
	满意度指标	群众满意度	群众满意度	≥95%	≥95%

国家级保护区补助项目绩效目标表

项目名称	中华穿山甲野外科学观测研究站建设			
主管部门	广东省林业局		用款单位	广东内伶仃福田国家级自然保护区管理局
实施期限	起始年度	2024	终止年度	2024
预算金额（万元）	立项总金额	310	当年度金额	310
项目概述	中华穿山甲野外科学观测研究站建设，一是进行修缮改造包括办公区（会议室、接待室、办公室）、功能区（自然教育室、实验室、动物救护收容室、无人机房）、辅助设施、野外作业区等；二是购置一批办公、研究、实验、科普宣教等设施设备。			
实施周期总目标	通过本项目的实施，建设集监测、研究、试验、示范为一体的中华穿山甲野外科学观测研究站，对于摸清中华穿山甲对栖息地植物、环境的利用，以及影响其种群扩繁的因素，从而更全面准确的掌握保护区内中华穿山甲等濒危物种的种群分布情况，有着非常重要的意义。并通过种群分布情况划分重点保护区域，合理分布保护投入力量，做到精准保护，提高保护成效，增加穿山甲生存机会，为中华穿山甲的保护管理提供科学依据。			
当年度目标	通过本项目的实施，建设集监测、研究、试验、示范为一体的中华穿山甲野外科学观测研究站，对于摸清中华穿山甲对栖息地植物、环境的利用，以及影响其种群扩繁的因素，从而更全面准确的掌握保护区内中华穿山甲等濒危物种的种群分布情况，有着非常重要的意义。并通过种群分布情况划分重点保护区域，合理分布保护投入力量，做到精准保护，提高保护成效，增加穿山甲生存机会，为中华穿山甲的保护管理提供科学依据。			

	一级指标	二级指标	三级指标	指标解释	实施周期指标值	当年度指标值
绩效指标	产出指标	数量指标	配套设施完成率	反映年度实际完成配套设施量占（调整后的）计划完成配套设施量的比率。	100%	100%
		质量指标	验收合格率	反映项目完成质量	100%	100%
		时效指标	任务按时完成率	反映项目按计划完成情况	100%	100%
	效益指标	可持续影响指标	是否为实际管理、科研、科普提供数据和素材（是/否）	反映项目成果服务于实际应用的情况	是	是
	满意度指标	群众满意度	群众满意度	满意度指标	≥95%	≥95%

国家级保护区补助项目绩效目标表

项目名称	广东内伶仃福田国家级自然保护区趣味故事编制			
主管部门	广东省林业局		用款单位	广东内伶仃福田国家级自然保护区管理局
实施期限	起始年度	2024	终止年度	2024
预算金额（万元）	立项总金额	95	当年度金额	95
项目概述	本项目力求以国内外高水平科普读物、文创设计为参照，编写印刷《内伶仃岛猕猴趣味故事》和《福田红树林鸟类趣味故事》等2本科普读物，设计制作科普宣传品。以创新设计为核心，深度挖掘保护区鸟类、猕猴的生态与社会内涵，以趣味性兼具通俗性的语言让人们了解、认识多姿多彩的野生动物（猕猴和鸟类为主）的生活、繁殖和栖息地，了解美丽中国丰富多彩的生物多样性，引导大家树立热爱自然、尊重自然、顺应自然、保护自然的生态文明理念，进一步激发公众对于人与自然和谐共生意识的共鸣。			
实施周期总目标	完成2本科普读物编写和一批科普宣传品设计制作，其中鸟类趣味故事正式出版、猕猴趣味故事达到可出版要求			
当年度目标	完成2本科普读物编写和一批科普宣传品设计制作，其中鸟类趣味故事正式出版、猕猴趣味故事达到可出版要求			

	一级指标	二级指标	三级指标	指标解释	实施周期指标值	当年度指标值
绩效指标	产出指标	数量指标	《鸟类趣味故事》科普读物出版（本）	科普读物出版印刷数量	≥2000	≥2000
			科普宣传品设计制作（套）	宣传品设计制作的类别	≥5	≥5
		数量指标	配套设施完成率	反映年度实际完成配套设施量占（调整后的）计划完成配套设施量的比率。	100%	100%
		质量指标	验收合格率	反映项目完成质量	100%	100%
		时效指标	任务按时完成率	反映项目按计划完成情况	100%	100%
	效益指标	可持续影响指标	是否为实际管理、科研、科普提供数据和素材（是/否）	反映项目成果服务于实际应用的情况	是	是
	满意度指标	群众满意度	群众满意度	满意度指标	≥95%	≥95%

国家级保护区补助项目绩效目标表

<table>
<tr><td colspan="2">项目名称</td><td colspan="6">中华白海豚宣传能力提升项目</td></tr>
<tr><td colspan="2">主管部门</td><td colspan="3">广东省林业局</td><td>用款单位</td><td>珠江口中华白海豚国家级自然保护区</td></tr>
<tr><td colspan="2">实施期限</td><td>起始年度</td><td colspan="2">2024</td><td>终止年度</td><td>2024</td></tr>
<tr><td colspan="2">预算金额（万元）</td><td>立项总金额</td><td colspan="2">75万元</td><td>当年度金额</td><td>75万元</td></tr>
<tr><td colspan="2">实施周期总目标</td><td colspan="6">提升公众对中华白海豚的关注度，吸引更多人参观保护区科普园，提升参观体验，在校园内营造中华白海豚氛围，让师生了解中华白海豚，提高保护意识，同时体现管理局在中华白海豚保育工作等方面，在粤港澳大湾区，乃至全国的重要影响力，打造具有全国中华白海豚示范意义的科普阵地。</td></tr>
<tr><td colspan="2">当年度目标</td><td colspan="6">提升公众对中华白海豚的关注度，吸引更多人参观保护区科普园，提升参观体验，在校园内营造中华白海豚氛围，让师生了解中华白海豚，提高保护意识，同时体现管理局在中华白海豚保育工作等方面，在粤港澳大湾区，乃至全国的重要影响力，打造具有全国中华白海豚示范意义的科普阵地。</td></tr>
<tr><td rowspan="6">绩效指标</td><td rowspan="2">产出指标</td><td rowspan="2">数量指标</td><td>中华白海豚宣传日活动</td><td>活动</td><td>1次</td><td>1次</td></tr>
<tr><td>参会人员</td><td>数量</td><td>≥100人</td><td>≥100人</td></tr>
<tr><td>产出指标</td><td>时效指标</td><td>任务按时完成率</td><td>反映项目按计划完成情况</td><td>100%</td><td>100%</td></tr>
<tr><td rowspan="2">效益指标</td><td>经济效益指标</td><td>增加社区旅游收益（是/否）</td><td>增加收益</td><td>是</td><td>是</td></tr>
<tr><td>可持续影响指标</td><td>媒体宣传</td><td>级别</td><td>省级及以上媒体报道</td><td>省级及以上媒体报道</td></tr>
<tr><td>满意度指标</td><td>群众满意度</td><td>群众满意度</td><td>满意度指标</td><td>≥95%</td><td>≥95%</td></tr>
</table>

附件6

湿地保护修复补助情况表

序号	项目单位	项目名称	金额（万元）
合计			1200
省级及中央驻穗单位			600
1	广东湛江红树林国家级自然保护区管理局	湛江红树林国际重要湿地自然教育基地建设规划及野外宣教点建设项目	480
2	广东南澎列岛海洋生态国家级自然保护区管理局	广东南澎列岛国际重要湿地海洋垃圾清理项目	120
市县单位			600
3	广州市海珠区湿地保护管理办公室	海珠湿地生态巡护管理及生物多样性科研宣教项目	400
4	南雄市孔江国家重要湿地管理处	广东省南雄市孔江国家重要湿地2024年湿地保护能力提升项目	200

附件7

湿地保护修复补助项目绩效目标表

项目名称	湛江红树林国际重要湿地宣教与动态监测能力提升			
主管部门	广东省林业局		用款单位	广东湛江红树林国家级自然保护区管理局
实施期限	起始年度	2024年	终止年度	2024年
预算金额（万元）	立项总金额	480	当年度金额	480
项目概述	为更好保护和管理好湛江红树林国际重要湿地，充分发挥湛江红树林国际重要湿地宣教职能，进一步提高红树林周边社区红树林保护意识和科普教育水平，同时更好对湛江红树林国际重要湿地进行动态监测，建设完成雷高镇红树林自然教育基地科普宣教能力提升、湛江红树林国际重要湿地动态监测系统等，进一步提升基础设施服务水平，将湛江红树林国际重要湿地打造成为绿美广东建设的靓丽名片。			
实施周期总目标	1、雷高镇红树林自然教育基地科普宣教展示设计及布展1套；2、湛江红树林国际重要湿地动态监测系统1套。			
当年度目标	1、雷高镇红树林自然教育基地科普宣教展示设计及布展1套；2、湛江红树林国际重要湿地动态监测系统1套。			

	一级指标	二级指标	三级指标	指标解释	实施周期指标值	当年度指标值
绩效指标	产出指标	数量指标	科普展示设计及布展（套）	反映科普展示设计及布展完成数量情况	1	1
			动态监测系统（套）	反映动态监测系统完成数量情况	1	1
		时效指标	任务按时完成率（%）	反映工作任务按计划时间完成情况	100%	100%
	效益指标	社会效益指标	是否为实际管理、科研、科普提供数据和素材（是/	反映项目成果服务于实际应用的情况	是	是
		生态效益指标	维护湿地生态系统健康稳定（稳定）	反映项目设施对维护湿地生态系统健康稳定的情况。	稳定	稳定
		可持续影响指标	湿地项目实施对保持湿地生态系统功能稳定的影响（长期/短期、3-5年）	反映项目实施对保持湿地生态系统功能稳定的影响情况。	长期	长期
	满意度指标	群众满意度指标	群众满意度（%）	反映项目实施服务对象满意度情况	≥95%	≥95%

湿地保护修复补助项目绩效目标表

项目名称	广东南澎列岛国际重要湿地海洋垃圾清理项目			
主管部门	广东省林业局		用款单位	广东南澎列岛海洋生态国家级自然保护区管理局
实施期限	起始年度	2024年	终止年度	2024年
预算金额（万元）	立项总金额	120	当年度金额	120
项目概述	本项目拟开展湿地内海洋垃圾清理，通过租用专业工具船艇，不定期开展湿地内海洋垃圾清理。利用渔网拖拽法清理海漂垃圾，以人工收集法清理以往遗弃的作业渔网，并将所收集的垃圾移交当地垃圾处理厂进行无公害处理。			
实施周期总目标	清理湿地内海洋垃圾，创造了一个更美好的湿地环境，进一步提升公众湿地保护意识。			
当年度目标	清理湿地内海洋垃圾，创造了一个更美好的湿地环境，进一步提升公众湿地保护意识。			

绩效指标	一级指标	二级指标	三级指标	指标解释	实施周期指标值	当年度指标值
	产出指标	数量指标	海洋垃圾清理	反映湿地内海洋垃圾清理的范围	广东南澎列岛国际重要湿地范围内	广东南澎列岛国际重要湿地范围内
		质量指标	项目验收率（%）	反映项目验收合格率情况	100%	100%
		时效指标	任务按时完成率（%）	反映工作任务按计划时间完成情况	100%	100%
	效益指标	可持续影响指标	湿地保护修复对保持湿地生态系统功能是否有积极影响	反映湿地保护修复对保持湿地生态系统功能稳定的影响情况	是	是
	满意度指标	群众满意度指标	湿地辖区及周边群众满意度（%）	反映群众对工作开展的满意度情况	≥95%	≥95%

湿地保护修复补助项目绩效目标表

项目名称	2024年广东广州海珠国际重要湿地生态巡护管理及生物多样性科研宣教项目			
主管部门	广东省林业局		用款单位	广州市海珠区湿地保护管理办公室
实施期限	起始年度	2024	终止年度	2024
预算金额（万元）	立项总金额	400	当年度金额	400
项目概述	根据生态系统完整性，落实《中华人民共和国湿地保护法》规定，在广东广州海珠国际重要湿地范围，通过湿地巡护管理、湿地生物资源调查、科普宣教体系优化提升等工作，力争在维持原有生态特征的基础上，优化提升湿地生态服务功能，持续为公众提供多样化、多场景、高品质的科普教育服务，打造人与自然和谐共生的绿美广东，向世界展示生态文明建设成果的。			
实施周期总目标	①通过第三方聘请临时巡护人员约8人； ②完成国际重要湿地所在的行政管理区域的湿地资源调查及濒危鸟种的孵育、野化及科普宣教1套； ③完成调查监测报告2份； ④完成高畦深沟场景提升和科普牌1套； ⑤完成生态艺术再生自然空间作品征集及科普标识标牌系统建设1套；			
当年度目标	本项目2024年一次性投入资金，同年度完成项目建设，项目绩效年度目标与总体目标一致。			

	一级指标	二级指标	三级指标	指标解释	实施周期指标值	当年度指标值
绩效指标	产出指标	数量指标	调查面积（公顷）	反映调查面积情况	≥751	≥751
			完成调查报告（份）	反映完成调查方案数量情况	≥2	≥2
		质量指标	验收合格率（%）	反映项目验收合格率情况	100%	100%
		时效指标	任务按时完成率（%）	反映工作任务按计划时间完成情况	100%	100%
	效益指标	生态效益指标	维护湿地生态系统健康稳定稳定（是/否）	反映项目设施对维护湿地生态系统健康稳定的情况	是	是
		可持续影响指标	湿地保护修复对保持湿地生态系统功能稳定的影响（长期/短期、3-5年）	反映湿地保护修复对保持湿地生态系统功能稳定的影响情况	长期	长期
	满意度指标	群众满意度指标	湿地辖区及周边群众满意度（%）	反映群众对工作开展的满意度情况	≥95%	≥95%

湿地保护修复补助项目绩效目标表

项目名称	广东省南雄市孔江国家重要湿地2024年湿地保护能力提升项目			
主管部门	广东省林业局		用款单位	南雄市孔江国家湿地公园管理处
实施期限	起始年度	2024年	终止年度	2024年
预算金额（万元）	立项总金额	200	当年度金额	200
实施周期总目标	本项目主要包括三部分内容，通过本项目实施一方面可提高湿地保护管理基础能力，通过购置防灾减灾物资，加强重要湿地巡护人员物资储备与应急能力；二是开展湿地科研监测，扩大重要湿地智能监测点范围，加强水源地水质监测，并加强对周边游客人为活动的监控监测；三是提升孔江国家重要湿地宣教系统设施建设水平，维护升级改造原有宣教牌示系统，做好湿地生态惠民，让游客共享湿地绿意空间。			
当年度目标	本项目主要包括三部分内容，通过本项目实施一方面可提高湿地保护管理基础能力，通过购置防灾减灾物资，加强重要湿地巡护人员物资储备与应急能力；二是开展湿地科研监测，扩大重要湿地智能监测点范围，加强水源地水质监测，并加强对周边游客人为活动的监控监测；三是提升孔江国家重要湿地宣教系统设施建设水平，维护升级改造原有宣教牌示系统，做好湿地生态惠民，让游客共享湿地绿意空间。			

	一级指标	二级指标	三级指标	指标解释	实施周期指标值	当年度指标值
绩效指标	产出指标	数量指标	巡护、监测船浮动码头（平方米）	反映巡护、监测船浮动码头数量的情况。	≥30	≥30
			游客监控监测与语音提醒系统（处）	反映游客监控监测与语音提醒系统数量的情况。	≥15	≥15
			水鸟智能监测点（处）	反应水鸟智能监测点数量情况。	≥4	≥4
			水文、水质监测站设备购置（套）	反映水文、水质监测站设备数量的情况。	≥2	≥2
		质量指标	成果验收合格率（%）	反映工作成果验收通过情况。	100%	100%
		时效指标	任务按时完成率（%）	反映工作任务按计划时间完成情况。	100%	100%
	效益指标	生态效益指标	湿地生态系统生态效益发挥明显（是/否）	反映湿地生态系统生态效益发挥变化情况。	是	是
		可持续影响指标	为重要湿地管理提供数据支撑（是/否）	反映重要湿地管理的可持续影响情况。	是	是
	满意度指标	群众满意度指标	群众满意度（%）	反映公众对项目实施的满意度情况。	≥95%	≥95%

附件8

古树名木保护补助情况表

序号	项目单位	项目名称	金额（万元）
合计			110
1	广东省林业局	广东省一级古树和名木抢救复壮（第二批）	60
2	广东省林业局	古树名木监测救护	50

附件9

古树名木保护补助项目绩效目标表

<table>
<tr><td colspan="2">项目名称</td><td colspan="5">古树名木监测救护</td></tr>
<tr><td colspan="2">主管部门</td><td colspan="2">广东省林业局</td><td>用款单位</td><td colspan="2">广东省林业局</td></tr>
<tr><td colspan="2">实施期限</td><td>起始年度</td><td>2024</td><td>终止年度</td><td colspan="2">2024</td></tr>
<tr><td colspan="2">预算金额（万元）</td><td>立项总金额</td><td>50</td><td>当年度金额</td><td colspan="2">50</td></tr>
<tr><td colspan="2">项目概述</td><td colspan="5">开展广东省一级古树名木视频监控运维工作。一是对828套视频监控硬件进行维护，确保设备的正常使用；二是租赁云服务器、购买移动卡流量、软件维护等维持古树名木视频展示平台各项功能的正常运行。三是将现有851个古树名木视频监控转接入省林业局新建设的古树名木展示平台。</td></tr>
<tr><td colspan="2" rowspan="2">总体绩效目标</td><td colspan="3">实施周期总目标</td><td colspan="2">当年度目标</td></tr>
<tr><td colspan="3">开展全省828株一级古树名木视频监控设备运维工作，保障古树名木视频监控平台正常运行使用。</td><td colspan="2">开展全省828株一级古树名木视频监控设备运维工作，保障古树名木视频监控平台正常运行使用。</td></tr>
<tr><td rowspan="6">绩
效
指
标</td><td>一级指标</td><td>二级指标</td><td>三级指标</td><td>实施周期指标值</td><td colspan="2">当年度指标值</td></tr>
<tr><td rowspan="4">产出指标</td><td>数量指标</td><td>广东省一级古树名木视频监控运维（株）</td><td>828株</td><td colspan="2">828株</td></tr>
<tr><td>质量指标</td><td>古树名木视频监控在线率（%）</td><td>≥90%</td><td colspan="2">≥90%</td></tr>
<tr><td rowspan="2">时效指标</td><td>完成时间</td><td>2024年12月底前</td><td colspan="2">2024年12月底前</td></tr>
<tr><td>任务按时完成率</td><td>≥90%</td><td colspan="2">≥90%</td></tr>
<tr><td>效益指标</td><td>生态效益指标</td><td>提高古树名木保护程度（是/否）</td><td>是</td><td colspan="2">是</td></tr>
<tr><td>满意度指标</td><td>服务对象满意度指标</td><td>服务对象满意度</td><td>≥95%</td><td colspan="2">≥95%</td></tr>
</table>

古树名木保护补助项目绩效目标表

项目名称	广东省一级古树和名木抢救复壮			
主管部门	广东省林业局		用款单位	广东省林业局
实施期限	起始年度	2024	终止年度	2024
预算金额（万元）	立项总金额	60	当年度金额	60
项目概述	针对全省古树名木生长现状，组织开展重要古树名木现场调查，全面诊断古树名木健康状况，准确判定影响古树名木健康的障碍因子，并采取科学的保护复壮措施，有助于提升全省古树名木保护与管理水平，助力“绿美广东”建设。项目内容包括：1、在全省范围内筛选50株长势衰弱的一级古树和名木开展健康诊断，编制“一树一策”抢救复壮方案；2、按照抢救复壮方案，对50株一级古树和名木开展抢救复壮。			
总体绩效目标	实施周期总目标		当年度目标	
	完成全省50株一级古树和名木生长监测分析，编制“一树一策”抢救复壮方案；完成50株一级古树和名木抢救复壮工作。		完成全省50株一级古树和名木生长监测分析，编制“一树一策”抢救复壮方案；完成50株一级古树和名木抢救复壮工作。	

	一级指标	二级指标	三级指标	实施周期指标值	当年度指标值
绩效指标	产出指标	数量指标	一级古树和名木抢救复壮	50株	50株
		质量指标	一级古树和名木抢救复壮合格率	≥90%	≥90%
		时效指标	完成时间	2024年11月底前	2024年11月底前
	效益指标	社会效益指标	抢救复壮一级古树和名木成效	较为显著	较为显著
	满意度指标	服务对象满意度指标	服务对象满意度	≥95%	≥95%

公开方式：主动公开

抄送：财政部、国家林业和草原局，省档案馆，财政部广东监管局。

广东省财政厅办公室　　2024 年 7 月 31 日印发

云浮市科学技术局

云科函〔2023〕115号

关于下达云浮市2023年创新创业团队项目的通知

各县（市）科技局,云城区、云安区工信局，云浮新区科创局，各有关单位：

根据《中共云浮市委人才工作领导小组印发<关于推进人才云聚强市工程的意见>的通知》(云委人才〔2023〕1 号) 中《产业人才项目实施方案（试行)》规定，云浮市 2023 年创新创业团队项目已评审完毕。经市科技局党组审定、报市委人才工作领导小组办公室备案，决定对温氏食品集团股份有限公司等 6 个单位申报的创新团队项目予以立项(名单详见附件)。

现将项目下达给你们。项目承担单位要严格执行项目合同规定，规范资金使用，确保项目高质量实施。项目所在地县级科技主管部门要会同项目审核职能部门做好县级财政分担资金的申请工作，同时加强协调联系和指导跟踪服务，推进项目全面完成。

附件：云浮市 2023 年创新团队项目立项名单



云浮市科学技术局

2023 年 10 月 23 日

附件:

云浮市2023年创新团队项目立项名单

项目承担单位	项目名称	项目负责人	资助金额（万元）			所属区域
			总额	市县分担		
				市财政	县财政	
温氏食品集团股份有限公司	种猪健康高效养殖（疫病防控和精准营养）创新团队	王松波	200	60	140	新兴县
广东嵩达新材料有限公司	高性能光固化树脂创新团队	孙启龙	200	60	140	郁南县
云浮市物联网研究院有限公司	物联网数字化畜禽养殖技术的研究与产业化推广团队	周皓恩	200	60	140	新兴县
罗定市谷盈畜牧业有限公司	楼房养猪智慧化创新团队	冯大春	200	60	140	罗定市
广东壹诺科技股份有限公司	高性能有机纤维增强树脂复合材料创新团队	廖作桂	200	60	140	郁南县
新兴县五叶茗农业科技有限公司	特色茶树新品种培育创新团队	张旭	200	60	140	新兴县
			1200	360	840	——

项目编号：CYRC202306

文件编号：云科函〔2023〕115号

云浮市2023年产业创新团队
项目合同书

项　目　名　称：特色茶树新品种培育创新团队

项目起止时间：2023年5月-2026年5月

管理单位（甲方）：云浮市科学技术局

承担单位（乙方）：新兴县五叶茗农业科技有限公司

通讯地址：新兴县太平镇社圩村民委员会岱山寺牌坊路口侧

联　系　方　式：电话　0766-2937456

项　目　负　责　人：张旭　联系电话：13539883664

项　目　联　系　人：李国勋　联系电话：13826866339

乙方所在地县或市级科 技主管部门：新兴县科技局

一、项目实施内容

1、现有基础，包括团队前期准备、申报单位条件和项目知识产权等情况；

1.1 团队前期准备

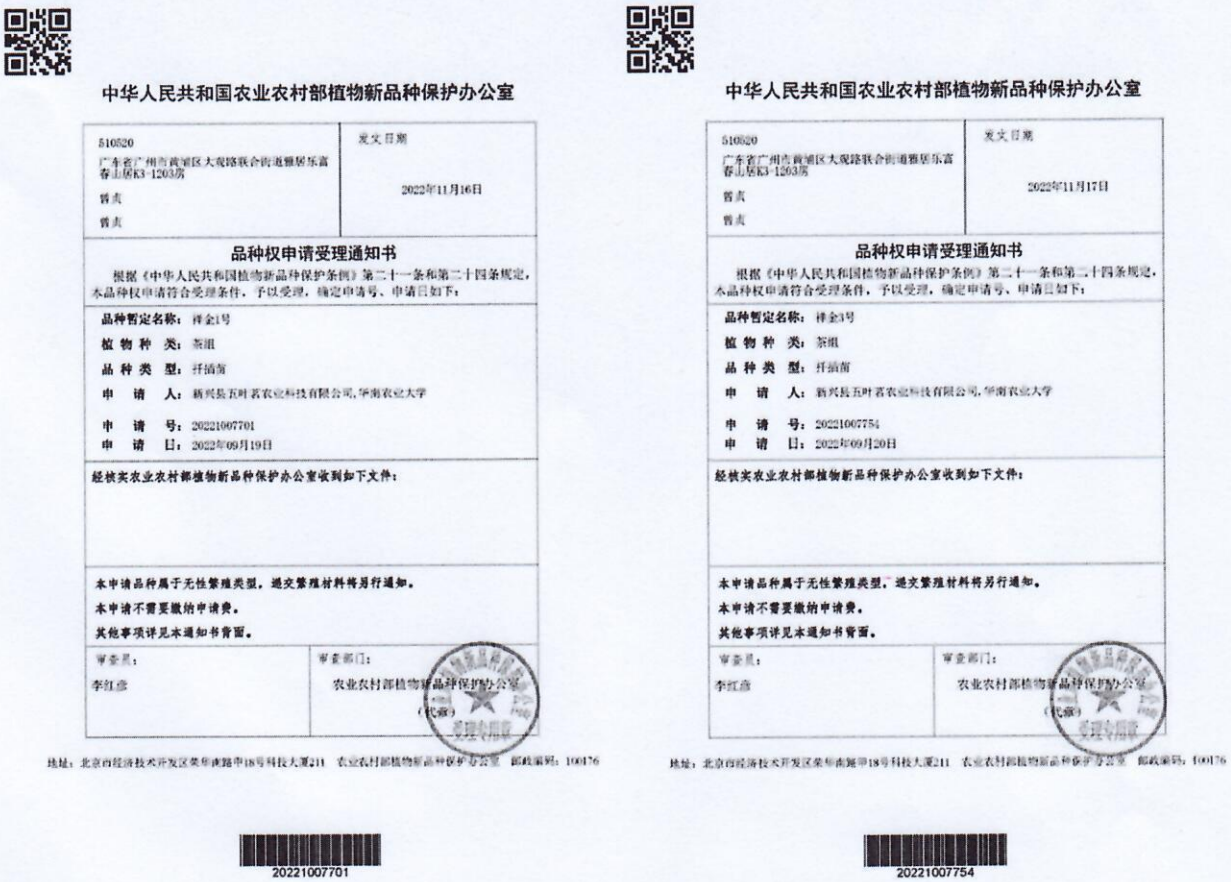
1）新品种选育进展





图 1 “禅金”茶树品种

如图 1 所示，本公司已与待引进团队在前期研究中选育得到性状稳定的优质茶树新品种——“禅金 1 号”和“禅金 3 号”，经无性繁殖方式扩繁，目前种植面积已达 30 亩。两个新品种已在农业农村部申报植物新品种权（图 2）。



中华人民共和国农业农村部植物新品种保护办公室

510520
广东省广州市黄埔区大观路联合街道雅居乐富春山居K3-1203房
暂未
暂未

发文日期
2022年11月16日

品种权申请受理通知书

根据《中华人民共和国植物新品种保护条例》第二十一条和第二十四条规定，本品种权申请符合受理条件，予以受理，确定申请号、申请日如下：

品种暂定名称：禅金1号
植物种类：茶组
品种类型：扦插苗
申请人：新兴县五叶茗农业科技有限公司,华南农业大学
申请号：20221007701
申请日：2022年09月19日

经核实农业农村部植物新品种保护办公室收到如下文件：

本申请品种属于无性繁殖类型，递交繁殖材料将另行通知。
本申请不需要缴纳申请费。
其他事项详见本通知书背面。

审查员：
李红彦

审查部门：
农业农村部植物新品种保护办公室
（代章）

地址：北京市经济技术开发区荣华南路甲18号科技大厦211 农业农村部植物新品种保护办公室 邮政编码：100176

20221007701

中华人民共和国农业农村部植物新品种保护办公室

510520
广东省广州市黄埔区大观路联合街道雅居乐富春山居K3-1263房
暂未
暂未

发文日期
2022年11月17日

品种权申请受理通知书

根据《中华人民共和国植物新品种保护条例》第二十一条和第二十四条规定，本品种权申请符合受理条件，予以受理，确定申请号、申请日如下：

品种暂定名称：禅金3号
植物种类：茶组
品种类型：扦插苗
申请人：新兴县五叶茗农业科技有限公司,华南农业大学
申请号：20221007754
申请日：2022年09月20日

经核实农业农村部植物新品种保护办公室收到如下文件：

本申请品种属于无性繁殖类型，递交繁殖材料将另行通知。
本申请不需要缴纳申请费。
其他事项详见本通知书背面。

审查员：
李红彦

审查部门：
农业农村部植物新品种保护办公室
（代章）

地址：北京市经济技术开发区荣华南路甲18号科技大厦211 农业农村部植物新品种保护办公室 邮政编码：100176

20221007754

图 2 “禅金 1 号”和“禅金 3 号”植物新品种权申请受理通知书

2）生化成分分析进展

茶多酚是影响成茶香气和滋味浓厚的主要物质。英红九号茶多酚平均含量为22.49%，禅金1号茶多酚平均含量为18.18%，禅金3号茶多酚平均含量为19.06%（图3A）。黄化茶树的特征性化学成分含量会发生较大变化，其中氨基酸含量显著增加。英红九号游离氨基酸的平均含量为3.68%，禅金3号游离氨基酸的平均含量为5.06%，禅金1号单株游离氨基酸最高可达9.1%，平均含量为7.74%（图3B）。英红九号的咖啡碱含量平均值为3.49%；禅金1号的咖啡碱含量为4.71%；禅金3号的咖啡碱含量平均值为5.39%（图3C）。

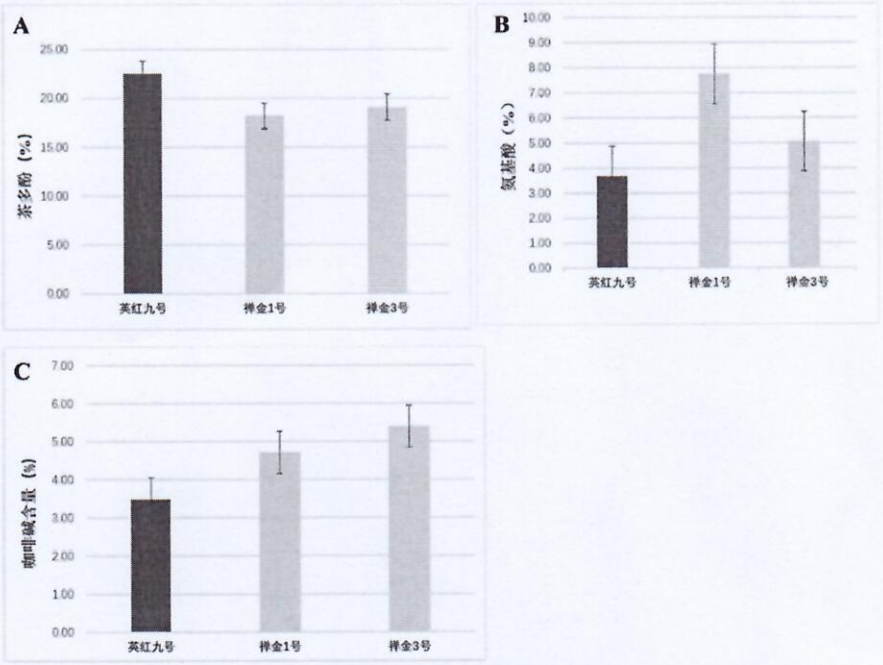


图3 茶叶内在生化成分分析

3）适制性研究进展

分别对“禅金”品种进行红茶、绿茶适制性研究，发现该品种非常适合加工高档绿茶。具有清汤黄叶、滋味甘醇、回甘强烈、香气具浓郁的熟板栗风味等特征。

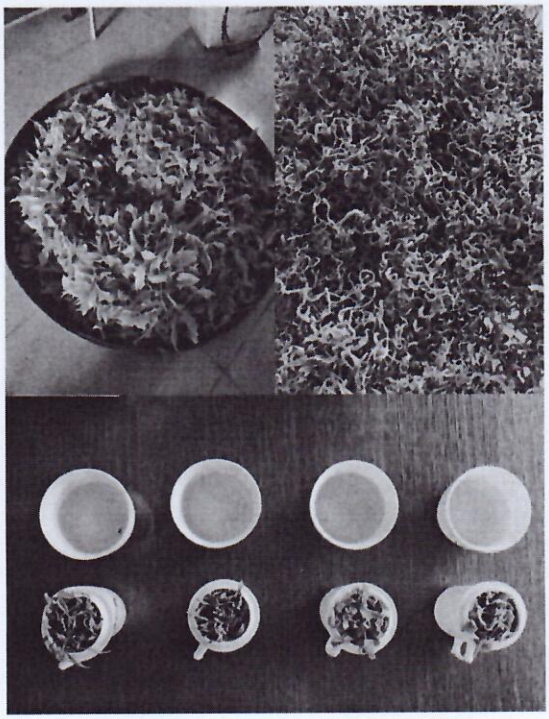


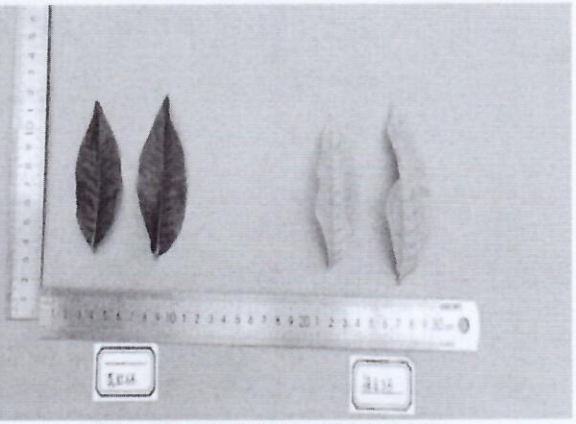
图4 “禅金”茶加工与感官评价

4）叶片颜色机理研究进展

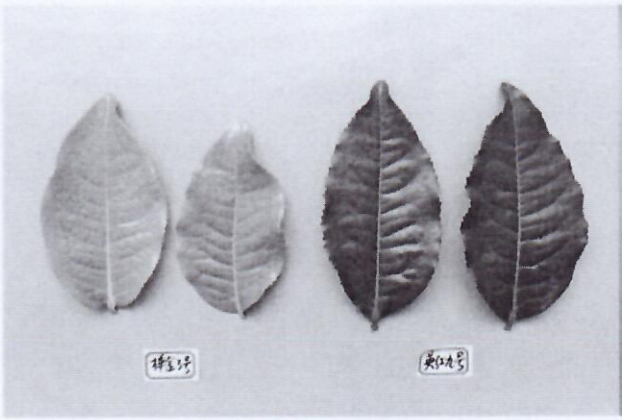
1、禅金 3 号与近似种英红九号春季一芽二叶差异对比



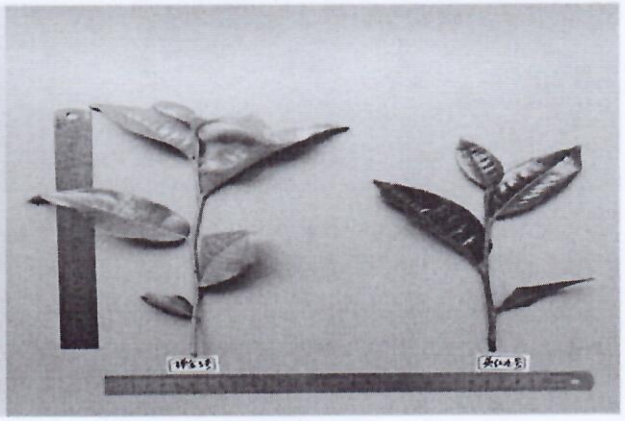
2、禅金 3 号与近似种英红九号新芽第二叶差异对比



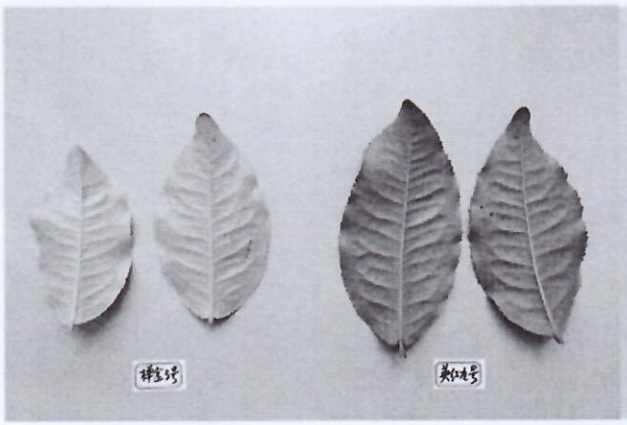
3、禅金 3 号与近似种英红九号成熟叶差异对比



4、禅金 3 号与近似种英红九号枝条差异对比



5、禅金 3 号与近似种英红九号叶背差异对比



6、禅金 3 号与近似种英红九号叶尖差异对比

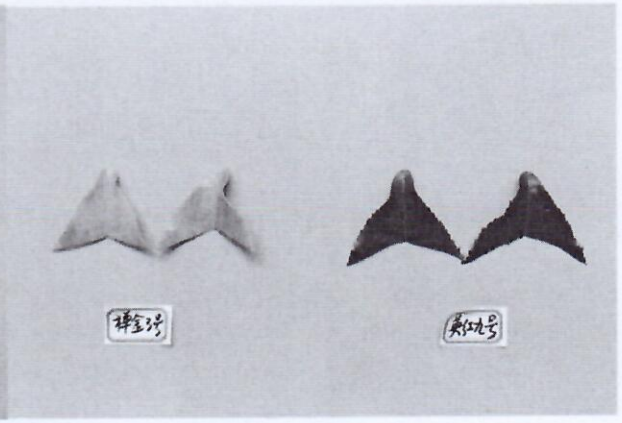


图 5 “禅金 3 号”与“英红九号”形态学对比

“禅金3号”是“英红九号”的黄色芽变植株（图5）。如图6所示，“禅金”品种中叶绿素a和叶绿素b的含量都极低，对照品种“英红九号”中叶绿素a和b的含量是“禅金”品种的13.8和40倍。同样，“英红九号”的类胡萝卜素含量要高于黄化突变品种“禅金”的含量。

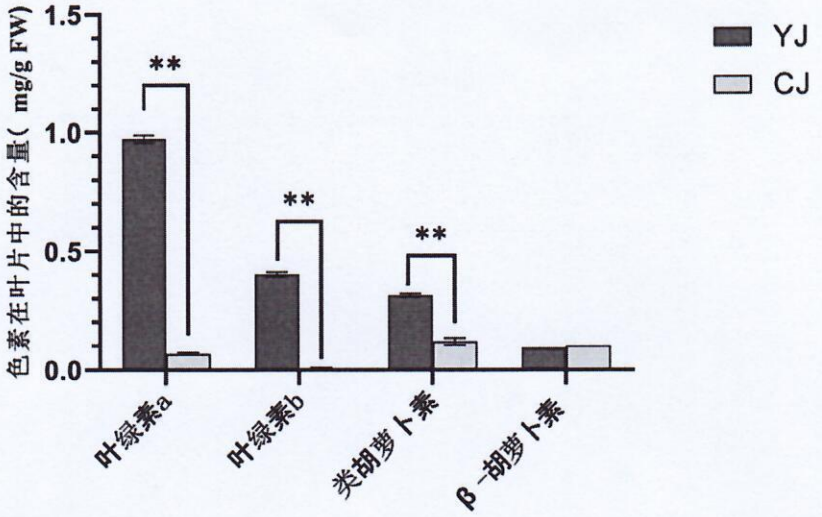


图6 色素在叶片中的含量

注:CJ(禅金品种)；YJ（英红九号）

为解析“禅金”品种叶片的黄化机理，我们以“英红九号”为对照，采用转录组技术分析。共分析 116个代谢途径中有三个显著差异的途径，即“内质网中的蛋白质加工”、“植物-病原互作”和“内吞作用”途径，发现涉及叶色代谢相关的差异显著 13 个。

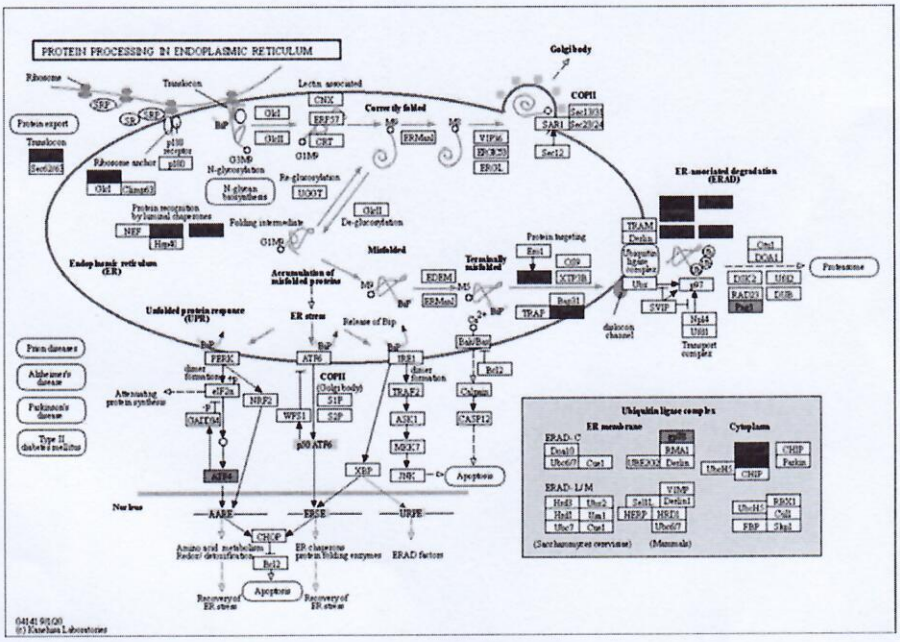


图 7 内质网中的蛋白质加工途径

5）缓解精神压力研究进展

“禅金 3 号”茶树品种的游离氨基酸经检测为 7.74%，氨基酸不但对茶汤的鲜爽滋味有重要作用，其组成还与茶叶保健功效密切相关。L-茶氨酸是茶树中含量最高的游离氨基酸（本品种含量高达 4%），是一种独特的非蛋白氨基酸，2014 年已被国家卫生和计划生育委员会批准为新资源食品。已有研究报道，茶氨酸具有预防糖尿病、保护神经系统和提高免疫力等保健作用。有研究发现，L-茶氨酸对焦虑、恐慌、抑郁和强迫症等精神疾病具有神经保护作用；长期服用 L-茶氨酸是安全的，并且能够改善重度抑郁障碍患者的抑郁症状。

慢性不可预知温和刺激（CUMS）动物抑郁模型是比较理想可靠的抑郁动物模型，它真实地模拟了抑郁症患者的某些病因和症状，运用冰水游泳、束缚、禁水、禁食、潮湿环境等应激源进行长期的温和刺激，使动物在一

定时期内承受巨大的精神压力，进而引发生理机能发生障碍，再通过强迫游泳、悬尾、旷场等行为学实验（图 8）验证动物的抑郁状态以及药物改善的情况。

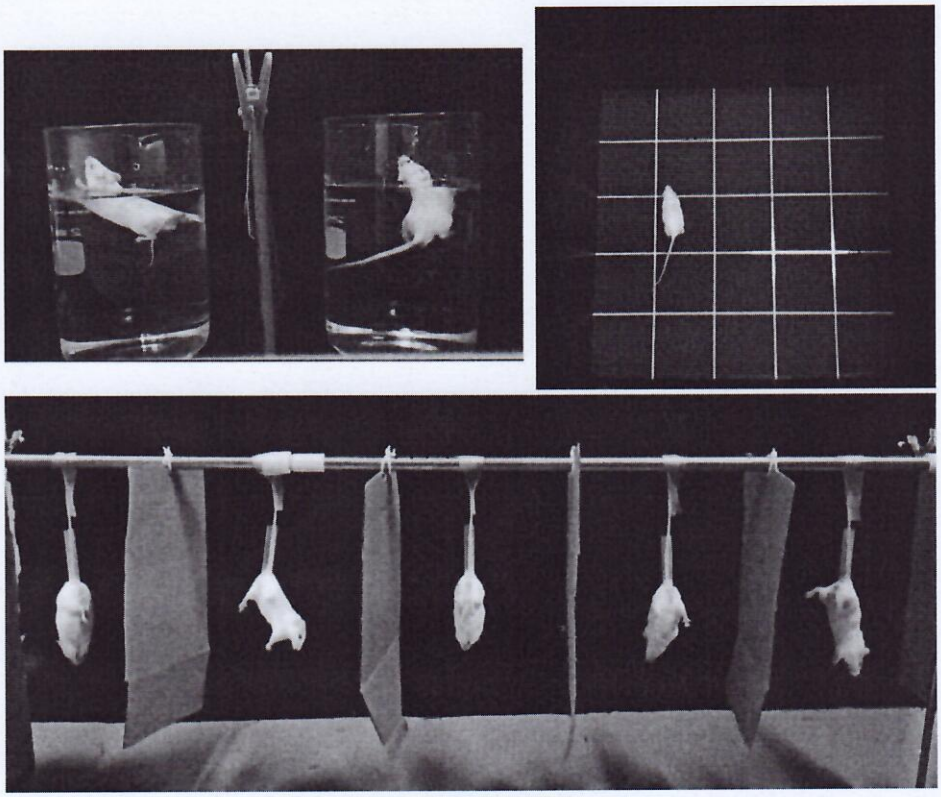


图8 小鼠动物行为学实验

1.2 申报单位条件

为了顺利实施本项目，本公司前期已经建设茶树普通扦插苗圃 30 亩，用于扩繁茶树新品种。收集种植云南大叶种茶树资源 100 亩，建设用于茶树新品系比较的实验茶园 20 亩。另外，建有茶叶加工厂一座，拥有红茶、绿茶、白茶等茶类的常规加工设备。

本公司拟与创新团队共同设计新建可自动喷灌的设施扦插苗圃1座（30万元），用于高效扩繁禅金茶树新品种；新建标准茶叶感官审评室一间（5万元），用于茶叶加工工艺感官评价；新建成分分析室一间（10万元），购置水分测定仪、紫外可见分光光度计等常规仪器设备，用于禅金新品种茶叶加工的品控。企业配套总投入45万元。

1.3 项目知识产权情况

1. 项目实施过程中所产生的知识产权，优先执行任务下达单位的知识产权管理政策，在此前提下，作如下规定：

①项目成果由新兴县五叶茗农业科技有限公司和华南农业大学双方共享，具体按照双方的贡献大小进行分配或双方另行商定。

②共同完成的项目成果的转让，须在双方同意的前提下进行，任何一方不得私自转让或许可实施。

2. 项目成果申报各级奖项，双方单位排名根据具体情况另行商定，人员排名原则上按贡献大小先后排名。

2、项目主要研究内容和拟解决的关键问题；

2.1 主要研究内容

1）新品种选育

从本地茶树品种自然变异植株中获得性状稳定的金黄色变异植株——“禅金”新品种。

2）内在生化品质分析

对影响茶叶品质的多种内在成分进行定量分析。

3）茶类适制性研究

通过前期内在成分分析数据、加工后成分变化以及感官评价，对禅金茶树品种的茶类适制性及其加工技术进行研究。

4）叶片金黄色变异的机制研究

叶绿素以及类胡萝卜素组成比例的变化，通常是叶片显示金黄色的原因，该变化一般可受温度或光照的影响，本研究将通过多组学手段对色素类次生代谢产物的合成途径进行分析，初步解析金黄色变异机理。

5）禅金茶缓解精神压力的作用及机制研究

禅金茶树品种中茶氨酸含量极高，而茶氨酸通常被认为具有调节情绪缓解精神压力的作用。本项目将通过细胞和动物模型，对禅金茶的缓解精神压力作用及其机制进行探讨。同时我们也期望通过对该功能活性的研究，从现代药理学的角度对“禅茶”的概念赋予新的解释。

2.2 拟解决的关键问题

1）如何从本地茶树资源中优选获得禅金茶树新品种？

本项目前期研究从本地茶树品种中筛选得到多株金黄色变异植株；在经扩大繁殖后，选取遗传性状稳定保持的植株进行内在品质成分分析和茶类适制性研究；经优选得到的品种再对其进行多组学分析，探讨其叶片金黄色变异机制；通过体内外模型，对茶汤的缓解精神压力作用及机制进行分析。经上述分析研究，能最终获得品质优异具有一定功能活性的禅金茶树新品种。

2）禅金茶树品种更适合加工成何种茶类？

通过前期对茶树叶片的氨基酸、茶多酚、咖啡碱、色素等关键品质成分进行定量分析，对禅金茶树新品种的茶类适制性进行初步评估；再通过不同的加工方式，试制成不同种类的茶，经感官评价、GC-MS 以及 LC-MS 结合分析，探讨该品种茶的适制性；最后针对特定的茶类，对其加工工艺进行优化，提高成品的品质。

3、项目主要研究方法、主要组织形式、技术路线和创新点；

3.1 主要研究方法

1）新品种选育

在本地茶树资源中发现的金黄色变异枝条，采用无性扦插扩繁，培育成禅金新品系。通过 DUS 测试，对其特异性、稳定性、一致性等进行系统调查，申报国家农业部植物新品种保护权，并进一步无性扩繁。（“禅金 1 号”和“禅金 3 号”两个禅金新品系已向国家农业农村部提交植物新品种权申请）

2）生化成分检测

茶多酚测定参照 GB/T 8313-2002、游离氨基酸测定参照 GB/T 8314-2002、生物碱和儿茶素单体测定采用高效液相色谱法。（色谱方法的建立参考我们已发表的文献：1. Xiao et al., 2021, Frontiers in Nutrition; 2. Zhang et al., 2017, Current Pharmaceutical Analysis; 3. Xiao et al., 2014, Journal of Integrative Agriculture; 4. Xiao et al., 2013, Journal of Separation Science.）

3）茶类适制性研究

通过前期分析，经初步评估后，对禅金新品种进行绿茶、白茶等多种茶类加工技术研究。以绿茶为例，发别对鲜叶日晒萎凋、杀青、揉捻、干燥等关键环节设计实验处理，以成茶感官审评得分结合 GC-MS 对挥发性成分的

分析以及 LC-MS 对非挥发性成分的分析，摸索最佳制茶工艺。茶叶感官审评参考国家标准方法。（本团队在茶叶加工方法及其设备方面拥有的专利如下：一种微生物发酵制作 GABA 茶的方法 CN201710352191；一种乌龙茶全自动做青机 CN201310436635；一种利用黄丝衣霉制备黑茶的方法 CN202110392912；一种 GABA 毛叶茶及其制备方法与应用 CN201510270285；一种清香型单丛茶及其制备方法与应用 CN201510271031；一种乌龙茶平台式全自动做青机控制系统及方法 CN201510698772；一种增加茶叶中 r-氨基丁酸含量的方法 CN02114156；一种乌龙茶连续做青方法及其应用 CN201610826425；一种利用红曲菌制备高没食子酸含量的黑茶的方法 CN202110170853；一种提高茶叶中表没食子儿茶素没食子酸酯含量的方法 CN201010582899）

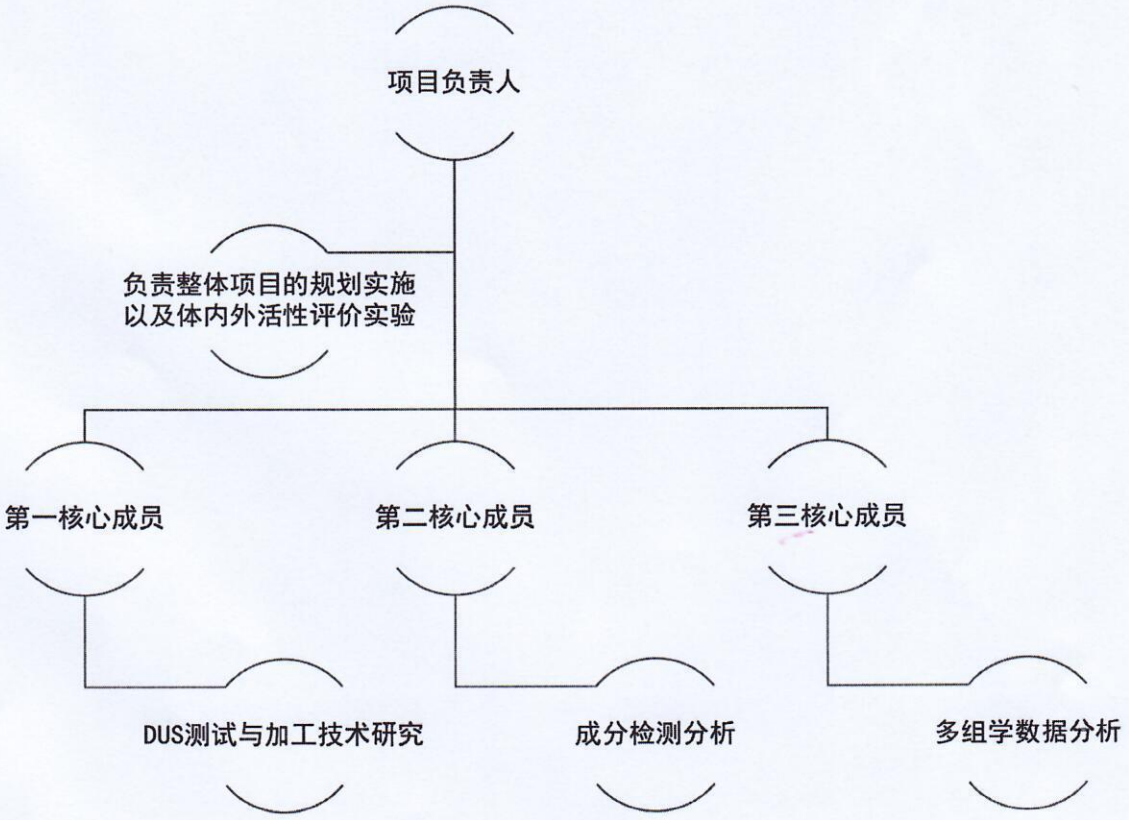
4）叶片金黄色变异的机理研究

转录组研究，将新品种鲜叶送相关生物科技公司完成转录组测序与基因注释，后续的代谢通路以及关键调控基因分析工作由本团队实验室完成。代谢组研究，基于 UPLC-MS/MS 检测平台、自建数据库以及多元统计分析相结合的手段研究样品间的代谢组差异。（组学研究方法参考我们已发表的文献：Mo et al., 2019, Food & Function）

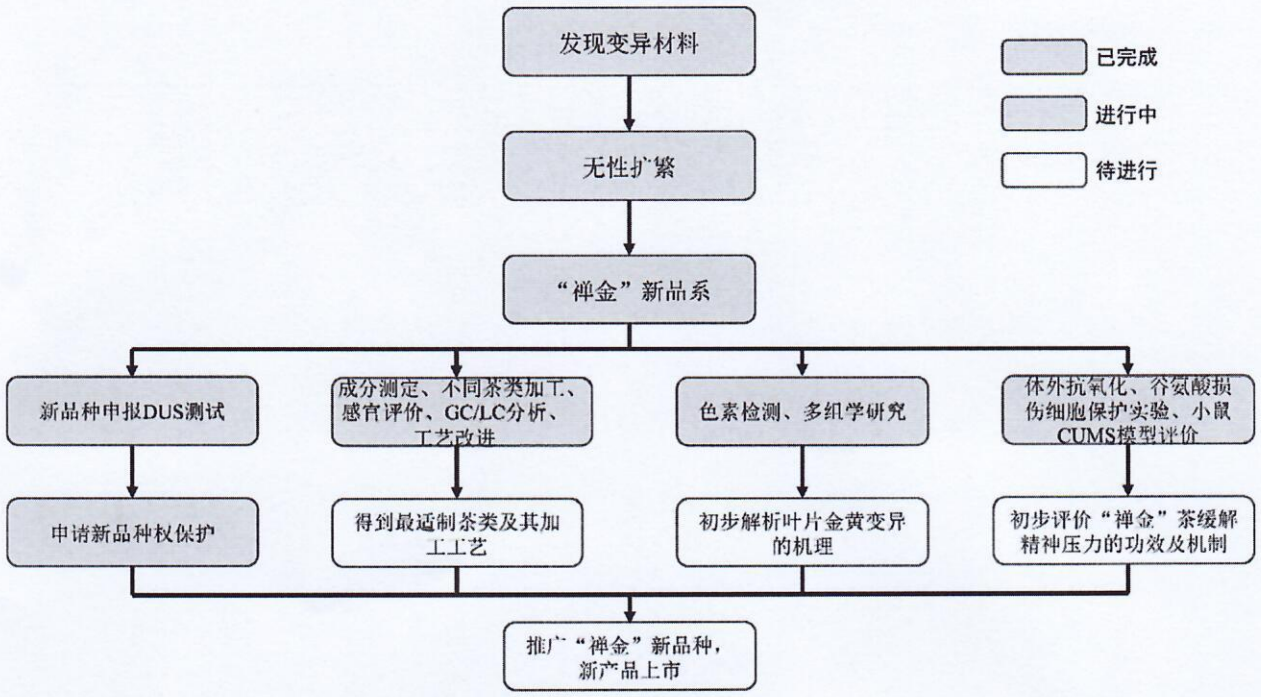
5）缓解情绪压力作用及机制研究

抗氧化活性评价（包括DPPH 自由基清除活性、ABTS+自由基清除率的测定、对羟基自由基（·OH）清除率的测定、总还原力测定等）；PC12细胞模型研究保护神经细胞谷氨酸损伤能力测定；CUMS构建小鼠情绪障碍模型，并通过对其行为学以及生理学指标进行分析，初步探讨作用及机制。（抗氧化试验方法参照我们课题组硕士毕业论文：谢曼卫，2021，茶树幼果生长特性及其多糖活性研究；细胞试验方法参照我们已发表的文献：1. Zhang et al., 2015, Chemical Research in Chinese Universities；2. Zhang et al., 2015, Chemical Research in Chinese Universities；行为学评价以及生理学相关实验操作参考我们已发表的文献：1. Xiao et al., 2021, Frontiers in Nutrition; 2. Cui et al., 2019, Molecular Pharmaceutics; 3. Teng et al., 2017, Food & Function）

3.2 主要组织形式



3.3 技术路线



3.4 创新点

项目首次从新兴本地茶树资源中选育获得黄叶茶树新品种，并对其叶片金黄色的形成机理开展多组学研究。大叶种一般适制红茶、普洱茶等，但本项目前期研究表明，禅金茶树新品种可能更适制高香绿茶，且春、夏、秋季绿茶均具有浓郁的熟板栗香。

4、项目实施后要达到的主要技术指标及技术突破。

1. 选育得到 2 个“禅金”茶树新品种并获得农业农村部植物新品种权授权；

2. 以“禅金”新品种为原料，经茶类适制性研究以及工艺优化后，得到一批“禅金”茶新产品，并附带整套完整的加工工艺；

3. 初步解析“禅金”茶叶片金黄色变异的机理；

4. 初步分析“禅金”茶缓解精神压力的作用及机制。

(以上填报内容要与申报书内容一致)

二、项目考核指标（以下指标按照申报书内容填写）

成果形式		数量（项/个/篇/名）		
		截止 2024 年 5 月	截止 2025 年 5 月	截止 2026 年 5 月
发明专利	申请		1	1
	授权			
实用新型	申请			
	授权			
国际专利（PCT）	申请			
	授权			
技术标准	国际标准			
	国家标准			
	行业标准			
	企业标准			
新产品		2（新品种权申请）		2（新品种权授权）
新材料				
新装备				
新工艺				2
新服务				
计算机软件（著作权）				
临床批文				
生产批件				
（医疗器械）注册证				
论文	发表总量	1		1
	SCI/EI 收录			1
	国内核心期刊（除 SCI/EI 收录外）	1		
专著总量				
科研获奖	总量			
	国家级			
	省部级			
	市级			

科研项目	总量			
	国家级			
	省部级			
	市级			
新增其他科研项目情况	总量			
	横向项目			
	单位内设项目			
人才培养	博士			1
	硕士		1	1
	科研骨干			
其他（如组织重要国际学术会议X次，孵化科技型企业X家等，由团队视情况自行填写）				

其他成果及形式说明：
（二）主要技术经济指标及社会效益

累计新增销售收入（万元）	2000
累计新增利税（万元）	500

其他主要技术经济指标及社会效益说明：

通过创新团队的引进，能帮助企业增强自身科研能力，促进高校科研团队与企业内部自身科研团队的融合,能有效的将基础研究与实际需求结合，让科研产品落地，真正做到产学研一体。同时，在创新团队帮助企业进一步搭建研发平台的过程中，既能根据企业自身特色和需求对常规的实验室进行定向改造，更好满足企业研发需求。通过与引进高校创新团队，还有利于企业在高校进行企业品牌文化的宣传，引入新的企业急需人才，充实企业自身研发实力。该项目的研究，既能以新兴本地特色茶叶品种为基础，通过企业+合作社+基地+农户的模式，促进云浮市政府提出的“资源经济”和“镇域经济”的发展；又能为云浮市以特色品牌的“林茶模式”发展林下经济提供优质的种质资源，为群策群力完成绿美广东计划交出一份属于自己的答卷。

三、项目进度和阶段目标

(一) 项目起止时间:	2023年5月-2026年5月
(二) 项目实施进度及阶段主要目标	
开始日期--结束日期	主要工作内容（限 500 字）
2023年 5月- 2023年 11月	以“禅金”新品种为原料，对其进行茶类适制性研究，并对加工工艺进行优化
2023年 11月- 2024年 5月	通过优化加工工艺，得到一批“禅金”茶新产品，并附带整套完整的加工工艺
2024年 5月- 2024年 11月	完成“禅金”茶金黄色变异机理研究所需的实验部分
2024年 11月- 2025年 5月	对常规实验以及组学实验产生的数据进行分析，初步解析变异机理
2025年 5月- 2025年 11月	完成“禅金”茶缓解精神压力的体外以及体内药效试验
2025年 11月- 2026年 5月	完成“禅金”茶缓解精神压力的机制实验，撰写结题报告

四、项目经费预算

（一）经费下达总额：贰佰万元，￥ 200万元 （其中：市财政负担60万元，县级财政负担140万元）

（二）经费拨付方式：市县财政按3:7比例分担

经费筹集情况：（单位：45万元）

总投入经费：(包含政府支持和自筹资金等总额)

项目总经费投入	项目下达经费	自筹资金				合计
		自有资金	贷款	地方政府投入	其它	
	200	45	0	0	0	245

其它政府部门、境外资金及其他资金投入情况说明：无

（二）经费预算（单位：245万元）

支出经费类别	经费构成及额度	
1.团队成员生活补助（按项目经费的40%开支）	成员1：张旭 金额：20万元 成员2：黄亚辉 金额：20万元 成员3：肖遂 金额：20万元 成员4：袁思思 金额：20万元 （成员数量按照团队情况自行增加或减少）	
2.科研活动开支（按项目经费的60%开支）	项目下达经费（万元）	自筹资金（万元）
（1）直接费用 （.项目承担单位根据实际情况作资金预算计划，不一定所列全部类别都设置相应费用）	科研经费总额： 120 其中包括： 一、直接费用：85.8 （一）设备费：0 （二）业务费：64 1..材料支出：42 2.测试化验加工支出：16 3.燃料动力支出：0 4.餐旅费/会议费/国际合作交流支出：4 5.出版/文献 /信息传播/知识产权事务支出：2 6.其他支出：0 （三）直接人力资源成本费：21.8 （如：工资性支出、劳务支出、专家咨询支出等）	科研经费总额： 45 其中包括： 一、直接费用：45 （一）设备费：5 （二）业务费：30 1..材料支出：30 2.测试化验加工支出： 3.燃料动力支出 4.餐旅费/会议费/国际合作交流支出： 5.出版/文献 /信息传播/知识产权事务支出： 6.其他支出： （三）直接人力资源成本费：10 （如：工资性支出、劳务支出、专家咨询支出等

（2）间接费用（项目承担单位根据实际情况作资金预算计划，不一定所列全部类别都设置相应费用）	二、间接费用：34.2 1.绩效支出：28.2 2.管理费用：6 (华南农业大学经费部分科研管理费6%) 3.其他间接费用：0	二、间接费用 1.绩效支出： 2.管理费用： 3.其他间接费用
其他需要说明的情况：项目下达经费50%（100万元）外拨合作单位华南农业大学，合作单位经按华南农业大学科研经费管理办法使用。		

填报说明：

（1）直接费用是指项目研究过程中发生的与之直接相关的费用。

1、设备费：与科研项目直接相关的计算类仪器设备、软件工具，及仪器设备的租赁、现有仪器设备的升级改造等支出。

2、业务费：项目研究过程中发生的与之直接相关的除设备费、人力资源成本费以外的其他支出。

3、直接人力资源成本费：参与项目研究的科研人员、科研辅助人员的工资性支出或劳务支出。

（2）间接费用是指项目承担单位在组织实施项目过程中发生的无法直接列支的相关费用，主要用于补偿项目承担单位为了项目研究提供的现有仪器设备及房屋，水、电、气、暖消耗，有关提高科研管理、服务能力等费用，以及绩效支出等（如绩效支出、管理费用、其他费用）。

五、人员信息

创新团队项目负责人：

序号	姓名	性别	学历	职称	身份证号码	人事关系所在单位	在本项目承担的工作任务	签名
1	张旭	男	博士研究生	讲师	430681198405180335	华南农业大学	负责主项目整体的规划、实施、协调、结果分析、品种申报、文章和专利的撰写等工作；负责体内外药效活性评价研究	

创新团队项目核心成员：

序号	姓名	性别	学历	职称	身份证号码	人事关系所在单位	在项目中承担的工作任务	签名
1	黄亚辉	男	博士研究生	研究员	43012119691118415X	华南农业大学	负责新品种选育及适应禅金新品种的加工技术研究	
2	肖遂	女	博士研究生	副教授	430103198402143022	华南农业大学	负责通过各种分析仪器对新品种的内在成分进行分析研究	
3	袁思思	女	硕士研究生	无	432524198602021244	新兴县王叶茗农业科技有限公司	负责多组学前处理以及后期的数据分析	

六、合同条款

第一条	甲方与乙方根据《中国人民共和国民法典》及国家有关法规和规定，为顺利完成云浮市2023年产业创新团队项目——特色茶树新品种培育创新团队项目实施（文件编号：云科函〔2023〕115号），经协商一致，特订立本合同，作为甲乙双方在项目实施管理过程中共同遵守的依据。
第二条	甲方的权利义务： 1.按合同书规定进行经费核拨的有关工作协调。 2. 根据甲方需要，在不影响乙方工作的前提下，定期或不定期对乙方项目的实施情况和经费使用情况进行检查或抽查。
第三条	乙方的权利义务： 1.人员名单、项目任务指标、来云工作时间、项目研究内容、项目预期取得的成果及目标与申报书保持一致，原则上不予调整。 2.确保落实自筹经费及有关保障条件。 3. 按合同书规定，对甲方核拨的经费实行专 款专用，单独列账，并随时配合甲方进行监督检查。 4. 使用财政资金采购设备、原材料等，按照有关规定，符合招标条件的须进行招标。 5. 项目实施完成或实施到一定程度，须提出验收或终止结题的申请，并按甲方要求做好项目结题验收工作。 6. 在实施期内，每年1月向甲方如实提交上年度工作情况报告，报告内容包含上年度项目进展情况、经费决算和取得的效果等。 7. 按照项目管理有关规定，提交科技报告或其他材料。
第四条	在履行本合同的过程中，如遇到财政计划改变等不可抗力情况，甲方对所核拨经费的数量和时间可进行相应变更。
第五条	在履行本合同过程中，如项目完成的进度加快或延缓，经双方协商，可对合同中经费年度下达计划 、项目进度和阶段目标进行相应变更。
第六条	在履行本合同的过程中，当事人一方发现可能导致项目整体或部分失败的情形时，应及时通知另一 方，并采取适当措施减少损失，没有及时通知并采取适当措施，致使损失扩大的，应当就扩大的损失承担责任。
第七条	在履行本合同的过程中，因出现在现有水平下无法克服的技术困难，致使项目失败或部分失败造成损失，1. 乙方应及时通知甲方，提供相关证据并予以说明。2. 甲方以已核拨的经费为最高限承担部分责任。
第八条	乙方违反约定造成项目工作停滞、延误或失败,未能通过验收,应承担违约责任。
第九条	本项目技术成果的归属、转让和实施技术成果所产生的经济利益的分享，除双方另有约定外，按国家和有关法规执行。
第十条	属技术保密的项目当事人双方订立技术保密条款，作为合同正式内容的一部分。
第十一条	根据项目具体情况，经双方协商订立的附加条款作为本合同正式内容的一部分。

第十二条	甲方可根据具体情况决定乙方是否需要单位担保，若需要保证单位，应订立担保条款，作为本合同正式内容一部分。
第十三条	本合同的争议应由双方本着协商一致的原则解决，当合同需要更改或解除时，双方应订立变更条 款或协议，仲裁和诉讼在甲方所在地进行。
第十四条	本合同一式三份，各份具有同等效力。甲方存一份，乙方存一份，丙方存一份。本合同自签字之日起生效，有效期至项目验收。各方均应负合同的法律责任，不应受机构、人事变动而影响。
第十五条	违约责任： 违反本合同约定，违方应承担违约责任。 1. 违反本合同第三条第一项约定，乙方应当承担违约责任，承担方式和违约金额如下： （1）合同解除。 （2）乙方退还甲方已核拨的经费，并自行承担由此引起的损失。 2. 违反本合同第八条约定，乙方应当承担违约责任，承担方式和违约金额如下： （1）退还甲方已核拨的经费。 （2）按已核拔经费的20%支付违约金。
第十六条	保密条款： 1. 本合同保密内容范围为：无 2. 本合同保密期限为：无 3. 乙方应与可能知悉保密内容的人员签订技术秘密保护协议。 4. 各方应建立技术秘密保护制度： 5. 属技术保密的项目必须经市负责技术保密部门审查后，确定可否发表或用于国际合作和交流。
第十七条	保证条款（可由保证人和被保证人另行约定） 1. 当乙方不履行或不完全履行本合同，以及没有或没有完全承担违约责任时，保证人承担一般担保责任。 说明： 1. 本合同书中，凡是当事人约定无需填写的条款，应在该条款的空白处划（/）。 2. 委托代理人签订本合同书的，应出具合法、有效的委托书。

七、本合同签约各方

管理单位（甲方）：云浮市科学技术局

（盖章）

单位地址：广东省云浮市吉祥中路25号

法定代表人（或授权代表）：

（签章）

联系人（经办人）姓名：

（签章）

E-mail： kjj8921136@163.com

联系电话：0766-8921136

2023 年 10 月 27 日

承担单位（乙方）：

（盖章）

单位地址：新兴县太平镇社圩村民委员会岱山寺牌坊路口侧

法定代表人（或法人代理）：

（签章）

联系人（项目主管）姓名：

（签章）

E-mail：13826866339@139.com

联系电话：0766-2937456

开户单位名称：新兴县五叶茗农业科技有限公司

开户银行：广东新兴农村商业银行股份有限公司新城支行

开户帐号：80020000015939397

2023年 10月 25日

乙方主管部门（丙方）：

（盖章）

单位地址：新兴县新城镇茅园路46号

法定代表人（或法人代理）：

（签章）

联系人（项目主管）姓名：

（签章）

E-mail：

联系电话：0766-2896166

开户单位名称：新兴县科学技术局

开户银行：广东新兴农村商业银行股份有限公司簕洲支行

开户帐号：80020000008866619

2023年 10月 25日

云浮市科学技术局政府信息公开

索引号：	11445300007175663E/2024-00127	分类：	
发布机构：	云浮市科学技术局	成文日期：	2024-10-10
名称：	关于云浮市2024年省科技创新战略专项资金（2024年科技创新支撑“百千万工程”）拟立项项目的公示		
文号：		发布日期：	2024-10-10
主题词：			

关于云浮市2024年省科技创新战略专项资金（2024年科技创新支撑“百千万工程”）拟立项项目的公示

发布日期：2024-10-10 浏览次数：233

各有关单位：

云浮市2024年省科技创新战略专项资金（2024年科技创新支撑“百千万工程”）项目经组织申报、专家评审、入库等程序，经研究，择优选取85个项目作为拟立项项目。现将拟立项项目名单（见附件）予以公示，公示期为5个工作日。

对公示内容有异议的，请于公示期内以书面形式向市科技局提出，并提供事实证据，签署真实姓名或加盖单位公章，注明联系方式，否则不予受理。

公示时间：2024年10月10日至2024年10月15日

地址：云浮市云城区吉祥中路25号云浮市科学技术局

联系方式：0766-8921010

附件：云浮市2024年省科技创新战略专项资金（2024年科技创新支撑“百千万工程”）拟立项项目名单

云浮市科学技术局

2024年10月9日

附件

云浮市2024年省科技创新战略专项资金（2024年科技创新支撑“百千万工程”）拟立项项目名单

单位：万元

序号	项目名称	申报单位	立项金额
科技型中小企业关键技术攻关			
1	动力电池无卤阻燃聚碳酸酯薄膜关键技术开发与产业化	铨盛（云浮）新型聚合物有限公司	15
2	长寿命耐高温的新能源电感技术攻关	广东乔晶电子科技有限公司	15
3	集成整流电流检测续流IGBT模块的研究与应用	广东瑞淞电子科技有限公司	15
4	基于RF无线互联的智能化红外超低功耗烟雾报警器	罗定市宝捷电子有限公司	15
5	昆虫提取物在生物医药领域的研发与应用	广东泽和诚生物科技有限公司	15

序号	项目名称	申报单位	立项金额
科创平台提质增效			
6	多模式切换电控空气悬架系统容错控制研究与产业化	广东溢康通空气弹簧有限公司	30
7	环保型HAA体系干混消光型粉末涂料用聚酯树脂的研发与产业化	广东伊诗德新材料科技有限公司	30
8	直流快速充电桩电源模块核心部件的研究与应用	磁电实业（罗定）有限公司	30
省实验室分中心高质量发展			
9	禽重要免疫抑制病防控关键技术研究与应用	岭南现代农业科学与技术广东省实验室云浮分中心	50
专业镇产业技术创新发展			
10	簕竹镇家禽专业镇产业技术创新发展研究	簕竹镇人民政府	100
11	罗定市太平豆豉鸡创新专业镇建设	罗定市太平镇人民政府	100
12	建城镇无核黄皮专业镇产业技术创新发展研究	郁南县建城镇人民政府	100
13	前锋镇产业技术创新研究与应用示范	云浮市云城区前锋镇人民政府	100
重大科技任务协同攻关（“揭榜挂帅”项目）			
14	新能源汽车用高性能铝合金型材关键制造技术应用	广东新合铝业有限公司	100
现代农业技术研究与应用			
15	多工序一体化罗竹笼身加工设备及关键技术研究应用	罗定市恒兆蒸笼有限公司	15
16	桂枝饮片生产线人工智造研究与应用	广东越润农业发展有限公司	15
17	G型产气荚膜梭菌致病机制研究及口服疫苗研发与推广应用	岭南现代农业科学与技术广东省实验室云浮分中心	15

序号	项目名称	申报单位	立项金额
18	华南优质籼稻有机富硒种植技术的示范推广	云浮市云威农业科技有限公司	15
19	山茶油物理压榨与全酶法精炼技术研究与应用	广东五季丰油茶科技有限公司	15
"农村科技特派员团队重点派驻任务"专题			
20	优质农产品产加销一体化体系构建	广东省农业科学院 果树研究所	8
21	云城区前锋镇甘薯产业科技支撑	广东省农业科学院 作物研究所	8
22	思劳镇马铃薯、贡柑、南药、竹笋、辣椒等农业种植技术提升及土壤提质增效	仲恺农业工程学院 资源与环境学院	8
23	以科技服务助力腰古镇重点产业高质量发展	仲恺农业工程学院、广州市农业农村科学院	8
24	"禅金"茶树新品种配套技术研究与示范	华南农业大学 林学与风景园林学院	8
25	花生产业提质增效技术示范与推广	仲恺农业工程学院 资源与环境学院、马克思主义学院	8
26	云浮市云安区白石镇荔枝产业提升及绿美乡村建设	仲恺农业工程学院 园艺园林学院	8
27	高村镇特色农业种养与加工技术示范推广	广东省农业科学院 蚕业与农产品加工研究所	8
28	农业种植与水产养殖技术提升	广东省农业科学院 农业资源与环境研究所	8
29	科技助力镇安"百千万工程"典型镇发展项目	广东省农业科学院 农业经济与信息研究所	8
30	肉桂、果蔬和肉鸽高效生产加工技术应用与示范	仲恺农业工程学院 机电工程学院	8
31	橄榄绿色高产矮化栽培技术研究与应用	广东云浮中医药职业学院 中药学院	8

序号	项目名称	申报单位	立项金额
32	农业信息化建设、豆豉鸡预制菜产品质量安全溯源	仲恺农业工程学院 信息科学与技术学院	8
33	特色南药（三丫苦、岗梅）高值化精深加工关键技术研发及推广应用	广东药科大学 药学院	8
34	罗定市华石镇特色农业产业科技提升与信息化建设	仲恺农业工程学院 信息科学与技术学院	8
35	加益香水柠檬高效种植技术示范与产业化应用	广东省农业科学院 果树研究所	8
36	果蔬绿色种植及市场信息化技术研发	仲恺农业工程学院 农业与生物学院	8
37	罗定市黎少镇特色农产品优质栽培与加工科技支撑	仲恺农业工程学院 轻工食品学院	8
38	利用“富氢水”种植技术及深加工等产业帮扶对接蒲塘镇	佛山职业技术学院 新能源与节能环保工程学院	8
39	罗镜镇丝苗米新品种引进及标准化栽培技术推广应用	广东省农业科学院 水稻研究所	8
40	肉桂资源的高值化综合利用研究与应用	广东药科大学 食品科学学院	8
41	科技赋能泗纶，强化联农带农，促进镇域经济高质量发展	仲恺农业工程学院 资源与环境学院	8
42	生江镇果蔬三产业融合发展及特色农旅产业提质增效技术支撑与服务	仲恺农业工程学院 农业与生物学院	8
43	玉米种植、菌菇栽培等关键技术指导与示范	仲恺农业工程学院 农业与生物学院	8
44	肉桂、茶叶、黑榄（乌榄）产业化加工关键技术提升及技术帮扶	暨南大学 生命科学技术学院	8
45	匙羹藤种植加工、稻虾共养等关键技术指导与示范	仲恺农业工程学院 农业与生物学院	8

序号	项目名称	申报单位	立项金额
46	文旅特色、农产品网络直播推广	广州城建职业学院 人文学院	8
47	特色南药种植与加工技术研究	广东药科大学 医药化工学院	8
48	饲料鳜工厂化循环水高效育苗、养成技术示范推广应用	中国水产科学研究院珠江水产研究所	8
49	龟鳖健康养殖技术服务	中国水产科学研究院珠江水产研究所	8
50	六祖镇文旅产业高质量发展	广东白云学院 工商管理学院	8
51	特色农产品加工产业技术提升	广东省农业科学院 蚕业与农产品加工研究所	8
52	青梅新品种选育与产业化关键技术创新与应用	仲恺农业工程学院 农业与生物学院	8
53	农村水环境治理及农林废弃物资源化	佛山科学技术学院 环境与化学工程学院	8
54	鱼稻共生特色种养、水产生态智慧养殖与污水处理技术应用与示范	仲恺农业工程学院 资源与环境学院	8
55	粮、果、茶作物品质栽培技术服务与示范推广	广东省农业科学院 农业资源与环境研究所	8
56	种植及加工技术、乡村建设	佛山科学技术学院 食品科学与工程学院	8
57	新兴县稔村镇优质特色水果产业科技支撑	广东省农业科学院 果树研究所	8
58	特色农产品加工技术研究及应用推广	仲恺农业工程学院 机电工程学院	8
59	新兴县水台镇特色水果产业提质增效技术推广及应用	广东省农业科学院 设施农业研究所	8
60	蚕桑高效种养关键技术示范与推广	广东省农业科学院 蚕业与农产品加工研究所	8

序号	项目名称	申报单位	立项金额
61	岭南特色果蔬标准化种植加工技术引进与示范	仲恺农业工程学院 轻工食品学院	8
62	无核黄皮栽培与产地加工技术示范推广及林下经济开发	中国热带农业科学院农产品加工研究所	8
63	国潮乡村文旅规划与建设	广东白云学院 创新创业学院	8
64	油茶的栽培、加工技术引进与示范	广东轻工职业技术学院 轻工化工学院	8
65	优质蚕桑新品种及高值化加工利用技术引进与示范	广东省农业科学院 蚕业与农产品加工研究所	8
66	郁南县桂圩镇肉桂种植技术帮镇扶村项目	东莞理工学院 中法联合学院	8
67	历洞镇特色食用菌栽培技术示范与推广	肇庆学院 环境与化学工程学院	8
68	乡村农文旅资源挖掘与文旅融合发展研究与应用示范	广东工业大学 管理学院	8
69	南江口镇特色水果及农作物种植技术研究与应用	肇庆学院 生命科学学院	8
70	作物优质高效栽培技术服务与示范推广	广东省农业科学院 农业资源与环境研究所	8
71	特色经济作物种植加工与畜牧养殖技术引进与示范	仲恺农业工程学院 轻工食品学院	8
72	大水面淡水渔业健康养殖技术应用与示范	中国水产科学研究院 珠江水产研究所	8
73	郁南县宝珠镇经济果树产业提质增效科技支撑	广东省农业科学院 果树研究所	8
74	畜禽水产养殖与特色果蔬种植加工技术引进与示范	广东省农业科学院 动物科学研究所	8
科普阵地培育与建设项目			
75	四一八小学科普基地建设	郁南县四一八小学	5

序号	项目名称	申报单位	立项金额
76	激光加工技术科普阵地培育与建设	罗定职业技术学院	5
77	人工智能科普阵地的培育与建设	罗定职业技术学院	5
78	青少年科技创新“育苗计划”系列活动	郁南县青少年宫	5
79	郁南县消防科普教育培育	郁南县消防救援大队	5
80	人工智能科普活动基地建设	罗定市喜耀粤西学校	5
“百千万工程”县域创新基地建设			
81	新兴县“百千万工程”县域创新基地建设	新兴县科学技术局	50
82	云城区“百千万工程”县域创新基地建设	云城区工业和信息化局	30
83	郁南县“百千万工程”县域创新基地建设提升	郁南县科学技术局	50
84	罗定市“百千万工程”县域布局设点建设	罗定市中医药发展促进中心	50
85	云安区“百千万工程”县域创新基地建设	云浮市云安区工业和信息化局	30

项目编号：KTP20240934

文件编号：云科函〔2024〕90号

云浮市农村科技特派员团队重点派驻任务合同书

重点派驻任务名称：“禅金”茶树新品种配套技术研究与示范

业 务 类 型：科技支撑“百千万工程”

管 理 单 位（甲方）：云浮市科学技术局

承 担 单 位（乙方）：华南农业大学

通 讯 地 址：广州市天河区五山路483号

邮 政 编 码：510642　　单位电话：85286065

团队负责人：张旭　　联系电话：13539883664

团队联系人：张旭　　联系电话：13539883664

县（市、区）科技部门（丙方）：云浮市云安区工业和信息化局

云浮市科学技术局

二零二四年制

一、派驻任务基本情况表

派驻任务名称	“禅金”茶树新品种配套技术研究与示范
派驻乡镇	云浮市云安区石城镇
起止时间（第一年）	2024 年 9 月 1 日至 2025 年 8 月 31 日
经费资助	8 万元
任务内容摘要（200 字以内）：	
广东作为我国茶叶的重要产区，品牌形象主要集中在红茶和乌龙茶上，绿茶品牌形象相对模糊，不利于产业的长期稳定发展。素有“中国石材之都”美誉的云浮，近年来致力于传统产业转型升级发展绿色经济。茶叶种植在这里因其独特的山地气候有着悠久的历史，且受客家文化影响，当地传统茶产品以绿茶为主，并曾以其特有的品质和风味远销海外。本课题组在云浮本地茶树群体中，通过人工培育得到叶色金黄的“禅金”系列新品种，氨基酸含量极高，多酚类物质含量适中，适制高品质绿茶并具有清汤黄叶、滋味甘醇、熟板栗香浓郁等特点。因此，推广种植“禅金”系列茶树新品种，在云浮地区打造区域性公用绿茶品牌，有助于传承和保护当地茶文化，填补广东茶叶品牌的空缺，同时还能助力“百千万工程”全面推进乡村振兴，打造人与自然和谐共生的“绿美广东”。	
项目已受财政资金资助情况	□国家（部委）财政资金资助 □省级财政科技资金资助□省级财政其他部门资金资助 □地市财政资金资助 □其他 ✓无 简要说明（限 100 字）
其它需要说明的问题（限 100 字）：	

二、重点派驻任务内容

（一）乡镇对接基础（200字以内）

云浮迳心岭，有着优越独特的地形地貌，海拔较高、群山耸峙，冬春之际多云雾，光热、水分适宜于茶树生长，这得天独厚的生态环境，使得"迳心茶"成为了具有400多年历史的云浮知名茶叶品牌。"迳心茶"有着当地农家独特炒制工艺，制作出的绿茶既保持了普通绿茶的清新鲜香，又具有其特有的铁锅"炒香"，整体香味别具一格，但目前尚未大规模种植适制绿茶的优良茶树品种。本团队基于云浮本地茶树品种选育的"禅金1号"新品种氨基酸含量极高，多酚类物质含量适中，并且在产量上能保持大叶种高产的优势，且扦插扩繁成活率高，由该品种制备得到的绿茶具有清汤黄叶、滋味甘醇、熟板栗香浓郁等特点。本团队已由云浮市科技局创新团队项目支持，引进至新兴县五叶茗农业科技有限公司，推广"禅金"茶树新品种。因此，从品种资源、地理位置以及团队实力层面，本团队均具备帮扶石城镇发展特色茶叶品牌的能力。

（二）任务内容（拟开展相关工作）

1）"禅金"茶树快速扩繁技术研究

针对"禅金"茶树品种特性，从母本园管理、扦插时间、苗床建设、苗圃水肥管理以及取苗时间、方法等方面摸索嫁接和嫩枝扦插繁殖技术，制定"禅金"茶树快速扩繁技术规程。

2）"禅金"茶树无公害栽培技术研究

针对"禅金"茶树特性，从茶树修剪、施肥、病虫害防治等方面进行技术集成，研究制定"禅金"茶树无公害栽培技术规程。

3）"禅金"茶树提香增质加工技术研究

GC-MS香气物质检测和HPLC标志性成分检测，结合感官评审，探索形成具有迳心独特加工工艺的"禅金1号"绿茶加工技术规程。

（三）绩效目标

1、种植推广"禅金1号"新品种，建立配套的母本园和繁殖苗圃；研究制定"禅金"茶树快速扩繁和无公害栽培技术规程1套；

2、制备得到1个优质绿茶新产品：研究制定"禅金"1号绿茶加工技术规程1套。

三、重点派驻任务考核指标

（一）主要任务考核指标

预期指标成果形式		各指标完成数量（项/个/篇/名）	
		三年拟完成数量	该年度完成数量（第一年）
累计帮扶天数		180	60
服务带动农户数量（户）		9	3
服务企业、合作社、农民协会等机构（个）		1	1
发明专利	申请		
	授权		
实用新型	申请		
	授权		
技术标准	国际标准		
	国家标准		
	行业标准		
	企业标准		
引进新品种（种）		1	1
推广新技术（个）		1	0
建立示范基地（个）		1	0
为当地引进项目（个）			
为当地引进资金（万元）			
举办培训场次（场）		6	2
培训农户或技术人员（人次）		60	20
帮助受援对象增收（元）			
论文	发表总量		
	其中：SCI/EI 收录		
	国内核心期刊（除 SCI/EI 收录外）		
其他将提供的研究开发成果及形式（创新特色、成果宣传推介措施等，200 字以内）			
以新品种茶树研发“禅金”系列适心茶新产品 1-3 款。			

（二）项目完成预计达到经济效益情况：

项目预期累计新增销售收入（万元）	0
项目预期累计新增利税（万元）	0
其他经济指标：新增产值（万元）	0

（三）项目完成预计带动社会效益情况（300字以内）：

以云浮本地特色茶叶品种为基础，结合迳心当地特色加工工艺，通过企业+合作社+基地+农户的模式，促进云浮市政府提出的“资源经济”和“镇域经济”的发展，助力“迳心茶”老品牌焕新，推动石城特色镇的建设。

四、经费预算情况表

项目经费（农村科技特派员相关资金实行“包干制”，可结合本单位实际情况，制定实施本单位农村科技特派员资金管理制度，确保资金支出用于支持保障农村科技特派员派驻任务实施。）

经费类别	财政经费
（一）直接费用	5.12
1. 设备费	
2. 业务费	3.52
3. 直接人力资源成本	1.6
（二）间接费用	2.88
1.绩效支出	2.4
2.管理费用	0.48
3.其它间接费用	
合计	8

其他需说明的情况：

五、特派员派出单位基本情况表

单位基本信息					
单位名称	华南农业大学			统一社会信用代码	12440000455416 5634
注册资金	311733 万元	所在地区	广州天河区	银行信用等级	AAA
单位性质	其他	所属行业	高等教育	单位级别	省属
职工总人数	3401 人		其中：科研人员	2283 人	
2023 年度研发经费	63000.00 万元		2023 年度总收入	万元	
是否科技特派员派出单位			✓是 □否		
项目承担单位简介（200 字以内）	华南农业大学是国家“双一流”建设高校，现有教职工 3380 人，其中专任教师 2360 人（正高级 478 人，副高级 893 人）；中国科学院院士 1 人、中国工程院院士 2 人，国家级人才项目获得者 70 人，省级人才项目获得者 128 人；国家级教学名师 4 人。拥有 14 个国家级科研平台、122 个省部级科研平台和 4 个广东省高校特色新型智库。学校高度重视产学研合作与社会服务，设立了乡村振兴研究院和新农村发展研究院，校地企共建产学研新型研发机构 57 个；与政府共建乡村振兴研究院地方分院 4 个、新农村发展研究院地方分院 4 个，建设永根科技站站点 67 个（含 3 个海外站点）。				

近三年承担科技计划项目数量			
级别 数量及金额 级别	国家级	省级	市级
项目数量（项）	720	750	778
财政资助金额（万元）	73000.00	62000.00	27300.00

建立创新平台情况			
工程技术开发中心		博士后科研工作站	
企业重点实验室		其它	

六、特派员团队人员信息

团队负责人：

序号	姓名	性别	出生年月	职务	职称	最高学位	所在单位	身份证号码	在本项目中承担的工作任务	签字
1	张旭	男	1984 年 5 月	无	讲师	博士	华南农业大学	430681198405180335	项目总体设计与实施	

团队成员：

序号	姓名	性别	出生年月	职务	职称	最高学位	所在单位	身份证号码	在本项目中承担的工作任务	签字
2	曾贞	女	1970 年 9 月	无	副研究员	硕士	华南农业大学	430111197009170484	示范基地规划和建设	
3	肖遂	女	1984 年 2 月	无	副教授	博士	华南农业大学	430103198402143022	茶叶加工与内在品质分析	

七、合同条款

条款	内容
第一条	甲方、乙方、丙方根据《中华人民共和国民法典》《省级科技计划项目任务书管理细则》《广东省农村科技特派员科技助力百县千镇万村高质量发展行动计划（2023-2026）》以及广东省科技厅印发的《农村科技特派员助力“百千万工程”管理工作指引（2024-2026 年）》等有关文件规定，经协商一致，特订立本合同，作为甲乙丙三方在项目实施管理过程中共同遵守的依据。
第二条	甲方的权利义务： 1.甲方作为项目管理单位，根据项目管理相关规定做好项目实施指导监督，根据项目监督管理需要，单独或联合其他部门定期或不定期对项目的实施情况和经费使用情况等进行检查或抽查。 2.按照项目任务书规定做好经费核拨。 3.负责辖区内农村科技特派员助力“百千万工程”的工作衔接和协调指导，推动农村科技特派员与辖区内县镇村涉农主体对接。 4.负责指导有关乡镇（驻镇工作队）提高对农村科技特派员工作的重视，协调有关乡镇（驻镇工作队）为农村科技特派员在基层开展工作提供一定条件保障，指导有关乡镇（驻镇工作队）为农村科技特派员提供客观公正的工作成效证明。
第三条	乙方的权利义务： 1.乙方作为特派员派出单位，应落实有关保障条件，与团队负责人、团队成员充分沟通协调，按时按计划完成各阶段工作任务，积极配合甲方和其他部门做好年度考核评价工作。统筹协调相关资源，配合省、市、县科技行政主管部门做好本单位农村科技特派员管理工作，鼓励探索创新农村科技特派员工作机制。 2.结合本单位实际情况，制定实施本单位农村科技特派员资金管理制度，确保资金支出用于支持保障农村科技特派员派驻任务实施。 3.负责督促落实本单位农村科技特派员承担的派驻任务及专项资金的支出和监管，收集本单位典型案例，开展宣传报道，及时将本单位农村科技特派员助力“百千万工程”工作情况报送科技行政主管部门。 4.帮扶期间，乙方应密切联系和协助对接帮扶镇开展工作，全力完成甲方安排的科技帮扶任务。并督促派出团队做好工作台账、工作成效等相关材料的收集整理和填报工作。

第四条	丙方的权利义务： 1.丙方作为县级科技主管部门，承担重点派驻任务实施的业务指导和监督管理责任。 2.在监督管理过程中，积极协助甲方研究解决存在问题，协同推进重点派驻任务顺利实施。
第五条	涉及农村科技特派员团队人员、对接地区、任务目标等工作重大调整变更，农村科技特派员团队应通过派出单位（乙方），及时与当地科技行政主管部门（甲方和丙方）商议并报送书面材料，地市科技行政主管部门（甲方）根据实际情况进行处理反馈，并将反馈结果报送省级科技行政主管部门备案。
第六条	乙方违反合同书规定未完成派驻任务的,导致未能通过考核验收,应承担违约责任。
第七条	本合同技术成果的归属、转让和实施技术成果所产生的经济利益分享，除项目单位和项目成员另有约定外，按国家和有关法规执行。
第八条	协议在履行过程中发生争议的，应通过共同协商方式解决，产生严重后果或重大影响、要求变更或解除协议的，应及时报告省级科技管理部门，在省科技管理部门指导和协调下进行争议事项处理。
第九条	本任务书一式四份，各方各存一份，报省科技管理部门1份，均具同等法律效力，自签字之日起生效。各方均应承担任务书的法律责任，不受机构、人事变动的影响。
第十条	其他未尽事宜，由各方友好协商解决。

八、本合同签约各方

管理单位（甲方）：云浮市科学技术局 单位地址：广东省云浮市云城区云城街道吉祥中路 25 号 法定代表人（或授权代表）： 联系人（经办人）姓名： 电子邮箱： 联系电话：0766-8921360	（盖章） （签章） （签章） 2024 年 12 月 6 日
承担单位（乙方）：华南农业大学 单位地址：广州市天河区五山路 483 号 法定代表人（或授权代表）：薛红卫 联系人（项目主管）姓名：张旭 电子邮箱：zhangxu@scau.edu.cn 联系电话：13539883664 开户单位名称：华南农业大学 开户银行：中国工商银行广州五山支行 开户帐号：3602002609000310520	（盖章） （签章） （签章） 2024 年 12 月 2 日
派驻单位所在县（市、区）科技部门（丙方）：云浮市云安区工业和信息化局 单位地址：广东省云浮市云安区六都镇白沙塘行政综合区康云路 法定代表人（或授权代表）： 联系人（经办人）姓名： 电子邮箱：yakj1@126.com	（盖章） （签章） （签章） 2024 年 12 月 4 日

十、附件目录（有需要附加说明的材料可附上）

序号	附件名称	页码

林

受理编号：c1730550100137　　项目编号：2017A020208048

文件编号：粤科规财字[2017]50号

广东省省级科技计划项目

合同书

项目名称：高GABA-无咖啡因速溶茶的研发

专项资金类别：公益研究与能力建设

计划类别：农村科技领域

项目起止时间：2017-01-01　至　2019-12-31

管理单位(甲方)：广东省科学技术厅

承担单位(乙方)：华南农业大学

乙方主管部门(丙方)：华南农业大学

通讯地址：广东省广州市天河区五山路483号

邮政编码：510642　　单位电话：020-38632819

项目负责人：张旭　　联系电话：15901624655

项目联系人：张旭　　联系电话：13539883664

2017A020208048

广东省科学技术厅
二〇一七年制

（广东科技微信公众号）

（受理纸质材料二维码）

一、研发内容和关键技术

主要研究内容：

本研究选用广东南昆山不含咖啡因的毛叶茶为原料，拟先通过厌氧处理提高GABA合成中关键酶谷氨酸脱羧酶（GAD）活性，同时再增加该酶底物谷氨酸（Glu）的含量，两方面共同作用利用茶叶自身代谢提高内在成分GABA的含量，经优化后的方法不影响其余内含物的含量和茶叶本身特有的风味；再将高GABA毛叶茶制作成不同类型的茶制品，如普洱茶、红茶、乌龙茶等；之后用不同浓度乙醇溶液或水对茶进行浸提，HPLC跟踪进行条件优化，确定合适的提取溶剂、温度和时间后，比较喷雾干燥和冷冻干燥对样品形态、稳定性、水溶性等的影响，选择适宜的干燥方式，最终研发得到一批风味不同的高GABA-无咖啡因速溶茶产品。

拟解决的关键问题：

1）如何通过不添加外源性GABA的方式提高茶叶自身GABA含量，且不影响茶叶本身的品质。我们通过厌氧处理和增加底物浓度两方面共同作用提高GABA含量，经HPLC和GC-MS分别检测其余内含物以及香气成分，证明在提高GABA含量的同时不影响茶叶自身风味；

2）怎样保证速溶茶产品中有效成分的含量。我们拟通过HPLC建立高GABA-无咖啡因茶的指纹图谱，在速溶茶工艺优化的过程中，用HPLC进行跟踪比对，监控主要活性成分的变化，以确定最佳条件。

技术路线：

厌氧处理技术优化→提高GABA含量→加工得到高GABA无咖啡因毛叶茶→建立HPLC检测方法→优化提取条件和干燥条件→确定速溶茶加工工艺→得到高GABA无咖啡因速溶茶产品

创新点：

1）本项目选取广东南昆山特有的无咖啡因野生茶树品种——毛叶茶做为原料，在采用本课题组已申请专利的厌氧法处理叶片提高其内在GABA含量后，得到的高GABA-无咖啡因毛叶茶能充分发挥GABA促进睡眠、降低血压、提高脑活力等功效，同时毛叶茶内丰富的茶氨酸以及茶多酚类物质对于GABA的功效具有多靶点协同作用，不易产生机体耐药性，其作用效果好于直接服用GABA单体物质。

2）在制备得到不同风味的高GABA-无咖啡因速溶茶后，通过HPLC的方法对于内在主要活性成分进行监控，能在满足消费者便于携带、易吸收、口味多样的同时，还能保证每一次饮用能得到数量明确且一致的已知功能性成分。

2017A020220048

二、项目考核指标

1.项目完成后提供的研究开发成果及形式（须明确产品、专利、版权、标准等成果的类型及数量）

成果形式		成果数量	成果形式		成果数量
发明专利	申请	1	引进人才(人)		
	授权		培养人才(人)		
实用新型专利	申请		科技人才奖励(人)		
	授权		技术标准制定	牵头(个)	
外观设计专利	申请			参与(个)	
	授权		科技报告(篇)		
国外专利	PCT受理		软件著作权(项)		
	授权		论文论著(篇)		1
获得国家级奖项(项)			其中：被收录论文数(篇)	SCI	
获得省级奖项(项)				EI	
新服务(项)				ISTP	
新产品（或新材料、新装备、新品种（系））		1	新工艺（或新方法、新模式、新技术）		
创新载体项目必填		技术服务数量（项）			
		服务企业数量（家）			
科技金融项目必填		开展培训宣讲活动场次(次)			
		服务企业数量(家)			
		帮助企业融资(万元)			
		引进专业机构(家)			
院士工作站项目必填		引进院士及其团队科技成果转化数量			
		院士开展的战略咨询和技术指导次数			
		院士年进站次数			
		院士及院士团队年进站时间			
软科学项目必填		决策咨询报告(篇)			
		研究总报告(篇)			
		研究中期报告(篇)			
		研究分报告(篇)			
		调研报告(篇)			
		专著(篇)[须注明“广东省软科学研究计划项目(项目编号：)资助”]			
		核心期刊论文(篇)[以第一作者发表，须注明“广东省软科学研究计划项目(项目编号：)资助”]			
		培养人才(人)			

2017A020208048

	获国家级奖项(项)	
	获省级奖项(项)	
	其他	

2.其他成果及形式说明：

本项目将研发得到一系列风味类型不同的高GABA-无咖啡因速溶茶产品，通过与本地企业联合，占领无咖啡因保健茶市场，本品能消除咖啡因过度症状和成瘾性，提高茶叶自身GABA含量后，发挥茶叶内在多成分的协同作用，达到促睡眠、降血压、提高脑活力的功效。

3.主要技术经济指标及社会效益

累计新增销售收入（万元）	
累计新增利税（万元）	

4.其他主要技术经济指标及社会效益说明：

γ-氨基丁酸（GABA）片做为药品，被用于改善睡眠、调节血压以及缓解脑功能的衰退等。本研究增加了茶叶中天然的GABA含量，无任何茶叶外源性物质添加，避免了化学合成以及微生物发酵过程中可能带来的杂质污染；同时由于毛叶茶中不含有咖啡因，消除了咖啡因对GABA的拮抗作用，以及咖啡因自身带来的成瘾性，充分发挥茶叶内含物质对GABA的协同作用，相较于GABA单体而言，不易产生耐药性。长期睡眠不足者以及失眠和高血压并发者可长期饮用本产品，许多症状较轻的患者甚至可以不必服用相关药品，仅通过日常饮茶方式达到改善睡眠降低血压的目的，真正将功能性食品的概念灌输到日常生活中。

项目负责人（签章）：　　年　　月　　日

2017A020208048

三、项目进度和阶段目标

开始日期	结束日期	主要工作内容
2017-01-01	2017-12-31	采集样品，通过厌氧处理提高GABA含量，制备出不同类型的高GABA-无咖啡因毛叶茶；
2018-01-01	2018-12-31	对速溶茶的提取和干燥工艺进行摸索和优化，对HPLC检测方法进行方法学的研究；
2019-01-01	2019-12-31	建立HPLC检测方法，确定速溶茶加工工艺，得到高GABA-无咖啡因速溶茶产品，项目验收。

2017A020208048

四、承担、参与单位工作分工及经费分配情况

承担/参与单位名称（盖章）	工作分工	总经费分摊（万元）	省科技厅经费分配（万元）
华南农业大学	承担本项目的所有研究工作	15.00	15.00
	合计	15.00	15.00

2017A020208048

五、项目总经费及省科技厅经费预算

1.省科技厅经费下达总额：（大写）壹拾伍万圆整；（小写 ）15万元；						
2.省科技厅经费拨付方式：**一次性拨款**						
3.省科技厅经费年度下达计划：（大写）壹拾伍万圆整；（小写 ）15万元；						
分期			经费(万元)			
第1期			15			
4.总经费开支预算计划：						
经费筹集情况：						（单位：万元）
总投入经费：15.00						
	省科技厅经费	自筹资金				合计
		自有资金	贷款	地方政府投入	其它	
已投入经费：						
新增经费：	15.00					15.00
政府部门、境外资金及其他资金投入情况说明：						

2017A020208048

新增经费预算：				（单位：万元）
	新增经费总额		省科技厅经费	
支出经费	经费额	用途说明	经费额	用途说明
基建费：				
1、直接费用：	14.25		14.25	
(1)设备费：				
(2)材料费：	8.00	试剂、药品、耗材等	8.00	试剂、药品、耗材等
(3)测试化验加工外协费：				
(4)燃料动力费：				
（5）差旅费/会议费/国际合作与交流费：	1.25	收集材料、调查性状、参加会议等出差用	1.25	收集材料、调查性状、参加会议等出差用
（6）出版/文献/信息传播/知识产权事务费：	1.00	论文发表、著作出版、申报专利等	1.00	论文发表、著作出版、申报专利等
（7）劳务费：				
（8）人员费：	4.00	研究生及临时工工资等	4.00	研究生及临时工工资等
（9）专家咨询费：				
（10）直接费用其他支出：				
（11）科技金融服务体系其他费用：				
①信用评级补贴：				
②大赛场租：				
③特派员奖励与补贴：				
2、间接费用：	0.75		0.75	
（1）间接成本：				
（2）管理成本：				
（3） 绩效支出：				
合计：	15.00		15.00	

特别提醒：2017年3月份，广东省《关于进一步完善省级财政科研项目资金管理等政策的实施意见（试行）》（粤委办〔2017〕13号）出台，对间接费用比例、劳务费开支范围、人员费用安排等进行了调整优化。为及时拨付2017年度科研经费，平台直接提取申报书相关信息生成合同书并进行了预签订，但各项目负责人、承担单位、主管部门须认真领会相关文件精神，在合同书签订完成后2个月内通过平台提请项目经费变更或确认，对相关经费开支进行细化完善，否则，将影响其科研信用评级或申报新的省级科技项目。

2017A020200048

六、人员信息

项目负责人情况

姓名	年龄	性别	职称	职务	学历	在项目中承担的任务	所在单位	签名
张旭	33	男	讲师	无	博士研究生	在本项目中承担组织、协调，以及品控HPLC检测方法的建立。	华南农业大学	

主要研究开发人员

姓名	年龄	性别	职称	职务	学历	在项目中承担的任务	所在单位	签名
黄亚辉	47	男	研究员	茶学系主任	博士研究生	负责品种选育以及关键加工技术的改进研究。	华南农业大学	
曾贞	46	女	副研究员	无	硕士研究生	负责提高GABA含量技术的研究	华南农业大学	
肖遂	32	女	助理研究员	无	博士研究生	负责茶叶内在化学成分的分析	华南农业大学	
滕杰	28	男	未取得	无	硕士研究生	负责茶叶加工及深加工研究	华南农业大学	
蒋陈凯	26	女	未取得	无	本科	负责特异茶树资源的研究与利用	华南农业大学	

2017A020208046

七、承担、参与单位合作

无

2017A020208048

八、合同条款

第一条	甲方与乙方根据《中华人民共和国合同法》及国家有关法规和规定，为顺利完成（2017）年**高GABA-无咖啡因速溶茶的研发**专项项目（项目编号： **2017A020208048** ）经协商一致，特订立本合同，作为甲乙双方在项目实施管理过程中共同遵守的依据。
第二条	甲方的权利义务： 1.按合同书规定进行经费核拨的有关工作协调。 2.根据甲方需要，在不影响乙方工作的前提下，定期或不定期对乙方项目的实施情况和经费使用情况进行检查或抽查。 3.根据《广东省科技计划项目信用管理办法(试行)》对乙方进行科技计划信用管理。
第三条	乙方的权利义务： 1.确保落实自筹经费及有关保障条件。 2.按合同书规定，对甲方核拨的经费实行专款专用，单独列账，并随时配合甲方进行监督检查。 3.使用财政资金采购设备、原材料等，按照《广东省实施〈中华人民共和国招标投标法〉办法》有关规定，符合招标条件的须进行招标。 4.项目实施完成或实施到一定程度，须按照《广东省省级科技计划项目结题管理的实施细则（试行）》提出验收或终止结题的申请，并按甲方要求做好项目结题工作。 5.在每年1月向甲方如实提交上年度工作情况报告，报告内容包含上年度项目进展情况、经费决算和取得的效果等。 6.按照国家和省有关规定，每年须提交年度科技报告；项目验收时，须提交验收科技报告。
第四条	在履行本合同的过程中，如出现广东省相关政策法规重大改变等不可抗力情况，甲方有权对所核拨经费的数量和时间进行相应调整。
第五条	在履行本合同过程中，需要对项目起止时间、项目经费使用（包括自筹经费、经费分配及经费支出预算等）、项目内容（包括研发内容、技术指标、经济指标及成果指标等）、项目名称、项目承担单位（包括承担单位更名、承担单位替换）、参与单位、项目负责人和成员等进行变更的，甲乙双方按照《广东省省级科技计划项目合同书管理的 实施细则（试行）》有关规定执行。
第六条	在履行本合同的过程中，当事人一方发现可能导致项目整体或部分失败的情形时，应及时通知另一方，并采取适当措施减少损失，没有及时通知并采取适当措施，致使损失扩大的，应当就扩大的损失承担责任。
第七条	本项目技术成果的归属、转让和实施技术成果所产生的经济利益的分享，除双方另有约定外，按国家和广东省有关法规执行。

第八条	属技术保密的项目，甲乙双方应另行订立技术保密条款，作为本合同正式内容的一部分，与本合同具有同等效力。
第九条	根据项目具体情况，经双方另行协商订立的附加条款，作为本合同正式内容的一部分，与本合同具有同等效力。
第十条	本合同的争议应由双方本着协商一致的原则解决，如双方协商不成的，则应向甲方所在地法院提起诉讼。
第十一条	保密条款： 1.本合同保密内容范围为： 无 2.本合同保密期限为： 无 3.乙方应与可能知悉保密内容的人员签订技术秘密保护协议。 4.各方应建立技术秘密保护制度。 5.属技术保密的项目必须经省负责技术保密部门审查后，确定可否发表或用于国际合作和交流。
第十二条	甲方可根据具体情况决定乙方是否需要单位担保，若需要保证单位，应订立担保条款，作为本合同正式内容一部分。当乙方不履行或不完全履行本合同，以及没有或没有完全承担违约责任时，乙方的保证单位承担连带保证责任。
第十三条	本合同一式六份，各份具有同等效力。甲方存三份，乙方存二份，丙方存一份，本合同自签字之日起生效，有效期至项目结题后一年内。各方均应负合同的法律责任，不应受机构、人事变动的影响。
说明：本合同书中，凡是当事人约定无需填写的内容，应在空白处划（/）。	

2017A020208048

九、本合同签约各方

管理单位（甲方）：　广东省科学技术厅　（盖章）

单位地址：　连新路171号

法定代表人（或授权代表）：　黄宁生　（签章）

立项责任人：　刘世伟　（签章）

2017 -07- 26
年　月　日

承担单位（乙方）：　华南农业大学　（盖章）

二级部门：　华南农业大学林学与风景园林学院

单位地址：　五山路483号

法定代表人（或法人代理）：　陈晓阳　（签章）

联系人（项目主管）姓名：　石睿　（签章）

Email：　kjcgxk@scau.edu.cn

电话：　020-85285390　/　13430350923

开户单位名称：　华南农业大学

开户银行及帐号：　广东广州工行五山支行　3602002609000310520

2017年 7月 2日
年　月　日

乙方主管部门（丙方）：　华南农业大学　（盖章）

单位地址：　五山路483号

法定代表人（或法人代理）：　陈晓阳　（签章）

2017年 7月 2日
年　月　日

2017A020208048

任务书编号：2023E04J0211

广州市科技计划项目

任务书

项目名称：GABA茶加工技术示范推广

承担单位：华南农业大学

项目负责人：张旭

计划类别：创新环境计划

专题名称：2023年度农村科技特派员专题

方向名称：市内帮扶方向

组织单位：华南农业大学

起止时间：2023-04-01 至 2025-03-31

主管处室：农村和社会发展科技处

广州市科学技术局制

二〇二三年

广州市科技项目任务书2023-03-30

填写说明

1.任务书甲方为广州市科学技术局；乙方为项目承担单位；丙方为项目组织单位。

2.任务书基于项目申报书转换而成，请按照“广州科技大脑”提示在线填写核实，若存在不填写内容的栏目，请用“无”表示；任务书中的单位名称应为规范全称，并与单位公章一致。

3.乙方与合作单位的合作协议自动从项目申报书中读取，如需变化调整，须待任务书签订后，按要求及时办理重大变更。

4.乙方完成项目任务书在线填写，依次提交丙方和甲方审核确认后，按要求登录“穗好办”APP完成电子签章。不具备电子签章条件的单位，经与业务主管处室沟通对接后，可下载电子版项目任务书用A4纸双面打印装订签章；一式六份报甲方和丙方签章，其中甲方两份丙方两份，项目承担单位和项目负责人各一份。

5.涉密项目请在“广州科技大脑”下载项目任务书模板，按保密要求离线填写报送。

6.项目申报书是项目任务书填报的重要依据，未经甲方许可，乙方不得修改考核指标，调整主要研究内容。项目任务书将作为项目实施管理、验收结题和监督评估的重要依据。

7.项目任务书中的“备注”，包括重要的必须补充的内容。

8.“广州科技大脑”是项目管理过程中重要通知和文书的电子送达平台。为确保电子送达渠道畅通，乙方和项目负责人应及时更新维护“广州科技大脑”的单位和个人信息。

广州市科技项目任务书2023-03-30

一、项目基本信息

项目名称	GABA茶加工技术示范推广			
计划类别	创新环境计划		专题名称	2023年度农村科技特派员专题
方向名称	市内帮扶方向			
指南发布日期	2022-04-15			
项目开始时间	2023-04-01		项目结束时间	2025-03-31
资助方式	竞争性前资助		市财政科技经费(万元)	10
广东省技术领域	农业技术植物产品加工(农产品加工、保鲜等)；			
承担单位	华南农业大学			
服务对象	广州喆道茶业有限公司			
	姓名	办公电话	手机号码	电子邮箱
特派员	张旭	020-85280256	13539883664	zhangxu@scau.edu.cn
项目联系人	张旭	020-85280256	13539883664	zhangxu@scau.edu.cn
承担单位法人	刘雅红	020-85280001	13602706880	kjcgxk@scau.edu.cn
项目概述	茶叶中含有多种能起到改善抑郁状态的物质，如γ-氨基丁酸（GABA）、茶氨酸以及茶多酚类等。其中γ-氨基丁酸（GABA）早已被开发成药品，具有改善睡眠、调节血压、缓解脑功能衰退等功效。2009 年卫生部批准GABA为新资源食品，添加到茶饮料和果汁饮料等产品中，用于开发功能性食品。而茶叶自身就含有一定量的内源性GABA，在通过适当的加工方法能大幅提高其含量，使得茶叶有潜力成为不依赖于外源性GABA添加的功能性食品。本课题组在前期研究中已得到一条能在不影响茶叶自身风味的同时，大幅提高茶叶内在GABA含量的技术路线（广东省科技厅项目见附件），通过该方法制备得到的GABA茶在小鼠实验中能表现出显著的抗抑郁作用（中科院一区论文见附件）。本项目以茶叶为研究对象，利用干法厌氧处理等方法，提高GABA合成底物Glu的含量及关键酶GAD的活性，用以在茶叶内富集其自身的内源性GABA，再以其为原料制作成GABA红茶、白茶、乌龙茶等一系列产品，同时选取GABA、儿茶素以及生物碱等几个标志性物质建立HPLC分析方法，为产品的质量标准控制提供检测方法。针对企业进行优化并推广应用，已确保产品稳定可靠。			

广州市科技局任务书2023-03-30

二、承担单位基本情况

单位名称	华南农业大学	统一社会信用代码	124400004554165634
注册时间	1952-01-01	单位类型	高等院校
注册地址	广东省广州市天河区五山路483号		
办公地址	广东省广州市天河区五山路483号		
联系人	姓名	倪慧群	
	手机号码	15920301530	
	电子邮箱	kjcgxk@scau.edu.cn	
开户银行	广东广州工行五山支行		
开户户名	华南农业大学		
银行账号	3602002609000310520		

广州市科技项目任务书2023-03-30

三、服务对象基本情况

服务对象名称	广州喆道茶业有限公司	单位类型	农业高新技术企业
所属地区	广东省广州市番禺区洛浦街西三工业区开发南路1号A幢四楼201	统一社会信用代码	91440101MA5AT2ME35
服务法人对象	姓名	吴江华	
	联系电话	18922794125	
联系人	姓名	莫冲	
	办公电话	020-36164540	
	手机号码	13826098299	
	公司地址	广东省广州市番禺区洛浦街西三工业区开发南路1号A栋四楼201	
基本情况	广州喆道茶业有限公司自2017年开始，通过控股、参股等方式建立了自己的核心原料基地，到2020年，建立了安溪、福安、武夷山、都匀、眉山、贺州、凤庆、横县等八大核心产区。2018年在广州设立生产基地，产品包括红茶、绿茶、乌龙茶、调味茶、代用茶等，2020年扩建广州生产基地，建立从烘焙、精选、除杂、拼配等精制茶叶的全体系生产质量保障体系，年产能2000吨。主要从事精制茶加工;非酒精饮料、茶叶批发;固体饮料制造;茶饮料及其他饮料制造;茶叶作物及饮料作物批发等业务。现经营状况良好，客户超过500家餐饮连锁企业，20000家终端门店。		
技术需求	近年来，随着人们消费水平的提升和消费观念的升级以及对健康、时尚、新潮、个性的追求，同时伴随着传统（茶）文化的复兴，新式茶饮以其趣味性、时尚感、参与感、体验感、健康便捷、口感优良且多样等特征受到了广大年轻消费群体（以90后为主）的普遍欢迎，成为了互联网时代的新风口，受到了资本市场的追捧，并成为茶叶消费的新趋势和茶业经济新的增长点。新式茶饮是以优质原叶茶（以红茶、乌龙茶为主）为核心原料，辅以不同萃取方式提取的浓缩液，并加入新鲜牛奶、新鲜水果、果汁、进口奶油、天然动物奶油、软欧包等材料调制而成的饮料，具有代表性的如芝士红茶、奶盖茶、碳焙乌龙奶茶等。该公司在深耕新式茶饮市场的同时，急需寻求新的突破口，即功能性新式茶饮。如何以茶叶自身为原料，运用新的加工工艺，使得茶叶中的功能性成分含量大幅提升，进而起到显著的保健功效，在后续产品研发中可与多种已知的药食同源植物或中药材搭配，开发出品类众多的具有明确		

广州市科技项目任务书2023-03-30

	保健功效的无添加绿色功能性茶饮。这是该公司目前以及今后相当长一段时间内急需发展的方向。
前期合作基础	本申请人所在的专业为中药资源与开发，而团队中多位老师和学生均在茶学专业，常年致力于从植物特别是茶叶中提取有效成分，我们团队与该企业已有多年合作关系。 一、从质量控制方法入手指导企业改进提取工艺。由于茶叶原材料批次之间存在差异的特点，在公司向客户提供浓缩茶汤时，难以保证货品质量的稳定性。因此，本团队从茶叶挥发性成分和非挥发性成分两方面入手，为企业制定质量控制标准以及相应的监测方法。在非挥发性成分方面，我们以茶叶的总浸提率、黄酮含量、生物碱含量等为指标，通过建立常规的分析方法，购买旋转蒸发仪、分光光度计等常规仪器设备，在企业内部即可低成本建立质量控制实验室；而香气等挥发性成分的质量控制则由本团队通过我们已配备的气相色谱- 质谱联用仪进行分析。通过本团队实验室和企业自身的质检实验室协作，共同保障了该企业产品的稳定性。 二、常年派驻本科生和研究生到企业实习。企业与高校建立实习基地的关系，有利于双方的共同成长。一方面本团队的学生能通过深入企业，将书本和实验室所学到的知识落到实处，同时也能解决企业在生产过程中所面临的问题，成为高校与企业之间的桥梁；另一方面，企业在接收本团队的学生后，能将其安排在加工、质检等多个环节中，能指导企业自身员工进行仪器设备的操作，也能在一定程度上节约人力成本。

广州市科技项目申报系统 2023-03-30

四、特派员及团队成员信息

特派员	姓名	张旭	证件类型	身份证	证件号码	430681198405180335	性别	男
	出生日期	1984-05-18	民族	汉族	国籍	中国	学历	博士研究生
	学位	博士	学位授予国家（或地区）	中国	职务	教师	职称	中级
	所学专业	药学	手机号码	13539883664	办公电话	020-85280256	电子邮箱	zhangxu@scau.edu.cn

特派员团队成员（含特派员）

序号	姓名	证件类型	证件号码	年龄	职务	职称	学位	分工	所在单位	手机号码
1	张旭	身份证	430681198405180335	38	教师	中级	博士	项目负责人	华南农业大学	13539883664
2	肖遂	身份证	430103198402143022	38	讲师	中级	博士	协助指导质控检测方法的建立	华南农业大学	13802408977
3	黄亚辉	身份证	430121196911 18415X	52	研究员	正高级	博士	协助指导茶叶加工	华南农业大学	13501513191

广州市科技项目任务书 2023-03-30

五、特派员工作、服务经历

1.工作经历

序号	所在城市	起止时间	工作单位	行政职务	专业技术职务（职称）
1	湖南省长沙市芙蓉区湖南省农产品加工研究所	2009-07-01 至 2010-05-01	湖南省农科院农产品加工研究所	农产品开发和食品检验	无

特派员近3年技术领域和成果情况	本人常年致力于功能性食品和药食同源产品的研发，通过成分分析、功能验证和感官评价相结合的手段，开发新的加工工艺，进而得到新的产品；然后在分子、细胞以及动物的水平上，对产品的活性机制进行深入的探讨；研究成果用于申请发明专利、发表高水平学术论文以及申请各类科研项目。我们课题组与多家食品、保健品以及药品生产企业有着紧密的合作，利用这一套研发模式，帮助企业成功开发拥有自主知识产权的新产品，真正做到产学研一体化。 近三年中，本人在广东省科技厅获得的1项工艺研究与能力建设项目《高GABA-无咖啡因速溶茶的研发》顺利结题，在该课题中研发得到了一项新的加工技术并获得了一系列新产品，对GABA茶的成分以及体内抗抑郁功效研究已撰写论文发表在中科院一区期刊《Food & Function》.

2.服务经历

序号	所在城市	服务时间	技术服务内容
1	广东省云鼎柑普茶业有限公司	2018-03-01 至 2021-12-31	指导全生晒柑普茶的加工生产，协助企业制定行业标准；对柑普茶内在成分进行分析，通过体内外实验对其多种生物活性进行评价。

特派员开展科技推广服务工作基础简介	自2018年开始，本团队与云鼎柑普茶业有限公司一起对全生晒柑普茶的加工工艺、内在品质成分以及各项功能活性进行研究。本人实地指导并参与了柑普茶的制作到成分分析

广州市科技项目信息平台2023-03-30

	以及功能研究等工作。其中科研成果抗抑郁分析论文已在SCI二区期刊《Frontiers in Nutrition》发表，抗肿瘤活性分析报告和香气成分GC-MS分析报告已在国内核心期刊《现代食品科技》发表；以该科技推广内容为基础，申请到广东省自然基金1项；为推动产品生产的安全化、标准化，云鼎柑普公司建立了产品相关标准（包括：工艺标准、安全标准和生产标准），由广东省农业农村厅推荐，华南农业大学和云鼎柑普公司负责起草的《全生晒柑普茶生产技术规程》，已在广东省市场监督管理局审批立项。

广州市科技项目任务书2023-03-30

六、工作进度安排

1.需要实施的技术和内容

本项目选用茶鲜叶为原料，先通过厌氧处理提高GABA合成中关键酶谷氨酸脱羧酶（GAD）活性，同时增加该酶底物谷氨酸（Glu）的含量，两方面共同作用利用茶叶自身代谢提高内在成分GABA的含量，经优化后的方法不影响其余内含物的含量和茶叶本身特有的风味；再将高GABA毛叶茶制作成不同类型的茶制品，如红茶、白茶、乌龙茶等；之后用水对茶进行浸提，确定合适的提取溶剂、温度和时间后，对浸膏的水浸出率、茶多酚总量、总游离氨基酸含量、生物碱含量等进行常规成分分析，再选取GABA、儿茶素单体以及生物碱建立HPLC质量控制分析方法，利用多种检测手段保证产品的稳定性，最终研发得到一批风味不同的GABA茶产品。

本项目将根据广州喆道茶业有限公司的实际情况，包括场地、设备等，对我们的技术路线进行优化后，提出一条适合于该企业大规模生产的技术路线，并提供相应的质量控制方法，在将其向企业推广后，开发得到一系列GABA茶产品。

2.项目实施进度安排

序号	起止时间	主要工作内容
1	2023-04-01 至 2023-09-30	优化用于提升茶叶GABA含量的厌氧处理方法，得到高GABA含量的茶叶原料
2	2023-10-01 至 2024-03-31	优化茶叶加工工艺，制备得到一系列GABA茶产品
3	2024-04-01 至 2024-09-30	建立质量控制检测方法
4	2024-10-01 至 2025-03-31	将成套技术向企业进行推广应用

注：以半年为单位填报

广州市科技项目任务书2023-03-30

七、特派员预期成果

（一）预期代表性成果

指南指标
（一）根据服务对象的需求，示范推广农业新技术（或新品种、新工艺、新方法、新装备等），每个项目实施期内完成示范推广农业新技术（或新品种、新工艺、新方法、新装备等）不少于3个（项）。 （二）开展科技下乡，为服务对象开展多种形式技术服务，举办技术培训（或现场会、展示会等）活动，或开展农业科普宣传活动，向服务对象及相关群体制作并发放有关农业科技资料或视频，每个项目实施期内组织开展科技下乡活动不少于5场（次）。 （三）撰写项目实施工作总结报告，在媒体宣传报道典型经验做法、工作成效与亮点等情况。项目实施期内，每个项目至少在申报单位官方网站上报道相关内容不少于1篇。项目完成后，提交项目结题验收报告1份，附加盖服务对象公章的服务评价函。

（二）预期一般性成果

经济价值
至2020年底，全国新式茶饮市场规模将突破千亿元，2021年预计将突破1100亿元。而据中商产业研究院和欧睿预测，2022 年我国功能性食品市场规模将突破 6000 亿元。因此，开发具有功能性的新式茶饮具有广阔的市场潜力。

社会价值

广州市科技项目任务书2023-03-30

当下消费者对健康养生的需求旺盛，而养生群体也呈现出低龄化的趋势，而企业要做的就是满足年轻人的核心诉求。年轻消费者对于成分的选择更加谨慎，在购买产品之前会研究成分表，这些消费习惯都为我们开发的具有明确功能成分的GABA茶产品奠定了良好的和庞大的消费基础。

文化价值
新式茶饮正在迎来“大航海时代”，成为中式茶饮文化和中国传统茶文化走向世界的新载体，新式茶饮有利于提升我国茶叶全球影响力，更有助于文化价值观念和传统茶文化的输出。未来，功能性的新式茶饮文化将进一步向欧洲、北美、澳洲等地区输出，直接或间接地推动中国茶文化走向世界。

广州市科技项目任务书2023-03-30

十、备注

专题补充约定条款： *甲方对未履行勤勉尽责义务的相关责任主体，自作出处理结论之日起，依照法律法规规定或任务书约定实施惩戒5年，取消相关责任主体申报市科技计划项目、申领市科技计划项目经费的资格。*

广州市科技项目任务书2023-03-30

项目承担单位（乙方）及项目负责人承诺书

承诺书

本单位/本人作为广州市科技计划项目承担单位/项目负责人，将严格遵守广州市科技计划管理相关规定，严格履行自身责任，加强对项目组人员及合作单位的管理，在此郑重承诺：

（一）确保与本项目有关的全部材料真实、合法、有效，未侵犯其他方知识产权等权利，不存在多头申报、重复申报行为；

（二）严格遵守《广州市科技创新条例》《广州市科技计划项目管理办法》《广州市科技计划项目经费管理办法》《广州市科技计划科技报告管理办法》等相关规定，实施项目和经费管理；

（三）严格遵守国家、省、市关于科研诚信和科技伦理的有关法律、法规，相关政策以及各项规定，加强项目实施过程中的科研诚信及科技伦理管理，恪守科研道德准则。

如有违反，本单位/本人愿意接受相关部门做出的各项处理决定，包括但不限于终止项目、停拨经费、核减经费、追回经费，取消一定期限广州市科技计划项目申报资格，记入科研失信行为数据库，将不良行为向社会公开等。

项目承担单位：华南农业大学

日期：2023年03月22日

项目负责人：张旭

日期：2023年03月22日

广州市科技项目任务书2023-03-30

任务书签署

甲乙丙三方根据《广州市科技计划项目管理办法》《广州市科技计划项目经费管理办法》《广州市科技计划科技报告管理办法》等有关文件规定，以及有关法律、政策和管理要求，签署本任务书。

签订地点：广州市越秀区

广州市科学技术局（甲方）：广州市科学技术局
局项目经办人：夏万志　　联系电话：83124147
责任处室负责人：赵晓曦

2023年03月30日

项目承担单位（乙方）：华南农业大学
二级部门：华南农业大学林学与风景园林学院
项目负责人：张旭
项目经费汇入账号
账户名：华南农业大学　　账号：3602002609000310520
开户银行：广东广州工行五山支行
财务负责人：肖斐

2023年03月22日

组织单位（丙方）：华南农业大学
项目经办人：倪慧群

2023年03月22日

广州市科技项目任务书2023-03-30

广东省林业局文件

粤林财〔2022〕8号

广东省林业局关于下达2023年度省级财政事业发展性支出项目计划的通知

局机关有关处（室），局直属有关单位，有关项目单位：

根据《广东省林业局林业项目全过程绩效管理办法（试行）》《广东省林业局关于进一步规范项目绩效管理的通知》要求，为进一步夯实项目前期准备，提高项目成熟度，确保做到预算一经批复即可执行，现将2023年度省级财政事业发展性支出项目计划下达给你们，并将有关事项通知如下：

一、严格论证评估重大项目

立项总额超过500万元的项目，项目单位须按照《广东省财政厅关于印发<广东省省级财政绩效评估指南>的通知》（粤财绩

〔2020〕3 号）要求，组织编制绩效评估报告并于 11 月 25 日前报送归口处室。归口处室审核汇总后，连同自身使用的相关重大项目绩效评估报告，于 11 月 30 日前书面报规划财务处。

本次绩效评估报告是在下达项目计划后补充报送，但以后年度将在项目入库阶段报送，并将作为项目纳入规划财务处项目库和部门项目库的必要条件。

二、科学编制项目实施方案（作业设计、合同）

审批或备案的实施方案、作业设计以及签订的科研项目合同，是项目执行、检查、评价、验收的最重要依据。项单位目须按照《广东省林业局关于进一步规范项目绩效管理的通知》要求及参考格式，及时编制项目实施方案。其中，造林抚育类项目编制的作业设计、科研类项目签订的科研项目合同，视同项目实施方案。以上请于 11 月 25 日前报归口业务处室审批或备案，其中业务处室自身使用项目需报请局领导批准。（该项工作不用报规划财务处）。

三、规范制定项目资金支出计划和项目实施计划

请各项目单位认真填报《项目实施工作计划统计表》《项目资金支出计划统计表（时间）》《项目资金支出计划统计表（支出内容）》，并于**11 月 10 日前**报送归口处室，归口处室审核汇总并连同自身使用的项目计划情况，于**11 月 15 日前**书面报规划财务处。

根据省财政厅提高年初预算到位率的要求，本次项目相关计划自2023年1月起分月填报,其中资金支出计划每月填累计额度，原则上6月底不低于50%，10月底不低于95%，全年支付完毕。项目资金支出计划和项目实施计划将嵌入预算系统和“双监控”系统，并据此监测和通报各单位支出进度。

四、其他注意事项

(一)项目计划是年度省级财政事业发展性支出项目立项依据。

（二）本次同步将各二级项目的绩效目标一并下达，项目单位要做好绩效运行监控，确保年度绩效目标如期实现。

（三）涉及土地（房屋)、投审、消防、节能、环保等的项目，要及时开展相关工作，确保项目具备相关要素。

（四）涉及政府采购的项目，要尽快明确采购需求、采购方式、代理的选定，并及时开展政府采购意向公开等工作。

附件：1.2023年度自然资源事务专项资金—生态林业建设及

自然保护地体系建设（第一批）项目计划

2.2023年度海洋事业费及海洋赔偿款项目计划

3.2023年度省级以上公益林效益补偿省统筹项目计划

4. 各二级项目绩效目标

5. 项目实施工作计划统计表及资金支出计划统计表格式

6. 广东省林业局关于进一步规范项目绩效管理的通知

广东省林业局

2022 年 10 月 24 日

（联系人：梁海燕；电话：020-81825078）

公开方式：不公开

校稿：梁海燕

广东省林业局办公室　　2022 年 10 月 24 日印

附件1：

2023年度自然资源事务专项资金—生态林业建设及自然保护地体系建设（第一批）项目计划

50000

单位：万元

序号	项目单位	项目名称	立项总额	实施周期	2023年计划安排额度	政策任务	归口处室	备注
	一、生态林业建设　合计		**54490.48**		**44435.06**			
	140001-广东省妇女联合会　汇总		**200.00**		**200.00**			
1	140001-广东省妇女联合会	广东省巾帼油茶园	200.00	1年实施	200.00	森林资源培育	改革发展处	
	156003-华南农业大学　汇总		**2060.00**		**1540.00**			
2	156003-华南农业大学	自然保护地建设与乡村振兴的融合机制及实现模式	110.00	2年实施	90.00	林业生态保护建设	保护地处	该项目共110万元，其中2023年安排90万元；2024年计划安排20万元。
3	156003-华南农业大学	雷州市雷高镇小微湿地保护修复试点	80.00	1年实施	80.00	林业生态保护建设	湿地处	
4	156003-华南农业大学	半野化状态下林麝养殖	50.00	1年实施	50.00	林业生态保护建设	动植物处	
5	156003-华南农业大学	广东省中华穿山甲栖息地不同类型生境白蚁分布调查	50.00	1年实施	50.00	林业生态保护建设	动植物处	
[illegible]	[illegible]	[illegible]	[illegible]	[illegible]	[illegible]	[illegible]	[illegible]	
7	156003-华南农业大学	南昆山毛叶茶种质资源的收集保存	30.00	1年实施	30.00	林业生态保护建设	动植物处	
[illegible]	[illegible]	[illegible]	[illegible]	[illegible]	[illegible]	[illegible]	[illegible]	
9	156003-华南农业大学	全省林木种质资源调查（5个市）	750.00	3年实施	250.00	森林资源培育	林场种苗处	该项目共750万元，其中2022年已安排250万元；2023-2024年每年计划安排250万元。
10	156003-华南农业大学	基于高碳汇目标的造林树种筛选和林分结构研究	300.00	1年实施	300.00	森林资源培育	科技处	科研项目
11	156003-华南农业大学	紫薇属树种种质创新与产业化利用研究	150.00	1年实施	150.00	森林资源培育	科技处	科研项目
12	156003-华南农业大学	油茶新品种选育及高效开发利用关键技术研究	150.00	1年实施	150.00	森林资源培育	科技处	科研项目
13	156003-华南农业大学	广东丘陵山地“林-草-羊”生态循环种养模式构建与示范	150.00	1年实施	150.00	森林资源培育	科技处	科研项目
14	156003-华南农业大学	黄粱木抗寒抗旱四倍体品种创制	50.00	1年实施	50.00	森林资源培育	科技处	科研项目
15	156003-华南农业大学	石碌含笑和诗琳通木兰抗逆性育种与繁育	20.00	1年实施	20.00	森林资源培育	林场种苗处	
16	156003-华南农业大学	油茶良种选育与繁育	20.00	1年实施	20.00	森林资源培育	林场种苗处	
17	156003-华南农业大学	火炬松和木荷良种选育繁育	20.00	1年实施	20.00	森林资源培育	林场种苗处	

项目批准号	32170401
申请代码	C0209
归口管理部门	
依托单位代码	51064208A0499-0932



国家自然科学基金

资助项目计划书

（预算制项目）

资助类别：面上项目

亚类说明：

附注说明：

项目名称：青钱柳叶中潜在活性成分的诱导发掘及主要活性成分的结构衍化生成机制

直接费用：58万元　　执行年限：2022.01-2025.12

负 责 人：谭建文

通讯地址：广州市天河区五山路483号华南农业大学林学与风景园林学院

邮政编码：510642　　电　　话：13268017610

电子邮件：jwtan@scau.edu.cn

依托单位：华南农业大学

联 系 人：唐家林　　电　　话：020-85280070

填表日期：2021年10月21日

国家自然科学基金委员会制

Version：1.006.510

国家自然科学基金资助项目计划书填报说明

（预算制项目）

一、项目负责人收到《国家自然科学基金资助项目批准通知》（以下简称《批准通知》）后，请认真阅读本填报说明，参照国家自然科学基金相关项目管理办法和新修订的《国家自然科学基金资助项目资金管理办法》（以下简称《资金管理办法》，请查阅国家自然科学基金委员会官方网站首页“政策法规”栏目），按《批准通知》的要求认真填写和提交《国家自然科学基金资助项目计划书》（以下简称《计划书》）。

二、填写《计划书》时要科学严谨、实事求是、表述清晰、准确。《计划书》经国家自然科学基金委员会相关项目管理部门审核批准后，将作为项目研究计划执行、检查和验收的依据。

三、《计划书》各部分填写要求如下：

（一）简表：由系统自动生成。

（二）摘要及关键词：各类获资助项目都应当填写中、英文摘要及关键词。

（三）项目组主要成员：计划书中列出姓名的项目组主要成员由系统自动生成，与申请书原成员保持一致，不可随意调整。如果《批准通知》所附“项目评审意见及修改意见表”中“修改意见”栏目有调整项目组成员相关要求的，待项目开始执行后，按照项目成员变更程序另行办理。

（四）资金预算表：根据批准的项目资助额度，按规定调整项目预算，并按照《国家自然科学基金项目计划书预算表编制说明》填报资金预算表和预算说明书。

（五）正文：

1. 面上项目、地区科学基金项目：如果《批准通知》所附“项目评审意见及修改意见表”中“修改意见”栏目没有修改要求的，只需选择“研究内容和研究目标按照申请书执行”即可；如果《批准通知》中上述栏目明确要求调整研究期限或研究内容等的，须选择“根据研究方案修改意见更改”并填报相关修改内容。

2. 重点项目、重点国际（地区）合作研究项目、重大项目、国家重大科研仪器研制项目、原创探索计划项目：须选择“根据研究方案修改意见更改”，根据《批准通知》的要求填写研究（研制）内容，不得自行降低、更改研究目标（或仪器研制的技术性能与主要技术指标、验收技术指标等）或缩减研究（研制）内容。此外，还要突出以下几点：

（1）研究的难点和在实施过程中可能遇到的问题（或仪器研制风险），拟采用的研究（研制）方案和技术路线；

（2）项目主要参与者分工，合作研究单位（如有）之间的关系与分工，重大项目还需说明课题之间的关联；

（3）详细的年度研究（研制）计划。

3. 创新研究群体项目：须选择“根据研究方案修改意见更改”，按下列提纲撰写：

（1）研究方向；

（2）结合国内外研究现状，说明研究工作的学术思想和科学意义（限两个页面）；

（3）研究内容、研究方案及预期目标（限两个页面）；

（4）年度研究计划；

（5）研究队伍的组成情况。

4. 基础科学中心项目：须选择“根据研究方案修改意见更改”，根据《批准通知》的要求和现场考察专家组的意见和建议，进一步完善并细化研究计划，按下列提纲撰写：

（1）五年拟开展的研究工作（包括主要研究方向、关键科学问题与研究内容）；

（2）研究方案（包括骨干成员之间的分工及合作方式、学科交叉融合研究计划等）；

（3）年度研究计划；

（4）五年预期目标和可能取得的重大突破等；

（5）研究队伍的组成情况。

5. 对于其他类型项目，参照面上项目的方式进行选择和填写。

简表

项目负责人信息	姓　　名	谭建文	性 别	男	出生年月	1975年12月	民 族	土家族
	学　　位	博士			职称	教授		
	是否在站博士后	否		电子邮件		jwtan@scau.edu.cn		
	电　　话	13268017610		个人网页				
	工 作 单 位	华南农业大学						
	所 在 院 系 所	林学与风景园林学院						
依托单位信息	名　　称	华南农业大学					代码	51064208A0499
	联 系 人	唐家林		电子邮件		kycjhk@scau.edu.cn		
	电　　话	020-85280070		网站地址		http://kjc.scau.edu.cn/		
合作单位信息	单 位 名 称							
项目基本信息	项 目 名 称	青钱柳叶中潜在活性成分的诱导发掘及主要活性成分的结构衍化生成机制						
	资 助 类 别	面上项目			亚 类 说 明			
	附 注 说 明							
	申 请 代 码	C0209:植物化学			H3402:天然药物化学			
	基 地 类 别							
	执 行 年 限	2022.01-2025.12						
	直 接 费 用	58万元						

项目摘要

中文摘要：

青钱柳具有高的应用开发潜力，但常规的植物化学研究尚未能有效充分地揭示其功效活性物质基础。前期研究显示，防御信号JA-Ile的功能类似物CR和CGM能有效诱导青钱柳叶中部分成分发生结构转化而生成积累具相关抗糖尿病、抗MRSA和抑制肿瘤细胞生长等重要活性的潜在高价值化合物，但具体潜在高价值活性成分的结构与活性及主要活性成分自相关构成型成分衍化生成的机制过程等均有待揭示。本项目将利用CR和CGM的显著诱导效能，拟对青钱柳叶中的潜在活性成分实施系统的诱导发掘，并利用色谱层析和现代波谱等技术来分析青钱柳潜在活性成分的具体结构与活性，以及通过解析可诱导成分与构成型成分间于结构转化层面的动态相关性，来推进构建主要活性成分自相关构成型成分转化生成的路径机制过程。项目将可望能自青钱柳叶中发掘出系列具高应用潜质的活性成分，以及揭示主要活性成分的衍化生成路径过程机制，可为推进青钱柳更有效的开发利用提供科学依据。

Abstract：

Cyclocarya paliurus is a plant with high potential for application and development, but conventional phytochemical studies have yet not sufficiently revealed its functional and active substance basis. Our recent pre-study have shown that both CR and CGM, two structural and functional analogues of JA-Ile, can effectively induce transformation of some constitutive chemicals to generate and accumulate potential bioactive components in the leaves of C. paliurus, respectively, and among those induced components, potential high-value compounds with important biological activities, including obvious anti-diabetes, anti-MRSA and inhibiting the growth of cancer cells, are included. However, the structures and activities of those induced specific active components, as well as the detailed structural transformation processes of the main active components derived from related constitutive chemicals are all needing to be revealed. By using the significant induction potential of CR and CGM, this project will systematically explore the potential bioactive ingredients in C. paliurus leaves. The structures and bioactivities of those potential bioactive ingredients in C. paliurus leaves will also be detailedly analyzed by means of chromatographic and modern spectroscopic techniques, etc. Besides, the structural transformation mechanism of the main active components will further be constructed by promoting the analysis of the dynamic correlation between the inducible components and the constitutive components at the level of structural transformation. It is predictable that this project will discover a series of bioactive compounds with high application potential from the leaves of C. paliurus, and the structural transformation processes of some of those major induced bioactive components will also be revealed. It is highly possible that this project will achieve a valuable scientific basis for a more effective development and utilization of C. paliurus.

关键词(用分号分开)：药用植物；活性成分；化学成分；天然产物；次生代谢产物

Keywords(用分号分开)： medicinal plants; bioactive compounds; chemical constituents; natural products; secondary metabolites

项目组主要成员

编号	姓名	出生年月	性别	职称	学位	单位名称	电话	证件号码	项目分工	每年工作时间（月）
1	谭建文	1975.12	男	教授	博士	华南农业大学	13268017610	430104197512304634	项目负责人	7
2	肖遂	1984.02	女	助理研究员	博士	华南农业大学	020-85280256	430103198402143022	诱导分析、活性分析	5
3	张旭	1984.05	男	讲师	博士	华南农业大学	020-85280256	430681198405180335	诱导剂制备、化学转化分析	5
4	欧阳锦逵	1992.01	男	博士生	硕士	华南农业大学	020-85280256	445224199201011670	分离纯化、结构鉴定	8
5	刘少博	1996.06	男	博士生	学士	华南农业大学	020-85280256	410421199606241011	诱导分析、活性分析	8
6	钱涛	1994.09	男	硕士生	学士	华南农业大学	020-85280256	340823199409285310	提取分离、化学转化分析	9
7	娄涛	1999.01	女	硕士生	学士	华南农业大学	020-85280256	342225199901016245	植物培育、植物材料收集	9
8	洪鑫发	1993.09	男	硕士生	学士	华南农业大学	18820123471	340822199309291637	植物培养、提取分离	6

总人数	高级	中级	初级	博士后	博士生	硕士生
8	1	2			2	3

国家自然科学基金预算制项目预算表

项目批准号：32170401　　项目负责人：谭建文　　金额单位：万元

序号	科目名称	金额
1	一、基金资助项目直接费用合计	58.0000
2	1、 设备费	0.6000
3	其中：设备购置费	0.0000
4	2、 业务费	43.4000
5	3、 劳务费	14.0000
6	二、 其他来源资金	0.0000
7	三、 合计	58.0000

注：请按照项目研究实际需要合理填写各科目预算金额。

预算说明书

（请按照《国家自然科学基金项目计划书预算表编制说明》等的有关要求，按照政策相符性、目标相关性和经济合理性原则，实事求是编制项目预算。填报时，直接费用应按设备费、业务费、劳务费三个类别填报，每个类别结合科研任务按支出用途进行说明。填报时，对单价≥50万元的设备详细说明,对单价＜50万元的设备费用分类说明，**对合作研究单位资质及资金外拨情况、自筹资金进行必要说明。**）

本项目直接费用预算共58.00万元，依据的各项预算开支说明如下。

1、设备费：共0.6万元

高压和中压液相仪等现有仪器设备升级改造和维修维护：0.6万

2、业务费：共43.4万元

（1）材料费：共26.80万元

所需试剂、药品及耗材品购置费：20.80万（4×5.20万/年）

色谱材料费：4.80万（正相材料2.00万，反相材料2.80万）

植物材料费：1.20万（4×0.30万/年）

（2）测试化验加工费：共10.00万元

GC-MS、LC-MS测试费：1.60万（4×0.40万/年）

核磁和质谱（含高分辨）测试费：8.00万（4年×2.00万/年）

红外/旋光等测试费：0.40万（4×0.10万/年）

（3）燃料动力费：共0.00万元

本项目无此项预算

（4）差旅/会议/国际合作与交流费：共3.6万元

参加3次相关学术会议与交流：2.4万（共8人次平均每人次0.3万）

平时机动实验与调研差旅等：1.20万

（5）出版/文献/信息传播费/知识产权事务费：共4.00万元

发表论文版面费、印刷费：2.20万

专利申请费：1.20万

电脑网络费、资料查询费：4年×0.15万元/年＝0.60万

（6）其他支出：无

3、劳务费：共14.00万元

博士研究生劳务费：5.76万（2人4年共计48人月，平均0.12万/人月）

硕士研究生劳务费：6.24万（3人4年共计104人月，平均0.06万/人月）

临时聘用人员劳务费：1.60万（1人×10月×0.16万/人月）

专家咨询费：0.40万元（聘请咨询专家2人次×0.20万/人次）

报告正文

研究内容和研究目标按照申请书执行。

国家自然科学基金项目负责人、依托单位承诺书

国家自然科学基金项目负责人承诺书

本人郑重承诺：我接受国家自然科学基金的资助，严格遵守中共中央办公厅、国务院办公厅《关于进一步加强科研诚信建设的若干意见》《关于进一步弘扬科学家精神加强作风和学风建设的意见》等规定，及国家自然科学基金委员会关于资助项目管理、项目资金管理等各项规章，在《计划书》填写及项目执行过程中：

（一）按照《批准通知》《国家自然科学基金资助项目计划书填报说明》的要求填写《计划书》，未自行降低、更改目标任务或约定要求，或缩减研究（研制）内容；

（二）树立“红线”意识，严格履行科研合同义务，按照《计划书》负责实施本项目（批准号：32170401），切实保证研究工作时间，按时报送有关材料，及时报告重大情况变动，不违规将科研任务转包、分包他人，不以项目实施周期外或不相关成果充抵交差；

（三）遵守科研诚信、科研伦理规范和学术道德，认真开展研究工作，对资助项目发表的论著和取得的研究成果按规定进行标注，反对无实质学术贡献者“挂名”，不在成果署名、知识产权归属等方面侵占他人合法权益，并如实报告本人及团队成员发生的违背科研诚信要求的任何行为；

（四）尊重科研规律，弘扬科学家精神，严谨求实，追求卓越，反对浮夸浮躁、投机取巧，不人为夸大学术或技术价值，不传播未经科学验证的现象和观点；

（五）将项目资金全部用于与本项目研究工作相关的支出，并结合科研活动需要，科学合理安排项目资金支出进度。

如违背上述承诺，本人愿接受国家自然科学基金委员会和相关部门做出的各项处理决定。

项目负责人（签字）：

年　　月　　日

依托单位科研管理部门：	依托单位财务管理部门：
负责人（签章）： 年　　月　　日	负责人（签章）： 年　　月　　日

国家自然科学基金项目依托单位承诺书

我单位同意承担上述国家自然科学基金项目，将保证项目负责人及其研究队伍的稳定和研究项目实施所需的条件，严格遵守国家自然科学基金委员会有关资助项目管理、项目资金管理和科研诚信管理等各项规定，并督促实施。

依托单位（公章）

年　　月　　日

国家自然科学基金资助项目签批审核表

本栏目由自然科学基金委填写	科学处审查意见： 负责人（签章）： 年　　月　　日
	科学部审查意见： 负责人（签章）： 年　　月　　日

受理编号：c23140500000915

项目编号：2023A1515012805

文件编号：粤基金字〔2023〕2号

广东省基础与应用基础研究基金项目

任务书

2023A1515012805

项目名称： 银合欢豆荚和叶中潜在功能活性成分发掘研究

项目类别： 广东省自然科学基金-面上项目

项目起止时间： 2023-01-01　至　2025-12-31

管理单位（甲方）： 广东省基础与应用基础研究基金委员会

依托单位（乙方）： 华南农业大学

通讯地址： 广东省广州市天河区五山路483号

邮政编码： 510642　　**单位电话：** 020-85283435

项目负责人： 谭建文　　**联系电话：** 13268017610

（广东科技微信公众号）　　（查看任务书信息）　　（受理纸质材料二维码）

广东省基础与应用基础研究
基金委员会
二〇二〇年制

填写说明

一、项目任务书内容原则上要求与申报书相关内容保持一致，不得无故修改。

二、项目承担单位通过广东省科技业务管理阳光政务平台下载项目任务书，按要求完成签名盖章后扫描上传到广东省科技业务管理阳光政务平台。

三、签名盖章说明。请分别在单位工作分工及经费分配情况页、人员信息页、签约各方页等地方按要求签字或盖章，签章不合规或错漏将不予受理。其中，人员信息页要求所有参与人员本人亲笔签名，代签或印章无效，漏签将不予受理。

四、本任务书自签字并加盖公章之日起生效，各方均应负本任务书的法律责任，不应受机构、人事变动影响。

五、根据《广东省科学技术厅广东省则政厅关于深入推进省基础与应严础研究基金项目经费使用“负面清单+包干制”改革试点工作的通知》（粤科规范字[2022]2号），2022年度及以后立项资助的全部省基金项目（包括省自然科学基金、省市联合基金、省企联合基金项自等）均适用“负面清单+包干制”，项目提交申请书和任务书时无需编制费用明细科目预算。

2023A1515012015

一、主要研究内容和要达到的目标

1. 研究内容

（1）银合欢豆荚醇提取物中潜在功能活性成分的系统分离纯化和结构鉴定

收集相应银合欢植物豆荚材料采用乙醇进行功能成分提取获得相应醇提取物，进而采用前期已建立的萃取分部过程步骤，具体分步萃取获得对应银合欢豆荚提取物的活性部位，继而针对所获活性部位具体分离纯化其中的潜在主要功能活性成分，并就分离所获各单体成分进行基于现代波谱技术的结构解析与鉴定。包括：

a. 所获银合欢豆荚材料醇提取物活性部位中潜在主要功能活性成分的系统分离纯化；

b. 自银合欢豆荚相应醇提取物活性部位系统分离所获具体单体成分的化学结构分析；

（2）银合欢受CGM诱导的叶中潜在主要功能活性成分富集分离纯化和结构鉴定

实施对所选银合欢叶对应的CGM诱导实验，收集获得对应受诱导的银合欢叶样品材料并富集提取和萃取，获得潜在活性部位，进而在受诱导前后叶样品液相对比分析图谱的指导下，进一步自受诱导银合欢叶的萃取活性部位分离纯化其中的潜在主要功能活性化合物（即受诱导成分），并就各具体单体成分进行基于现代波谱技术的结构分析鉴定。包括：

a. 银合欢受CGM诱导叶的材料收集以及相应活性部位的萃取分部获取；

b. 银合欢受CGM诱导叶相应提取物中潜在功能活性成分的系统分离纯化；

c. 自银合欢受CGM诱导叶提取物中分离所获具体单体成分的结构分析鉴定；

（3）自银合欢豆荚和受诱导叶中分离鉴定的各具体单体成分相关重要生物活性的分析评测

对自银合欢豆荚和受诱导叶提取物的相应活性部位分离所获的各具体单体成分开展抗菌、抑制α-糖苷酶和抑制肿瘤细胞等重要生物活性的分析评测，以明确具体成分在抗菌、抗糖尿病和抗肿瘤等方面潜在重要的价值用途。包括：

a. 对分离鉴定的各单体成分进行抗多种人体病原菌的生物活性分析评测分析；

b. 对分离鉴定的各单体成分进行抑制α-糖苷酶和DPP-IV酶的生物活性测试分析，揭示抗糖尿病相关潜在活性化合物；

c. 对分离鉴定的各单体成分进行针对SF-286和K562等肿瘤细胞株的细胞毒活性测试分析，揭示抗肿瘤潜质活性化合物；

（4）基于成分系统分离鉴定和重要生物活性评测的银合欢综合开发利用价值的再评测分析

即结合本项目的新研究进展结果，对银合欢综合开发利用的潜质价值进行新基础的综合分析评价。

2. 研究目标

实现对银合欢豆荚和受CGM诱导叶中潜在主要活性成分的分离纯化和结构鉴定，发掘出其中具新结构和在相关抗菌、抗糖尿病和抗肿瘤等方面具高应用潜质的功能活性化合物，为推进银合欢更具有效性的综合开发利用提供基础和科学依据。

2023A1515012807

二、项目预期获得的研究成果及形式

<table>
<tr><td rowspan="3">论文及专著情况</td><td colspan="2">国家统计源刊物以上刊物发表论文（篇）</td><td colspan="2">3</td><td colspan="2">科技报告（篇）</td><td colspan="2">1</td></tr>
<tr><td colspan="2">其中被SCI/EI/ISTP收录论文数（篇）</td><td colspan="2">2</td><td colspan="2">培养人才（人）</td><td colspan="2">2</td></tr>
<tr><td colspan="2">专著（册）</td><td colspan="2"></td><td colspan="2">引进人才（人）</td><td colspan="2"></td></tr>
<tr><td rowspan="3">专利情况(项)</td><td colspan="2">发明专利</td><td colspan="2">实用新型专利</td><td colspan="2">外观设计专利</td><td colspan="2">国外专利</td></tr>
<tr><td>申请</td><td>授权</td><td>申请</td><td>授权</td><td>申请</td><td>授权</td><td>申请</td><td>授权</td></tr>
<tr><td>2</td><td>1</td><td></td><td></td><td></td><td></td><td></td><td></td></tr>
</table>

2023A1515012805

三、项目进度和阶段目标

（一）项目起止时间： 2023-01-01 至 2025-12-31		
（二）项目实施进度及阶段主要目标:		
开始日期	结束日期	主要工作内容
2023-01-01	2023-12-31	实施并完成对银合欢豆荚提取物中潜在主要功能活性成分系统的分离纯化与结构分析鉴定工作；并针对分离自银合欢豆荚的具体单体成分完成其针对糖苷酶和DPP-IV酶的活性分析；启动并推进银合欢受诱导剂诱导叶组织材料的收集富集工作。
2024-01-01	2024-12-31	对分离自银合欢豆荚的各具体单体成分推进完成其相关抗人体病原菌和抑制肿瘤细胞生长等重要生物活性的分析评测；另在完成银合欢受CGM诱导叶组织材料收集富集工作的基础上，推进完成对银合欢受诱导叶组织材料所含潜在活性成分的总提取和对大部分潜在主要功能活性成分的分离纯化与结构鉴定。完成发表SCI论文1-2篇，申请发明专利1件。
2025-01-01	2025-12-31	完成对银合欢受诱导剂诱导叶提取物中剩余部分潜在主要功能活性成分的分离纯化与结构鉴定；完成对分离自银合欢受诱导叶的各具体单体成分于抗人体病原菌、相关抗糖尿病以及相关抗癌等所设定重要功能活性的分析评测，进而对银合欢综合开发利用潜质价值进行新的综合分析评价。完成发表SCI论文1-2篇，申请专利1件。进行课题的总结，完成结题报告。

2023A1515012877

四、项目总经费及省基金委经费预算

1.省基金委经费下达总额： （大写）壹拾万圆整；（小写 ）10万元；					
2.省基金委经费年度下达计划：					
年度	2023 年	年	年	年	年
经费(万元)	10.00				

2023A1515012805

五、人员信息

项目负责人

姓名	证件号码	年龄	性别	职称	学历	在项目中承担的任务	所在单位	签名
谭建文	430104197512304634	48	男	教授	博士研究生	项目负责人	华南农业大学	谭建文

项目组主要成员

姓名	证件号码	年龄	性别	职称	学历	在项目中承担的任务	所在单位	签名
张旭	430681198405180335	39	男	讲师	博士研究生	分离鉴定、活性分析	华南农业大学	张旭
刘少博	410421199606241011	27	男	未取得	博士研究生	分离鉴定、诱导分析	华南农业大学	刘少博
娄涛	342225199901016245	24	女	未取得	硕士研究生	植物培育、活性分析	华南农业大学	娄涛
张善炫	440981199308133257	30	男	未取得	硕士研究生	植物培育、诱导分析	华南农业大学	张善炫
刘梦飞	360732200107220044	22	女	未取得	硕士研究生	植物培育、提取分离	华南农业大学	刘梦飞

2023A1515011005

六、工作分工及财政经费分配

承担/参与单位名称（盖章）	工作分工	省级财政科技资金分配（万元）
华南农业大学	全面负责本项目的各项工作。	10.00
	合计	10.00

2023A1515012805

七、任务书条款

第一条 甲方与乙方根据《中华人民共和国民法典》及国家有关法规和规定，按照《广东省科学技术厅关于广东省基础与应用基础研究基金（省自然科学基金、联合基金等）项目管理的实施细则（试行）》《广东省省级科技计划项目验收结题工作规程（试行）》等规定，为顺利完成（2023）年银合欢豆荚和叶中潜在功能活性成分发掘研究专项项目（文件编号：粤基金字〔2023〕2号 ）经协商一致，特订立本任务书，作为甲乙双方在项目实施管理过程中共同遵守的依据。

第二条 甲方的权利义务：

1.按任务书规定进行经费核拨的有关工作协调。

2.根据甲方需要，在不影响乙方工作的前提下，定期或不定期对乙方项目的实施情况和经费使用情况进行检查或抽查。

3.根据《广东省科研诚信管理办法(试行)》等规定对乙方进行科技计划信用管理。

第三条 乙方的权利义务：

1.确保落实自筹经费及有关保障条件。

2.按任务书规定，对甲方核拨的经费实行专款专用，单独列账，并随时配合甲方进行监督检查。

3.经费使用按照广东省级财政科研项目经费使用等有关规定进行管理。

4.项目依托单位应制定经费使用“负面清单+包干制”内部管理制度并报甲方备案。

5.使用财政资金采购设备、原材料等，按照《广东省实施〈中华人民共和国招标投标法〉办法》有关规定，符合招标条件的须进行招标。

6.项目任务书任务完成后，或任务书规定的任务、指标及经费投入等提前完成的，乙方可提出验收结题申请，并按甲方要求做好项目验收结题工作。

7.若项目发生需要终止结题的情况，乙方须提出终止结题申请，并按甲方要求做好项目终止结题工作。

8.在每年规定时间内向甲方如实提交上年度工作情况报告，报告内容包含上年度项目进展情况、经费决算和取得的成果等。

9.按照国家和省有关规定，提交科技报告及其他材料。

10.利用甲方的经费获得的研究成果，项目负责人和参与者应当注明获得“广东省基础与应用基础研究基金（英文：Guangdong Basic and Applied Basic Research Foundation）（项目编号）”资助或作有关说明。

11.乙方要恪守科学道德准则，遵守科研活动规范，践行科研诚信要求，不得抄袭、剽窃他人科研成果或者伪造、篡改研究数据、研究结论；不得购买、代写、代投论文，虚构同行评议专家及评议意见；不得违反论文署名规范，擅自标注或虚假标注获得科技计划（专项、基金等）等资助；不得弄虚作假，骗取科技计划（专项、基金等）项目、科研经费以及奖励、荣誉等；不得有其他违背科研诚信要求的行为。

12.确保本项目开展的研究工作符合我国科技伦理管理相关规定。

第四条 在履行本任务书的过程中，如出现广东省相关政策法规重大改变等不可抗力情况，甲方有权对所核拨经费的数量和时间进行相应调整。

2023A1515012805

第五条 在履行本任务书的过程中，当事人一方发现可能导致项目整体或部分失败的情形时，应及时通知另一方，并采取适当措施减少损失，没有及时通知并采取适当措施，致使损失扩大的，应当就扩大的损失承担责任。

第六条 本项目技术成果的归属、转让和实施技术成果所产生的经济利益的分享，除双方另有约定外，按国家和广东省有关法规执行。

第七条 根据项目具体情况，经双方另行协商订立的附加条款，作为本任务书正式内容的一部分，与本任务书具有同等效力。

第八条 本任务书一式三份，各份具有同等效力。甲、乙方及项目负责人各执一份，三方签字、盖章后即生效，有效期至项目结题后一年内。各方均应负任务书的法律责任，不应受机构、人事变动的影响。

第九条 乙方必须接受甲方聘请的本项目任务书监理单位的监督和管理。监理单位按照甲方赋予的权利对本项目任务书的履行进行审核、进度调查，对项目任务书变更、经费使用情况进行监督管理及组织项目验收。

说明：1.本任务书中，凡是当事人约定无需填写的内容，应在空白处划（/）。

2.委托代理人签订本任务书的，应出具合法、有效的委托书。

2023A1515012805

八、本任务书签约各方

管理单位（甲方）：　　广东省基础与应用基础研究基金委员会　（盖章）

法定代表人（或法人代理）：　曾路　（签章）

2023 年　02 月　14 日

依托单位（乙方）：　华南农业大学　（盖章）

法定代表人（或法人代理）：　刘雅红　（签章）

联系人（项目主管）姓名：　倪慧群　（签章）

Email：　kjcgxk@scau.edu.cn

电话：　020-85283435　/　15920301530

开户单位名称：　华南农业大学

开户银行名称：　广东广州工行五山支行

开户银行帐号：　3602002609000310520

2023 年 3 月 6 日

联系人（项目负责人）姓名：　谭建文　（签名）

Email：　jwtan@scau.edu.cn

电话：　13268017610

2023 年 2 月 20 日

20231515012805

受理编号：c21140500001405

项目编号：2021A1515012153

文件编号：粤基金字〔2021〕4号

广东省基础与应用基础研究基金项目

合同书

2021A1515012153

项目名称：全生晒柑普茶品质特征的形成及其抗抑郁活性物质与作用机理研究

项目类别：广东省自然科学基金-面上项目

项目起止时间：2021-01-01 至 2023-12-31

管理单位（甲方）：广东省基础与应用基础研究基金委员会

依托单位（乙方）：华南农业大学

通讯地址：广东省广州市天河区五山路483号

邮政编码：510642 单位电话：020-85283435

项目负责人：肖遂 联系电话：13802408977

（广东科技微信公众号） （查看合同书信息） （受理纸质材料二维码）

广东省基础与应用基础研究
基金委员会
二〇二〇年制

填写说明

一、项目合同书/任务书内容原则上要求与申报书相关内容保持一致，不得无故修改。

二、项目承担单位通过广东省科技业务管理阳光政务平台下载项目合同书/任务书，按要求完成签名盖章后提交至省科技厅受理窗口。

三、签名盖章说明。请分别在单位工作分工及经费分配情况页、人员信息页、签约各方页等地方按要求签字或盖章，签章不合规或错漏将不予受理。其中，人员信息页要求所有参与人员本人亲笔签名，代签或印章无效，漏签将不予受理。

四、本合同书/任务书自签字并加盖公章之日起生效，各方均应负本任务书的法律责任，不应受机构、人事变动影响。

2021A1515012153

一、主要研究内容和要达到的目标

主要研究内容：

1、全生晒柑普茶日晒过程特征成分的变化研究

a 香气成分解析：采用HS-SPME-GC-MS技术解析全生晒柑普茶香气成分的来源以及它们在15天日晒过程中的形成变化规律；

b 非挥发性成分解析：采用UPLC-Q-TOF-MS技术解析全生晒柑普茶非挥发性成分的来源以及它们在15天日晒过程中的形成变化规律；

c 感官评价：对全生晒柑普茶的香气品质和风味品质进行感官评价，结合化合物分析结果阐明全生晒柑普茶特有的香气成分和风味物质，挖掘由它们带来的品质特点。

2、全生晒柑普茶抗抑郁活性物质的辨识与验证

a 动物模型评价抗抑郁效果：通过小鼠强迫游泳实验和小鼠悬尾实验建立两个抗抑郁小鼠行为模型，对不同日晒时间和不同剂量的柑普茶提取物的抗抑郁效果进行评价。

b “谱效关系”辨识活性物质：采用UPLC-Q-TOF-MS指纹图谱分析日晒过程中各柑普茶样品的化学成分差异，根据小鼠抗抑郁行为模型分析日晒过程中各柑普茶样品的药效差异；结合“谱”、“效”信息，通过相关分析法、多元回归分析、热图分析、主成分分析等手段辨识全生晒柑普茶抗抑郁活性物质；

c 活性物质验证：分离纯化全生晒柑普茶抗抑郁活性物质，通过小鼠抗抑郁行为模型验证它们的药效。

3、全生晒柑普茶活性物质抗抑郁作用机理研究

a 血清代谢轮廓分析：分别取对照组、模型组、给药组（最佳药效剂量）的小鼠眼眶静脉血，采用UPLC-Q-TOF-MS技术分析小鼠血清内源性代谢物的组间差异；

b 海马组织代谢轮廓分析：分别取对照组、模型组、给药组（最佳药效剂量）的小鼠前额叶处两侧的海马组织，采用UPLC-Q-TOF-MS技术分析小鼠海马组织内源性代谢物的组间差异；

c 潜在生物标记物和相关信号通路的鉴定：对上述代谢物检测所得数据通过PCA和OPLS-DA分析，获得VIP值和S-plot图，发现能够代表组间差异的潜在的标记物，根据HMDB、KEGG、METLIN、Metabo Analyst 等数据库对这些潜在的生物标记物进行筛选辨认，找到与全生晒柑普茶活性物质抗抑郁相关的信号通路。

研究目标：

1、 揭示全生晒柑普茶日晒过程香气成分和非挥发性成分的来源及形成变化规律，阐明全生晒柑普茶感官品质的物质基础，挖掘其特征香气和风味物质；

2、 通过“谱效关系”阐明全生晒柑普茶与抗抑郁相关的活性物质；

3、采用“非靶标代谢组学”技术探索全生晒柑普茶活性物质在小鼠体内通过影响哪些代谢标志物的合成积累以及通过哪些代谢途径发挥抗抑郁的功效。

2021A1515012153

二、项目预期获得的研究成果及形式

论文及专著情况	国家统计源刊物以上刊物发表论文（篇）		1		科技报告（篇）		1	
	其中被SCI/EI/ISTP收录论文数（篇）		1		培养人才（人）			
	专著（册）				引进人才（人）			
专利情况(项)	发明专利		实用新型专利		外观设计专利		国外专利	
	申请	授权	申请	授权	申请	授权	申请	授权

2021A1515012153

三、项目进度和阶段目标

（一）项目起止时间： 2021-01-01 至 2023-12-31		
（二）项目实施进度及阶段主要目标:		
开始日期	结束日期	主要工作内容
2021-01-01	2021-12-31	完成全生晒柑普茶特征成分的形成变化规律研究
2022-01-01	2022-12-31	完成全生晒柑普茶抗抑郁活性物质的辨识和药效评价研究
2023-01-01	2023-12-31	完成小鼠血清样本和海马组织的内源性代谢物研究，初步揭示全生晒柑普茶活性物质的抗抑郁作用机理

2021A1515012153

四、项目总经费及省基金委经费预算

1.省基金委经费下达总额： （大写）壹拾万圆整；（小写 ）10万元；

2.省基金委经费年度下达计划：

年度	2021 年	年	年	年	年
经费(万元)	10.00				

3.总经费及省基金委经费开支预算计划：

经费筹集情况： （单位：万元）

省基金委经费	自筹资金				合计
	自有资金	贷款	地方政府投入	其它	
10.00	0	0	0	0	10.00

政府部门、境外资金及其他资金投入情况说明：	

与本项目相关的其他经费来源	（单位：万元）
其他计划资助经费：	0
单位配套经费：	0
其他经费资助：	0
其他经费来源合计：	0.00

2021A1515012153

五、人员信息

项目负责人

姓名	证件号码	年龄	性别	职称	学历	在项目中承担的任务	所在单位	签名
肖遂	430103198402143022	37	女	助理研究员	博士研究生	项目负责人	华南农业大学	肖遂

项目组主要成员

姓名	证件号码	年龄	性别	职称	学历	在项目中承担的任务	所在单位	签名
张旭	430681198405180335	37	男	讲师	博士研究生	抗抑郁动物实验及作用机制研究	华南农业大学	张旭
曾贞	430111197009170484	51	女	副研究员	硕士研究生	柑普茶活性成分研究	华南农业大学	曾贞
周梦珍	441623199511131020	26	女	未取得	本科	柑普茶化学成分研究	华南农业大学	周梦珍

六、工作分工及经费分配

承担/参与单位名称（盖章）	工作分工	总经费分摊（万元）	省基金委经费分配（万元）
华南农业大学	1、完成项目申报书内所有研究内容，包括：揭示全生晒柑普茶日晒过程香气成分和非挥发性成分的来源及形成变化规律，阐明全生晒柑普茶感官品质的物质基础，挖掘其特征香气和风味物质； 通过“谱效关系”阐明全生晒柑普茶与抗抑郁相关的活性物质；采用“非靶标代谢组学”技术探索全生晒柑普茶活性物质在小鼠体内通过影响哪些代谢标志物的合成积累以及通过哪些代谢途径发挥抗抑郁的功效。 2、撰写科技报告和发表相关论文 3、完成项目经费决算	10.00	10.00
	合计	10.00	10.00

七、合同条款

第一条 甲方与乙方根据《中华人民共和国合同法》及国家有关法规和规定，为顺利完成（2021）年全生晒柑普茶品质特征的形成及其抗抑郁活性物质与作用机理研究 专项项目（文件编号：粤基金字〔2021〕4号）经协商一致，特订立本合同，作为甲乙双方在项目实施管理过程中共同遵守的依据。

第二条 甲方的权利义务：

1.按合同书规定进行经费核拨的有关工作协调。

2.根据甲方需要，在不影响乙方工作的前提下，定期或不定期对乙方项目的实施情况和经费使用情况进行检查或抽查。

3.根据《广东省科技计划项目信用管理办法(试行)》对乙方进行科技计划信用管理。

第三条 乙方的权利义务：

1.确保落实自筹经费及有关保障条件。

2.乙方是项目资金管理的责任主体，应当建立健全科研项目资金管理制度，严格按照省科技经费使用范围和有关规定管好用好财政资金；应当按合同书规定，对甲方核拨的经费实行专款专用，单独列账，并随时配合甲方进行监督检查。

3.实施“包干制”的面上项目及青年基金项目，依托单位应参照国家杰出青年科学基金试点项目经费使用“包干制”要求，制定经费使用“包干制”内部管理规定。项目经费支出应实际用于研发活动相关支出，使用范围限于设备费、材料费、测试化验加工费、燃料动力费、差旅/会议/国际合作与交流费、出版/文献/信息传播/知识产权事务费、劳务费、专家咨询费、依托单位管理费用、绩效支出以及其他合理支出。依托单位管理费用由依托单位根据实际管理支出情况与项目负责人协商确定。绩效支出由项目负责人根据实际科研需要和相关薪酬标准自主确定，依托单位按照现行工资制度进行管理。其余用途经费无额度限制，由项目负责人根据实际需要自主决定使用。项目验收时应提交经费决算表。

4.项目负责人是项目资金使用的直接责任人，对资金使用的合规性、合理性、真实性和相关性承担法律责任。

5.使用财政资金采购设备、原材料等，按照《广东省实施〈中华人民共和国招标投标法〉办法》有关规定，符合招标条件的须进行招标。

6.项目合同任务完成后，或合同书规定的任务、指标及经费投入等提前完成的，乙方可按照《广东省省级科技计划项目结题管理实施细则（试行）》提出验收结题申请，并按甲方要求做好项目验收结题工作。

7.若项目发生需要终止结题的情况，乙方须按照《广东省省级科技计划项目结题管理的实施细则（试行）》提出终止结题申请，并按甲方要求做好项目终止结题工作。

8.在每年规定时间内向甲方如实提交上年度工作情况报告，报告内容包含上年度项目进展情况、经费决算和取得的成果等。

9.按照国家和省有关规定，提交科技报告及其他材料。

10.利用甲方的经费获得的研究成果，项目负责人和参与者应当注明获得“广东省基础与应用基础研究基金（英文：Guangdong Basic and Applied Basic Research Foundation）（项目编号）”资助或作有关说明。

11.乙方要恪守科学道德准则，遵守科研活动规范，践行科研诚信要求，不得抄袭、剽窃他人科研成果或者伪造、篡改研究数据、研究结论；不得购买、代写、代投论文，虚构同行评议专家及评议意见；不得违反论文署名规范，擅自标注或虚假标注获得科技计划（专项、基金等）等资助；不得弄虚作假，骗取科技计划（专项、基金等）项目、科研经费以及奖励、荣誉等；不得有其他违背科研诚信要求的行为。

12.确保本项目开展的研究工作符合我国科研伦理管理相关规定。

第四条 在履行本合同的过程中，如出现广东省相关政策法规重大改变等不可抗力情况，甲方有权对所核拨经费的数量和时间进行相应调整。

第五条 在履行本合同的过程中，当事人一方发现可能导致项目整体或部分失败的情形时，应及时通知另一方，并采取适当措施减少损失，没有及时通知并采取适当措施，致使损失扩大的，应当就扩大的损失承担责任。

第六条 本项目技术成果的归属、转让和实施技术成果所产生的经济利益的分享，除双方另有约定外，按国家和广东省有关法规执行。

第七条 根据项目具体情况，经双方另行协商订立的附加条款，作为本合同正式内容的一部分，与本合同具有同等效力。

第八条 本合同一式三份，各份具有同等效力。甲、乙方及项目负责人各执一份，三方签字、盖章后即生效，有效期至项目结题后一年内。各方均应负合同的法律责任，不应受机构、人事变动的影响。

第九条 乙方必须接受甲方聘请的本项目合同监理单位的监督和管理。监理单位按照甲方赋予的权利对本项目合同的履行进行审核、进度调查，对项目合同变更、经费使用情况进行监督管理及组织项目验收。

说明：1.本合同书中，凡是当事人约定无需填写的内容，应在空白处划（/）。

2.委托代理人签订本合同书的，应出具合法、有效的委托书。

2021A1515012153

八、本合同签约各方

管理单位（甲方）：　　广东省基础与应用基础研究基金委员会　（盖章）

法定代表人（或法人代理）：　曾路　（签章）

2021 年　03 月　25 日

依托单位（乙方）：　华南农业大学　（盖章）

法定代表人（或法人代理）：　刘雅红　（签章）

联系人（项目主管）姓名：　安沛（基金类基础科、实验室平台办、海外名师人事处）　（签章）

Email：　414484016@qq.com

电话：　020-85283435　/　13535577893

开户单位名称：　华南农业大学

开户银行名称：　广东广州工行五山支行

开户银行帐号：　3602002609000310520

2021年04月12日

年　月　日

联系人（项目负责人）姓名：　肖遂　（签名）

Email：　suixiao@outlook.com

电话：　13802408977

2021 年 4 月 9 日

SCAULIB202518653

检索证明

根据委托人提供的论文材料，委托人**华南农业大学 张旭** 15 篇论文收录情况如下表。

序号	论文名称	发表刊物及发表的年月卷期/页码等	作者排名	论文等级	作者文中单位	收录情况	影响因子	中科院大类分区
1	Short-term steaming during processing impacts the quality of Citri Reticulatae 'Chachi' peel	FOOD CHEMISTRY 出版年：2024 出版日期：JUL 30 卷期：447 页码：- 文献号：138964 文献类型：Article	共同通讯作者（排名最后）	T2 类	华南农业大学林学与风景园林学院	SCI	IF2-year=9.8 IF5-year=9.7 （2024）	农林科学 1 区 Top 期刊：是 （2025）
2	CKLF instigates a "cold" microenvironment to promote MYCN-mediated tumor aggressiveness	SCIENCE ADVANCES 出版年：2024 出版日期：MAR 15 卷期：10 11 页码：- 文献号：eadh9547 文献类型：Article	并列第一作者	T2 类	华南农业大学林学与风景园林学院	SCI	IF2-year=12.5 IF5-year=14.1 （2024）	综合性期刊 1 区 Top 期刊：是 （2025）
3	Differences in the components of Neolamarckia cadamba from different provenance and the drug resistance reversal activity of characteristic alkaloid	INDUSTRIAL CROPS AND PRODUCTS 出版年：2022 出版日期：OCT 15 卷期：186 页码：- 文献号：115145	共同通讯作者	T2 类	华南农业大学林学与风景园林学院	SCI	IF2-year=5.9 IF5-year=6.0 （2022）	农林科学 1 区 Top 期刊：是 （2022）

华南农业大学图书馆SCAULIB202518653 查用检索专用章

		文献类型：Article						
4	Design and synthesis of epigallocatechin (EGC) analogs selective to inhibit α-amylase over α-glucosidases via the incorporation of caffeine acid and its derivatives	BIOORGANIC CHEMISTRY 出版年：2022 出版日期：FEB 卷期：119 页码：- 文献号：105515 文献类型：Article	共同通讯作者	T2 类	华南农业大学 林学与风景园林学院	SCI	IF2-year=5.1 IF5-year=5.3 （2022）	化学 1区 Top 期刊：是 （2022）
5	Flavor Characteristics of Ganpu Tea Formed During the Sun-Drying Processing and Its Antidepressant-Like Effects	FRONTIERS IN NUTRITION 出版年：2021 出版日期：MAR 24 卷期：8 页码：- 文献号：647537 文献类型：Article	共同通讯作者（排名最后）	A 类	华南农业大学 林学与风景园林学院	SCI	IF2-year=6.59 IF5-year=6.873 （2021）	农林科学 2区 Top 期刊：否 （2021）
6	α-naphthoflavone-derived cytochrome P450 (CYP)1B1 degraders specific for sensitizing CYP1B1-mediated drug resistance to prostate cancer DU145: Structure activity relationship	BIOORGANIC CHEMISTRY 出版年：2021 出版日期：NOV 卷期：116 页码：- 文献号：105295 文献类型：Article	共同通讯作者	A 类	华南农业大学 林学与风景园林学院	SCI	IF2-year=5.307 IF5-year=5.321 （2021）	化学 2区 Top 期刊：是 （2021）

华南农业大学图书馆SCAULIB20251853
华南农业大学图书馆 学术信息检索专用章

7	Advance in Anti-tumor Mechanisms of Shikonin, Alkannin and their Derivatives	MINI-REVIEWS IN MEDICINAL CHEMISTRY 出版年：2018 卷期：18 2 页码：164-172 文献类型：Review	第一作者	B 类	华南农业大学林学与风景园林学院	SCI	IF2-year=2.842 IF5-year=2.952 （2018）	医学 3 区 Top 期刊：否 （2018）
8	A treasure reservoir of genetic resource of tea plant (Camellia sinensis) in Dayao Mountain	GENETIC RESOURCES AND CROP EVOLUTION 出版年：2018 出版日期：JAN 卷期：65 1 页码：217-227 文献类型：Article	共同通讯作者（排名最后）	B 类	华南农业大学林学与风景园林学院	SCI	IF2-year=1.296 IF5-year=1.423 （2018）	农林科学 3 区 Top 期刊：否 （2018）
9	Chemical compositions of Pu'er tea fermented by Eurotium Cristatum and their lipid-lowering activity	LWT-FOOD SCIENCE AND TECHNOLOGY 出版年：2018 出版日期：DEC 卷期：98 页码：204-211 文献类型：Article	共同通讯作者（排名最后）	A 类	华南农业大学林学与风景园林学院	SCI	IF2-year=3.714 IF5-year=4.0 （2018）	工程技术 2 区 Top 期刊：否 （2018）
10	Quality components and antidepressant-like effects of GABA green tea	FOOD & FUNCTION 出版年：2017 出版日期：SEP 1 卷期：8 9 页码：3311-3318 文献类型：Article	共同通讯作者（排名最后）	T2 类	华南农业大学林学与风景园林学院	SCI	IF2-year=3.289 IF5-year=3.685 （2017）	农林科学 1 区 Top 期刊：是 （2017）

华南农业大学图书馆SCAU[B]20251853
华南农业大学图书馆 信息检索专用章

11	STUDY ON THE ANTI-TUMOR ABILITY OF NIAOWANGZHONG GREEN TEA	JOURNAL OF FOOD BIOCHEMISTRY 出版年：2017 出版日期：FEB 卷期：41 1 页码：- 文献号：e12305 文献类型：Article	共同通讯作者（排名最后）	B 类	华南农业大学林学与风景园林学院	SCI	IF2-year=1.552 IF5-year=1.328 （2017）	生物 4 区 Top 期刊：否 （2017）
12	An Approach for Searching Bioactive Compounds from Traditional Chinese Plant Food and Herb Medicines by Investigating Spectrum-Effect Relationships	CURRENT PHARMACEUTICAL ANALYSIS 出版年：2017 卷期：13 5 页码：417-426 文献类型：Article	第一作者	B 类	华南农业大学林学与风景园林学院	SCI	IF2-year=0.859 IF5-year=0.756 （2017）	医学 4 区 Top 期刊：否 （2017）
13	柑普提取物对 HepG2 和 SGC-7901 肿瘤细胞系的抗增殖作用	现代食品科技 出版年：2020 卷期： 页码：- 文献号： 文献类型：	通讯作者	C 类	华南农业大学林学与风景园林学院	北大核心	无	无
14	茶学专业实践教育改革研究	福建茶叶 出版年：2016 卷期： 页码：- 文献号： 文献类型：	第一作者	C 类	华南农业大学林学与风景园林学院	CNKI	无	无

华南农业大学图书馆SCAULIB20251206153
华南农业大学图书馆 版权所有 仅供借阅专用章

15	中药资源综合利用与产品开发课程特色初探	教育教学论坛 出版年：2020 卷期： 页码：- 文献号： 文献类型：	通讯作者	普刊类	华南农业大学林学与风景园林学院	CNKI	无	无

说明：论文等级和中科院大类分区按《华南农业大学学术论文评价方案（试行）》划分。

报告免责声明:如未盖章,报告无效

检索员：刘汉忠

华南农业大学图书馆

2025-07-09

华南农业大学图书馆SCAULIB20251865

BENTHAM SCIENCE



Search here... 0 Search Articles



ISSN (Print): 1389-5575
ISSN (Online): 1875-5607

Download PDF Flyer

Mini-Reviews in Medicinal Chemistry

All Open Access articles of this journal are also available on ScienceDirect.

Impact Factor: 3.3

Indexed in: Scopus, SCI Expanded, MEDLINE/PubMed... *View all*

Volume 25 , Issues 22, 2025

Active Special Issues | Submit Now | Purchase Full Issue

Institutional Members

Limited-Time Complimentary Open Access Offer

Get free Open Access by submitting your article on or before August 31st, 2025. **This offer applies to general articles only.**



Volume 18, Issue 2 , 2018

Biography

Meet Our Editorial Board Member

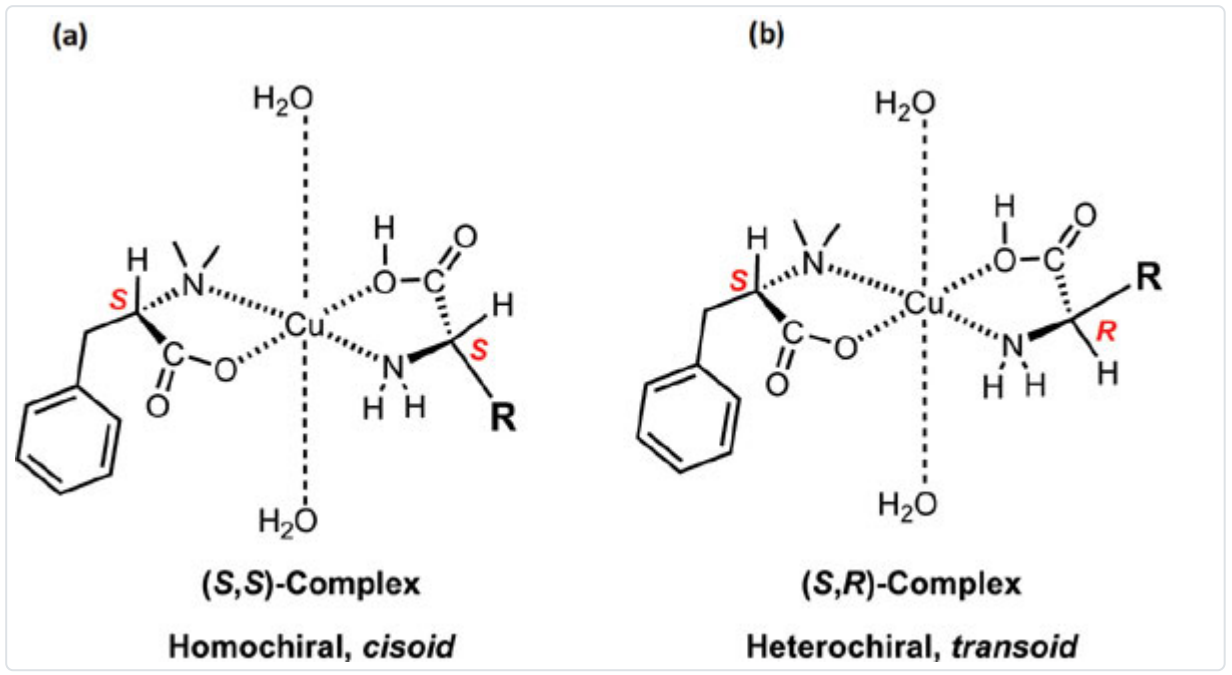
Pp: 87-87
Author(s): Gil Bar-Sela
DOI: 10.2174/1389557518021801081654l1

Download PDF File | Cite

Review Article

Elucidation of the Chromatographic Enantiomer Elution Order Through Computational Studies

Pp: 88-97
Author(s): Roccaldo Sardella, Federica Ianni, Antonio Macchiarulo, Lucia Pucciarini, Andrea Carotti* and Benedetto Natalini
DOI: 10.2174/1389557516666161018143629

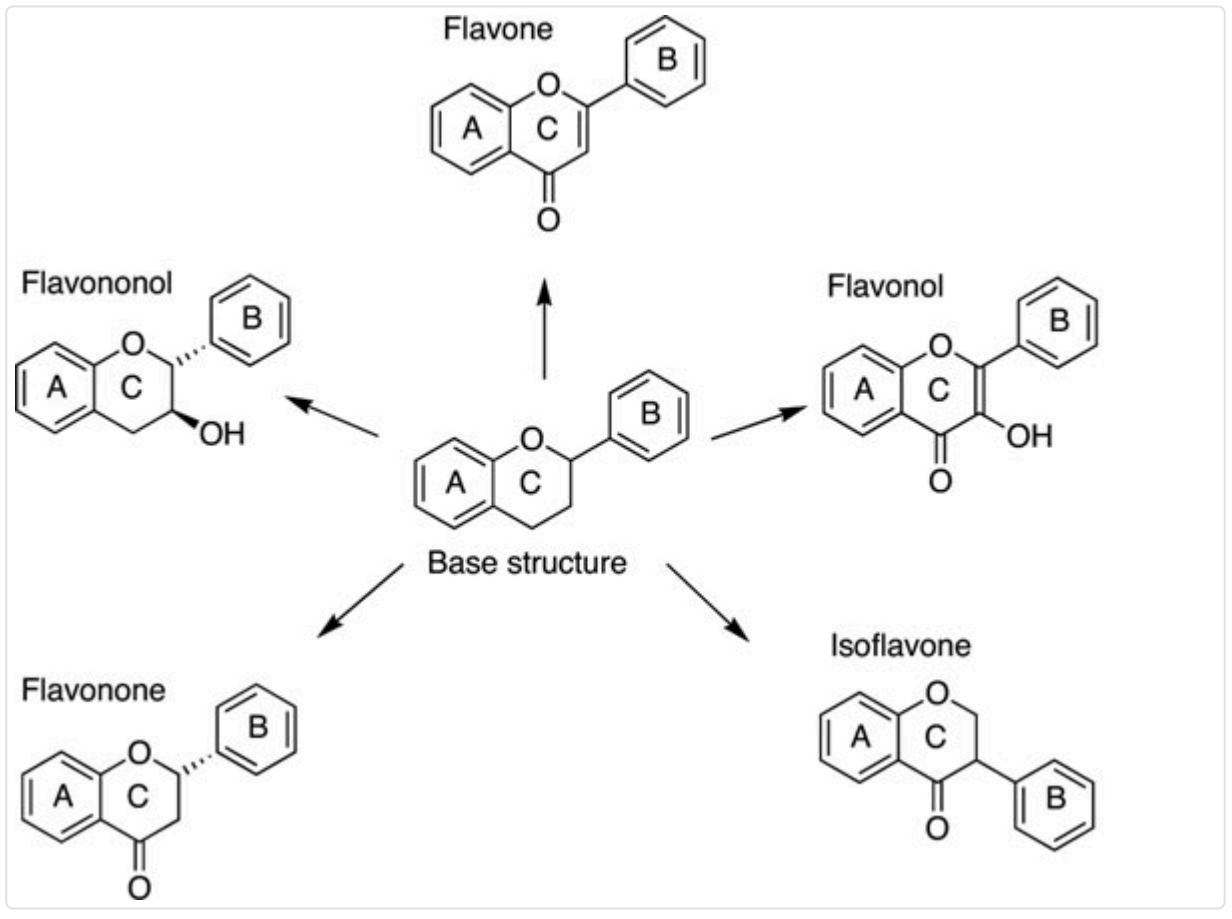


Add to Wish List | Purchase PDF | Cite

Review Article

Recent Advances on 3-Hydroxyflavone Derivatives: Structures and Properties

Pp: 98-103
Author(s): Burcu Butun, Gulacti Topcu and Turan Ozturk*
DOI: 10.2174/1389557517666170425102827

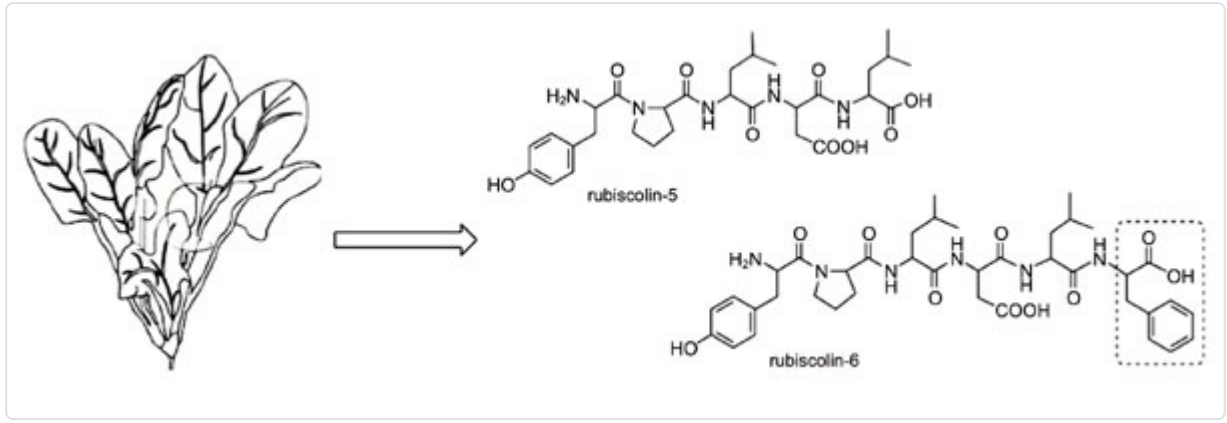


Add to Wish List | Purchase PDF | Cite

Review Article

Rubiscolins - Highly Potent Peptides Derived from Plant Proteins

Pp: 104-112
Author(s): Renata Perlikowska* and Anna Janecka
DOI: 10.2174/1389557517666170426160703

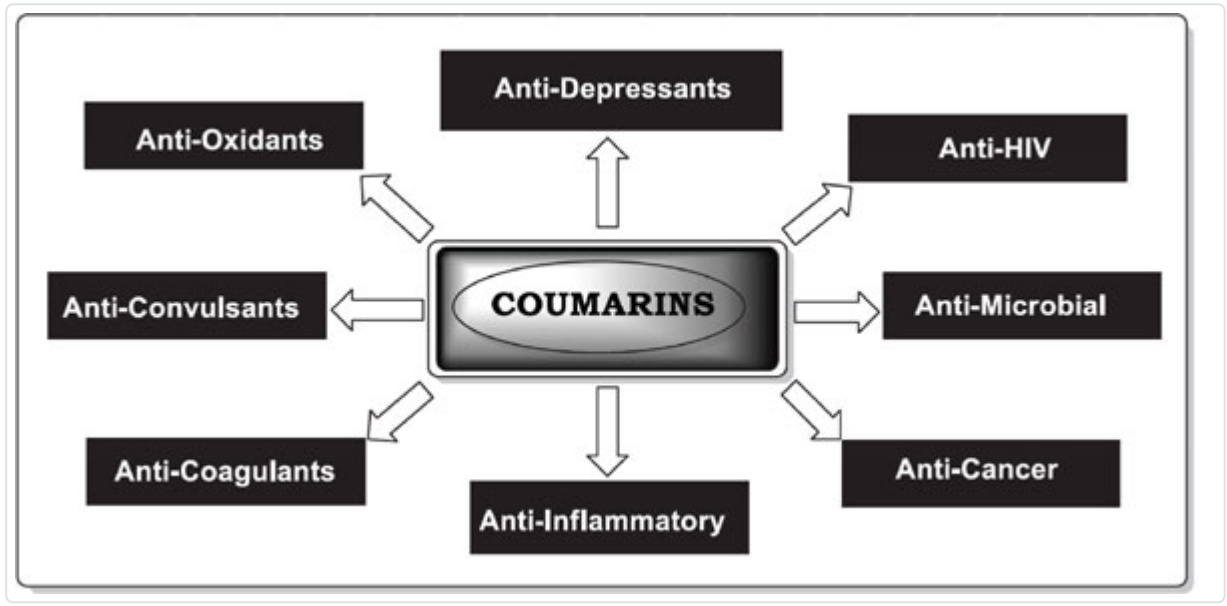


Add to Wish List | Purchase PDF | Cite

Review Article

A Review on Pharmacological Properties of Coumarins

Pp: 113-141
Author(s): Devulapally Srikrishna, Chandraiah Godugu and Pramod Kumar Dubey*
DOI: 10.2174/1389557516666160801094919

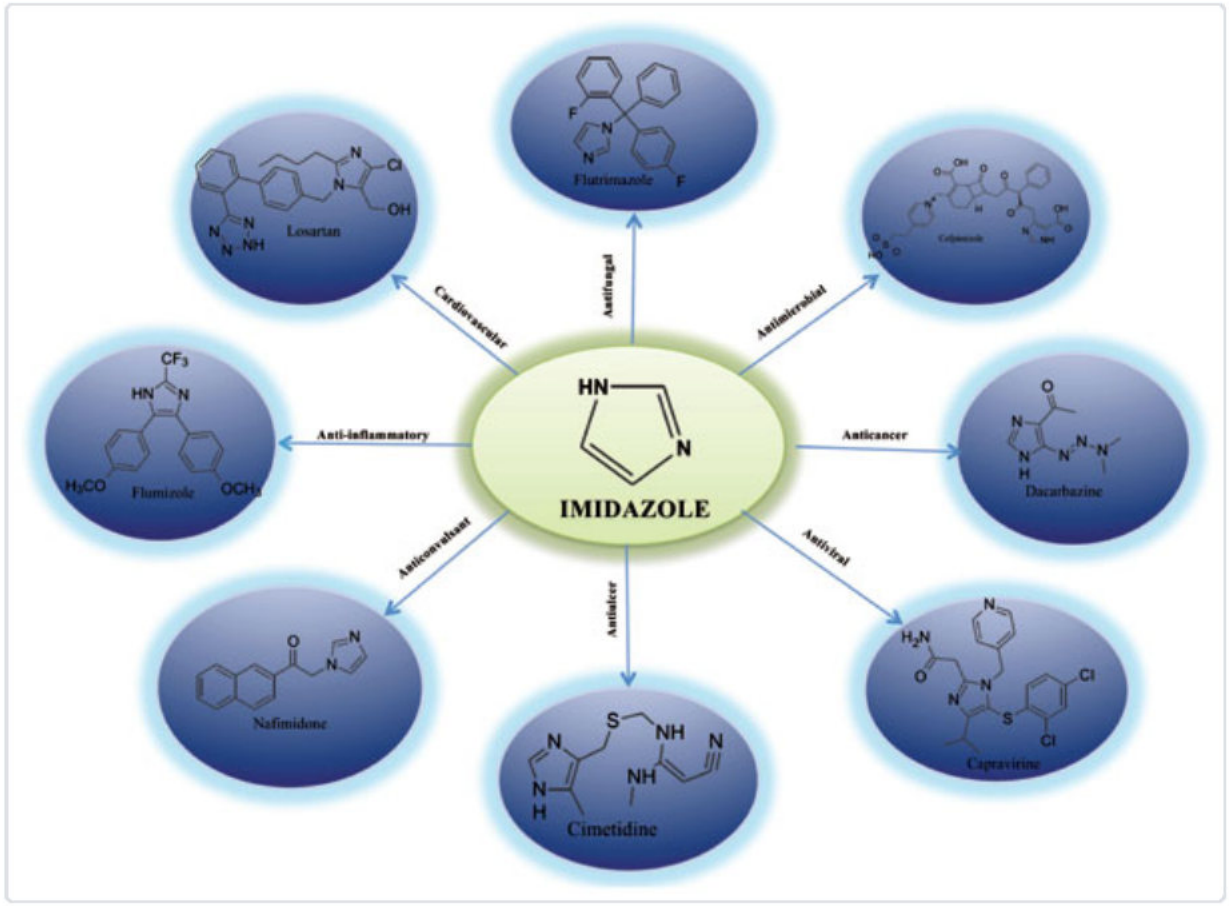


Add to Wish List | Purchase PDF | Cite

Review Article

Imidazole: An Essential Edifice for the Identification of New Lead Compounds and Drug Development

Pp: 142-163
Author(s): Nishtha Shalmali, Md. Rahmat Ali and Sandhya Bawa*
DOI: 10.2174/1389557517666170228113656

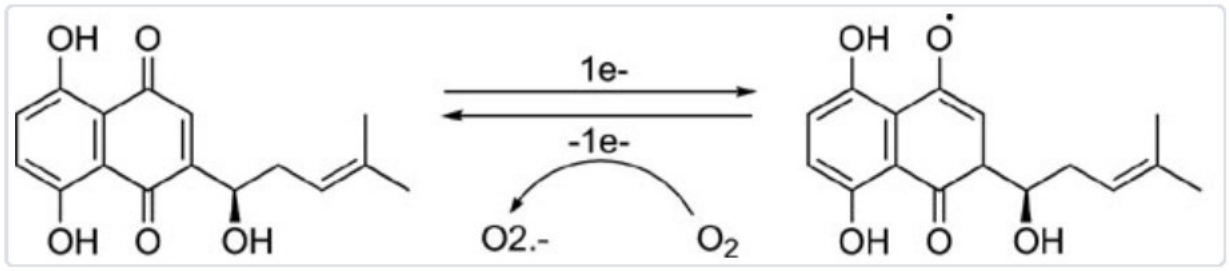


Add to Wish List | Purchase PDF | Cite

Review Article

Advance in Anti-tumor Mechanisms of Shikonin, Alkannin and their Derivatives

Pp: 164-172
Author(s): Xu Zhang, Jia-Hua Cui, Qing-Qing Meng, Shao-Shun Li, Wen Zhou* and Sui Xiao*
DOI: 10.2174/1389557517666170228114809



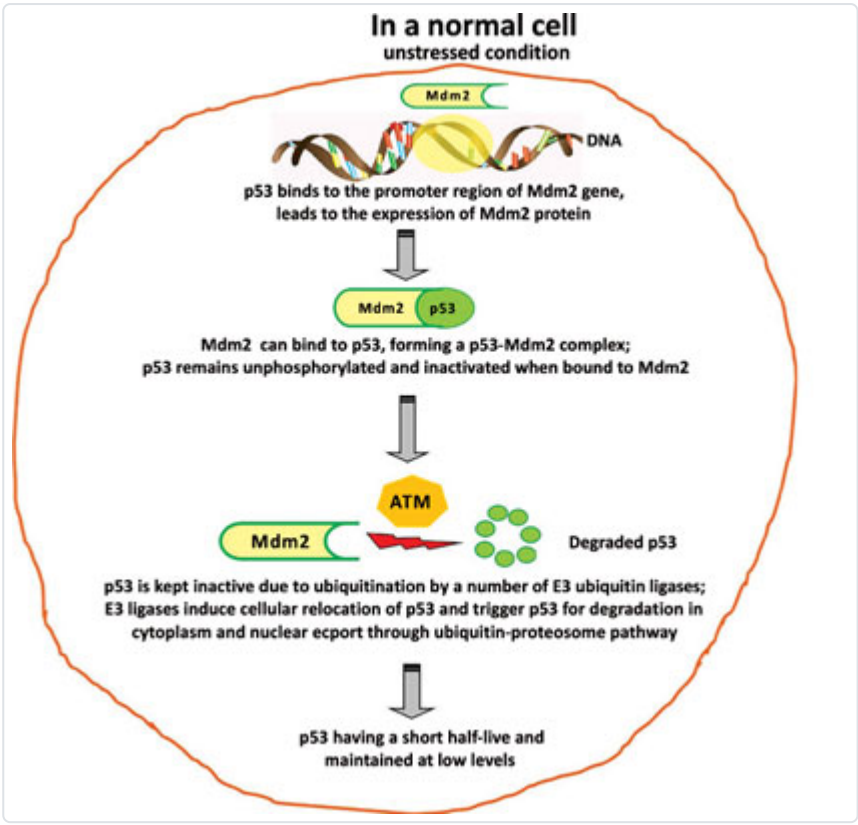
Add to Wish List | Purchase PDF | Cite

Review Article

open access plus

Nutlin-3, A p53-Mdm2 Antagonist for Nasopharyngeal Carcinoma Treatment

Pp: 173-183
Author(s): Voon Yee-Lin*, Wong Pooi-Fong and Alan Khoo Soo-Beng
DOI: 10.2174/1389557517666170717125821

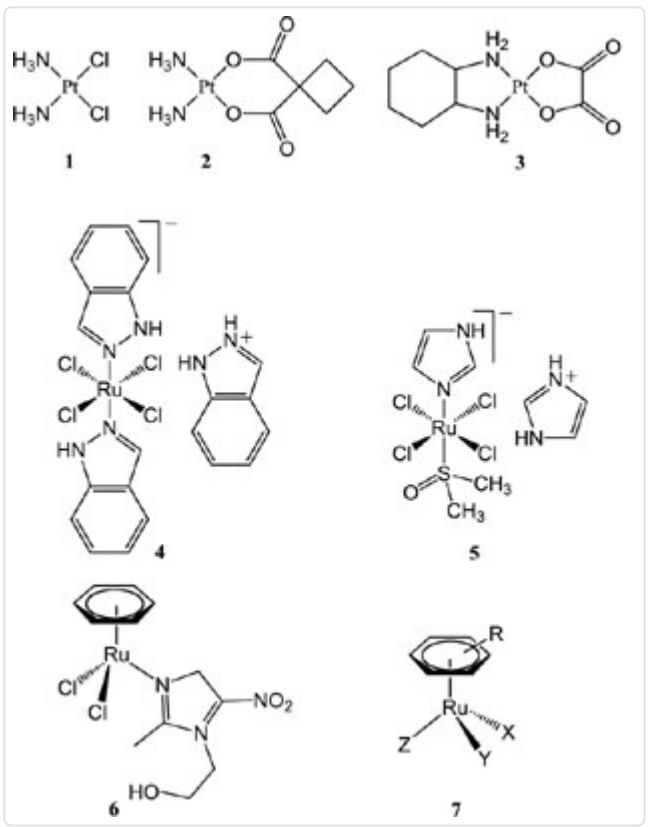


Download PDF File | Cite

Review Article

Design of Ru-arene Complexes for Antitumor Drugs

Pp: 184-193
Author(s): Wei Su, Yuchun Li and Peiyuan Li*
DOI: 10.2174/1389557517666170510113453



Add to Wish List | Purchase PDF | Cite

Impact

Impact Factor:

Current: 3.3
5 - Year: 4.1

Impact Factor Journals

CiteScore:

7.8

Track Manuscript

Type manuscript code Track

Submissions

Subscribe



Journal Information

- About Journal
- Editorial Board
- Meet the Guest Editor(s)
- Current Issue
- **Volumes /Issues**

For Authors

For Editors

For Reviewers

Explore Articles

Open Access

For Visitors

THE INTERNATIONAL MEDICINE AND BIOSCIENCES CONFERENCE 2026

22nd in the series of Eureka Science Translational Medicine Conferences

Publish in Impact Factor & Scopus-Indexed Journals!
Exclusive Opportunity for TIMBC Conference Participants

Call for Papers and Presentations

Submit Abstract Now!



BENTHAM SCIENCE

Quick Links

Journals | Books | Submit Articles | Alerting Services | Open Access Policy | Funding Agencies | Endorsements | Author's Comments & Reviews | Newsletters | Press Release | Terms and Conditions

COUNTER RELEASE 5 COMPLIANT

© 2025 Bentham Science Publishers | Privacy Policy

Send Orders for Reprints to reprints@benthamscience.ae

Mini-Reviews in Medicinal Chemistry, 2018, *18*, 164-172

REVIEW ARTICLE

Advance in Anti-tumor Mechanisms of Shikonin, Alkannin and their Derivatives

Xu Zhang[1], Jia-Hua Cui[3], Qing-Qing Meng[3], Shao-Shun Li[3], Wen Zhou[2,*] and Sui Xiao[1,*]

[1]*Guangdong Key Laboratory for Innovative Development and Utilization of Forest Plant Germplasm, College of Forestry and Landscape Architecture, South China Agricultural University, Guangzhou 510642, China;* [2]*School of Chinese Meteria, Medica, Guangzhou University of Chinese Medicine, E. 232, Waihuan Rd, University Town, Panyu, Guangzhou, 510006;* [3]*School of Pharmacy, Shanghai Jiaotong University, 800 Dongchuan Road, Shanghai 200240, China*

ARTICLE HISTORY

Received: April 16, 2016
Revised: August 14, 2016
Accepted: February 22, 2017

DOI:
10.2174/1389557517666170228114809

Abstract: Shikonin, alkannin and their derivatives, the main ingredient of *Lithospermum erythrorhizon* and *Arnebia euchroma (Royle) Johnst* native to Inner Mongolian and Northwest of China respectively, hold promising potentials for antitumor effects *via* multiple-target mechanisms. This review will emphasize the importance of their antitumor activity in apoptosis, necroptosis and immunogenic cell death, and expound the relationship of their antitumor activity and naphthoquinone scaffold that could generate ROS and alkylating agent. Meanwhile, the antitumor mechanisms of naturally-occurring shikonin, alkannin and their derivatives, which were divided into the direct interaction involved in alkylating agent, covalently binding the DNA and protein, as well as the indirect interaction mediated by ROS, nonspecifically influencing the mitochondria or multiple signal pathways, will be systematically summarized and discussed.

Keywords: Alkannin, anti-tumor mechanisms, bioalkylation, DNA, ROS, shikonin.

1. INTRODUCTION

Lithospermum erythrorhizon (L.erythrorhizon), a perennial hebaceous plant belonging to the *Boraginaceae* and *Lithospermum*, is originated in China. The medicinal properties of *L.erythrorhizon* roots are applied to treat burn-wounding in traditional Chinese medicine [1]. *L.erythrorhizon Sieb. et Zucc* is native to Inner Mongolia and Northeast of China. Its major active components are shikonin and its derivatives, and all the configurations are *R*. The *Arnebia euchroma (Royle) Johnst* originates from Xinjiang Uygur Autonomous Region of China. Its major effective contents are alkannin and its derivatives, but their configurations belong to *S*. Shikonin, alkannin and their derivatives display many biological activities including wounds healing [2], anti-inflammatory [3, 4], anti-bacterial [5], anti-viral [6], anti-thrombotic activities [7, 8] and so on.

*Address correspondence to these authors at the Guangdong Key laboratory for innovative Development and Utilization of Forest Plant Germplasm, College of Forestry and Landscape Architecture, South China Agricultural University, Guangzhou 510642, China; Tel:/Fax: +86 2085280256; E-mail: suixiao@outlook.com; and School of Chinese Meteria, Medica, Guangzhou University of Chinese Medicine, E. 232, Waihuan Rd, University Town, Panyu, Guangzhou, 510006, China; E-mail: wzhou60@sjtu.edu.cn

Since U. S. National Cancer Institute (NCI) firstly reported [9] that alkannin and its derivatives exhibited cytotoxicities to KB cells *in vitro* in 1974, more and more researchers have been focusing on the anti-tumor activities of shikonin, alkannin and their derivatives. Herein, we will review and shed light on the antitumor mechanisms of shikonin, alkannin and their derivatives from the indirect and direct interaction aspects.

2. ANTI-TUMOR ACTIVITIES OF SHIKONIN, ALKANNIN AND THEIR DERIVATIVES

Apoptosis is a process of programmed cell death that is responsible for cell clearance in normal tissues. Morphologically, membrane-enclosed apoptotic bodies which are phagocytosed and digested by nearby resident cells are formed, and no associated inflammations take place [10]. Biologically, there are some particular cellular markers such as DNA fragmentation, caspase activation, Bid cleavage, and cytochrome *c* release. Shikonin, alkannin and their derivatives are capable of inducing many kinds of tumor cell lines to be apoptotic in a time- and dose-dependent manner, such as the promotion of cell cycle arrest at G0/G1 phase, the reduction of the mitochondrial membrane potential, and the activation of caspase 3 expression in HaCaT cells [11]; up-

1875-5607/18 $58.00+.00 © 2018 Bentham Science Publishers

Mini-Reviews in Medicinal Chemistry

regulation of p53, down-regulation of cyclin-dependent protein kinase 4 and the reduced release of cytochrome *c* in A375-S2 cells [12]; chromatin condensation, DNA fragmentation and activation of caspase 3 in HL60 cell line [13, 14]; the distribution of cell cycle, the disruption of mitochondrial membrane potential, and the change of the expression of Bax and Bcl-2 in Hep G2 cells [15].

Necrosis has been considered as an unregulated and uncontrollable process before the discovery of necroptosis. Necroptosis has been used to designate one specific type of programmed necrosis that is regulated by receptor-interacting protein 1 (RIP1), receptor-interacting protein 3 (RIP3) and mixed lineage kinase domain-like (MLKL) [16]. Necroptosis was induced by shikonin, that showed some characteristics distinct from apoptosis in MCF-7 and HEK293, such as a morphology of necrotic cell death, loss of plasma membrane integrity, the cell death hampered by necrostatin-1 (Nec-1), a specific necroptosis inhibitor, and so on [17]. Further investigation performed by the same group demonstrated that the naturally-occurring shikonin analogues (deoxyshikonin, acetylshikonin, isobutyrylshikonin, *β,β*-dimethylacrylshikonin, isovalerylshikonin, α-methyl-*n*-butylshikonin) could circumvent drug resistance, initiating another unique apoptosis death pathway----necroptosis [18]. Shikonin-induced necroptosis could be reverted to apoptosis in the presence of Nec-1, due to the permeability conversion from mitochondrial inner membrane to mitochondrial outer membrane [19].

Immunogenic cell death (ICD) is a cell death form that can stimulate an immune response against dying or dead cell antigens, the dying, stressed or injured cells release or exposed molecules on their surface that function as signals for the innate immune system were called damage-associated molecular patterns (DAMPs). The molecular phenotype of ICD has been characterized according to changes in DMAPs, including heat shock proteins (HSP), high mobility group box 1 (HMGB1), calreticulin (CRT), glucose-related protein (GRP) and others [20, 21]. On the basis of their distinct actions to induce endoplasmic reticulum (ER) stress, ICD inducers are classified into two categories, type I or II, and shikonin was categorized as type I ICD inducer [22]. Shikonin can increase the expression of five DAMPs in the treated tumor cell lysates and the induction of ICD in carcinoma cells, and shikonin-treated tumor cell lysate could be further employed to elicit more strong *in vivo* anti-tumor activity for a dendritic cell (DC)-based cancer vaccine [23, 24].

3. RELATIONSHIP BETWEEN THE ANTI-TUMOR ACTIVITIES AND NAPHTHAZARIN MOTHER NUCLEUS

The antitumor activities of skinonin, alkaninn and their derivatives are largely attributed to their naphthoquinone mother nucleus. On one hand, indirectly affecting oxidation stress of cells by the generation of superoxide radical (ROS), and on the other hand, directly interacting with intracellular DNA and protein through the bioalkylation.

Many naturally-occurring naphthoquinone compounds have exhibited anti-tumor activities, mainly due to the generation of reactive oxygen species (ROS) of their naphthoquinone scaffold [25-27]. Shikonin and its derivatives are no exception that are capable of producing ROS to participate in and regulate the biological processes. The detailed mechanism of ROS generation of shikonin is shown in Fig. (**1**). The generation of semi-quinone radical of naphthazarin ring undergoes a one-electron transfer reduction with the help of NADPH-cytochrome P450 reductase, followed by self-oxidation of this radical back to quinone in the presence of oxygen molecule. During this oxidation-reduction process, a large amount of ROS is simultaneously produced to influence the cellular and mitochondrial membrane potentials [28].

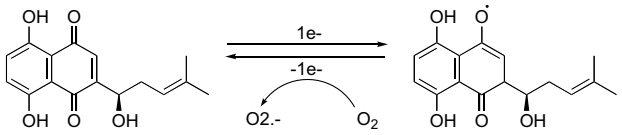


Fig. (1). The mechanism of ROS generated by shikonin.

Furthermore, a potent alkylating agent derived from the same structure is also the main mode of antitumor mechanism, which may capture intracellular nucleophiles, such as DNA, protein or reduced glutathione, to generate non-specific cytotoxicity [29]. The alkylation of shikonin is achieved by the nucleophilic displacement of chiral carbon on the side chain (Fig. **2**) as well as the Michael addition of naphthoquinone ring (Fig. **3**), both of which may take place simultaneously to inhibit the growth of cancer cells.

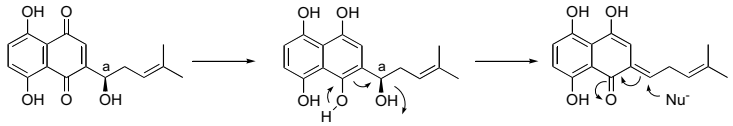


Fig. (2). The alkylated mechanism of shikonin by nucleophilic substitution.

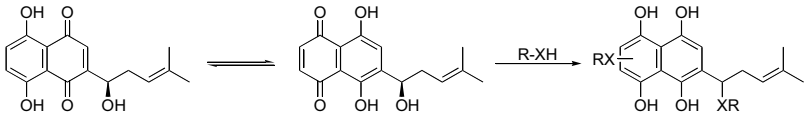


Fig. (3). The mechanism of alkylation of shikonin by Michael addition.

4. THE MECHANISMS UNDERLYING THE ANTI-TUMOR ACTIVITIES OF SHIKONIN, ALKANNIN AND THEIR DERIVATIVES

For decades, more and more attention was turned to anti-tumor activity of shikonin, alkannin and their derivatives, mainly ascribing to their powerful effects and high tolerance to cancerous cells *via* multi-target mechanisms. Function is largely dependent on its corresponding structure. As we analyzed above, the structures of shikonin, alkannin and their derivatives can produce ROS or alkylating agent, maybe even both, to exert an anti-neoplastic effect. ROS generated from their naphthoquinone has a significant influence on mitochondria and multiple signal pathways including ERK, JNK, P38 and ERK5/BMK1, ultimately killing tumor cells, and this process is an indirect interaction mode and ROS is a key mediator. On the other hand, alkylating agent originated from naphthoquinone and its side chain (Fig. **2**) can target DNA or proteins in cells and covalently bind them, thereby inhibiting the activity of target DNA and protein to induce cell apoptosis, this mode is a direct interaction that shikonin, alkannin and their derivatives attack related proteins or enzymes. To sum up, the discussion of the antitumor mechanisms of shikonin, alkannin and their derivatives from two aspects, indirect interaction and direct interaction, will be a brand-new perspective so far.

4.1. Cell Death Indirectly Induced by ROS

4.1.1. Induction of Cellular Apoptosis by ROS

For camptothecin, vinblastine and adriamycin [30], the most important mechanism underlying their antitumor activities is that ROS generated from these compounds induces cancer cells to undergo apoptosis. Also, ROS from shikonin, alkonin and their derivatives brings about significant consumption of intracellular reduced glutathione (GSH) and increased concentration of Ca^{2+} [31]. The accumulation of ROS gives rise to oxidative stress to cell [32]. Subsequently, *c*-Jun N-terminal kinase (JNK), extracellular signal-regulated kinase (ERK) and p38 signaling pathways were influenced [33-35], accompanying with the release of cytochrome *c* and Smac/DIABLO, up-regulation of the expression of p53 and Bax, down-regulation of the expression of Bcl-2 and Bcl-xL, activation of caspase-9 and caspase-3, dissociation of poly ADP-ribose polymerase (PARP), DNA damage, finally leading to cell apoptosis [36-38]. These changes are in accordance with those treated by the first-line anti-tumor drugs, implying that ROS made cancer cells suffer from apoptosis [39-42].

4.1.1.1. Interference with the MAPKs Signal Pathway

The mitogen-activated protein kinase (MAPK) is a kind of serine-threonine kinase widely distributed in cells. MAPK could transmit the signal from cytoplasm to nucleus where it plays important roles in the processes of cell proliferation, cell differentiation, apoptosis and so on. To data, MAPKs are consisted of some significant signal pathways such as ERK, JNK, P38 and ERK5/BMK1. Each of them has high specificity and independent functions, However, to some extent, they have crosstalk with each other [43].

ERK1 and ERK2 are two subtypes of ERK belonging to the super family of MAPKs, just like ERK5, JNK and P38. The phosphorylated MAPKs could transmit the received signals from membranes to nucleus through signaling cascade, transduction and propagation. Phosphatases could dephosphorylate threonine and tyrosine residues in the activation loop of ERK. The activated ERKs, in turn, regulate several physiological responses, such as proliferation, migration, differentiation and death [44]. Abnormity of this signaling pathway is thought to result in the cell proliferation out of control, and correlates with carcinogenesis. Shikonin could induce apoptosis in cancer cells through regulation of phosphorylation of ERKs in many different kinds of cancer cells, for instance, it can promote the phosphorylation level of ERK in Hela cells and osteosarcoma cells [45-46] or inhibit the activities of ERK1/2 in human gastric cancer cells and epidermoid carcinoma cells [47, 48].

To date, there are two major apoptotic pathways: the extrinsic (or death receptor) pathway and the intrinsic (or mitochondrial) pathway [49]. All the JNK subtypes (JNK1, JNK2, and JNK3) take part in the apoptotic pathways. The mechanisms of JNK-mediated apoptosis are divided into nucleus- and mitochondria-targeted signaling pathways. The phosphorylated JNK could be translocated to nucleus where it phosphorylates and transactivates *c*-Jun. The phosphorylation of *c*-Jun leads to the formation of AP-1. JNK-AP-1 pathway is involved in the increased expression of pro-apoptotic genes and/or a decrease in the expression of pro-survival genes. In addition, the activated JNK translocates to mitochondria, phosphorylates BH3-only member of Bcl2-family apoptotic proteins, or activates Bax in membrane channels to release the pro-apoptotic proteins such as cytochrome *c* [50]. It was reported that treatment of K562 cells with shikonin resulted in a rapid generation of ROS, subsequently activated the stress-related JNK pathway, released cytochrome *c* and Smac/DIABLO, and activated the caspase, thereby leading to apoptosis [33]. This results were in consistent with another report that shikonin induced the generation of ROS as well as caspase 3-dependent apoptosis [51], meanwhile, the JNK activity was apparently elevated in shikonin-treated AGS human stomach carcinoma cells, therefore, shikonin-induced apoptosis in AGS cell line was caspase- and JNK-dependent pathways.

The p38 MAPK signaling pathway permits cells to integrate a large number of external signals and responds appropriately by generating a plethora of different biological effects [52]. It is generally believed that p38 MAPK-induced apoptosis covers translocation of Bax to the mitochondria and the increase in Bax/Bcl-2 ratio, release of cytochrome *c*, and activation of caspase-9 and caspase-3 [53]. Shikonin-induced ROS is capable of activating ASK1 by decreasing the phosphorylation of Ser83 and dissociating the negative regulator *p*21, leading to the activation of p38 MAPK and the induction of apoptosis [54]. Acetylshikonin, one of shikonin derivatives, has been reported to induce apoptosis in OSCC cells mediated by ROS as well as G2 cell cycle arrest, and acetylshikonin treatment can enhance the phosphorylation level of JNK and p38 MAPK [55].

4.1.1.2. Triggering the Mitochondrial Apoptotic Pathway

The mitochondria-mediated apoptosis pathway is one of research hotspots in the field of cell apoptosis. A variety of apoptotic signals stimulate the pro-apoptotic BH3-only proteins, and destroy the balance between anti-apoptotic and pro-apoptotic Bcl-2 family of proteins, and then change the permeability of the outer mitochondrial membrane (OMM), and finally release pro-apoptotic proteins from mitochondria [56]. Mitochondrial permeability transition pore (MPT) is another potential mechanism for release of pro-apoptotic proteins from mitochondria, the open pore in the inner mitochondrial membrane (IMM) leads to the swelling of the matrix and the rupture of the OMM [57]. Cytochrome *c* from mitochondria induces formation of the Apaf-1/cytochrome *c* complex and the activation of procaspase-9, and then the activated caspase-9 cleaves and activates caspase-3, caspase-6, and caspase-7, ultimately leading to DNA fragmentation and cell death [58].

Treated with low concentration of shikonin for a short time, the significantly inhibitory effect on the proliferation of A375-S2 cells was observed [59]. Later on, further research discovered that the expression of P53 protein was enhanced after treatment for 9 h, and the expression of Bax was up-regulated but the expression of Bcl-xL was down-regulated during 3-24 h. Noticeably, the release of cytochrome *c* was observed after 12 h. Liu *et al.* [60] indicated that the proliferation of the papillary thyroid cancer cell lines K1 and W3 was inhibited by shikonin in a dose- and time-dependent manner, and changes in typical apoptotic morphological and higher apoptosis rates were observed, and no obvious cell cycle arrest was found. The results were further supported by real-time PCR analysis that shikonin increased the expression of Bax and caspase-3 and obviously up-regulated the expression of Bcl-2, and finally resulted in apoptosis. Wiench *et al.* [31] proposed that a number of recent findings regarding the cellular effects of shikonin were downstream events of the mitochondrial pathway of apoptosis, and that shikonin could directly target to mitochondria where it caused the overproduction of ROS and an increase in intracellular calcium levels, leading to breakdown of the mitochondrial membrane potential. Again, Shikonin inhibited the proliferation of human TT medullary thyroid carcinoma cells in a dose- and time-dependent manner *via* the mitochondrial signaling pathway, demonstrating that the increase in the expression levels of Bcl-2/Bax, the reduction of mitochondrial membrane potential and the activation of the caspase-9/caspase-3 enzyme-associated reactions [61].

4.1.2. Necroptosis Induced by ROS

RIP1-RIP3 pronecrotic complex was a prerequisite for TNFα-induced programmed necrosis. Shikonin-treated MDA-MB-468 cells displayed that an increase in the ROS levels, a reduction in mitochondrial membrane potential and necroptosis were associated with a significant increase in RIP_1K and RIP_3K expressions. The main route of cell death induced by shikonin was thus thought as RIP_1K-RIP_3K mediated necroptosis [62]. The similar conclusion was drawn that shikonin could induce the formation of RIP1-RIP3 complex, and cause cell necroptosis in NIH3T3 cells [63]. It was worth noticing that this kind of cell death could be reversed by a ROS scavenger, *N*-acetylcysteine (NAC), the RIP1-RIP3 complex was interfered with NAC as well. Furthermore, ROS has been identified as a critical mediator of necroptosis because it can promote necroptosis by stabilizing the RIP1/RIP3 necrosome complex *via* a potential positive feedback loop [64, 65]. Therefore, all the results have pointed out that the generation of ROS from naphthoquinone mother nucleus might be involved in the induction of necroptosis.

4.2. Direct Targeting to DNA or Protein

Some nucleophilic groups like sulfydryl and aliphatic amidogen exist in DNA and protein, and they play very important roles in the maintenance of the functions of biomolecules. Anti-cancer property of naphthoquinone scaffold maybe due to the reason that shikonin, alkannin and their derivatives can react with intracellular DNA and protein, ultimately resulting in cell death.

4.2.1. Inhibition of Nuclear Factor kB (NF-kB)

NF-kB proteins are a family of transcription factors that have been shown to be constitutively activated in many kinds of leukemias and solid tumors. NF-*k*B regulates the expression of a large number of genes involved in cell growth, apoptosis and differentiation [66]. With increase in the concentrations of shikonin, protein levels and gelatinolytic activities of MMP-9 were suppressed in a highly metastatic adenoid cystic carcinomas cell line ACC-M [67], and further significant anti-invasion and anti-migration activities were exhibited. But TNF-α, a specific stimulator of NF-kB pathway, could increase the NF-kB activity to inhibit the expression level of MMP-9. Therefore, anti-invasion and anti-migration activities of shikonin partly brought about down-regulation of NF-kB-mediated MMP-9 expression. More than 40 natural products (including shikonin) possessed inhibitory activities on NF-kB. Shikonin functioned as a Michael acceptor for the cysteine residue of p65 protein of NF-kB, and played a key role in the inhibition of the NF-kB pathway [68].

4.2.2. Inhibition of Topoisomerases

DNA topoisomerases are a class of enzymes that change the topological state of DNA by breaking and rejoining the phosphodiester backbone of DNA [69]. Because of their continuous proliferation and frequent DNA replication, the cancer cells are more sensitive to the inhibitors of topoisomerases than the normal ones. Camptothecin and etoposide, the clinical antitumor drugs, are the representative drugs of Topo I and Topo II inhibitors, respectively. 2- and 6-acyl-5,8-dimethoxy-1,4-naphthoquinone (DMNQ) derivatives against DNA topoisomerase I and their cytotoxicity *in vitro* were assessed, and they exhibited more inhibitory potency than the positive control [70]. Meanwhile, when Topo I was pre-incubated with 6-hexanoyl-DMNQ, its activity decreased in a time-dependent manner. After a further study, the inhibition of Topo I was confirmed to be one of their antitumor mechanisms, mainly depending on the redox cycle. SH-7, a shikonin derivative, exhibited obvious cytotoxicity against the MDR cell lines, and its cytotoxicity was ascribed to sig-

nificantly inhibitory effects on Topo I and Topo II, further displaying the selective inhibition that it was much stronger on Topo II than on Topo I. Moreover, SH-7 could stabilize Topo II-DNA cleavable complex and elevate the expression of phosphorylated-H2AX [71], while shikonin could weakly block Topo I-mediated DNA relaxation, and could not convert pUC19 DNA to a supercoiled state from a relaxed state. Although the biochemical and structural results suggest that shikonin is not a DNA intercalator, it was found to displace SYBR green, a known minor groove binding dye, from binding to DNA in the PCR reaction. Thus, shikonin is considered as a better groove binder to exhibit the inhibition of Topo II-mediated DNA relaxation [72].

4.2.3. Inhibition of Protein Tyrosine Kinases (PTKs)

Protein tyrosine kinases (PTKs) are a large family of enzymes responsible for catalyzing the phosphorylation of tyrosine residues of proteins. Phosphorylation of tyrosine residues plays a very important role in the control of cell growth, metabolism, differentiation and apoptosis [73]. However, PTKs would easily lead to the emergence of malignancy due to the mutation, overexpression and autocrine paracrine stimulation. Therefore, the selective tyrosine kinase inhibitors could be applied as a new mode of cancer therapy to block the constitutive oncogenic activation in cancer cells [74]. *β*-HIVS, a shikonin derivative isolated from *Lithospermium radix*, efficiently induced cell death in two types of lung cancer cells, due to their selective inhibition of protein tyrosine kinase activity [75]. *β*-HIVS also had more pronounced inhibition against EGFR and *v*-Src than shikonin, and *β*-HIVS was pointed out as a competitive inhibitor with PTK peptide substrate. However, the chemical structure of *β*-HIVS does not resemble that of any other PTK inhibitors, probably suggesting that the different inhibition mechanism of *β*-HIVS against PTK is to interfere with phosphorylation.

4.2.4. Inhibition of Telomerase

A telomere is a region of repetitive nucleotide sequences at the end of chromatid, which is shortened in each chromosome replication. Telomere length can be maintained by telomerase reverse transcriptase, which adds DNA sequence repeats to the 3' end of DNA strands in the telomere regions. Telomerase activation has been observed in 90% of all types of human tumors [76], and the activated telomerase can eliminate process of death, the absence of apoptosis-induction pathways and persistent activation of mitosis. Human telomerase has been proposed as a highly selective target for antitumor therapeutics. G-quadruplexes (G-tetrads or G_4-DNA) structure fold into intra-molecular quadruplex helix structures through Hoogsten hydrogen-bonding in the G-rich oligonucleotides of telomeric DNA. This structure can hide 3'-end of the DNA from telomerase and thereby inhibit the activity of telomerase to maintain length of telomere. Shikonin had been found to complex with G_4-DNA through multiple binding sites, and thus inhibit the activity of telomerase [77]. Either, shikonin and alkannin glycosides had exhibited much stronger binding activity with G_4-DNA than its corresponding shikonin and alkannin do, and had the potential anticancer activity *via* its inhibition against human telomerase [78].

4.2.5. Inhibition of Pyruvate Kinase-M_2 (PKM2)

PKM2 catalyzes the last but rate-limiting step in glycolysis, a central metabolic pathway to mainly produce ATP for cancer cells, through the transphosphorylation from phosphoenolpyruvate to ADP. Increased expression of PMK2, which has been observed in various cancer cell lines and in the samples from cancer patients, is necessary for tumor growth [79]. Chen *et al.* [80] designed a series of experiments to "fish" shikonin-targeted protein from MCF cell lysate using shiknin-conjugated sepharose-6B. Fortunately, the specific combination of shikonin and PKM2 was obtained, probably indicating that PKM2 is a potential target of shikonin. The further results obtained by the same group demonstrated that shikonin and alkannin inhibited the cellular glycolytic rate in a concentration-dependent manner by selectively inhibiting the activity of PKM2 but not those of PKM1 and PKL. Although All the PKL, PKM1 and PKM2 could bound to solid-phase shikonin, selective inhibition of shikonin on PKM2 was mainly dependent on the allosteric region of PKM2 with the exception of a common domain for binding shikonin. The hypothesis was testified by another experiment that shikonin can suppress PKM2 activation to inhibit glycolysis in the early stage of carcinogenesis induced by 12-*O*-tetradecanoylphorbol 13-acetate [81]. All the results mentioned above indicated that shikonin might be useful in chemoprevention for human cancers through interfering with the energy metabolism of cancer cells.

4.2.6. Dysfunction of Heterogeneous Nuclear Ribonucleoprotein A1 (hnRNPA1)

HnRNPA1 was shown to be an important substrate of enzyme A that can affect nuclear export activity of newly synthesized RNA and disrupt pre-mRNA splicing, and result in the production of ICD [82]. Molecular affinity between shikonin and more than 27,000 human protein and peptides *via* a molecular docking was compared, and then hnRNPA1 was found to exhibit the highest binding/docking affinity with shikonin [83]. Subsequently, an antibody pull-down assay in combination with LC-MS/MS analysis, and isothermal titration calorimetry analysis was used to confirm the direct binding relationship between shikonin and hnRNPA1. Based on the computer modeling analysis, together with the result that shikonin-treatment could disrupt hnRNPA1-mediated nuclear export activity of the newly synthesized RNA into the cytosol, two binding sites for shikonin/hnRNPA1 complex were proposed. The binding sites were thought to probably interfere with the RNA-binding domain of hnRNPA1. Interestingly, alternative splicing between PKM1 and PKM2 was also regulated by hnRNPA1 activity, shikonin may regulate PKM splicing through an indirect mechanism with the exception of the direct inhibition on PKM2.

CONCLUSION

Programmed cell death (PCD) plays an important role during maintenance of tissue homoeostasis and elimination of damaged cells [84]. The concept of apoptosis used to equate with the concept of PCD, but subsequently growing number of people have recognized that apoptosis is just one

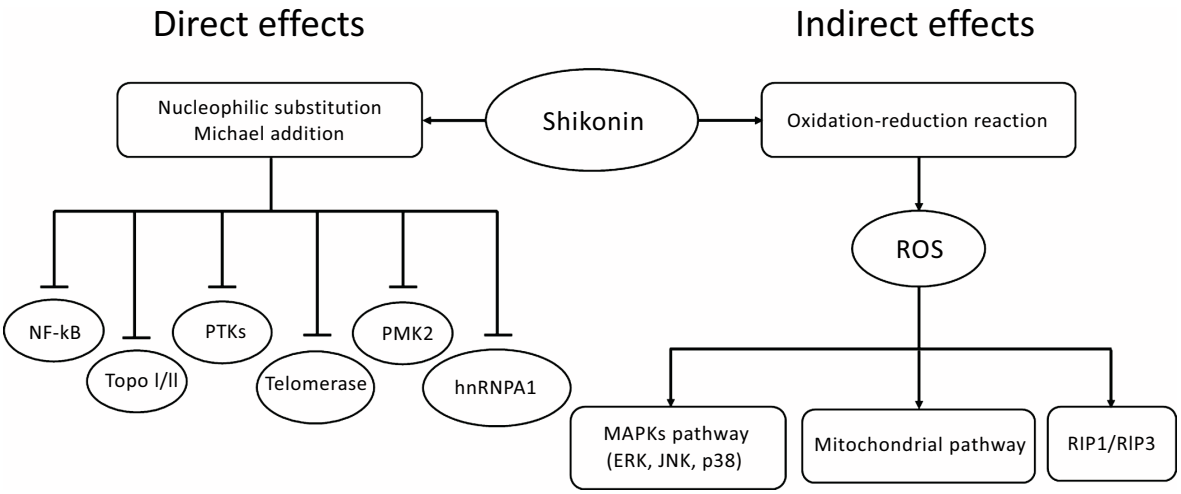


Fig. (4). The probable mechanisms of the antitumor activity of shikonin. NF-kB (nuclear factor kB), Topo (topoisomerase), PTKs (protein tyrosine kinases), PMK2 (pyruvate kinase M2), ROS (reactive oxygen species), MAPKs (mitogen-activated protein kinases), ERK (extracellular signal-regulated kinase), JNK (c-Jun N-terminal kinase), p38 (P38 mitogen-activated protein kinases).

of the type of PCD (type I PCD). There are other two types of PCD, autophagy (type II PCD) and necroptosis (type III PCD), and all the three types are easily distinguished by their morphological differences. Shikonin, alkannin and their derivatives are capable of inducing type I and type III PCD [85]. It is generally accepted that low concentrations of shikonin, alkannin and their derivatives mainly induced cell death by apoptosis, and at high concentrations they induced cell death by necroptosis [18, 32, 86, 87]. Necroptosis can induce proinflammatory to result in immunological responses. Although apoptosis can't trigger proinflammatory, some apotosis inducer can initiate immunogenic apoptosis. Moreover, shikonin can't induce ER stress coupled with ROS generation, so it can be categorized as type I ICD inducer [85]. Since shikonin, alkannin and their derivatives display many characteristics similar to those caused by ROS, and this phenomenon could be eliminated or attenuated by ROS scavenger. Variation of MAPK signal, mitochondrial pathway, caspases cascade reaction and so on, were considered as the downstream events of ROS generation. Additionally, as small molecules with the potent alkylating ability, shikonin, alkannin and their derivatives can easily bind to intracellular DNA or protein, and induce the cell death. In conclusion, from the angel of the indirect effects and direct effects, the mechanisms of antitumor activity of shikonin, alkoanin and their derivativesare summarized in Fig. (**4**). On one hand, because of the generation of superoxide radicals and potential bioalkylation, the naphthazarin ring of shikonin, alkannin and their derivatives possess significant potential antitumor activities and multi-targeting antitumor mechanisms. On the other hand, this structure is also the source of the unwanted toxic side effects. Therefore, none of the shikonin, alkannin and their derivatives has entered into clinical trials as an antitumor drug to date.

Our research group has been working on the structural modifications of shikonin, alkannin and their derivatives, aiming to down-regulate the ROS generation and bioalkylation level, and maintain their antitumor activity and increase the selectivity. 5,8-dimethoxy-1,4-naphthoquinone derivatives exhibit a greater selectivity *in vitro*, and more potential inhibition as well as less toxicity *in vivo* [88]. Now we designed and synthesized 1, 4, 5, 8-tetramethoxynaphthalene and 5, 8-dimethoxy-1, 4- dioximenaphthalene derivatives in order to further shield the carbonyl groups. DCFH-DA was used as a ROS-capturing reagent in MCF-7 cells, and the results from the determination of ROS experiments have shown that these compounds significantly decreased ROS generation. Meanwhile, *p*-thiocresol was applied to react with these compounds to determine their ability of alkylation, but no trace of alkylation product was obtained. These results have demonstrated that these compounds almost have no ROS generation and bioalkylation [89]. As we expected, 1, 4, 5, 8-tetramethoxynaphthalene derivatives have not any antitumor activity. However, 5,8-dimethoxy-1,4-dioximenaphthalene derivatives unexpectedly displayed excellent antiproliferative activity [90] and selectivity against HCT-116 cell lines, which are more potent than lead compound shikonin *in vitro* and have potential inhibition against CT-26 xenografted tumor *in vivo* comparable to 5-Fu. More importantly, 5,8-dimethoxy-1,4-dioximenaphthalene scaffold was fairly stable in rat liver microsomes *in vitro* [91]. In summary, a promising class of shikonin, alkannin and their derivatives with great antitumor activity both *in vitro* and *in vivo* were found. The mechanisms underlying their antitumor activities are significantly different from those of the lead compound shikonin and alkannin. This discovery will open a new avenue to modify scaffold of shikonin and alkannin to be an effective antitumor agent.

LIST OF ABBREVIATIONS

CRT	=	Calreticulin
DAMPs	=	Damage-associated Molecular Patterns
DC	=	Dendritic Cell
DMNQ	=	5,8-Dimethoxy-1,4-naphthoquinone
ER	=	Endoplasmic Reticulum

ERK = Extracellular Signal-regulated kinase
G4-DNA = G-quadruplexes
GRP = Glucose-related Protein
HMGB1 = High Mobility Group Box 1
HSP = Heat Shock Proteins
ICD = Immunogenic Cell Death
IMM = Inner Mitochondrial Membrane
JNK = c-jun N-terminal kinase
MAPK = Mitogen-activated Protein Kinase
MLKL = Mixed Lineage Kinase Domain-like
MPT = Mitochondrial Permeability Transition Pore
NAC = N-acetylcysteine
Nec-1 = Necrostatin-1
NF-kB = Nuclear Factor kB
OMM = Outer Mitochondrial Membrane
PARP = Poly ADP-ribose Polymerase
PKM2 = Pyruvate kinase-M2
PTKs = Protein Tyrosine Kinases
RIP1 = Receptor-interacting Protein 1
RIP3 = Receptor-interacting Protein 3
ROS = Reactive Oxygen Species
Topo = Topoisomerase

CONSENT FOR PUBLICATION

Not applicable.

CONFLICT OF INTEREST

The authors declare no conflict of interest, financial or otherwise.

ACKNOWLEDGEMENTS

This work was supported by National Natural Science Foundation of China (81373274), the Youth Science Funds of National Natural Science Foundation of China (31402245), and the funds of College of Forestry and Landscape Architecture, South China Agricultural University for Young Scholar(201609).

REFERENCES

[1] Luo, X.-y.; Li, M.-h.; Lu, l.; Luo, Y.-l.; Zhang, N. Research progress of pharmacological action and application of lithospermum erythrorhizon. Sieb. et Zucc. *J. Dalian Univ.,* **2004**, *25*(2), 80-83.
[2] Mani, H.; Sidhu, G.; Singh, A.; Gaddipati, J.; Banaudha, K.; Raj, K.; Maheshwari, R. Enhancement of wound healing by shikonin analogue 93/637 in normal and impaired healing. *Skin Pharmacol. Physiol.,* **2003**, *17*(1), 49-56.
[3] Singh, B.; Sharma, M.; Meghwal, P.; Sahu, P.; Singh, S. Anti-inflammatory activity of shikonin derivatives from Arnebia hispidissima. *Phytomedicine,* **2003**, *10*(5), 375-380.
[4] Tanaka, S.; Tajima, M.; Tsukada, M.; Tabata, M. A comparative study on anti-inflammatory activities of the enantiomers, shikonin and alkannin. *J. Nat. Prod.,* **1986**, *49*(3), 466-469.
[5] Liu, M.; Ohuchi, T.; Ieiri, T.; Ohe, M.; Matsuzaki, S. Shikonin has potent antibacterial activity against methicillin-resistant *Staphylococcus aureus* (MRSA). *Dokkyo J. Med. Sci.,* **1996**, *23*, 63-69.
[6] Luo, X.-y.; Li, M.-h.; Lun, Y.-z.; Lv, L.; Teng, M.-j.; Luo, Y.-l.; Zhang, N. Antiviral activity of Shikonin on parainfluenza viruses. *Chin. Trad. Herbal Drugs,* **2005**, *36*(4), 568-571.
[7] Chang, Y.-S.; Kuo, S.-C.; Weng, S.-H.; Jan, S.-C.; Ko, F.-N.; Teng, C.-M. Inhibition of platelet aggregation by shikonin derivatives isolated from *Arnebia euchroma*. *Planta Med.,* **1993**, *59*(5), 401-404.
[8] Ko, F.-N.; Lee, Y.-S.; Kuo, S.-C.; Chang, Y.-S.; Teng, C.-M. Inhibition on platelet activation by shikonin derivatives isolated from *Arnebia euchroma*. *Biochimica et Biophysica Acta (BBA)-Mol. Cell Res.,* **1995**, *1268*(3), 329-334.
[9] Driscoll, J.; Hazard Jr, G.; Wood Jr, H.; Goldin, A. Structure-antitumor activity relationships among quinone derivatives. *Cancer Chemother. Reports Part 2,* **1974**, *4*(2), 1.
[10] Kerr, J.F.R.; Winterford, C.M.; Harmon, B.V. Apoptosis. Its significance in cancer and cancer therapy. *Cancer,* **1994**, *73*(8), 2013-2026.
[11] Jing, H.; Sun, W.; Fan, J.; Zhang, Y.; Yang, J.; Jia, J.; Li, J.; Guo, J.; Luo, S.; Zheng, Y. Shikonin induces apoptosis of HaCaT cells *via* the mitochondrial, Erk and Akt pathways. *Mol. Med. Reports,* **2016**, *13*(4), 3009-3016.
[12] Wu, Z.; Wu, L.; Li, L.; Tashiro, S.-i.; Onodera, S.; Ikejima, T. p53-mediated cell cycle arrest and apoptosis induced by Shikonin *via* a caspase-9-dependent mechanism in human malignant melanoma A375-S2 cells. *J. Pharmacol. Sci.,* **2004**, *94*(2), 166-176.
[13] Gao, D.; Hiromura, M.; Yasui, H.; Sakurai, H. Direct reaction between shikonin and thiols induces apoptosis in HL60 cells. *Biol. Pharmaceut. Bull.,* **2002**, *25*(7), 827-832.
[14] Duan, D.; Zhang, B.; Yao, J.; Liu, Y.; Fang, J. Shikonin targets cytosolic thioredoxin reductase to induce ROS-mediated apoptosis in human promyelocytic leukemia HL-60 cells. *Free Rad. Bio Med.,* **2014**, *70*, 182-193.
[15] Yingkun, N.; Lvsong, Z.; Huimin, Y. Shikonin inhibits the proliferation and induces the apoptosis of human HepG2 cells. *Can. J. Physiol. Pharm.,* **2010**, *88*(12), 1138-1146.
[16] Chen, D.; Yu, J.; Zhang, L. Necroptosis: an alternative cell death program defending against cancer. *Biochimica et Biophysica Acta (BBA) – Rev. Cancer,* **2016**, *1865*(2), 228-236.
[17] Han, W.; Li, L.; Qiu, S.; Lu, Q.; Pan, Q.; Gu, Y.; Luo, J.; Hu, X. Shikonin circumvents cancer drug resistance by induction of a necroptotic death. *Am. Associat. Cancer Res.,* **2007**, *6*(5), 1641-1649.
[18] Xuan, Y.; Hu, X. Naturally-occurring shikonin analogues – A class of necroptotic inducers that circumvent cancer drug resistance. *Cancer Lett.,* **2009**, *274*(2), 233-242.
[19] Han, W.; Xie, J.; Li, L.; Liu, Z.; Hu, X. Necrostatin-1 reverts shikonin-induced necroptosis to apoptosis. *Apoptosis,* **2009**, *14*(5), 674-686.
[20] Yang, N.-S.; Lin, T.-J. Molecular basis of shikonin-induced immunogenic cell death: insights for developing cancer therapeutics. *Receptor Clin. Investig.,* **2016**, *3*(1), e1234.
[21] Krysko, D. V.; Garg, A. D.; Kaczmarek, A.; Krysko, O.; Agostinis, P.; Vandenabeele, P. Immunogenic cell death and DAMPs in cancer therapy. *Nat. Rev. Cancer,* **2012**, *12*(12), 860-875.
[22] Inoue, H.; Tani, K. Multimodal immunogenic cancer cell death as a consequence of anticancer cytotoxic treatments. *Cell. Death Differ.,* **2014**, *21*(1), 39-49.
[23] Chen, H.-M.; Wang, P.-H.; Chen, S.-S.; Wen, C.-C.; Chen, Y.-H.; Yang, W.-C.; Yang, N.-S. Shikonin induces immunogenic cell death in tumor cells and enhances dendritic cell-based cancer vaccine. *Cancer Immunol. Immunother.,* **2012**, *61*(11), 1989-2002.
[24] Lin, T.-J.; Lin, H.-T.; Chang, W.-T.; Hsiao, P.-W.; Yin, S.-Y.; Yang, N.-S. Shikonin-enhanced cell immunogenicity of tumor vaccine is mediated by the differential effects of DAMP components. *Mol. Cancer,* **2015**, *14*(1), 174.
[25] El-Najjar, N.; Chatila, M.; Moukadem, H.; Vuorela, H.; Ocker, M.; Gandesiri, M.; Schneider-Stock, R.; Gali-Muhtasib, H. Reactive oxygen species mediate thymoquinone-induced apoptosis and activate ERK and JNK signaling. *Apoptosis,* **2010**, *15*(2), 183-195.
[26] Hussain, A. R.; Ahmed, M.; Ahmed, S.; Manogaran, P.; Platanias, L. C.; Alvi, S. N.; Al-Kuraya, K. S.; Uddin, S. Thymoquinone suppresses growth and induces apoptosis *via* generation of reactive oxygen species in primary effusion lymphoma. *Free Radic. Bio. Med.,* **2011**, *50*(8), 978-987.
[27] Lu, J.-J.; Bao, J.-L.; Wu, G.-S.; Xu, W.-S.; Huang, M.-Q.; Chen, X.-P.; Wang, Y.-T., Quinones derived from plant secondary metabolites as anti-cancer agents. *Anti-Cancer Agents Med. Chem. (Formerly Curr. Med. Chem.-Anti-Cancer Agents),* **2013**, *13*(3), 456-463.

[28] Papageorgiou, V. P.; Assimopoulou, A. N.; Couladouros, E. A.; Hepworth, D.; Nicolaou, K. The chemistry and biology of alkannin, shikonin, and related naphthazarin natural products. *Angewandte Chemie Intl. Ed.,* **1999**, *38*(3), 270-301.

[29] Moore, R.E.; Scheuer, P.J. Nuclear magnetic resonance spectra of substituted naphthoquinones. influence of substituents on tautomerism, anisotropy, and stereochemistry in the naphthazarin system. *J. Org. Chem.,* **1966**, *31*(10), 3272-3283.

[30] Simizu, S.; Takada, M.; Umezawa, K.; Imoto, M. Requirement of caspase-3 (-like) protease-mediated hydrogen peroxide production for apoptosis induced by various anticancer drugs. *J. Biol. Chem.,* **1998**, *273*(41), 26900-26907.

[31] Wiench, B.; Eichhorn, T.; Paulsen, M.; Efferth, T. Shikonin directly targets mitochondria and causes mitochondrial dysfunction in cancer cells. *Evid.-Based Complement. Altern. Med.,* **2012**, *2012*, 1-15.

[32] Piao, J.-L.; Cui, Z.-G.; Furusawa, Y.; Ahmed, K.; Rehman, M. U.; Tabuchi, Y.; Kadowaki, M.; Kondo, T. The molecular mechanisms and gene expression profiling for shikonin-induced apoptotic and necroptotic cell death in U937 cells. *Chem-Biol. Interact.,* **2013**, *205*(2), 119-127.

[33] Mao, X.; Yu, C. R.; Li, W. H.; Li, W. X., Induction of apoptosis by shikonin through a ROS/JNK-mediated process in Bcr/Abl-positive chronic myelogenous leukemia (CML) cells. *Cell. Res.,* **2008**, *18*(8), 879-888.

[34] Papaiahgari, S.; Zhang, Q.; Kleeberger, S. R.; Cho, H.-Y.; Reddy, S. P. Hyperoxia stimulates an Nrf2-ARE transcriptional response *via* ROS-EGFR-PI3K-Akt/ERK MAP kinase signaling in pulmonary epithelial cells. *Antioxid. Redox Signal.,* **2006**, *8*(1-2), 43-52.

[35] Gong, K.; Li, W. Shikonin, a Chinese plant-derived naphthoquinone, induces apoptosis in hepatocellular carcinoma cells through reactive oxygen species: A potential new treatment for hepatocellular carcinoma. *Free Radic. Bio. Med.,* **2011**, *51*(12), 2259-2271.

[36] Lech, T.; Sadlik, J. Copper concentration in body tissues and fluids in normal subjects of southern Poland. *Biol. Trace Elem. Res.,* **2007**, *118*(1), 10-15.

[37] Hsu, P.-C.; Huang, Y.-T.; Tsai, M.-L.; Wang, Y.-J.; Lin, J.-K.; Pan, M.-H. Induction of apoptosis by shikonin through coordinative modulation of the Bcl-2 family, p27, and p53, release of cytochrome c, and sequential activation of caspases in human colorectal carcinoma cells. *J. Agr. Food Chem.,* **2004**, *52*(20), 6330-6337.

[38] Cheng, H.-M.; Qiu, Y.-K.; Wu, Z.; Zhao, Y.-F. DNA damage induced by shikonin in the presence of Cu (II) ions: potential mechanism of its activity to apoptotic cell death. *J. Asian Nat. Prod. Res.,* **2011**, *13*(01), 12-19.

[39] Jung, C. H.; Kim, J. H.; Hong, M. H.; Seog, H. M.; Oh, S. H.; Lee, P. J.; Kim, G. J.; Kim, H. M.; Um, J. Y.; Ko, S.-G. Phenolic-rich fraction from Rhus verniciflua Stokes (RVS) suppress inflammatory response *via* NF-κB and JNK pathway in lipopolysaccharide-induced RAW 264.7 macrophages. *J. Ethnopharmacol.,* **2007**, *110*(3), 490-497.

[40] Kook, S.-H.; Son, Y.-O.; Chung, S.-W.; Lee, S.-A.; Kim, J.-G.; Jeon, Y.-M.; Lee, J.-C., Caspase-independent death of human osteosarcoma cells by flavonoids is driven by p53-mediated mitochondrial stress and nuclear translocation of AIF and endonuclease G. *Apoptosis,* **2007**, *12*(7), 1289-1298.

[41] Iwashita, K.; Kobori, M.; Yamaki, K.; Tsushida, T., Flavonoids inhibit cell growth and induce apoptosis in B16 melanoma 4A5 cells. *Biosci. Biotechnol. Biochem.,* **2000**, *64*(9), 1813.

[42] Yang, L.-H.; Ho, Y.-J.; Lin, J.-F.; Yeh, C.-W.; Kao, S.-H.; Hsu, L.-S. Butein inhibits the proliferation of breast cancer cells through generation of reactive oxygen species and modulation of ERK and p38 activities. *Mol. Med. Reports,* **2012**, *6*(5), 1126-1132.

[43] Wei, X.-Y. The relationship between p38 MAPK pathway and cancer. *Practical J. Cancer,* **2009**, *24*(1), 101-103.

[44] Murphy, L.O.; Blenis, J. MAPK signal specificity: the right place at the right time. *Trends Biochem. Sci.,* **2006**, *31*(5), 268-275.

[45] Wu, Z.; Wu, L.-J.; Tashiro, S.; Onodera, S.; Ikejima, T. Phosphorylated extracellular signal-regulated kinase up-regulated p53 expression in shikonin-induced HeLa cell apoptosis. *Chin. Med. J. Peking,* **2005**, *118*(8), 671-677.

[46] Chang, I.-C.; Huang, Y.-J.; Chiang, T.-I.; Yeh, C.-W.; Hsu, L.-S. Shikonin induces apoptosis through reactive oxygen species/ extracellular signal-regulated kinase pathway in osteosarcoma cells. *Biol. Pharm. Bull.,* **2009**, *33*(5), 816-824.

[47] Lee, M.-J.; Kao, S.-H.; Hunag, J.-E.; Sheu, G.-T.; Yeh, C.-W.; Hseu, Y.-C.; Wang, C.-J.; Hsu, L.-S. Shikonin time-dependently induced necrosis or apoptosis in gastric cancer cells *via* generation of reactive oxygen species. *Chem-Biol. Interact.,* **2014**, *211*, 44-53.

[48] Singh, F.; Gao, D.; Lebwohl, M. G.; Wei, H. Shikonin modulates cell proliferation by inhibiting epidermal growth factor receptor signaling in human epidermoid carcinoma cells. *Cancer Lett.,* **2003**, *200*(2), 115-121.

[49] Elmore, S. Apoptosis: a review of programmed cell death. *Toxicol. Pathol.,* **2007**, *35*(4), 495-516.

[50] Dhanasekaran, D. N.; Reddy, E. P. JNK signaling in apoptosis. *Oncogene,* **2008**, *27*(48), 6245-6251.

[51] Ko, H.; Kim, S.; Shim, S.; Chang, H.; Ha, C. Shikonin induces the apoptotic cell death *via* regulation of p53 and Nrf2 in AGS human stomach carcinoma cells. *Biomol. Therapeut.,* **2016**, *24*(5), 501-509.

[52] Cuadrado, A.; Nebreda, A. R. Mechanisms and functions of p38 MAPK signalling. *Biochem. J.,* **2010**, *429*(3), 403-417.

[53] Xue, L. U.; Chun, L. I.; Yong-Kun, W.; Kun, J.; Xiao-Dong, G. A. I. Sorbitol induces apoptosis of human colorectal cancer cells *via* p38 MAPK signal transduction. *Oncol. Lett.,* **2014**, *7*(6), 1992-1996.

[54] Ahn, J.; Won, M.; Choi, J.-H.; Kim, Y.; Jung, C.-R.; Im, D.-S.; Kyun, M.-L.; Lee, K.; Song, K.-B.; Chung, K.-S. Reactive oxygen species-mediated activation of the Akt/ASK1/p38 signaling cascade and p21Cip1 downregulation are required for shikonin-induced apoptosis. *Apoptosis,* **2013**, *18*(7), 870-881.

[55] Kim, D. J.; Lee, J. H.; Park, H. R.; Choi, Y. W. Acetylshikonin inhibits growth of oral squamous cell carcinoma by inducing apoptosis. *Arch. Oral. Biol.,* **2016**, *70*, 149-157.

[56] Orrenius, S. Mitochondrial regulation of apoptotic cell death. *Toxicol. Lett.,* **2004**, *149*(1), 19-23.

[57] Haeberlein, S. L. B. Mitochondrial function in apoptotic neuronal cell death. *Neurochem. Res.,* **2004**, *29*(3), 521-530.

[58] Li, P.; Nijhawan, D.; Budihardjo, I.; Srinivasula, S. M.; Ahmad, M.; Alnemri, E. S.; Wang, X. Cytochrome c and dATP-dependent formation of Apaf-1/Caspase-9 complex initiates an apoptotic protease cascade. *Cell,* **1997**, *91*(4), 479-489.

[59] Wu, Z.; Wu, L.-j.; Tashiro, S.; Onodera, S.; Ikejima, T., Studies on the mechanisms of shikonin-induced A375-S2 cell apoptosis. *Chin. Pharmacol. Bull.,* **2005**, *21*(2), 202-205.

[60] Liu, C.; Yin, L.; Chen, J.; Chen, J. The apoptotic effect of shikonin on human papillary thyroid carcinoma cells through mitochondrial pathway. *Tumor Biol.,* **2014**, *35*(3), 1791-1798.

[61] Tang, X.; Zhang, C.; Wei, J.; Fang, Y.; Zhao, R.; Yu, J. Apoptosis is induced by shikonin through the mitochondrial signaling pathway. *Mol. Med. Reports,* **2016**, *13*(4), 3668-3674.

[62] Shahsavari, Z.; Karami-Tehrani, F.; Salami, S.; Ghasemzadeh, M. RIP1K and RIP3K provoked by shikonin induce cell cycle arrest in the triple negative breast cancer cell line, MDA-MB-468: necroptosis as a desperate programmed suicide pathway. *Tumor Biol.,* **2016**, *37*(4), 4479-4491.

[63] Park, S.; Shin, H.; Cho, Y. Shikonin induces programmed necrosis-like cell death through the formation of receptor interacting protein 1 and 3 complex. *Food Chem. Toxicol.,* **2013**, *55*, 36-41.

[64] Schenk, B.; Fulda, S. Reactive oxygen species regulate Smac mimetic/TNF[alpha]-induced necroptotic signaling and cell death. *Oncogene,* **2015**, *34*(47), 5796-5806.

[65] Fulda, S., Regulation of necroptosis signaling and cell death by reactive oxygen species. *Biol. Chem.,* **2016**, *397*(7), 657-660.

[66] Suh, J.; Rabson, A. B. NF-κB activation in human prostate cancer: Important mediator or epiphenomenon? *J. Cell. Biochem.,* **2004**, *91*(1), 100-117.

[67] Min, R.; Zun, Z.; Min, Y.; Wenhu, D.; Wenjun, Y.; Chenping, Z. Shikonin inhibits tumor invasion *via* down-regulation of NF-κB-mediated MMP-9 expression in human ACC-M cells. *Oral Dis.,* **2011**, *17*(4), 362-369.

[68] Schumacher, M.; Dicato, M.; Diederich, M. NF-κB Inhibitors from Terrestrial Plants Reported in 2011. *J. Food Drug Anal.,* **2012**, *20*.

[69] Liu, L. DNA topoisomerase poisons as antitumor drugs. *Ann. Rev. Biochem.,* **1989**, *58*(1), 351-375.

[70] Song, G.-Y.; Kim, Y.; Zheng, X.-G.; You, Y.-J.; Cho, H.; Chung, J.-H.; Sok, D.-E.; Ahn, B.-Z. Naphthazarin derivatives (IV): synthesis, inhibition of DNA topoisomerase I and cytotoxicity of 2-or 6-acyl-5, 8-dimethoxy-1, 4-naphthoquinones. *Eur. J. Med. Chem.,* **2000**, *35*(3), 291-298.

[71] Yang, F.; Chen, Y.; Duan, W.; Zhang, C.; Zhu, H.; Ding, J. SH-7, a new synthesized shikonin derivative, exerting its potent antitumor activities as a topoisomerase inhibitor. *Intl. J. Cancer,* **2006**, *119*(5), 1184-1193.

[72] Chen, C.; Shanmugasundaram, K.; Rigby, A.C.; Kung, A.L. Shikonin, a natural product from the root of Lithospermum erythrorhizon, is a cytotoxic DNA-binding agent. *Eur. J. Pharm. Sci.,* **2013**, *49*(1), 18-26.

[73] Radha, V.; Nambirajan, S.; Swarup, G. Association of Lyn tyrosine kinase with the nuclear matrix and cell-cycle-dependent changes in matrix-associated tyrosine kinase activity. *Eur. J. Biochem.,* **1996**, *236*(2), 352-359.

[74] Paul, M.K.; Mukhopadhyay, A.K. Tyrosine kinase - role and significance in cancer. *Intl. J. Med. Sci.,* **2004**, *1*(2), 101-115.

[75] Hashimoto, S.; Xu, Y.; Masuda, Y.; Aiuchi, T.; Nakajo, S.; Uehara, Y.; Shibuya, M.; Yamori, T.; Nakaya, K. β-hydroxyisovalerylshikonin is a novel and potent inhibitor of protein tyrosine kinases. *Cancer Sci.,* **2002**, *93*(8), 944-951.

[76] Shay, J. W.; Bacchetti, S. A survey of telomerase activity in human cancer. *Eur. J. Cancer,* **1997**, *33*(5), 787-791.

[77] Lu, Q.; Liu, W.; Ding, J.; Cai, J.; Duan, W. Shikonin derivatives: synthesis and inhibition of human telomerase. *Bioorg. Med. Chem. Lett.,* **2002**, *12*(10), 1375-1378.

[78] He, H.; Bai, L.-P.; Jiang, Z.-H. Synthesis and human telomeric G-quadruplex DNA-binding activity of glucosaminosides of shikonin/alkannin. *Bioorg. Med. Chem. Lett.,* **2012**, *22*(4), 1582-1586.

[79] Tamada, M.; Suematsu, M.; Saya, H. Pyruvate kinase M2: Multiple faces for conferring benefits on cancer cells. *Clin. Cancer Res.,* **2012**, *18*(20), 5554-5561.

[80] Chen, J.; Xie, J.; Jiang, Z.; Wang, B.; Wang, Y.; Hu, X. Shikonin and its analogs inhibit cancer cell glycolysis by targeting tumor pyruvate kinase-M2. *Oncogene,* **2011**, *30*(42), 4297-4306.

[81] Li, W.; Liu, J.; Zhao, Y. PKM2 inhibitor shikonin suppresses TPA-induced mitochondrial malfunction and proliferation of skin epidermal JB6 cells. *Mol. Carcinog.,* **2012**, *53*(5), 403-12.

[82] Rajani, D. K.; Walch, M.; Martinvalet, D.; Thomas, M. P.; Lieberman, J. Alterations in RNA processing during immune-mediated programmed cell death. *Proc. Nat. Acad. Sci.,* **2012**, *109*(22), 8688-8693.

[83] Yin, S.; Efferth, T.; Jian, F.; Chen, Y.; Liu, C.; Wang, A.; Chen, Y.; Hsiao, P.; Yang, N. Immunogenicity of mammary tumor cells can be induced by shikonin *via* direct binding-interference with hnRNPA1. *Oncotarget,* **2016**, *7*(28), 43629-43653.

[84] Ouyang, L.; Shi, Z.; Zhao, S.; Wang, F. T.; Zhou, T. T.; Liu, B.; Bao, J. K. Programmed cell death pathways in cancer: a review of apoptosis, autophagy and programmed necrosis. *Cell. Proliferat.,* **2012**, *45* (6), 487-498.

[85] Inoue, H.; Tani, K. Multimodal immunogenic cancer cell death as a consequence of anticancer cytotoxic treatments. *Cell Death Differentiat.,* **2014**, *21*(1), 39-49.

[86] Wada, N.; Kawano, Y.; Fujiwara, S.; Kikukawa, Y.; Okuno, Y.; Tasaki, M.; Ueda, M.; Ando, Y.; Yoshinaga, K.; Ri, M. Shikonin, dually functions as a proteasome inhibitor and a necroptosis inducer in multiple myeloma cells. *Intl. J. Oncol.,* **2015**, *46*(3), 963-972.

[87] Zhao, Q.; Assimopoulou, A. N.; Klauck, S. M.; Damianakos, H.; Chinou, I.; Kretschmer, N.; Rios, J.-L.; Papageorgiou, V. P.; Bauer, R.; Efferth, T. Inhibition of c-MYC with involvement of ERK/JNK/MAPK and AKT pathways as a novel mechanism for shikonin and its derivatives in killing leukemia cells. *Oncotarget,* **2015**, *6*(36), 38934.

[88] Zhou, W.; Zhang, X.; Xiao, L.; Ding, J.; Liu, Q.-H.; Li, S.-S. Semisynthesis and antitumor activity of 6-isomers of 5, 8-O-dimethyl acylshikonin derivatives. *Eur. J. Med. Chem.,* **2011**, *46*(8), 3420-3427.

[89] Wang, R.; Zhang, X.; Song, H.; Zhou, S.; Li, S. Synthesis and evaluation of novel alkannin and shikonin oxime derivatives as potent antitumor agents. *Bioorg. Med. Chem. Lett.,* **2014**, *24*(17), 4304-4307.

[90] Zhang, X.; Cui, J.; Zhou, W.; Li, S., Design, synthesis and anticancer activity of shikonin and alkannin derivatives with different substituents on the naphthazarin scaffold. *Chem. Res. Chin. Univ.,* **2015**, *31*(3), 394-400.

[91] Zhang, X.; Wang, R.-B.; Zhou, W.; Xiao, S.; Meng, Q.-Q.; Li, S.-S. Antitumor activity of DMAKO-05, a novel shikonin derivative, and its metabolism in rat liver microsome. *AAPS Pharm SciTech,* **2014**, *16*(2), 259-266.

BENTHAM SCIENCE

REGISTER TO OUR FREE NEWSLETTER FOR UPDATES

Search here...

0



ISSN (Print): 1573-4129
ISSN (Online): 1875-676X

Download PDF Flyer

Current Pharmaceutical Analysis

Impact Factor: 0.6

Indexed in: Scopus, SCI Expanded, JCR... *View all*

Volume 20 , Issues 9, 2024

Back | Journal Home | Call For Paper | Institutional Members

Limite
Compleme
Of

Publish R
Articles
Char

Volume 13, Issue 5, 2017

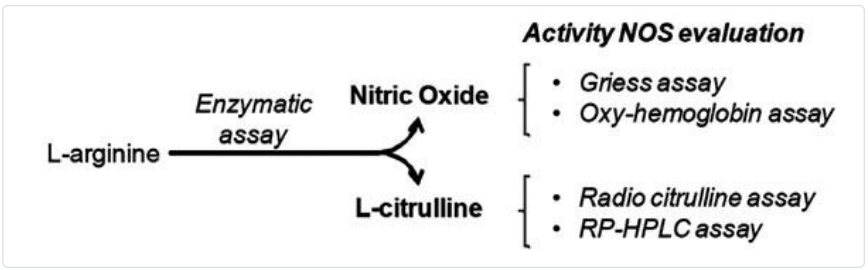
Review Article

Methods to Evaluate the Activity of Nitric Oxide Synthase

Pp: 411-416

Author(s): Marialuigia Fantacuzzi*, Alessandra Ammazzalorso, Barbara De Filippis, Letizia Giampietro, Cristina Maccallini and Rosa Amoroso

DOI: 10.2174/1573412912666160916154405

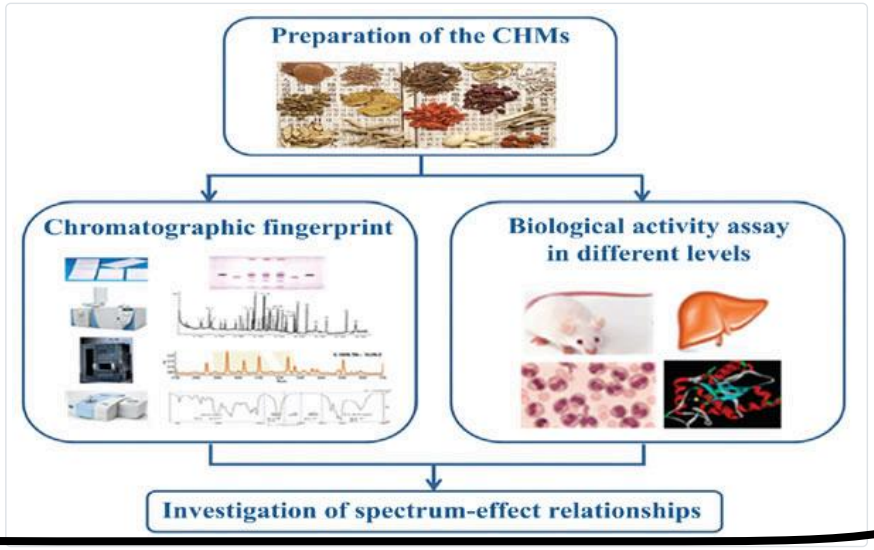


Add to Wish List | Purchase PDF

Research Article

An Approach for Searching Bioactive Compounds from Traditional Chinese Plant Food and Herb Medicines by Investigating Spectrum–Effect Relationships

Pp: 417-426
Author(s): Xu Zhang, Li-Fang Zhang, Chen-Yuan Cai, Fei-Qun Xue* and Sui Xiao*
DOI: 10.2174/1573412912666160616105314

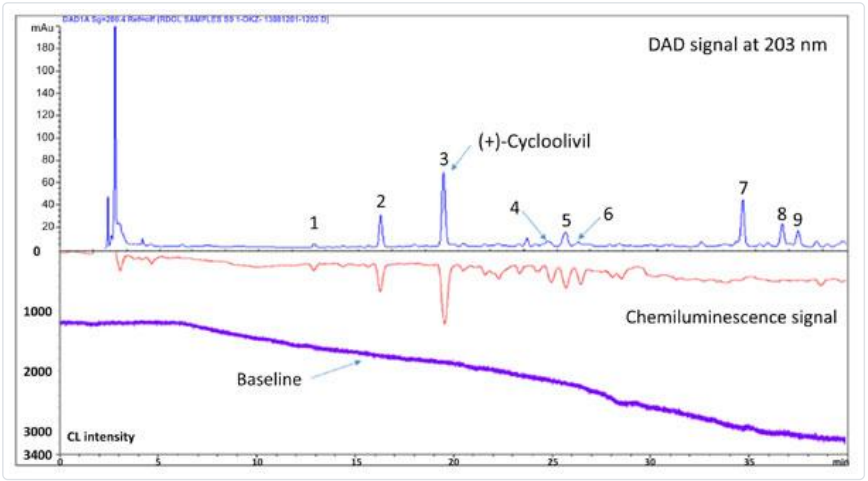


Add to Wish List | Purchase PDF

Research Article

Identification of Antioxidative Components in *ChuanKeZhi* Injection and Discussion on Its Quality Control Method

Pp: 427-432
Author(s): Shuai Sun*, Hailing Liu, Yijuan Xu, Longgang Guo, Shunjun Xu, Liu Yang and Peishan Xie
DOI: 10.2174/1573412912666160919115110



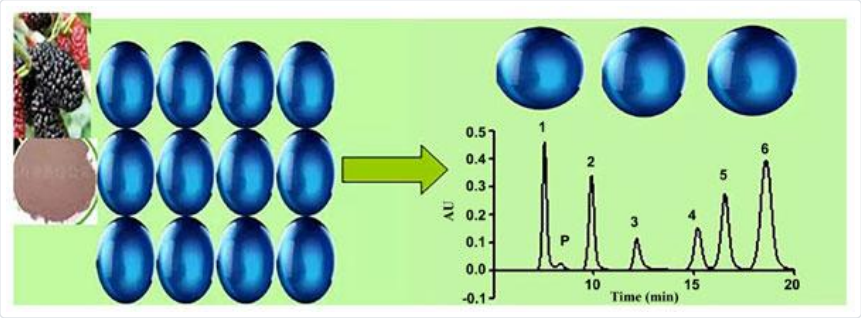
Add to Wish List | Purchase PDF

Research Article

open access plus

Compositional Monosaccharide Analysis of *Morus nigra* Linn by HPLC and HPCE Quantitative Determination and Comparison of Polysaccharide from *Morus nigra* Linn by HPCE and HPLC

Pp: 433-437
Author(s): Xiao-Li Ma*, Feng Feng Song, Hui Zhang, Xie Huan and Song Ya Li
DOI: 10.2174/1573412913666170330150807

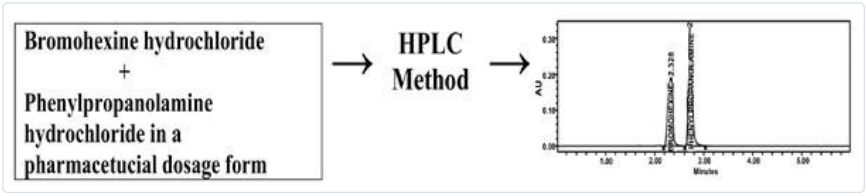


Download PDF File

Research Article

Analytical Method Development and Validation for Concurrent Determination of Bromohexine and Phenylpropanolamine by Reverse Phase-HPLC Method

Pp: 438-445
Author(s): Kishor Kumar Erukulla and S. R. Suseem*
DOI: 10.2174/1573412912666161004144334

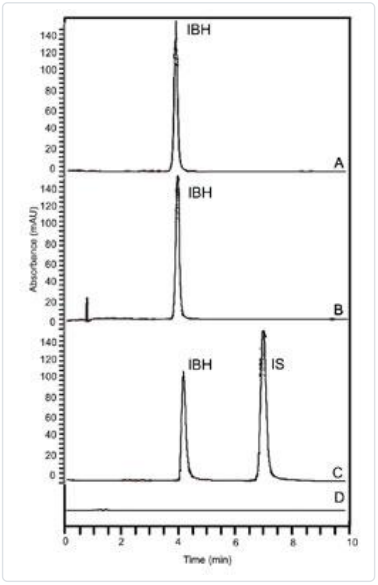


Add to Wish List | Purchase PDF

Research Article

Quantitative Determination and Validation of Ivabradine-HCl in Pharmaceutical Formulation and Rabbit Plasma by High Performan ce Liquid Chromatography Method

Pp: 446-451
Author(s): Nazar Muhammad Ranjha, Abdul Majeed*, Ikhlaq Hussain and Muhammad Fawad Rasool
DOI: 10.2174/1573412913666161213105900

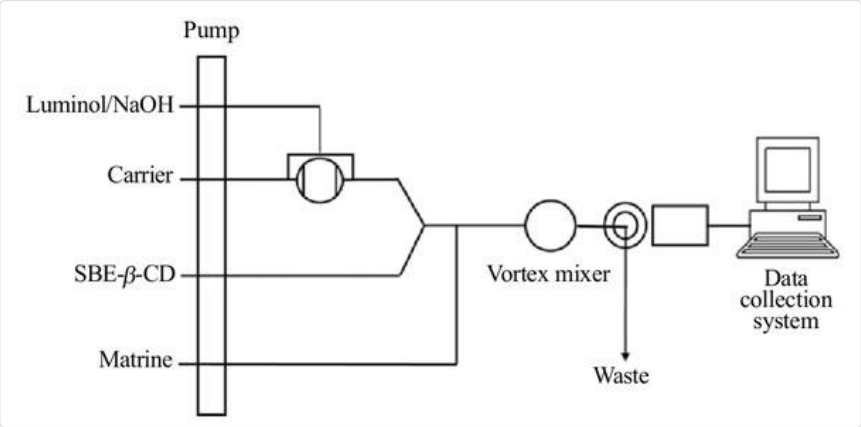


Add to Wish List | Purchase PDF

Research Article

A Highly Sensitive Chemiluminescence Method and Application in Rapid Pharmacokinetic Study of Matrine in Rat Plasma

Pp: 452-461
Author(s): Xun-Yu Xiong*, Hong-Jiang Yu and Ye-Fei Nan
DOI: 10.2174/1573412913666161110111715

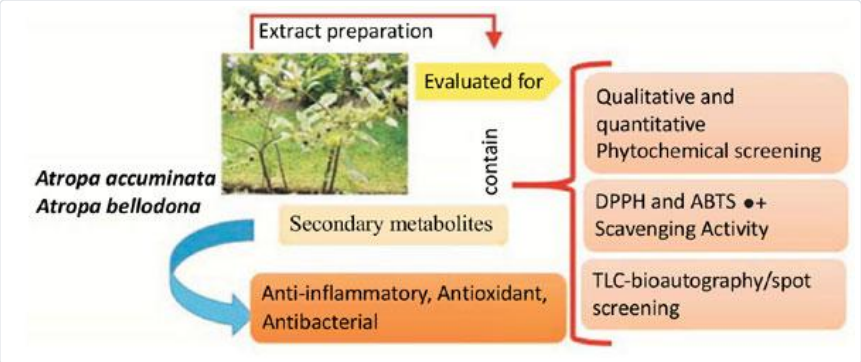


Add to Wish List | Purchase PDF

Research Article

Analysis of TLC-Bioautography and TLC-Spot Visualization of *Atropa accuminata* and *Atropa belladonna* Extracts as Antioxidant and Antibacterial Agents Against Human Pathogenic Bacteria

Pp: 462-472
Author(s): Saeeda Hussain, Muhammad Babar, Sozana Kousar, Samna Wazir, Farwa Fareed, Farooq Latif, Saiqa Andleeb and Shaukat Ali*
DOI: 10.2174/1573412913666170117162851

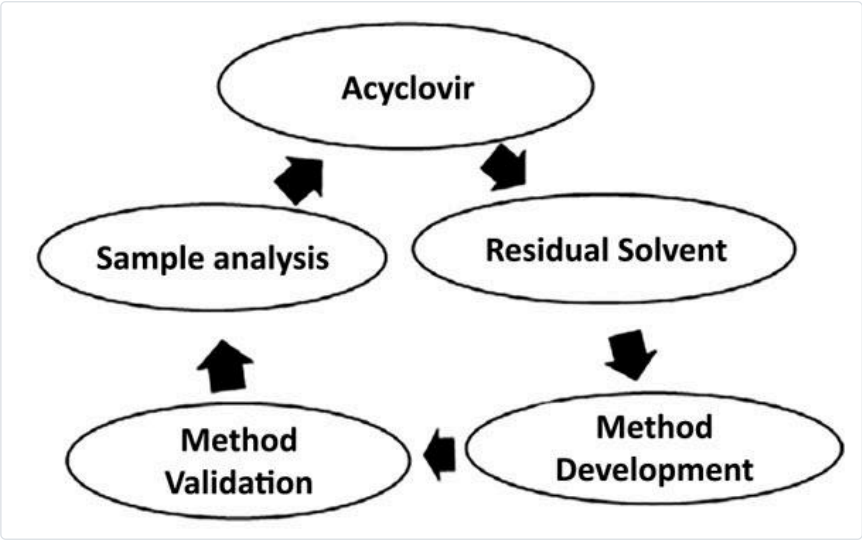


Add to Wish List | Purchase PDF

Research Article

Identification and Determination of Potential Impurities Present in the Acyclovir Drug Substance by GC-MS

Pp: 473-480
Author(s): Natarajan Sivanandham* and Kempegowda Bommanadoddi Kempegowda
DOI: 10.2174/1573412913666170321110612

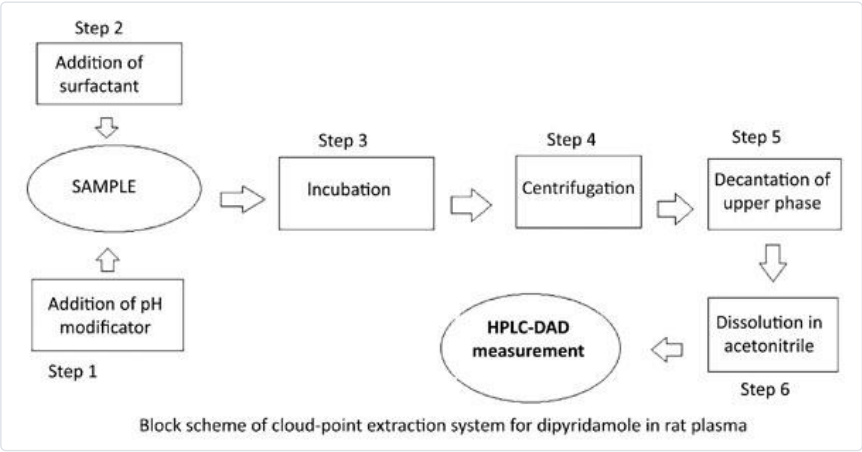


Add to Wish List | Purchase PDF

Research Article

Cloud-Point Extraction Coupled with High-Performance Liquid Chromatography for the Determination and Pharmacokinetic Study of Dipyridamole in Rat Plasma

Pp: 481-487
Author(s): Jiajia Li, Yulan Li, Jingjing Liu, Min Liu and Kang Li*
DOI: 10.2174/1573412913666170329143017



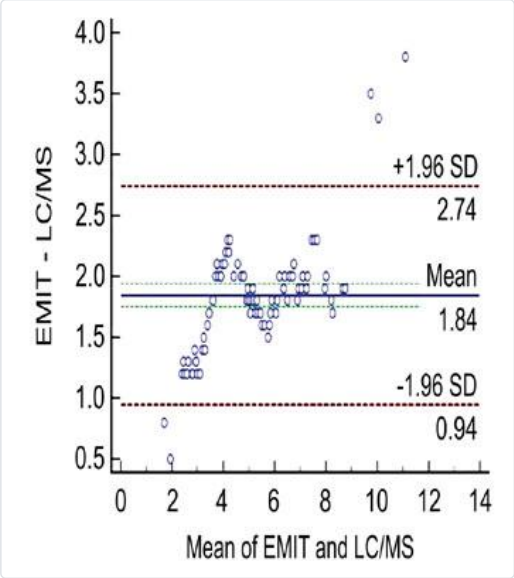
Block scheme of cloud-point extraction system for dipyridamole in rat plasma

Add to Wish List | Purchase PDF

Research Article

Comparative Study of LC/MS and EMIT in Therapeutic Monitoring of Carbamazepine and its Clinical Applications

Pp: 488-493
Author(s): Abdul Sami Shaikh, Fanlong Bu, Huanjun Liu, Chunmei Geng, Pingli Li, Meimei Gao, Rui Zhang* and Ruichen Guo*
DOI: 10.2174/1573412913666170427120250



Add to Wish List | Purchase PDF

FIND YOUR INSTITUTION

Journal Information

About Journal

Editorial Board

Current Issue

Volumes /Issues

For Authors

For Editors

For Reviewers

Explore Articles

Open Access

For Visitors

BENTHAM SCIENCE



Quick Links

Journals | Books | Submit Articles | Alerting Services | Open Access Plus (Gold Open Access) | Funding Agencies | Online Store | Endorsements | Author's Comments & Reviews | Newsletters | Press Release | Terms and Conditions



© 2024 Bentham Science Publishers | Privacy Policy

Current Pharmaceutical Analysis, 2017, *13*, 417-426

RESEARCH ARTICLE

An Approach for Searching Bioactive Compounds from Traditional Chinese Plant Food and Herb Medicines by Investigating Spectrum–Effect Relationships

Xu Zhang[a,c], Li-Fang Zhang[b], Chen-Yuan Cai[b], Fei-Qun Xue[b,*] and Sui Xiao[a,c*]

[a]*College of Forestry and Landscape Architecture, South China Agricultural University, 510642, Guangzhou, China;* [b]*Key Laboratory of Veterinary Drug Safety Evaluation and Residues Research, Shanghai Veterinary Research Institute, Chinese Academy of Agricultural Sciences, 200241, Shanghai, China;* [c]*Guangdong Key Laboratory for Innovative Development and Utilization of Forest Plant Germplasm, 510642, Guangzhou, China*

ARTICLE HISTORY

Received: April 7, 2016
Revised: June 9, 2016
Accepted: June 16, 2016

DOI:
10.2174/1573412912666160616105314

Abstract: ***Background:*** *Acalypha australis* Linn. (*A. australis*) was a kind of traditional Chinese plant food with high nutrition and was usually used to treat diarrhoea and other bacterial diseases clinically in China. The purpose of this paper was to establish a rapid and effective approach for searching bioactive compounds from *A. australis* species.

Method: The chromatographic fingerprints were established using ultra-performance liquid chromatography/mass spectrometry (UPLC/MS), and the antibacterial activities were also studied with agar-diffusion and broth microdilution methods. Moreover, correlational analysis, stepwise regression and partial least-square regression were performed to explore the relationship between the compositions and bioactivities and to identify the active compounds from *A. australis*. All the characteristic peaks in the UPLC/MS fingerprint were separated with semi-preparative HPLC and subsequently confirmed with ultra-performance liquid chromatography/time-of-flight mass spectrometry (UPLC-Q-TOF-MS).

Result: Apart from nicotinic acid, gallic acid, protocatechuic acid, *p*-hydroxybenzoic acid, australisin, and quercetin, $C_{13}H_8O_8$, $C_{22}H_{12}O_{13}$ and $C_{27}H_{22}O_{18}$ were first found to be the main antibacterial components in *A. australis*. Among them, seven were identified by the "spectrum–effect relationship" strategy, while two minor active compounds were not conjectured in this study.

Conclusion: This work successfully provides a general model that combined the chromatographic fingerprint and bioactivity assay to study the spectrum–effect relationships, which could be used to discover the primary active ingredients in traditional Chinese plant food and herb medicines.

Keywords: Chinese herb medicines, *Acalypha australis* Linn., spectrum-effect relationships, bioactive compound, chromatographic fingerprints, antibacterial activity.

1. INTRODUCTION

Chinese herbal medicines (CHMs) have been widely used among billions of people around the world for thousands of years. Extracts from these medical plants contain a variety of chemical compositions with potent biological activities. Unfortunately, screening and analysing the bioactive compounds they contained contain are often extremely difficult because of their complex nature. However, the screening and analysis of bioactive compounds in CHMs are very important for the pharmaceutical discovery process. In the traditional method, all the defined compounds in these medical plants are separated and used for the bioactivity assay one by one to seek the lead compound [1, 2]. Apparently, the traditional approach is time consuming, arduous and unsuitable for drug discovery from CHMs. Researchers need a drug discovery procedure that can hit the target as accurately, quickly and profitably as possible. Some techniques have been widely applied to search for new drug leads, such as biotechnology, on-line screening approaches, affinity chromatography and bioassay-guided fractionation [3-9]. However, all these strategies have drawbacks and limitation in-

*Address correspondence to these authors at the College of Forestry and Landscape Architecture, South China Agricultural University, 483 Wushan road, Tianhe, Guangzhou. 510642, People's Republic of China; Tel:/Fax: +86-20-85280256
Shanghai Veterinary Research Institute, Chinese Academy of Agricultural Sciences, Key Laboratory of Veterinary Drug Safety Evaluation and Residues Research, 518 Ziyue road, Minhang, Shanghai 200241, People's Republic of China; Tel:/Fax: +86 21 3429 3396;
E-mails: suixiao@outlook.com, fqxue@outlook.com

1875-676X/17 $58.00+.00 © 2017 Bentham Science Publishers

Current Pharmaceutical Analysis

cluding special apparatus, rigorous experimental conditions, increased running costs and synergistic active constituents that may be reduced or may disappear upon the isolation procedure [10]. Therefore, new alternative approaches for active compound discovery should be established, taking into consideration the unique characteristics of CHMs.

Biological activity is largely dependent on the combination of the different active components of CHMs. With When the amount and proportion of the active components varying, the biological activity changes accordingly. Certain relationships exist between the chemical composition and the biological activity of CHMs. Synthetic analytical methods, such as chromatographic fingerprint [11-18] that is indicative of the combined constituents, are suitable for investigating the characteristics of CHMs. The application of the UPLC/MS system has been gaining considerable interest. This system adpoted in the research on CHMs can dramatically improve peak resolution, sensitivity and speed of analysis [19, 20]. Coupled with bioactivity assay, certain chemometrics and statistics methods, the UPLC/MS chromatographic fingerprint was beneficial to explore the relationship between the chemical composition and biological activity (spectrum–effect relationships) of CHMs [21-24]. This approach to rapidly and accurately search for the active compounds from CHMs is possible.

Acalypha australis Linn. (*A. australis*) was a kind of traditional Chinese plant food with high nutrition and was also used as the model herb plant in the present study to explore feasibility of this approach for screening active compounds from CHMs. *A. australis* with obvious appearance is usually used as a folk medicine to treat diarrhoea and other bacterial diseases, and it grows in farmlands and roadsides in most provinces of China [25]. This herb medicine was found to show strong antibacterial activity against the most prevalent two pathogenic bacteria *Aeromonas hydrophila (A. hydrophila)* and *Aeromonas sobria (A. sobria*), especially in marine lives. Thus, in the present study, UPLC/MS was applied to establish the chromatographic fingerprints of *A. australis*. The growth of *A. hydrophila* and *A. sobria* was selected as antibacterial models to evaluate the biological activities of samples from various sources. Aided by certain chemometrics and statistics methods like correlational analysis, stepwise regression and partial least-squares regression, the combination of UPLC/MS fingerprints and antibacterial activities was use to define the active compounds of *A. australis*. This work aimed at providing a reasonable strategy of spectrum–effect relationships for identifying active compounds from CHMs.

2. MATERIALS AND METHODS

2.1. Reagents and Materials

The reference standards of nicotinic acid, gallic acid, protocatechuic acid, p-hydroxybenzoic acid and quercetin were obtained from the National Institute for the Control of Pharmaceutical and Biological Products of China, Beijing, China. Berberine hydrochloride was obtained from Aladdin Reagent Company (Shanghai, China). The purity of all compounds was more than 98%. HPLC-grade acetonitrile and formic acid were purchased from Fisher Chemicals (Pittsburgh, PA, USA). Water was purified using a Milli-Q water purification system (Millipore, Bedford, MA, USA). *A. australis* samples were purchased from the Chinese herbal medicine markets in several provinces of China and authenticated by Professor LiHong Wu (Institute of Chinese Materia Medica, Shanghai University of Traditional Chinese Medicine, Shanghai, China). The voucher specimens were deposited at the Shanghai Veterinary Research Institute, Chinese Academy of Agricultural Sciences (Shanghai, China). The raw herbs were labelled according to their species, sources and harvesting times (Table **1**).

Aeromonas hydrophila (A. hydrophila) (0388) and *Aeromonas sobria (A. sobria*) (0398) were incubated in Mueller–Hinton (MH) broth and then adjusted to yield approximately 10^7 CFU/mL of each culture in fresh MH broth. The strains were supplied by the National Pathogen Collection Center for Aquatic Animals (Shanghai, China). The aforementioned bacterial suspension was prepared prior to use in the antibacterial assay.

2.2. Analyses of UPLC/MS Fingerprints

Chromatographic fingerprints of *A. australis* from various sources were performed on a Waters ACQUITY™ SQD with UPLC/MS system (Waters, Milford, MA, USA). The conditions of the instrument and the preparation of reference standard solutions and sample solutions were described in detail in our previous published paper [26]. Precision and repeatability of this method were evaluated by analysing five replicate injections of one sample and injections of five samples prepared independently from S1 (Table **1**), respectively. The stability study of the sample was performed at different intervals over 24 h (0, 2, 4, 8, 16 and 24 h).

The reference fingerprint was created using the professional software Similarity Evaluation System for chromatographic fingerprint of Traditional Chinese Medicine, (TCM) devised by the Chinese Pharmacopoeia Committee (Version 2004A). The median method was from a general comparison of the chromatograms of 14 tested samples. The similarity values between the reference fingerprint and the chromatograms of *A. australis* samples were calculated using this software [27].

Hierarchical clustering analysis (HCA) of the *A. australis* samples S1 to S14 was performed using the SPSS statistics software (SPSS for Windows 18.0, SPSS Inc., USA). The ward linkage method was applied [28].

2.3. Antibacterial Assay

The sample preparation for the antibacterial experiments and the processes of the antibacterial assay had been described in detail in our published paper [26].

2.4. Establishment of Spectrum–Effect Relationships

2.4.1. Correlational Analysis (CA) Method

To determine the antibacterial constituents in the UPLC/MS fingerprints of *A. australis*, CA was used to explore the association between the area values of common characteristic peaks and antibacterial activities. In the present study, the relevance and variation tendency between these two sets of variables were evaluated by CA using the SPSS

Table 1. ***A. australis*** **samples with voucher number, species, origin, collection time and the antibacterial activities on** ***A. hydrophila*** **and** ***A. sobria.***

Sample No.	Species	Origin	Collection time	*Aeromonas hydrophila*		*Aeromonas sobria*	
				Inhibition zone (mm)	MIC (mg/mL)	Inhibition zone (mm)	MIC (mg/mL)
1	*A. australis* (Purple stems)	Anhui	August 2010	30.1±0.7	0.781	29.2±0.6	0.781
2	*A. australis* (White stems)	Hunan	August 2011	28.4±0.8	1.563	27.8±0.7	1.563
3	*A. australis* (Purple stems)	Hunan	July 2011	37.7±0.6	0.781	36.0±1.0	0.781
4	*A. australis* (White stems)	Guangdong	July 2011	35.9±1.0	0.781	35.1±0.8	0.781
5	*A. australis* (Purple stems)	Jiangsu	May 2009	29.1±0.5	0.781	28.0±0.5	0.781
6	*A. australis* (White stems)	Shanghai	June 2011	25.6±1.3	3.125	24.8±1.1	3.125
7	*A. australis* (Purple stems)	Shanghai	June 2011	32.0±1.5	0.781	32.4±0.6	0.781
8	*A. australis* (Purple stems)	Jiangsu	July 2011	38.5±0.8	0.391	36.3±1.4	0.391
9	*A. australis* (Purple stems)	Jilin	July 2011	26.9±0.6	1.563	27.0±1.3	1.563
10	*A. australis* (Purple stems)	Hubei	June 2011	27.2±1.3	1.563	27.4±1.2	1.563
11	*A. australis* (Purple stems)	Yunnan	July 2011	30.4±1.4	0.781	30.1±1.0	0.781
12	*A. australis* (Purple stems)	Anhui	July 2011	31.4±0.9	0.781	30.9±0.7	0.781
13	*A. australis* (Purple stems)	Henan	July 2011	29.5±0.6	0.781	28.8±0.7	0.781
14	*A. australis* (Purple stems)	Jiangsu	April 2012	12.3±1.0	25.000	10.9±0.8	25.000

Inhibition zone was measured by the agar-diffusion method at a concentration of 100 mg/mL of crude extract. MIC value was measured by broth microdilution method.
All data were given as the average between three separated tests. Mean value of inhibition zone n = 3 ± standard error. Inhibition zone (mm) including the diameter of hole (6mm).

statistics software (SPSS for Windows 18.0, SPSS Inc., USA).

2.4.2. Stepwise Regression (SR) Method

The area values of the common characteristic peaks in the UPLC/MS fingerprint of *A. australis* were regarded as independent variables, and the values of antibacterial activities were regarded as dependent variables. SR was performed using the SPSS statistics software (SPSS for Windows 18.0, SPSS Inc., USA) to pick out the most important independent variables (active compounds) that significantly affected the dependent variables (antibacterial effect).

2.4.3. Partial Least-Square Regression (PLSR)

PLSR was applied in this work to correlate the UPLC/MS fingerprint data (*X*-matrix) with related antibacterial activity data (*Y*-matrix). First, the original variables were transformed into a set of integrated variables that could explain the most information from the original variables. The values of variable importance in projection (VIP) of these independent variables (characteristic peaks) were then investigated, and values greater than 1 meant that those independent variables (characteristic peaks) can significantly explain the information on the dependent variables [29]. PLSR was performed using the SPSS statistics software (SPSS for Windows 18.0, SPSS Inc., USA).

2.5. Isolation and Identification of Antibacterial Compounds

2.5.1. Isolation of Antibacterial Compounds

The sample preparation and the isolation processes of the chemical compounds of *A. australis with* semi-preparative HPLC have been described in detail in our published paper [26].

2.5.2. UPLC-Q –TOF-MS Analysis

The controls and samples were analysed on a Triple TOF 4600 MS/MS system (AB SCIEX, Foster City, CA, USA) coupled to Waters UPLC ACQUITY^{TM} system. The chromatographic conditions had have been described in our published paper [26]. The mass spectrometer was operated in the positive or negative ESI mode with a Duo Spray TM source (AB SCIEX, USA), and the mass range was set at m/z 100–800. The following parameter settings were also used: 5500 V ion spray voltage, 700 °C ion source heater, 35 psi curtain gas and 45 psi ion source gas. The MS/MS experiments were run as 150 ms accumulation time for TOF/MS and 80 ms accumulation time in the MS/MS experiments. The collision energy was 35 eV, and the collision energy spread was 15 in the MS/MS experiments [30, 31].

3. RESULTS

3.1. UPLC/MS Fingerprints and Similarity Evaluation

Based on careful selection of the extraction process and the UPLC/MS analytical conditions described in our previous paper [26], the results of methodology validation showed that the relative standard deviation for precision was less than 3% and that for reproducibility was less than 3.98%. The storage stability was less than 3.06% of the 20 common peaks in the UPLC/MS fingerprints. All the results indicated that the method of fingerprint analysis was valid and satisfactory. The UPLC/MS fingerprints of *A. australis* samples from various sources were then obtained under the optimal conditions, and the reference atlas was created by similarity evaluation system (Fig. **1**). Twenty peaks with large areas and good segregation were regarded as "common peaks", and the average relative retention time and average peak area (n = 3) of the 20 common peaks were shown in Table **2**. The coefficients of variance (C.V. %) of the peak areas of the 20 common peaks were within the range of 12.0%–49.2%, showing that the amount of each constituent varied significantly in different samples. The similarities between the reference atlas and the entire chromatographic profiles of 14 batches of *A. australis* samples were evaluated, and the correlation coefficients were 0.963, 0.912, 0.971, 0.981, 0.938, 0.898, 0.969, 0.990, 0.927, 0.892, 0.951, 0.935, 0.924 and 0.836. The results showed that the entire chromatograms of the samples from various sources revealed significant differences.

3.2. Antibacterial Activities of the *A. australis* Samples

In the investigation of the antibacterial activities against *A. hydrophila* and *A. sobria*, the zones of inhibition ranged from 10.9 mm to 38.5 mm, and the MIC values ranged from 0.391 mg/mL to 25 mg/mL for the extracts of 14 various samples (Table **1**). In this study, the obvious difference of the samples in antibacterial activities was probably associated with their different species, origin, collection time and so on. Essentially, these abovementioned reasons resulted in variances in the amount and proportion of the active ingredients among different samples. The general results showed that the magnitude of the antibacterial activities of the *A. australis* samples on *A. hydrophila* and *A. sobria* was S8 > S3 > S4 > S7 > S12 > S11 > S1 > S13 > S5 > S2 > S10 > S9 > S6 > S14. Sample 8, with the smallest MIC value and the

Table 2. The average relative retention time and peak area of each common peak.

Peak Number	Relative Retention Time[a]	Average Peak Area of Every Common Peak														
		S1[a]	S2[a]	S3[a]	S4[a]	S5[a]	S6[a]	S7[a]	S8[a]	S9[a]	S10[a]	S11[a]	S12[a]	S13[a]	S14[a]	C.V.[b](%)
1	2.92	591381	458622	687934	700003	482760	494829	573278	603451	422415	512933	543105	681899	567243	120690	27.5
2	6.3	333986	268382	465196	524836	357843	65378	447303	596405	115125	191579	429411	399591	369771	274346	43.7
3	7.35	145937	163450	136597	122587	74720	141267	91065	116750	58375	127257	54872	84060	68882	122587	32.7
4	7.96	118820	132891	109440	187611	101622	121947	234514	156343	136018	281417	148525	96932	140708	128201	34.9
5	10.75	237990	243525	218619	304406	182643	348683	199247	276733	210317	381891	406797	249059	166039	226921	28.4
6	12.41	145112	132253	156133	168991	126743	108374	178175	183686	121232	113885	165317	148785	137764	62453	23.1
7	14.14	310614	347397	490443	388268	318788	241135	449573	408703	265656	286092	376007	367833	335136	85828	29.7
8	14.62	332571	430386	348221	410823	359959	356047	352134	391260	293445	469512	449949	336483	313008	38734	29.6
9	16.98	973640	963806	1003145	1032649	924467	678598	914632	983475	934301	688433	1022815	993310	944136	672697	14.2
10	18.63	280061	247327	327344	341893	254601	238880	312796	363716	113713	110550	294610	323707	250964	98203	34.6
11	20.02	700200	558268	993528	927293	662352	60723	898906	946217	174085	287065	775898	756974	615041	293327	49.2
12	21.01	284346	358523	370886	296708	280225	333797	445063	412095	420337	267862	288467	255499	473909	317313	20.7
13	21.54	763677	1078132	970318	826568	718754	943365	664848	898443	916412	1006256	637895	1042194	557035	583988	21.1
14	22.13	441459	388676	417467	374281	455855	427064	369482	479847	470250	364684	623801	407870	398273	431862	15.3
15	24.48	312980	324903	283172	238461	304038	244422	336826	298076	265288	226538	211634	217595	315961	271249	15.3
16	27.17	257739	364851	267781	381588	358157	391629	324684	334726	301253	311295	351462	284517	291212	341421	12.8
17	30.15	359760	348399	340826	325678	268873	302956	337039	378695	287808	371121	299169	310530	257513	280234	12.0
18	30.97	296763	309666	348374	395683	537614	387082	339772	430091	356976	520410	279559	503206	481702	326869	22.1
19	31.95	414023	314795	400337	359276	307951	283999	249783	342168	349011	437975	379806	263469	434553	338780	17.4
20	34.92	349538	250950	337588	274850	244975	259913	283813	298750	352525	233025	328625	253948	230038	268875	15.2

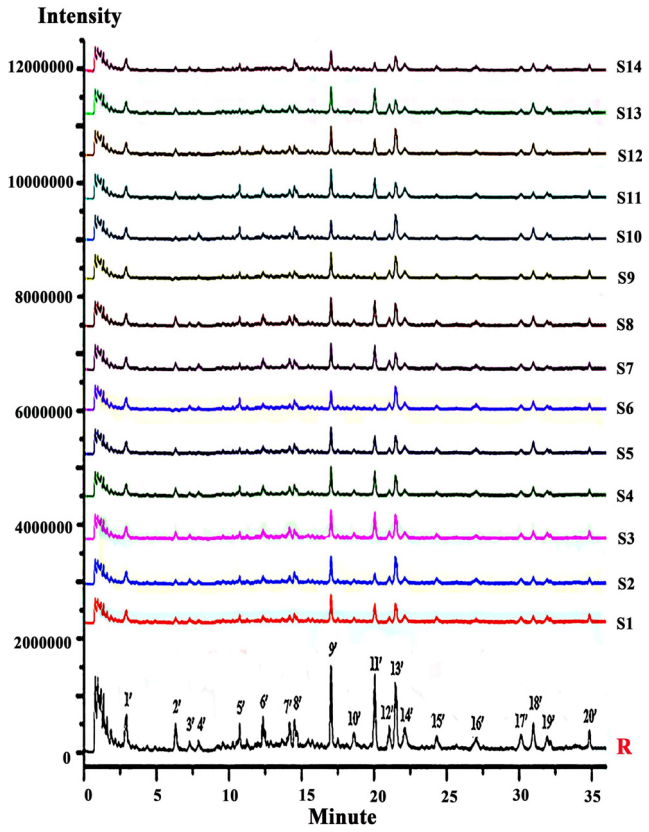


Fig. (1). The UPLC/MS fingerprints of the extracts of *A. australis* from various sources and the reference atlas (R) from the fourteen chromatograms.

largest zones of inhibition, had the strongest antibacterial activity, whereas sample 14 had the weakest activity. Samples 8 and 14 were collected from Jiangsu Province and belonged to the same species, but these two samples were collected at different harvesting times. It seemed that collection time significantly influenced the antibacterial activity of *A. australis*. Furthermore, different antibacterial activities were found in samples 2, 8, 9, 11, 12 and 13, all of these samples were collected at the same harvesting time and belonged to the same species, however, these samples were harvested from Hunan, Jiangsu, Jilin, Yunnan, Anhui and Henan provinces, respectively. This results indicated that the given activities were likely related to the production region of *A. australis*. In addition, strong activities of samples 3 and 7 were exhibited from the *A. australis* species with purple stems, whereas weak activities of samples 2 and 6 were displayed from the *A. australis* species with white stems. Thus, maybe species was an important contribution factor to the antibacterial activity of this herb.

3.3. Spectrum–Effect Relationships

3.3.1. Results of the HCA

To assess the clustering tendency, HCA of the 14 samples was performed, to reveal natural groupings of the data set. The results of the HCA analysis were shown in Fig. (**2**). The samples could be clearly divided into three clusters: cluster I was formed including samples 1, 3, 4, 8, 7 and 11;

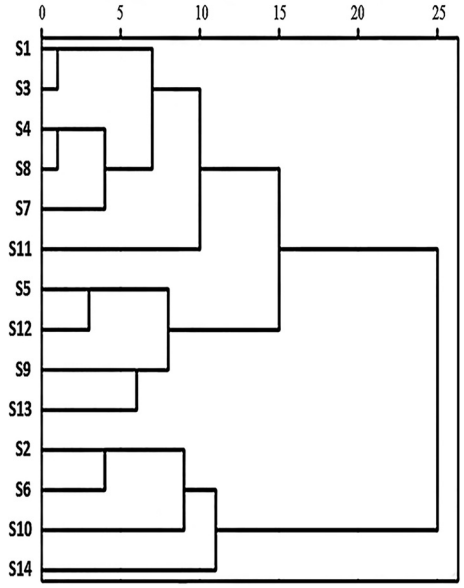


Fig. (2). HCA of UPLC/MS fingerprints of *A. australis* from various samples. The HCA of samples 1 to 14 was performed using SPSS 18.0 statistics software (SPSS for Windows 18.0, SPSS Inc., USA). A method called Ward Linkage was applied.

cluster II consisted of samples 5, 12, 9 and 13; and cluster III consisted of samples 2, 6, 10 and 14. These results showed that the similarities between the reference fingerprint and the entire chromatographic profiles of samples from cluster I were higher than those of samples from clusters II and III. In other words, the internal qualities of the *A. australis* samples from cluster I had close relationships with themselves, but were quite different from the ones in clusters II and III. Thus, the results of the HCA analysis agreed well with the visual comparison of the entire chromatographic profiles of the 14 test samples.

3.3.2. Results of the CA

CA was used to investigate the spectrum–effect relationships between the area values of the 20 common peaks in the UPLC/MS fingerprints and the values of the antibacterial activities on the growth of *A. hydrophila* and *A. sobria*. The correlation coefficients between the common peaks and the antibacterial activities were shown in Table **3**. The general results showed that positive correlations existed between almost all the common peaks and the antibacterial activities, excepting peak numbers 3, 14 and 16 in the UPLC/MS fingerprint. Furthermore, the antibacterial activities against the growth of *A. australis* on *A. hydrophila* and *A. sobria* had a close correlation with peak numbers 1, 6, 7, 9, 10 and 11 in the UPLC/MS fingerprint. The correlation coefficients between these peaks and antibacterial activities were in the range of 0.7261–0.9383. Thus, the compounds with peaks 1, 6, 7, 9, 10 and 11 might be the antibacterial ingredients of *A. australis*. The relationship of the antibacterial effects and chemical structures of these compounds was further required to be affirmed by other analytical methods.

3.3.3. Results of the SR Analysis

The average relative peak areas of the 20 common peaks in Table **2** were set as the independent variables ($X1$ to $X20$),

Table 3. The correlation coefficient between the common peaks in UPLC/MS fingerprints and the antibacterial activities.

Peak No.	*Aeromonas hydrophila*	*Aeromonas sobria*
1	0.9186	0.9303
2	0.6541	0.6135
3	-0.0170	-0.5650
4	0.0726	0.1342
5	0.0263	0.0466
6	0.9137	0.9232
7	0.9286	0.9383
8	0.6951	0.7358
9	0.7399	0.7356
10	0.8155	0.7866
11	0.7523	0.7261
12	0.1729	0.1749
13	0.3082	0.3134
14	0.0060	-0.0112
15	0.0883	0.0696
16	-0.1801	-0.1843
17	0.4647	0.4596
18	0.1247	0.1255
19	0.0724	0.0607
20	0.2486	0.0240

and the values of antibacterial activities in Table **1** were set as the dependent variables (Y) for the multiple regression analysis. The SR equation of all variables was $Y = 7.588 + 3.415E-5X_7 + 2.006E-5X_1$ ($R^2 = 0.862$). The results indicated that the antibacterial activity of *A. australis* exhibited a close correlation with peaks 1 and 7, which might be the antibacterial compounds in the UPLC/MS fingerprint. The correlation of the antibacterial effects and chemical structuress of peak 1 and peak 7 was needed to be affirmed by other analytical methods.

3.3.4. Results of the PLSR

In the present study, the original variables were reassembled into new integrated variables by multiple linear transformation, and these new variables had no correlation between themselves. In other words, several principal components were replaced and derived from the original variables by data processing. These principal components would keep as much information of the original variables as possible, and the variance was used to measure the explanatory power for the information from the original variable. The VIP values of each independent variable reflected the importance for explaining the dependent variables; VIP > 1 generally indicated that the importance was significant.

As shown in Table **4**, 78.9% information of the original independent variables and 99% information of original dependent variables could be explained by the first seven principal components. X1, X2, X6, X7, X8, X9, X10 and X11 were fit to the linear regression of the first seven principal components separately. Peak numbers 1, 2, 6, 7, 8, 9, 10 and 11 had VIP > 1, as shown in Table **5**, indicated that these peaks in the UPLC/MS fingerprint might exert important effects on the antibacterial activity of *A. australis.* The association of the antibacterial effects and chemical structures of these peaks was needed to be affirmed by other analytical methods.

3.4. Confirmation of the Active Compounds

3.4.1. Confirmation of Effectiveness of the Targeted Peaks

All the compounds of the crude extract of *A. australis* were isolated by the optimal conditions of semi-preparative HPLC method described in our previous paper [26]. The antibacterial activities of these compounds were measured on the growth *A. hydrophila* and *A. sobria*. As shown in Table **6**, peak numbers 1, 2, 6, 7, 9, 10, 11, 12 and 17 in the UPLC/MS fingerprint showed antibacterial activities on the tested organisms. Apart from the nine aforementioned peaks, the remaining peaks in the UPLC/MS fingerprint were completely ineffective. The results showed that most of the effective peaks of *A. australis*

Table 4. Proportion of variance explained of PLSR on UPLC/MS fingerprints.

Latent Factors	Statistics				
	X Variance	Cumulative X Variance	Y Variance	Cumulative Y Variance (R-square)	Adjusted R-square
1	0.314	0.314	0.883	0.883	0.873
2	0.126	0.440	0.042	0.925	0.911
3	0.101	0.541	0.022	0.947	0.932
4	0.070	0.611	0.017	0.965	0.949
5	0.059	0.670	0.009	0.973	0.957
6	0.066	0.736	0.008	0.982	0.966
7	0.053	0.789	0.008	0.990	0.977

Table 5. VIP of PLSR on UPLC/MS fingerprints.

Variables	Latent Factors						
	1	2	3	4	5	6	7
X1	1.712	1.694	1.674	1.668	1.670	1.663	1.664
X2	1.196	1.222	1.209	1.219	1.217	1.213	1.209
X3	0.137	0.159	0.309	0.308	0.333	0.357	0.363
X4	0.231	0.256	0.257	0.341	0.340	0.346	0.356
X5	0.026	0.113	0.292	0.289	0.297	0.308	0.312
X6	1.720	1.681	1.661	1.647	1.640	1.633	1.627
X7	1.744	1.707	1.687	1.673	1.666	1.659	1.653
X8	1.351	1.381	1.366	1.355	1.351	1.345	1.343
X9	1.427	1.398	1.388	1.378	1.390	1.384	1.389
X10	1.447	1.417	1.419	1.417	1.422	1.417	1.416
X11	1.399	1.402	1.387	1.387	1.382	1.377	1.372
X12	0.310	0.331	0.392	0.466	0.478	0.483	0.488
X13	0.558	0.673	0.667	0.661	0.680	0.695	0.700
X14	0.001	0.127	0.126	0.146	0.176	0.176	0.182
X15	0.170	0.213	0.239	0.242	0.243	0.247	0.266
X16	0.412	0.410	0.459	0.492	0.503	0.541	0.573
X17	0.859	0.839	0.834	0.846	0.843	0.843	0.841
X18	0.263	0.486	0.548	0.543	0.542	0.550	0.597
X19	0.178	0.194	0.356	0.398	0.396	0.424	0.477
X20	0.457	0.449	0.469	0.482	0.483	0.533	0.580

were conjectured in our study, except for peaks 12 and 17, having exceedingly weak antibacterial activities on the test organisms. As shown in Table **6**, peaks 2 and 11 were the main antibacterial compounds, and the rest of the conjectured effective peaks were the auxiliary antibacterial compounds of *A. australis.* In other words, almost all the antibacterial compounds of *A. australis* could be identified by investigating the spectrum–effect relationship.

Table 6. Effectiveness confirmation and structural identification of the active compounds of *A. australis.*

Peak No.	*Aeromonas hydrophila*		*Aeromonas sobria*		Ion Mode	Rt (min)	MI(f)/MI(c) (Da)	Error (ppm)	Fragment Ion	Chemical Formula	Compound
	Inhibition Zone	MIC	Inhibition Zone	MIC							
1	10.9±0.5	0.312	10.5±0.7	0.312	+	2.75	124.0393/ 124.03922	-0.7	78,50	C6H5NO2	nicotinic acid
2	39.1±0.6	0.039	36.1±1.3	0.019	+	6.47	171.0288/ 171.02876	-0.2	153,125,107,81	C7H6O5	gallic acid
6	25.6±1.0	0.156	26.8±1.2	0.078	+	11.74	155.03389/ 155.0338	-0.6	137,109,93	C7H6O4	protocatechuic acid
7	11.4±0.4	0.312	10.2±0.5	0.312	+	14.73	139.03897/ 139.03889	-0.6	121,93,77	C7H6O3	p-hydroxybenzoic acid
9	25.3±0.9	0.156	23.0±0.8	0.156	+	17.7	293.0301/ 293.0292	3.1	247,219,191,153	C13H8O8	—
10	20.9±0.9	0.156	21.3±0.6	0.156	-	19.56	484.0409/ 484.0421	2.0	301,275,169,125	C22H12O13	—
11	28.3±0.5	0.039	25.6±1.2	0.039	-	20.08	633.0713/ 633.0733	2.3	463,301,275	C27H22O18	—
12	10.1±0.3	0.625	9.6±0.5	0.625	+	22.9	355.02959/ 355.02958	0	337,301,291,247,181	C14H10O11	Austrslisin
17	8.4±0.6	1.563	8.0±0.7	1.563	+	31.89	303.04993/ 303.05008	+0.5	285,257,229,153	C15H10O7	quercetin

Inhibition zone was measured by the agar-diffusion method at a concentration of 5 mg/mL of each compound. MIC value was measured by broth microdilution method. All data were given as the average between three separated tests. Mean value of inhibition zone n = 3 ± standard error. Inhibition zone (mm) including the diameter of hole (6mm). Structural identification was investigated by UPLC/Q-TOF system: MI (f) means measured value and MI (c) means theoretical value.

3.4.2. Structure Identification of the Targeted Peaks

To obtain the accurate molecular weight of the bioactive compounds, peak numbers 1, 2, 6, 7, 9, 12 and 17 in the UPLC/MS fingerprint were determined by UPLC/Q–TOF system in positive ionisation mode, Peak numbers 1, 2, 6, 7, 9, 12 and 17 were verified as compounds with [M–H]+ of 124.03922, 171.02876, 155.03380, 139.03889, 293.02920, 355.02958 and 303.05008, respectively. Peak 10 and peak 11 were determined by UPLC/Q–TOF system in negative ionisation mode as compounds with [M–H]- of 484.04210 and 633.07330, respectively. Peak numbers 1, 2, 6, 7, 12 and 17 were further verified as nicotinic acid, gallic acid, protocatechuic acid, p-hydroxybenzoic acid, australisin and quercetin by comparison with the standard substances. The molecular formula of peak numbers 9, 10 and 11 were verified as $C_{13}H_8O_8$, $C_{22}H_{12}O_{13}$ and $C_{27}H_{22}O_{18}$ from their accurate molecular weight and characteristic fragment ions. The definite chemical structures of these three compounds should be affirmed by other analytical methods. All the results described above are listed in Table **6**.

4. DISCUSSION

In the present study, the UPLC/MS system was applied to establish the fingerprints of *A. australis*, and antibacterial assay was selected to evaluate it's pharmacological function. The UPLC/MS fingerprints and antibacterial activities of 14 samples from various sources were then combined to investigate and search for the antibacterial compounds of *A. australis.* By descriptive statistics of the characteristic peaks in the fingerprint, the amount and proportion of the components

in *A. australis* were found to be significantly different among the 14 test samples. The antibacterial effects of these samples were also found to be widely divergent, and the difference between the highest activity and the lowest activity was 64 times. Samples 3, 4 and 8, with the strongest antibacterial activities, were collected in the same cluster analysed by HCA, and the similarities between the reference fingerprints and the entire chromatographic profiles of these samples also showed the highest values. By contrast, samples 6, 10 and 14 with the weakest antibacterial activities were collected in the other cluster, and these samples have the lowest values of similarities between the reference fingerprint and their entire chromatographic profiles. The results demonstrated that the similarity evaluation of the UPLC/MS fingerprint from various samples could reflect the inherent quality of *A. australis* to a certain extent.

The possible active compounds of *A. australis* were conjectured, coupled with the aid of CA, SR and PLSR. CA could evaluate the correlation between the characteristic peaks in the fingerprint and the pharmacological function of CHMs. The SR method could pick out the most important independent variables (characteristic peaks) that significantly affected the dependent variables (biological activities) to establish a regression model. The PLSR method could simplify to process data, and establish a regression model and then investigate the correlation between two sets of variates at the same time. Through the statistical approaches described above, peak numbers 1, 2, 6, 7, 8, 9, 10 and 11 in the UPLC/MS fingerprint were conjectured as the antibacterial compounds of *A. australis* in this study.

To verify the reliability and viability of the method of spectrum–effect relationships, semi-preparative HPLC was applied to separate all the characteristic peaks in the UPLC/MS fingerprint, and antibacterial assay was performed on these purified compounds one by one. The chemical structures of those confirmed antibacterial compounds were then verified by UPLC/Q–TOF system and validated by comparison with relevant standard substances. Hence, seven antibacterial compounds of *A. australis* were identified by the spectrum–effect relationships, and only two minor active compounds were not conjectured in our present study.

CONCLUSION

Essentially, the relationship of the chemical components of CHMs and biological activity is typically causal. When the amount and proportion of chemical components varied, its pharmacological function changed accordingly. Thus, the strategy of "spectrum–effect relationships" provided a model that combined chromatographic fingerprints of chemical components and modern pharmacological bioassay to elucidate the complexity of CHMs. Identification of bioactive compounds was carried out, comparing the chromatographic fingerprints of the CHMs samples and establishing the relationships between the chemical ingredients and the biological activities through certain statistical methods. The "spectrum–effect relationship" approach greatly increased the effectiveness of drug discovery, which represented an important and potential way to searching for bioactive compounds in CHMs.

LIST OF ABBREVIATIONS

CHMs	=	Chinese Herb Medicines
A.australis	=	*Acalypha australis* Linn
UPLC/MS	=	Ultra-Performance Liquid Chromatography/Mass Spectrometry
A.hydrophila	=	*Aeromonas hydrophila*
A.sobria	=	*Aeromonas sobria*
MIC	=	Minimum Inhibitory Concentration
HCA	=	Hierarchical Clustering Analysis
CA	=	Correlational Analysis
SR	=	Stepwise Regression
PLSR	=	Partial Least-Square Regression
VIP	=	Values of Variable Importance In Projection
UPLC/Q–TOF	=	Ultra-Performance Liquid Chromatography/Time-of-Flight Mass Spectrometry

CONFLICT OF INTEREST

The authors declare no conflict of interest, financial or otherwise.

ACKNOWLEDGEMENTS

The authors appreciated the support of Key Laboratory of Animal Parasitology of Ministry of Agriculture for providing laboratory apparatus. We gratefully acknowledge financial support provided theYouth Science Funds of National Natural Science Foundation of China (31402245).

COMPLIANCE WITH ETHICAL STANDARDS

Funding: Supported by National Natural Science Funds for Young Scholar (31402245).

Supported by the funds of College of Forestry and Landscape Architecture, South China Agricultural University for Young Scholar (201606).

Ethical approval: This article does not contain any studies with human participants or animals performed by any of the authors.

INFORMED CONSENT

Not applicable.

REFERENCES

[1] Harvey, A.L. Natural products in drug discovery. *Drug Discov. Today*, **2008**, *13*(19-20), 894-901.

[2] Li, J.W.; Vederas, J.C. Drug discovery and natural products: End of an era or an endless frontier? *Science*, **2009**, *325*(5937), 161-165.

[3] Koehn, F.E.; Carter, G.T. The evolving role of natural products in drug discovery. *Nat. Rev. Drug. Discov.*, **2005**, *4*(3), 206-220.

[4] Huang, X.; Kong, L.; Li, X.; Chen, X.; Guo, M.; Zou, H. Strategy for analysis and screening of bioactive compounds in traditional Chinese medicines. *J. Chromatogr. B Analyt. Technol. Biomed. Life Sci.*, **2004**, *812*(1-2), 71-84.

[5] Su, X.; Hu, L.; Kong, L.; Lei, X.; Zou, H. Affinity chromatography with immobilized DNA stationary phase for biological fingerprinting analysis of traditional Chinese medicines. *J. Chromatogr. A*, **2007**, *1154*(1-2), 132-137.

[6] Mao, X.; Kong, L.; Luo, Q.; Li, X.; Zou, H. Screening and analysis of permeable compounds in Radix Angelica Sinensis with immobilized liposome chromatography. *J. Chromatogr. B Analyt. Technol. Biomed. Life Sci.*, **2002**, *779*(2), 331-339.

[7] Wang, H.; Zou, H.; Ni, J.; Kong, L.; Gao, S.; Guo, B. Fractionation and analysis of Artemisia capillaris Thunb. by affinity chromatography with human serum albumin as stationary phase. *J. Chromatogr. A*, **2000**, *870*(1-2), 501-510.

[8] Lam, K.S. New aspects of natural products in drug discovery. *Trends Microbiol.*, **2007**, *15*(6), 279-289.

[9] Yang, D.Z.; An, Y.Q.; Jiang, X.L.; Tang, D.Q.; Gao, Y.Y.; Zhao, H.T.; Wu, X.W. Development of a novel method combining HPLC fingerprint and multi-ingredients quantitative analysis for quality evaluation of traditional Chinese medicine preparation. *Talanta*, **2011**, *85*(2), 885-890.

[10] Cheng, Y.Y.; Wang, Y.; Wang, X.W. A causal relationship discovery-based approach to identifying active components of herbal medicine. *Comput. Biol. Chem.*, **2006**, *30*(2), 148-154.

[11] Fabri, R.L.; Aragao, D.M.; Florencio, J.R.; Pinto, N.C.; Mattos, A.C.; Coelho, P.M. Chromatographic fingerprint analysis and effects of the medicinal plant species Mitracarpus frigidus on adult Schistosoma mansoni worms. *Biomed. Res. Int.*, **2014**, *2014*, 1-10.

[12] Liu, X.; Wang, X.L.; Wu, L.; Li, H.; Qin, K.M.; Cai, H. Investigation on the spectrum-effect relationships of Da-Huang-Fu-Zi-Tang in rats by UHPLC-ESI-Q-TOF-MS method. *J. Ethnopharmacol.*, **2014**, *154*(3), 606-612.

[13] Song, L.; Wang, S.; Duan, X.; Liu, X.; Li, Z.; Nie, L. Chromatographic fingerprint combined with content of asperosaponin VI and antioxidant activity for quality evaluation of wine-fried Dipsaci Radix. *Nat. Prod. Commun.*, **2014**, *9*(6), 773-778.

[14] Zheng, Q.; Zhao, Y.; Wang, J.; Liu, T.; Zhang, B.; Gong, M. Spectrum-effect relationships between UPLC fingerprints and bioactivities of crude secondary roots of Aconitum carmichaelii Debeaux (Fuzi) and its three processed products on mitochondrial growth coupled with canonical correlation analysis. *J. Ethnopharmacol.*, **2014**, *153*(3), 615-623.

[15] Custers, D.; Canfyn, M.; Courselle, P.; De Beer, J.O.; Apers, S.; Deconinck, E. Headspace-gas chromatographic fingerprints to discriminate and classify counterfeit medicines. *Talanta*, **2014**, *123*, 78-88.

[16] Sun, J.; Chen, P. Chromatographic fingerprint analysis of yohimbe bark and related dietary supplements using UHPLC/UV/MS. *J. Pharm. Biomed. Anal.*, **2012**, *61*, 142-149.

[17] Leung, K.S.; Fu, C. Improved chromatographic assessment of Chinese medicinal products by multi-chemical classes analysis. *Planta Med.*, **2009**, *75*(10), 1171-1179.

[18] Yao, H.; Li, S.; Hu, J.; Chen, Y.; Huang, L.; Lin, J. Chromatographic fingerprint and quantitative analysis of seven bioactive compounds of *Scutellaria barbata*. *Planta Medica.*, **2011**, *77*(4), 388-393.

[19] Zhu, Y.; Zheng, Q.; Sun, Z.; Chen, Z.; Zhao, Y.; Wang, Z. Fingerprint-efficacy study of Radix Aconiti Lateralis Preparata (Fuzi) in quality control of Chinese herbal medicine. *J. Therm. Anal. Calorim.*, **2014**, *118*(3), 1763-1772.

[20] Wang, X.; Sun, W.; Sun, H.; Lv, H.; Wu, Z.; Wang, P. Analysis of the constituents in the rat plasma after oral administration of Yin Chen Hao Tang by UPLC/Q-TOF-MS/MS. *J. Pharm. Biomed. Anal.*, **2008**, *46*(3), 477-490.

[21] Kvalheim, O.M.; Chan, H.Y.; Benzie, I.F.F.; Szeto, Y.T.; Tzang, H.C.; Mok, K.W. Chromatographic profiling and multivariate analysis for screening and quantifying the contributions from individual components to the bioactive signature in natural products. *Chemometr. Intell. Lab.*, **2011**, *107*(1), 98-105.

[22] Jiao, L.; Xue, Z.; Wang, G.; Wang, X.; Li, H. Application of Fourier transform to preprocessing chromatographic fingerprints of Traditional Chinese Medicine. *Chemometr. Intell. Lab.*, **2014**, 141-148.

[23] Yang, W.L.; Hu, M.H.; Chen, S.W.; Wang, Q.; Zhu, S. Identification of adulterated cocoa powder using chromatographic fingerprints of polysaccharides coupled with principal component analysis. *Food. Anal. Methods*, **2015**, 1-8.

[24] Yu, X.; Liu, Q.; Xie, Z.; Lam, S.; Xu, X. Chromatographic fingerprint analysis of exocarpium citri grandis by high-performance liquid chromatography coupled with diode-array detector. *Food. Anal. Methods*, **2014**, *8*, 1-8.

[25] Reiersen, B.; Kiremire, B.T.; Byamukama, R.; Andersen, M.O. Anthocyanins acylated with gallic acid from chenille plant, Acalypha hispida. *Phytochemistry*, **2003**, *64*(4), 867-871.

[26] Xiao, S.; Zhang, L.F.; Zhang, X.; Li, S.M.; Xue, F.Q. Tracing antibacterial compounds from Acalypha australis Linn. by spectrum-effect relationships and semi-preparative HPLC. *J. Sep. Sci.*, **2013**, *36*(9-10), 1667-1676.

[27] Long, T.; Yu, J.; Huang, Y.; Shi, Z.; Xu, L. Rapid fingerprint analysis of Radix Scutellariae by UFLC-DAD. *J. Chromatogr. Sci.*, **2013**, *51*(10), 939-42.

[28] Zou, P.; Hong, Y.; Koh, H.L. Chemical fingerprinting of Isatis indigotica root by RP-HPLC and hierarchical clustering analysis. *J. Pharm. Biomed. Anal.*, **2005**, *38*(3), 514-520.

[29] Tantishaiyakul, V.; Worakul, N.; Wongpoowarak, W. Prediction of solubility parameters using partial least square regression. *Int. J. Pharm.*, **2006**, *325*(1-2), 8-14.

[30] Alam, M.A.; Aljenoobi, F.I.; Almohizea, A.M.; Ahad, A.; Raish, M. Validated UPLC-MS method for pharmacokinetic investigations of cyclosporine-A in blood. *Curr. Pharm. Anal.*, **2015**, *11*(3), 210-215.

[31] de Souza, S.R.; Inoue, F.Y.; Camargo, T.S.; Malheiros, S.; da Silva, A.M.L.; Bresolin, R.M.B. Rapid HILIC method for assay and dissolution analysis of rivastigmine hydrogen tartrate from hydrophilic matrix. *Curr. Pharm. Anal.*, **2014**, *10*(3), 169-174.

ScienceDirect

Food Chemistry
Supports open access

16.3 CiteScore | 8.5 Impact Factor

Submit your article ↗ | Guide for authors

Menu | Search in this journal

Volume 447

30 July 2024

Previous vol/issue | Next vol/issue

Receive an update when the latest issues in this journal are published

Sign in to set up alerts

Full text access

Editorial Board

Article 139250

View PDF

General Section: Reviews

Review article · Full text access

Recent advances in artificial intelligence towards the sustainable future of agri-food industry

Pinku Chandra Nath, Awdhesh Kumar Mishra, Ramesh Sharma, Biswanath Bhunia, ... Kandi Sridhar

Article 138945

View PDF Article preview

Review article · Full text access

Casein-based hydrogels: Advances and prospects

Yuxi Yang, Qunna Xu, Xinyi Wang, Zhongxue Bai, ... Jianzhong Ma

Article 138956

View PDF Article preview

Review article · Full text access

The dual function of calcium ion in fruit edible coating: Regulating polymer internal crosslinking state and improving fruit postharvest quality

Yiqin Zhang, Qi Kong, Ben Niu, Ruiling Liu, ... Haiyan Gao

Article 138952

View PDF Article preview

Review article • *Open access*

In vitro and *in vivo* assessment of AFB1 and OTA toxic effects and the beneficial role of bioactive compounds. A systematic review

Massimo Frangiamone, Álvaro Lázaro, Alessandra Cimbalo, Guillermina Font, Lara Manyes

Article 138909

View PDF Article preview

Review article • Full text access

Human milk sphingomyelin: Function, metabolism, composition and mimicking

Yuying Yuan, Junying Zhao, Qian Liu, Yan Liu, ... Lijun Chen

Article 138991

View PDF Article preview

Review article • Full text access

Recent trends in design of healthier fat replacers: Type, replacement mechanism, sensory evaluation method and consumer acceptance

Yuanxue Gao, Yan Zhao, Yao Yao, Shuping Chen, ... Yonggang Tu

Article 138982

View PDF Article preview

Review article • Full text access

Review on toxicology and activity of tomato glycoalkaloids in immature tomatoes

Li-hao Wang, De-hong Tan, Xue-song Zhong, Mei-qi Jia, ... Lin Shi

Article 138937

View PDF Article preview

Review article • Full text access

Nanotechnology-based optical sensors for Baijiu quality and safety control

Wei Dong, Zhen Fan, Xiaolong Shang, Mengjun Han, ... Bo Deng

Article 138995

View PDF Article preview

Review article • Full text access

Recent advances in metal oxide nanozyme-based optical biosensors for food safety assays

Jing Qin, Ningning Guo, Jia Yang, Jing Wei

Article 139019

View PDF Article preview

Review article • Full text access

Traceability of chemicals from *Tripterygium Wilfordii* Hook. f. in raw honey and the potential synergistic effects of honey on acute toxicity induced by celastrol and triptolide

Tian Xiao, Li Yang, Fan Yang, Guang Nie, ... Yajie Zheng

Article 139044

View PDF Article preview

General Papers

Research article • Full text access

Enhanced oxidase mimic activity of raspberry-like *N*-doped Mn_3O_4 with oxygen vacancies for efficient colorimetric detection of gallic acid coupled with smartphone

Tao Zhou, Daqing Chen, Haoran Li, Danhua Ge, Xiaojun Chen

Article 138919

View PDF Article preview

Research article • Full text access

Trehalose-conjugated lentil-casein protein complexes prepared by structural interaction: Effects on water solubility and protein digestibility

Mohammad Alrosan, Ali Madi Almajwal, Ali Al-Qaisi, Sana Gammoh, ... Khalid Bani-Melhem

Article 138882

View PDF Article preview

Research article ● Full text access

Ionic liquid-enhanced silica aerogels for the specific extraction and detection of aflatoxin B1 coupled with a smartphone-based colorimetric biosensor

Wenpeng Jiang, Qingli Yang, Huixiao Duo, Wei Wu, Xiudan Hou

Article 138917

View PDF Article preview

Research article ● Full text access

Characterization of alkaloids and phenolics in *Nitraria roborowskii* Kom. fruit by UHPLC-triple-TOF-MS/MS and its sucrase and maltase inhibitory effects

Di Wu, Sirong Jiang, Gongyu Wang, Luya Wang, ... Huilan Yue

Article 138743

View PDF Article preview

Research article ● Full text access

The novel angiotensin-I-converting enzyme inhibitory peptides from *Scomber japonicus* muscle protein hydrolysates: QSAR-based screening, molecular docking, kinetic and stability studies

Baobei Wang, Hui Zhang, Yuxi Wen, Wenwen Yuan, ... Chao Zhao

Article 138873

View PDF Article preview

Research article ● Full text access

Hydroxyl-containing triazine-based conjugated microporous polymers for solid phase extraction of fluoroquinolone antibiotics in the environment and food samples

Lu-Shu Meng, Xiao-Li Wang, Xia Wang, Lei Ji, ... Ru-Song Zhao

Article 138867

View PDF Article preview

Research article ● Full text access

Fluorescent carbon dots in situ polymerized biodegradable semi-interpenetrating tough hydrogel films with antioxidant and antibacterial activity for applications in food industry

Abdulhakeem Alzahrani

Article 138905

View PDF Article preview

Research article ● Full text access

Bimetallic Fe/Ni metal organic framework-based hypoxanthine biosensor for early monitoring of freshness changes of aquatic products

Zhuoran Li, Limin Cao, Jianxin Sui, Lei Wang, ... Kaiqiang Wang

Article 138902

View PDF Article preview

Research article ● *Open access*

Important roles of coarse particles in pasting and gelling performance of different pulse flours under high-temperature heating

Dong-Jin Lee, Fan Cheng, Dongxing Li, Ke Ding, ... Yongfeng Ai

Article 138896

View PDF Article preview

Research article ● *Open access*

Evaluation of Iron Chlorin e6 disappearance and hydrolysis in soil and garlic using salting-out assisted liquid-liquid extraction coupled with high-performance liquid chromatography and ultraviolet-visible detection

Wenwen Zhou, Jian Chen, Rendan Zhou, Jian Xiao, ... Baotong Li

Article 138960

View PDF Article preview

Research article ● Full text access

Exploring the composition and potential uses of four hops varieties through different extraction techniques

Aleksandra Cvetanović Kljakić, Miha Ocvirk, Ksenija Rutnik, Iztok Jože Košir, ... Gökhan Zengin

Article 138910

View PDF Article preview

Research article ● Full text access

The underlying reasons for the efficient extraction of peanut oil by aqueous ethanol combined with roasting conditioning pretreatment

Sicheng Wang, Yubao Guo, Dan Xie, Liyou Zheng, ... Zhenzhen Wang

Article 138934

View PDF Article preview

Research article ● Full text access

Comparison of the physical stability, microstructure and protein-lipid co-oxidation of O/W emulsions stabilized by L-arginine/L-lysine-modified soy protein hydrolysate

Bin Zhu, Jinjie Yang, Jingjing Dou, Yijie Ning, ... Yang Li

Article 138901

View PDF Article preview

Research article ● Full text access

Screening method for the analysis of Rhodamine B in chili powder

G. Thomas Knecht, Noah Froelich, Andres D. Campiglia

Article 138936

View PDF Article preview

Research article ● Full text access

Development of a tamarind-based functional beverage with partially-hydrolyzed agave syrup and the health effects of its consumption in C57BL/6 mice

Román Cardona-Herrera, Tannia Alexandra Quiñones-Muñoz, Elena Franco-Robles, César Ozuna

Article 138935

View PDF Article preview

Research article ● Full text access

A novel dual-activatable ultrasensitive chemiluminescent probe for mercury (II) monitoring: From rational design to multiple application

Ting Luo, Shuai Huang, Shuaige Bai, Bin Feng, ... Wenbin Zeng

Article 138954

View PDF Article preview

Research article ● Full text access

Polyphenolic profile and *in vitro* biological activity of Serbian orange (skin fermented white) wines

Ivana Beara, Tatjana Majkić, Ljiljana Milovanović, Emilija Svirčev, Ljilja Torović

Article 138933

View PDF Article preview

Research article ● Full text access

A colorimetry-enhanced tri-functional film with high stability by polyphenol-anthocyanin co-pigmentation/conjugate: New prospect for active intelligent food packaging

Rui Li, Haoyu Feng, Shancan Wang, Di Zhuang, Jie Zhu
Article 138927

View PDF Article preview

Research article ● Full text access

Valorization and protection of anthocyanins from strawberries (*Fragaria×ananassa* Duch.) by acidified natural deep eutectic solvent based on intermolecular interaction

Hao Huang, Shengrong Guo, Yanqun Xu, Fatima-ezzahra Ettoumi, ... Kejun Cheng
Article 138971

View PDF Article preview

Research article ● Full text access

Encapsulation of 4-terpineol with β-cyclodextrin: Inclusion mechanism, characterization and relative humidity-triggered release

Chuanxiang Cheng, Yujie Lei, Tiantian Min, Yushan Zhang, Jin Yue
Article 138926

View PDF Article preview

Research article ● Full text access

Short-term steaming during processing impacts the quality of Citri Reticulatae 'Chachi' peel

Shiheng Chen, Ziying Chen, Dylan O'Neill Rothenberg, Yong Long, ... Xu Zhang
Article 138964

View PDF Article preview

Research article ● Full text access

Deep learning-assisted flavonoid-based fluorescent sensor array for the nondestructive detection of meat freshness

Min Li, Jianguo Xu, Chifang Peng, Zhouping Wang
Article 138931

View PDF Article preview

Research article ● Full text access

Rapid analysis and authentication of Chinese propolis using nanoelectrospray ionization mass spectrometry combined with machine learning

Ruiyue Wang, Liangliang Qu, Yiran Wang, Yijiao Qu, ... Zongxiu Nie
Article 138928

View PDF Article preview

Research article ● Full text access

Colorimetric aptasensor utilizing MOF-235 with exceptional peroxidase-like activity for the detection of oxytetracycline residues in raw milk

Long Wang, Xia Lu, Yan Zhang, Yuxin Wang, ... Wupeng Ge
Article 138966

View PDF Article preview

Research article ● Full text access

Inoculation fermentation with *Lactobacillus fermentum* L28 and *Staphylococcus epidermidis* S24 for improving the protein degradation of air-dried goose

Mangang Wu, Chen Gu, Likun Duan, Peipei Yin, ... Hai Yu
Article 138955

View PDF Article preview

Research article ● Open access

Targeted and untargeted metabolomics reveals meat quality in grazing yak during different phenology periods on the Qinghai-Tibetan Plateau

Tongqing Guo, Qian Zhang, Xungang Wang, Xianli Xu, ... Shixiao Xu

Article 138855

View PDF Article preview

Research article ● Full text access

Unraveling the relationship between aroma characteristics and lipid profile of abalone (*Haliotis discus hannai*) during seasonal fluctuation and thermal processing

He-He Tian, Yu-Lian Li, Xu-Song Wang, Xu-Hui Huang, ... Lei Qin

Article 138949

View PDF Article preview

Research article ● Full text access

Effects of different thawing methods on physical and physicochemical properties of frozen dough and quality of corresponding steamed bread

Fan Zhang, Jinying Guo, Peiyao Li, Fen Zhao, ... Can Cui

Article 138932

View PDF Article preview

Research article ● Full text access

A sustainable and efficient strategy for bioconverting naringin to L-rhamnose, 2R-naringenin, and kaempferol

Mengfan Lu, Simin Liu, Jiamei Liu, Linguo Zhao, Jianjun Pei

Article 138942

View PDF Article preview

Research article ● Full text access

Development, characterization and *Lactobacillus plantarum* encapsulating ability of novel C-phycocyanin-pectin-polyphenol based hydrogels

Ziyi Zhu, Ying Wu, Yejun Zhong, Hui Zhang, Junzhen Zhong

Article 138918

View PDF Article preview

Research article ● Full text access

Formation mechanism, environmental sensitivity and functional characteristics of succinylated ovalbumin/ε-polylysine electrostatic complexes: The roles of succinylation modification and ε-polylysine combination

Ru-yi Zhang, Hui-min Zhang, Tian-zhu Guan, Zhi-rong Wang, ... Sheng-qi Rao

Article 138951

View PDF Article preview

Research article ● Full text access

Luminescent carbon dots-rooted polysaccharide crosslinked hydrogel adsorbent for sensitive determination and efficient removal of Cu^{2+}

Jingkun Li, Liying Wang, Guoyong Jiang, Yuqi Wan, ... Fuwei Pi

Article 138977

View PDF Article preview

Research article ● Full text access

Carbon dots and covalent organic frameworks based FRET immunosensor for sensitive detection of *Escherichia coli* O157:H7

Sunli Wang, Nini Liang, Xuetao Hu, Wenting Li, ... Jiyong Shi

Article 138663

View PDF Article preview

Research article ● Full text access

Insight into the improvement mechanism of gel properties of pea protein isolate based on the synergistic effect of cellulose nanocrystals and calcium ions

Jinglei Zhang, Huajian Xu, Huixia Liu, Wenqi Wang, ... Yaqing Xiao

Article 138975

View PDF Article preview

Research article • *Open access*

Effects of post-fermentation addition of green tea extract for sulfur dioxide replacement on Sauvignon Blanc wine phenolic composition, antioxidant capacity, colour, and mouthfeel attributes

Yi Yang, Zhijing Ye, Yunxuan Qin, Sreeni Pathirana, ... Paul A. Kilmartin

Article 138976

View PDF Article preview

Research article • Full text access

Plasma-activated water in combination with coconut exocarp flavonoids emerge as promising preservation technique for golden pompano: Impact of the treatment sequence

Chengyan Gao, Mantong Zhao, Xinwen Wang, Jiamei Wang, ... Dayong Zhou

Article 138981

View PDF Article preview

Research article • Full text access

Development of a self-reinforced starch-derived film with biocompatibility and mechanical properties

Liping Wang, Dexiang Li, Lei Ye, Chaohui Zhi, ... Ming Miao

Article 138974

View PDF Article preview

Research article • Full text access

Development of a processing factor prediction model for pesticides in processed tomato foods using elastic net regularization

Yuki Yamasaki, Kosuke Nakamura, Nao Kashiwabara, Shinji Chiba, ... Tomoaki Tsutsumi

Article 138943

View PDF Article preview

Research article • Full text access

Smart nano-inks based on natural food colorant for screen-printing of dynamic shelf life of shrimp

Atiyeh Mehrzad, Asma Verdian, Mahboobe Sarabi-Jamab

Article 138963

View PDF Article preview

Research article • Full text access

Effects of synergistic modification using alkalis and guar gum on the pasting, rheological, and microstructural properties of germinated highland barley starch gels

Wentao Pan, Xin Qi, Mingyue Shen, Yi Chen, ... Jianhua Xie

Article 138986

View PDF Article preview

Research article • Full text access

Application of ultrasound treatment in pork marination: Effects on moisture migration and microstructure

Lina Guo, Xinyan Zhang, Chen Hong, Ning Liu, ... Haile Ma

Article 138950

View PDF Article preview

Research article • Full text access

Effects of freeze-thaw cycles on the quality of Hot-dry noodles: From the moisture, starch, and protein characteristics

Liuyu Wan, Xiude Wu, Peng Xu, Yaonan Xing, ... Xuedong Wang

Article 138996

View PDF Article preview

Research article ● Full text access

Insight into the mechanisms of combining direct current magnetic field with phosphate in promoting emulsifying properties of myofibrillar protein

Kun Yang, Rongshuo Chi, Jingjiao Jiang, Jing Ma, ... Yuanhua Zhou

Article 138990

View PDF Article preview

Research article ● Full text access

Kinetic and thermodynamic-based studies on the interaction mechanism of novel *R. roxburghii* seed peptides against pancreatic lipase and cholesterol esterase

Hao Yin, Jiangxiong Zhu, Yu Zhong, Danfeng Wang, Yun Deng

Article 139006

View PDF Article preview

Research article ● Full text access

Preparation of limonin monoclonal antibody and establishment of a sensitive icELISA for analyzing limonin in citrus and herbal samples

Di Sun, Yifan Liu, Zihui Jin, Bo Xu, ... Yongliang Cui

Article 138989

View PDF Article preview

Research article ● *Open access*

High pressure-assisted enzymatic hydrolysis potentiates the production of quinoa protein hydrolysates with antioxidant and ACE-inhibitory activities

Ludmilla de Carvalho Oliveira, Cristina Martinez-Villaluenga, Juana Frias, María Elena Cartea, ... Elena Peñas

Article 138887

View PDF Article preview

Research article ● Full text access

Electrochemiluminescence detection of diazinon in vegetables based on the synergistic interaction of WO_{3-x} dots with Au@SiO_2 nanocapsules

Wenzheng Liu, Haifang Wang, Peisen Li, Chengqiang Li, ... Xia Sun

Article 139011

View PDF Article preview

Research article ● Full text access

Strategies for using magnetic beads in enhanced deep eutectic solvent-mechanochemical extraction of natural products from orange peels

Zhaoyang Wang, Wuxia Ge, Wentao Bi, David Da Yong Chen

Article 139004

View PDF Article preview

Research article ● Full text access

Investigation of the role of sodium chloride on wheat starch multi-structure, physicochemical and digestibility properties during X-ray irradiation

Haiyu Luo, Danyang Liang, Qing Liu, Yue Zheng, ... Wenhao Li

Article 139012

View PDF Article preview

Research article ● Full text access

Simultaneous determination of advanced glycation end products and heterocyclic amines in roast/grilled meat by UPLC-MS/MS

Mingyu Li, Chunjiang Zhang, Zhenyu Wang, Na Liu, ... Dequan Zhang

Article 138930

View PDF Article preview

Research article ● Full text access

Multispectral detection of dietary fiber content in Chinese cabbage leaves across different growth periods
Shaoliang Zhang, Xin Duan, Xinglong Yan, Xiaoxue Yuan, ... Aixia Gu
Article 138895

View PDF Article preview

Research article ● Full text access
Polyglycerol polyricinoleate and lecithin stabilized water in oil nanoemulsions for sugaring Beijing roast duck: Preparation, stability mechanisms and color improvement
Xinshuo Yao, Wendi Teng, Jinpeng Wang, Ying Wang, ... Jinxuan Cao
Article 138979

View PDF Article preview

Research article ● Full text access
Improvement of the drying quality of blueberries by catalytic infrared blanching combined with ultrasound pretreatment
Xingrui Bei, Xiaojie Yu, Cunshan Zhou, Abu ElGasim A. Yagoub
Article 138983

View PDF Article preview

Research article ● Full text access
Investigating the impact of lipid molecules and heat transfer on aroma compound formation and binding in roasted chicken skin: A UHPLC-HRMS and GC-O-MS study
Ruotong Nie, Zhenyu Wang, Huan Liu, Xiangru Wei, ... Dequan Zhang
Article 138877

View PDF Article preview

Research article ● Full text access
Machine learning-enabled high-throughput industry screening of edible oils
Peishan Deng, Xiaomin Lin, Zifan Yu, Yuanding Huang, ... Weng Kung Peng
Article 139017

View PDF Article preview

Research article ● Full text access
The cathodically pretreated boron-doped diamond electrode as an environmentally friendly electrochemical tool for the detection and monitoring of mesotrione in food samples
Aleksandar Mijajlović, Vesna Stanković, Filip Vlahović, Slađana Đurđić, ... Dalibor Stanković
Article 138993

View PDF Article preview

Research article ● Full text access
High enrichment and sensitive measurement of oxytetracycline in tea drinks by thermosensitive magnetic molecular imprinting based magnetic solid phase extraction coupled with boron doped carbon dots
Zhi Li, Shuangying Li, Liushan Jiang, Jingwen Niu, ... Chunmao Chen
Article 138998

View PDF Article preview

Research article ● Full text access
Lipidomics analysis of rice bran during storage unveils mechanisms behind dynamic changes in functional lipid molecular species
Xuan Liu, Zhong Li, Bo OuYang, Weifei Wang, ... Yonghua Wang
Article 138946

View PDF Article preview

Research article ● Full text access
In-situ investigation of supercooling behaviour during high-pressure shift freezing of pure water and sucrose solution
Zhiwei Zhu, Jiayu Mai, Tian Li, Da-Wen Sun, ... Zhe Wang

Article 138980

View PDF Article preview

Research article ● Full text access

Enhanced antibacterial activity of bovine milk exosome-based drug formulation against bacterial pathogens

Qingjun Xu, Shuo Yang, Kai Zhang, Ying Liu, ... Shaoqi Qu

Article 139034

View PDF Article preview

Research article ● Full text access

Simulated *in vitro* infant digestion and lipidomic analysis to explore how the milk fat globule membrane modulates fat digestion

Yue Pan, Yibo Liu, Jiayi Zhao, Liqin Cui, ... Chao Gao

Article 139008

View PDF Article preview

Research article ● Full text access

Carboxymethylcellulose-induced depletion attraction to stabilize high internal phase Pickering emulsions for the elderly: 3D printing and β-carotene delivery

Jingjie Hou, Guixin Tan, Afeng Wei, Shan Gao, ... Yunze Ma

Article 139028

View PDF Article preview

Research article ● Full text access

Insight into the solubilization mechanism of wheat gluten by protease modification from conformational change and molecular interaction perspective

Weixiao Li, Qianxin Zhou, Jianxia Xu, Shanlong Zhu, ... Yaqing Xiao

Article 138992

View PDF Article preview

Research article ● Full text access

Novel salty peptides derived from bovine bone: Identification, taste characteristic, and salt-enhancing mechanism

Haiyan Wang, Di Chen, Wenjing Lu, Yali Dang, ... Chaogeng Xiao

Article 139035

View PDF Article preview

Research article ● Full text access

Identification of lentils (*Lens culinaris* Medik) from Eglouvi (Lefkada, Greece) based on rare earth elements profile combined with chemometrics

Theopisti Lymperopoulou, Kalliopi Balta-Brouma, Lamprini-Areti Tsakanika, Constantina Tzia, ... Fotios Tsopelas

Article 138965

View PDF Article preview

Research article ● Full text access

Nano-palladium-decorated bismuth sulfide microspheres on a disposable electrode integrated with smartphone-based electrochemical detection of nitrite in food samples

Kiattisak Promsuwan, Jenjira Saichanapan, Asamee Soleh, Kasrin Saisahas, ... Warakorn Limbut

Article 138987

View PDF Article preview

Research article ● Full text access

Aggregation-induced emission nanoparticles facilitating multicolor lateral flow immunoassay for rapid and simultaneous detection of aflatoxin B1 and zearalenone

Yi Zhang, Guoxin Chen, Xirui Chen, Xiaxia Wei, ... Xiaolin Huang

Article 138997

View PDF Article preview

Research article ● Full text access

Controlling soft rot of green pepper by bacteriocin paracin wx3 and its effect on storage quality of green pepper

Lanhua Yi, Teng Qi, Xiaofen Li, Kaifang Zeng

Article 138962

View PDF Article preview

Research article ● Full text access

Edible Sea urchins *Echinus esculentus* from Norwegian waters- Effect of season on nutritional quality and chemical contaminants

Imen Hamed, Dionysios Tsoukalas, Anita Nordeng Jakobsen, Junjie Zhang, ... Jørgen Lerfall

Article 139032

View PDF Article preview

Research article ● Full text access

Evaluation of biological activity and prebiotic properties of proanthocyanidins with different degrees of polymerization through simulated digestion and *in vitro* fermentation by human fecal microbiota

Xiaoyi Chen, Shuai Liu, Hong Song, Chunlong Yuan, Junjun Li

Article 139015

View PDF Article preview

Research article ● Full text access

Unraveling the binding mechanism between soybean protein isolate and selected bioactive compounds

Yves Harimana, Bertrand Muhoza, Philip Munyandamutsa, Javzan Gankhuyag, ... Yang Li

Article 139031

View PDF Article preview

Research article ● *Open access*

Novel procedures for olive leaves extracts processing: Selective isolation of oleuropein and elenolic acid

Serena Fiorito, Chiara Collevecchio, Roberto Spogli, Francesco Epifano, Salvatore Genovese

Article 139038

View PDF Article preview

Research article ● Full text access

Impact of high-pressure processing on hemolymph, color, lipid globular structure and oxidation of the edible portion of blood clams

Suriya Palamae, Wattana Temdee, Jirakrit Saetang, Umesh Patil, ... Soottawat Benjakul

Article 138948

View PDF Article preview

Research article ● Full text access

Rapidly enrichment and detection of per-and polyfluoroalkyl substances in foods using a novel bifunctional covalent organic framework

Jing Gong, Xingyuan Zhang, Rongyao Liang, Juanqiong Ma, ... Qiongfeng Liao

Article 139016

View PDF Article preview

Research article ● Full text access

Uncovering the Counterfeit: A study of whiskey authenticity through volatile organic compound fingerprinting, aroma and color sensory analysis

Vítor Luiz Caleffo Piva Bigão, Jonas Joaquim Mangabeira da Silva, Murilo Henrique Anzolini Cassiano, Bruno Ruiz Brandão da Costa, ... Bruno Spinosa De Martinis

Article 139023

View PDF Article preview

Research article ● Full text access

A new PdMOF-loaded molecularly imprinted polyaniline nanocatalytic probe for ultratrace oxytetracycline with SERS technique

Zhiyu Qin, Youjun Zhang, Guiqing Wen, Zhiliang Jiang

Article 139041

View PDF Article preview

Research article ● Full text access

Direct elemental analysis of plant oils by inductively coupled plasma mass spectrometry: Simple sample dilution combined with oxygen introduction into the plasma

Filip Gregar, Jakub Grepl, David Milde, Tomáš Pluháček

Article 139010

View PDF Article preview

Research article ● Full text access

Metabolomic insights into the browning inhibition of fresh-cut apple by hydrogen sulfide

Chen Chen, Jiani Xie, Jie Gang, Mingyu Wang, ... Aili Jiang

Article 139005

View PDF Article preview

Research article ● *Open access*

Assessment of anthropogenic particles content in commercial beverages

Cristina Socas-Hernández, Pablo Miralles, Javier González-Sálamo, Javier Hernández-Borges, Clara Coscollà

Article 139002

View PDF Article preview

Research article ● Full text access

Effect of vine leaves processing on Azoxystrobin, Fenazaquin and Indoxacarb residues dissipation: processing factors and consumer safety assessment

Liliane Majed, Salem Hayar, Sylvie Dousset, Britt Marianna Maestroni, Khaled El Omari

Article 139065

View PDF Article preview

Research article ● Full text access

Pickering emulsion stabilized by grass carp myofibrillar protein via one-step: Study on microstructure, processing stability and stabilization mechanism

Xuehua Zhang, Zhongbo Liu, Wenzheng Shi

Article 139014

View PDF Article preview

Research article ● Full text access

Characteristics of casein phosphopeptides in Chinese human milk and its correlation with infant growth: A cross-sectional study

Muke Han, Kaifeng Li, Yuehui Fang, Baorong Chen, ... Yajun Xu

Article 139007

View PDF Article preview

Research article ● Full text access

Quality and flavor development of solid-state fermented surimi with *Actinomucor elegans*: A perspective on the impacts of carbon and nitrogen sources

Yicheng Ding, Wenjia He, Wangli Dai, Xiaoben Xie, ... Xuxia Zhou

Article 139053

View PDF Article preview

Research article ● Full text access

The effect of extraction methods on the components and quality of *Camellia oleifera* oil: Focusing on the flavor and lipidomics

Wenquan Zeng, Xudong Liu, Yan Chao, Yiying Wu, ... Changzhu Li
Article 139046

View PDF Article preview

Research article ● Full text access

Novel hydrocolloids synthesized by polyphenols grafted onto chitosan: A promising coating to inhibit PhIP formation during pan-frying of golden pompano fillets

Mantong Zhao, Zhongyuan Liu, Ying Sun, Haohao Shi, ... Xuanri Shen
Article 139029

View PDF Article preview

Research article ● Full text access

Development of UV-Vis spectroscopy-based analysis method for determination of tin(IV) in epilobium parviflorum (hoary willowherb) tea using deep eutectic solvent based preconcentration

Ozan Yağmuroğlu
Article 139036

View PDF Article preview

Research article ● Full text access

Simulating the behavior of antioxidant to explore the mechanisms of oxidative stability in Pickering emulsion

Zhibin Chen, Zijun Zhao, Wenbo Wang, Qianyi Ye, Jie Xiao
Article 138291

View PDF Article preview

Research article ● Full text access

Inhibitory effects and mechanisms of phenolic compounds in rapeseed oil on advanced glycation end product formation in chemical and cellular models *in vitro*

Huihui Liu, Ruiying Zhang, Wen Wang, Xiaoyang Xia, ... Xia Xiang
Article 139056

View PDF Article preview

Research article ● Full text access

Ultra-trace Ag doped carbon quantum dots with peroxidase-like activity for the colorimetric detection of glucose

Wei Tan, Guixiang Yao, Hang Yu, Yanzhi He, ... Hongbin Wang
Article 139020

View PDF Article preview

Page 1 of 2

Previous vol/issue Next vol/issue

ISSN: 0308-8146

Copyright © 2024 Elsevier Ltd. All rights are reserved, including those for text and data mining, AI training, and similar technologies.

ELSEVIER

All content on this site: Copyright © 2025 Elsevier B.V., its licensors, and contributors. All rights are reserved, including those for text and data mining, AI training, and similar technologies. For all open access content, the relevant licensing terms apply.

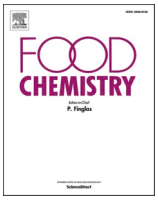
Food Chemistry 447 (2024) 138964



Contents lists available at ScienceDirect

Food Chemistry

journal homepage: www.elsevier.com/locate/foodchem





Short-term steaming during processing impacts the quality of Citri Reticulatae 'Chachi' peel

Shiheng Chen [a,1], Ziying Chen [b,1], Dylan O'Neill Rothenberg [a], Yong Long [c], Huafeng Li [d], Xiaoyang Zeng [a], Zhen Zeng [a], Xiaoli Mo [a], Dunying Wu [a], Yinghong Liao [b], Yahui Huang [a,*], Sui Xiao [b,**], Xu Zhang [b,**]

[a] Department of Tea Science, College of Horticulture, South China Agricultural University, Guangzhou, China
[b] Guangdong Key Laboratory for Innovative Development and Utilization of Forest Plant Germplasm, College of Forestry and Landscape Architecture, South China Agricultural University, Guangzhou, China
[c] Center of Logistics Management, Shenzhen Customs, Shenzhen, China
[d] Guangdong Maoming Agriculture & Forestry Technical College, Maoming, China

ARTICLE INFO

Keywords:
Short-term steaming
Peel of Citri Reticulatae 'Chachi'
Irritation
Medicinal and food homology

ABSTRACT

Citrus peel is a commonly used food-medicine material in the production of fast-moving consumer goods (FMCGs). For instance, Ganpu tea is manufactured by combining the peel of Citri Reticulatae 'Chachi' (PCRC) with Pu-erh tea. The alleviated irritation of PCRC through years of aging makes Citri reticulatae Pericarpium a traditional Chinese medicine. Herein, we introduced short-term steaming into the processing of PCRC to favor the quick removal of its irritation while retaining its food-medicine properties. Sensory evaluation and volatile component analysis showed that 60-s steaming reduced irritation of freshly prepared PCRC. Biological evaluations indicated no effects of steaming on the neuroprotective activity of PCRC. The process increased the contents of several bioactive ingredients, including hesperidin, nobiletin, tangeretin, and synephrine. In addition, physical indications of accelerating PCRC aging were observed. Taken together, our findings suggest that short-term steaming may offer a promising new possibility for enhancing the quality of citrus peel.

1. Introduction

Citrus peel, also known as "Jupi" in China, is a well-known food-medicine dual-use material in the production of popular fast-moving consumer goods (FMCGs). A common way to consume citrus peel is by drying it, then infusing it in hot water and drinking it. The traditional process of preparing medicinal-grade peel of Citri Reticulatae 'Chachi' (PCRC), known as "Chenpi", involves picking fresh citrus, cleaning, cutting, and removing the pulp, withering the peel, sun-drying, then aging for several years. According to traditional Chinese medicine, aged PCRC regulates "Qi" flow to strengthen the spleen and dry dampness, reducing phlegm. It is mainly used to treat abdominal distension, lack of appetite, vomiting, diarrhea, and coughing with phlegm (National Pharmacopoeia Commission, 2020). Modern pharmacology studies indicate that the chemical constituents of PCRC include flavonoids, volatile oils, polysaccharides, and alkaloids (Luo et al., 2019), with the predominant bioactive component reported to be flavonoids, particularly flavonoid glycosides and polymethoxyflavonoids (Fu et al., 2018). PCRC possesses broad-spectrum pharmacological activities, such as anti-asthmatic (Fu, Zou, An, Yu, & Tang, 2019), antioxidant (Liang et al., 2021), anti-inflammatory (Shen, Jiang, Zhu, & Qin, 2017), antitumor (Somasundaram et al., 2012), and anti-neuroinflammatory properties (Ho & Kuo, 2014).

The traditional aging process alters the properties and efficacy of PCRC to better suit the clinical needs of traditional medicine (Wang, Huang, Zhang, Juan, & Liu, 2012). In fact, prior to aging, PCRC is generally not considered suitable for direct consumption due to its potential to damage the gastrointestinal tract. Therefore, the aging process is necessary to convert and degrade the irritant components in PCRC, and enhance its medicinal value (Zhang et al., 2022). Citrus peel FMCG companies would prefer that consumers consume their product immediately after purchase to increase product turnover rate. At the same

* Corresponding author.
** Corresponding authors.
E-mail addresses: 13501513191@163.com (Y. Huang), suixiao@outlook.com (S. Xiao), zhangxu919@hotmail.com (X. Zhang).
[1] These authors contributed equally to the work.

https://doi.org/10.1016/j.foodchem.2024.138964
Received 10 November 2023; Received in revised form 19 February 2024; Accepted 4 March 2024
Available online 8 March 2024
0308-8146/© 2024 Elsevier Ltd. All rights reserved.

time, however, they seek to underscore the age-associated value of their product to increase its market value. Of course, the above-mentioned traditional approach to preparing PCRC requires specialized storage facilities and considerable time, which significantly increases production cost.

A potential solution to this issue may be found in the processing methods of Ganpu tea, a popular type of FMCG that combines PCRC with Pu-erh tea. In Ganpu Tea processing, to remove the pungent/irritating taste of PCRC, a common method is to treat Pu-erh tea-filled PCRC at high temperatures for several minutes before drying (Zhou et al., 2023). While notably effective at removing undesirable flavor attributes, this process nonetheless remains imperfect. In particular, the risks associated with heat treatment including potential damage to the active ingredients, which may impede their bioactivities and subsequent transformation during the aging process.

To address these issues, the present study meticulously examines the effects of short-term steam treatment on PCRC. Specifically, we explore in detail how this process may be optimized for significant reductions in pungent/irritating taste without corresponding losses in ingredient bioactivity or the capacity of PCRC to undergo further age-induced transformations over time. In our previous study, we surprisingly found that the content of flavonoids and methoxyflavonoids in PCRC, such as quercetin, hesperidin, and nobiletin, increased during sun-drying without steaming (Xiao et al., 2021). Based on the theory of "food and medicine continuum" (Yao, He, & Xiao, 2023), these compounds are critical for PCRC as a food-medicine dual-use product, and merit careful attention during the aging process of Chenpi. Currently, it is unknown whether short-term steaming can remove the pungent flavors of PCRC while maintaining its key food-medicine properties.

In the present study, short-term steaming of different times was applied to PCRC, followed by direct sun drying to obtain the study samples. Human sensory evaluation, along with E-nose and headspace-solid phase microextraction-gas chromatography–mass spectrometry (HS-SPME-GC–MS), was applied to analyze the underlying mechanism of reduced irritation and milder taste. The differences in volatile metabolites between samples with and without steam after one year of storage were compared to understand the impact of steam treatment on flavor during aging. Several key active components in PCRC were quantified using high-performance liquid chromatography (HPLC). Considering aged PCRC is a commonly used herb for depression therapy in traditional Chinese medicine (Yu, Shao, Fu, Zhou, & Chen, 2021), with observed antidepressant-like effects in animal experiments (Li, Chen, Chen, Yi, & Liu, 2014), an *in vitro* neuroprotective model was used to evaluate the pharmacological activity of PCRC.

Additionally, non-targeted metabolomics technology was employed to study all metabolites of the samples after one year of aging, offering insights into the early period of aging and intrinsic compositional changes of PCRC. Overall, this research provides a comprehensive analysis of the effects of short-term steaming on the quality of citrus peel during processing, including the material basis for irritation, intrinsic active components, and the pharmacological activity of PCRC. These findings may guide and enhance the processing of both PCRC and traditional "Chenpi".

2. Materials and methods

2.1. Plant material

Citrus reticulata 'Chachi' were selected for the purpose of this study, following the picking standards of collecting mature citrus (National Pharmacopoeia Commission, 2020). The mature *citrus reticulata* 'Chachi' were collected in November 2021 in Xinhui, Guangdong.

2.2. Chemicals

Methanol, acetonitrile, isopropanol, and formic acid were HPLC-grade and purchased from Thermo Fisher (USA). The standards for HPLC analysis included synephrine (≥98%, CAS: 94–07-5), hesperidin (≥98%, CAS: 520–26-3), nobiletin (≥98%, CAS: 478–01-3), tangeretin (≥98%, CAS: 481–53-8) and 7-methoxyflavone (≥98%, CAS: 22395–22-8) and were purchased from Shanghai Yuanye Bio-Technology Co., Ltd. (Shanghai, China). L-Glutamic acid, the total antioxidant capacity assay kit (ABTS and DPPH), and Hoechst 33258 staining solution were purchased from Sangon Biotech (Shanghai, China). 3-(4,5-dimethylthi-azol-2-yl)-2,5-diphenyltetrazolium bromide (MTT), dimethyl sulfoxide (DMSO), Dulbecco's minimal essential medium (DMEM), phosphate buffered saline (PBS), and fetal bovine serum (FBS) were purchased from Sigma-Aldrich Co. (St. Louis, Mo, USA). PC12 cells were purchased from Kunming Institute of Zoology (Yunnan, China).

2.3. Samples

Following the picking of mature *Citrus reticulata* 'Chachi' in November, the surface impurities were first cleaned with water. Secondly, we applied the traditional processing method to cut the citrus, assuring the pedicle connected the whole pericarp while removing the pulp. Thirdly, we steamed the citrus peels in a steaming apparatus (SZQ-ZBTR-50, Guangdong, China) for 0 s (S0), 20 s (S2), 40 s (S4), 60 s (S6) and 90 s (S9). Fourthly, citrus peels were evenly spreading in a cool and ventilated place for 4 h, allowing water to slowly evaporate and the texture of the peels to become soft. Finally, samples were placed in the sun for 4 days, until the moisture content of the citrus peel fell below 13%, in accordance with the Chinese Pharmacopoeia (version 2020). The detailed parameters of steaming apparatus used in the steaming treatment are shown in Table S1.

Each PCRC sample (a mixture of 30 individual citrus peels) was first disassembled and mixed evenly, then divided into three groups. The first group was placed in a dry and ventilated room to age for one year (AS0, AS2, AS4, AS6, AS9). During aging, PCRC samples were exposed to sunlight twice per year to avoid mildew. The second group was used for sensory evaluation immediately after drying in the sun (S0, S2, S4, S6, S9). The third group was dried completely by vacuum freeze-drying machine after drying in the sun and ground into a homogeneous powder using a mill, then stored at −20 °C for analysis (powder of S0, S2, S4, S6, S9). The processing diagram was shown in Fig. 1.

2.4. Sensory evaluation

At present, there is no standard evaluation method for PCRC consumed as a tea beverage. The sensory evaluation of PCRC samples subjected to steaming for different time was performed by 8 professional tea tasters from the Department of Tea Science at South China Agricultural University, in accordance with the Methodology for Sensory Evaluation of Tea (GB/T 23776–2018) with some modifications. The PCRC samples were blindly coded with random numbers and placed on a plate. The sample (3.0 g) was infused with 150 mL of 100 °C distilled water for 5 min. Then, appearance, aroma, taste and pungency level of PCRC samples were described by the sensory evaluation panel. Description standards are described in Table S2.

2.5. E-nose measurement

The PEN3 E-nose (Airsense Analytics GmbH, Germany) was applied to determine the volatile substances. The PEN3 E-nose utilizes 10 different metal oxide sensors as the sensor array. The performance description of the E-nose gas sensor array is characterized in Table S3.

Before detection, 1.0 g PCRC powder was weighed and placed in a headspace vial sealed with cling film. The headspace vial was heated in a 90 °C heater (MiniH-100D, Hangzhou, China) for 5 min, then left undisturbed for 30 min to reach the headspace equilibrium. Next, zero gas (indoor air filtered with standard activated carbon) was pumped into the cleaning channel for 180 s and sensors were reset. Sampling was carried

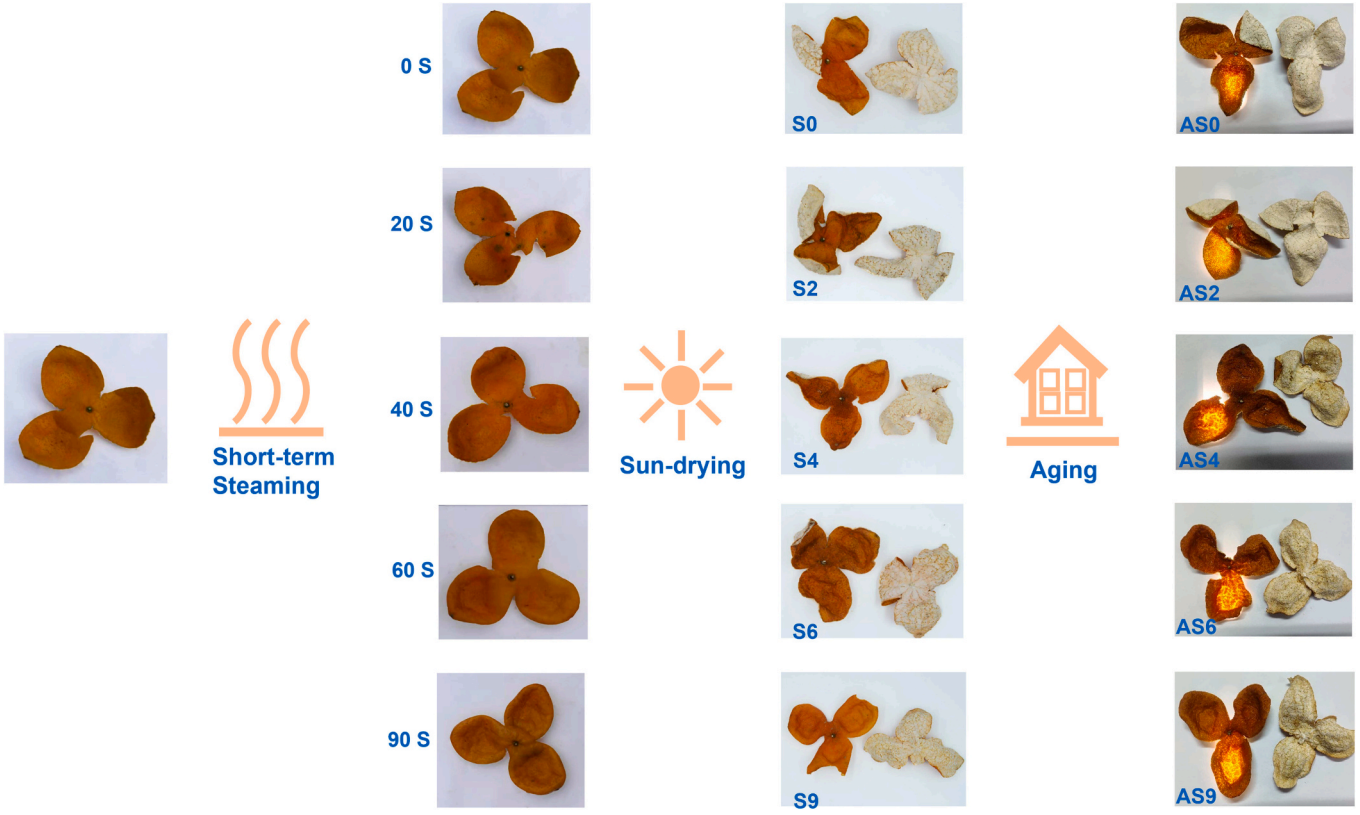


Fig. 1. Images of the PCRC under different treaments and stages of processing.

out with measurement time of 120 s and a pre-sampling time of 5 s. The injection flow rate was set to 300 mL/min. Each sample was measured in triplicate.

2.6. Analysis of HS-SPME-GC–MS

2.6.1. Headspace solid-phase microextraction (HS-SPME)

1.0 g PCRC powder was weighed and placed in a 25 mL headspace vial sealed with cling film, then was heated in the 90 °C heater (MiniH-100D, Hangzhou, China) for 45 min. At the same time, the fiber CAR/PDMS (Supelco, Bellefonte, PA) of 75 μm thickness was exposed to the headspace of the sample for 45 min. Once the extraction time had ended, the fiber was removed from the vial and placed in the injection port of the gas chromatograph for the rapid desorption of analytes. A desorption time of 3 min with an injection temperature of 230 °C was sufficient to desorb the analytes from the fiber. After desorption from the fiber the headspace of the sample went into contact with the stationary phase in the column. The fiber was cleaned before each microextraction to prevent contamination using a blank GC–MS run with the same conditions mentioned above.

2.6.2. GC–MS analysis

The volatile compounds of PCRC were analyzed by GC–MS (Shimadzu, Kyoto, Japan), equipped with a Rxi-5sil column (30 mm × 0.25 mm × 0.25 μm), and identified by mass spectrometry in the NIST 11 database. A high-purity helium (99.999%) flow used in the split injection mode (20:1) was set at 1.0 mL/min. The temperature of the GC injector was maintained at 230 °C. The oven was initiated at 60 °C (2 min), ramped up to 130 °C at 3 °C/min, held for 2 min, ramped up to 210 °C at 5 °C/min, then remained for 5 min. The temperature of ion source (EI) and desolvation were set at 230 °C and 250 °C, respectively. The collision energy was 70 eV and the scan range was 35–350 *m/z*.

2.7. HPLC analysis

The analytical samples were prepared as follows: 0.2 g of the PCRC powder was weighed and extracted with 25 mL of 100% methanol by ultrasonic processing (power: 300 W, frequency: 40 kHz) for 45 min. The extracts were centrifuged for 10 min to obtain supernatants, which were filtered through a 0.22 μm membrane for HPLC analysis. Three replicates were performed for each sample.

The determination was performed using a high-performance liquid chromatography (HPLC) system (Agilent Technologies Inc., USA), equipped with a XDB-C18 column (5 μm, 4.6 mm × 150 mm, Agilent Technologies Inc., USA). The mobile phase included eluents A (0.2% formic acid) and B (acetonitrile). The flow rate was 1 mL/min, and the detection wavelength was set to 255 nm. The gradient elution conditions were as follows: 0–3 min, 10% B; 3–5 min, linear gradient increase to 15% B; 5–8 min, linear gradient increase to 40% B; 8–15 min, linear gradient increase to 50% B; 15–17 min, linear gradient increase to 60% B; 17–20 min, linear gradient decrease to 10%. The injection volume was 10 μL, and the temperature of the column was maintained at 30 °C. The compounds, including synephrine, hesperidin, nobiletin, tangeretin and 7-methoxylflavone, were identified by HPLC, with the standards quantified using the external standard method of HPLC. The retention time, standard curve, limit of detection (LOD) and limit of quantification (LOQ) are listed in Table S4.

2.8. Bioactivity assays

2.8.1. Sample extraction

4.0 g PCRC powder was weighed and extracted by 100 mL of ultrapure water at 100 °C water for 60 min with stirring for every 5 min. After centrifugation for 10 min, residues were re-extracted as mentioned earlier. The two resultant supernatants were combined and concentrated, then dried by vacuum freeze-drying for 82 h.

2.8.2. Antioxidant activity assay

The total antioxidant capacity (T-AOC) assay kit (ABTS & DPPH) was performed to detect the antioxidant capacities of PCRC groups at concentrations of 0.5, 1, 2 and 4 mg/mL. Each treatment was performed in three replicates.

2.8.3. In vitro Neuroprotection assay

The neuroprotective effect of PCRC was determined by MTT assay and Hoechst 33258 staining methods. PC12 cells were seeded at a density of 7000 cells/well in 96-well culture plates, and then randomly divided into 6 groups: control group, Glu-induced group, and PCRC groups of 0.25, 0.5, 1 and 2 mg/mL. Cells were treated with PCRC extracts for 1 h before the exposure to 15 mM Glu. The MTT and staining by Hoechst 33258 were carried out after another 24 h. Each treatment was performed in three replicates.

2.9. Analysis of LC-MS untargeted metabolomics

The analytical samples were prepared as follows: 50 mg PCRC powder was extracted with grinding beads (6 mm) and 400 μL extracting solution (methanol: acetonitrile = 1:1(v: v)) containing four internal standards (L-2-chlorophenylalanine, etc.), then grinded in a frozen tissue grinder at −10 °C for 6 min. Samples were treated with ultrasonic extraction for 30 min at low temperature (5 °C, 40 KHz), completely precipitated at −20 °C for 30 min, then centrifuged at 13000 *g* for 15 min at 4 °C. The obtained supernatants were filtered through a 0.22 μm membrane for analysis. In addition, 20 μL supernatant was removed from each sample and mixed as samples for quality control (QC). Each treatment was performed in three replicates.

Nontargeted metabolomic analysis was performed by an ultra performance liquid chromatography tandem fourier transform mass spectrometry system (UHPLC-Q Exactive HF-X, Thermo Ferrier, USA). The separation of chemical compounds was conducted using an ACQUITY UPLC HSS T3 column (100 mm × 2.1 mm, 1.8 μm; Waters, Milford, USA). The mobile phase included eluents A (5% acetonitrile containing 0.1% formic acid) and B (47.5% acetonitrile, 47.5% isopropyl alcohol and 5% water with 0.1% formic acid). The injection volume was 3 μL and the column temperature was 40 °C. The detailed mobile phase

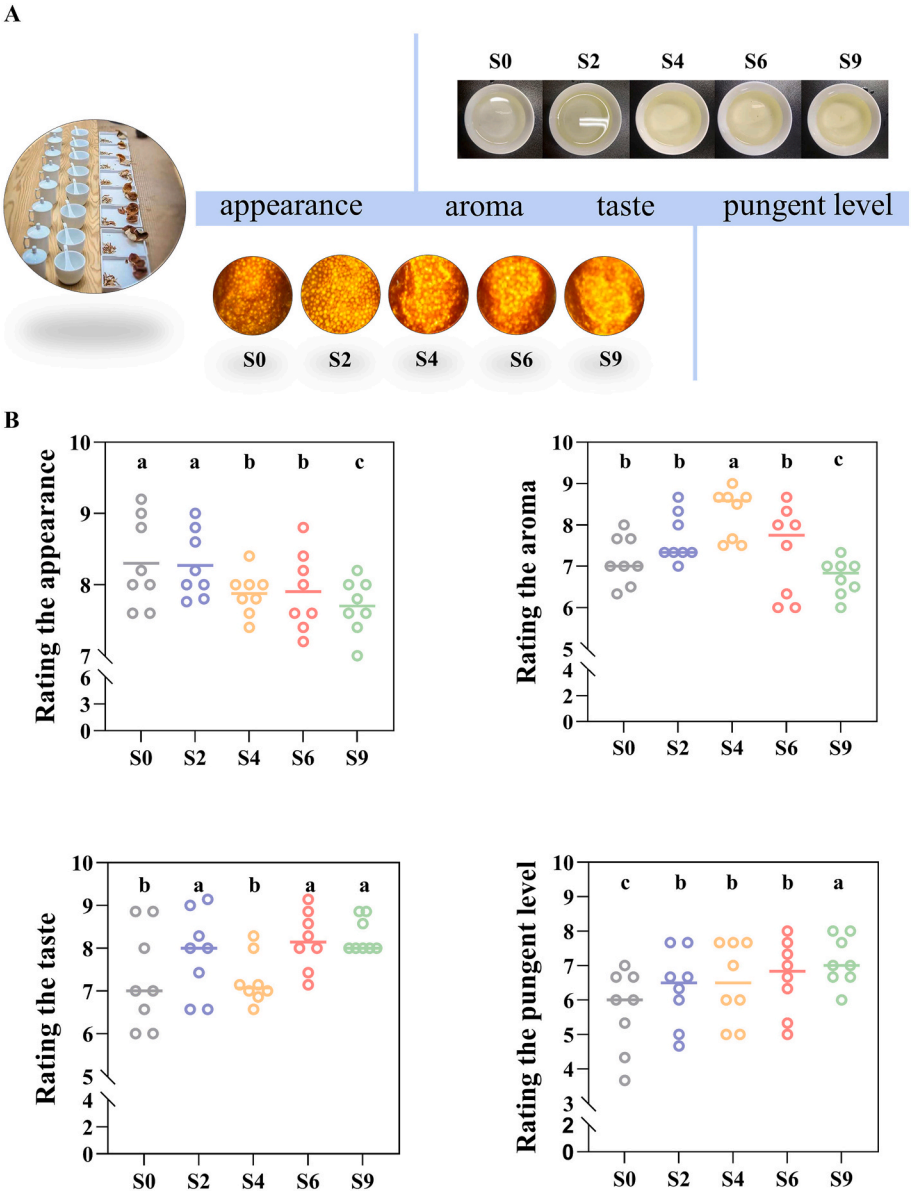


Fig. 2. (A) Images from sensory evaluation of appearance, aroma, taste and pungent level of PCRC. (B) Sensory scores of the appearance, aroma, taste and pungent level by 8 persons, each circle point represents one score. Statistical analyses were performed using ANOVA, followed by Duncan's multiple range test ($p < 0.05$).

elution conditions were listed in Table S5. The positive ESI parameters were set at follows: capillary voltage, 3.5 kV; capillary temperature, 325 °C; drying gas temperature, 425 °C; gas flow rate, 15 L/min; and full-scan mass analysis from *m/z* 70–1050.

2.10. Software and statistical analysis

The figures were obtained using the software TBtools (version 2.037), Origin 2021, Excel software (Excel 2021) and GraphPad Prism 9.0. The data are presented as mean ± standard deviation (SD) of three replicates. Each sample was a mixture of 30 individual citrus peels from one treatment. The statistical analysis of datasets (one-way analysis of variance, Duncan's test, $p < 0.05$) was performed using SPSS 22.0.

3. Results and discussion

3.1. Sensory evaluation

Sensory evaluation is crucial in determining the acceptability of PCRC among consumers. In this study, a multi-person sensory evaluation was conducted to assess the appearance, aroma, taste, and pungency level of PCRC. Fig. 2A shows the effects of short-term steaming on the appearance of PCRC, focusing on the oil lumen, an essential organelle responsible for synthesizing and storing volatile substances (Ge, Deng, Zeng, & Deng, 2022). Results revealed that the 20 s steam treatment resulted in a full oil lumen, and under strong light, boundaries between the oil lumen became more distinct and transparent compared to the untreated control group. However, as the steaming time increased, oil lumen shape started to deteriorate. By 90 s of steaming, most of the intervals between the oil lumen had collapsed, and the clear shape of the oil lumen disappeared. Consequently, the appearance scores gradually decreased with increasing steaming time past 20 s (Fig. 2B).

Next, we evaluated aroma following a 5 min infusion of the peels in hot water. Aroma score increased during the first 40 s of steaming, possibly due to the evaporation of low boiling-point volatile substances. Although the score of the 60 s-steam treatment was higher than that of the unsteamed sample, aroma score had begun to decrease. Treated with 90 s, the aroma score significantly decreased compared to that of the unsteamed sample. This may be attributed to the generation of new components, the evaporation of low boiling point compounds, or that most of the oil lumen had been damaged due to continuous high-temperature steaming.

Regarding the sensory evaluation of taste, nearly all treatments led to a significant improvement in the softness mouthfeel. Notably, when the steaming time reached 60 s, the differences in taste ratings became smaller. Continuing to 90 s, no further improvement on the taste was found. Evaluating the pungency level, PCRC pungency decreased continuously with increasing steaming time.

Overall, a short-term steaming of 60 s or less improved the softness of PCRC-infused water and reduced the overall pungency level without seriously damaging the structure of the oil lumen, ultimately contributing to milder, more aromatic, and more mellow PCRC flavor.

3.2. Analysis of volatile metabolites based on E-nose measurement and HS-SPME-GC–MS

To gain a deeper understanding of the volatile compounds responsible for the pungent taste of PCRC, we utilized the E-nose to conduct a preliminary analysis of principal components. The signal values of 10 sensors in response to volatile substances from different PCRC samples were recorded (Fig. 3A). The sensors W2W and W1W were found to be the most sensitive to changes of volatile composition in the different PCRC sample treatments. This observation suggested that the main volatile substances of PCRC may consist of aromatic compounds and terpenes. HS-SPME-GC–MS identified specific volatile metabolites in PCRCs (Table S6), consistent with predictions made by the E-nose sensor, that terpenes were the most abundant components. As steaming time increased to 60 s (Fig. 3B), the total aldehydes content initially decreased, and then increased, however remained below the level of S0 (untreated control). In contrast, the terpenes increased with steaming time. Based on the sensory evaluation results, short-term steaming may reduce the presence of spicy aldehydes and potentially transform them into terpenes, as was observed in previous research (Han & Jiang, 2021). A detailed analysis of the effects of different steaming times on various volatile metabolites revealed four major trend patterns (Fig. 3C-F), discussed below.

Volatile metabolites illustrated in Fig. 3C significantly increased and then decreased during short-term steaming. They consisted of thymol (spicy and grassy flavor with strong antioxidant and antifungal activity) (Ding et al., 2023), a-terpineol (lilac flavor) (Yang et al., 2023), 4-(1-methylethenyl)-1-cyclohexene-1-carboxaldehyde (spicy, wood and citrus taste) (Hobbs et al., 2016), and linalool (French lavender scent with multi-bioactive properties, e.g. antidepressive and neuroprotective) (Pereira, Severino, Santos, Silva, & Souto, 2018). This change trend may be a result of enzymatic reactions. Initially, the rate of enzymatic reaction increased with the rise in temperature, but enzyme denaturation and inactivation caused by prolonged exposure to excessive heat resulted in a decrease in reaction rate (Arcus & Mulholland, 2020).

Fig. 3D demonstrated that, as steaming time increased, certain metabolites experienced a continuous decrease, suggesting that they may not be able to withstand high temperatures. These metabolites included 1-hydroxy-2-propanone (found in tobacco, beer, and honey and used in the synthesis of drugs, spices, and dyes) (Wu, Liu, & Pan, 2016); 1-penten-3-one (spicy and garlic odor) (Liao et al., 2023), and l-(+)-ascorbic acid 2,6-dihexadecanoate (strong antioxidant, antimicrobial, antitumor properties) (Huang et al., 2010; Karthikeyan, Velmurugan, Donio, Michaelbabu, & Citarasu, 2014). Furthermore, 2-(methylamino)-benzoic acid-methyl ester can be considered a significant factor in identifying the authenticity of PCRC, with its concentration in Chenpi observed to decrease with extended storage time (Lian, Chen, & Wu, 2018).

Several metabolites were generated de novo with short-term steaming (Fig. 3E). (*E*, *E*)-2,4-heptadienal and (*Z*)-9,17-octadecadienal were produced during the early stages of steaming. Additionally, 3,7,11,15-tetramethyl-2-hexadecen-1-ol, is a common volatile component in plants with previously measured antioxidant and antiviral effects (Akkoyunlu & Dulger, 2022; Kalasariya et al., 2022; Vitalini, Iriti, Orlando, & Garzoli, 2022), and a potential quorum-sensing inhibitor (QSI) that significantly slowed the process of microbial spoilage (Cui et al., 2022). Thus, short-term steaming provided a way to produce several new metabolites with notable bioactive properties.

Fig. 3F indicated that with increasing steaming time, 24 metabolites significantly increased in concentration, terpenes being the most abundant. Terpenes are essential components of fruit aroma, playing a key role in fruit aroma development during ripening or storage (Liat et al., 2010; Wang et al., 2023). Notably, D-limonene, that increased the most with the extension of steaming time, was considered to be crucial for the formation of a characteristic aroma in Chenpi essential oil (Li, Lin, Feng, & Zhao, 2024). Collectively, changes in these volatile metabolites can preliminarily reveal the material basis for short-term steaming in the reduced irritation of PCRC.

3.3. Changes in volatile metabolites of PCRC after aging 1 year

Based on our aforementioned findings, a 60-s steaming treatment was the most suitable for reducing the pungent taste of PCRC. After analyzing the volatile components of freshly processed PCRC and identifying components that affected the taste irritation, we aged a 60-s steaming sample for one year (AS6) to study the changes in volatile components during the early aging stage. Table S7 shows the specific volatile substances found in AS6 and the control group (AS0, 1 year aged

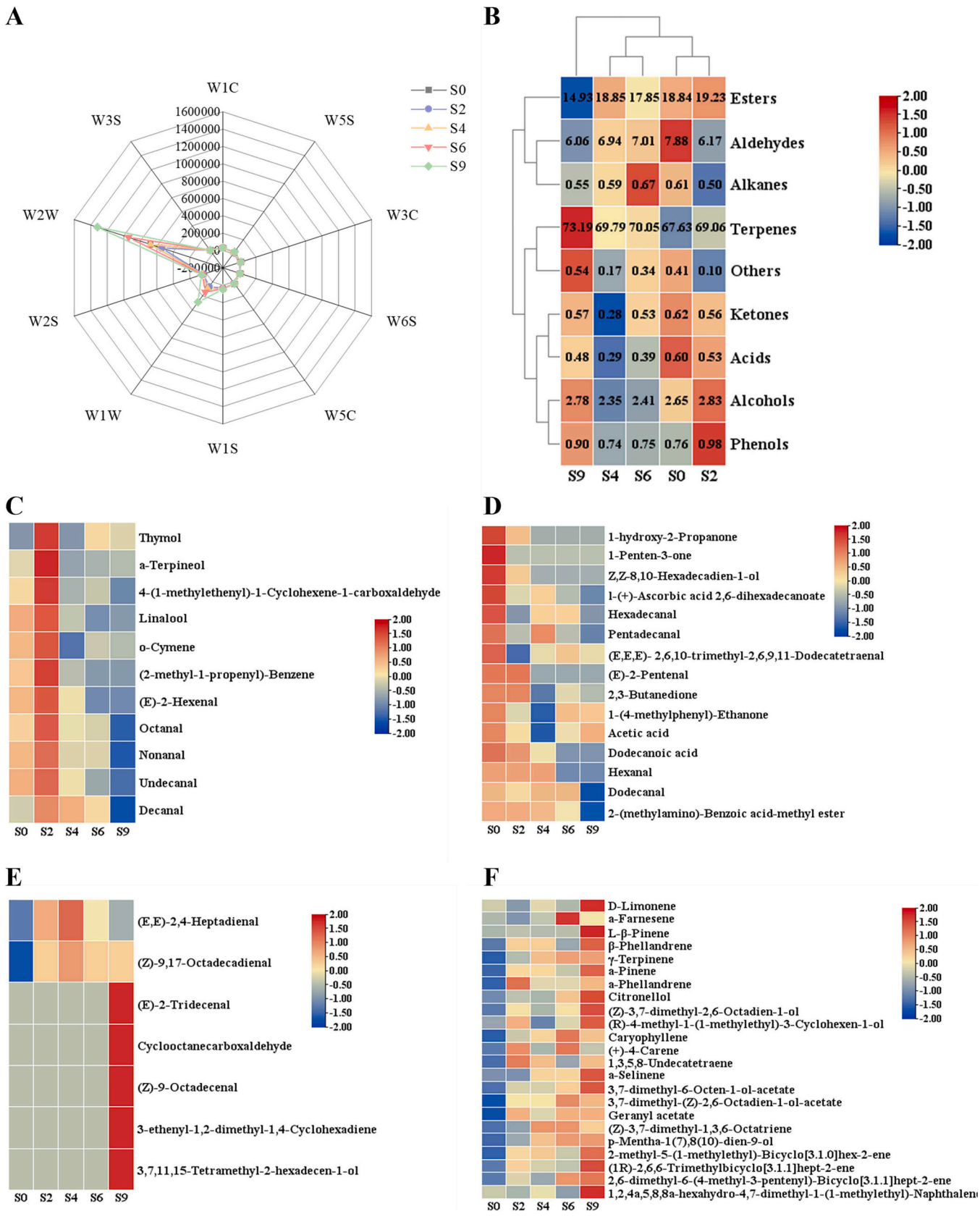


Fig. 3. (A) Radar diagram of E-nose response signal value; (B) The changes in various components of S0, S2, S4, S6, S9; the numerical values represent the proportion of each type of volatile metabolite in each sample. (C-F) Heat map of the levels of volatile metabolites under steaming treatment, including metabolites that increased until 20 s then decreased (C), declined steadily with steaming time (D), were generated de novo under steam treatment (E), or increaesd steadily with steaming time (F).

but not steamed). As shown in Fig. 4A, 84 volatile components were detected in AS0, and 87 detectable volatile components were detected in AS6. Among them, 64 components were shared in AS0 and AS6, 20 components were unique to AS0, and 23 components were unique to AS6. The unique components of AS0 included 9 aldehydes, 5 alcohols, 3 terpenes, 1 acid, 1 ester, and 1 ketone, while the unique components of AS6 included 2 aldehydes, 6 alcohols, 5 terpenes, 2 acids, 1 ester, 3 ketones, and 4 other components.

The main aroma components in both AS0 and AS6 were similar (Fig. 4B), with terpenes accounting for the largest proportion, followed by esters, aldehydes, ketones, alcohols, and phenols. Notably, steaming treatment significantly increased the overall concentrations of PCRC aroma compounds during the aging period, except for aldehydes.

Analyzing the top 20 substances in abundance (Fig. 4C), it was observed that, except for D-limonene, (*E*, *E*, *E*)-2,6,10-trimethyl-2,6,9,11-dodecatetraenal and *β*-myrcene, the contents of most substances increased with steaming during the aging process of PCRC. The content of the only aldehyde listed in the top 20 substances, (*E*, *E*, *E*)-2,6,10-trimethyl-2,6,9,11-dodecatetraenal, with an orange flavor (Wang et al., 2022) decreased with steaming. 2-(methylamino)-benzoic acid-methyl ester, a unique component of PCRC, exhibited a significant increase after aging (Lian et al., 2018). The higher level in AS6 indicated that short-term steaming contributed to an increase in 2-(methylamino)-benzoic acid-methyl ester in early aging stage. D-limonene, with a high concentration in PCRC, was considered a precursor of various aroma components (Wang et al., 2008). The decrease of D-limonene and the increase of α-terpineol and γ-terpinene in AS6 emphasized that the short-term steaming sample might accelerate the conversion of some aroma components. Additionally, when PCRC was used in high doses in clinical treatment, a reduced content of D-limonene was beneficial in mitigating gastrointestinal side effects such as nausea, vomiting, and diarrhea (Vigushin et al., 1998).

The irritating nature of PCRC not only affects taste, but also affects the gastrointestinal tract. In Guangdong, China, aged PCRC used for medicinal purposes involves a long time steaming treatment before infusion in water, which helps reduce irritation to the gastrointestinal tract. This traditional Chinese processing method was believed to speed up the aging process of PCRC and reduce its irritating effects (Zhang et al., 2022). The comparison between samples that were first steamed, and aged (AS0 and AS6) and those that were aged and then steamed (P0, P1, P8, and P60), as depicted in Fig. S1, revealed similar trends in the changes of terpenes, esters, ketones, and phenols. Therefore, short-term

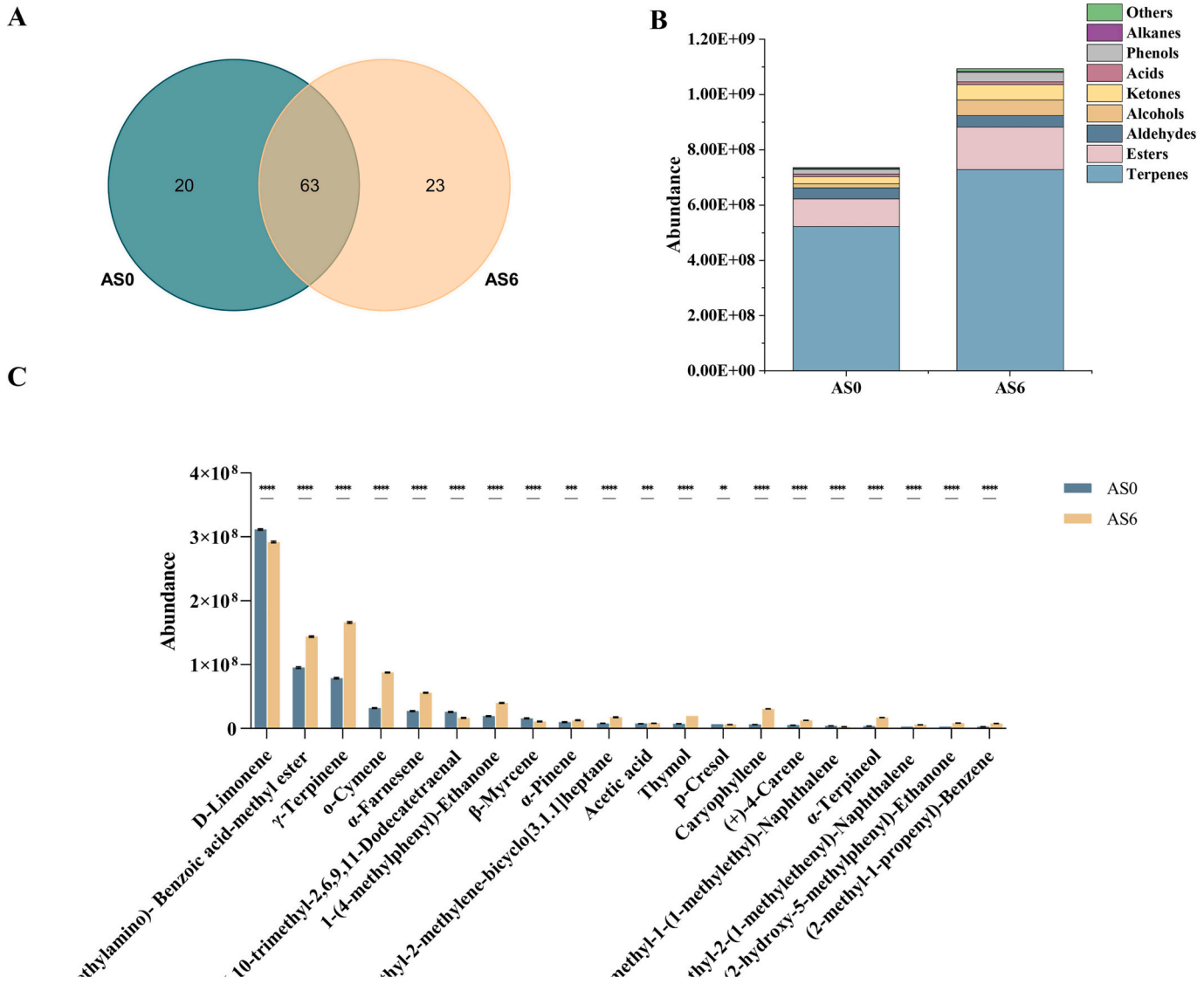


Fig. 4. (A) Venn diagram of volatile metabolites of AS6 vs AS0; (B) Total content of volatile metabolites of AS6 vs AS0. (C) The change of the top 20 volatile metabolites in abundance of AS6 vs AS0. The statistical analyses were performed using ANOVA, followed by LSD test, $*p < 0.05$, $**p < 0.01$, $***p < 0.001$, $****p < 0.0001$.

steaming may effectively accelerate the aging process of PCRC and potentially reduce its irritating effects on taste and the gastrointestinal tract.

3.4. Analysis of pharmacological activity and characteristic components

The value of PCRC exists not only in its unique flavor, but also in its properties of food medicine homology. To assess the pharmacological activity of PCRC, a PC12 cell line, demonstrated to exhibit typical neuronal characteristics (Gong, Zhou, Gong, & Qin, 2020), was used in a neuroprotection assay. Treatment of PC12 cells with 5 mM Glu alone for 24 h significantly induced cell apoptosis and led to cell death in approximately 50% of cells. Addition of various concentrations of PCRC resulted in a significant improvement on the cell viability. Short-term steaming treatment with varying time did not impair this effect (Fig. 5A). At a concentration of 0.5 mg/mL, PCRC alone did not exhibit cytotoxic activity toward PC12 cells (Fig. S2). In the case of S6 and S0 samples used for respective treatment, 100% protection of PC12 cells from Glu-induced apoptosis was observed (Fig. 5B).

Excessive Glu can damage the nervous system and lead to neurological dysfunction (Elena, Benny, & Connie, 2015; Juan et al., 2022; Kim & Na, 2016), and Glu-induced oxidative stress can cause apoptosis (Chang, Chen, Liaw, Peng, & Peng, 2020). Given that antioxidant activity was a well-known core biological activity of PCRC, we investigated the antioxidant activity of PCRC before and after short-term steaming using the ABTS and DPPH methods. Results showed that the in vitro antioxidant activity of PCRC was significantly enhanced by short-term steaming for 20 s, however gradually decreased with increasing steaming time. When steaming exceeded 60 s, the antioxidant activity was significantly lower than that of the unsteamed sample (Fig. 5C-D). It can be seen that, although the antioxidant effect was important for PCRC, it was only one aspect of the mechanism by which PCRC exerted neuroprotection.

The pharmacological activity of PCRC has often been associated with its intrinsic flavonoids. We determined the content of one alkaloid and four flavonoids, three of which are required for the Chinese Pharmacopoeia (hesperidin, nobiletin, and tangeretin), then investigated the effect of short-term steaming treatment on these characteristic active components in citrus peel. Each PCRC sample analyzed with HPLC is shown in Fig. 5E, while Fig. 5F presents the contents of synephrine, hesperidin, nobiletin, tangeretin and 7-methoxylflavone in each sample (Quantitative analysis methods for validation were provided in Table S4). The contents of hesperidin, nobiletin and tangeretin in unsteamed and steamed samples met the requirements of the Chinese Pharmacopoeia (Table S8), and were increased under short-term steaming treatment. 7-methoxylflavone as a precursor of polymethoxy flavonoid synthesis (Gang & Berim, 2016), decreased significantly with 90-s steaming, possibly leading to the observed increase in the contents of polymethoxyflavonoids in that treatment group. Surprisingly, the content of synephrine, the most abundant alkaloid in PCRC, with effective antidepressant-like activity (Kim et al., 2001), increased continuously with increasing steaming time. Consistent with a previous study (Xu, Chen, & Wang, 2011), synephrine in Chenpi increased with increasing steaming time. The increased concentration of such active components offers one potential explanation for how steamed PCRC maintained its neuroprotective effects despite a reduced antioxidant capacity.

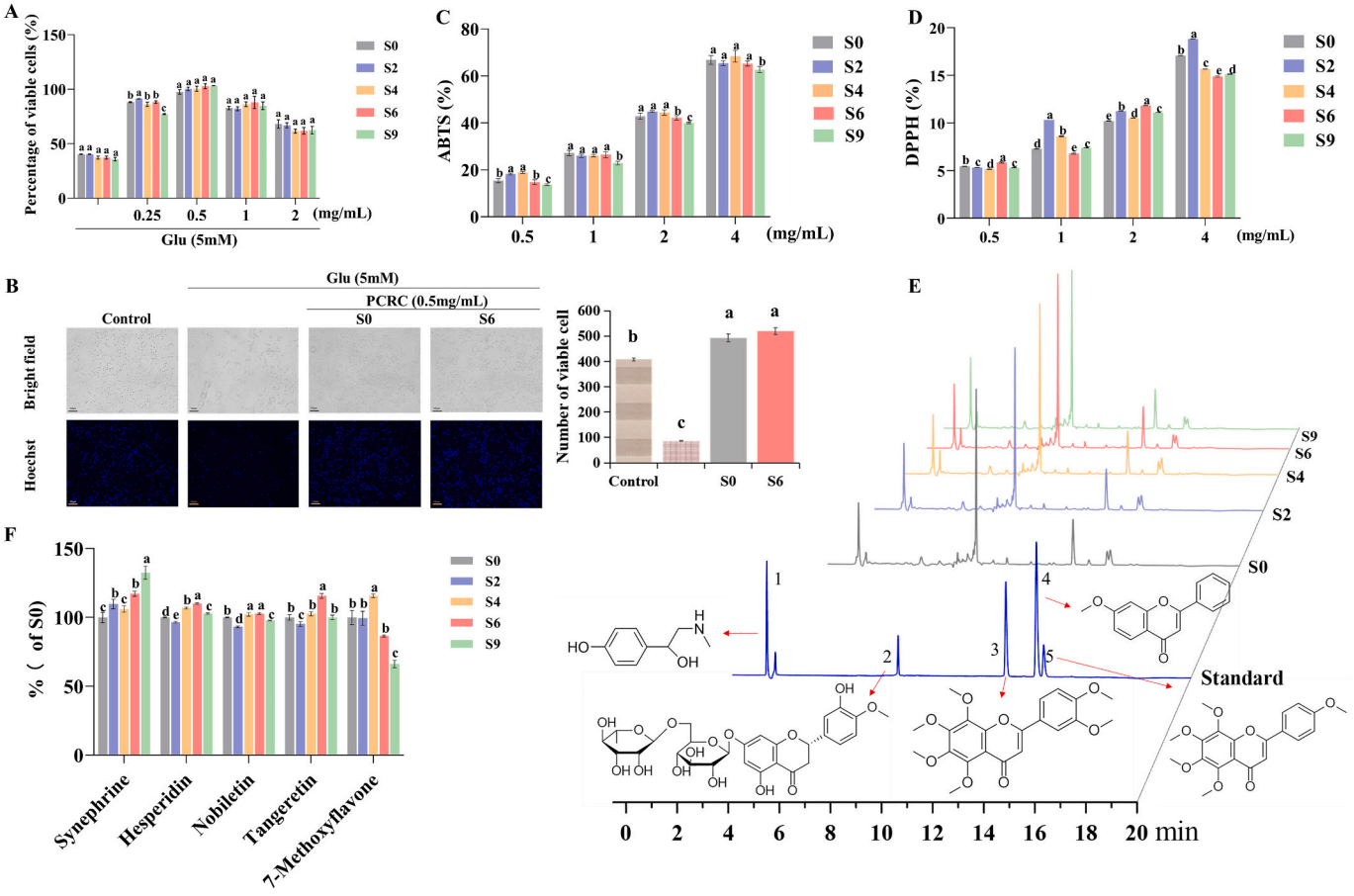


Fig. 5. (A) The neuroprotection on the Glu-induced PC12 of all PCRC treatment groups. (B) Cell survival analyzed by Hoechst 33258 staining; (C, D) The antioxidant activity of PCRC with methods of ABTS and DPPH; (E) The HPLC fingerprints of PCRC, 1. Synephrine, 2. Hesperidin, 3. Nobiletin, 4. 7-Methoxylflavone, 5. Tangeretin; (F) The contents of Synephrine, Hesperidin, Nobiletin and Tangeretin, 7-Methoxylflavone. The statistical analyses were performed using ANOVA, followed by LSD test, $*p < 0.05$, $**p < 0.01$.

Together, short-term steaming did not damage the neuroprotective capacity of PCRC in an *in vitro* model, and the increase of characteristic alkaloids and flavonoids by this treatment may provide new directions for the processing of Chenpi.

3.5. Non-targeted metabolomics analysis of PCRC after aging for 1 year

We compared and analyzed the total metabolites of AS0 and AS6. The score plot for the principal component analysis demonstrated that AS0 and AS6 were well distinguished and completely separated, indicating distinct differences between the two samples (Fig. 6A). A total of 917 differential metabolites were screened for AS0 and AS6, with 402 up-regulated components and 515 down-regulated ones (Fig. 6B). Lipids and lipid-like molecules were predominantly down-regulated, likely due to high temperatures decomposing them into more mild hydrocarbons. Organic acids and their derivatives were mostly upregulated. Natural organic acids like citric acid, malic acid, and ascorbic acid had various beneficial functions including antibacterial, anti-inflammatory, antioxidant, and immune regulation effects (Jeong et al., 2017; Koriem & Tharwat, 2023; Maity, Majumder, Pal, Saha, & Mukhopadhyay, 2023; Yang, Tang, Xiao, Du, & Li, 2018). Organic heterocyclic compounds fall into two categories; lipid heterocyclic rings and aromatic heterocyclic rings. In general, the ring system of aromatic heterocyclic compounds was stable and presented aromaticity, leading to the aroma enrichment of PCRC caused by short-term steaming. Additionally, a downward trend in organic oxygen compounds may indicate that they were decomposed into unstable and easily degradable oxygen-containing free radicals after heating (Fig. 6C-D).

Changes in the up-regulated and down-regulated substances were similar to those observed between samples S6 and S0 (Fig. S3), implying that PCRC treated with short-term steaming may still taste milder than unsteamed PCRC after aging. To further confirm this hypothesis, we conducted a sensory evaluation for PCRC that had been aged for a longer period (two years of aging). We found that the steamed PCRCs were milder in terms of taste, and pungent level with the extension of the short-term steaming time (Fig. S4).

Flavonoids are the main active ingredients of PCRC, playing a crucial role in its properties of food medicine homology (Zheng et al., 2013). To compare the differences in flavonoids between steam-treated and untreated samples after one year of aging (AS6 and AS0), we screened the top 9 flavonoids in abundance (Fig. 6E), with chemical structures shown in Fig. S5. The content of methoxyflavonoids in AS6 was not lower than that of AS0, and the levels of hesperidin, sinensetin, 5,6,7,8,3′,4′,5′-heptamethoxyflavone and neohesperidin in AS6 were significantly higher than those in AS0. Concomitant with our findings, previous research found a significant increase in the content of methoxyflavonoids in Chenpi during the first four years of aging (Yang et al., 2022).

Several compounds presently detected in PCRC have various therapeutic properties. Hesperidin exhibited cerebroprotective effects by acting as an antioxidant and anti-apoptotic agent against oxidative damages caused by cerebral ischemia-reperfusion (Praveen et al., 2020). Sinensetin, also known as 5,6,7,3′,4′-pentamethoxyflavone, was a novel and highly potent second-generation flavonoid chemosensitizer. It displayed notable medicinal benefits, including a high therapeutic index, and functioned as a non-transportable inhibitor of p-glycoprotein (Choi et al., 2002). Neohesperidin, a flavanone glycoside commonly occuring in citrus fruits, demonstrated various biological activities, ranging from food ingredient to therapeutic agent. A broad range of therapeutic and biological activities of neohesperidin were also reported in the treatment of various complex disorders, including neurodegenerative, hepatocardiac, infectious, allergic, and inflammatory diseases (Akhter, Arman, Tayab, Islam, & Xiao, 2022).

In summation, 60-s steaming treatment accelerated the early stage of PCRC aging, and enhanced its food-medicine dual-use properties. However, after two years aging, sensory evaluation revealed that although 90-s steaming treatment had a milder taste, the highest content of characteristic flavonoids was detectable in the 20-s steamed samples

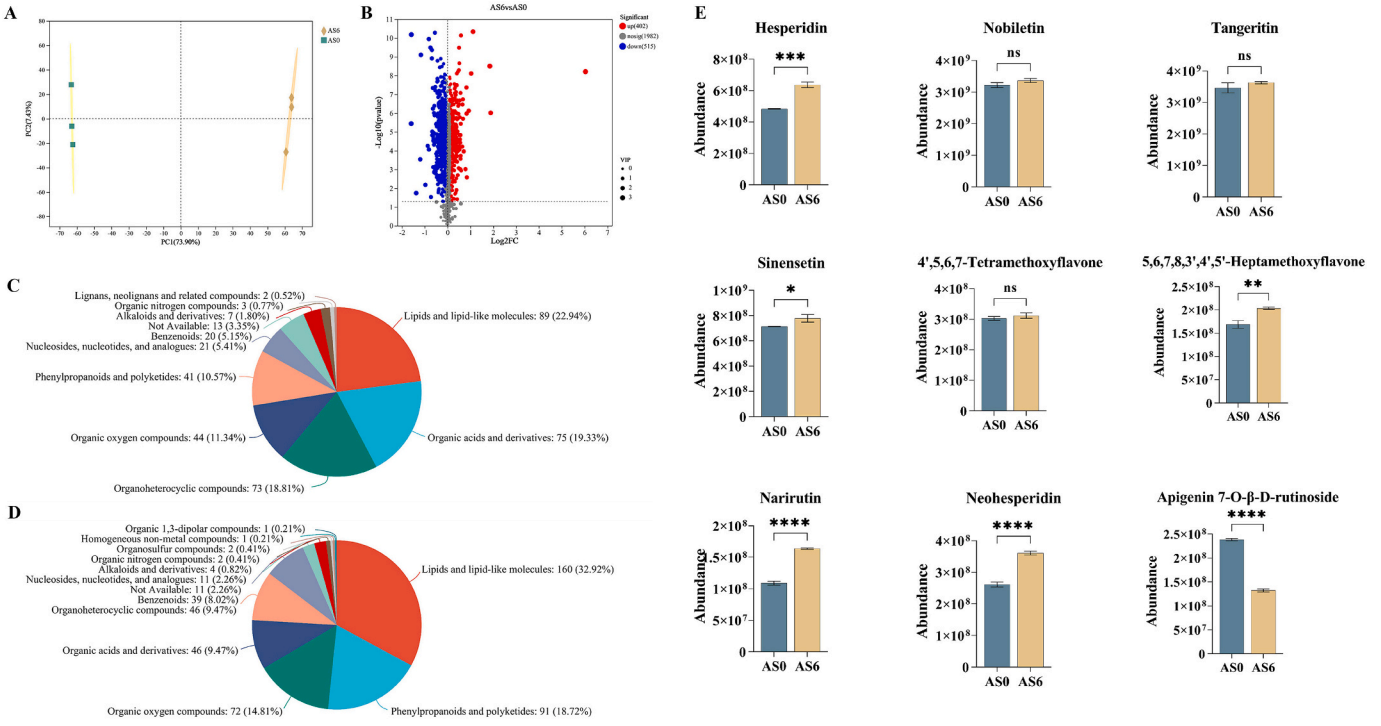


Fig. 6. (A) PCA score scatter plot composed of all metabolites of AS6 vs AS0; (B) Volcano plot of the differential metabolites of AS6 vs AS0; (C) Pie chart of the number of different types of up-regulated substances; (D) Pie chart of the number of different types of down-regulated substances. (E) The change of the top 9 flavonoids in abundance of AS6 vs AS0; The statistical analyses were performed using ANOVA, followed by LSD test, $*p < 0.05$, $**p < 0.01$, $***p < 0.001$, $****p < 0.0001$.

(Fig. S6). These results suggest that extending the steam time accelerated the aging process of citrus peel, however for medicinal purposes, a short-term steaming of 20 s was more conducive to the accumulation of active components. Therefore, when considering food medicine homology, it's important not to blindly extend the short-term steaming for the sake of reducing irritation.

4. Conclusions

In this study, the effects of short-term steaming on the citrus peel component were explored. Sensory evaluation and volatile component analysis revealed that an appropriate steaming time effectively reduced the sensory irritation of PCRC. Moreover, short-term steaming of PCRC during the early aging period showed similar changes to traditional steaming methods for "Chenpi," indicating that short-term steaming was the ideal alternative approach to reducing gastrointestinal irritation and the accelerated aging process of PCRC during subsequent storage.

We also assessed the *in vitro* neuroprotective activity of PCRC and analyzed its intrinsic pharmacodynamic components. The results demonstrated that short-term steaming tended to reduce antioxidant activity. However, despite a loss in antioxidant capacity, the neuroprotective activity of steam-treated PCRC was maintained, which may relate to the increased contents of methoxyflavonoids and synephrine resulting from steam treatment. Non-targeted metabolomics analysis after one year of aging revealed, compared to the unsteamed PCRC, 60 s-steamed PCRC had a higher flavonoid content, especially methoxyflavonoids. This observation coincided with a milder flavor in the steamed PCRC. Moreover, significant increases in alkaloids and methoxyflavonoids may provide additional health benefits. Taken together, short-term steaming introduced in the processing of citrus peel effectively reduced the irritation of PCRC and improved its food-medicine dual-use properties, suggesting increased overall quality and application value.

Ethical statement

There is no coercion to participate, full disclosure of study requirements and risks, written or verbal consent of participants, no release of participant data without their knowledge, ability to withdraw from the study at any time. The products tested were safe for consumption.

Informed consent

Participants gave informed consent via the statement "I agree to participate in this sensory evaluation and give my consent for information about my evaluation to be published in a journal" where an affirmative reply was required to enter the sensory evaluation.

CRediT authorship contribution statement

Shiheng Chen: Writing – review & editing, Writing – original draft, Software, Project administration, Methodology, Investigation. **Ziying Chen:** Writing – review & editing, Writing – original draft, Software, Methodology, Investigation. **Dylan O'Neill Rothenberg:** Writing – review & editing, Writing – original draft, Methodology. **Yong Long:** Resources, Methodology. **Huafeng Li:** Methodology. **Xiaoyang Zeng:** Methodology. **Zhen Zeng:** Software, Methodology. **Xiaoli Mo:** Methodology. **Dunying Wu:** Methodology. **Yinghong Liao:** Methodology. **Yahui Huang:** Writing – review & editing, Writing – original draft, Supervision, Funding acquisition, Conceptualization. **Sui Xiao:** Writing – review & editing, Writing – original draft, Supervision, Funding acquisition, Conceptualization. **Xu Zhang:** Writing – review & editing, Writing – original draft, Supervision, Project administration, Funding acquisition, Conceptualization.

Declaration of competing interest

The authors declare no competing financial interests.

Data availability

Data will be made available on request.

Acknowledgments

This work was financially supported by the Guangzhou Rural Science and Technology Commissioner Special Project (No. 2023E04J0211), and General project of Natural Science Foundation of Guangdong Province (No. 2021A1515012153).

Appendix A. Supplementary data

Supplementary data to this article can be found online at https://doi.org/10.1016/j.foodchem.2024.138964.

References

Akhter, S., Arman, M., Tayab, M., Islam, M., & Xiao, J. (2022). Recent advances in the biosynthesis, bioavailability, toxicology, pharmacology, and controlled release of citrus neohesperidin. *Critical Reviews in Food Science and Nutrition, 1-20*. https://doi.org/10.1080/10408398.2022.2149466

Akkoyunlu, A., & Dulger, G. (2022). Chemical composition and in vitro antimicrobial, antioxidant, and antiproliferative studies of the Lamium galeobdolon L. (L.) essential oil. *Russian Journal of Bioorganic Chemistry, 48*(6), 1240–1246. https://doi.org/10.1134/S1068162022060048

Arcus, V., & Mulholland, A. (2020). Temperature, dynamics, and enzyme-catalyzed reaction rates. *Annual Review of Biophysics, 49*, 163–180. https://doi.org/10.1146/annurev-biophys-121219-081520

Chang, C., Chen, K., Liaw, K., Peng, C., & Peng, R. (2020). Astaxanthin protects PC12 cells against homocysteine- and glutamate-induced neurotoxicity. *Molecules (Basel, Switzerland), 25*(1), 214. https://doi.org/10.3390/molecules25010214

Choi, C., Sun, K., An, C., Yoo, J., Hahm, K., Lee, I., Kim, & Y.. (2002). Reversal of P-glycoprotein-mediated multidrug resistance by 5,6,7,3′,4′-pentamethoxyflavone (Sinensetin). *Biochemical and Biophysical Research Communications, 295*(4), 832–840. https://doi.org/10.1016/S0006-291X(02)00755-6

Cui, F., Xi, L., Wang, D., Tan, X., Li, J., & Li, T. (2022). Functional magnetic nanoparticles combined with molecular dynamics technology to screen quorum sensing inhibitiors from natural substances: Accurate, efficient and high throghput. In *The 19th annual conference of China society of food science and technology*. https://doi.org/10.26914/c.cnkihy.2022.051105

Ding, J., Liu, C., Huang, P., Zhang, Y., Hu, X., Li, H., … Qin, W. (2023). Effects of thymol concentration on postharvest diseases and quality of blueberry fruit. *Food Chemistry, 402*, Article 134227. https://doi.org/10.1016/j.foodchem.2022.134227

Elena, D., Benny, B., & Connie, S. (2015). Emerging mechanisms and treatments for depression beyond SSRIs and SNRIs. *Biochemical Pharmacology, 95*(2), 81–97. https://doi.org/10.1016/j.bcp.2015.03.011

Fu, M., An, K., Xu, Y., Chen, Y., Wu, J., Yu, Y., & Ti, H. (2018). Effects of different temperature and humidity on bioactive flavonoids and antioxidant activity in pericarpium Citri reticulata (Citrus reticulata 'chachi'). *LWT- Food Science and Technology, 93*, 167–173. https://doi.org/10.1016/j. lwt.2018.03.036

Fu, M., Zou, B., An, Z., Yu, Y., & Tang, D. (2019). Anti-asthmatic activity of alkaloid compounds from pericarpium citri reticulatae (citrus reticulata 'chachi'). *Food & Function, 10*(2), 903–911. https://doi.org/10.1039/c8fo01753k

Gang, D., & Berim, A. (2016). Methoxylated flavones: Occurrence, importance, biosynthesis. *Phytochemistry Reviews, 15*(3), 363–390. https://doi.org/10.1007/s11101-015-9426-0

Ge, X., Deng, S., Zeng, K., & Deng, L. (2022). Effects of storage temperature on plastid structure and related gene expression during coloring of mandarin fruit peel after harvest. *Journal of Food Science and Technology, 40*(05). https://doi.org/10.12301/spxb202200165

Gong, W., Zhou, Y., Gong, W., & Qin, X. (2020). Coniferyl ferulate exerts antidepressant effect via inhibiting the activation of NMDAR-CaMKII-MAPKs and mitochondrial apoptotic pathways. *Journal of Ethnopharmacology, 251*, Article 112533. https://doi.org/10.1016/j.jep.2019.112533

Han, M., & Jiang, H. (2021). Analysis of volatile components from raw product and processed products of Citri Reticulatae Pericarpium by HS-SPME-GC-MS combined with stoichiometry. *China Journal of Traditional Chinese Medicine, 36*(05).

Ho, S., & Kuo, C. (2014). Hesperidin, nobiletin, and tangeretin are collectively responsible for the anti-neuroinflammatory capacity of tangerine peel (citri reticulatae pericarpium). *Food and Chemical Toxicology, 71*, 176–182. https://doi.org/10.1016/j.fct.2014.06.014

Hobbs, C., Taylor, S., Beevers, C., Lloyd, M., Bowen, G., Lillford, L., … Hayashi, S. (2016). Genotoxicity assessment of the flavouring agent, perillaldehyde. *Food and Chemical Toxicology*. https://doi.org/10.1016/j.fct.2016.08.029

Huang, B., Ban, X., He, J., Tong, J., Tian, J., & Wang, Y. (2010). Comparative analysis of essential oil components and antioxidant activity of extracts of Nelumbo nucifera from various areas of China. *Journal of Agricultural and Food Chemistry, 58*(1), 441–448. https://doi.org/10.1021/jf902643e

Jeong, H., Choi, Y., Lee, J., Lee, B., Kim, W., & Kang, H. (2017). Anti-inflammatory activity of citric acid-treated wheat germ extract in lipopolysaccharide-stimulated macrophages. *Nutrients, 9*(7), 730. https://doi.org/10.3390/nu9070730

Juan, T., Julieta, R., Juan, B., Lila, C., Federico, L., Julieta, S., … Daniela, D. (2022). A metabotropic glutamate receptor 3 (mGlu3R) isoform playing neurodegenerative roles in astrocytes is prematurely up-regulated in an Alzheimer's model. *Journal of Neurochemistry, 161*(4), 366–382. https://doi.org/10.1111/jnc.15610

Kalasariya, H., Patel, N., Gacem, A., Alsufyani, T., Reece, L., Yadav, V., … Jeon, B. (2022). Marine alga Ulva fasciata-derived molecules for the potential treatment of SARS-CoV-2: An in silico approach. *Marine Drugs, 20*(9). https://doi.org/10.3390/md20090586

Karthikeyan, S., Velmurugan, S., Donio, M., Michaelbabu, M., & Citarasu, T. (2014). Studies on the antimicrobial potential and structural characterization of fatty acids extracted from Sydney rock oyster Saccostrea glomerata. *Annals of Clinical Microbiology and Antimicrobials, 13*, 332. https://doi.org/10.1186/s12941-014-0057-x

Kim, K., Kim, H., Jung, J., Woo, R., Kim, H., Suh, H., … Song, D. (2001). Characterization of antidepressant-like effects of p-synephrine stereoisomers. *Naunyn-Schmiedeberg's Archives of Pharmacology, 364*(1), 21–26. https://doi.org/10.1007/s002100100416

Kim, Y., & Na, K. (2016). Role of glutamate receptors and glial cells in the pathophysiology of treatment-resistant depression. *Progress in Neuro-Psychopharmacology and Biological Psychiatry, 70*(3), 117–126. https://doi.org/10.1016/j.pnpbp.2016.03.009

Koriem, K., & Tharwat, H. (2023). Malic acid improves behavioral, biochemical, and molecular disturbances in the hypothalamus of stressed rats. *Journal of Integrative Neuroscience, 22*(4), 98. https://doi.org/10.31083/j.jin2204098

Li, C., Chen, X., Chen, S., Yi, L., & Liu, Q. (2014). Extracts from Pericarpium citri improve behaviors and hippocampal BDNF in mice exposed to chronic mild unpredictable stress. *Chinese Journal of Experimental Traditional, 20*(19), 151–155. https://doi.org/10.13422/j.cnki.syfjx.2014190151

Li, H., Lin, L., Feng, Y., & Zhao, M. (2024). Exploration of optimal preparation strategy of Chenpi (pericarps of Citrus reticulata Blanco) flavouring essence with great application potential in sugar and salt-reduced foods. *Food Research International, 175*, Article 113669. https://doi.org/10.1016/j.foodres.2023.113669

Lian, X., Chen, M., & Wu, L. (2018). Determination of dimethyl anthranilate and β-myrcene in Xinhui pericarpium citri reticulatae by UPLC-MS-MS. *Food Science and Technology, 43*(11), 4. https://doi.org/10.13684/j.cnki.spkj.2018.11.053

Liang, S., Wen, Z., Tang, T., Liu, Y., Liu, Y., Dang, F., … Wu, H. (2021). Study on flavonoid and bioactivity features of the pericarp of Citri Reticulatae "chachi" during storage. *Arabian Journal of Chemistry, 15*(3). https://doi.org/10.1016/j.arabjc.2021.103653

Liao, Y., Wang, C., Gao, Z., Pan, Z., Peng, M., Ma, J., … Guo, J. (2023). Anti-obesity mechanism of Ganpu tea revealed by microbiome, metabolome and transcriptome analyses. *Food Chemistry, 412*, Article 135048. https://doi.org/10.1016/j.foodchem.2022.135048

Liat, S., Moshe, S., Ahuva, F., Einat, B., Doron, H., Or, E., … Eyal, Y. (2010). Citrus fruit flavor and aroma biosynthesis: Isolation, functional characterization, and developmental regulation of Cstps1, a key gene in the production of the sesquiterpene aroma compound valencene. *The Plant Journal, 36*(5), 664–674. https://doi.org/10.1046/j.1365-313x.2003.01910.x

Luo, Y., Zeng, W., Huang, K., Li, D., Chen, W., Yu, X., & Ke, X. (2019). Discrimination of Citrus reticulata Blanco and Citrus reticulata'Chachi' as well as the Citrus reticulata'Chachi' within different storage years using ultra high performance liquid chromatography quadrupole/time-of-flight mass spectrometry based metabolomics approach. *Journal of Pharmaceutical and Biomedical Analysis, 171*, 218–231. https://doi.org/10.1016/j.jpba.2019.03.056

Maity, J., Majumder, S., Pal, R., Saha, B., & Mukhopadhyay, P. (2023). Ascorbic acid modulates immune responses through Jumonji-C domain containing histone demethylases and Ten eleven translocation (TET) methylcytosine dioxygenase. *BioEssays, 45*(11), Article e2300035. https://doi.org/10.1002/bies.202300035

National Pharmacopoeia Commission. (2020). *Pharmacopoeia of the People's Republic of China, One Sections* (pp. 199–200). Beijing: China Medical Science and Technology Press.

Pereira, I., Severino, P., Santos, A., Silva, A., & Souto, E. (2018). Linalool bioactive properties and potential applicability in drug delivery systems. *Colloids and Surfaces. B, Biointerfaces, 171*, 566–578. https://doi.org/10.1016/j.colsurfb.2018.08.001

Praveen, P., Sunil, K., Kavya, M., Sai, A., Raghu, B., Deepika, K., … C.. (2020). Cerebroprotective potential of hesperidin nanoparticles against bilateral common carotid artery occlusion reperfusion injury in rats and in silico approaches. *Neurotoxicity Research, 37*(2), 264–274. https://doi.org/10.1007/s12640-019-00098-8

Shen, C., Jiang, J., Zhu, W., & Qin, O. (2017). Anti-inflammatory effect of essential oil from citrus aurantium l. var. amara engl. *Journal of Agricultural and Food Chemistry, 65*(39), 8586–8594. https://doi.org/10.1021/acs.jafc.7b02586

Somasundaram, S., Price, J., Pearce, K., Shuck, R., Jayaprakasha, G., & Patil, B. (2012). Citrus limonin lacks the antichemotherapeutic effect in human models of breast cancer. *Journal of Nutrigenetics and Nutrigenomics, 5*(2), 106–114. https://doi.org/10.1159/000336921

Vigushin, D., Poon, G., Boddy, A., English, J., Halbert, G., Pagonis, C., … Coombes, R. (1998). Phase I and pharmacokinetic study of D-limonene in patients with advanced cancer. Cancer research campaign phase I/II clinical trials committee. *Cancer Chemotherapy and Pharmacology, 42*(2), 111–117. https://doi.org/10.1007/s002800050793

Vitalini, S., Iriti, M., Orlando, F., & Garzoli, S. (2022). Chemical composition and in vitro antimicrobial, antioxidant, and antiproliferative studies of the Lamium galeobdolon L. (L.) essential oil. *Sustainable Chemistry and Pharmacy, 25*. https://doi.org/10.1016/j.scp.2022.100607

Wang, J., Huang, Q., Zhang, Y., Juan, S., & Liu, J. (2012). Current situation of the long-stored TCM research and exploration of the ideas. *China Pharmacy, 23*(15), 1433–1435. https://doi.org/10.6039/j.issn.1001-0408.2012.15.36

Wang, P., Wang, H., Zou, J., Chen, L., Chen, H., Hu, Y., … Liu, Y. (2023). Electronic nose and head space GC-IMS provide insights into the dynamic changes and regularity of volatile compounds in Zangju (*Citrus reticulata* cv. Manau Gan) peel at different maturation stages. *Molecules, 28*(14), 5326. https://doi.org/10.3390/molecules28145326

Wang, R., Liu, B., Sun, J., Xu, J., Kong, B., & Zhang, N. (2022). Volatile aroma analysis of tangerine peel. *Fine Chemicals, 39*(02). https://doi.org/10.13550/j.jxhg.20210836, 321-329+410.

Wang, Y., Yi, L., Liang, Y., Li, H., Yuan, D., Gao, H., & Zeng, M. (2008). Comparative analysis of essential oil components in *Pericarpium Citri Reticulatae Viride* and *Pericarpium Citri Reticulatae* by GC-MS combined with chemometric resolution method. *Journal of Pharmaceutical and Biomedical Analysis, 46*(1), 66–74. https://doi.org/10.1016/j.jpba.2007.08.030

Wu, L., Liu, X., & Pan, Z. (2016). New synthesis of hydroxyacetone. *Chemical Reagents, 38*(10), 3. https://doi.org/10.13822/j.cnki.hxsj.2016.10.023

Xiao, S., Huang, J., Huang, Y., Lai, H., Zheng, Y., Liang, D., … Zhang, X. (2021). Flavor characteristics of ganpu tea formed during the sun-drying processing and its antidepressant-like effects. *Frontiers in Nutrition, 8*, Article 647537. https://doi.org/10.3389/fnut.2021.647537

Xu, X., Chen, K., & Wang, J. (2011). Comparative study on the content of synephrine in "Guang chenpi" and "Qingpi" before and after processing. *Henan Traditional Chinese Medicine, 31*(07). https://doi.org/10.16367/j.issn.1003-5028.2011.07.055

Yang, J., Tang, C., Xiao, J., Du, W., & Li, R. (2018). Influences of epigallocatechin gallate and citric acid on Escherichia coli O157:H7 toxin gene expression and virulence-associated stress response. *Letters in Applied Microbiology, 67*(5), 435–441. https://doi.org/10.1111/lam.13058

Yang, M., Jiang, Z., Wen, M., Wu, Z., Zha, M., Xu, W., … Zhang, L. (2022). Chemical variation of chenpi (Citrus peels) and corresponding correlated bioactive compounds by LC-MS metabolomics and multibioassay analysis. *Frontiers in Nutrition, 9*, Article 825381. https://doi.org/10.3389/fnut.2022.825381

Yang, X., Zhao, S., Deng, Y., Xu, W., Wang, Z., Wang, W., … Liu, D. (2023). Antibacterial activity and mechanisms of α-terpineol against foodborne pathogenic bacteria. *Applied Microbiology and Biotechnology, 107*, 6641–6653. https://doi.org/10.1007/s00253-023-12737-4

Yao, R., He, C., & Xiao, P. (2023). 'Food and medicine continuum' in the East and West: Old tradition and current regulation. *Chinese Herbal Medicines, 15*(01), 6–14. https://doi.org/10.1016/j.chmed.2022.12.002

Yu, B., Shao, X., Fu, X., Zhou, M., & Chen, C. (2021). Study on composition characteristics and mechanism of anti-depression traditional Chinese medicine compound based on literature mining and correlation analysis. *Chinese Traditional and Herbal Drugs, 52*(11), 9. https://doi.org/10.7501/j.issn.0253-2670.2021.11.022

Zhang, X., Zhang, Y., Zhang, D., Meng, J., Sun, Y., Wang, S., … Cao, H. (2022). Processing of Citri Reticulatae Pericarpium: A review. *Chinese Journal of Experimental Traditional Medical Formulae, 28*(17), 267. https://doi.org/10.13422/j.cnki.syfjx.20212053

Zheng, G., Zhou, P., Yang, H., Li, Y., Li, P., & Liu, E. (2013). Rapid resolution liquid chromatography–electrospray ionisation tandem mass spectrometry method for identification of chemical constituents in Citri Reticulatae Pericarpium. *Food Chemistry, 136*(02), 604–611. https://doi.org/10.1016/j.foodchem.2012.08.040

Zhou, J., Zhang, X., Liu, W., Zhang, Q., Wu, Y., & Wu, L. (2023). Widely targeted metabolomics analysis of the main bioactive compounds of Ganpu tea processing through different drying methods. *LWT, 189*, Article 115501. https://doi.org/10.1016/j.lwt.2023.115501

ScienceDirect

Industrial Crops and Products

Supports open access

9.7 CiteScore | 5.9 Impact Factor

Submit your article | Guide for authors

Menu | Search in this journal

Volume 186

15 October 2022

Previous vol/issue | Next vol/issue

Receive an update when the latest issues in this journal are published

Sign in to set up alerts

Full text access

Editorial Board

Article 115352

View PDF

Fats and oils

Research article • Full text access

3D Weft-knitted spacer fabrics (WKSFs) coated with silica aerogels as oil intercepting sorbents for use in static and dynamic water tests

Syed Rashedul Islam, Mohammed Kayes Patoary, Amjad Farooq, Tayyab Naveed, ... Jinhua Jiang

Article 115169

View PDF Article preview

Research article • Full text access

Sustainable production of azelaic acid from vegetable oils over a heterogeneous catalyst

Aakriti Sood, Rahul Upadhyay, Sushil K. Maurya

Article 115139

View PDF Article preview

Research article • Full text access

Comparison of chemical composition and activities of essential oils from fresh leaves of *Pelargonium graveolens* L'Herit. extracted by hydrodistillation and enzymatic pretreatment combined with a solvent-free microwave extraction method

Liang Wei, Huiying Yang, Hui Li, Minghua Zhu, ... Yuangang Zu

Article 115204

View PDF Article preview

Research article • Full text access

Physicochemical and textural properties of natural cosmeceutical fats prepared from interesterified oil blends consisting of palm olein and palm kernel oil

Zhen Zhang, Xiaodong Xie, Wan Jun Lee, Yong Wang
Article 115195

View PDF Article preview

Research article • Full text access

^{1}H NMR-based analytical method: A valid and rapid tool for the epoxidation processes

Tommaso Cogliano, Rosa Turco, Vincenzo Russo, Martino Di Serio, Riccardo Tesser
Article 115258

View PDF Article preview

Research article • Full text access

Seven underutilized species of the Fabaceae family with high potential for industrial application as alternative sources of oil and lipophilic bioactive compounds

Anna Grygier, Suryakant Chakradhari, Katarzyna Ratusz, Magdalena Rudzińska, ... Paweł Górnaś
Article 115251

View PDF Article preview

Research article • Full text access

Analysis of the effects of mepiquat chloride priming on the seedling growth-promoting in cotton under salt stress by multi-omics

Ning Wang, Xiangru Wang, Qian Qi, Asif Iqbal, ... Gentu Yan
Article 115296

View PDF Article preview

Non-food bioactive products

Research article • Full text access

The phenotypic diversity of *Schisandra sphenanthera* fruit and SVR model for phenotype forecasting

Xiaorui Wang, Min Yan, Xinxin Wang, Zhiting Wu, ... Wei Gu
Article 115162

View PDF Article preview

Research article • Full text access

Differences in the components of *Neolamarckia cadamba* from different provenance and the drug resistance reversal activity of characteristic alkaloid

Mingxia Nie, Jingyuan Huang, Jiaoli Huang, Ziying Chen, ... Sui Xiao
Article 115145

View PDF Article preview

Research article • Full text access

Apiaceae essential oil nanoemulsions as effective wheat protectants against five arthropod pests

Nickolas G. Kavallieratos, Erifili P. Nika, Anna Skourti, Diego Romano Perinelli, ... Filippo Maggi
Article 115001

View PDF Article preview

Research article • Full text access

Genome assembly provided new insights into the *Cinnamomum burmannii* evolution and D-borneol biosynthesis differences between chemotypes

Fangping Li, Shilin Huang, Yu Mei, Bingqi Wu, ... Jihua Wang
Article 115181

View PDF Article preview

Research article • Full text access

Spatial and temporal patterns of secoiridoid and xanthone biosynthetic pathways during early development of *Centaurium erythraea* Rafn, as altered by ploidy level

Biljana Filipović, Marijana Skorić, Uroš Gašić, Milan Dragićević, ... Danijela Mišić
Article 115146

View PDF Article preview

Research article • Full text access

Untargeted metabolomics study of *Lonicerae japonicae flos* processed with different drying methods via GC-MS and UHPLC-HRMS in combination with chemometrics

Shu-Fang Li, Xiao-Meng Guo, Xue-Fei Hao, Shu-Hui Feng, ... Yong-Jie Yu
Article 115179

View PDF Article preview

Research article • Full text access

Cell-type-specific H^+-ATPase activity and antioxidant enzymes improve the *Echinacea purpurea* L. Moench tolerance to salinity stress at different NO_3^-/NH_4^+ ratios

Fatemeh Ahmadi, Abbas Samadi, Ebrahim Sepehr, Amir Rahimi, Sergey Shabala
Article 115199

View PDF Article preview

Research article • Open access

Opportunities and challenges for sustainable production and processing of *Rosa damascena* in Bulgaria

Mariyana Shishkova, Boryana Ivanova, Rositsa Beluhova-Uzunova, Adelina Harizanova
Article 115184

View PDF Article preview

Research article • Full text access

Micro and nanoencapsulation of bioactive compounds for agri-food applications: A review

Jorge L. Guía-García, Ana V. Charles-Rodríguez, M. Humberto Reyes-Valdés, Francisca Ramírez-Godina, ... María L. Flores-López
Article 115198

View PDF Article preview

Research article • Full text access

Temperature-responsive surfactant-free microemulsion solvent: Preparation, characterization and application of extraction hydrophobic and hydrophilic components in plant matrix

Jian-Dong Wang, Zi-Hui Cai, Yuan-Hang Chang, Yan-Qiu Wang, ... Yu-Jie Fu
Article 115216

View PDF Article preview

Research article • Full text access

Evaluation of the extracts from the renewable parts in *Garcinia subelliptica* as natural sunscreen additives

Ying-Hao Yeo, Fu-Lan Hsu, Yi-Lin Chen, Tzu-Cheng Chang
Article 115214

View PDF Article preview

Research article • Full text access

Physical properties of Ashwagandha seeds (*Withania somnifera* L.) – A medicinal crop

T.M. Anandakumar, Devendra Kumar, B. Shivanna, Rakesh Kumar
Article 115233

View PDF Article preview

Research article ● Full text access

Transcriptome and metabolite profiling analyses reveal the molecular mechanism underlying the characteristic accumulation of anthocyanins and flavonols in *Fritillaria unibracteata* and *F. delavayi.*

Qiyan Chen, Yan Li, Hongping Han, Yonggui Ma, ... Yanjie Zhang
Article 115183

View PDF Article preview

Research article ● Full text access

Untargeted metabolomics used to describe the chemical composition and antimicrobial effects of the essential oil from the leaves of *Guatteria citriodora* Ducke

Diego Pereira de Souza, José Francisco de Carvalho Gonçalves, Josiane Celerino de Carvalho, Karyne Kathlen Guedes da Silva, ... Alberdan Silva Santos
Article 115180

View PDF Article preview

Short communication ● Full text access

Oil from *kopyor* coconut (*Cocos nucifera var. Kopyor*) for cosmetic application

Khafid Mahbub, Islamiati Dewi Octaviani, Ika Yuni Astuti, Sisunandar Sisunandar, Binar Asrining Dhiani
Article 115221

View PDF Article preview

Research article ● Full text access

Extracts of selected Lamiaceae species as promising antidiabetics: Chemical profiling, *in vitro* and *in silico* approach combined with dynamical modeling

Mariana Oalđe Pavlović, Tanja Lunić, Stefan Graovac, Marija Mandić, ... Bojan Božić
Article 115200

View PDF Article preview

Research article ● Full text access

How does *Flourensia microphylla* extract affect polyphenolic composition, antioxidant capacity, and antifungal activity?

Dennise A. Carrillo-Lomelí, Diana Jasso de Rodríguez, Víctor M. Moo-Huchin, Lorena Ramón-Canul, ... Fidel M. Peña-Ramos
Article 115248

View PDF Article preview

Research article ● Full text access

Supercritical fluid extraction of dried Surangi flowers (*Mammea suriga*)

Viplav Hari Pise, Bhaskar N. Thorat
Article 115268

View PDF Article preview

Research article ● Full text access

Enhancing the affinity and adsorption efficiency of *Glochidion ericarpum* Champ leave extract to cotton for colouristic and functional properties integrating trimethyl chitosan and ultrasonic technique

Yuyang Zhou, Benjamin Tawiah, Lili Wang, Qing Li
Article 115255

View PDF Article preview

Research article ● Full text access

Evaluation of *in vitro* anti-acne activities of *Ocimum basilicum* L. water extract

Yu Zhang, Huaming He, Dexian Wang, Liya Song, Congfen He
Article 115205

View PDF Article preview

Research article ● Full text access

Sambucus nigra L. cell cultures produce main species-specific phytochemicals with anti-inflammatory properties and *in vitro* ACE2 binding inhibition to SARS-CoV2

Anete Borodušķe, Madara Balode, Ilva Nakurte, Marta Berga, ... Heiko Rischer
Article 115236

View PDF Article preview

Research article ● Full text access

Together is better: poly(tannic acid) nanorods functionalized polysaccharide hydrogels for diabetic wound healing

Shengye You, Yijing Huang, Ruiting Mao, Yajing Xiang, ... Xiaoliang Qi
Article 115273

View PDF Article preview

Review article ● Full text access

Research progress on the biosynthesis and metabolic engineering of the anti-cancer drug camptothecin in *Camptotheca acuminate*

Xiaoxuan Fan, Xinting Lin, Qingyan Ruan, Jingyi Wang, ... Xiaolong Hao
Article 115270

View PDF Article preview

Research article ● Full text access

Climate change adversely affects the medicinal value of *Aconitum* species in Alpine region of Indian Himalaya

Sudeep Chandra, Vaishali Chandola, Zarkha Sultan, C.P. Singh, ... M.C. Nautiyal
Article 115277

View PDF Article preview

Research article ● Full text access

Development, characterization, insecticidal and sublethal effects of *Bunium persicum* and *Ziziphora clinopodioides*-based essential oil nanoemulsions on *Culex quinquefasciatus*

Diego Romano Perinelli, Roman Pavela, Giulia Bonacucina, Cecilia Baldassarri, ... Angelo Canale
Article 115249

View PDF Article preview

Research article ● Full text access

Tyrosinase inhibition of major secondary metabolites isolated from endangered *Meconopsis bhutanica* Tosh.Yoshida & Grey-Wilson

Zheng-Hao Yin, Yuan-Fei Li, Kang Li, Yu Gong, ... Li-Mei Li
Article 115280

View PDF Article preview

Research article ● *Open access*

Three candidate 2-(2-phenylethyl)chromone-producing type III polyketide synthases from *Aquilaria sinensis* (Lour.) Gilg have multifunctions synthesizing benzalacetones, quinolones and pyrones

Mengjun Xiao, Binbin Wang, Yanan Feng, Peiwen Sun, ... Jianhe Wei
Article 115263

View PDF Article preview

Review article ● Full text access

Tropane alkaloids (hyoscyamine, scopolamine and atropine) from genus *Datura*: extractions, contents, syntheses and effects

Zhiwen Shi, Wenjin Zou, Zhiming Zhu, Ziwen Xiong, ... Zhenglin Zhu
Article 115283

View PDF Article preview

Research article ● Full text access

In vitro propagation from seeds and enhanced synthesis of podophyllotoxin from root callus of *SinoPodophyllum hexandrum* Royle T.S. Ying (Himalayan Mayapple) – An endangered medicinal plant

Neha Sharma, Manisha Thakur, Pooja Sharma, Bhupender Dutt, Yash Pal Sharma
Article 115300

View PDF Article preview

Research article ● Full text access

Integration of LC/MS-based molecular networking and molecular docking allows in-depth annotation and prediction of the metabolome: A study of *Salvia miltiorrhiza* Bunge

Shiqi Wang, Yuekai Su, Jingyu Li, Yongping Lu, ... Jianhua Wang
Article 115298

View PDF Article preview

Research article ● Full text access

Constituents of the roots of *Physochlaina physaloides* (L.) G. Don promote apoptosis and cell cycle arrest by inhibiting the Wnt/β-catenin pathway in gastric and liver cancer cells

Wei Wei, Kai Cheng, Huan Lu, Yansen Yang, ... Yingchun Wang
Article 115262

View PDF Article preview

Natural rubber and resins

Research article ● Full text access

The contribution mechanism of furfuryl alcohol treatment on the dimensional stability of plantation wood

Xiaoshuang Shen, Sheng Yang, Gaiyun Li, Shengquan Liu, Fuxiang Chu
Article 115143

View PDF Article preview

Research article ● Full text access

Genetic variability of traits of the laticiferous system and association with rubber yield in juvenile and adult rubber tree progenies

Lígia Regina Lima Gouvêa, Mario Luíz Teixeira de Moraes, Elaine Cristine Piffer Gonçalves, Marcela Aparecida de Moraes, Paulo Gonçalves
Article 115225

View PDF Article preview

Bioenergy - crops and processing

Research article ● Full text access

Genomic identification of ARF transcription factors and expression analysis in *Cannabis sativa* L

Libing Zhang, Rui Guan, Guangli Li, Kexin Su, ... Aijia Ji
Article 115118

View PDF Article preview

Research article ● Full text access

Probing the mechanism of green solvent solubilization of hemicellulose based on molecular dynamics simulations

Weixian Wang, Yi Kong, Jianjun Peng, Bin Li, Huanfei Xu
Article 115159

View PDF Article preview

Research article ● Full text access

Metabolomics and transcriptomics analysis of vitro growth in pitaya plantlets with different LED Light spectra treatment

Wenjing Huang, Guangzhu Yang, Dandan Liu, Qian Li, ... Jun Ma

Article 115237

View PDF Article preview

Research article ● Full text access

Hydrogen production from cotton stalk over Ni-La catalysts supported on spent bleaching clay via hydrothermal gasification

Yan-qing Song, Sonil Nanda, Wen-jie Cong, Jie Sun, ... Janusz A. Kozinski
Article 115228

View PDF Article preview

Research article ● Full text access

Evaluation of harvest time effects on the combustion quality of warm- and cool-season perennial grasses in two contrasting semi-arid environments

Alpaslan Kusvuran, Recep Irfan Nazli, Veyis Tansi, Hasan Huseyin Ozturk, Dilek Bostan Budak
Article 115260

View PDF Article preview

Research article ● Full text access

Estimating technological parameters and stem productivity of sugarcane treated with rock powder using a proximal spectroradiometer Vis-NIR-SWIR

Marlon Rodrigues, Everson Cezar, Glaucio Leboso Alemparte Abrantes dos Santos, Amanda Silveira Reis, ... Marcos Rafael Nanni
Article 115278

View PDF Article preview

Fibres, proteins and carbohydrates

Research article ● Full text access

Prediction of the equilibrium moisture content based on the chemical composition and crystallinity of natural fibres

Nick Sweygers, Delphine E.C. Depuydt, Samuel Eyley, Wim Thielemans, ... Aart Willem Van Vuure
Article 115187

View PDF Article preview

Research article ● Full text access

Synthesis of magnetic polypyrrole modified sodium alginate nanocomposite with excellent antibacterial properties and optimization of dye removal performance using RSM

Mahsa Sadeghnezhad, Mohsen Ghorbani, Maryam Nikzad
Article 115192

View PDF Article preview

Short communication ● Full text access

Remarkable toughness reinforcement of elastomer with cellulose microgel: Employing polymer matrix and cellulose nanofiber network as the continuous phase and energy dissipation agent

Bin Sun, Ziting Yuan, Kai Li, Wei Tang, ... Yuxin Liu
Article 115227

View PDF Article preview

Research article ● Full text access

A novel polysaccharide from *Boletus edulis*: Extraction, purification, characterization and immunologic activity

Shasha Yu, Rongjie Ma, Xiaodan Dong, Haiyu Ji, Anjun Liu
Article 115206

View PDF Article preview

Research article ● Full text access

Comparison of polysaccharides in ginseng root cultures and cultivated ginseng and establishment of high-content uronic acid plant synthesis system

Junping He, Juan Wang, Geyuan Qi, Lu Yao, ... Wenyuan Gao
Article 115155

View PDF Article preview

Research article ● Full text access

Eco-friendly flame retardant and smoke suppression coating containing boron compounds and phytic acids for nylon/cotton blend fabrics

Jian Liu, Peng Qi, Dan Meng, Lu Li, ... Sheng Zhang
Article 115239

View PDF Article preview

Research article ● Full text access

Rich variant phenotype of *Gossypium hirsutum L.* saturated mutant library provides resources for cotton functional genomics and breeding

Yunxiao Wei, Yongming Liu, Abid Muhammad Ali, Rong Xiao, ... Rui Zhang
Article 115232

View PDF Article preview

Research article ● Full text access

Application of poly(lactic acid)-grafted cellulose nanofibers as both inhibitor and reinforcement for 3D-printable tough polydicyclopentadiene composites via frontal ring-opening metathesis polymerization

Ruoteng Ma, Shaoning Wang, Lisha Ma, Bowen Li, ... Zhiguo Wang
Article 115217

View PDF Article preview

Research article ● Full text access

Highly efficient and low pollution catalytic oxidation of ramie degumming by NHPI

Shu Yang, Chongwen Yu, Bin Zhang, Peihua Zhang, ... Wenbo Zhang
Article 115189

View PDF Article preview

Research article ● Full text access

Renewable phosphorous-based flame retardant for lignocellulosic fibers

Karina Antoun, Melek Ayadi, Roland El Hage, Michel Nakhl, ... Nicolas Brosse
Article 115265

View PDF Article preview

Research article ● Full text access

Comparative plastome analyses and genomic resource development in wild rice (*Zizania* spp., Poaceae) using genome skimming data

Ruisen Lu, Min Chen, Yu Feng, Na Yuan, ... Xiaoqin Sun
Article 115244

View PDF Article preview

Research article ● Full text access

Controllable fabrication of nanofibrillated cellulose supported HKUST-1 hierarchically porous membranes for highly efficient removal of formaldehyde in air

Zicheng Chen, Xiangyang He, Jing Ge, Guangyuan Fan, ... Guanhua Wang
Article 115269

View PDF Article preview

Research article ● Full text access

Facile fabrication of antibacterial and fire-safety multifunctional cotton fabric with a triazine-phosphonate N-halamine

Shijie Wang, Denghui Xu, Ping Zhu, Zhiming Jiang
Article 115261

View PDF Article preview

Research article ● Full text access

Cotton fiber quality response to nitrogen depends on source-sink process, boll growth habit, and weather condition

Mojtaba Hassanzadehdelouei, Sami Ul-Allah, Ahad Madani
Article 115279

View PDF Article preview

Research article ● Full text access

Adopting different cotton cropping systems may regulate the spatiotemporal variation in soil moisture and affect the growth, WUE and yield of cotton

Fengqi Wu, Beifang Yang, Simeng Guo, Weibin Huang, ... Yabing Li
Article 115259

View PDF Article preview

Research article ● Full text access

Characterization of a new natural cellulose fiber from *Enhalus acoroides* and its potential application

Jaruwan Mayakun, Piramon Klinkosum, Thitirat Chaichanasongkram, Sukanya Sarak, Kaewta Kaewtatip
Article 115285

View PDF Article preview

Research article ● Full text access

Efficient and practical bioconversion strategy of xylose-rich corncob for prebiotic *Bacillus subtilis* production

Xutong Ma, Xinlu Liu, Yong Xu
Article 115274

View PDF Article preview

Research article ● Full text access

Environmental friendly bio-dyeing of silk using *Alkanna tinctoria* based Alkannin natural dye

Fazal-ur-Rehman, Shahid Adeel, Salman Liaqat, Muhammad Hussaan, ... Haddar Wafa
Article 115301

View PDF Article preview

Research article ● Full text access

Preparation of green magnetic hydrogel from cellulose nanofibril (CNF) originated from soybean residue for effective and rapid removal of copper ions from waste water

Peiyi Li, Hezhen Liu, Miaomiao Zhou, Haozhe Lei, ... Bingyao Zhou
Article 115257

View PDF Article preview

Review article ● Full text access

Preparation, structure-function relationship and application of *Grifola umbellate* polysaccharides

Binghang Li, Gangliang Huang
Article 115282

View PDF Article preview

Research article ● Full text access

Down-regulating a fiber-specific KCR like gene *GhKCRL1* suppressed fiber elongation through blocking the synthesis of sphingolipids in fiber cell

Qian Meng, Qiaoling Wang, Fan Xu, Qian Chen, ... Ming Luo
Article 115290

View PDF Article preview

Research article ● Full text access

A rapid and efficient method of microwave-assisted extraction and hydrolysis and automatic amino acid analyzer determination of 17 amino acids from mulberry leaves

Ping-Yue Wang, Fei-Fan Shuang, Jia-Xin Yang, Yu-Xiong Jv, ... Dong-Yang Zhang
Article 115271

View PDF Article preview

Bio-based Materials from Crops

Research article ● Full text access

Interactions between biofiller-modified polymeric composites and wood-rotting fungi in terms of their biotechnological applications

Beata Podkościelna, Anna Matuszewska, Dawid Stefaniuk, Marta Ruminowicz-Stefaniuk, ... Magdalena Jaszek
Article 115125

View PDF Article preview

Research article ● Full text access

Weavable and wearable strip-shaped supercapacitors from bamboo cellulose nanofibers

Qunhao Wang, Tian Xia, Zhuo Zheng, Jiangqi Zhao, ... Canhui Lu
Article 115174

View PDF Article preview

Research article ● Full text access

In situ formation of polymethylsiloxane nanofilaments on pristine cotton stalk with natural interconnected pores for rapid and recyclable organic solvents absorption

Tao Liu
Article 115176

View PDF Article preview

Research article ● Full text access

Characterization of industry grade soybean wax for potential applications in natural fiber reinforced composite (NFRC) filaments

Athira Nair Surendran, Kameswara Pavan Kumar Ajjarapu, Arulselvan Akilan Arumugham, Kunal Kate, Jagannadh Satyavolu
Article 115163

View PDF Article preview

Research article ● Full text access

Miscanthus and Sorghum as sustainable biomass sources for nanocellulose production

Marta Babicka, Magdalena Woźniak, Monika Bartkowiak, Barbara Peplińska, ... Izabela Ratajczak
Article 115177

View PDF Article preview

Research article ● Full text access

Photo-selective nets influence physiology, growth, yield and quality of turmeric (*Curcuma longa* L.)

B.S. Harish, K. Umesha, R. Venugopalan, B.N. Maruthi Prasad
Article 115202

View PDF Article preview

Research article ● Full text access

Lignin-rich cellulose nanocrystals from coir fiber treated with ionic liquids: Preparation and evaluation as pickering emulsifier

Priscilla F.O. Ferreira, André L.S. Pereira, Morsyleide F. Rosa, Rílvia S. de Santiago-Aguiar
Article 115119

View PDF Article preview

Research article ● Full text access

Novel *Lagenaria siceraria* peel waste based cellulose nanocrystals: Isolation and rationalizing H-bonding interactions

Radheesh Sharma Meda, Somya Jain, Shiva Singh, Chhavi Verma, ... Pradip K. Maji
Article 115197

View PDF Article preview

Research article ● Full text access

Woven cattail leaf slips for large-scale, high-efficient and salt-resistant solar water evaporation

Yan Sun, Lingling Fan, Wenfeng Zheng, Dezhan Ye, ... Jie Xu
Article 115185

View PDF Article preview

Research article ● Full text access

Almond shell nanocellulose: Characterization and self-assembling into fibers, films, and aerogels

Juri Fukuda, You-Lo Hsieh
Article 115188

View PDF Article preview

Research article ● Full text access

Freezing-induced interfacial growth of polypyrrole layers on hierarchical carbon aerogels for robust ultrasensitive pressure sensors

Ziheng Li, Lumin Chen, Mengya Mu, Houyong Yu, ... Xiang Chen
Article 115215

View PDF Article preview

Research article ● Full text access

Structure-property relationships in Japanese knotweed – The potential of using the stem for composite applications

Timo Wunsch, Milan Kelch, Vincent Röhl, Hansjörg Wieland, ... Jörg Müssig
Article 115191

View PDF Article preview

Research article ● *Open access*

Pine sawdust modification using Fenton oxidation for enhanced production of high-yield lignin-containing microfibrillated cellulose

Ari Ämmälä, Juho Antti Sirviö, Henrikki Liimatainen
Article 115196

View PDF Article preview

Research article ● Full text access

Preparation and performance of fluorescent transparent bamboo

Zihao Wang, Jiewei Tong, Bingbin Kuai, Jingshu Gao, ... Liping Cai
Article 115222

View PDF Article preview

Research article ● Full text access

A novel pH-responsive charge reversal nanospheres based on acetylated histidine-modified lignin for drug delivery

Conghua Yi, Qinghe Xu, Dongjie Yang, Miao Wang
Article 115193

View PDF Article preview

Research article ● Full text access

Cellulose template designed porous ZnO based catalysts with different valence copper for solar photocatalytic CO_2 conversion

Chun Shi, Lili Zhang, Zhengjun Shi, Jinxia Ma, Zhiguo Wang
Article 115223

View PDF Article preview

Research article ● Full text access

Non-isocyanate polyurethane from sweet potato residual and the application in food preservation

Yumiao Yang, Hui Cao, Yankun Wang, Jianbo Zhao, ... Di Cai
Article 115224

View PDF Article preview

Research article ● Full text access

Effect of different biomass species and pyrolysis temperatures on heavy metal adsorption, stability and economy of biochar

Wei Liao, Xiong Zhang, Shujia Ke, Jingai Shao, ... Hanping Chen
Article 115238

View PDF Article preview

Research article ● Full text access

A comparative evaluation of statistical empirical and neural intelligence modeling of *Manihot esculenta*-derived leaves extract for optimized bio-coagulation-flocculation of turbid water

Heri Septya Kusuma, Andrew Nosakhare Amenaghawon, Handoko Darmokoesoemo, Yantus A.B. Neolaka, ... Chinedu L. Anyalewechi
Article 115194

View PDF Article preview

Research article ● Full text access

A new approach for the use of cellulose-rich solids from biorefinery in the formulation of gel-like materials

Cynthia Hopson, Victoria Rigual, Juan C. Domínguez, M. Virginia Alonso, ... Francisco Rodríguez
Article 115230

View PDF Article preview

Research article ● Full text access

Ball-milled Bi_2MoO_6/biochar composites for synergistic adsorption and photodegradation of methylene blue: Kinetics and mechanisms

Yidan Luo, Aofeng Zheng, Mingshan Xue, Yu Xie, ... Bin Gao
Article 115229

View PDF Article preview

Research article ● Full text access

Preparation and characterization of a bio-based rigid plastic based on gelatinized starch cross-linked with furfural and formaldehyde

Jun Zhang, Bowen Liu, Yunxia Zhou, Hisham Essawy, ... Guanben Du
Article 115246

View PDF Article preview

Research article ● Full text access

3D printing of crude lignocellulosic biomass extracts containing hemicellulose and lignin

E. Gokce Bahcegul, Erinc Bahcegul, Necati Ozkan
Article 115234

View PDF Article preview

Research article ● Full text access

Novel stretchable fiber-shaped fluidic nanogenerators fabricated from carbonized lignin/thermoplastic polyurethane

Jiawen Gao, Hanxiao Zhang, Qiannan Zhang, Siqi Li, ... Hongbin Liu
Article 115240

View PDF Article preview

Research article ● Full text access

Wood based quasi-solid-state Zn-air battery with dual honeycomb-like porous carbon and cationic nanocellulose film

Chenglong Qiu, Lei Zhang, Baobin Wang, Guihua Yang, ... Jiachuan Chen
Article 115242

View PDF Article preview

Research article ● Full text access

Screening of dual targeted inhibitors of 5-lipoxygenase and cyclooxygenase-2 from *Oroxylum indicum* by off-line two-dimensional liquid chromatography coupled with mass spectrometry

Xin-jie Cheng, De-zhi Kong, Ya-hui Li, Guang-li Bian, De-qiang Li
Article 115243

View PDF Article preview

Research article ● Full text access

Fabrication of sustainable and durable superwetting cotton fabrics with plant polyphenol for on-demand oil/water separation

Dan-Dan Hu, Yi-Dong Li, Yunxuan Weng, Hua-Qiao Peng, Jian-Bing Zeng
Article 115264

View PDF Article preview

Research article ● Full text access

Study on the correlation between the puncture impact performance of arc-shaped bamboo splits and bamboo ages

Bin Huang, Hao Jia, Benhua Fei, Lin Chen, ... Fengbo Sun
Article 115252

View PDF Article preview

Research article ● Full text access

Self-healing modified liquefied lignocellulosic cross-linked bio-based polymer for controlled-release urea

Hongyu Tian, Lina Zhang, Xiao Sun, Jing Cui, ... Panfang Lu
Article 115241

View PDF Article preview

Research article ● Full text access

Pyrogallol loaded thermoplastic cassava starch based films as bio-based oxygen scavengers

Juthathip Promsorn, Nathdanai Harnkarnsujarit
Article 115226

View PDF Article preview

Review article ● Full text access

Zein - a plant-based material of growing importance: New perspectives for innovative uses

Ana Caroline Jaski, Francielle Schmitz, Rayta Paim Horta, Larissa Cadorin, ... Lizandra Maria Zimmermann
Article 115250

View PDF Article preview

Page 1 of 2

Previous vol/issue

Next vol/issue

ISSN: 0926-6690

Copyright © 2024 Elsevier B.V. All rights reserved

ELSEVIER

All content on this site: Copyright © 2024 Elsevier B.V., its licensors, and contributors. All rights are reserved, including those for text and data mining, AI training, and similar technologies. For all open access content, the Creative Commons licensing terms apply.

RELX™

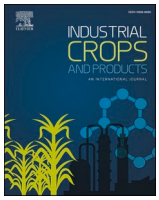
Industrial Crops & Products 186 (2022) 115145



Contents lists available at ScienceDirect

Industrial Crops & Products

journal homepage: www.elsevier.com/locate/indcrop





Differences in the components of *Neolamarckia cadamba* from different provenance and the drug resistance reversal activity of characteristic alkaloid

Mingxia Nie [a,b,1], Jingyuan Huang [c,1], Jiaoli Huang [a], Ziying Chen [a], Lazi Lin [a], Fulan Luo [a], Xu Zhang [a,*], Sui Xiao [a,*]

[a] Guangdong Key Laboratory for Innovative Development and Utilization of Forest Plant Germplasm, College of Forestry and Landscape Architecture, South China Agricultural University, Guangzhou, China
[b] Guangzhou Quality Supervision and Testing Institute, Guangzhou, China
[c] University of Massachusetts at Amherst, Amherst, MA, USA

ARTICLE INFO

Keywords:
Neolamarckia cadamba
UPLC-MS fingerprint
Spectrum-effect relationship
P-gp inhibitor

ABSTRACT

Neolamarckia cadamba (Roxb.) Bosser (Rubiaceae) is a fast-growing and economically important tree in Asia, which has a wide range of biological and pharmacological activities. Using the UPLC-MS fingerprints of the barks of N. cadamba that sampled from 12 different provenance (10 trees per provenance) in a provenance trail, the difference in the components of these samples was visualized. Analyzing the spectrum data and the cytotoxic activity, the relationships of chemical composition and in vitro anti-tumor activity had been established. It was noted that 3α-dihydrocadambine (3a-Dhc), one of the characteristic components in N. cadamba, could bind to the active pocket of P-glycoprotein (P-gp), and then inhibit its efflux activity, leading to reverse the adriamycin (ADR) resistance in MCF7/ADR cells with no toxicity. Taken together, our data pointed out that N. cadamba in different families had high but different contents of cadambine alkaloids, and the UPLC-MS fingerprint could be a powerful tool for guiding the variety breeding, and Sample 12, the provenance from Mengla County, may be a valued source for the best prospect of anti-tumor application. More importantly, 3a-Dhc could be a potential lead for developing a P-gp inhibitor with high potency and low toxicity.

1. Introduction

Neolamarckia cadamba (Roxb.) Bosser (Rubiaceae), broadly known as "Miracle tree", belongs to Rubiaceae family, which is a tropical evergreen and fast-growing tree mainly distributed in south and south-east Asia, such as India, China, Thailand and so on (Pandey and Negi, 2016). In Indonesia *N. cadamba* has been planted on a large scale for reforestation and afforestation since the 1930s, because it grows fast on a variety of soils and resists diseases and pests (Krisnawati et al., 2011). This kind of evergreen and fast-growing tree, *N. cadamba,* is highly suitable for agroforestry systems for higher economic returns in a short period (Saravanan, 2019), especially when combined with economic crops on steep slopes, the increasing diameter and height of the *N. cadamba* can reduce the rate of surface run-off and potential soil erosion, as a result, the survival rate, ground coverage, and yield of crops under a forest was significantly enhanced (Karyati et al., 2021). Since *N. cadamba* is the excellent characteristics of the fiber, nutritive and phytochemistry, it has been utilized for the wood industry and traditional medicine (Pandey et al., 2018). The 7–10 years growth rotation and lightweight hardwood of *N. cadamba* make it suitable for producing plywood, paper, and furniture (Mok and Ho, 2019). The fruit is also an abundant and edible source of nutritional components being the anti-oxidative activity (Sarkar et al., 2019). And the Charaka Samhita, a well-known ancient Indian medical treatise, mentions the use of leaves for treating wounds and pimples (Pandey and Negi, 2016). The extract of its leaves can cure some kinds of infection and pain due to the presence of alkaloids, tannins, steroids, saponins, and glycosides (Golla et al., 2018). The anti-diabetic effects in the rat model are observed when administrated with the extract of the roots (Acharyya et al., 2010) and flowers (Munira et al., 2020), respectively. Actually, the bark has a

* Corresponding authors.
E-mail addresses: zhangxu919@hotmail.com (X. Zhang), suixiao@outlook.com (S. Xiao).
[1] Contributed equally to the work.

https://doi.org/10.1016/j.indcrop.2022.115145
Received 7 February 2022; Received in revised form 9 May 2022; Accepted 26 May 2022
0926-6690/© 2022 Elsevier B.V. All rights reserved.

wide application for traditional medicine in numerous countries including India and Bangladesh. Moreover, it cures the inflammation of the throat and eyes, and even treat tumor, alone or mix with other plants (Pandey and Negi, 2016).

Extracts from fruits (Mishra et al., 2018), leaves (Chandel et al., 2016; Jamil et al., 2019; Singh et al., 2013), and barks (Fatima et al., 2016; Kumar et al., 2015) of *N. cadamba* have been demonstrated to be effective in killing many kinds of cancer cell lines in vitro. The methanolic extract of *N. cadamba* (MEAC) exhibits antitumor activity on Ehrlich ascites carcinoma (Dolai et al., 2012) and Dalton's lymphoma ascites cells (Dolai et al., 2016a). MEAC treatment could modulate the ratio of pro-apoptotic and anti-apoptotic proteins via the Bax upregulation and Bcl-2 downregulation, resulting in cancer cell apoptosis (Dolai et al., 2016b). However, to date there is no paper to integrally study the antitumor relationship of the components in the bark of *N. cadamba*. As we known, the biological activity of the plant is largely dependent on the different amounts and proportions of the chemical components, and certain chemometrics could quantitatively detect the chemical components and display them in the form of a chromatographic fingerprint. As our previous research, the establishment of the relationship of the chemical component and biological activity is achieved by an appropriate statistics method that could convert the diverse bioactivity and chemical components to spectrum-effect relationship (Xu et al., 2017). Therefore, to explore the antitumor relationship of the chemical ingredients, the *N. cadamba* resources from different provenances as the best experimental materials are applied for establishing the spectrum-effect relationship.

In this study the difference in the intrinsic chemical constituents of *N. cadamba* from different sources has been analyzed for the first time. A UPLC-MS fingerprint method has been established to help future selective breeding and study the spectral-effect relationship. The correlation of the peaks in the fingerprint and the cytotoxicity to breast cancer cells MCF-7 has been figured out. The isolated and purified alkaloid 3a-Dhc has demonstrated to be nontoxic against MCF-7 sensitive cells, however, and reverse the ADR resistance towards MCF7/ADR cells. Further in vitro cell experiments and molecular docking simulation reveal that 3a-Dhc can inhibit the efflux activity of P-gp via binding to its the active site. Combined with the discovery of biosynthesis path of cadambine (Zhao et al., 2021), our finding will lay a the new strategy for further development and utilization of cadambine and its derivatives.

2. Materials and methods

2.1. Chemicals

Methanol, acetonitrile, and formic acid were HPLC-grade and supplied by Fisher (Pittsburg, PA, USA). Deionized water obtained from a Milli-Q water system (Millipore, Bedford, MA, USA). dimethyl sulfoxide (DMSO), Rnase-A, propidium iodide (PI), 5-fluorouracil, Adriamycin and 3-(4,5-Dimethylthi-azol-2-yl)-2,5 -diphenyltetrazolium bromide (MTT) were purchased from Sigma-Aldrich (St. Louis, Mo, USA). All other reagents were of analytical grade.

2.2. Plant material

N. cadamba barks were collected in a five-year-old *N. cadamba* provenance trial established in Guangzhou, Guangdong province (23°14′ N, 113°37′ E), with an average annual temperature of 21.8 °C and annual rainfall of 2137 mm. Each sample was a mixture of 10 individual trees from one provenance. The collected barks were dried at 60 ℃ to be constant and were milled into fine 60-mesh-sieve powder, then stored at 4 °C. These raw materials were labeled according to their original provenances (Fig. 1).

2.3. Preparation of plant extracts

Approximately 10 g of the prepared powder sample was accurately weighed and extracted using a ultrasonic wave method for 30 min with 150 mL different extraction solvent (deionized water/ethyl alcohol/ethyl acetate/petroleum/ dichloromethane). The extraction solvent was treated through vacuum filtering (deionized water/ethyl alcohol/ethyl acetate) or centrifuging (petroleum/ dichloromethane). The filter liquor or supernatant liquor was dried by vacuum freeze-drying machine to bark extract. The sample solutions were diluted to 10 mg/mL with the corresponding extraction solvent and each treatment was performed in triplicate for fingerprint analysis.

2.4. UPLC-MS fingerprint analysis

2.4.1. UPLC-MS conditions

UPLC-MS fingerprints were analyzed by Waters ACQUITY QDA with UPLC system (Waters, Milford, MA, USA). An ACQUITY UPLC BEH C18 column (2.1 mm × 100 mm id,1.7 μm,waters) was applied for

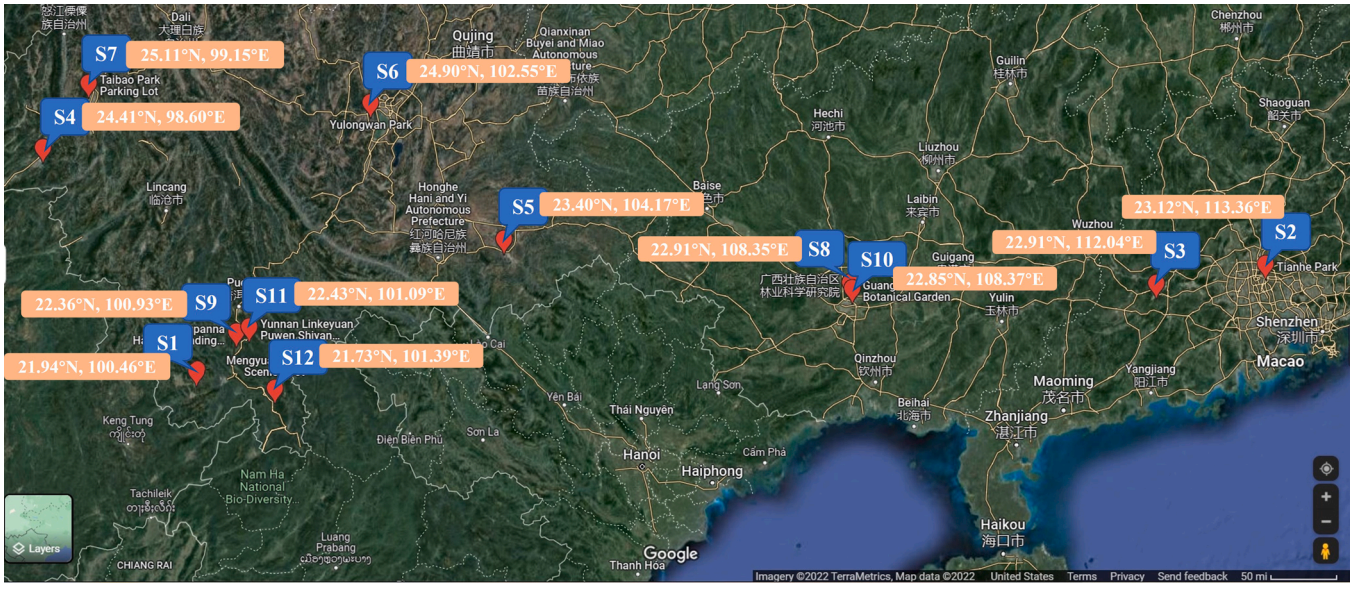


Fig. 1. The *N. cadamba* samples labeled with their provenances.

chromatographic separations. The column and auto-sampler were kept at 40 °C and 20 °C, respectively. 5 μL of sample solutions was injected into the above system. The mobile phase included eluents A (0.2% formic acid, v/v) and B (acetonitrile), which run at a flow rate of 0.3 mL/min. Mobile-phase B was increased from 5% to 10% over 0–10 min, from 10% to 20% over 10–30 min, from 20% to 35% over 30–40 min, from 35% to 65% over 40–60 min, and from 65% to 93% over 60–80 min. The mass spectrometer coupled with the full scan patten (*m/z* 50–1000) in the presence of positive electrospray ionization was operated. MS parameters for the analysis were listed as follows: the temperatures of ion source and desolvation gas were set at 100 and 300 °C, respectively; nitrogen was used as desolvation gas at the flow rate of 500 L/h; the capillary and cone voltages were 3.5 kV and 25 V, respectively.

2.4.2. UPLC-MS fingerprint analysis

Repeatability and precision of chromatograms *of N. cadamba* extracts were analysed through five replicate injections and five injections of each sample prepared independently from S11, respectively. Stability was analysed through the same sample at different intervals for 2 d (0, 2, 4, 8, 16, 24, and 48 h).

2.5. Preparative liquid chromatography

Preparative HPLC was developed on a GALAK EF-C18 column (19 mm × 250 mm, 5 μm; Waters) using a HP PLUS 100D system (Waters, Milford, MA, USA) equipped with a ultraviolet detector, and a fraction collector. The mobile phase consisting of solvent A (0.2%, v/v formic acid) and solvent B (acetonitrile) was used at a flow rate of 20 mL/min. Mobile-phase B was maintained at 10% over 8 min, increased from 10% to 20% over 8–26 min, and to 30% at 53 min. Final concentration of 100 mg/mL of the tested sample solution was diluted with methyl alcohol. The injection volume was 5 mL. The detector was set at 280 nm. The refining and identification of fractions of *N. cadamba* have acquired with rotary evaporator, vacuum freeze-drying machine and UPLC/MS analysis.

2.6. Cell lines and culture

The human breast cancer cells MCF-7 were purchased from Cell Bank of the Chinese Academy of Sciences (Shanghai, China). Adriamycin-resistant Cells MCF-7/ADR were obtained from Sun Yat-Sen Memorial Hospital. These cells were cultured in RPMI-1640 medium (Hyclone, USA) supplemented with 10% fetal bovine serum (Gibco, USA) and 1% penicillin-streptomycin (Hyclone, USA).

2.7. MTT assay

MCF-7 cells or MCF-7/ADR cells at 70–80% confluency were plated overnight into 96-well plates (1×10^4 cells/mL). Then, cells were treated with extracts or compounds at various indicated concentrations, or buffer alone (vehicle control) for 48 h. The supernatant was discarded, 100 μL medium and 10 μL MTT solution was added for another 4 h incubation, then add 100 μL of DMSO after the medium was aspirated. The OD absorbance was recorded at 570 nm with a Mutiskan MK3 microplate reader (Thermo, USA). IC_{50} was calculated by Probit analysis with IBM SPSS statistics software (21.0).

2.8. ADR efflux assay

The cells were pre-incubated in RMPI-1640 medium (1 μM ADR) for 1 h, and then cultured in an ADR-free medium for another 1.5 h with or without compounds. cells were observed and analyzed with a FACSCalibur flow cytometer (BD Biosciences, USA).

2.9. Western blotting

Cell lysates were prepared in RIPA buffer (50 mM Tris-HCl pH 7.4, 150 mM NaCl, 1 mM EDTA, 0.1% SDS, 1% NP-40, 0.5% sodium deoxycholate) supplemented with protease and phosphatase inhibitor cocktail (Thermo Scientific). Protein concentrations were quantified via RC DCTM Protein Assays (Bio-Rad, USA). 20 μg lysate was separated on 10% Bis-Tris protein gels (Invitrogen, USA), transferred to a PVDF membrane (Millipore, USA), blocked in 5% non-fat milk for 60 min, and then incubated overnight at 4 °C with primary antibodies. Primary antibodies included anti-P glycoprotein (1:1000, Proteintech 22336-1-AP) and anti-Actin antibodies (1:1000, Santa Cruz Biotechnology sc-47778). Secondary antibodies included Goat anti-Rabbit IgG (H+L) HRP, and Goat anti-Mouse IgG (H+L) HRP (Pierce, USA). Proteins were detected by ECL chemiluminescence detection kits (Pierce, USA), while autoradiographs were obtained with a GelDoc XR system (Bio-Rad, USA). Quantification analysis was performed using ImageJ software.

2.10. Docking

Docking experiments were performed with AutoDock Vina (Trott and Olson, 2010), a suite of automated docking tools. In this study, the nanodisc-reconstituted structure of P-gp was obtained from the Protein Data Bank server (PDB code: 6QEX). The brief steps of docking are summarized as follows: first, the HETATOMs including water and ligands were removed from the P-gp protein, and the energy of both the protein and ligand was minimized; secondly, the grid box was set based on the binding pocket of P-gp and the configuration document was written with an exhaustiveness parameter of 400, which indicated the number of runs; finally, the docking started with an AutoDock Vina run. With similar parameters, the docking process was repeated in triplicate to improve the accuracy of the results. The docking results were analyzed with Discovery Studio Visualizer 2020 and the PyMOL Molecular Graphics System, Version 2.0 Schrödinger, LLC. The interactions were studied in terms of ligand interactions, binding affinity (Kcal/mol), and RMSD.

2.11. Statistical analysis and heap map

Multiple regression analysis was used to evaluate the spectrum-effect relationships regarding the values of peak areas in the UPLC-MS fingerprints and the antitumor effects of 12 samples using SPSS V21 software. The heat map was created with Morpheus (https://software.broadinstitute.org/morpheus/).

3. Results

3.1. Optimization of the extraction

Breast cancer cell line MCF-7 was used as a cell model for the evaluation of anti-tumor activity. The antitumor activities of a series of extracts of *N. cadamba* from extraction solvents were assessed by the viability of MCF-7 cells. Extraction solvents with the polarities ranging from high to low were deionized water, ethyl alcohol, ethyl acetate, dichloromethane, and petroleum, respectively. The antiproliferation activity of various extracts against MCF-7 cells was ranked as follows: ethyl acetate extract > ethyl alcohol extract > dichloromethane extract > petroleum extract > deionized water extract. The antitumor activity of these treated groups was significantly higher than that of the untreated group (Fig. 2A). The inhibition ratio toward MCF-7 cells treated with the ethyl acetate extract at 50 μg/mL, 100 μg/mL and 500 μg/mL were 33.3% ($p < 0.01$), 58.6% ($p < 0.01$), and 86% ($p < 0.01$), respectively, indicating that the antitumor activity of ethyl acetate extract was in a dose-dependent manner.

The significantly different cytotoxicity toward MCF-7 cancer cells of extracts of *N. cadamba* from various extraction solvents was observed in

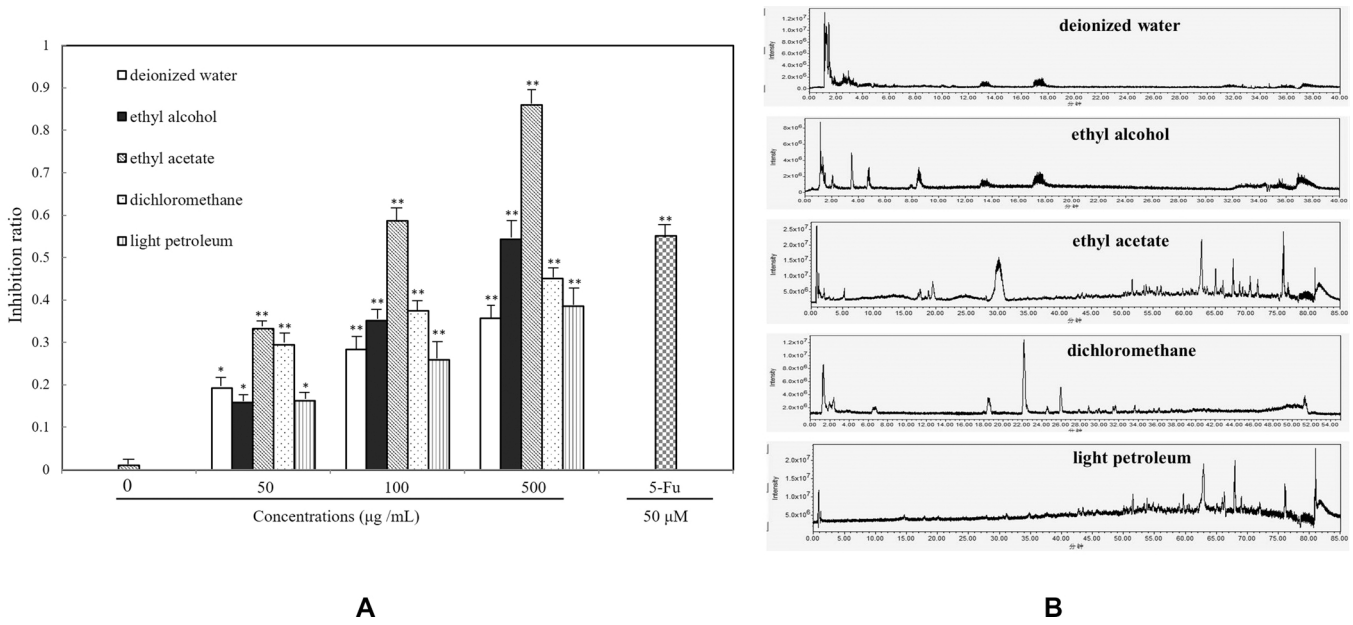


Fig. 2. The inhibition ratio of MCF-7 cells in vitro (A) by *N. cadamba* bark extracts obtained from different polarities extraction solvents; (B) UPLC pictures of different extracts of *N. cadamba* bark treated with five extraction solvents.

Fig. 2A. This may be ascribed to their different chemical compositions (Fig. 2B). Treated with the water extract, ethyl alcohol extract, ethyl acetate extract, dichloromethane extract, and petroleum extract at 500 μg/mL, the inhibition ratio towards MCF-7 cells was 35.7% ($p < 0.01$), 54.3% ($p < 0.01$), 86% ($p < 0.01$), 45% ($p < 0.01$) and 38.5% ($p < 0.01$), respectively, possibly indicating that ethyl acetate with medium polarity could contain more active compositions than the other extraction solvents. As seen in Fig. 2B, the types and contents of compounds in ethyl acetate extract were significantly more than that of the other extract. The detailed conditions of the extraction process described in Section 2.3 was the optimal extraction for use in the further experiments.

3.2. Discovery and optimization of UPLC-MS fingerprints

To obtain better chromatograms, three analytical columns including ACQUITY UPLC BEH phenyl, ACQUITY UPLC BEH C18, and ACQUITY UPLC HSS T3 were compared. ACQUITY UPLC BEH C18 column was selected because of the best resolution of separated peaks. Other chromatographic variables and MS parameters were described in Section 2.4.1 and also optimized. After screening the optimized conditions and careful selection of linear gradient elution, the complete separation of all the target peaks was finally achieved. Precision, repeatability, and storage stability of the UPLC-MS fingerprints was below 4% for both retention times and peak areas of common peaks, implying that this obtained methodology was totally feasible. The results also emphasized that the method of UPLC-MS for the fingerprint analysis was valid and satisfactory.

The UPLC-MS fingerprints of twelve *N. cadamba* bark extracts and the reference atlas created by the Chinese Pharmacopoeia Committee were shown in Fig. 3. Forty peaks with large areas and good segregation were regarded as common peaks. Similarities between the atlases of twelve *N. cadamba* bark extracts and the reference atlas were 0.941, 0.976, 0.931, 0.971, 0.955, 0.957, 0.948, 0.981, 0.952, 0.977, 0.928 and 0.978, respectively. It can be inferred from these results that the atlas of S2, S4, S8, S10, S12 had high similarities with the reference atlas, while the similarities of S1, S3 and S11 were low. Furthermore, retention times of peaks 6 and 7, as well as the common peaks from 35 min to 50 min, varied greatly in these twelve samples. These ingredients with significant differences could be the main reason for the difference in the

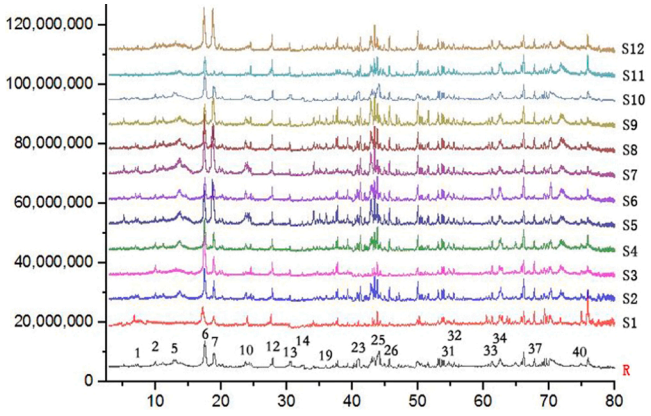


Fig. 3. The UPLC-MS fingerprints of the twelve *N. cadamba* bark extracts and the reference atlas.

antitumor activity of twelve *N. cadamba* bark extracts. So we next wanted to identify the specific components that regulate the antitumor activity and explain their antitumor action mechanisms.

3.3. Spectrum-effect relationships of UPLC-MS fingerprints and antitumor effects

A heatmap analysis was applied to visualize the difference of the relative contents of forty components in the twelve *N. cadamba* bark extract samples. The relationships of the chemical components and antitumor activities were reflected in Fig. 4. Each column represented the twelve samples and each row meant the forty common peaks of the UPLC/MS fingerprints. A color-coded scale grading from red to blue responded to the relative content of forty components shifting from high to low. An orange color-coded scale grading from dark to light matched the antitumor activities towards MCF-7 shifting from high to low. A purple color-coded scale grading from dark to light corresponded to the correlation index of the forty components and antitumor effects shifting from high to low. As shown in Fig. 4, the obvious difference in the relative content of the components of the twelve samples tested was observed. The relevance to the antitumor activities of some components,

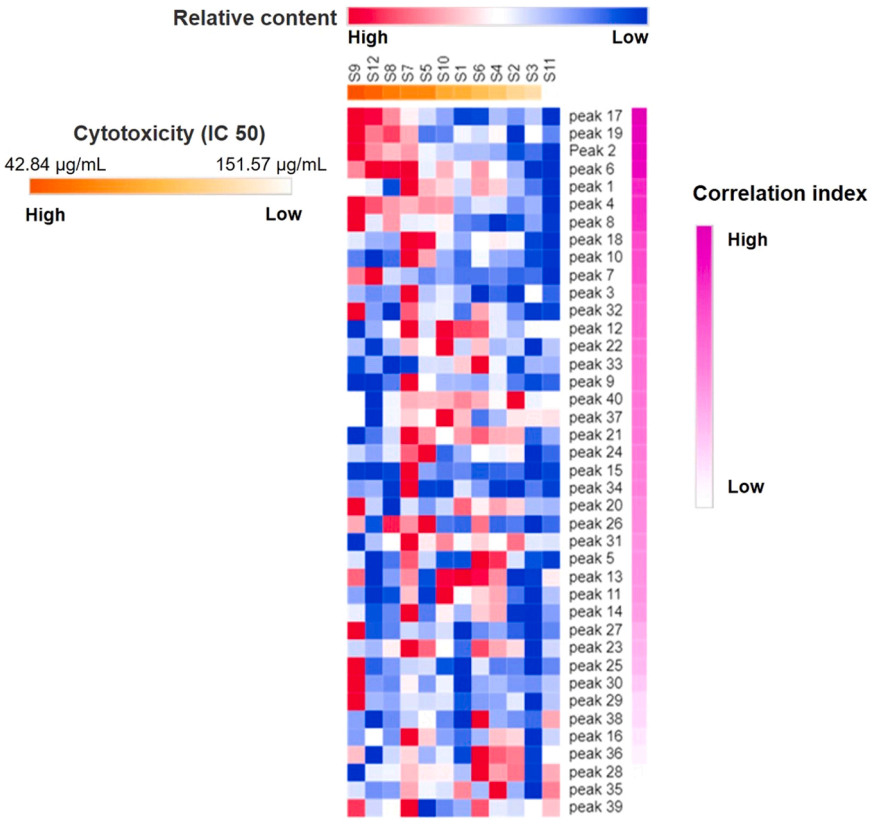


Fig. 4. Heatmap analysis of the correlation of chemical components and antitumor activities.

such as peaks 17, 19, 2, 6, 1, 4, 8, 18, 10, and 7 was much stronger than that of the rest peaks. The lower IC_{50} values of cytotoxicity to MCF7 was, the stronger the antitumor effects of *N. cadamba* bark extract exhibited. Samples 9, 12, 8, and 7 showed higher antitumor activities in comparison with other samples, possibly ascribing to the higher relative content of the above potential active components. From Fig. 3, the relative content of the potential active components was low except peaks 6 and 7. According to the UPLC-MS fingerprints (Fig. 3), peaks 6 and 7 were high peak area but obviously different among all of the tested samples. Consistent with the rank of the correlation index, peaks 6 and 7 were in the fourth and tenth place, respectively, probably implying that two peaks might be the representative components of *N. cadamba* in the antitumor activities. Therefore, understanding the antitumor activity and the action mechanisms of peaks 6 and 7 will guide the selective breeding to increase the amount of the species. Subsequently, we decided to purify and identify the structures of peaks 6 and 7, and further investigated the antitumor activity and their potential mechanisms.

3.4. Isolation and identification of the active fractions

From the above research results, we found that peaks 6 and 7 played an essential role in the antitumor activity of *N. cadamba* bark extracts. The content of the two components was the highest peak area and varied conspicuously among twelve samples. The peaks 6 and 7 were obtained by fraction collections operated as the optimized conditions described in Section 2.5. As depicted in Fig. 5, the fractions of peaks 6 and 7 were collected and identified by the established UPLC-MS system. These two components were baseline separated with satisfactory resolution and with the purities of 95.5% and 96.1%, respectively. Meantime, we compared retention times and MS data of the isolated fractions with the standard substances, validating that the molecular structures of peaks 6 and 7 were 3β-isodihydrocadambine (3β-Idhc) and 3α-dihydrocadambine (3a-Dhc), respectively (Fig. 5).

3.5. Synergistic effects of 3a-Dhc with clinical antitumor drug Adriamycin (ADR)

To further verify the accuracy of the antitumor activity, we investigated the cytotoxicity of peak 6 (3β-Idhc) and peak 7 (3a-Dhc) in vitro. We found that, after co-incubation with MCF7 cells for 72 h, 3β-Idhc showed an acceptable antitumor activity and the IC_{50} was 25.1 μM. But the IC_{50} of 3a-Dhc was above 100 μM, and in comparison with negative control, no difference at the highest concentration of 3a-Dhc was observed. Since the previous regression analysis showed 3a-Dhc exhibited some correlation to cytotoxicity, we chose ADR sensitive cell line MCF7 and ADR-resistant cell line (MCF7/ADR) as cell evaluation models to explore the potential synergistic effect of 3a-Dhc. As seen in Table 1, 3a-Dhc could not increase the antitumor activity of ADR in the sensitive cell line, but 3a-Dhc demonstrated a strong reversal of MCF7/ADR cells. The reversal result was similar to that of the positive drug verapamil. 10 μM of verapamil can change the resistance index from 45.6 to 4.0, and 100 μM 3a-Dhc could also decrease this index to 15. Although the concentration of 3a-Dhc is 10 times than that of the positive drug verapamil, no toxicity of 3a-Dhc itself against cell lines appeared at this concentration. More importantly, the reversal tendency similar to that of verapamil, a specific P-glycoprotein (Pg-p) inhibitor, emphasized 3a-Dhc achieved the synergistic effects with ADR via probably inhibiting Pg-p.

3.6. Inhibition of 3a-Dhc on P-glycoprotein efflux function

Because of the high expression of P-gp/ABCB1 in MCF7/ADR cells, ADR as the substrate of P-gp was pumped out of the cell and resulted in ADR resistance. In this study we examined the effect of 3a-Dhc on the efflux of ADR in MCF7/ADR cells by flow cytometry (Fig. 6A). The mean

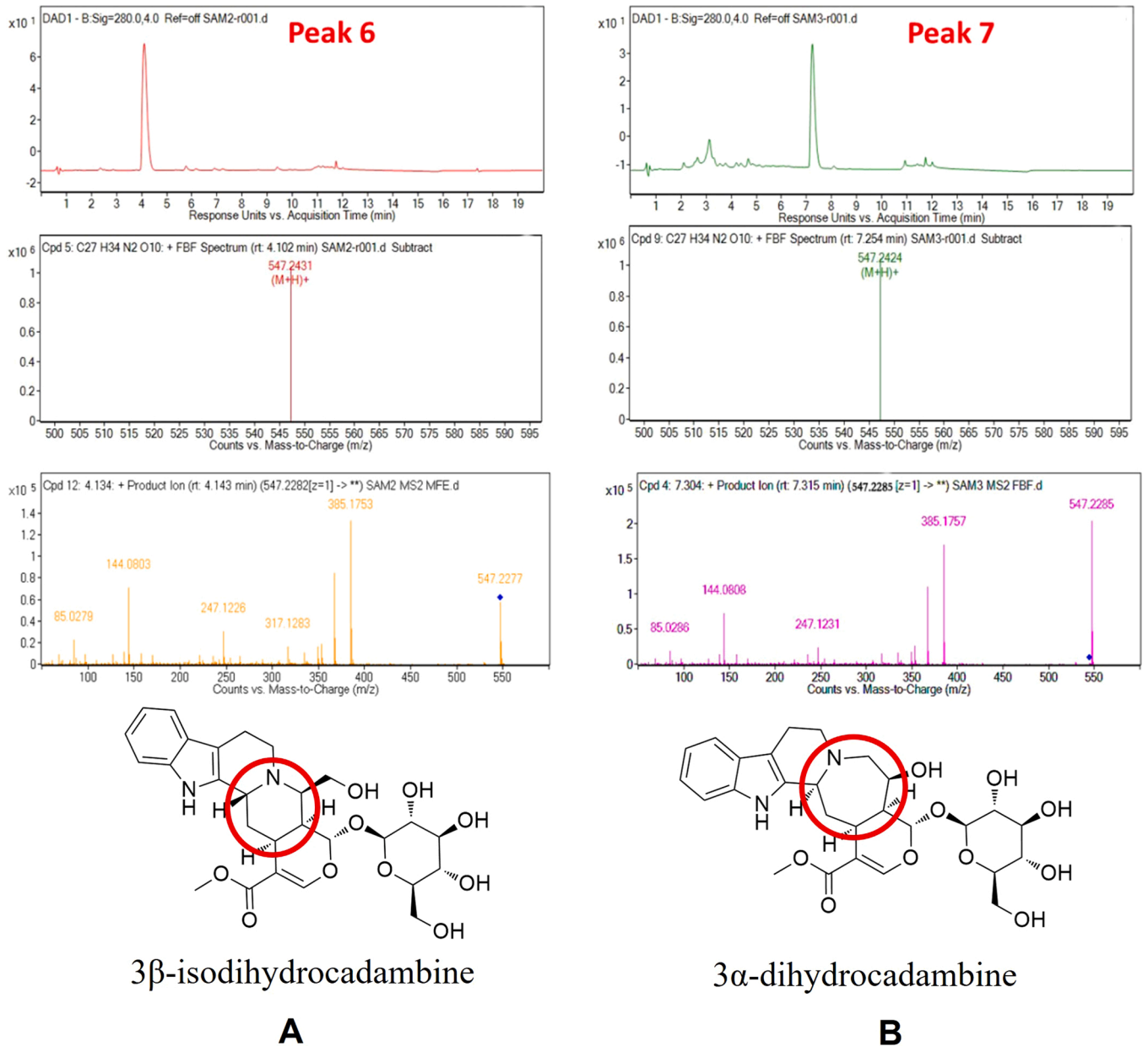


Fig. 5. UPLC-MS chromatogram and the molecular structures of 3β-isodihydrocadambine (A) and 3α-dihydrocadambine (B).

Table 1
Elimination of anticancer drug-resistance in MCF-7/ADR cells.

Compounds	IC_{50} (μM)		Resistance[a] Index
	MCF-7	MCF-7/ADR	
Adriamycin	1.21 ± 0.34	55.18 ± 6.21	45.6
+10 μM Verapamil	1.08 ± 0.26	4.32 ± 1.44	4.0
+10 μM 3α-Dihydrocadambine	1.13 ± 0.15	40.31 ± 3.55	30.8
+50 μM 3α-Dihydrocadambine	1.05 ± 0.19	29.77 ± 4.68	28.4
+100 μM 3α-Dihydrocadambine	1.24 ± 0.28	18.62 ± 2.74	15.0
100 μM 3α-Dihydrocadambine	> 100	> 100	

[a] Resistance index is defined as the IC_{50} of MCF-7/ADR resistant cell line relative to the parental MCF-7 cells.

fluorescent index of ADR increased from 11.3 to 275.2 by 10 μM of verapamil, indicating P-gp inhibitor can enhance the accumulation of ADR inside the cell by inhibiting the efflux function of P-gp. 100 μM of 3a-Dhc also could increase the fluorescent index to 162.5, which meant that 3a-Dhc was capable of inhibiting P-gp efflux function. Furthermore, we detected the expression of P-gp protein in MCF7/ADR cells. As shown in Fig. 6B, treated with 100 μM of 3a-Dhc for 72 h could not alter the expression of P-gp, illustrating that the inhibition of 3a-Dhc could suppress the efflux function of P-gp other than the downregulation of P-gp expression.

3.7. Molecular docking study of 3a-Dhc and P-gp

To further confirm our speculation that 3a-Dhc is an inhibitor of P-gp, molecular docking was performed using the Autodock Vina docking platform to determine the interaction of 3a-Dhc and P-gp. The human P-gp (PDB ID: 6QEX) was studied by Alam et al. for its interactions with the inhibitor zosuquidar as well as the anti-cancer drug Taxol, and the binding pocket of P-gp was determined as well (Alam et al., 2019). As shown in Fig. 7A, 3a-Dhc fitted tightly in the active site of P-gp with a binding energy of − 10.1 kcal/mol. According to the two-dimensional docking results (Fig. 7B), the A-ring and B-ring of 3a-Dhc were sandwiched by the phenyl ring of Trp232 and Phe343 through π-π

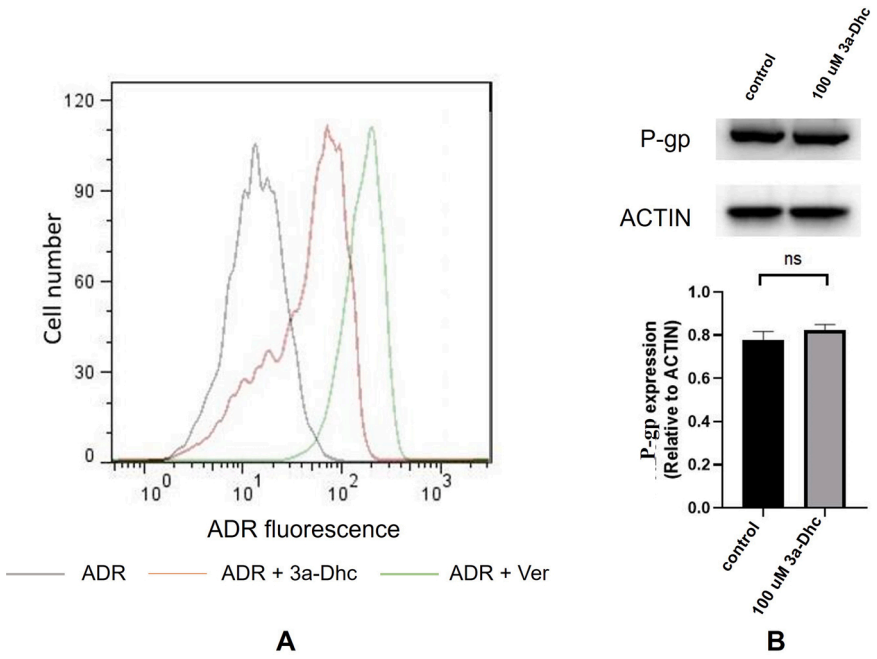


Fig. 6. Inhibitory effects of 3α-dihydrocadambine (3a-Dhc) on human P-gp. (A) 3a-Dhc significantly increased intracellular fluorescence of Adriamycin (ADR) as compared with the untreated control. Verapamil (Ver) was used as a positive control. (B) P-gp protein levels were quantified by WB in MCF7/ADR cells with or without 3a-Dhc treatment for 72 h.

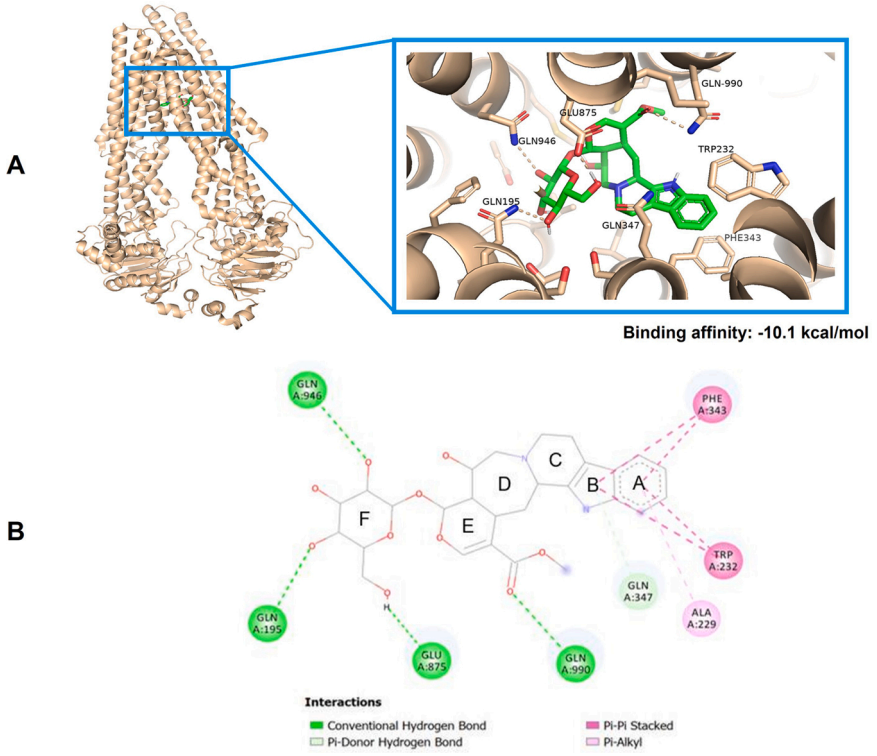


Fig. 7. Ribbon diagram of human P-gp bound to 3a-Dhc (A) and two-dimensional docking results (B). Relevant hydrogen bonds are shown in dashed lines.

interactions. The A-ring also had the π-alkyl interaction with Ala229. The hydroxyl groups on the F-ring and the carboxyl on the E-ring formed conventional hydrogen bonds with Gln195, Gln946, Glu875, and Gln990, respectively. Overall, the docked pose as well as the binding affinity indicated that 3a-Dhc was a potent small molecule that can bind to P-gp.

4. Discussion

Eucalyptus plantations expand quickly in China because of the fast-growing and high-yield characteristics and the economic and medical value of eucalyptus oil (Hua et al., 2016). Due to the problems of the ecological environment caused by large-scale planting of a single species, people have been looking for alternative trees (Wei and Zhu, 2019).

N. cadamba, an economically important fast-growing tree, is being developed for the paper and wood industry. Meanwhile, because of the bioactive components, *N. cadamba* are widely used for traditional medicine (Li et al., 2019), food supplements (Pandey et al., 2018), and feed additives (He et al., 2019). Our research has found that, using the UPLC-MS fingerprints, the components of the barks of *N. cadamba* from different genealogies exhibited obvious chemical diversity, especially in the feature components, such as cadambine and its derivatives. It is known that chemical differentiation is related to both the growing environment and genetic genes (Zhao et al., 2012). The former has been considered as the key point to the medical value in traditional Chinese medical herbs collected from the famous-region drug in specific area (Wang et al., 2018). Though there is a significant difference in plant secondary metabolites in our samples, the feature constituents of *N. cadamba* are not lost with the migration. The phenomenon indicates that the generation of cadambine and other characteristic components is more related to genetic genes rather than the growing environments such as temperature, moisture, and soil. Therefore, the difference in cadambine alkaloids among families provides the theoretical basis for future breeding. As well, the UPLC-MS fingerprint analysis we established is a useful tool for selective breeding for *N. cadamba* as a potential alternative species of eucalyptus.

Another useful application of the established UPLC-MS fingerprint of *N. cadamba* is in search of the active components using the spectrum-effect relationship. Unlike the traditional method for identifying single compounds, the spectrum-effect relationship study can more intuitively and holistically understand the association of the bioactivity potency and the content of internal components in *N. cadamba*. In the development and utilization of *N. cadamba* the bioactivity of high-content characteristic components should be paid attention to, and these components can guide more effectively guide the application of the extract of *N. cadamba*. Several peaks, including the highest characteristic peaks 6 and 7, have been found to be a strong correlation with cytotoxicity against MCF7 cells. 3β-Idhc (peak 6) displays certain cytotoxicity in MCF7 cells, which is in agreement with the results of the spectrum-effect relationship. But 3a-Dhc (peak 7) fails to exhibit any cytotoxicity even at the highest concentration. Furthermore, 3a-Dhc can significantly reverse the resistance index of MCF-7/ADR cells when co-administrated with ADR. The observation is possibly due to the rigid chemical structure of a six-membered ring of 3β-Idhc shifted to the flexible chemical structure of a seven-membered ring of 3a-Dhc. Noticeably, 3a-Dhc with a seven-membered ring contained in the scaffold overcomes drug resistance without any toxicity. Besides, with the further in-depth study of the biological activity of cadambine and its derivatives as the characteristic components abundant in almost every sample, the accumulation of these characteristic secondary metabolites will be chemical substance marks for evaluating the nutrient and medicinal value of *N. cadamba*. Considering the utilization of active ingredients and the in vitro cytotoxicity, S12 (the provenance is Mengla County, Xishuangbanna Dai Autonomous Prefecture) with the highest content of 3a-Dhc and almost the strongest cytotoxicity is considered to have the greatest application potential in anti-tumor.

The multidrug resistance (MDR) that cancer cells develop resistance to a variety of structurally anticancer drugs, is a major problem in the therapy of breast cancer (Perez, 2008). P-gp has a wide tissue distribution and is a broad-spectrum multidrug efflux pump, involving in the transport of cationic hydrophobic compounds out of cells (Aller et al., 2009). A high expression level of P-gp has been investigated as a predictor of cross-resistance to structurally unrelated chemotherapeutics (Trock et al., 1997) and is found to be associated with a higher grade, lymph node involvement, shorter overall survival, and a shorter progression-free period in breast cancer patients (Surowiak et al., 2005). To reverse the cancer MDR, lots of studies have focused on the inhibition of P-gp efflux function. Verapamil, one of the first generation of P-gp inhibitors, unspecifically binds to other transporters, leading to unpredictable pharmacokinetics (Ferry et al., 1996). Dexverapamil, a typical drug of the second-generation inhibitors, has less toxicity than the previous generation, however, and it affects the metabolism of other drugs because of the inhibition of hepatic microsomal enzymes (Amin, 2013). Although the third generation tariquidar with an acceptable toxicity and a potent P-gp inhibition in phase I trial fails during phase III, and the side effects in combination with carboplatin or vinorelbine are the main reason for its failure (Kelly et al., 2011). Now, inspired by the clinical phase I stage P-gp inhibitor tetrandrine/CBT-01®, a natural isoquinoline alkaloid, more researchers are seeking other alkaloids for cancer resistance reversal (Joshi et al., 2017). In this study, we found a alkaloid derivative 3a-Dhc can inhibit P-gp efflux function, and then effectively reverse the ADR resistance in MCF7/ADR cells. The most important finding is that alkaloid 3a-Dhc specific for the inhibition of P-gp rarely exhibits cytotoxicity to MCF7 cells. In the following researches, we are going to perform structural modification of the lead compound 3a-Dhc in combination with the molecule docking results, for purpose of getting 3a-Dhc-derived P-gp inhibitors with higher specificity and lower toxicity.

5. Conclusion

In summary, the fingerprints of *N. cadamba* were successfully established using the UPLC-MS system. The difference in the chemical compositions of *N. cadamba* from various provenances was determined with the UPLC-MS assay, laying a solid material foundation for guiding future variety selective breeding. After analyzing the spectrum-effect fingerprints, 3β-Idhc, the characteristic alkaloids of *N. cadamba*, exhibited an obvious cytotoxicity to MCF-7 cells in vitro, and another analog 3a-Dhc was demonstrated to reverse the ADR resistance in MCF7/ADR cells through inhibiting P-gp activity, accompanying no toxicity to MCF-7 sensitive and resistant cells. This kind of a nucleus structure having a flexible seven-membered ring as the lead scaffold hold great potentials for developing novel P-gp inhibitors with lower toxicity and higher efficacy. From the above compelling evidences, sample 12 acquired from the original provenance of Mengla County may be an source for the best prospect of anti-tumor application.

CRediT authorship contribution statement

Mingxia Nie: Resources, Methodology, Formal analysis, Validation, Investigation. **Jingyuan Huang**: Software, Formal analysis, Writing – review & editing. **Jiaoli Huang**: Investigation, Validation. **Ziying Chen**: Investigation, Validation. **Lazi Lin**: Investigation, Validation. **Fulan Luo:** Investigation, Validation. **Xu Zhang:** Conceptualization, Methodology, Writing – original draft, Supervision, Project administration. **Sui Xiao:** Conceptualization, Formal analysis, Investigation, Resources, Supervision, Writing – review & editing, Funding acquisition.

Declaration of Competing Interest

The authors declare that they have no known competing financial interests or personal relationships that could have appeared to influence the work reported in this paper.

The authors declare that they have no conflicts of interest.

Acknowledgments

TThis work was financially supported by the General project of Natural Science Foundation of Guangdong Province (No. 2021A1515012153), and Project of Strengthening Guangdong Province with Traditional Chinese Medicine (No. 20201248). We thank Dr. Kunxi Ouyang for assistance with sampling and providing provenance information.

References

Acharyya, S., Dash, G.K., Mondal, S., Dash, S.K., 2010. Studies on glucose lowering efficacy of the Anthocephalus cadamba (Boxb.) Miq. roots. Int. J. Pharma Bio Sci. 1, 1–9.

Alam, A., Kowal, J., Broude, E., Roninson, I., Locher, K.P., 2019. Structural insight into substrate and inhibitor discrimination by human P-glycoprotein. Science 363, 753–756.

Aller, S.G., Yu, J., Ward, A., Weng, Y., Chittaboina, S., Zhuo, R., Harrell, P.M., Trinh, Y. T., Zhang, Q., Urbatsch, I.L., Chang, G., 2009. Structure of P-glycoprotein reveals a molecular basis for poly-specific drug binding. Science 323, 1718–1722.

Amin, M.L., 2013. P-glycoprotein inhibition for optimal drug delivery. Drug Target Insights 7, 27–34.

Chandel, M., Kumar, M., Sharma, U., Kumar, N., Singh, B., Kaur, S., 2016. Isolation and characterization of flavanols from Anthocephalus cadamba and evaluation of their antioxidant, antigenotoxic, cytotoxic and COX-2 inhibitory activities. Rev. Bras. Farmacogn. Braz. J. Pharmacogn. 26, 474–483.

Dolai, N., Karmakar, I., Suresh Kumar, R.B., Kar, B., Bala, A., Haldar, P.K., 2012. Evaluation of antitumor activity and in vivo antioxidant status of Anthocephalus cadamba on Ehrlich ascites carcinoma treated mice. J. Ethnopharmacol. 142, 865–870.

Dolai, N., Islam, A., Haldar, P.K., 2016a. Antiproliferative activity and apoptosis inducing mechanism of Anthocephalus cadamba on Dalton's lymphoma ascites cells. Iran. J. Pharm. Res. 15, 505–514.

Dolai, N., Islam, A., Haldar, P.K., 2016b. Methanolic extract of Anthocephalus cadamba induces apoptosis in Ehrlich ascites carcinoma cells in experimental mice. Indian J. Pharmacol. 48, 445–449.

Fatima, N., Ahmad, M., Ansari, J., Khan, H., Rastogi, N., Srivastava, S., Ahmad, S., Ali, Z., 2016. Antiproliferative and antioxidant studies of Anthocephalus cadamba Rox. Miq. Bark. Indian J. Pharm. Sci. 78, 525–531.

Ferry, D.R., Traunecker, H., Kerr, D.J., 1996. Clinical trials of p-glycoprotein reversal in solid tumours. Eur. J. Cancer 32, 1070–1081.

Golla, V.S.K., Kumari, D.A., Nilesh, K.F., Kumar, C.S.P., 2018. Preliminary phytochemical investigation and bioloical evaluation of the leaves of Neolamarckia cadamba. World J. Pharm. Res. 7, 851–865.

He, L., Wang, C., Zhou, W., Zhang, Q., Chen, X., 2019. Effect of additives on fermentation characteristics, nutrient values and in vitro fermentation profile of Neolamarckia cadamba leaf silage. South Afri. J. Anim. Sci. 49, 644–653.

Hua, F., Wang, X., Zheng, X., Fisher, B., Wang, L., Zhu, J., Tang, Y., Yu, D.W., Wilcove, D. S., 2016. Opportunities for biodiversity gains under the world's largest reforestation programme. Nat. Commun. 7, 12717.

Jamil, M.M.A., Rahman, N.A.A., Ishak, D.N.F.M., Adon, M.N., Choon, C.C., Ambar, R., Wahab, R.A., 2019. Combined effect of Neolamarckia cadamba leaves and electroporation method on HeLa cell anti-proliferation process. In: Proceedings of the 9th IEEE International Conference on Control System, Computing and Engineering (ICCSCE), pp. 226–229.

Joshi, P., Vishwakarma, R.A., Bharate, S.B., 2017. Natural alkaloids as P-gp inhibitors for multidrug resistance reversal in cancer. Eur. J. Med. Chem. 138, 273–292.

Karyati, K., Sarminah, S., Karmini, K., Akbar, A.M., Hermansyah, R., 2021. Conservation and economic aspects of a combination of forestry-agricultural crops (Neolamarckia cadamba-Phaseolus vulgaris) and terrace systems in different slope classes. ST-JSSA 18, 98–106.

Kelly, R.J., Draper, D., Chen, C.C., Robey, R.W., Figg, W.D., Piekarz, R.L., Chen, X., Gardner, E.R., Balis, F.M., Venkatesan, A.M., Steinberg, S.M., Fojo, T., Bates, S.E., 2011. A pharmacodynamic study of docetaxel in combination with the P-glycoprotein antagonist tariquidar (XR9576) in patients with lung, ovarian, and cervical cancer. Clin. Cancer Res. 17, 569–580.

Krisnawati, H., Kallio, M., Kanninen, M., 2011. Anthocephalus cadamba Miq.: Ecology, Silviculture and Productivity. Center for International Forestry Research (CIFOR).

Kumar, D., Tejaswi, C., Rasamalla, S., Mallick, S., Pal, B.C., 2015. Bio-assay guided isolation of anti-cancer compounds from Anthocephalus Cadamba Bark. Nat. Prod. Commun. 10, 1934578×1501000807.

Li, J., Zhang, D., Que, Q., Chen, X., Ouyang, K., 2019. Plant regeneration and Agrobacterium-mediated transformation of the miracle tree Neolamarckia cadamba. Ind. Crop. Prod. 130, 443–449.

Mishra, D.P., Khan, M.A., Yadav, D.K., Rawat, A.K., Singh, R.K., Ahamad, T., Hussain, M. K., Saquib, M., Khan, M.F., 2018. Monoterpene indole alkaloids from Anthocephalus cadamba fruits exhibiting anticancer activity in human lung cancer cell line H1299. ChemistrySelect 3 (8468–8472).

Mok, P.-K., Ho, W.-S., 2019. Rapid in vitro propagation and efficient acclimatisation protocols of Neolamarckia cadamba. Asian J. Plant Sci. 18, 153–163.

Munira, S., Nesa, L., Islam, M.S., Begum, Y., Rashid, M.A., Sarker, M.R., Ahmed, T., 2020. Antidiabetic activity of Neolamarckia cadamba (Roxb.) Bosser flower extract in alloxan-induced diabetic rats. Clin. Phytosci. 6, 33.

Pandey, A., Negi, P.S., 2016. Traditional uses, phytochemistry and pharmacological properties of Neolamarckia cadamba: a review. J. Ethnopharmacol. 181, 118–135.

Pandey, A., Chauhan, A.S., Haware, D.J., Negi, P.S., 2018. Proximate and mineral composition of Kadamba (Neolamarckia cadamba) fruit and its use in the development of nutraceutical enriched beverage. J. Food Sci. Technol. 55, 4330–4336.

Perez, E.A., 2008. Impact, mechanisms, and novel chemotherapy strategies for overcoming resistance to anthracyclines and taxanes in metastatic breast cancer. Breast Cancer Res. Treat. 114, 195.

Saravanan, S., 2019. Neolamarkia cadamba-a potential tree species for domestication through agroforestry system. Int. J. Environ. Agric. Biotechnol. 12, 375–380.

Sarkar, M., Hasan, M., Bhowmick, S., Hussain, J., Haque, M., Khan, M.A., Hossain, S., 2019. Evaluation of the anti-oxidative, erythrocyte membrane stabilizing effect and nutritional status of Neolamarckia cadamba Fruit. Am. J. Food Nutr. 7, 6–12.

Singh, S., Ishar, M.P.S., Saxena, A.K., Kaur, A., 2013. Cytotoxic effect of Anthocephalus cadamba Miq. leaves on human cancer cell lines. Pharmacogn. J. 5, 127–129.

Surowiak, P., Materna, V., Matkowski, R., Szczuraszek, K., Kornafel, J., Wojnar, A., Pudelko, M., Dietel, M., Denkert, C., Zabel, M., Lage, H., 2005. Relationship between the expression of cyclooxygenase 2 and MDR1/P-glycoprotein in invasive breast cancers and their prognostic significance. Breast Cancer Res. 7, R862–R870.

Trock, B.J., Leonessa, F., Clarke, R., 1997. Multidrug resistance in breast cancer: a meta-analysis of MDR1/gp170 expression and its possible functional significance. J. Natl. Cancer Inst. 89, 917–931.

Trott, O., Olson, A.J., 2010. AutoDock Vina: improving the speed and accuracy of docking with a new scoring function, efficient optimization, and multithreading. J. Comput. Chem. 31, 455–461.

Wang, X., Feng, L., Zhou, T., Ruhsam, M., Huang, L., Hou, X., Sun, X., Fan, K., Huang, M., Zhou, Y., Song, J., 2018. Genetic and chemical differentiation characterizes top-geoherb and non-top-geoherb areas in the TCM herb rhubarb. Sci. Rep. 8, 9424.

Wei, R., Zhu, W., 2019. Adaptability and growth of a fast-growing Neolamarckia cadamba (Roxb.) bosser clone in the south subtropical region of China. Open J. For. 9, 419–438.

Xu, Z., Li-Fang, Z., Chen-Yuan, C., Fei-Qun, X., Sui, X., 2017. An approach for searching bioactive compounds from traditional Chinese plant food and herb medicines by investigating spectrum–effect relationships. Curr. Pharm. Anal. 13, 417–426.

Zhao, X., Hu, X., OuYang, K., Yang, J., Que, Q., Long, J., Zhang, J., Zhang, T., Wang, X., Gao, J., Hu, X., Yang, S., Zhang, L., Li, S., Gao, W., Li, B., Jiang, W., Nielsen, E., Chen, X., Peng, C., 2021. Chromosome-level assembly of the Neolamarckia cadamba genome provides insights into the evolution of cadambine biosynthesis. Plant J. 109, 891–908.

Zhao, Z., Guo, P., Brand, E., 2012. The formation of daodi medicinal materials. J. Ethnopharmacol. 140, 476–481.

Contents lists available at ScienceDirect

Bioorganic Chemistry

journal homepage: www.elsevier.com/locate/bioorg

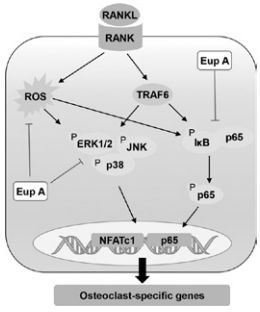
Graphical Abstracts/Bioorganic Chemistry 119 (2022) ii-xxi

REGULAR ARTICLES

105511

Euphoesulatin A prevents osteoclast differentiation and bone loss via inhibiting RANKL-induced ROS production and NF-κB and MAPK signal pathways

Yu-ting Zhang, Chen Hu, Song-xuan Zhang, Hui-hao Zhou, Jun Xu, Jian-da Ma, Lie Dai and Qiong Gu

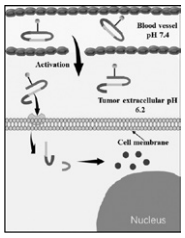


105510

Construction of synergistic pH/H_2O_2-responsive prodrug for prolonging blood circulation and accelerating cellular internalization

Jun Liu, Shuang Si, Jinyi Xu, Peng Xue and Kaipeng Li

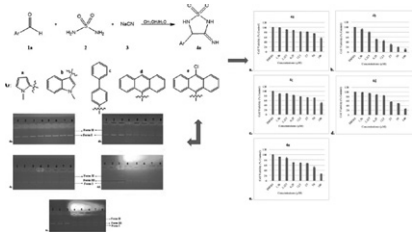
To achieve controlled shielding of loaded drugs in the biodistribution and blood circulation, we have proposed that the shielding group (5′-DFUR) as the encapsulating to create a promising framework for overcoming the stability in the blood circulation. The prodrugs coupled with bisboronate group could be selectively activated by H_2O_2 in tumor sites. Using this approach, the stability and stimulus responsive properties of prodrug as stable surrogates could synergistically achieve effectively prevented premature doxifluridine release and achieved prompt intracellular release during intracellular trafficking. Therefore, the probe, could provide a promising framework for overcoming the stability in the blood circulation and achieving drug release in acidic tumor environments.



105517

3-Imino derivative-sulfahydantoins: Synthesis, in vitro antibacterial and cytotoxic activities and their DNA interactions

Ceren Başkan, Aliye Gediz Ertürk, Birsen Aydın and Belgin Sırıken

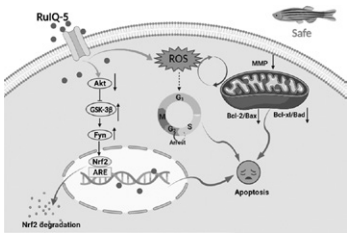


105516

Cyclometalated Ru(II)-isoquinoline complexes overcome cisplatin resistance of A549/DDP cells by downregulation of Nrf2 via Akt/GSK-3β/Fyn pathway

Lanmei Chen, Jie Wang, Xianhong Cai, Suxiang Chen, Jingjing Zhang, Baojun Li, Weigang Chen, Xinhua Guo, Hui Luo and Jincan Chen

The cellular uptake, *in vitro* cytotoxicities on 2D planar cell and 3D MCTSs, *in vivo* toxicity, cell apoptosis studies and mechanism of overcomimg cisplatin resistance in A549/DDP cells by new cyclometalated ruthenium(II)-isoquinoline complex **RuIQ-5** have been extensively explored by ICP-MS, MTT assay, 3D MCTSs model, zebrafish embryos model, flow cytometry, immunofluorescence staining and other fluorescence staining experiment by inverted fluorescence microscope, as well as western blot experimental techniques.



105519

Systemic pharmacological verification of *Baixianfeng decoction* regulating TNF-PI3K-Akt-NF-κB pathway in treating rheumatoid arthritis

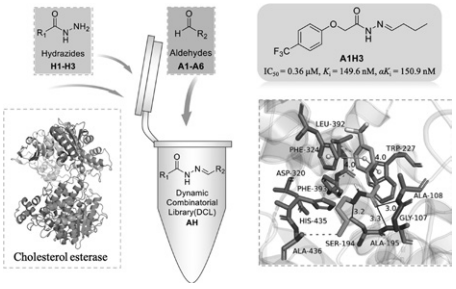
Xin Wei, Renpeng Zhou, Yong Chen, Ganggang Ma, Yang Yang, Chao Lu, Weiping Xu and Wei Hu

The cellular uptake, *in vitro* cytotoxicities on 2D planar cell and 3D MCTSs, *in vivo* toxicity, cell apoptosis studies and mechanism of overcomimg cisplatin resistance in A549/DDP cells by new cyclometalated ruthenium(II)-isoquinoline complex **RuIQ-5** have been extensively explored by ICP-MS, MTT assay, 3D MCTSs model, zebrafish embryos model, flow cytometry, immunofluorescence staining and other fluorescence staining experiment by inverted fluorescence microscope, as well as western blot experimental techniques.

105520

Identification and synthesis of selective cholesterol esterase inhibitor using dynamic combinatorial chemistry

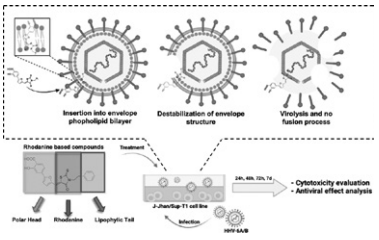
Shuang Zhao, Yao Wu and Lei Hu



105518

Synthesis and biological evaluation of novel rhodanine-based structures with antiviral activity towards HHV-6 virus

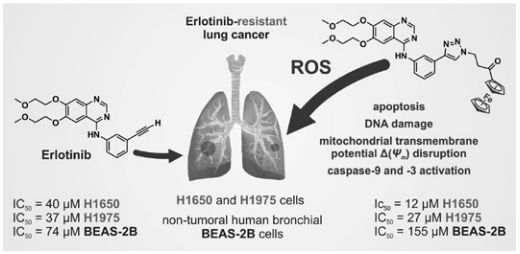
Valentina Gentili, Giulia Turrin, Paolo Marchetti, Sabrina Rizzo, Giovanna Schiuma, Silvia Beltrami, Virginia Cristofori, Davide Illuminati, Greta Compagnin, Claudio Trapella, Roberta Rizzo, Daria Bortolotti and Anna Fantinati



105514

Click ferrocenyl-erlotinib conjugates active against erlotinib-resistant non-small cell lung cancer cells *in vitro*

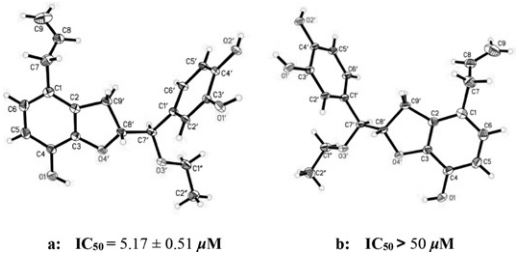
Przemysław Biegański, Martina Godel, Chiara Riganti, Daniel Fábio Kawano, Joanna Kopecka and Konrad Kowalski



105522

New enantiomeric lignans and new meroterpenoids with nitric oxide release inhibitory activity from *Piper puberulum*

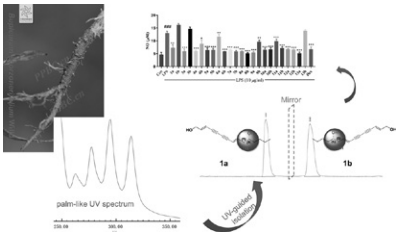
Yuan-kun Zheng, Ya-qi Wang, Bao-jun Su, Heng-shan Wang, Hai-bing Liao and Dong Liang



105521

UV-guided isolation of enantiomeric polyacetylenes from *Bupleurum scorzonerifolium* Willd. with inhibitory effects against LPS-induced NO release in BV-2 microglial cells

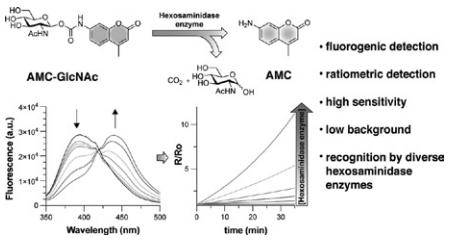
Wei Hong, Da Liu, Peng Zhao, Shu-Yan Qin, Yu-Fei Xi, Rui Guo, Xiao-Xiao Huang, Shao-Jiang Song and Dan-Qi Li



105532

Multifunctional fluorescent probes for high-throughput characterization of hexosaminidase enzyme activity

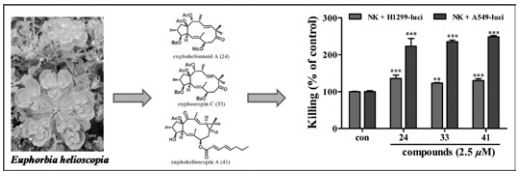
Shaochi Wang, Alexandra P. Breslawec and Myles B. Poulin



105534

Diterpenoids from *Euphorbia helioscopia* and their enhancement of NK cell-mediated killing of NSCLC cells

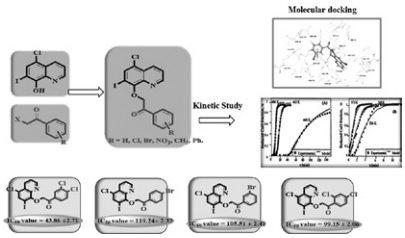
Hong-yan Mu, Chen-yuan Gong, Ru-jun Zhang, Zhen-hua Chen, Shi-guo Zhu and Wei-min Zhao



105506

Synthesis of new clioquinol derivatives as potent α-glucosidase inhibitors; molecular docking, kinetic and structure–activity relationship studies

Shoukat Wali, Atia-tul-Wahab, Saeed Ullah, Maria Aqeel Khan, Shahid Hussain, Muniza Shaikh, Atta-ur-Rahman and M. Iqbal Choudhary

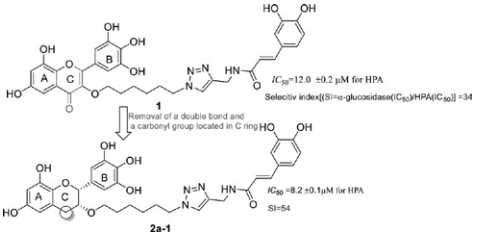


105515

Design and synthesis of epigallocatechin (EGC) analogs selective to inhibit α-amylase over α-glucosidases *via* the incorporation of caffeine acid and its derivatives

Wenming Chen, Cui Zhou, Jiansheng Chen, Meizhu Wang, Fang Zhou, Chunmei Wang, Xu Zhang and Wen Zhou

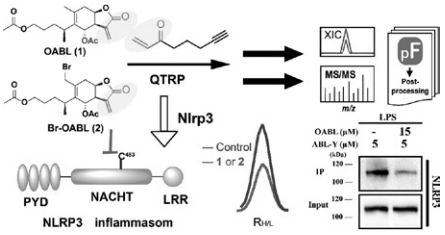
Taking human pancreatic α-amylase (HPA) inhibitor **1** as the lead, the influence of methylation of caffeic acid, the length of a liker, a double bond of a linker on the inhibition activity and selectivity of EGC-based conjugates was explored. Accordingly, conjugate **2a-1** with a superior inhibition activity and higher selectivity toward HPA held great potentials in developing the anti-diabetes mellitus drugs.



105536

Identification of NLRP3 as a covalent target of 1,6-*O*,*O*-diacetylbritannilactone against neuroinflammation by quantitative thiol reactivity profiling (QTRP)

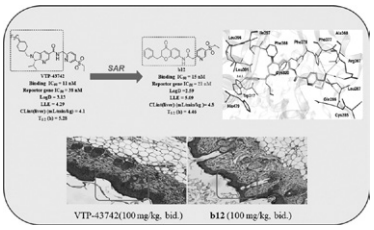
Min-Ran Wang, Lan-Fang Huang, Cong Guo, Jing Yang, Shuai Dong, Jiang-Jiang Tang and Jin-Ming Gao



105483

Discovery of *N*-(2-benzyl-4-oxochroman-7-yl)-2-(5-(ethylsulfonyl) pyridin-2-yl) acetamide (b12) as a potent, selective, and orally available novel retinoic acid receptor-related orphan receptor γt inverse agonist

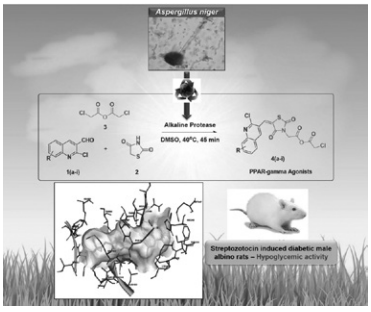
Lei Chen, Mei Su, Qiu Jin, Chun-Gu Wang, Israa Assani, Mu-Xuan Wang, Shi-Feng Zhao, Shen-Min Lv, Jia-Wei Wang, Bo Sun, Yan Li and Zhi-Xin Liao



105533

Biocatalytic one pot three component approach: Facile synthesis, characterization, molecular modelling and hypoglycemic studies of new thiazolidinedione festooned quinoline analogues catalyzed by alkaline protease from *Aspergillus niger*

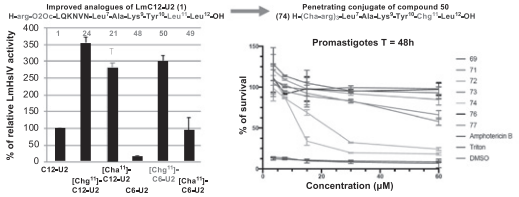
Gangadhara Angajala, Valmiki Aruna, Pasupala Pavan and Pulikanti Guruprasad Reddy



105539

The C-terminal segment of *Leishmania major* HslU: Toward potential inhibitors of LmHslVU activity

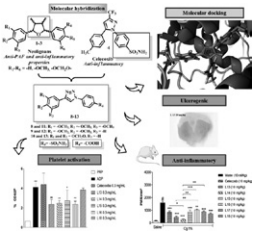
Priyanka Singh, Krishnananda Samanta, Ndeye Mathy Kebe, Grégory Michel, Baptiste Legrand, Vera E. Sitnikova, Andrey V. Kajava, Michel Pagès, Patrick Bastien, Christelle Pomares, Olivier Coux and Jean-François Hernandez



105485

Anti-inflammatory, ulcerogenic and platelet activation evaluation of novel 1,4-diaryl-1,2,3-triazole neolignan-celecoxib hybrids

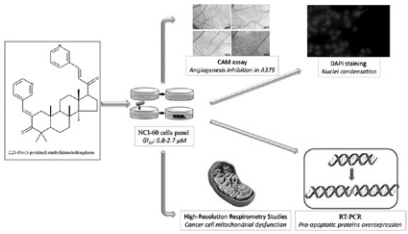
Josyelen L. Felipe, Tatiana B. Cassamale, Leticia D. Lourenço, Diego B. Carvalho, Amarith R. das Neves, Rita C.F. Duarte, Maria G. Carvalho, Monica C. Toffoli-Kadri and Adriano C.M. Baroni



105535

Hollongdione arylidene derivatives induce antiproliferative activity against melanoma and breast cancer through pro-apoptotic and antiangiogenic mechanisms

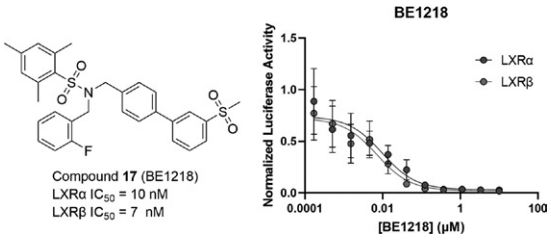
Irina Smirnova, George Drăghici, Oxana Kazakova, Lavinia Vlaia, Stefana Avram, Alexandra Mioc, Marius Mioc, Ioana Macaşoi, Cristina Dehelean, Adrian Voicu and Codruţa Şoica



105540

Synthesis and structure activity relationship of the first class of LXR inverse agonists

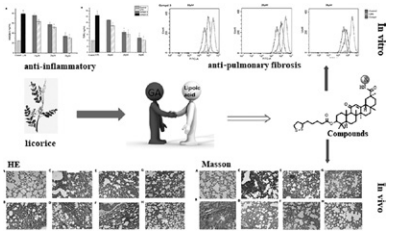
Bahaa Elgendy, Kristine Griffett, Lamees Hegazy, Paolo Di Fruscia, Kirby Sample, Emmalie Schoepke, Theodore M. Kamenecka and Thomas P. Burris



105542

Synthesis and anti-inflammatory activities of glycyrrhetinic acid derivatives containing disulfide bond

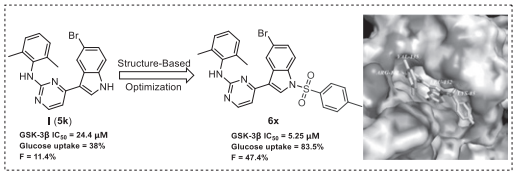
Qiuping Zhang, Yanni Wang, Zongyuan Wang, Eyad Abdulwhab Hamoud Mohammed, Quanyi Zhao, Dian He and Zhen Wang



105537

Structure-Based design of Marine-derived Meridianin C derivatives as glycogen synthase kinase 3β inhibitors with improved oral bioavailability: From aminopyrimidyl-indoles to the sulfonyl analogues

Shuwen Han, Wei Zhou, Chunlin Zhuang and Fener Chen



105541

Discovery of pyrido[3,4-*b*]indol-1-one derivatives as novel non-covalent Bruton's tyrosine kinase (BTK) inhibitors

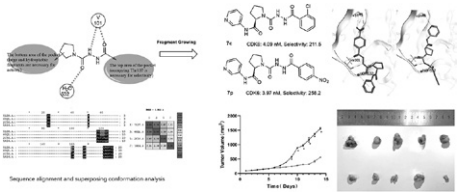
Dou Dou, Wenjie Sha, Yanyan Diao, Rongrong Su, Yunjin Qiao, Zhixiao Yu, Zhenjiang Zhao, Honglin Li, Zhuo Chen and Yufang Xu



105547

Synthesis and identification of a novel skeleton of *N*-(pyridin-3-yl) proline as a selective CDK4/6 inhibitor with anti-breast cancer activities

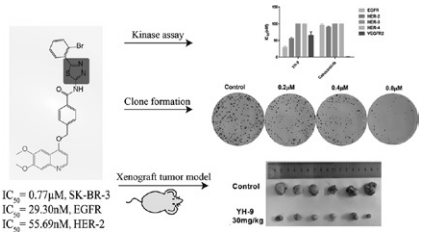
Jing-wei Liang, Wan-qiu Li, Qing-yang Nian, Si-hua Xie, Lulu Yang and Fan-hao Meng



105469

Discovery of *N*-(1,3,4-thiadiazol-2-yl)benzamide derivatives containing a 6,7-methoxyquinoline structure as novel EGFR/HER-2 dual-target inhibitors against cancer growth and angiogenesis

Xin-yang Li, De-pu Wang, Shuai Li, Wen-han Xue, Xin-hua Qian, Kai-li Liu, Yu-heng Li, Qi-qi Lin, Gang Dong, Fan-hao Meng and Ling-yan Jian

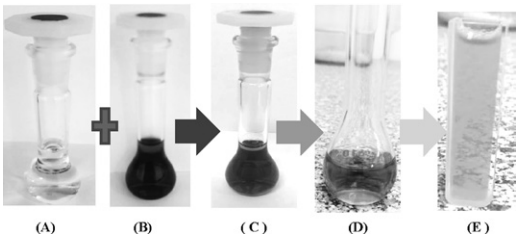


105553

Novel synthesis of antibacterial pyrone derivatives using kinetics and mechanism of oxidation of azithromycin by alkaline permanganate

Samia M. Ibrahim, Nora Saad, Mahmoud M. Ahmed and Mohamed Abd El–Aal

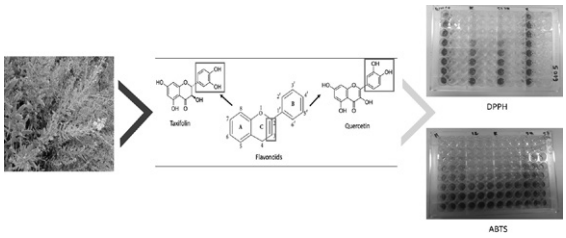
The color degradation of $KMnO_4$ during the oxidation process: Oxidation states: (A) AZ in 0.01 moldm^{-3} NaOH; (B) MnO_4^- in 0.01 moldm^{-3} NaOH; (C) Violet Mn (VII) ion; (D) Green Mn(VI) ion; (E) Yellow Mn (IV) in the oxidation of AZ by alkaline permanganate.



105551

Isolation, identification, and activity evaluation of antioxidant components from *Inula viscosa:* A bioguided approach

Ikrame Zeouk, Ines Sifaoui, Amel Ben Jalloul, Khadija Bekhti, Isabel L. Bazzocchi, José E. Piñero, Ignacio A. Jiménez and Jacob Lorenzo-Morales

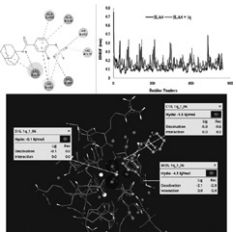


105545

Discovery of urease inhibitory effect of sulfamate derivatives: Biological and computational studies

Sumera Zaib, Muhammad Tayyab Younas, Seyed-Omar Zaraei, Imtiaz Khan, Hanan S. Anbar and Mohammed I. El-Gamal

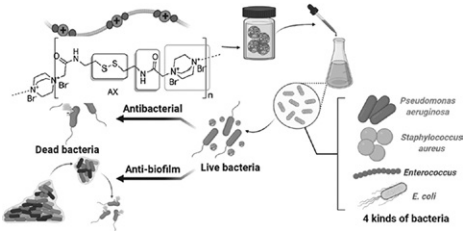
Figure representing the 2D interactions, RMSF and visual/ investigative modes of the docked pose of compound **1q** within the active site of urease.



105550

Antibacterial, antibiofilm, anti-inflammatory, and wound healing effects of nanoscale multifunctional cationic alternating copolymers

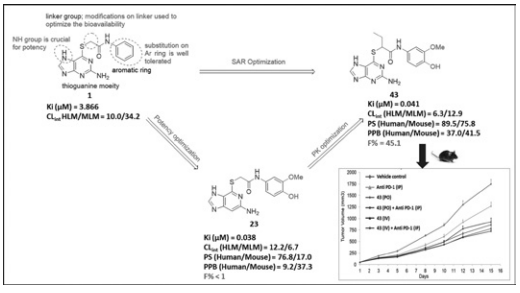
Seyyed Emad Hooshmand, Arefeh Ebadati, Elaheh Sadat Hosseini, Amir Hossein Vahabi, Mojgan Oshaghi, Reza Rahighi, Yasin Orooji, Mirza Ali Mofazzal Jahromi, Rajender S. Varma, Michael R. Hamblin and Mahdi Karimi



105549

Design, synthesis and biological evaluation studies of novel small molecule ENPP1 inhibitors for cancer immunotherapy

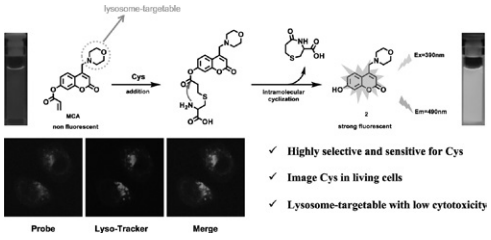
Mukesh Gangar, Sandeep Goyal, Digambar Raykar, Princy Khurana, Ashwita M. Martis, Avijit Goswami, Ishani Ghoshal, Ketul V. Patel, Yadav Nagare, Santosh Raikar, Apurba Mukherjee, Rajath Cyriac, Jean-François Paquin and Aditya Kulkarni



105558

A coumarin-based fluorescent probe for specific detection of cysteine in the lysosome of living cells

Guowei Lu, Jianning Dong, Congbin Fan, Yayi Tu and Shouzhi Pu

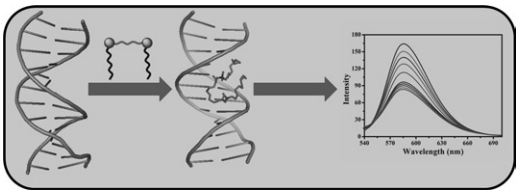


105555

Exploring the binding mode of ester-based cationic gemini surfactants with calf thymus DNA: A detailed physicochemical, spectroscopic and theoretical study

Mohd Akram, Hira Lal and Kabir-ud-Din

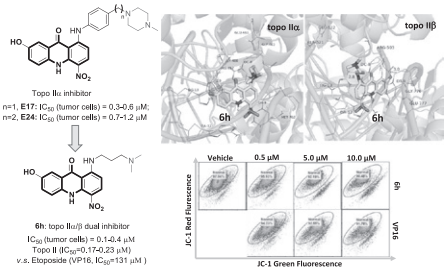
We describe herein the interaction of C_m-E2O-C_m gemini surfactants (m = 12, 14 and 16) with calf thymus deoxyribonucleic acid (ctDNA) by employing tensiomeric, different spectroscopic and computational studies. The obtained results suggested that the concerned gemini surfactants have been interacted with ctDNA *via* intercalation binding mode rather than groove binding.



105543

Structural optimizations and bioevaluation of *N*-substituted acridone derivatives as strong topoisomerase II inhibitors

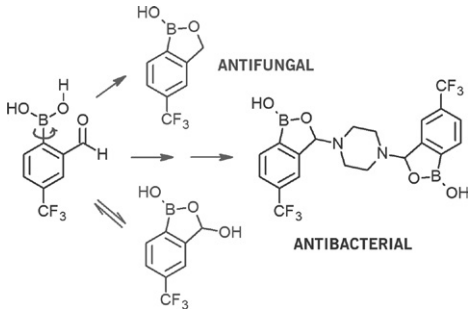
Zhi-Ying Li, Guang-Sen Xu, Yu-Liang Song and Xun Li



105560

Synthesis, structure, properties and antimicrobial activity of *para* trifluoromethyl phenylboronic derivatives

Agnieszka Adamczyk-Woźniak, Magdalena Tarkowska, Zofia Lazar, Ewa Kaczorowska, Izabela D. Madura, Anna Maria Dabrowska, Jacek Lipok and Dorota Wieczorek

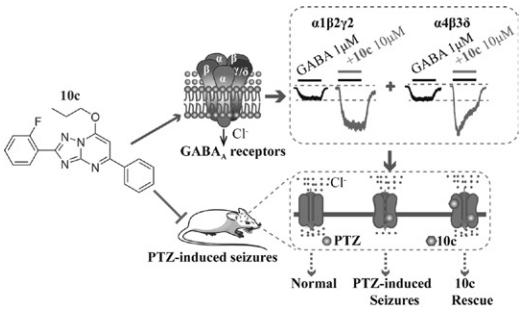


105565

Discovery of 7-alkyloxy- [1,2,4] triazolo[1,5-a] pyrimidine derivatives as selective positive modulators of $GABA_{A1}$ and $GABA_{A4}$ receptors with potent antiepileptic activity

Jun Wu, Zhipeng Hou, Yan Wang, Liping Chen, Chengxi Lian, Qingfei Meng, Chaoying Zhang, Xiufen Li, Longjiang Huang and Haibo Yu

In searching for better efficacy of anticonvulsants with clear action mechanism, a series of 7-alkoxy - [1,2,4] triazolo [1,5-a] pyrimidine derivatives were designed and synthesized. Among them, compound **10c** showed more pronounced anticonvulsant activities. Further mechanism study indicated that the anticonvulsant activity of compound **10c** mainly depended on its potentiating effect on $GABA_A$ receptors, especially $GABA_{A1}$ and $GABA_{A4}$.

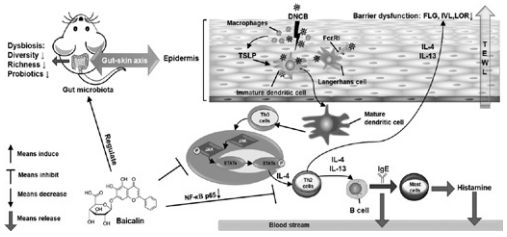


105538

Baicalin ameliorates 2,4-dinitrochlorobenzene-induced atopic dermatitis-like skin lesions in mice through modulating skin barrier function, gut microbiota and JAK/STAT pathway

Lan Wang, Yan-Fang Xian, Steven King Fan Loo, Siu Po Ip, Wen Yang, Wood Yee Chan, Zhi-Xiu Lin and Justin Che Yuen Wu

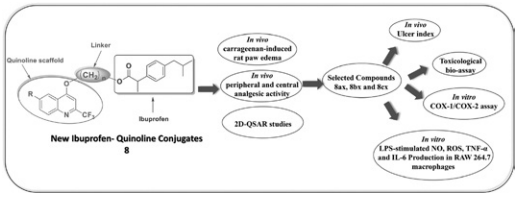
Baicalin significantly inhibited dorsal skin thickening as well as trans-epidermal water loss, and restricted the infiltration of mast cells and epidermal thickening in dorsal skin of mice. Additionally, baicalin obviously decreased the levels IgE, histamine, MCP-1 and TSLP in serum and level of IL-4 in the dorsal skin of DNCB-treated mice. Moreover, baicalin also markedly up-regulated the protein expression levels of FLG, IVL, and LOR, but inhibited the activation of NF-γB and JAK/STAT pathways in the dorsal skin of DNCB-treated mice. Furthermore, baicalin significantly restored the abundance of probiotics in the gut microbiota induced by DNCB in mice.



105557

Design and synthesis of ibuprofen-quinoline conjugates as potential anti-inflammatory and analgesic drug candidates

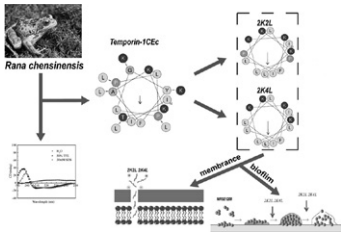
Amany M. Ghanim, Adel S. Girgis, Benson M. Kariuki, Nermin Samir, Mona F. Said, Anwar Abdelnaser, Soad Nasr, Mohamed S. Bekheit, Mohamed F. Abdelhameed, Ahmad J. Almalki, Tarek S. Ibrahim and Siva S. Panda



105544

Membrane mechanism of temporin-1CEc, an antimicrobial peptide isolated from the skin secretions of *Rana chensinensis*, and its systemic analogs

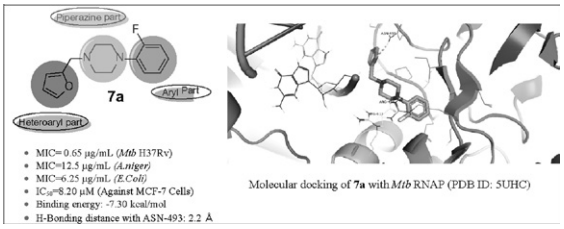
Fangyu Ji, Ying Zhao, Fengquan Jiang and Dejing Shang



105568

Design, synthesis, biological screening and molecular docking studies of novel multifunctional 1,4-di (aryl/heteroaryl) substituted piperazine derivatives as potential antitubercular and antimicrobial agents

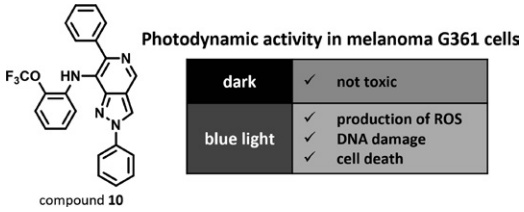
Bruktawit Mekonnen Sanka, Dereje Mamo Tadesse, Endale Teju Bedada, Ephriem T. Mengesha and Neelaiah Babu G.



105570

Synthesis of *N*-aryl-2,6-diphenyl-2*H*-pyrazolo[4,3-*c*]pyridin-7-amines and their photodynamic properties in the human skin melanoma cell line G361

Beatričė Razmienė, Veronika Voj\xC3\xA1čková, Eva Řezníčková, Lukáš Malina, Vaida Dambrauskienė, Martin Kubala, Robert Bajgar, Hana Kolářová, Asta Žukauskaitė, Eglė Arbačiauskienė, Algirdas Šačkus and Vladimír Kryštof

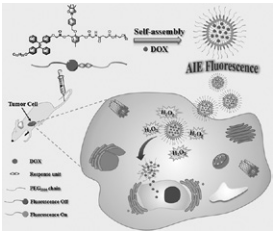


105559

H_2O_2-Responsive amphiphilic polymer with aggregation-induced emission (AIE) for DOX delivery and tumor therapy

Ya-Xuan Liang, Xue-Yi Sun, De-Zhong Xu, Jun-Ru Huang, Quan Tang, Zhong-Lin Lu and Rui Liu

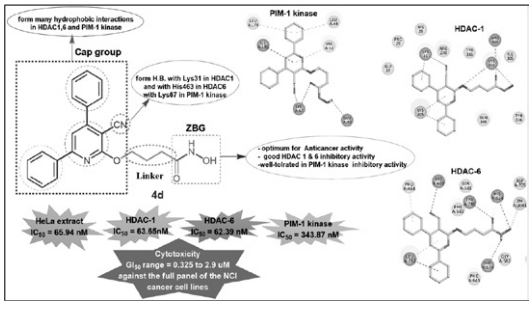
Schematic diagram of formation, transport and release DOX of **TBP**@DOX micelles.A TPE modified H_2O_2-responsive amphiphilic polymer, **TBP**, was designed and synthesized for the efficient loading, tracing and selectively triggered release of doxorubicin for tumor inhibition *in vitro* and *in vivo*.



105564

Utilization of cyanopyridine in design and synthesis of first-in-class anticancer dual acting PIM-1 kinase/HDAC inhibitors

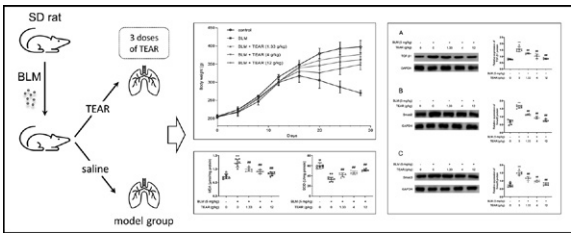
Amr K.A. Bass, El-Shimaa M. Nageeb, Mona S. El-Zoghbi, Mamdouh F.A. Mohamed, Mohamed Badr and Gamal El-Din A. Abuo-Rahma



105546

Total extract of Anemarrhenae Rhizoma attenuates bleomycin-induced pulmonary fibrosis in rats

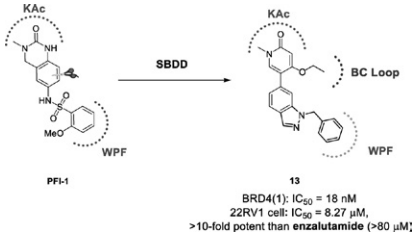
Xue-Bin Shen, Da-Li Ding, Li-Zhen Yu, Jin-Zhong Ni, Yao Liu, Wei Wang, Li-Min Liu and Si-Hui Nian



105575

Design, synthesis, and evaluation of novel pyridone derivatives as potent BRD4 inhibitors for the potential treatment of prostate cancer

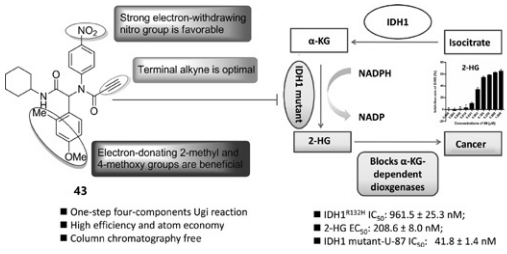
Wenhua Jiang, Xiaohui Wang, Chengxia Shu, Qiangqiang Hou, Kexin Yang and Xiaoxing Wu



105569

Discovery of linear unnatural peptides as potent mutant isocitrate dehydrogenase 1 inhibitors by Ugi reaction

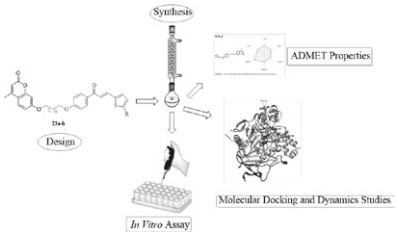
Xuechen Zhou, Mengzhu Zheng, Na Zhao, Yixin Hu, Kaiyin Yang, Junfeng Huo, Guangyuan Liu, Jiangeng Huang, Lixia Chen, Yirong Zhou and Hua Li



105572

Novel thiophene Chalcones-Coumarin as acetylcholinesterase inhibitors: Design, synthesis, biological evaluation, molecular docking, ADMET prediction and molecular dynamics simulation

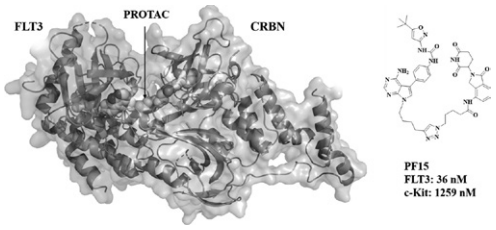
Aso Hameed Hasan, Sankaranarayanan Murugesan, Syazwani Itri Amran, Subhash Chander, Mohammed M. Alanazi, Taibi Ben Hadda, Sonam Shakya, Mohammad Rizki Fadhil Pratama, Basundhara Das, Subhrajit Biswas and Joazaizulfazli Jamalis



105508

Degrading FLT3-ITD protein by proteolysis targeting chimera (PROTAC)

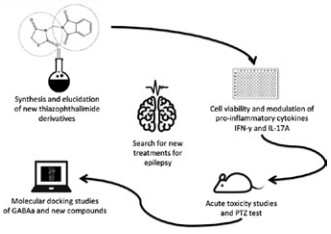
Yong Chen, Xue Yuan, Minghai Tang, Mingsong Shi, Tao Yang, Kongjun Liu, Dexin Deng and Lijuan Chen



105548

Synthesis of novel thiazolidinic-phthalimide derivatives evaluated as new multi-target antiepileptic agents

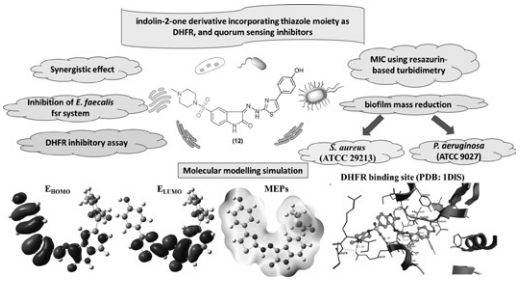
Maria Cecilia V.A. de Oliveira, Douglas C.F. Viana, Anderson A. Silva, Michelly C. Pereira, Filipe S. Duarte, Maira G.R. Pitta, Ivan R. Pitta and Marina G.R. Pitta



105571

Development of novel indolin-2-one derivative incorporating thiazole moiety as DHFR and quorum sensing inhibitors: Synthesis, antimicrobial, and antibiofilm activities with molecular modelling study

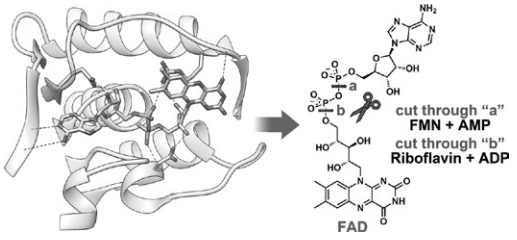
Abdullah Y. Alzahrani, Yousry A. Ammar, Mohammed Abu-Elghait, Mohamed A. Salem, Mohammed A. Assiri, Tarik E. Ali and Ahmed Ragab



105561

The role of remote flavin adenine dinucleotide pieces in the oxidative decarboxylation catalyzed by salicylate hydroxylase

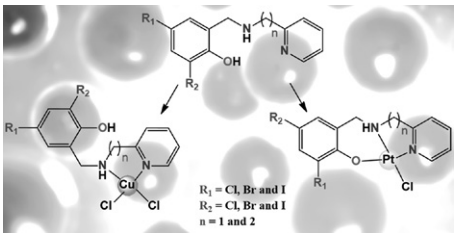
Mozart S. Pereira, Simara S. de Araújo, Ronaldo A.P. Nagem, John P. Richard and Tiago A.S. Brandão



105556

Platinum(II) and Copper(II) complexes of asymmetric halogen-substituted [NN′O] ligands: Synthesis, characterization, structural investigations and antiproliferative activity

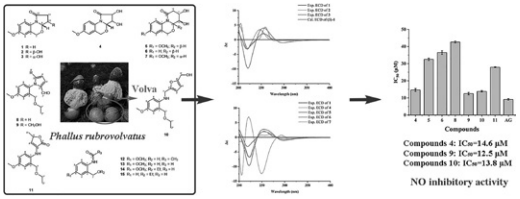
Hadi Amiri Rudbari, Arezoo Saadati, Mahnaz Aryaeifar, Olivier Blacque, Jose V. Cuevas-Vicario, Rui Cabral, Luis R. Raposo and Alexandra R. Fernandes



105577

New aniline derivatives from the volva of *Phallus rubrovolvatus* and their anti-inflammatory activity

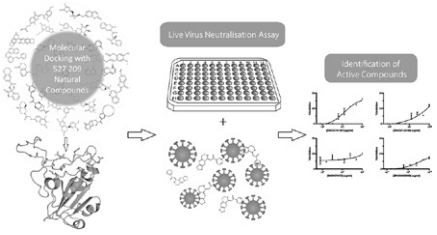
Jianhua Lv, Lan Yao, Shiyu Li, Jing Dong, Mingyu Ye, Dongyu Fan, Changtian Li, Fenghua Tian and Yu Li



105574

Virtual screening and *in vitro* validation of natural compound inhibitors against SARS-CoV-2 spike protein

Helen Power, Jiadai Wu, Stuart Turville, Anupriya Aggarwal, Peter Valtchev, Aaron Schindeler and Fariba Dehghani

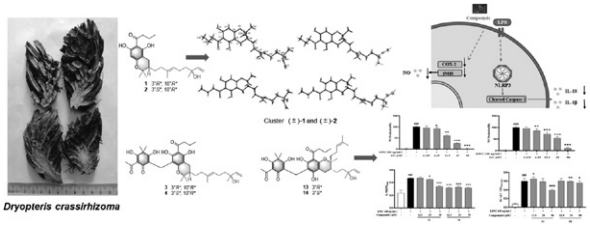


105567

Structure elucidation, biogenesis, and bioactivities of acylphloroglucinol-derived meroterpenoid enantiomers from *Dryopteris crassirhizoma*

Ping Hai, Kairui Rao, Na Jiang, Dan Liu, Ruirui Wang, Yuan Gao, Xiaocong Liu, Sihao Deng, Yu Zhou, Xuanqin Chen, Xiaonian Li and Rongtao Li

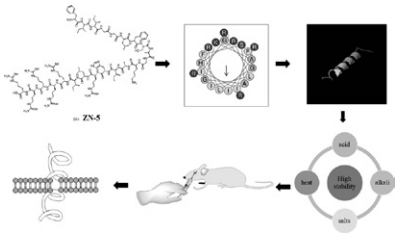
Eighteen novel acylphloroglucinol meroterpenoid enantiomers were isolated from the rhizomes of *Dryopteris crassirhizoma*. Anti-inflammatory, antiviral, and antifungal activities were assessed. The anti-inflammatory mechanism of compounds **13** and **14** were investigated.



105583

Rational design and synthesis of Oreoch-2 analogues as efficient broad-spectrum antimicrobial peptides

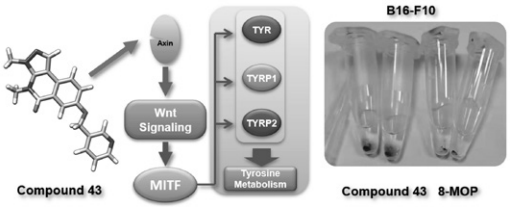
Na Zhang, Xiaotong Gu, Di Song, Panpan Zhang, Nan Zhang, Weijin Chen, Shengli Ji, Yunkun Qi and Shutao Ma



105582

Design, synthesis and structure-activity relationship optimization of phenanthridine derivatives as new anti-vitiligo compounds

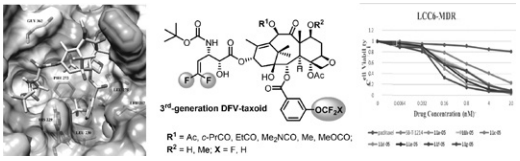
Bi-juan Yang, Shi-rui Fan, Xin-fang Zhang, Jie-yun Cai, Ting Ruan, Zheng-rui Xiang, Juan Ren, Xiao-jiang Hao and Duo-zhi Chen



105578

Design, synthesis and SAR study of Fluorine-containing 3rd-generation taxoids

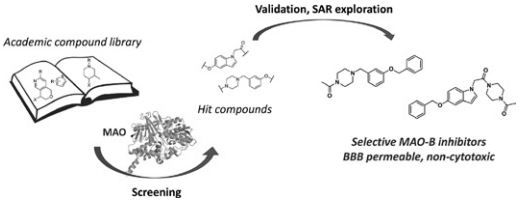
Changwei Wang, Lei Chen, Yi Sun, Wanrong Guo, Adam K. Taouil and Iwao Ojima



105581

Indoles and 1-(3-(benzyloxy)benzyl)piperazines: Reversible and selective monoamine oxidase B inhibitors identified by screening an *in-house* compound library

Damijan Knez, Martina Hrast, Rok Frlan, Anja Pišlar, Simon Žakelj, Janko Kos and Stanislav Gobec

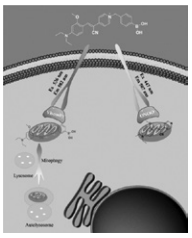


105484

A bifunctional fluorescence probe for dual-channel detecting of mitochondrial viscosity and endogenous/exogenous peroxynitrite

Minglu Li, Yue Huang, Shengmei Song, Shaomin Shuang and Chuan Dong

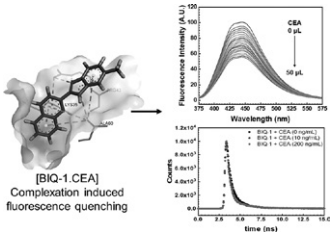
We designed and synthesized a novel fluorescence probe (**PV**) for dual-detecting viscosity and $ONOO^-$, which was capable of detecting of mitochondrial viscosity fluctuations during LPS and starvation-induced mitophagy.



105490

An abiotic fluorescent probe for the detection and quantification of carcinoembryonic antigen

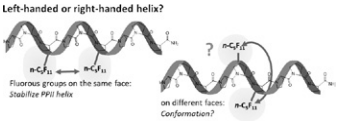
Jung-Seop Lee, In-ho Song, Shrikant Dashrath Warkad, Gyu Seong Yeom and Satish Balasaheb Nimse



105491

Design and synthesis of fluorinated peptides for analysis of fluorous effects on the interconversion of polyproline helices

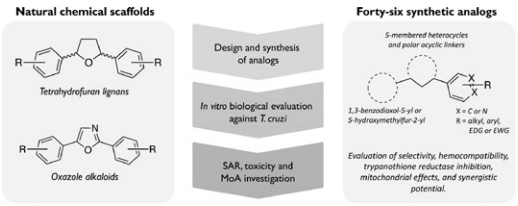
Meng-Che Li, Ying-Jie Liu, Kuang-Cheng Hsu, Tse-Hsueh Lin, Chih-Wei Lin, Jia-Cherng Horng and Sheng-Kai Wang



105492

Natural-product-inspired design and synthesis of two series of compounds active against *Trypanosoma cruzi:* Insights into structure–activity relationship, toxicity, and mechanism of action

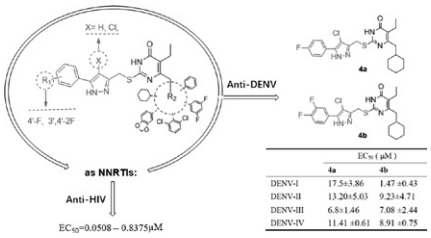
Rafael da Rosa, Bibiana Paula Dambrós, Milene Höehr de Moraes, Lucie Grand, Maïwenn Jacolot, Florence Popowycz, Mario Steindel, Eloir Paulo Schenkel and Lílian Sibelle Campos Bernardes



105494

C6-structural optimizations of 2-aryl-1*H*-pyrazole-*S*-DABOs: From anti-HIV to anti-DENV activity

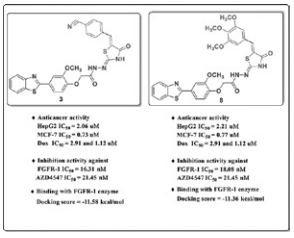
Ruo-Mei Rui, Cheng-Run Tang, Chun-Tao Zhang, Wen-Kai Pan, Kai Gan, Rong-Hua Luo, Zi-Qian Wei, Fan-Shun Jing, Si-Ming Huang, Liu-Meng Yang, Yi-Ming Li, Yue-Ping Wang, Wei-Lie Xiao, Hong-Bing Zhang, Yong-Tang Zheng and Yan-Ping He



105504

Synthesis, anticancer evaluation and molecular docking of new benzothiazole scaffolds targeting FGFR-1

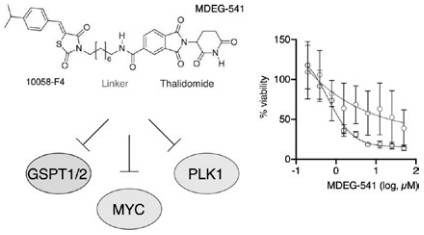
Eman A. Abd El-Meguid, Eman M. Mohi El-Deen, Gaber O. Moustafa, Hanem M. Awad and Eman S. Nossier



105505

A novel Cereblon E3 ligase modulator with antitumor activity in gastrointestinal cancer

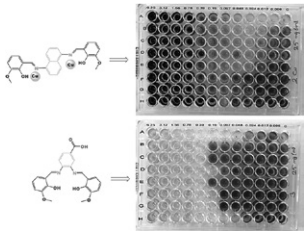
Svenja Lier, Andreas Sellmer, Felix Orben, Stephanie Heinzlmeir, Lukas Krauß, Christian Schneeweis, Zonera Hassan, Carolin Schneider, Arlett Patricia Gloria Schäfer, Herwig Pongratz, Thomas Engleitner, Rupert Öllinger, Anna Kuisl, Florian Bassermann, Christoph Schlag, Bo Kong, Stefan Dove, Bernhard Kuster, Roland Rad, Maximilian Reichert, Matthias Wirth, Dieter Saur, Siavosh Mahboobi and Günter Schneider



105507

Ortho-hydroxy bioactive schiff base compounds: Design, comprehensive characterization, photophysical properties and elucidation of antimicrobial and mutagenic potentials

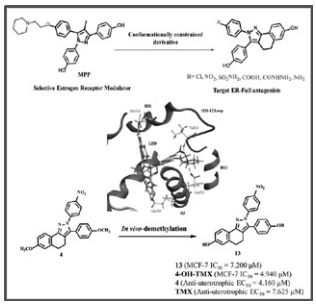
Israa Nıbras Qader Qader, İhsan Obalı, Halil İsmet Uçan, Ahmet Uysal, Aslıhan Yılmaz Obalı and Mustafa Kul



105554

Structure-based design and synthesis of conformationally constrained derivatives of methyl-piperidinopyrazole (MPP) with estrogen receptor (ER) antagonist activity

Mahmoud A. Ragab, Mohamed Elagawany, Hoda Daabees, Al-Shaimaa F. Ahmed, Eman M. Awad, Cyrielle Billon, Bahaa Elgendy, Khaled A.M. Abouzid and Shaymaa E. Kassab

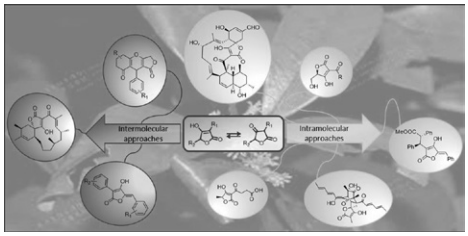


REVIEW ARTICLES

105552

Recent advances in the synthesis of naturally occurring tetronic acids

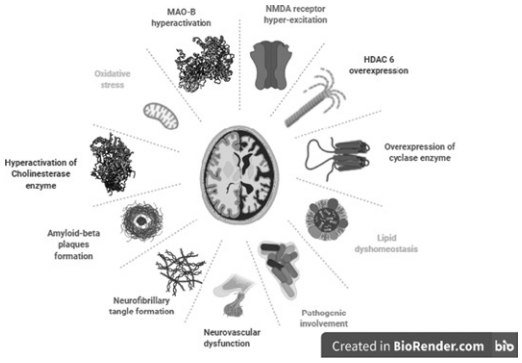
Salvatore Princiotto, Lalith Jayasinghe and Sabrina Dallavalle



105562

The molecular mechanism, targets, and novel molecules in the treatment of Alzheimer's disease

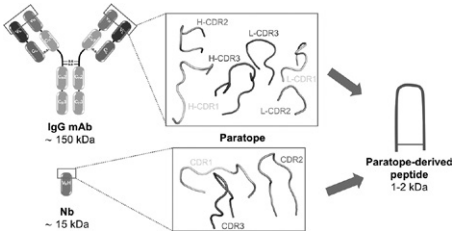
Akash Verma, Digambar Kumar Waiker, Bhagwati Bhardwaj, Poorvi Saraf and Sushant K. Shrivastava



105563

Downsizing antibodies: Towards complementarity-determining region (CDR)-based peptide mimetics

Kevin Van holsbeeck, José C. Martins and Steven Ballet



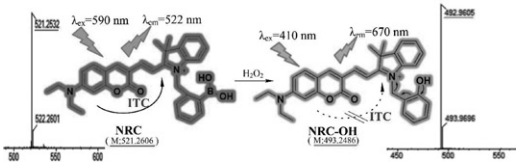
PRELIMINARY COMMUNICATIONS

105513

A near-infrared, colorimetric and ratiometric fluorescent sensor with high sensitivity to hydrogen peroxide and viscosity for solutions detection and imaging living cells

Daili Liu, Gaofei Chen and Guiqian Fang

Proposed sensing mechanism of **NCR** with H_2O_2.

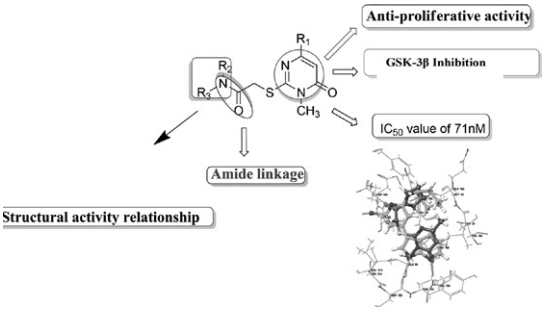


105512

Design, synthesis, *in vitro* antiproliferative evaluation and GSK-3β kinase inhibition of a new series of pyrimidin-4-one based amide conjugates

Imran Khan, Mushtaq A. Tantray, Hinna Hamid, Mohammad Sarwar Alam, Kalicharan Sharma and Prashant Kesharwani

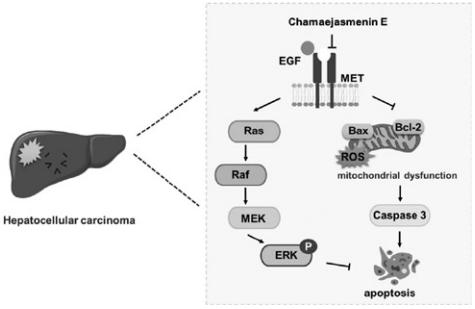
ADMET predictions indicate good drug like properties.Compound *4i* could serve as a potential hit candidate.Further structural optimization might give novel anticancer therapeutics.



105509

Chamaejasmenin E from *Stellera chamaejasme* induces apoptosis of hepatocellular carcinoma cells by targeting c-Met *in vitro* and *in vivo*

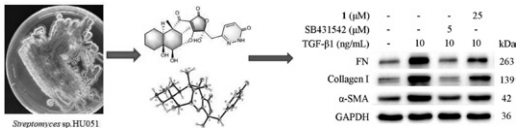
Xiao-Qi Yu, Qiu-Lin Yan, Shuai Shen, Zhuo-Yang Cheng, Xiao-Xiao Huang, Guo-Dong Yao and Shao-Jiang Song



105573

Tetrodecadazinone, a novel tetrodecamycin-pyridazinone hybrid with anti-liver fibrosis activity from *Streptomyces* sp. HU051

Ruo-Xi Liu, Shi-Fan Ma, Yi-Li Chen, Lie-Feng Ma, Ji-Dong Wang and Zha-Jun Zhan



105584

Corrigendum to "Daphnegiravone D from *Daphne giraldii* induces cell death by targeting ATR in Hep3B cells" [Bioorg. Chem. 110 (2021) 104802]

Xin-Yue Shang, Xiao-Qi Yu, Guo-Dong Yao and Shao-Jiang Song

Bioorganic Chemistry 119 (2022) 105515

Contents lists available at ScienceDirect

Bioorganic Chemistry

journal homepage: www.elsevier.com/locate/bioorg

Design and synthesis of epigallocatechin (EGC) analogs selective to inhibit α-amylase over α-glucosidases *via* the incorporation of caffeine acid and its derivatives

Wenming Chen [a,1], Cui Zhou [b,c,1], Jiansheng Chen [d], Meizhu Wang [c], Fang Zhou [a], Chunmei Wang [b,e,*], Xu Zhang [d,*], Wen Zhou [b,e,*]

[a] Department of Pharmaceutical Production Center & TCM and Ethnomedicine Development International Laboratory, The First Hospital of Hunan University of Chinese Medicine, 95, Shaoshan Rd, Changsha, Hunan 410007, China
[b] Shanghai Veterinary Research Institute, Chinese Academy of Agricultural Sciences, 200241 Shanghai, China
[c] School of Pharmaceutical Sciences, Guangzhou University of Chinese Medicine, University Town, Waihuan Rd., Panyu, Guangzhou 510006, China
[d] College of Forestry and Landscape Architecture, South China Agricultural University, 510642, China
[e] Key Laboratory of Veterinary Chemical Drugs and Pharmaceutics, Ministry of Agriculture and Rural, Affairs, Shanghai Veterinary Research Institute, Chinese Academy of Agricultural Sciences, Shanghai 200241, China

ARTICLE INFO

Keywords:
HPA inhibitors
EGC
Selectivity
Caffeic acid
Antidiabetic drug

ABSTRACT

Natural products are a promising and underappreciated reservoir for the preferred chemical scaffolds in the search of antidiabetic drugs. In this study twenty-one EGC-based derivatives selective to inhibit human pancreatic α-amylase (HPA), the enzyme at the top of the starch digestion pyramid, have been designed and synthesized in terms of the lead myricetin-caffeic acid conjugate **1** reported ever. We focus on methylation of caffeic acid, length of a liker, a double bond contained in the linker on the inhibition activity and selectivity of EGC-based conjugates. As a result, methylation of caffeic acid and the length of a linker affect significantly the activity and selectivity of EGC-based conjugates, but the effect of a double in caffeic acid is limited. Conjugate **2a-1** having a six-carbon-atom linker fused to EGC and caffeic acid demonstrates the most ponent inhibitory activity to HPA and its selectivity towards HPA over α-glucosidase by far superior to that construct **1**. Molecular docking studies reveal that conjugate **2a-1** accommodates well to the active site of HPA with four hydrogen bonds in the form of the preorganization of two moieties EGC and caffeic acid *via* π-stacking interaction. Collectively, conjugating caffeic acid and EGC with an appropriate linker possibly provides a new strategy for finding the specific HPA inhibitors in the discovery of anti-diabetes mellitus drugs.

1. Introduction

Diabetes mellitus (DM) ranks as the third most prevalent disease characterized by hyperglycemia [1]. By 2035, estimated 592 million individuals worldwide will be tormented by DM [2]. Normalization of blood glucose prevents hyperglycemia and its resultant complications development. Glycemic control in the treatment of DM, however, is toughly achieved by the currently antihyperglycemic agents, including insulins, sulphonylureas, biguanides, thiazolidinediones, α-glucosidase inhibitors, glucagon-like peptide-1 agonists, and dipeptidyl peptidase-IV inhibitors, even with a combination of multiple agents with different action mechanisms [3,4]. Off-target of antidiabetic drugs leading to unexpected adverse effects including diarrhoea, nausea, and weight gain, compromises the clinical applications [5,6]. So it is still urgent that the persistent efforts to develop potentially antidiabetic agents with novel mechanisms and no side effects.

Controlling postprandial hyperglycemia is a promising therapeutic solution to DM [7]. An increasing postprandial blood glucose largely comes from starch degradation under the combined action of enzymes human pancreatic α-amylase (HPA) and α-glucosidase in the small intestine [8]. Principal cleavage of starch by HPA affords linear or branched malto-oligosaccharides followed by further degradation into glucose with α-glucosidase [9]. The inhibition of HPA or α-glucosidase that digests starch and malto-oligosaccharides is an attractive strategy

* Corresponding authors at: Shanghai Veterinary Research Institute, Chinese Academy of Agricultural Sciences, 200241 Shanghai, China (C. Wang and W. Zhou).
E-mail addresses: wangchunmei@shvri.ac.cn (C. Wang), zhangxu@126.com (X. Zhang), zhouwen60@126.com (W. Zhou).
[1] Contributed equally to this work.

https://doi.org/10.1016/j.bioorg.2021.105515
Received 25 October 2021; Received in revised form 16 November 2021; Accepted 21 November 2021
Available online 5 December 2021
0045-2068/© 2021 Elsevier Inc. All rights reserved.

for preventing hyperglycosemia. Clinically, α-glucosidase inhibitors acarbose, miglitol and voglibose exhibit obvious poor patient compliances due to deleterious gastrointestinal side effects from the fermentation of malto-oligosaccharides that originates from the starch degraded by HPA [10]. Theoretically, HPA responsible for catalyzing the initial step in the hydrolysis of starch into shorter oligosaccharides is a more promising target over α-glucosidase. Selectively inhibiting HPA activity to block the formation of oligosaccharides may be of considerable medical relevance in the treatment of DM.

Natural products (NPs) have become the important resources of bioactive agents in the discovery of anti-DM drugs [2]. In a screening campaign for potential HPA inhibitors, many flavonols display a considerably weak affinity and poor specificity to HPA [11–13], but flavonol glycoside montbretin A (mbA) being a $K_i = 8$ nM against HPA raises our concern [14]. Enzymatically controlled degradation and activity assays of mbA unfold that the core structure responsible for high-affinity includes two moieties myricetin (Fig. 1) and caffeic acid [15]. In the mbA-HPA binding complex, internal π-stacking interactions of myricetin and caffeic acid favor the formation of the optimal hydrogen bonds, and weak interactions of HPA and the linker disaccharide of mbA hint the feasibility of a non-sugar linker instead of a noninteracting liker disaccharide [16]. A simplified inhibitor (Figs. 1, 1) in which two moieties myricetin and caffeic acid are tethered *via* a simple alkyl chain nicely validates this observation [15]. More importantly, such structure simplifications and replacements open up the possibilities and directions for synthetically tractable analogs able to inhibit HPA activity with high efficacies and low side effects.

From the mbA-HPA cocrystal complex reported, we dissect the binding mode of the myricetin fragment and the active site of HPA [15]. No interaction of any residues is observed with all the atoms on C ring of myricetin except O_1, emphasizing that a carbonyl group and a double bond are non-essential groups. The replacement of a carbonyl group and a double bond in ring C with a methylene and a single bond, respectively, may not only have no influence on HPA activity, but also extend a structural scope from flavonols to flavanols. To date, no experimental evidence is provided to testify the feasibility of structural modifications. Naturally occurring (-) epigallocatechin (EGC) is similar to myricetin except for lack of a carbonyl group and a double bond (Fig. 1), affording a representative structure for the above exploration. As we known, EGC mainly exists in the form of (-) epigallocatechin gallate (EGCG) that is a potent antidiabetic agent mainly through the inhibition of α-glucosidase [17–22]. Recently, molecular simulation technology and experimental data demonstrate EGCG could bind to and inhibit HPA, highlighting the structure basis for recognizing to HPA [23,24]. Moreover, this kind of the complex structures in which EGC takes place of myricetin possibly continue to keep limiting their uptake from the gut, contributing to them being stayed in the correct locale for HPA inhibition.

In search of EGC-caffeic acid conjugates selective towards HPA over α-glucosidase, various linkers with the appropriate and constrained geometry, and different caffeic acid derivatives will be explored. In the present study, taking the reported simplified analog **1** as a template compound, caffeic acid derivatives and an EGC scaffold are joined with a varying alkyl linker to afford target derivatives (Fig. 2). The replacement of one of its hydroxyl groups with a methoxyl group on caffeic acid scaffold leads to a sharp decrease in the binding of HPA,[14] so three substitution modes are used to investigate the influence of a hydroxyl group of caffeic acid on HPA activity. The role of a double bond contained in caffeic acid derivatives **3a-b** in the inhibition of HPA is to be validated using reduction manipulation. Meantime, the importance of a linker is to be investigated by compounds **4a-d** where EGC is directly coupled to different substituted caffeic acid derivatives. Selectivity toward HPA over α-glucosidase of all the newly synthesized EGC-based conjugates are assessed, and accordingly the corresponding structure-activity relationships are summarized, for purpose of establishing a promising strategy for finding the specific HPA inhibitors to treat DM.

2. Results and discussion

2.1. Chemistry

The synthetic routes of all the EGC-caffeic acid conjugates were demonstrated in Scheme 1. Coupling of caffeic acid derivatives (**5a-d**) and prop-2-yn-1-amine yielded alkynes (**6a-d**) in high yields. EGC scaffold was prepared from commercially available EGCG (**7**) in the presence of potassium carbonate. After systematic comparison of numerous protection groups for ester **7**, chloromethyl ether (MOMCl) was selected to synthesize target compounds **2a-1**, **2a-2**, **2a-3**, **2a-4**, **2b-1**, **2b-2**, **2b-3**, **2b-4** and **2c,** leaving a double bond intact upon removal of the protection groups. From the ^{1}H NMR spectrum analysis, all the hydroxyl groups of ester **7** were etherified by methoxymethyl groups to afford protected **8** due to 16 protons appearing at peaks 5.24–5.02. Protected **9** with an EGC scaffold was achieved by hydrolysis of

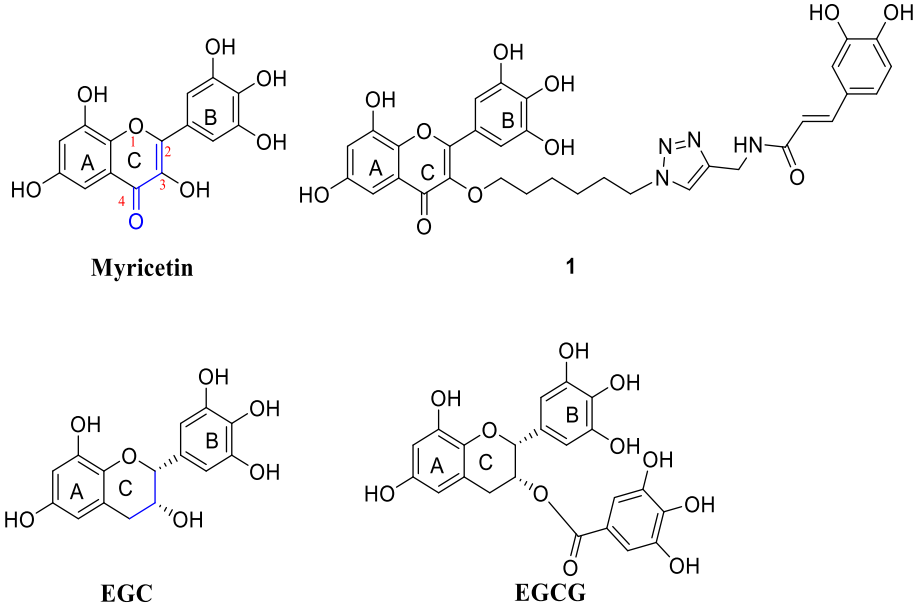


Fig. 1. Structures of myricetin, inhibitor **1**, EGC and EGCG.

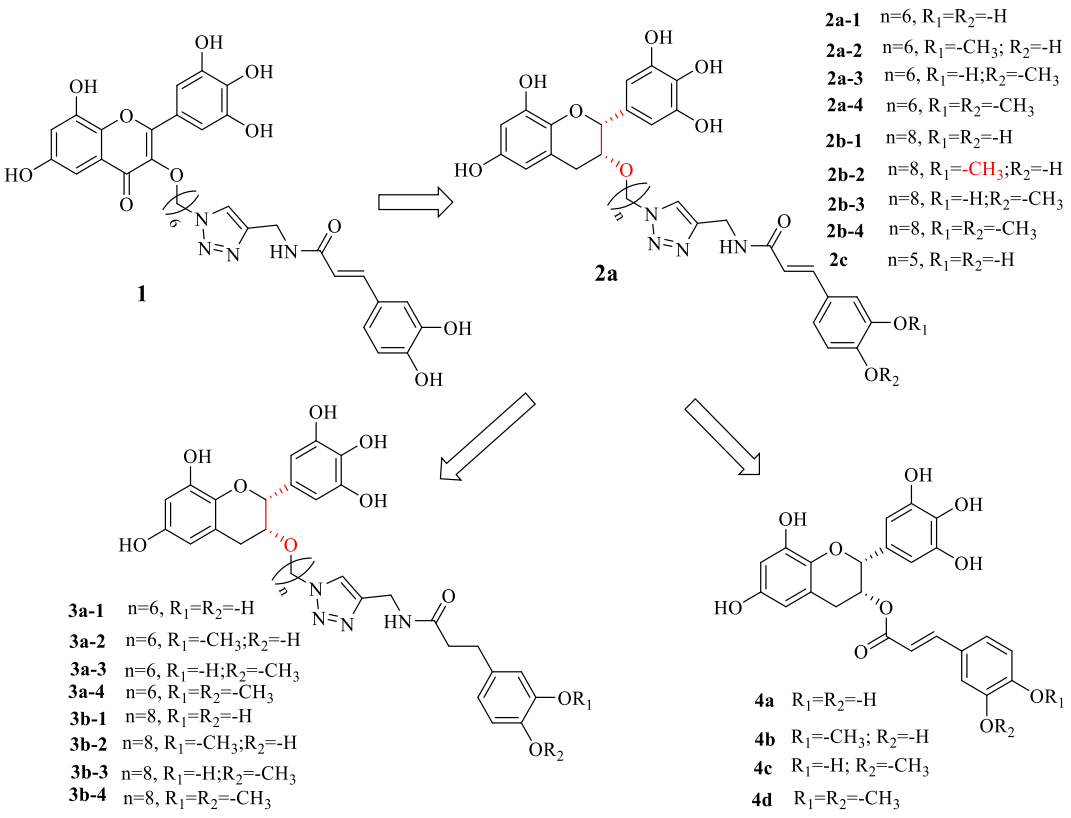
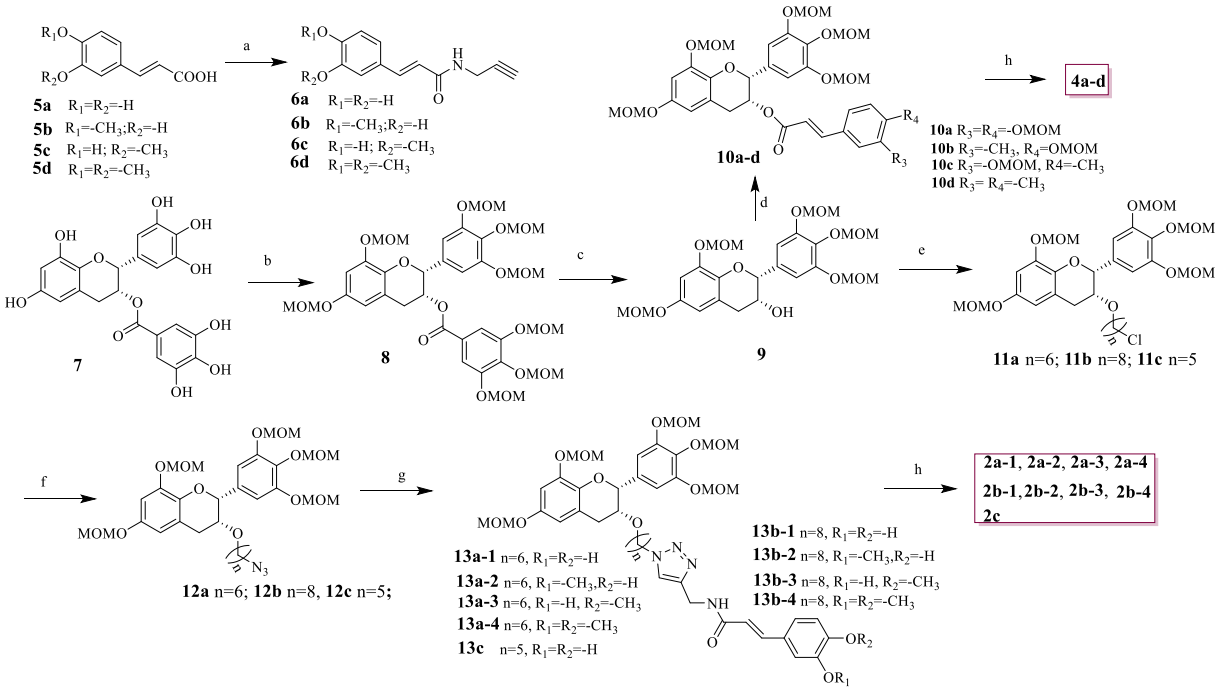


Fig.2. Design of EGC-derived conjugates.



Scheme 1. The synthesis of EGC-caffeic acid derivatives (**2a-1, 2a-2, 2a-3, 2a-4, 2b-1, 2b-2, 2b-3, 2b-4** and **2c**). Condition and reagents: a) prop-2-yn-1 amine, HOBT, EDCI; b) NaH, CH_3OCH_2Cl, r.t.; c) K_2CO_3, dimethoxy- methane/methanol (V/V = 1/1); d) EDCI, DAMP, unseparated methoxy-methylated **5a-c** or **5d**; e) NaH, anhydrous DMF, 1-bromo-6-chlorohexane for **11a**, 1-bromo-8-chlorooctane for **11b**, 1-bromo-5-chloropentane for **11c**; f) sodium azide, anhydrous DMF, 60 ℃; g) copper (II) sulfate pentahydrate, sodium ascorbate, *t*-BuOH/CH_3CN/ H_2O = 2/1/1(V/V/V), **6a-d**; h) 12 M HCl, DCM/CH_3OH = 4/1 (V/V).

construct **8** in an 85% yield. In the presence of 3- (ethyl-iminomethylideneamino)-*N*, *N*-dimethylpropan-1-amine, hydrochloride (EDCI) and dimethylaminopyridine (DMAP), direct esterification of compound **9** with unseparated methoxymethylated **5a-c** [25] or compound **5d** followed by deprotection of **10a-d** with 12 M HCl afforded target compounds **4a-d** in acceptable yields, respectively.

Next, 1-bromo-6-chlorohexane, 1-bromo-8-chlorooctane or 1-bromo-5-chloropentane was linked to a pendent hydroxyl group of construct **9**. Substitution of unseparated **11a-c** with excessive sodium azide afforded the corresponding constructs **12a-c** in high yields. With alkynes **6a-d** and azides **12a-b** in hand, click reaction system was adopted that included copper (II) sulfate pentahydrate and sodium ascorbate dissolved in *t*-BuOH and CH_3CN and H_2O (V/V/V = 2/1/1) [27]. As expected, 1,4-*trans*-trizoles (**13a-1**, **13a-2**, **13a-3**, **13a-4**, **13b-1**, **13b-2**, **13b-3** and **13b-4**) were smoothly produced in more than 74% yields. Removal of all the methoxymethyl groups from the above 1,4-*trans* trizoles with 12 M HCl provided target EGC-caffeic acid conjugates (**2a-1**, **2a-2**, **2a-3**, **2a-4**, **2b-1**, **2b-2**, **2b-3** and **2b-4**) in 37%-46% yields, respectively (Scheme 1). Analogously, compound **2c** was prepared by the click reaction of alkyne **6a** and azide **12c** followed by deprotection of construct **13c** with 12 M HCl.

To further evaluate the influence of a double bond of caffeic acid, we synthesized a series of EGC-phenylpropionic acid conjugates (**3a-1**, **3a-2**, **3a-3**, **3a-4**, **3b-1**, **3b-2**, **3b-3** and **3b-4**). As demonstrated in Scheme 2, different from a protecting group of the EGC-caffeic acid analogues (Scheme 1), benzyl bromide was selected to cap the hydroxyls of EGCG **7** for the following simultaneous deprotection and double bond reduction. The ^{1}H NMR spectra analysis revealed benzylation of all the hydroxyl groups of ester **7** due to 16 protons found at peaks 4.5–4.9. Compound **15** carrying a pendent hydroxyl group was observed after careful hydrolysis, accompanying with release of a gallate. Like constructs **11a-b**, 1-bromo-6-chlorohexane and 1-bromo-8 chlorooctane were introduced to **15**, providing the corresponding ethers **16a-b**. Substitution of **16a-b** with excessive sodium azide afforded compounds **17a-b** at 60 ℃, which further reacted with alkynes **6a-d** in the click reaction system [26] to produce 1,4-*trans*-trizole derivatives (**18a-1**, **18a-2**, **18a-3**, **18a-4**, **18b-1**, **18b-2**, **18b-3** and **18b-4**), respectively. All the key intermediates were double-validated to be correct using

^{1}HNMR and ^{13}C NMR spectra. Finally, hydrogenation debenzylation of the above 1,4-*trans* trizole derivatives yielded target EGC-phenylpropionic acid conjugates lacking a double bond (**3a-1**, **3a-2**, **3a-3**, **3a-4**, **3b-1**, **3b-2**, **3b-3** and **3b-4**). From the ^{1}H NMR spectra analysis, two hydrogen atoms characteristic of a *trans*-double bond disappeared, verifying that hydrogenation debenzylation was thorough.

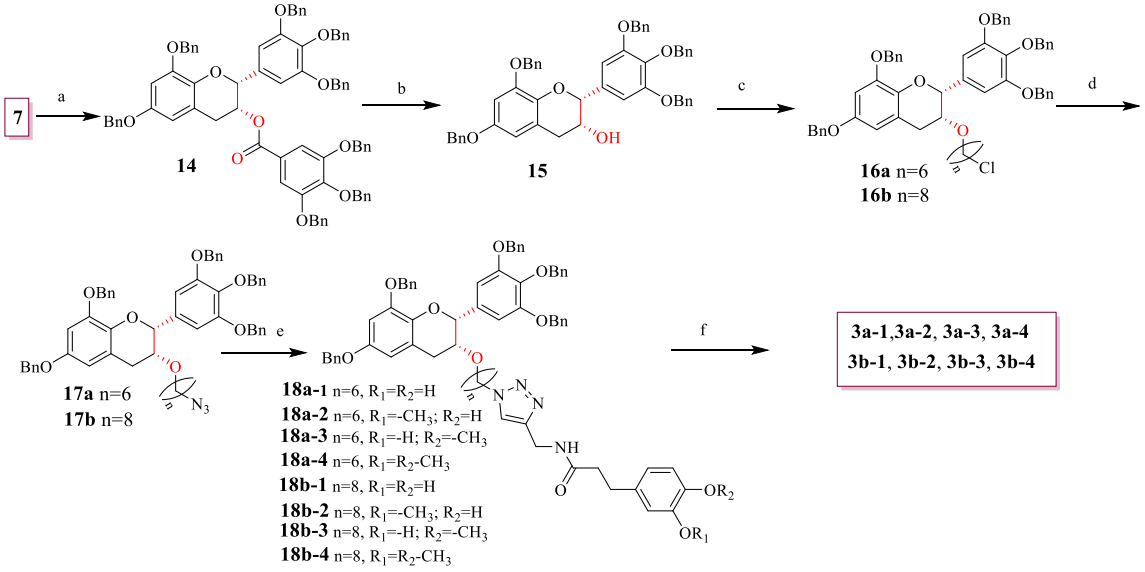
2.2. Enzymatic inhibition assessment for HPA and α-glucosidase

Twenty-one EGC-derived conjugates had been designed and synthesized, and then their inhibitory activity against α-glucosidase [27] and α-amylase [14,28,29] were next evaluated according to the previous reports with minor modifications. α-glucosidase from *S. cerevisiae* and HPA were acted as enzyme evaluation models. The most robust assay of α-glucosidase and HPA depended on a synthetic aryl glycoside substrate that was enzymatically cleaved to yield a chromophoric product, the release of which can be continuously monitored. For the α-glucosidase inhibition assay, *p*-nitrophenol glucopyranoside (*p*-NPG) was applied as a reaction indicator, while an ideal substrate 2-chloro-4-nitrophenyl-4-*O*-*β*-D-maltotrioside (G3CNP) that was characteristic of a high extinction coefficient (e = 11 $mm^{-1}cm^{-1}$) and the *pK*a of the chloro-nitrophenyl leaving group (*pK*a = 5.45) considerably lower than the pH value of this assay (pH = 7), was selected for the HPA inhibition assay. Clinical anti-MD drug acarbose and simplified analogue **1** were used as positive compounds. The selectivity index (SI) of all the tested compounds was defined as the ratio of IC_{50} of α-glucosidase to IC_{50} of HPA. To confirm the feasibility of EGC substituting for myricetin, we first tested the inhibitory activity of conjugates **1**, **2a-1**, **4a** and their structural compositions including EGC and caffeic acid against HPA and α-glucosidase and resultant selectivity. As shown in Table 1, in comparison with

Table 1
Inhibitory activities of conjugates **1**, **2a-1** and **4a** against human pancreatic α-amylase (HPA) and α-glucosidase and their resultant selectivity.

Compds No.	α-glucosidase (IC_{50} μM)[a,b]	HPA (IC_{50} μM)[a,b]	SI[c]
2a-1	450.7 ± 2.8	8.2 ± 0.1	54
4a	40.4 ± 3.6	325.2 ± 13.3	0.1
1	410.4 ± 5.4	12.0 ± 0.2	34
EGCG **(7)**	4.3 ± 0.04	146.5 ± 4.5	0.03
EGC	537.1 ± 2.4	136.7 ± 3.6	3.9
myricetin	436.8 ± 5.6	152.3 ± 2.1	2.8
acarbose	263.5 ± 2.3	1234.09 ± 21.3	0.2
caffeic acid	740.3 ± 3.7	1654.8 ± 31.5	0.4

[a] The average of IC_{50} values measured from three independent experiments.
[b] Data as mean ± standard deviations (SD).
[c] SI means that selectivity index that is the ratio of α-glucosidase (IC_{50}) to HPA (IC_{50}).



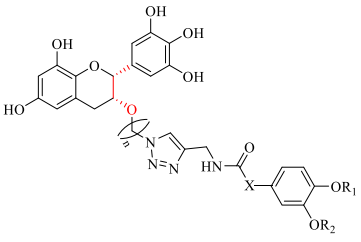
Scheme 2. The synthesis of EGC-phenylpropionic acid conjugates (**3a-1, 3a-2, 3a-3, 3a-4, 3b-1, 3b-2, 3b-3** and **3b-4**). Condition and reagents: a) benzyl bromide, K_2CO_3; b) K_2CO_3, dimethoxymethane/methanol (V/V = 1/1); c) NaH, anhydrous DMF, 1-bromo-6-chlorohexane for **16a**, 1-bromo-8-chlorooctane for **16b**; d) sodium azide, anhydrous DMF, 60℃; e) copper (II) sulfate pentahydrate, **5a-d**, sodium ascorbate, *t*-BuOH/CH_3CN/H_2O = 2/1/1(V/V/V); f) 10% Pd/C, hydrogen gas, DCM/MeOH = 4/1 (V/V).

clinical drug acarbose that was an α-glucosidase inhibitor, conjugates **2a-1** and **1** displayed more potent inhibition activity towards HPA over α-glucosidase. Although the inhibitory activity of EGC-caffeic acid conjugate **2a-1** against both enzymes was slightly superior to that of the template **1**, its SI increased significantly. Interestingly, the selectivity of EGC towards HPA over α-glucosidase was similar to that of myricetin bound to the active site of HPA (SI = 3.9 for EGC *vs* 2.8 for myricetin), [15] probably laying the structural foundation for specific HPA inhibitors.

Attachment of a gallic acid moiety to ring C of EGC formed EGCG **7**, contributing to an obvious preference for α-glucosidase. However, caffeic acid being weak inhibition activity and poor selectivity towards HPA was introduced to EGC with a linker, leading to a sharp increase in the selectivity of construct **2a-1** to HPA. Removal of a linker between moieties EGC and caffeic acid resulted in conjugate **4a** more sensitive toward α-glucosidase, which accorded with the trend of a gallic acid

Table 2

Inhibitory activities of EGC analogs against HPA and *α*-glucosidase and their resultant selectivity.



Compds No.	X	n	R_1	R_2	α-glucosidase (IC_{50} μM)[a,b]	HPA (IC_{50} μM)[a,b]	Selectivity[c]
2a-1		6	-H	-H	450.7 ± 2.8	8.2 ± 0.1	54
2a-2		6	-H	$-CH_3$	343.3 ± 13.8	197.4 ± 1.7	1.7
2a-3		6	$-CH_3$	-H	410.3 ± 4.4	230.4 ± 3.3	1.8
2a-4		6	$-CH_3$	$-CH_3$	530.6 ± 5.8	1562.6 ± 3.6	0.3
2b-1		8	-H	-H	240.7 ± 3.4	70.3 ± 2.9	3.4
2b-2		8	$-CH_3$	-H	218.7 ± 5.6	314.2 ± 9.5	0.7
2b-3		8	-H	$-CH_3$	410.7 ± 4.4	1907.0 ± 4.5	0.2
2b-4		8	$-CH_3$	$-CH_3$	326.3 ± 17.3	2907.5 ± 4.5	0.1
2c		5	-H	-H	398.6 ± 5.3	698.6 ± 5.1	0.6
3a-1		6	-H	-H	423.7 ± 1.9	33.4 ± 2.6	12.7
3a-2		6	$-CH_3$	-H	515.8 ± 7.5	167.3 ± 6.4	3.1
3a-3		6	-H	$-CH_3$	432.5 ± 2.8	220.6 ± 7.2	1.9
3a-4		6	$-CH_3$	$-CH_3$	620.7 ± 6.4	1572.7 ± 7.7	0.4
3b-1		8	-H	-H	453.4 ± 4.8	150.6 ± 1.2	3.0
3b-2		8	$-CH_3$	-H	335.4 ± 3.6	286.7 ± 10.1	1.2
3b-3		8	-H	$-CH_3$	389.7 ± 9.8	258.2 ± 2.6	1.5
3b-4		8	$-CH_3$	$-CH_3$	286.3 ± 4.5	1750.5 ± 3.7	0.2
4a			-H	-H	40.4 ± 3.6	325.2 ± 13.3	0.1
4b			$-CH_3$	-H	60.7 ± 6.2	2134.6 ± 8.7	0.03
4c			-H	$-CH_3$	48.3 ± 5.2	1734.6 ± 7.2	0.03
4d			$-CH_3$	$-CH_3$	60.4 ± 4.1	1932.6 ± 9.6	0.03
1		6	H	H	410.4 ± 5.4	12.0 ± 0.2	34

[a] The average of IC_{50} values measured from three independent experiments.
[b] Data as mean ± standard deviations (SD).
[c] The ratio of α-glucosidase (IC_{50}) to HPA (IC_{50}).

introduced to EGC in the enzymatic inhibition activity. This partly highlighted that the moiety caffeic acid at location was remote from the active site of HPA [15]. These results also emphasized the importance of a linker dominating the inhibition selectivity between HPA and α-glucosidase.

The existence of a linker was demonstrated to be crucial to the selectivity to HPA from our above evaluation. Meantime, in the binding to HPA, the binding affinity of caffeic acid alone was weak, but the caffeic ester moiety removed from mbA caused a 100-fold loss in affinity [15], emphasizing the necessity of the caffeate scaffold. Caffeic acid moiety favored the potent inhibition of mbA by the preorganization of myricetin *via* hydrophobic stacking and optimally hydrogen bonds with the active site of HPA, presenting a completely new mode of HPA inhibition. The conformation pre-formation of mbA bound to the HPA enzyme in solution was observed in NMR studies [15]. To further explore the effects of structural modification on a benzene ring, a double bond of caffeic acid, along with the length of a linker, on the inhibitory activity against HPA, we focused on methylating a hydroxyl group of caffeic acid, reducing a double bond and varying the length of a linker to compare the efficacy in inhibiting HPA and α-glucosidase. As illustrated in Table 2, with a growing number of the methyl groups modified on moiety caffeic acid, the inhibition activity of conjugates (8.2 ± 0.1 μM for **2a-1** *vs* 197.4 ± 1.7 μM for **2a-2** *vs* 230.4 ± 3.3 μM for **2a-3** *vs* 1562.6 ± 3.6 μM for **2a-4**) against HPA decreased sharply, resulting in the selectivity shifted from HPA to α-glucosidases. The similar tendency of other conjugates (**2b-1**, **2b-2**, **2c-3** and **2c-4**) was observed. The decreased inhibition activity was probably ascribed to the destruction of hydrogen bonds due to methylation, agreeing to the observation of the HPA-mbA complex with high-resolution 3D structure that the two aromatic rings of mbA stack in the active site and their hydroxyls interact with the essential amino acid residues of HPA [15].

When a linker was elongated from six carbon atoms (**2a-1**) to eight carbon ones (**2b-1**), the inhibitory activity declined a lot (8.2 ± 0.1 μM for **2a-1** *vs* 70.3 ± 2.9 μM for **2b-1**) and thus the selectivity to HPA decreased by about 15 times (SI = 54 for **2a-1** *vs* SI = 3.4 for **2b-1**). Shortening a linker from six carbon atoms (**2a-1**) to five carbon ones (**2c**), the similar observation was demonstrated (SI = 54 for **2a-1** *vs* SI = 0.6 for **2c**). These results obviously suggested a six-carbon-atom linker coupled to EGC was the optimal linker for π stacking of the two aromatic systems caffeic acid and EGC and hydrogen bonds forming with HPA. Elongation or shortening possibly damaged the hydrophobic stacking, and hydrogen bonding with crucial amino acid residues of HPA, and additional water-mediated interaction with other key active site residues. Besides, compared to conjugates EGC-caffeic acid derivatives (**2a-1**, **2a-2**, **2a-3** and **2a-4**), EGC-phenylpropionic acid conjugates (**3a-1**, **3a-2**, **3a-3** and **3a-4**) displayed the inferior inhibitory activity and poorer selectivity to HPA, however, the effect of a double bond was limited. For conjugates **4a-d**, the methylation of caffeic acid affected slightly α-glucosidase activity but significantly HPA activity. Taken together, caffeic acid with a weak binding affinity was an essential scaffold for EGC-based conjugates in the binding of HPA. The more the number of methyl groups of caffeic acid was, the less the activity and selectivity exhibited. The length of a linker dominated the sensitivity of conjugates modified towards HPA over α-glucosidase, and the optimal linker fused to the EGC moiety was demonstrated to be a six-carbon-atom one. A double bond contained in caffeic acid moiety had limited effects on the inhibition activity and resultant selectivity to HPA. Moreover, the inhibitory activity and selectivity of conjugate **2a-1** to HPA were superior to those of the lead **1**, further validating our hypothesis that EGC could replace myricetin and a double bond and a carbonyl group resided in C ring were non-essential groups for binding to HPA.

2.3. Molecular docking studies of HPA with respective conjugates 2a-1 and 1

To gain insight into the potential binding modes and rationalize the observed efficiency of HPA inhibition by EGC-based derivatives, compound **2a-1** as a potent HPA inhibitor we screened was selected for molecular docking studies based on PDB code: 4W93. As shown in Fig. 3 (**A**), compound **2a-1** tightly fitted the active site of HPA, and four hydrogen-bond interactions were observed between **2a and 1** and the residues R195, H305, H201 and Q63 of HPA *via* a hydroxyl group of caffeic acid, a hydroxyl group of B ring of moiety EGC, a hydroxyl group of A ring of moiety EGC and an *O* atom of amide in the linker, respectively. All these interactions helped compound **2a-1** to anchor in the binding site of HPA. Noticeably, compound **2a-1** bound to the active site of HPA in the form of π-stacking interactions of moieties A ring of

EGC and caffeic acid, which was similar as that of the lead **1** where two moieties myricetin and caffeic acid stacked (Fig. 3, **B**). But template **1** bound to the active site of HPA *via* forming three hydrogen bonds only through a hydroxyl group of caffeic acid, a hydroxyl group of B ring of myricetin with residues D197, R195 and H201 of HPA, respectively. These observation from molecular docking studies that conjugate **2a-1** had four hydrogen bonds interacting with HPA but only three hydrogen bonding appeared in the binding of reference compound **1** and HPA**,** gave reasonable explanations for the inhibitory activity of **2a-1** more potent than that of **1**. More importantly, hydrogen bond formation of caffeic acid with HPA emphasized the importance and necessary of the free hydroxyl group located on caffeic acid moiety for conjugates **2a-1** and **1**. Methylation able to block the hydrogen bond formation disfavored the inhibition activity of the modifying conjugates against HPA, which totally accorded with the results from the *in vitro* HPA inhibition activity.

3. Conclusion

In summary, to overcome the specificity problems that originated from currently available α-glucosidase inhibitors, twenty-one EGC-based derivatives that were selective inhibition targeted at only HPA, the enzyme at the top of the starch digestion pyramid, were designed and synthesized based on the simplified myricetin-caffeic acid conjugate **1**. The methylation of caffeic acid and the length of a liker affected significantly the inhibition activity and selectivity of EGC-based conjugates, but the effect of a double bond contained in the linker was demonstrated to be limited. Molecular docking experiments revealed that conjugate **2a-1** accommodated well to the active site of HPA by the preorganization of two compositions EGC and caffeic acid *via* four hydrogen-bond interactions. Our results supported the feasibility of finding the novel specific HPA inhibitors where EGC was instead of myricetin, highlighting the non-essential groups of a carbonyl group and a double bond in the C ring of myricetin in the binding of HPA. The *in vivo* detailed studies on blood sugar-lowering effects of compound **2a-1** are on-going evaluation using animal models in our lab.

4. Experimental section

All chemicals were of reagent grade quality or better, which were purchased from commercial suppliers and used with no further purification. Solvents were used as received or dried over molecular sieves. Column chromatography was performed on silica gel (100–200 mesh) purchased from Qingdao Ocean Chemical Factory. All the reactions were monitored by TLC (HSGF 254, Yantai Jiangyou Silica Gel Development Co. LTD). α-glucosidase (0.6 unit/mL) from *S. cerevisiae* (G5003) was purchased from Merck & Co. Inc., and human pancreas α-amylase was from Lee Biosolutions, Inc. All the key intermediates and final products were confirmed by ^{1}H NMR and ^{13}C NMR, which was recorded in a Bruker Avance 400 (^{1}H at 400 MHz, ^{13}C at 100 MHz), and chemical shifts were reported in parts per million using the residual solvent peaks

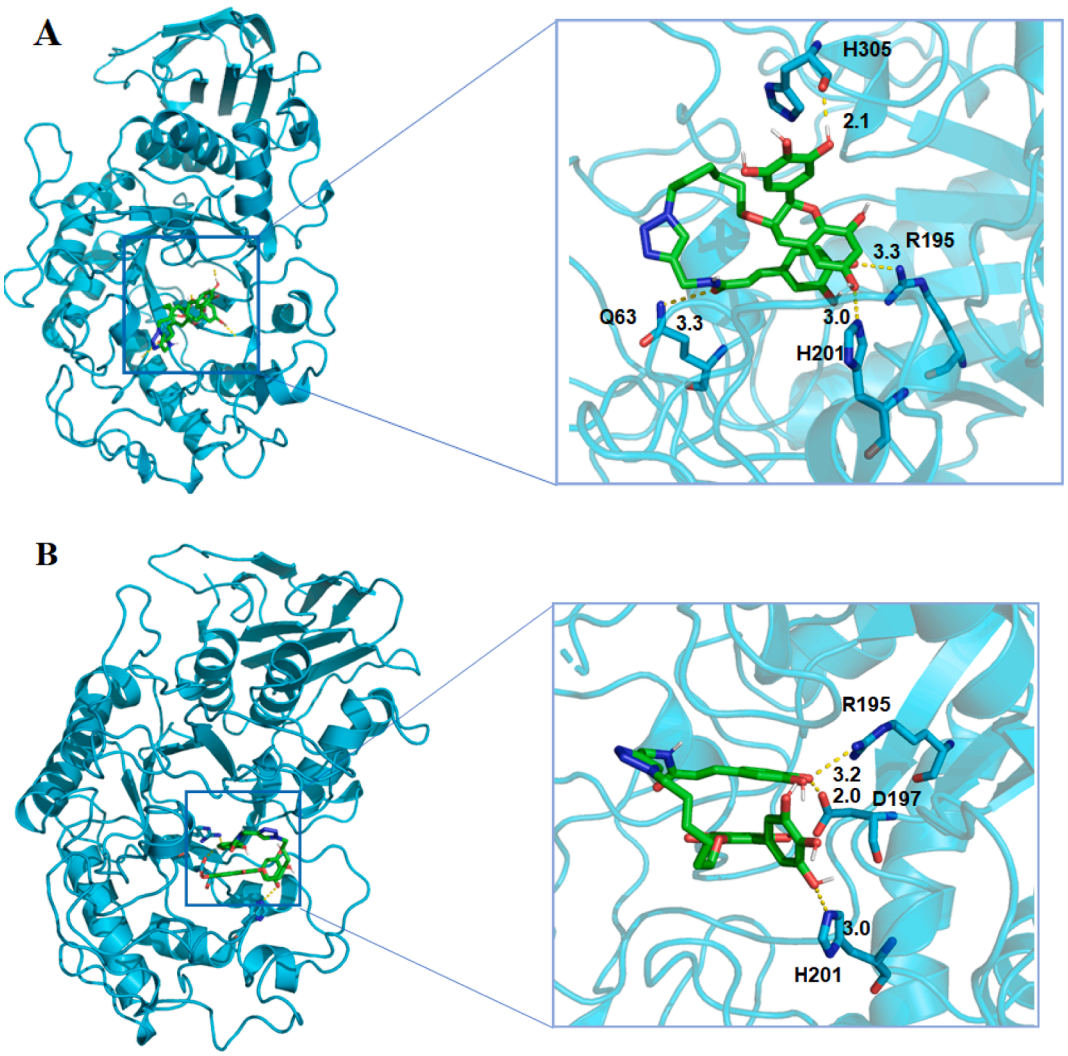


Fig. 3. The binding modes of conjugates **2a-1** (**A**) and **1** (**B**) with HPA (PDB. 4 W93) using molecular docking Autodock vina 1.1.2 software. (Ribbon diagram represents HPA protein, various colored sticks mean the molecular structures of conjugates **2a-1** and **1**, and amino acid residues of HPA, among of which a green color represents carbon atoms, a blue color means nitrogen atoms, and a red color represents oxygen atoms.) (For interpretation of the references to color in this figure legend, the reader is referred to the web version of this article.)

as internal standards ($CDCl_3$ = 7.26 ppm for ^{1}H NMR and 77.16 ppm for ^{13}C NMR, CD_3COCD_3 = 2.05 ppm for ^{1}H NMR and 206.68 and 29.92 ppm for ^{13}C NMR, CD_3OD = 3.31 ppm for ^{1}H NMR, and 49.00 ppm for ^{13}C NMR). Also, several final products were determined by electrospray ionization high resolution mass spectrometry (ESI-HRMS), recorded on AB Sciex triple TOF 5600 + system. The purity was more than 95%, and it was determined with C_{18}-column (250 × 4.6 mm, 5 μm, Agilent Eclipse Plus) run on Agilent Technologies 1260 infinity II.

4.1. Synthesis of (E)-N-((3-(5-((6,8-dihydroxy-4-oxo-2-(3,4,5-trihydroxyphenyl)-4H-chromen-3-yl)oxy)pentyl)–3H-pyrazol-5-yl) methyl)-3-(3,4-dihydroxyphenyl) acrylamide ***(1)***

The synthetic route of compound **1** was the same as that reported in reference 15.

^{1}H NMR (400 MHz, CD_3OD) δ 7.87 (s, 1H), 7.40 (s, J = 15.8 Hz, 1H), 7.19–7.08 (s 2H), 6.97 (s, 1H), 6.87 (d, J = 8.4 Hz, 1H), 6.73 (d, J = 8.4 Hz, 1H), 6.42–6.28 (m, 2H), 6.18 (d, J = 2.8 Hz, 1H), 4.53 (s, 2H), 4.34 (t, J = 8.0 Hz, 2H), 3.88 (t, J = 8.0 Hz, 2H), 1.88–1.78 (m, 2H), 1.75–1.66 (m, 2H), 1.49–1.36 (m, 2H); ^{13}C NMR (100 MHz, CD_3OD) δ 183.56, 180.07, 165.81, 163.11, 158.71, 158.43, 148.84, 146.78, 146.68, 142.78, 138.67, 137.82, 128.16, 124.45, 122.24, 122.21, 122.08, 117.91, 116.42, 115.05, 109.35, 105.92, 99.70, 94.65, 73.43, 51.40, 35.77, 30.86, 30.17, 24.08.

*4.2. Synthesis of (E)-3-(3,4-dihydroxyphenyl)-N-(prop-2-yn-1-yl) acrylamide (**6a**)*

Caffeic acid (1.8 g, 10 mmol) was dissolved in dry DMF, and 1-hydroxybenzotriazole (HOBT, 1.4 equiv.) and 1-ethyl-3-(3-dimethylaminopropyl) carbodiimide hydrochloride (EDCI, 1.6 equiv.) were added. The reaction mixture was stirred for 0.5 h at room temperature, and then the addition of propargylamine (1.2 equiv.) was performed. At the same temperature the reaction proceeded for another 6 h. Water was added to quench the reaction. Ethyl acetate extract was washed with 4% hydrochloride, water and statured brine in order, and the organic layer was condensed to obtain the crude residue, which was purified by silica gel-based chromatography column with a mixture of ethyl acetate and petroleum ether (V/V = 1/4) as an eluent to afford 1.7 g of **6a** as a light-yellow solid.

Yield, 80%.^{1}H NMR (400 MHz, CD_3COCD_3) δ 8.49 (d, J = 25.8 Hz, 1H), 8.24 (d, J = 19.6 Hz, 1H), 7.82–7.60 (m, 1H), 7.53–7.42 (m, 1H), 7.14–7.05 (m, 1H), 6.95 (dd, J = 8.0, 2.0 Hz, 1H), 6.85 (dd, J = 8.0, 2.0 Hz, 1H), 6.54–6.43 (m, 1H), 4.12 (m, 2H), 2.68 (t, J = 2.6 Hz, 1H).

4.3. Synthesis of (E)-3-(3-hydroxy-4-methoxyphenyl)-N-(prop-2-yn-1-yl)acrylamide (6b)

The synthetic procedure was similar to that of **6a**, only differing in a starting material caffeic acid replaced by isoferulic acid.

Yield, 80%. ^{1}H NMR (400 MHz, CD_3COCD_3) δ 7.49 (d, J = 15.7 Hz, 1H), 7.08 (d, J = 2.1 Hz, 1H), 7.02 (dd, J = 8.2, 2.0 Hz, 1H), 6.81 (d, J = 8.2 Hz, 1H), 6.44 (d, J = 15.7 Hz, 1H), 4.10 (d, J = 2.5 Hz, 2H), 3.85 (s, 3H), 2.63 (t, J = 2.6 Hz, 1H); ^{13}C NMR (100 MHz, CD_3COCD_3) δ 162.96, 149.25, 148.55, 141.31, 127.92, 122.65, 119.01, 116.09, 111.35, 81.42, 72.04, 56.17, 28.91.

4.4. Synthesis of (E)-3-(4-hydroxy-3-methoxyphenyl)-N-(prop-2-yn-1-yl)acrylamide (6c)

The synthetic procedure was similar to that of **6a**, only differing in a starting material caffeic acid replaced by ferulic acid.

Yield, 83%. ^{1}H NMR (400 MHz, CD_3OD) δ 7.82 (s, 1H), 7.60 (t, J = 5.6 Hz, 1H), 7.48 (d, J = 15.6 Hz, 1H), 7.12–7.07 (m, 1H), 7.02 (dd, J = 8.3, 2.1 Hz, 1H), 6.95 (d, J = 8.4 Hz, 1H), 6.53 (d, J = 15.6 Hz, 1H), 4.12 (dd, J = 5.6, 2.6 Hz, 2H), 3.86 (s, 3H), 2.67 (t, J = 2.6 Hz, 1H). ^{13}C NMR (100 MHz, CD_3COCD_3) δ 166.45, 150.31, 148.00, 141.42, 129.56, 121.92, 119.97, 114.43, 112.64, 81.72, 72.34, 56.57, 29.36.

4.5. Synthesis of (E)-3-(3,4-dimethoxyphenyl)-N-(prop-2-yn-1-yl) acrylamide (6d)

The synthetic procedure was similar to compound **6a**, only differing in a starting material isoferulic acid replaced by 3,4-dimethoxycinnamic acid.

Yield, 83%. ^{1}H NMR (400 MHz, CD_3COCD_3) δ 7.58 (t, J = 5.6 Hz, 1H), 7.51 (d, J = 15.6 Hz, 1H), 7.18 (d, J = 2.0 Hz, 1H), 7.12 (dd, J = 8.4, 2.0 Hz, 1H), 6.95 (d, J = 8.4 Hz, 1H), 6.58 (d, J = 15.6 Hz, 1H), 4.12 (dd, J = 5.6, 2.5 Hz, 2H), 3.84 (s, 3H), 3.83 (s, 3H), 2.67 (t, J = 2.5 Hz, 1H).

4.6. Synthesis of (2R, 3S)-6,8-bis(methoxymethoxy)-4-oxo-2-(3,4,5-tris (methoxy methoxy)phenyl)chroman-3-yl 3,4,5-tris(methoxymethoxy) benzoate (8)

Commercially available EGCG (2 g, 4.3 mmol) was taken up in anhydrous DMF (30 mL), and NaH coated with mineral oil (60%, 2.6 g, 65 mmol) and MOMCl (5.2 g, 65 mmol) were added in order. After being stirred for 48 h, ethyl acetate (200 mL) and water (100 mL) were added to quench the reaction mixture. The organic layer was washed with water and brine, and dried with anhydrous Na_2SO_4, and the filter was dried under reduced pressure to afford the crude residue, which was purified by silica gel chromatography column with a mixture of ethyl acetate and petroleum ether (V/V = 1/5) as an eluent to give 2.08 g of compound **8** as a light-yellow solid.

Yield, 60%.^{1}H NMR (400 MHz, $CDCl_3$) δ 7.40 (s, 2H), 6.96 (s, 2H), 6.47–6.40 (m, 2H), 5.25–5.00 (m, 18H), 3.59–3.26 (m, 26H); ^{13}C NMR (100 MHz, $CDCl_3$) δ 166.45, 150.76, 140.72, 125.98, 111.63, 98.57, 95.36, 95.32, 93.67, 93.65, 89.25, 89.23, 88.86, 88.84, 57.31, 56.49, 55.95, 52.33, 29.79.

4.7. Synthesis of (2R,3S)-3-hydroxy-6,8-bis(methoxymethoxy)-2-(3,4,5-tris(methoxy methoxy) phenyl)chroman-4-one (9)

To a solution of compound **8** (0.5 g, 0.6 mmol) dissolved in a mixture of methanol (5.0 mL) and glycol dimethyl ether (5.0 mL) was added anhydrous potassium carbonate (1.7 g, 12 mmol). The mixture was stirred for 5.0 h at room temperature. After all the starting materials were consumed, ethyl acetate (200 mL) and water (100 mL) were added in order. The organic layer was washed with water (30 mL) and brine (30 mL) in order, and dried with anhydrous Na_2SO_4, and filtered, and then condensed under the reduced pressure to obtain the crude residue, which was purified by a silica gel chromatography column with a mixture of ethyl acetate and petroleum ether (V/V = 1/5) as an eluent to afford 0.27 g of compound **9** as a yellow solid.

Yield, 85%. ^{1}H NMR (400 MHz, $CDCl_3$) δ 6.98 (s, 2H), 6.46–6.39 (m, 2H), 5.24–5.12 (m, 10H), 4.91 (s, 1H), 4.27 (d, J = 4.0 Hz, 1H), 4.16–4.06 (m, 1H), 3.65–3.60 (m, 3H), 3.52–3.46 (m, 12H), 3.03–2.85 (m, 2H); ^{13}C NMR (100 MHz, $CDCl_3$) δ 157.10, 156.84, 155.12, 151.33, 136.29, 134.53, 108.30, 102.58, 98.66, 97.94, 96.73, 95.47, 94.64, 94.60, 78.39, 66.42, 57.27, 56.50, 56.29, 56.17, 29.83.

4.8. General synthesis of conjugates 10a-d

To a solution of **9** dissolved in anhydrous DCM (10 mL) were added EDCI (2.2 equiv.), DMAP (2.2 equiv.) and unseparated methoxymethylated **5a-c** and **5d**. The reaction mixture was stirred for 12 h. Water was added to quench the reaction, and ethyl acetate was used to extract the target compound. The organic layer was washed with water and brine in order, and filtered, and then evaporated under reduced pressure. The residue obtained was further purified by flash chromatographic column with a mixture of ethyl acetate and petroleum (V/V = 1/5) as an eluent to afford a yellow solid **10a-d**, respectively.

10a, yield 76%, ^{1}H NMR (400 MHz, $CDCl_3$) δ 7.50 (d, J = 16.0 Hz, 1H), 7.31 (s, 1H), 7.19–7.04 (m, 2H), 7.00 (s, 2H), 6.50–6.35 (m, 2H), 6.30 (d, J = 16.0 Hz, 1H), 5.50 (s, 1H), 5.25–5.08 (m, 14H), 4.98 (s, 1H), 3.57 (s, 3H), 3.51–3.37 (m, 18H), 3.02 (s, 2H); ^{13}C NMR (100 MHz, $CDCl_3$) δ 166.45, 156.99, 156.45, 155.41, 150.85, 149.20, 147.26, 144.67, 136.09, 133.76, 128.78, 123.68, 116.44, 116.00, 115.37, 108.89, 102.36, 98.51, 97.82, 96.38, 95.36, 95.17, 95.07, 94.54, 94.48, 77.64, 67.65, 57.07, 56.31, 56.24, 56.19, 56.08, 29.69, 26.24.

10b, yield 81%, ^{1}H NMR (400 MHz, $CDCl_3$) δ 7.53 (d, J = 15.8 Hz, 1H), 7.18–6.90 (m, 5H), 6.44 (s, 2H), 6.33 (d, J = 15.8 Hz, 1H), 5.52 (s, 1H), 5.30–5.06 (m, 12H), 4.99 (s, 1H), 3.88 (s, 3H), 3.61–3.35 (m, 18H), 3.03 (d, J = 4.8 Hz, 2H); ^{13}C NMR (100 MHz, $CDCl_3$) δ 166.52, 157.03, 156.54, 155.49, 150.92, 149.77, 148.60, 144.89, 136.15, 133.82, 128.75, 122.58, 116.31, 115.65, 110.10, 108.94, 102.46, 98.57, 97.83, 96.46, 95.20, 94.60, 94.54, 77.73, 67.65, 57.14, 56.41, 56.27, 56.18, 56.15, 55.93, 26.33.

10c, yield 79%, ^{1}H NMR (400 MHz, $CDCl_3$) δ 7.51 (d, J = 16.0 Hz, 1H), 7.31 (s, 1H), 7.11 (d, J = 8.2 Hz, 1H), 7.01 (s, 2H), 6.85 (d, J = 8.3 Hz, 1H), 6.51–6.38 (m, 2H), 6.29 (d, J = 16.0 Hz, 1H), 5.52 (d, J = 3.9 Hz, 1H), 5.28–5.05 (m, 12H), 4.99 (s, 1H), 3.88 (s, 3H), 3.69–3.26 (m, 18H), 3.15–2.88 (m, 2H); ^{13}C NMR (100 MHz, $CDCl_3$) δ 166.61, 157.05, 156.53, 155.49, 151.78, 150.92, 146.73, 144.87, 136.15, 133.85, 127.51, 124.11, 115.97, 114.86, 111.49, 108.96, 102.46, 98.59, 97.91, 96.46, 95.49, 95.25, 94.64, 94.56, 77.74, 67.65, 57.17, 56.34, 56.29, 56.17, 56.01, 26.34.

10d, yield 90%, ^{1}H NMR (400 MHz, $CDCl_3$) δ 7.53 (d, J = 15.9 Hz, 1H), 7.08–6.97 (m, 4H), 6.83 (d, J = 8.4 Hz, 1H), 6.44 (s, 2H), 6.31 (d, J = 15.9 Hz, 1H), 5.52 (s, 1H), 5.26–5.08 (m, 10H), 5.00 (s, 1H), 3.89 (d, J = 1.6 Hz, 6H), 3.62–3.37 (m, 15H), 3.03 (d, J = 4.4 Hz, 2H) ; ^{13}C NMR (100 MHz, $CDCl_3$) δ 166.65, 157.10, 156.63, 155.58, 151.23, 151.00, 149.28, 145.08, 136.24, 133.91, 127.49, 123.01, 115.85, 111.02, 109.49, 109.04, 102.57, 98.66, 97.93, 96.55, 95.30, 94.71, 94.64, 77.83, 67.64, 57.23, 56.36, 56.28, 56.23, 56.07, 55.98, 26.42.

4.9. General synthesis of conjugates 4a-d

The yellow solid **10a** (100.0 mg, 0.13 mmol) obtained above was dissolved in a mixture of DCM (4 mL) and methanol (1 mL), and then use of 0.1 mL of 12 M HCl promoted removal of MOMCl. The mixture was stirred for 8 h at room temperature. Compound **4a** (18.1 mg) as a light-red powered solid was obtained with a preparative HPLC. Operated as **4a**, the target compounds **4b-d** were achieved by replacement **10a** with **10b-d**, respectively.

4a, yield, 30%. ^{1}H NMR (400 MHz, CD_3OD) δ 7.42 (d, J = 15.9 Hz,

1H), 6.99 (d, $J = 2.0$ Hz, 1H), 6.91 (dd, $J = 8.4$, 2.0 Hz, 1H), 6.74 (d, $J = 8.4$ Hz, 1H), 6.50 (d, $J = 3.0$ Hz, 2H), 6.19 (d, $J = 15.9$ Hz, 1H), 5.99–5.92 (m, 2H), 5.46 (d, $J = 4.2$ Hz, 1H), 4.95 (s, 1H), 2.97 (dd, 1H), 2.82 (dd, $J = 14.7$ Hz, 1H); ^{13}C NMR (100 MHz, CD_3OD) δ 168.63, 157.94, 157.85, 157.14, 149.69, 147.17, 146.73, 130.85, 127.80, 123.07, 119.08, 116.39, 115.23, 115.13, 106.83, 96.52, 95.79, 78.49, 69.79, 30.46.

4b, yield 32%.^{1}H NMR (400 MHz, CD_3OD) δ 7.50 (d, $J = 16.0$ Hz, 1H), 7.15 (d, $J = 2.0$ Hz, 1H), 7.04 (dd, $J = 8.4$, 2.0 Hz, 1H), 6.78 (d, $J = 8.4$ Hz, 2H), 6.53 (s, 2H), 6.29 (d, $J = 16.0$ Hz, 1H), 5.99–5.95 (m, 1H), 5.50–5.46 (m, 1H), 4.97 (s, 1H), 3.87 (s, 3H), 2.98 (dd, $J = 17.2$, 4.6 Hz, 1H), 2.85 (dd, $J = 17.2$, 2.6 Hz, 1H); ^{13}C NMR (100 MHz, CD_3OD) δ 168.59, 157.83, 157.78, 157.08, 157.06, 157.06, 150.49, 149.27, 147.07, 146.73, 133.79, 130.74, 127.77, 124.24, 116.32, 115.48, 111.67, 106.80, 99.31, 78.46, 69.81, 56.43, 26.72.

4c, yield, 31%, ^{1}H NMR (400 MHz, CD_3OD) δ 7.43 (d, $J = 16.0$ Hz, 1H), 7.05–6.95 (m, 2H), 6.89 (d, $J = 8.0$ Hz, 1H), 6.50 (t, $J = 2.4$ Hz, 2H), 6.23 (d, $J = 16.0$ Hz, 1H), 6.01–5.90 (m, 2H), 5.44 (s, 1H), 4.94 (s, 1H), 3.85 (t, $J = 2.4$ Hz, 3H), 2.97–2.82 (m, 2H); ^{13}C NMR (100 MHz, CD_3OD) δ 168.43, 157.93, 157.84, 157.13, 151.42, 147.85, 146.78, 146.72, 133.79, 130.70, 128.92, 122.92, 116.13, 114.83, 112.38, 106.81, 99.32, 96.51, 95.78, 78.47, 69.89, 56.32, 26.70.

4d, yield 33%.^{1}H NMR (400 MHz, CD_3OD) δ 7.49 (d, $J = 16.0$ Hz, 1H), 7.19–7.02 (m, 3H), 6.91 (d, $J = 8.4$ Hz, 2H), 6.51 (s, 2H), 6.31 (d, $J = 16.0$ Hz, 1H), 5.48–5.43 (m, 1H), 4.95 (s, 1H), 3.91–3.84 (m, 2H), 3.82 (d, $J = 3.5$ Hz, 6H), 2.97 (dd, $J = 17.4$, 4.6 Hz, 1H), 2.84 (dd, $J = 17.5$, 2.7 Hz, 1H); ^{13}C NMR (100 MHz, CD_3OD) δ 168.39, 157.84, 157.79, 157.05, 152.70, 150.64, 146.74, 146.65, 133.78, 130.72, 128.83, 124.15, 116.43, 112.45, 111.40, 106.78, 99.29, 78.43, 69.88, 56.46, 56.36, 26.72.

*4.10. Synthesis of (2R, 3S)-3-((6-chlorohexyl)oxy)-6,8-bis(methoxymethoxy)-2-(3,4,5-tris(methoxy methoxy)phenyl)chroman-4-one (**11a**)*

Compound **9** (2.0 g, 3.8 mmol) was dissolved in anhydrous DMF (30 mL), and NaH (750 mg, 18.8 mmol) was added in batches, and finally 1-bromo-6-chlorohexane (1.5 g, 7.7 mmol) was introduced dropwise. The mixture was stirred for 12 h at the room temperature. After all the starting material was consumed, the addition of water (10 mL) was used to carefully quench the mixture. Ethyl acetate was added to extract the target compound. The organic layer was washed with water (100 mL) and brine (50 mL), and dried with anhydrous Na_2SO_4, and filtered, and then condensed under the diminished pressure to afford the crude residue **11a** without further purification.

*4.11. Synthesis of (2R,3S)-3-((6-azidohexyl)oxy)-6,8-bis(methoxymethoxy)-2-(3,4,5-tris(methoxy methoxy)phenyl)chroman-4-one (**12a**)*

To a solution of crude residue **11a** obtained above dissolved in anhydrous DMF (15 mL) was added sodium azide (500 mg, 7.6 mmol), and the mixture was heated to 60 ℃ and stirred for 6 h. When the reaction was over, water (10 mL) was added to quench the reaction and then ethyl acetate was added. The organic layer was washed with water (100 mL) and brine (30 mL), and dried with anhydrous Na_2SO_4, and filtered, and then condensed under the diminished pressure to remove the solvent. The crude residue was further purified by a silica-gel column chromatogram with a mixture of petrol ether and ethyl acetate (V/V = 3/1) as an eluent to afford 257.5 mg of compound **12a** as a yellow solid.

Yield, 52% (in terms of compound **9**). ^{1}H NMR (400 MHz, $CDCl_3$) δ 6.97 (s, 2H), 6.35 (s, 2H), 5.31–4.99 (m, 10H), 4.88 (s, 1H), 3.93–3.76 (m, 1H), 3.58 (s, 3H), 3.50–3.39 (m, 12H), 3.37–3.07 (m, 4H), 2.96–2.85 (m, 1H), 2.73 (dd, $J = 17.1$, 4.4 Hz, 1H), 1.48–1.34 (m, 4H), 1.25–1.10 (m, 4H); ^{13}C NMR (100 MHz, $CDCl_3$) δ 156.71, 156.24, 155.37, 150.53, 135.94, 134.91, 109.15, 102.97, 98.43, 97.80, 96.03, 95.26, 94.39, 94.36, 77.88, 73.30, 69.46, 56.91, 56.08, 55.95, 55.80, 51.17, 29.27, 28.56, 26.24, 25.38, 24.67.

*4.12. Synthesis of (E)-N-((1-(6-(((2R,3R)-6,8-bis(methoxymethoxy)-2-(3,4,5-tris(methoxymethoxy) phenyl)chroman-3-yl)oxy)hexyl)-1H-1,2,3-triazol-4-yl)methyl)-3-(3,4-dihydroxy phenyl)acrylamide (**13a-1**)*

A three-necked bottle was charged with **12a** (1.0 g, 1.5 mmol) and **6a** (0.4 g, 1.8 mmol), and *t*-BuOH (10.0 mL) and CH_3CN (5.0 mL) were added to dissolve the above two compounds. Copper sulfate pentahydrate (14.0 mg) and sodium ascorbate (32.0 mg) were taken up in water (5 mL). The two above systems were combined and stirred fiercely for 12.0 h. After the reaction ended, the solvent was removed under reduced pressure to obtain the crude residue, which was further purified by column chromatogram over silica gel with a mixture of petrol ether and ethyl acetate (V/V = 2/1) to obtain 1.04 g of a light-yellow solid (**13a-1**).

Yield, 80 %. ^{1}H NMR (400 MHz, $CDCl_3$) δ 7.92 (s, 1H), 7.57–7.44 (m, 2H), 7.35 (d, $J = 15.4$ Hz, 1H), 6.93 (d, $J = 13.2$ Hz, 3H), 6.70 (s, 2H), 6.41–6.26 (m, 2H), 5.14 (s, 4H), 5.09 (d, $J = 7.8$ Hz, 4H), 5.02 (s, 2H), 4.84 (s, 1H), 4.50 (s, 2H), 4.16–3.97 (m, 2H), 3.82 (s, 1H), 3.55 (s, 3H), 3.47–3.30 (m, 12H), 2.89–2.77 (m, 4H), 2.14–1.89 (m, 2H), 1.70–1.51 (m, 2H), 1.35–1.21 (m, 2H), 1.22–1.00 (m, 4H); ^{13}C NMR (100 MHz, $CDCl_3$) δ 174.25, 167.17, 162.86, 156.68, 156.23, 155.34, 150.55, 146.97, 144.73, 144.40, 141.55, 135.80, 135.00, 126.94, 122.60, 121.80, 117.14, 115.36, 113.74, 109.02, 103.00, 98.46, 95.23, 94.39, 94.35, 77.90, 73.30, 69.37, 57.00, 56.15, 56.02, 55.85, 50.23, 36.55, 31.46, 29.82, 29.03, 25.92, 25.18.

*4.13. Synthesis of (E)-N-((1-(6-(((2R,3R)-6,8-bis(methoxymethoxy)-2-(3,4,5-tris(methoxymethoxy) phenyl)chroman-3-yl)oxy)hexyl)-1H-1,2,3-triazol-4-yl)methyl)-3-(3-hydroxy-4-methoxyphenyl)acrylamide (**13a-2**)*

The synthetic procedure of **13a-2** was similar to that of **13a-1**, except that a starting material **6a** was replaced by **6b**.

Yield, 75%. ^{1}H NMR (400 MHz, $CDCl_3$) δ 7.52 (s, 1H), 7.43 (d, $J = 15.6$ Hz, 1H), 7.29–7.22 (m, 1H), 6.93–6.86 (m, 3H), 6.76 (d, $J = 8.2$ Hz, 1H), 6.29 (s, 2H), 6.25 (d, $J = 15.6$ Hz, 1H), 5.16–4.99 (m, 10H), 4.81 (s, 1H), 4.51 (d, $J = 6.0$ Hz, 2H), 4.16–3.97 (m, 2H), 3.83–3.76 (m, 1H), 3.74 (s, 3H), 3.52 (s, 3H), 3.46–3.28 (m, 13H), 3.17–3.09 (m, 1H), 2.86–2.76 (m, 2H), 2.71–2.62 (m, 1H), 2.09–1.87 (m, 4H), 1.67–1.62 (m, 2H), 1.31–1.28 (m, 2H). ^{13}C NMR (100 MHz, $CDCl_3$) δ 166.56, 156.81, 156.38, 155.50, 150.67, 147.69, 147.00, 141.20, 135.97, 135.14, 128.31, 127.21, 122.47, 122.20, 117.97, 114.97, 109.90, 109.19, 103.11, 98.59, 97.99, 96.22, 95.39, 94.54, 94.52, 78.03, 73.39, 69.38, 57.13, 56.29, 56.16, 56.00, 55.88, 50.30, 31.95, 30.05, 26.08, 25.34, 22.72.

*4.14. Synthesis of (E)-N-((1-(6-(((2R,3R)-6,8-bis(methoxymethoxy)-2-(3,4,5-tris(methoxymethoxy) phenyl)chroman-3-yl)oxy)hexyl)-1H-1,2,3-triazol-4-yl)methyl)-3-(4-hydroxy-3-methoxyphenyl)acrylamide (**13a-3**)*

The synthetic procedure of **13a-3** was similar to that of **13a-1**, except that a starting material **6a** was replaced by **6c**.

Yield 86%. ^{1}H NMR (400 MHz, $CDCl_3$) δ 7.58 (s, 1H), 7.52–7.40 (m, 1H), 7.37–7.22 (m, 1H), 7.08 (s, 1H), 6.96 (s, 2H), 6.90 (d, $J = 8.4$ Hz, 1H), 6.74 (d, $J = 8.4$ Hz, 1H), 6.35 (d, $J = 6.4$ Hz, 2H), 5.29–5.00 (m, 10H), 4.86 (s, 1H), 4.57 (d, $J = 5.6$ Hz, 2H), 4.16 (t, $J = 7.2$ Hz, 2H), 3.82 (d, $J = 12.0$ Hz, 4H), 3.62–3.32 (m, 15H), 3.24–3.12 (m, 1H), 2.95–2.70 (m, 3H), 2.23–1.95 (m, 2H), 1.75–1.62 (m, 2H), 1.36–1.30 (m, 2H), 1.11–1.08 (m, 2H); ^{13}C NMR (100 MHz, $CDCl_3$) δ 166.63, 162.74, 156.78, 156.36, 155.48, 150.65, 148.53, 146.03, 140.89, 135.95, 135.12, 128.31, 122.52, 121.62, 118.59, 112.89, 110.74, 109.18, 103.12, 98.57, 97.96, 96.21, 95.37, 94.52, 94.49, 78.00, 73.34, 69.39, 57.11, 56.26, 56.14, 55.98, 55.88, 50.29, 31.17, 30.03, 29.69, 29.16,

26.06, 25.31.

*4.15. Synthesis of (E)-N-((1-(6-(((2R,3R)-6,8-bis(methoxymethoxy)-2-(3,4,5-tris(methoxymethoxy) phenyl)chroman-3-yl)oxy)hexyl)-1H-1,2,3-triazol-4-yl)methyl)-3-(3,4-dimethoxy phenyl)acrylamide (**13a-4**)*

The synthetic procedure of **13a-4** was similar to that of **13a-1**, except that a starting material **6a** was replaced by **6d**.

Yield 91%. ^{1}H NMR (400 MHz, $CDCl_3$) δ 7.59 (s, 1H), 7.51 (d, J = 15.6 Hz, 1H), 7.30 (d, J = 6.4 Hz, 1H), 7.06–6.92 (m, 4H), 6.78 (d, J = 8.4 Hz, 1H), 6.43–6.30 (m, 3H), 5.23–5.01 (m, 10H), 4.86 (s, 1H), 4.57 (d, J = 5.6 Hz, 1H), 4.16 (t, J = 7.6 Hz, 2H), 3.88–3.76 (m, 7H), 3.57 (s, 3H), 3.46–3.37 (m, 12H), 3.23–3.11 (m, 1H), 2.95–2.81 (m, 2H), 2.76–2.68 (m, 1H), 2.04 (d, J = 2.4 Hz, 1H), 1.74–1.65 (m, 2H), 1.35–1.23 (m, 4H), 0.84–0.79 (m, 2H); ^{13}C NMR (100 MHz, $CDCl_3$) δ 174.36, 166.42, 156.78, 156.34, 155.46, 150.63, 150.51, 149.03, 140.89, 135.93, 135.10, 127.80, 122.42, 121.91, 118.48, 111.03, 109.77, 109.14, 103.06, 98.54, 97.93, 96.17, 95.35, 94.50, 94.47, 77.99, 73.34, 69.32, 57.08, 56.24, 56.11, 55.95, 55.88, 55.80, 50.28, 30.02, 29.66, 29.13, 26.03, 25.31, 24.73.

*4.16. Synthesis of (E)-N-((1-(6-(((2R,3R)-5,7-dihydroxy-2-(3,4,5-trihydroxyphenyl) chroman-3-yl) oxy) hexyl)-1H-1,2,3-triazol-4-yl) methyl)-3-(3,4-dihydroxyphenyl) acrylamide (**2a-1**)*

Compound **13a-1** (50 mg, 0.06 mmol) was dissolved in a mixture of DCM (8 mL) and methanol (2 mL), and a solution of 12 M HCl (0.1 mL) was added. The mixture was stirred for 8 h at the room temperature. When the reaction was completed, the solvent was evaporated under the diminished pressure to obtain the crude residue, which was further purified with a reversed preparative HPLC to afford 13.1 mg of light-red powered solid (**2a-1**).

Yield, 35%. ^{1}H NMR (400 MHz, CD_3OD) δ 7.87 (d, J = 9.4 Hz, 1H), 7.43 (d, J = 15.6 Hz, 1H), 7.01 (t, J = 1.7 Hz, 1H), 6.90 (dt, J = 8.2, 2.6 Hz, 1H), 6.76 (dd, J = 8.2, 2.2 Hz, 1H), 6.53 (d, J = 8.9 Hz, 1H), 6.39 (d, J = 15.8 Hz, 3H), 6.01–5.82 (m, 1H), 4.53 (d, J = 8.2 Hz, 2H), 4.28 (dt, J = 20.7, 7.0 Hz, 3H), 3.92–3.78 (m, 1H), 3.67–3.55 (m, 1H), 3.52–3.45 (m, 1H), 3.20 (dt, J = 7.5, 4.0 Hz, 1H), 2.93–2.84 (m, 1H), 1.75 (dt, J = 13.2, 6.4 Hz, 2H), 1.43–1.26 (m, 6H). TOF-MS, *m/z*: [M + H$^+$], calcd for $C_{33}H_{37}N_4O_{10}^+$, 649.2504, found: 649.2510.

*4.17. Synthesis of (E)-N-((1-(6-(((2R,3R)-5,7-dihydroxy-2-(3,4,5-trihydroxyphenyl) chroman-3-yl)oxy)hexyl)-1H-1,2,3-triazol-4-yl) methyl)-3-(3,4-dihydroxyphenyl) acrylamide (**2a-2**)*

The preparation procedure of **2a-2** was similar to that of **2a-1**, only differing in the replacement of the starting material **13a** with **13b**.

Yield, 42%. ^{1}H NMR (400 MHz, CD_3OD) δ 7.85 (d, J = 7.6 Hz, 1H), 7.46 (d, J = 15.6 Hz, 1H), 7.10–7.06 (m, 1H), 6.99 (dd, J = 8.0, 2.4 Hz, 1H), 6.75 (dd, J = 8.0, 2.4 Hz, 1H), 6.56–6.28 (m, 3H), 4.74 (s, 1H), 4.64–4.39 (m, 3H), 4.32–4.14 (m, 2H), 3.89–3.74 (m, 4H), 3.48–3.37 (m, 1H), 3.20–3.11 (m, 1H), 2.88–2.79 (m, 1H), 2.64 (dd, J = 16.9, 4.4 Hz, 1H), 1.99 (s, 1H), 1.78–1.63 (m, 2H), 1.40–1.19 (m, 3H), 1.12–1.02 (m, 3H); ^{13}C NMR (100 MHz, CD_3OD) δ 169.15, 157.82, 157.51, 157.30, 149.92, 149.26, 146.76, 146.54, 142.70, 133.93, 133.40, 131.79, 128.12, 124.57, 123.36, 118.28, 116.46, 111.56, 107.29, 106.91, 100.10, 79.22, 75.46, 70.18, 56.38, 51.43, 35.76, 31.21, 31.15, 26.91, 26.34, 25.59. TOF-MS, *m/z*: [M + Na$^+$], calcd for $C_{34}H_{38}N_4NaO_{10}^+$, 685.2480, found: 685.2487.

*4.18. Synthesis of (E)-N-((1-(6-(((2R,3R)-5,7-dihydroxy-2-(3,4,5-trihydroxyphenyl) chroman-3-yl) oxy) hexyl)-1H-1,2,3-triazol-4-yl) methyl)-3-(3,4-dihydroxyphenyl) acrylamide (**2a-3**)*

The preparation procedure of **2a-3** was similar as that of **2a-1**, only differing in the replacement of the starting material **13a** with **13c**.

Yield, 43%. ^{1}H NMR (400 MHz, CD_3OD) δ 7.90 (d, J = 9.0 Hz, 1H), 7.52–7.43 (m, 1H), 7.09–6.99 (m, 2H), 6.93 (dd, J = 8.4, 7.2 Hz, 1H), 6.54 (d, J = 1.2 Hz, 1H), 6.49–6.40 (m, 2H), 5.97–5.82 (m, 2H), 4.59–4.53 (m, 2H), 4.31 (dt, J = 13.6, 7.2 Hz, 2H), 3.89 (d, J = 2.4 Hz, 3H), 3.64 (td, J = 7.4, 4.8 Hz, 1H), 3.54–3.44 (m, 2H), 3.22 (dt, J = 11.2, 6.4 Hz, 1H), 2.93–2.85 (m, 1H), 2.69 (dd, J = 16.8, 4.4 Hz, 1H), 1.82–1.59 (m, 4H), 1.37 (d, J = 16.8 Hz, 4H). TOF-MS, *m/z*: [M + Na$^+$], calcd for $C_{34}H_{38}N_4NaO_{10}^+$, 685.2480, found: 685.2484.

*4.19. Synthesis of (E)-N-((1-(6-(((2R,3R)-5,7-dihydroxy-2-(3,4,5-trihydroxyphenyl) chroman-3-yl)oxy)hexyl)-1H-1,2,3-triazol-4-yl) methyl)-3-(3,4-dimethoxyphenyl) acrylamide (**2a-4**)*

The preparation procedure of **2a-4** was similar as that of **2a-1**, only differing in the replacement of the starting material **13a** with **13d**.

Yield, 46%.^{1}H NMR (400 MHz, CD_3OD) δ 7.81 (d, J = 6.4 Hz, 1H), 7.43 (d, J = 15.6 Hz, 1H), 7.11–6.93 (m, 2H), 6.83 (dd, J = 8.4, 6.0 Hz, 1H), 6.45 (d, J = 6.0 Hz, 2H), 6.37 (d, J = 25.6 Hz, 1H), 4.69 (s, 1H), 4.51–4.43 (m, 2H), 4.28–4.10 (m, 2H), 3.78–3.70 (m, 7H), 3.46–3.30 (m, 1H), 3.14–3.04 (m, 1H), 2.84–2.72 (m, 1H), 2.59 (dd, J = 16.8, 4.2 Hz, 1H), 1.75–1.52 (m, 2H), 1.38–1.14 (m, 3H), 1.15–0.82 (m, 5H); ^{13}C NMR (100 MHz, CD_3OD) δ 168.94, 157.81, 157.50, 157.29, 152.22, 150.58, 146.74, 146.53, 145.82, 142.35, 133.40, 129.14, 124.61, 123.36, 119.16, 112.65, 111.32, 111.29, 107.31, 106.95, 100.12, 79.19, 75.42, 70.18, 56.43, 56.39, 51.46, 35.75, 31.11, 30.16, 26.90, 26.32, 25.59; TOF-MS, *m/z*: [M + Na$^+$], calcd for $C_{35}H_{40}N_4NaO_{10}^+$, 699.2637, found: 699.2640.

*4.20. Synthesis of (E)-N-((1-(8-(((2R,3R)-5,7-dihydroxy-2-(3,4,5-trihydroxyphenyl) chroman-3-yl)oxy)octyl)-1H-1,2,3-triazol-4-yl) methyl)-3-(3,4-dihydroxyphenyl) acrylamide (**2b-1**)*

The preparation procedure of **2b-1** was similar to that of **2a-1**, only differing in the replacement of the starting material **12a** with **12b**.

Yield, 37%. ^{1}H NMR (400 MHz, CD_3OD) δ 7.90 (s, 1H), 7.44 (d, J = 15.6 Hz, 1H), 7.10–6.70 (m, 7H), 6.40 (d, J = 15.6 Hz, 1H), 4.56 (s, 1H), 4.39 (m, 4H), 3.54 (t, J = 6.4 Hz, 1H), 3.35–3.21 (m, 1H), 3.07–2.85 (m, 1H), 2.73–2.60 (m, 2H), 2.52 (t, J = 6.4 Hz, 1H), 1.30–0.83 (m, 12H); TOF-MS, *m/z*: [M + Na$^+$], calcd for $C_{35}H_{40}N_4NaO_{10}^+$, 699.2637, found: 699.2634.

*4.21. Synthesis (E)-N-((1-(8-(((2R,3R)-5,7-dihydroxy-2-(3,4,5-trihydroxyphenyl) chroman-3-yl) oxy)octyl)-1H-1,2,3-triazol-4-yl) methyl)-3-(3-hydroxy-4-methoxy phenyl) acrylamide (**2b-2**)*

The preparation procedure of **2b-2** was similar as that of **2a-2**, only differing in the replacement of the starting material **12a** with **12b**.

Yield, 43%. ^{1}H NMR (400 MHz, CD_3OD) δ 7.69 (d, J = 2.8 Hz, 1H), 7.30 (d, J = 15.6 Hz, 1H), 6.89 (d, J = 1.8 Hz, 1H), 6.82 (dd, J = 8.4, 1.8 Hz, 1H), 6.61 (d, J = 8.4 Hz, 1H), 6.41–6.22 (m, 3H), 4.59 (s, 1H), 4.47–4.29 (m, 3H), 4.21–4.08 (m, 2H), 3.66 (s, 3H), 3.31–3.17 (m, 1H), 3.06–2.92 (m, 1H), 2.74–2.58 (m, 1H), 2.51 (dd, J = 16.8, 4.2 Hz, 1H), 1.69–1.57 (m, 2H), 1.28–0.76 (m, 12H); ^{13}C NMR (100 MHz, CD_3OD) δ 169.03, 157.79, 157.49, 157.30, 150.91, 147.82, 146.73, 146.49, 145.85, 142.48, 133.46, 131.63, 129.23, 124.67, 122.32, 118.82, 114.55, 112.48, 107.17, 106.98, 100.18, 79.24, 75.51, 70.71, 56.35, 51.65, 35.66, 31.09, 30.43, 30.02, 29.83, 27.25, 27.23, 26.81; TOF-MS, *m/z*: [M + Na$^+$], calcd for $C_{36}H_{42}N_4NaO_{10}^+$, 713.2793, found: 713.2796.

*4.22. Synthesis of (E)-N-((1-(8-(((2R,3R)-5,7-dihydroxy-2-(3,4,5-trihydroxyphenyl) chroman-3-yl)oxy)octyl)-1H-1,2,3-triazol-4-yl) methyl)-3-(4-hydroxy-3-methoxy phenyl)acrylamide (**2b-3**)*

The preparation procedure of **2b-3** was similar as that of **2a-3**, only differing in the replacement of the starting material **11a** with **11b**.

Yield, 43%. ^{1}H NMR (400 MHz, CD_3OD) δ 7.82 (d, J = 2.9 Hz, 1H), 7.36 (d, J = 15.6 Hz, 1H), 6.94 (d, J = 2.0 Hz, 1H), 6.88 (dd, J = 8.4, 2.0 Hz, 1H), 6.79 (dd, J = 8.4, 3.2 Hz, 1H), 6.45–6.28 (m, 3H), 4.68 (s, 1H), 4.49–4.45 (m, 2H), 4.30–4.22 (m, 2H), 3.78–3.72 (m, 4H), 3.39–3.29 (m, 1H), 3.14–3.05 (m, 1H), 2.79–2.70 (m, 1H), 2.59 (dd, J = 16.8, 4.4 Hz, 1H), 1.79–1.69 (m, 2H), 1.37–0.86 (m, 12H); ^{13}C NMR (100 MHz, CD_3OD) δ 169.11, 157.75, 157.43, 157.25, 149.80, 149.17, 146.70, 146.45, 145.94, 145.92, 142.68, 133.43, 131.61, 128.08, 124.50, 124.47, 123.35, 118.23, 116.44, 111.52, 107.15, 107.00, 100.18, 79.20, 75.44, 70.74, 56.37, 51.52, 35.73, 31.07, 30.40, 29.99, 29.97, 29.81, 27.21, 26.78. TOF-MS, *m/z*: [M + Na^+], calcd for $C_{36}H_{42}N_4NaO_{10}^+$, 713.2793, found: 713.2791.

*4.23. Synthesis of (E)-N-((1-(8-(((2R,3R)-5,7-dihydroxy-2-(3,4,5-trihydroxyphenyl) chroman-3-yl)oxy)octyl)-1H-1,2,3-triazol-4-yl) methyl)-3-(3,4-dimethoxyphenyl) acrylamide (**2b-4**)*

The preparation procedure of **2b-4** was similar as that of **2a-4**, only differing in the replacement of the starting material **11a** with **11b**.

Yield, 46 %.^{1}H NMR (400 MHz, CD_3OD) δ 7.87 (d, J = 3.7 Hz, 1H), 7.45 (d, J = 15.6 Hz, 1H), 7.13–6.98 (m, 2H), 6.87 (dd, J = 8.4, 2.8 Hz, 1H), 6.49–6.33 (m, 3H), 4.72 (s, 1H), 4.59–4.46 (m, 3H), 4.38–4.28 (m, 2H), 3.83–3.76 (m, 6H), 3.62–3.52 (m, 1H), 3.43–3.35 (m, 1H), 3.18–3.11 (m, 1H), 2.84–2.75 (m, 1H), 2.44 (dd, J = 16.0, 8.0 Hz, 1H), 1.85–1.73 (m, 2H), 1.39–0.96 (m, 12H); ^{13}C NMR (100 MHz, CD_3OD) δ 168.94, 157.74, 157.48, 156.81, 152.27, 150.62, 146.75, 146.52, 145.96, 142.31, 133.94, 131.75, 129.16, 124.56, 123.37, 119.14, 112.66, 111.31, 107.18, 106.97, 100.60, 81.27, 76.95, 70.47, 56.45, 56.39, 51.57, 35.74, 31.14, 30.64, 29.97, 29.90, 27.24, 27.22, 26.80. TOF-MS, *m/z*: [M + Na^+], calcd for $C_{37}H_{44}N_4NaO_{10}^+$, 727.2950, found: 727.2957.

*4.24. Synthesis of (E)-N-((1-(5-(((2R,3R)-6,8-bis(methoxymethoxy)-2-(3,4,5-tris(methoxymethoxy)phenyl)chroman-3-yl)oxy)pentyl)-1H-1,2,3-triazol-4-yl)methyl)-3-(3,4-dihydroxyphenyl)acrylamide (**13c**)*

The synthetic procedure of **13c** was similar to that of **13a-1**, except that a starting material **12a** was replaced by **12c**.

Yield, 86 %. ^{1}H NMR (400 MHz, $CDCl_3$) δ 7.49 (s, 1H), 7.38–7.30 (m, 1H), 7.19 (m, 1H), 7.04 (s, 1H), 7.00 (d, J = 8.0 Hz, 1H), 6.72 (s, 1H), 6.38 (d, J = 8.0 Hz, 2H), 5.34–5.07 (m, 11H), 4.91 (d, J = 12.0 Hz, 1H), 4.52 (s, 1H), 4.10 (t, J = 12.0 Hz, 1H), 3.62–3.36 (m, 18H), 3.27–3.11 (m, 1H), 2.97 (m, d, J = 20.0 Hz, 1H), 2.78–2.70 (m, 1H), 1.67–1.40 (m, 6H); ^{13}C NMR (100 MHz, $CDCl_3$) δ 167.23, 156.93, 156.90, 156.44, 155.57,155.52, 150.78, 147.17, 144.76, 141.77, 136.12, 135.97, 135.26, 135.11, 127.12, 122.37, 115.50, 109.32, 109.17, 103.13, 103.09, 98.68, 98.08, 96.29, 95.50, 94.65, 94.61, 78.13, 73.59, 69.57, 57.22, 56.41, 56.26, 56.11, 45.03 , 32.32, 29.81, 28.87, 24.90, 23.40.

*4.25. Synthesis of (E)-N-((1-(5-(((2R,3R)-6,8-dihydroxy-2-(3,4,5-trihydroxyphenyl)chroman-3-yl)oxy)pentyl)-1H-1,2,3-triazol-4-yl) methyl)-3-(3,4-dihydroxyphenyl)acrylamide (**2c**)*

The preparation procedure of **2c** was similar to that of **2a-1**, only differing in the replacement of the starting material **11a** with **13c**.

Yield, 48%. ^{1}H NMR (400 MHz, CD_3OD) δ 7.18–6.84 (m, 3H), 6.60–6.35 (m, 4H), 5.81 (d, J = 25.0 Hz, 1H), 4.63 (s, 1H), 4.23 (s, 1H), 4.13–3.91 (m, 2H), 3.93–3.82 (m, 1H), 3.78 (s, 1H), 3.68 (s, 1H), 3.30 (s, 1H), 3.22 (d, J = 12.4 Hz, 1H), 3.05(t, J = 7.8 Hz, 1H), 2.64–2.51 (m, 6H), 2.31 (t, J = 7.8 Hz, 1H), 1.80 (s, 1H), 1.54 (t, J = 8.4 Hz, 2H), 1.38–1.13 (m, 5H); TOF-MS, *m/z*: [M + Na^+], calcd for $C_{32}H_{34}N_4NaO_{10}^+$, 657.2167, found: 657.2172.

*4.26. Synthesis of (2R,3R)-5,7-bis(benzyloxy)-2-(3,4,5-tris(benzyloxy) phenyl) chroman-3-yl3,4,5-tris(benzyloxy)benzoate (**14**)*

Commercially available EGCG (2.0 g, 4.3 mmol*)* was taken up in anhydrous DMF (30 mL), and NaH coated with mineral oil (60%, 2.6 g, 65 mmol) and BnBr (11.2 g, 65 mmol) were added in order. The reaction was stirred for 48 h, and water (15 mL) was added slowly to quench the reaction, and ethyl acetate (200 mL) was used for extraction twice. The combined organic layer was washed with water and brine in order, and dried with anhydrous Na_2SO_4, and the filter was evaporated under reduced pressure to offer the crude residue, which was purified by a silica gel chromatography with a mixture of ethyl acetate and petroleum ether (V/V = 1/6) as an eluent to afford 3.7 g of compound **14** as a light-yellow solid.

Yield, 72%. ^{1}H NMR (400 MHz, $CDCl_3$) δ 7.42–7.04 (m, 42H), 6.65 (d, J = 11.4 Hz, 2H), 6.29 (dd, J = 21.7, 11.4 Hz, 2H), 5.59 (d, J = 11.4 Hz, 1H), 5.02–4.53 (m, 17H), 3.10–2.92 (m, 2H).

*4.27. Synthesis of (2R,3R)-5,7-bis(benzyloxy)-2-(3,4,5-tris(benzyloxy) phenyl) chroman-3-ol (**15**)*

To a solution of **14** (0.5 g, 0.42 mmol) dissolved in a mixture of methanol (5.0 mL) and glycol dimethyl ether (5.0 mL) was added potassium carbonate (0.46 g, 3.3 mmol) and a little water (15 μL), and the mixture was stirred for 5.0 h at room temperature. After all the starting materials were consumed, ethyl acetate (200 mL) and water (100 mL) were added in order. The organic layer was washed with water (50 mL) and brine (40 mL), and dried with anhydrous Na_2SO_4, and filtered, and then evaporated under reduced pressure to obtain the crude residue, which was purified by a silica gel column chromatography with a mixture of ethyl acetate and petroleum ether (V/V = 1/4) as an eluent to afford 263.9 mg of compound **15** as a yellow solid.

Yield, 83%. ^{1}H NMR (400 MHz, $CDCl_3$) δ 7.39–7.14 (m, 27H), 6.73 (s, 1H), 6.19 (d, J = 6.1 Hz, 1H), 5.11–4.67 (m, 11H), 4.16–4.07 (m, 1H), 3.99 (t, J = 2.2 Hz, 1H), 3.05–2.73 (m, 2H); ^{13}C NMR (100 MHz, $CDCl_3$) δ 158.93, 158.44, 153.16, 137.95, 137.11, 137.07, 137.04, 133.88, 128.74, 128.71, 128.67, 128.62, 128.58, 128.55, 128.31, 128.28, 128.21, 128.14, 128.05, 128.03, 127.99, 127.96, 127.77, 127.70, 127.67, 106.25, 105.69, 101.11, 78.69, 75.37, 71.46, 71.23, 70.29, 66.56, 28.25.

*4.28. Synthesis of (2R,3R)-6,8-bis(benzyloxy)-3-((6-chlorohexyl)oxy)-2-(3,4,5-tris(benzyloxy) phenyl)chromane (**16a**)*

Compound **15** (2.0 g, 2.6 mmol) was dissolved in anhydrous DMF (30 mL), and then NaH (530 mg, 22.1 mmol) was added in batches, and finally 1-bromo-6-chlorohexane (1.0 g, 5.0 mmol) was introduced dropwise. The mixture was stirred for 16 h at room temperature. After all the starting materials were consumed, the addition of water (10.0 mL) was used to carefully quench the mixture. Ethyl acetate (100 mL) was added to extract the target compound. The organic layer was washed with water and brine, and dried with anhydrous Na_2SO_4, and filtered, and then condensed under the diminished pressure to afford the crude residue, which was further purified by a silica-gel column chromatogram with a mixture of petrol ether and ethyl acetate (V/V = 5/1) as an eluent to afford 1.8 g of compound **16a** as a yellow solid.

Yield, 78%, ^{1}H NMR (400 MHz, $CDCl_3$) δ 7.42–6.95 (m, 25H), 6.74 (s, 2H), 6.22–6.11 (m, 2H), 5.07–4.77 (m, 10H), 4.17–3.92 (m, 1H), 3.69 (s, 1H), 3.37–2.99 (m, 4H), 2.99–2.56 (m, 2H), 1.63–1.51 (m, 2H), 1.27–1.17 (m, 3H), 1.09–0.94 (m, 2H), 0.85–0.75 (m, 1H); ^{13}C NMR (100 MHz, $CDCl_3$) δ 162.58, 158.65, 158.04, 155.50, 152.53, 137.94, 137.21, 137.17, 137.13, 137.02, 134.57, 129.77, 129.02, 128.79, 128.62, 128.57, 128.54, 128.52, 128.50, 128.47, 128.44, 128.41, 128.24, 128.21, 128.18, 128.15, 128.00, 127.92, 127.87, 127.84, 127.80, 127.78, 127.70, 127.60, 127.57, 127.54, 127.50, 127.46, 127.26, 106.70, 106.18, 105.57, 101.62, 78.28, 75.26, 73.90, 71.24,

70.12, 69.96, 69.66, 51.27, 29.75, 29.21, 28.56, 24.99, 23.21.

4.29. Synthesis of (2R,3R)-3-((6-azidohexyl)oxy)-5,7-bis(benzyloxy)-2-(3,4,5-tris (benzyl oxy)phenyl) chromane (**17a**)

To a solution of **16a** (1.0 g, 1.1 mmol) dissolved in anhydrous DMF (15.0 mL) was added sodium azide (378.0 mg, 5.8 mmol), and then the mixture was heated to 60 ℃ and stirred for 6.0 h. When the reaction was over, water (10 mL) was added to quench the reaction, and ethyl acetate (50 mL) was subsequently added. The organic layer was washed with water (100 mL) and brine (50 mL), and dried with anhydrous Na_2SO_4, and the filter was condensed under the diminished pressure. The crude residue was further purified by a silica-gel column chromatogram with a mixture of petrol ether and ethyl acetate (V/V = 5/1) as an eluent to afford 796 mg of compound **17a** as a yellow solid.

Yield, 82%. ^{1}H NMR (400 MHz, $CDCl_3$) δ 7.37–7.08 (m, 27H), 6.75 (s, 1H), 6.27–6.09 (m, 1H), 5.12–4.79 (m, 10H), 3.97 (s, 1H), 3.70 (s, 1H), 3.34–3.20 (m, 1H), 3.07–2.65 (m, 5H), 1.36–1.01 (m, 8H); ^{13}C NMR (100 MHz, $CDCl_3$) δ 158.71, 158.09, 155.56, 152.59, 152.43, 137.99, 137.23, 137.18, 137.06, 134.88, 134.61, 129.70, 128.72, 128.67, 128.62, 128.55, 128.52, 128.49, 128.40, 128.23, 128.20, 128.14, 128.04, 127.97, 127.92, 127.88, 127.85, 127.80, 127.78, 127.74, 127.62, 127.54, 127.51, 127.33, 127.31, 127.29, 127.26, 106.80, 106.27, 101.66, 94.87, 93.91, 78.33, 75.28, 73.97, 71.31, 71.05, 70.59, 70.18, 70.01, 51.32, 29.27, 28.61, 26.65, 25.05, 23.26.

4.30. Synthesis of N-((1-(6-(((2R,3R)-6,8-bis(benzyloxy)-2-(3,4,5-tris (benzyloxy) phenyl)chroman-3-yl)oxy)hexyl)-1H-1,2,3-triazol-4-yl) methyl)-3-(3,4-dihydroxy phenyl)propenamide (**18a-1**)

The synthetic procedure of **18a-1** was similar to that of **13a-1** except for the replacement of **12a** with **17a**.

Yield, 66 %. ^{1}H NMR (400 MHz, $CDCl_3$) δ 7.29–6.57 (m, 31H), 6.13 (d, J = 8.4 Hz, 1H), 5.88 (d, J = 15.6 Hz, 1H), 5.07–4.72 (m, 10H), 4.22 (s, 2H), 4.00–3.60 (m, 5H), 3.31–3.13 (m, 1H), 2.96–2.62 (m, 4H), 2.22–1.84 (m, 2H), 1.54–1.29 (m, 3H), 0.94–0.63 (m, 5H); ^{13}C NMR (100 MHz, $CDCl_3$) δ 167.26, 158.73, 158.13, 155.50, 152.57, 152.42, 147.12, 144.71, 141.96, 137.69, 137.13, 137.03, 137.00, 136.97, 134.99, 128.85, 128.76, 128.69, 128.65, 128.64, 128.60, 128.55, 128.50, 128.44, 128.40, 128.34, 128.23, 128.18, 128.09, 128.04, 127.91, 127.87, 127.84, 127.64, 127.61, 127.37, 127.34, 127.28, 122.94, 122.29, 117.14, 115.48, 113.84, 110.21, 106.46, 105.92, 101.64, 95.00, 94.06, 78.29, 75.47, 73.89, 71.29, 71.03, 70.24, 70.09, 69.25, 29.89, 29.82, 29.44, 28.92, 27.34, 24.95, 21.86.

4.31. Synthesis of N-((1-(6-(((2R,3R)-6,8-bis(benzyloxy)-2-(3,4,5-tris (benzyloxy) phenyl)chroman-3-yl)oxy)hexyl)-1H-1,2,3-triazol-4-yl) methyl)-3-(4-hydroxy-3-methoxyphenyl) propanamide (**18a-2**)

The synthetic procedure of **18a-2** was similar to that of **13a-2** except for the replacement of **12** with **17a**.

Yield, 65%. ^{1}H NMR (400 MHz, $CDCl_3$) δ 7.44–7.02 (m, 27H), 6.98–6.62 (m, 6H), 6.22–6.08 (m, 2H), 5.05–4.70 (m, 10H), 4.33 (t, J = 6.8 Hz, 2H), 4.09–3.83 (m, 3H), 3.78–3.49 (m, 4H), 3.36–3.19 (m, 1H), 3.10–2.55 (m, 5H), 1.58–1.43 (m, 2H), 1.27–1.14 (m, 4H), 0.94–0.88 (m, 2H), 0.86–0.71 (m, 2H); ^{13}C NMR (100 MHz, $CDCl_3$) δ 166.38, 158.63, 158.05, 155.48, 152.49, 152.34, 147.64, 146.94, 141.13, 137.80, 137.63, 137.10, 137.04, 136.97, 134.79, 128.71, 128.66, 128.61, 128.57, 128.53, 128.48, 128.46, 128.42, 128.35, 128.23, 128.09, 128.00, 127.96, 127.92, 127.74, 127.55, 127.51, 127.48, 127.28, 127.24, 127.19, 122.28, 122.19, 118.03, 114.93, 109.88, 106.45, 101.63, 94.88, 93.90, 78.30, 75.28, 73.79, 71.18, 70.92, 70.12, 69.95, 69.43, 55.88, 50.23, 34.93, 30.22, 29.73, 29.40, 29.35, 26.23, 25.50, 24.91.

4.32. Synthesis of N-((1-(6-(((2R,3R)-6,8-bis(benzyloxy)-2-(3,4,5-tris (benzyloxy) phenyl)chroman-3-yl)oxy)hexyl)-1H-1,2,3-triazol-4-yl) methyl)-3-(3-hydroxy-4-methoxyphenyl) propanamide (**18a-3**)

The synthetic procedure of **18a-3** was similar to that of **13a-3** except for replacement of **12** with **17a**.

Yield, 61% .^{1}H NMR (400 MHz, $CDCl_3$) δ 7.31–6.90 (m, 29H), 6.79–6.49 (m, 4H), 6.13 (d, J = 11.4 Hz, 2H), 5.00–4.55 (m, 11H), 4.46–4.16 (m, 2H), 4.12–3.75 (m, 4H), 3.77–3.48 (m, 4H), 3.36–3.09 (m, 1H), 2.97–2.53 (m, 3H), 1.52–1.38 (m, 2H), 1.32–1.02 (m, 5H), 1.01–0.65 (m, 3H); ^{13}C NMR (100 MHz, $CDCl_3$) δ 171.21, 166.44, 158.63, 158.04, 155.46, 152.55, 152.50, 152.35, 148.44, 146.01, 140.83, 137.74, 137.57, 137.07, 137.00, 136.97, 134.81, 128.64, 128.60, 128.56, 128.53, 128.49, 128.41, 128.35, 128.22, 128.12, 128.08, 127.98, 127.95, 127.92, 127.90, 127.74, 127.54, 127.50, 127.47, 127.28, 127.24, 127.19, 121.66, 118.64, 112.84, 110.70, 106.48, 105.97, 101.58, 94.90, 93.91, 78.22, 75.29, 73.80, 71.19, 70.93, 70.11, 69.97, 69.21, 60.44, 55.87, 50.21, 34.88, 29.95, 28.91, 24.88, 23.00, 21.07, 14.23.

4.33. Synthesis of N-((1-(6-(((2R,3R)-6,8-bis(benzyloxy)-2-(3,4,5-tris (benzyloxy)phenyl) chroman-3-yl)oxy)hexyl)-1H-1,2,3-triazol-4-yl) methyl)-3-(3,4-dimethoxy phenyl) propanamide (**18a-4**)

The synthetic procedure of **18a-4** was similar to that of **13a-4** except for replacement of **12** with **17a**.

Yield, 66%. ^{1}H NMR (400 MHz, $CDCl_3$) δ 7.55–7.29 (m, 10H), 7.26–6.67 (m, 22H), 6.25 (dd, J = 33.8, 15.8 Hz, 2H), 5.16–4.69 (m, 10H), 4.41 (d, J = 7.2 Hz, 2H), 4.07–3.87 (m, 4H), 3.72 (s, 6H), 3.39–3.20 (m, 1H), 3.20–2.64 (m, 3H), 1.65–1.48 (m, 2H), 1.27–1.10 (m, 4H), 1.07–0.86 (m, 4H); ^{13}C NMR (100 MHz, $CDCl_3$) δ 166.22, 166.19, 158.50, 157.92, 155.38, 152.36, 152.21, 150.36, 148.91, 137.70, 137.51, 137.16, 136.98, 136.91, 134.68, 128.54, 128.45, 128.39, 128.35, 128.28, 128.22, 128.08, 127.96, 127.88, 127.84, 127.78, 127.75, 127.60, 127.44, 127.40, 127.37, 127.34, 127.14, 127.10, 127.05, 122.25, 121.72, 118.53, 110.96, 109.88, 109.81, 106.34, 105.83, 101.51, 94.77, 93.75, 78.13, 75.13, 73.65, 71.03, 70.77, 69.96, 69.79, 69.31, 55.75, 55.68, 50.05, 34.78, 30.07, 29.59, 29.24, 26.10, 25.37, 14.11.

4.34. Synthesis of N-((1-(5-(((2R,3R)-5,7-dihydroxy-2-(3,4,5-trihydroxy phenyl) chroman-3-yl)oxy)pentyl)-1H-1,2,3-triazol-4-yl) methyl)-3-(3,4-dihydroxyphenyl) propenamide (**3a-1**)

Compound **18a-1** (100 mg, 0.09 mmol) was dissolved in a mixture of ethyl acetate (8.0 mL) and methanol (8.0 mL), and a catalytic amount of 20% Pd $(OH)_2$ was added. The mixture was stirred for 8 h at room temperature at the atmosphere of hydrogen gas. After the reaction was over, Pd $(OH)_2$ was filtered and the solvent was generally evaporated under the diminished pressure to obtain the crude residue, which was further purified with a reversed preparative HPLC to afford 24.2 mg of a light-red powered solid.

Yield, 41%. ^{1}H NMR (400 MHz, CD_3OD) δ 7.34 (s, 1H), 6.72–6.59 (m, 3H), 6.57–6.44 (m, 4H), 4.79 (s, 1H), 4.37 (s, 2H), 4.24 (t, J = 7.1 Hz, 2H), 3.85 (dt, J = 4.4, 2.4 Hz, 1H), 3.45 (dt, J = 9.8, 6.0 Hz, 1H), 3.21 (dt, J = 9.8, 6.0 Hz, 1H), 2.86 (dd, J = 16.8, 2.8 Hz, 1H), 2.77 (t, J = 7.2 Hz, 2H), 2.69 (dd, J = 16.8, 4.4 Hz, 1H), 2.46 (t, J = 7.2 Hz, 2H), 1.74–1.68 (m, 2H), 1.34–1.26 (m, 6H); ^{13}C NMR (100 MHz, CD_3OD) δ 175.42, 157.83, 157.54, 157.31, 146.55, 146.13, 144.63, 133.55, 133.42, 133.39, 131.77, 130.84, 124.07, 121.39, 120.75, 116.75, 116.34, 106.91, 100.10, 79.23, 75.56, 70.36, 51.42, 38.91, 35.62, 32.15, 31.27, 30.26, 27.00, 26.44; TOF-MS, m/z: [M + Na^+], calcd for $C_{33}H_{38}N_4NaO_{10}^+$, 673.2480, found: 673.2475.

*4.35. Synthesis of N-((1-(5-(((2R,3R)-5,7-dihydroxy-2-(3,4,5-trihydroxyphenyl) chroman-3-yl)oxy)pentyl)-1H-1,2,3-triazol-4-yl) methyl)-3-(3-hydroxy-4-methoxy phenyl) propenamide (**3a-2**)*

The synthetic procedure behaved as that of **3a-2**, the only difference was conducted that starting material **18a-2** was substituted for **18a-1**.

Yield, 44%.^{1}H NMR (400 MHz, CD_3OD) δ 7.34 (s, 1H), 6.76 (s, 1H), 6.69–6.58 (m, 3H), 6.50 (d, J = 2.8 Hz, 2H), 5.90 (d, J = 13.2 Hz, 1H), 4.78 (s, 1H), 4.39–4.35 (m, 2H), 4.22 (t, J = 7.6 Hz, 2H), 3.86–3.83 (m, 1H), 3.76 (s, 3H), 3.47–3.42 (m, 1H), 3.24–3.18 (m, 1H), 2.86–2.81 (m, 3H), 2.72–2.64 (m, 1H), 2.52–2.47 (m, 2H), 1.72–1.66 (m, 2H), 1.33–1.29 (m, 4H), 1.11–1.07 (m, 2H); ^{13}C NMR (100 MHz, CD_3OD) δ 175.38, 157.84, 157.54, 157.31, 153.07, 148.86, 148.83, 146.56, 146.26, 145.85, 133.50, 131.78, 130.84, 124.05, 121.90, 116.12, 113.22, 106.91, 100.10, 79.24, 75.54, 70.32, 56.33, 51.37, 38.89, 35.62, 32.35, 31.26, 30.25, 28.10, 26.98, 26.43; TOF-MS, *m/z*: [M + Na^+], calcd for $C_{34}H_{40}N_4NaO_{10}^+$, 687.2637, found: 687.2640.

*4.36. Synthesis of N-((1-(5-(((2R,3R)-5,7-dihydroxy-2-(3,4,5-trihydroxyphenyl) chroman-3-yl)oxy)pentyl)-1H-1,2,3-triazol-4-yl) methyl)-3-(4-hydroxy-3-methoxy phenyl) propenamide (**3a-3**)*

The synthetic procedure behaved as that of **3a-3**, the only difference was conducted that starting material **18a-3** substituted for **18a-1.**

Yield, 45%.^{1}H NMR (400 MHz, CD_3OD) δ 7.41 (s, 1H), 6.77 (d, J = 8.2 Hz, 2H), 6.71–6.54 (m, 3H), 6.51 (s, 2H), 4.78 (s, 1H), 4.37 (s, 2H), 4.22–4.12 (m, 2H), 3.88–3.81 (m, 1H), 3.77 (s, 3H), 3.50–3.41 (m, 1H), 3.22–3.14 (m, 1H), 2.88–2.65 (m, 4H), 2.50–2.39 (m, 2H), 1.65–1.54 (m, 2H), 1.41–1.27 (m, 4H), 1.09–0.98 (m, 2H); ^{13}C NMR (101 MHz, CD_3OD) δ 175.34, 157.82, 157.53, 157.29, 147.44, 147.34, 146.58, 146.03, 134.92, 133.39, 131.86, 131.78, 124.24, 120.61, 116.58, 112.86, 106.95, 106.93, 100.07, 79.19, 75.62, 70.22, 56.50, 51.49, 38.77, 35.55, 32.09, 30.96, 29.85, 25.59, 24.09. TOF-MS, *m/z*: [M + Na^+], calcd for $C_{34}H_{40}N_4NaO_{10}^+$, 687.2637, found: 687.2643.

*4.37. Synthesis of N-((1-(5-(((2R,3R)-5,7-dihydroxy-2-(3,4,5-trihydroxyphenyl) chroman-3-yl)oxy)pentyl)-1H-1,2,3-triazol-4-yl) methyl)-3-(3,4-dimethoxyphenyl) propenamide (**3a-4**)*

The synthetic procedure behaved as that of **3a-4**, the only difference was conducted that starting material **18a-4** substituted for **18a-1.**

Yield, 41%.^{1}H NMR (400 MHz, CD_3OD) δ 7.45 (s, 1H), 6.98–6.74 (m, 3H), 6.72 (d, J = 8.4 Hz, 1H), 6.50 (d, J = 2.8 Hz, 2H), 5.91 (d, J = 2.8 Hz, 1H), 4.78 (s, 1H), 4.37 (s, 2H), 4.25–4.16 (m, 2H), 3.87–3.79 (m, 1H), 3.75 (d, J = 7.6 Hz, 6H), 3.48–3.41 (m, 1H), 3.23–3.16 (m, 1H), 2.92–2.80 (m, 3H), 2.67 (d, J = 16.8 Hz, 1H), 2.54–2.44 (m, 2H), 1.69 (t, J = 7.6 Hz, 2H), 1.32 (dd, J = 18.0, 10.4 Hz, 6H); ^{13}C NMR (100 MHz, CD_3OD) δ 175.29, 157.85, 157.55, 157.33, 150.28, 148.86, 146.56, 146.15, 134.97, 133.43, 131.79, 130.84, 124.10, 121.74, 113.54, 113.12, 106.91, 100.09, 79.25, 75.53, 70.28, 56.55, 56.38, 51.36, 49.64, 38.79, 35.60, 32.29, 31.23, 30.25, 26.99, 26.44, 25.62; TOF-MS, *m/z*: [M + Na^+], calcd for $C_{35}H_{42}N_4NaO_{10}^+$, 701.2793, found: 701.2797.

*4.38. Synthesis of (2R,3R)-5,7-dibenzyl-3-((8-chlorooctyl)oxy)-2-(3,4,5-tribenzyl phenyl)chromane (**16b**)*

The synthetic procedure of **16b** was similar to that of **16a,** only differing in the replacement of 1-bromo-6-chlorohexane with 1-bromo-8-chlorooctane.

Yield, 75%. ^{1}H NMR (400 MHz, $CDCl_3$) δ 7.49–7.25 (m, 25H), 6.89 (s, 2H), 6.30 (d, J = 20.2 Hz, 2H), 5.15–4.88 (m, 11H), 3.80 (s, 1H), 3.48–3.32 (m, 2H), 3.26–3.11 (m, 2H), 3.03–2.75 (m, 2H), 1.73–1.64 (m, 2H), 1.42–1.31 (m, 4H), 1.29–1.24 (m, 3H), 1.16–1.12 (m, 3H); ^{13}C NMR (100 MHz, $CDCl_3$) δ 158.51, 157.91, 155.44, 152.37, 137.87, 137.74, 137.08, 137.03, 136.92, 134.53, 128.59, 128.45, 128.41, 128.34, 128.29, 128.04, 128.02, 127.97, 127.88, 127.82, 127.75, 127.72, 127.66, 127.63, 127.60, 127.56, 127.40, 127.36, 127.32, 127.13, 127.09, 127.06, 106.58, 101.60, 94.75, 93.70, 78.13, 75.10, 73.73, 71.03, 70.77, 69.92, 69.89, 69.75, 62.63, 33.99, 32.63, 29.63, 29.22, 28.66, 28.04, 25.90.

*4.39. Synthesis of (2R,3R)-3-((8-azidooctyl)oxy)-5,7-dibenzyl-2-(3,4,5-tribenzyl phenyl) chromane (**17b**)*

The synthetic procedure of **17b** behaved similarly as that of **17a.**

Yield 84%. ^{1}H NMR (400 MHz, $CDCl_3$) δ 7.45–7.16 (m, 25H), 6.82 (s, 2H), 6.24 (d, J = 17.1 Hz, 2H), 5.06–4.84 (m, 10H), 3.75 (s, 1H), 3.50 (t, J = 6.7 Hz, 1H), 3.45–3.25 (m, 1H), 3.15–2.88 (m, 4H), 2.76–2.72 (m, 1H), 1.56–1.33 (m, 4H), 1.20–0.96 (m, 8H); ^{13}C NMR (100 MHz, $CDCl_3$) δ 162.45, 158.53, 157.93, 155.44, 152.40, 137.89, 137.77, 137.11, 137.08, 137.06, 136.95, 134.54, 128.61, 128.48, 128.44, 128.36, 128.30, 128.24, 128.13, 128.06, 128.04, 127.98, 127.94, 127.89, 127.84, 127.77, 127.74, 127.70, 127.68, 127.64, 127.61, 127.59, 127.42, 127.38, 127.34, 127.14, 127.11, 127.11, 127.08, 106.61, 101.63, 94.77, 93.72, 78.16, 75.11, 73.75, 71.06, 69.95, 69.92, 69.78, 62.66, 51.23, 29.65, 29.29, 29.07, 28.66, 26.59, 25.92, 25.60.

*4.40. Synthesis of N-((1-(8-(((2R,3R)-6,8-bis(benzyloxy)-2-(3,4,5-tris (benzyloxy) phenyl) chroman-3-yl)oxy)octyl)-1H-1,2,3-triazol-4-yl) methyl)-3-(3,4-dihydroxy phenyl)propanamide (**18b-1**)*

The synthetic procedure of **18b-1** was similar to that of **18a-1** except for the replacement of **17a** with **17b**.

Yield, 63%. ^{1}H NMR (400 MHz, $CDCl_3$) δ 7.30–6.98 (m, 28H), 6.85–6.46 (m, 5H), 6.19–5.86 (m, 2H), 5.05–4.75 (m, 10H), 4.39–4.25 (m, 2H), 4.13–3.83 (m, 4H), 3.78–3.54 (m, 2H), 3.36–3.21 (m, 1H), 3.02–2.62 (m, 5H), 1.57–1.38 (m, 3H), 1.21–1.15 (m, 4H), 1.03–0.93 (m, 5H); ^{13}C NMR (100 MHz, $CDCl_3$) δ 162.85, 158.72, 158.12, 156.87, 155.96, 155.55, 152.62, 152.57, 152.42, 147.08, 144.65, 137.88, 137.74, 137.74, 137.44, 137.17, 137.06, 134.78, 128.87, 128.74, 128.69, 128.64, 128.59, 128.54, 128.49, 128.43, 128.36, 128.28, 128.21, 128.17, 128.08, 128.00, 127.94, 127.83, 127.64, 127.60, 127.31, 115.46, 106.64, 101.80, 94.95, 94.00, 78.36, 75.38, 73.91, 71.27, 70.99, 70.22, 70.05, 60.56, 50.55, 30.05, 29.83, 29.73, 29.31, 29.03, 26.47, 26.02, 25.02, 14.32, 14.26.

*4.41. Synthesis of N-((1-(8-(((2R,3R)-6,8-bis(benzyloxy)-2-(3,4,5-tris (benzyloxy) phenyl)chroman-3-yl)oxy)octyl)-1H-1,2,3-triazol-4-yl) methyl)-3-(4-hydroxy-3-methoxyphenyl) propanamide (**18b-2**)*

The synthetic procedure of **18b-2** was similar to that of **18a-2** except for replacement of **17a** with **17b**.

Yield, 62%. ^{1}H NMR (400 MHz, $CDCl_3$) δ 7.37–7.14 (m, 27H), 6.99–6.63 (m, 4H), 6.29–6.11 (m, 2H), 5.03–4.79 (m, 10H), 4.50–4.38 (m, 2H), 4.04–3.96 (m, 3H), 3.76–3.65 (m, 4H), 3.37–3.22 (m, 1H), 3.07–2.83 (m, 2H), 2.78–2.66 (m, 3H), 1.62–1.52 (m, 2H), 1.28–1.18 (m, 6H), 1.08–1.01 (m, 4H), 0.83–0.75 (m, 2H); ^{13}C NMR (100 MHz, $CDCl_3$) δ 166.52, 158.58, 158.00, 155.98, 155.82, 155.47, 153.21, 152.45, 152.30, 147.68, 146.97, 142.18, 141.12, 137.86, 137.34, 137.10, 136.96, 134.64, 128.63, 128.55, 128.53, 128.51, 128.45, 128.40, 128.30, 128.19, 128.14, 128.12, 128.04, 127.94, 127.85, 127.79, 127.69, 127.52, 127.50, 127.46, 127.22, 127.19, 127.14, 122.14, 118.00, 114.95, 110.03, 109.93, 106.56, 106.03, 101.68, 94.85, 93.84, 91.20, 78.27, 75.17, 71.13, 70.87, 70.83, 70.50, 70.07, 69.89, 55.87, 55.81, 50.29, 38.60, 30.06, 29.69, 29.62, 29.17, 28.97, 28.94, 26.40, 25.92.

*4.42. Synthesis of N-((1-(8-(((2R,3R)-6,8-bis(benzyloxy)-2-(3,4,5-tris (benzyloxy) phenyl)chroman-3-yl)oxy)octyl)-1H-1,2,3-triazol-4-yl) methyl)-3-(3-hydroxy-4-methoxyphenyl) propanamide (**18b-3**)*

The synthetic procedure of **18b-3** was similar to that of **18a-3** except for replacement of **17a** with **17b**.

Yield 60%. ^{1}H NMR (400 MHz, $CDCl_3$) δ 7.27–6.98 (m, 27H), 6.79–6.71 (m, 2H), 6.68–6.55 (m, 2H), 6.23–6.08 (m, 2H), 5.04–4.74 (m, 10H), 4.55–4.30 (m, 3H), 4.11–3.88 (m, 4H), 3.65 (d, J = 16.0 Hz, 4H), 3.36–3.16 (m, 1H), 2.98 (q, J = 7.2 Hz, 1H), 2.90–2.70 (m, 3H), 1.61–1.47 (m, 2H), 1.28–1.06 (m, 4H), 1.06–0.86 (m, 8H); ^{13}C NMR (100 MHz, $CDCl_3$) δ 166.58, 162.68, 158.58, 158.00, 155.47, 152.45, 152.30, 148.51, 146.03, 142.18, 140.86, 137.85, 137.33, 137.08, 136.96, 134.64, 128.63, 128.55, 128.52, 128.50, 128.44, 128.40, 128.36, 128.30, 128.27, 128.19, 128.14, 128.12, 128.04, 127.94, 127.85, 127.81, 127.79, 127.69, 127.52, 127.49, 127.46, 127.42, 127.21, 127.18, 127.14, 122.36, 121.55, 118.57, 112.95, 110.73, 110.02, 106.57, 106.04, 101.80, 101.70, 78.25, 75.21, 75.17, 71.13, 70.87, 70.49, 70.06, 69.90, 55.83, 50.26, 38.59, 34.80, 30.05, 29.68, 29.62, 29.19, 29.17, 28.94, 26.39, 25.91.

*4.43. N-((1-(8-(((2R,3R)-6,8-bis(benzyloxy)-2-(3,4,5-tris(benzyloxy) phenyl)chroman-3-yl)oxy)octyl)-1H-1,2,3-triazol-4-yl)methyl)-3-(3,4-dimethoxyphenyl)propanamide (**18b-4**)*

The synthetic procedure of **18b-4** was similar to that of **18a-4** except for replacement of **17a** with **17b**.

Yield 65%. ^{1}H NMR (400 MHz, $CDCl_3$) δ 7.31–6.98 (m, 26H), 6.94–6.78 (m, 3H), 6.77–6.56 (m, 3H), 6.16 (dd, J = 28.4, 12.8 Hz, 2H), 5.19–4.65 (m, 11H), 4.41 (d, J = 5.2 Hz, 2H), 4.12–3.89 (m, 3H), 3.77–3.57 (m, 7H), 3.38–3.13 (m, 1H), 3.03–2.94 (m, 1H), 2.92–2.60 (m, 3H), 1.60–1.45 (m, 2H), 1.23–1.09 (m, 4H), 1.04–0.84 (m, 8H); ^{13}C NMR (100 MHz, $CDCl_3$) δ 166.39, 158.66, 158.08, 155.53, 152.53, 150.61, 149.12, 141.05, 137.93, 137.82, 137.17, 137.02, 134.70, 128.70, 128.63, 128.60, 128.58, 128.52, 128.49, 128.47, 128.44, 128.22, 128.19, 128.10, 128.01, 127.93, 127.88, 127.84, 127.75, 127.58, 127.53, 127.50, 127.28, 127.25, 127.21, 122.03, 118.45, 111.10, 109.82, 106.64, 101.74, 94.90, 93.91, 78.37, 75.28, 73.86, 71.22, 70.15, 69.97, 69.94, 55.97, 55.90, 50.40, 34.84, 30.14, 29.76, 29.68, 29.25, 29.01, 26.45, 25.97, 24.97, 21.05.

*4.44. Synthesis of N-((1-(8-(((2R,3R)-5,7-dihydroxy-2-(3,4,5-trihydroxyphenyl) chroman-3-yl)oxy)octyl)-1H-1,2,3-triazol-4-yl) methyl)-3-(3,4-dihydroxyphenyl) propenamide (**3b-1**)*

The synthetic procedure of **3b-1** behaved similarly as that of **3a-1**, the only difference was conducted that starting material **18a-1** was substituted for **18b-1**.

Yield, 43%.^{1}H NMR (400 MHz, CD_3OD) δ 7.28 (s, 1H), 6.76 (s, 1H), 6.65(s, 1H), 6.63 (d, J = 3.6 Hz, 2H), 6.53 (d, J = 4.0 Hz, 1H), 6.50 (s, 2H), 5.34 (t, J = 4.0 Hz, 1H), 4.81 (s, 1H), 4.42–4.30 (m, 3H), 3.89 (q, J = 2.4 Hz, 1H), 3.50–3.42 (m, 1H), 3.24 (m, 1H), 2.87–2.67 (m, 5H), 2.48 (t, J = 8.0 Hz, 2H), 2.19 (t, J = 8.0 Hz, 2H), 2.06 (s, 1H), 2.03 (m, 1H), 1.82 (d, J = 7.2 Hz, 2H), 1.66–1.58 (m, 1H), 1.27 (m, 10H); TOF-MS, *m/z*: [M + Na^+], calcd for $C_{35}H_{42}N_4NaO_{10}^+$, 701.2793, found: 701.2781.

*4.45. Synthesis of N-((1-(8-(((2R,3R)-5,7-dihydroxy-2-(3,4,5-trihydroxyphenyl) chroman-3-yl)oxy)octyl)-1H-1,2,3-triazol-4-yl) methyl)-3-(3-hydroxy-4-methoxyphenyl) propenamide (**3b-2**)*

The synthetic procedure of **3b-2** behaved similarly as that of **3a-2**, the only difference was conducted that starting material **18a-2** was substituted for **18b-2**.

Yield, 46%. ^{1}H NMR (400 MHz, CD_3OD) δ 7.30 (s, 1H), 6.75 (s, 1H), 6.73–6.57 (m, 3H), 6.50 (d, J = 2.8 Hz, 2H), 5.95–5.84 (m, 1H), 4.78 (s, 1H), 4.36 (s, 2H), 4.34–4.25 (m, 2H), 3.85 (s, 1H), 3.77 (s, 3H), 3.46–3.40 (m, 1H), 3.26–3.17 (m, 1H), 2.88–2.79 (m, 3H), 2.69 (d, J = 16.7 Hz, 1H), 2.48 (t, J = 7.4 Hz, 2H), 1.83–1.75 (m, 2H), 1.33–1.30 (m, 2H), 1.20–1.15 (m, 4H), 1.11–1.03 (m, 4H); ^{13}C NMR (100 MHz, CD_3OD) δ 175.35, 157.82, 157.53, 157.31, 148.83, 146.51, 145.87, 136.85, 133.76, 133.48, 131.55, 130.84, 123.93, 121.94, 116.13, 113.26, 110.35, 106.91, 100.14, 79.22, 75.62, 70.80, 56.34, 51.44, 38.84, 35.62, 32.34, 31.24, 30.47, 30.07, 29.88, 27.27, 26.85, 25.75; TOF-MS, *m/z*: [M + Na^+], calcd for $C_{36}H_{44}N_4NaO_{10}^+$, 715.2950, found: 715.2942.

*4.46. Synthesis of N-((1-(8-(((2R,3R)-5,7-dihydroxy-2-(3,4,5-trihydroxyphenyl) chroman-3-yl)oxy)octyl)-1H-1,2,3-triazol-4-yl) methyl)-3-(4-hydroxy-3-methoxyphenyl) propenamide (**3b-3**)*

The synthetic procedure of **3b-3** behaved similarly as that of **3b-3**, the only difference was conducted that starting material **18a-3** was substituted for **18b-3**.

Yield, 42%. ^{1}H NMR (400 MHz, CD_3OD) δ 7.35 (s, 1H), 6.63 (d, J = 8.2 Hz, 1H), 6.58–6.41 (m, 3H), 6.37 (d, J = 1.2 Hz, 2H), 4.63 (s, 1H), 4.24 (s, 2H), 4.16 (t, J = 7.2 Hz, 2H), 3.72–3.67 (m, 1H), 3.64 (s, 3H), 3.28 (dt, J = 9.6, 6.4 Hz, 1H), 3.05 (dt, J = 9.6, 6.4 Hz, 1H), 2.70 (dd, J = 16.8, 2.8 Hz, 1H), 2.63 (t, J = 7.4 Hz, 2H), 2.55 (dd, J = 16.8, 4.4 Hz, 1H), 2.32 (t, J = 7.4 Hz, 2H), 1.69–1.61 (m, 2H), 1.21–1.15 (m, 2H), 1.07–1.01 (m, 4H), 0.96–0.89 (m, 4H); ^{13}C NMR (100 MHz, CD_3OD) δ 175.39, 157.77, 157.47, 157.28, 147.40, 147.28, 146.47, 146.46, 146.43, 145.98, 134.87, 133.44, 131.61, 131.53, 124.35, 120.62, 116.58, 112.84, 106.97, 106.94, 100.18, 79.21, 79.18, 75.53, 70.78, 56.48, 51.67, 38.71, 35.46, 32.05, 31.13, 30.44, 30.05, 29.86, 27.23, 26.82, 25.73; TOF-MS, *m/z*: [M + Na^+], calcd for $C_{36}H_{44}N_4NaO_{10}^+$, 715.2950, found: 715.2957.

*4.47. Synthesis of N-((1-(6-(((2R,3R)-5,7-dihydroxy-2-(3,4,5-trihydroxyphenyl) chroman-3-yl)oxy)hexyl)-1H-1,2,3-triazol-4-yl) methyl)-3-(3,4-dimethoxyphenyl) propenamide (**3b-4**)*

The synthetic procedure of **3b-4** behaved as that of **3a-4**, the only difference was conducted that starting material **18a-4** was substituted for **18b-4**.

Yield, 44%. ^{1}H NMR (400 MHz, CD_3OD) δ 7.45 (s, 1H), 6.99–6.76 (m, 3H), 6.73 (d, J = 8.4 Hz, 1H), 6.51 (d, J = 2.4 Hz, 2H), 5.35 (d, J = 5.2 Hz, 1H), 4.79 (s, 1H), 4.38 (s, 2H), 4.31 (t, J = 7.4 Hz, 2H), 3.88–3.83 (m, 1H), 3.77 (d, 6H), 3.48–3.41 (m, 1H), 3.25–3.18 (m, 1H), 2.90–2.82 (m, 3H), 2.74–2.66 (m, 1H), 2.53–2.46 (m, 2H), 1.40–1.32 (m, 4H), 1.22–1.14 (m, 4H), 1.13–1.06 (m, 4H); ^{13}C NMR (100 MHz, CD_3OD) δ 175.27, 157.82, 157.54, 157.32, 150.29, 148.87, 146.52, 135.22, 134.95, 133.48, 131.63, 130.84, 130.09, 124.00, 121.75, 113.56, 113.12, 106.94, 100.13, 79.25, 75.61, 70.76, 56.55, 56.39, 51.41, 38.76, 35.60, 32.29, 31.21, 30.83, 30.74, 29.87, 28.10, 27.27, 26.84; TOF-MS, *m/z*: [M + Na^+], calcd for $C_{37}H_{46}N_4NaO_{10}^+$, 729.3106, found: 729.3115.

4.48. HPLC purification condition

The preparation conditions for purifying all the target conjugates were as follows: 1) the mobile phases consisted of A and B, which were water containing 0.1% trifluoroacetic acid and acetonitrile, respectively; 2) the gradient system was adopted that phase A decreased gradually from 80% at 10.0 min to 40% at 40.0 min and recovered to 80% at 50.0 min, while phase B increased gradually from 20% at 10.0 min to 60% at 40.0 min and restored to 20% at 50.0 min; 3) the flow rate was 2 mL/min, and the detection wavelength was 254 nm; 4) the preparative separation column was 2QRBAX SB-C1 (ZORBAX SB-C18, 9.4 × 250 mm, 5 μm). The target products were collected and combined according to the corresponding the eluted peak.

4.49. α-glucosidase inhibition activity assays

According to the reported method [27], the α-glucosidase inhibition assay was performed with minor modifications. Different concentrations of target EGC-derived analogues (13.0, 26.0, 52.0, 104.0, 208.0, 416.0 and 833.0 μM) and 50 μL of α-glucosidase (0.6 unit/mL) from *S. cerevisiae* (G5003) in 0.1 M phosphate buffer (pH 6.5) were added to a 96-well microplate, and then the mixture was incubated for 10 min at 37 °C. 50 μL of *p*NPG (0.5 mM) as a substrate was added to initiate the reaction. At 37 °C, the 96-well microplate was incubated for an additional 20 min followed by addition of 50 μL of Na_2CO_3 (0.1 M) to terminate the reaction. Acarbose, EGCG and the template compound **1** were applied as reference compounds. The absorbance of the reaction mixture was detected at 405 nm by a microplate reader (Sunrise TM microplate absorbance reader, Tecan, Austria). The control was the same mixture except for the tested compound replaced by the phosphate buffer. The sample blank and control blank were the same mixtures as the corresponding sample and control, except that α-glucosidase was instead with phosphate buffer. The α-glucosidase inhibition activity (%) was calculated as: the inhibition activity (%) = $[(A_S - A_{SB})/(A_C - A_{CB})] \times 100\%$, where A_S, A_{SB}, A_C and A_{CB} are the absorbance of sample, sample blank, control and control blank, respectively. All the measurements for each compound tested were performed in triplicate. IC_{50} values were analyzed by Graphpad Prism 8.3.0.538.

4.50. HPA activity inhibition assays

The *in vitro* enzyme assay we adopted was in line with the hydrolytic cleavage of substrate 2-chloro-4-nitrophenyl-4-*O*-*β*-D-maltotrioside (G3CNP) by HPA with suitable modifications [24,28,29]. The HPA inhibition activities of all the newly synthesized compounds were expressed as half inhibitory concentration (IC_{50}) values. All the stock solutions of the tested compounds were immediately diluted with 50 mM Tris buffer to the desired concentration before use. 25 μL of the sample solution and 25 μL of 4.0 U/mL HPA (Lee Biosolutions, Inc) solution were mixed in a 96-well microtiter plate, and then 50 μL of the substrate solution (0.5 mM) was added to start the reaction. The reaction time was over 30 mins at 37℃. The assay was continuously monitored with a UV–Vis spectrophotometer (Sunrise TM microplate absorbance reader, Tecan, Austria) at 405 nm. A control without tested compounds or acarbose represented 100% HPA activity. The template compound **1** was used as a positive control. Absorption for each sample was measured in triplicate and each measurement repeated twice. IC_{50} values were analyzed by Graphpad Prism 8.3.0.538.

4.51. Molecular docking

Molecular docking studies were conducted to explore the binding mode between conjugates **2a-1** and **1** and HPA using Autodock vina 1.1.2. software [30]. The two-dimensional (2D) structure of the test compounds **2a-1** and **1** were drawn and then converted to 3D structure by ChemBioDraw Ultra 14.0 software. The three- dimensional (3D) structure of HPA (PDB code: 4w93) was downloaded from RCSB Protein Data Bank (http://www.rcsb.org/). The Autodock vina 1.1.2 package was applied to generate the docking input files. The docking ligand was prepared by merging non-polar hydrogen atoms and defining rotatable bonds. The search grids corresponding to HPA binding site were identified as center_x = -9.632; center _y = 4.341, and center _z = –23.107, and dimensions were: size _x = 29.451, size _y = 29.451; and size _z = 29.451. To increase the accuracy of molecular docking, the value of exhaustiveness was set at 20. Unless otherwise mentioned, the parameters used for Autodock vina docking were the default values. The best-scoring pose was chosen based on the Vina docking score, and was visually analyzed on PymoL 1.7.6 software (http://www.pymol.org/).

Declaration of Competing Interest

The authors declare that they have no known competing financial interests or personal relationships that could have appeared to influence the work reported in this paper.

Acknowledgements

The work is partly supported by the Natural Science Foundation of Hunan Province, China (Grant No. 2021JJ80064) and Scientific Research Fund of Hunan Provincial Education Department (Grant No. 18B231). We also appreciated Dr. Jinyun Dong for guiding us to perform the molecular docking.

References

[1] S.E. Inzucchi, Oral antihyperglycemic therapy for type II diabetes, JAMA 287 (2002) 360–372.
[2] L. Xu, Y. Li, Y. Dai, J. Peng, Natural products for the treatment of type 2 diabetes mellitus: pharmacology and mechanisms, Pharmacol. Res. 130 (2018) 451–465.
[3] J.B. Buse, R.R. Henny, J. Han, D.D. Kim, M.S. Fineman, A.D. Baron, Effects of exenatide (exendin-4) glycemic control over 30 weeks in sulfonylurea-treated patients with type 2 diabetes, Diabetes Care 27 (2004) 2628–2635.
[4] K. Donnan, L. Segar, SGLT2 inhibitors and metformin: dual antihyperglycemic therapy and the risk of metabolic acidosis in type 2 diabetes, Eur. J. Pharmacol. 846 (2019) 23–29.
[5] M.R. Loizzo, M. Marrelli, A. Pugliese, F. Conforti, F. Nadjafi, F. Menichini, R. Tundis, Crocus cancellatus subsp. Damascenus stigmas: chemical profile, and inhibition of a-amylase, a-glucosidase and lipase, key enzymes related to type 2 diabetes and obesity, J. Enzyme Inhib. Med. Chem. 31 (2016) 212–218.
[6] M.S. Akhter, P. Uppal, Toxicity of metformin and hypoglycemic therapies, Adv. Chronic Kidney D. 27 (2020) 18–30.
[7] V. Dionysios, M. Sofia, F.L. Fedon, K. Georgia, Glycemic index (GI) or Glycemic Load (GL) and dietary interventions for optimizing postprandial hyperglycemia in patients with T2 diabetes: a review, Nutrients 12 (6) (2020) 1561.
[8] H. Zhang, Y. Jiang, J. Pan, Y. Lv, J. Liu, S. Zhang, Y. Zhu, Effect of tea products on the in vitro enzymatic digestibility of starch, Food Chem. 243 (2018) 345–350.
[9] K.e. Wang, T. Qi, L. Guo, Z. Ma, G. Gu, M. Xiao, L. Lu, Enzymatic glucosylation of salidroside from starch by α-amylase, J. Agric. Food Chem. 67 (7) (2019) 2012–2019.
[10] A. Sujayev, P. Taslimi, E. Garibov, M. Karaman, M.M. Zangeneh, Novel cyclic thiourea derivatives of aminoalcohols at the presence of $AlCl_3$ catalyst as potent α-glucosidases and α-amylase inhibitors: synthesis, characterization, bioactivity investigation and molecular docking studies, Bioorg. Chem. 104 (2020), 104216, https://doi.org/10.1016/j.bioorg.2020.104216.
[11] E.L. Elena, H. Scheib, N. Frei, G. Williamson, M. Grigorov, C.J. Chou, Flavonoids for controlling starch digestion: structural requirements for inhibiting human alpha-amylase, J. Med. Chem. 51 (2008) 3555–3561.
[12] K. Yoshida, A. Hishida, O. Iida, K. Hosokawa, J. Kawabata, Flavonol caffeoylglycosides as alpha-glucosidase inhibitors from *Spiraea cantoniensis* flower, J. Agric. Food Chem. 56 (2008) 4367–4371.
[13] T. Manaharan, D. Appleton, H.M. Cheng, U.D. Palanisamy, Flavonoids isolated from *Syzygium aqueum* leaf extract as potential antihyperglycaemic agents, Food Chem. 132 (4) (2012) 1802–1807.
[14] C.A. Tarling, K. Woods, R. Zhang, H.C. Brastianos, G.D. Brayer, R.J. Andersen, S. G. Withers, The search for novel human pancreatic α-amylase inhibitors: high-throughput screening of terrestrial and marine natural product extracts, ChemBioChem 9 (2008) 433–438.
[15] L.K. Williams, X.H. Zhang, S. Caner, C. Tysoe, N.T. Nguyen, J. Wicki, D.E. Williams, J. Coleman, J.H. McNeill, V. Yuen, R.J. Andersen, S.G. Withers, G.D. Brayer, The amylase inhibitor montretin A reveals a new glucosidases inhibition motif, Nat. Chem. Biol. 2015 (11) (2015) 691–696.
[16] L.K. Williams, C. Li, S.G. Withers, G.D. Brayer, Order and disorder: differential structural impacts of myricetin and ethyl caffeate on human amylase, an antidiabetic target, J. Med. Chem. 55 (22) (2012) 10177–10186.
[17] D.Q. Li, Z.M. Qian, S.P. Li, Inhibition of three selected beverage extracts on alpha-glucosidase and rapid identification of their active compounds using HPLC-DAD-MS/MS and biochemical detection, J Agric. Food. Chem. 58 (2010) 6608–6613.
[18] H. Yang, A.L. Chan, V. LaVallo, Q. Cheng, Quantitation of alpha-glucosidase activity using fluorinated carbohydrate array and MALDI-TOF-MS, ACS Appl. Mater. Interfaces 8 (4) (2016) 2872–2878.
[19] C.L. Lin, J.K. Lin, Epigallocatechin gallate (EGCG) attenuates high glucose-induced insulin signaling blockade in human hepG2 hepatoma cells, Mol. Nutr. Food Res. 52 (2008) 930–939.
[20] S. Wolfram, D. Raederstorff, M. Preller, Y. Wang, S.R. Teixeira, C. Riegger, P. Weber, Epigallocatechin gallate supplementation alleviates diabetes in rodents, J. Nutr. 136 (2006) 2512–2518.
[21] M.C. Venables, C.J. Hulston, H.R. Cox, A.E. Jeukendrup, Green tea extract ingestion, fat oxidation, and glucose tolerance in healthy humans, Am. J. Clin. Nutr. 87 (2008) 778–784.

[22] Q.Q. Zhu, X.Y. Yang, X.J. Zhang, C.J. Yu, Q.Q. Pang, Y.W. Huang, X.J. Wang, J. Sheng, EGCG targeting Notch to attenuate renal fibrosis *via* inhibition of TGFβ/Smad3 signaling pathway activation in streptozotocin-induced diabetic mice, Food&Funct. 11 (2020) 9686–9695.

[23] J.A.H. Kaeswurm, B. Claasen, M.-P. Fischer, M. Buchweitz, Interaction of structurally diverse phenolic compounds with porcine pancreatic α-amylase, J. Agric. Food, Chem. 67 (40) (2019) 11108–11118.

[24] A.S.D'. Costa, N. Bordenave, Inhibition of starch digestion by flavonoids: role of flavonoid-amylase binding kinetics, Food Chem. 341 (2021), https://doi.org/10.1016/j.foodchem.2020.128256.

[25] B.F. Marcune, S. Karady, U.-H. Dolling, T.J. Novak, Methoxymethylation of alcohols, phenols, and avermectin aglycones using MOM-2-pyridylsulfide, J. Org. Chem. 64 (7) (1999) 2446–2449.

[26] P. Chen, S. Wang, C. Cao, W. Ye, M. Wang, C. Zhou, W. Chen, X.u. Zhang, K. Zhang, W. Zhou, α-naphthoflavone-derived cytochrome P450 (CYP)1B1 degraders specific for sensitizing CYP1B1-mediated drug resistance to prostate cancer DU145: Structure activity relationship, Bioorg. Chem. 116 (2021) 105295, https://doi.org/10.1016/j.bioorg.2021.105295.

[27] J.-Q. Zhao, Y.-M. Wang, Y.-L. Yang, Y. Zeng, Q.-L. Wang, Y. Shao, L.-J. Mei, Y.-P. Shi, Y.-D. Tao, Isolation and identification of antioxidant and α-glucosidase inhibitory compounds from fruit juice of *Nitraria tangutorum*, Food Chem. 227 (2017) 93–101.

[28] J.R. Homoki, A. Nemes, E. Fazekas, G. Gyémánt, P. Balogh, F. Gál, J. Al-Asri, J. Mortier, G. Wolber, L. Babinszky, J. Remenyik, Anthocyanin composition, antioxidant efficiency, and α-amylase inhibitor activity of different hungarian sour cherry varieties (*Prunus cerasus L.*), Food Chem. 194 (2016) 222–229.

[29] S. Justyna, B. Tina, P. Dominik, G. Sebastian, O. Ewa, F.M. Mtthias, E.C. Monika, Pancreatic lipase and α-amylase inhibitory activity of extracts from selected plant materials after gastrointestinal digestion *in vitro*, Food Chem. 355 (2021) 1–13, https://doi.org/10.1016/j.foodchem.2021.129414.

[30] X.B. Wang, Q. He, K.Q. Wu, T.N. Guo, X.Z. Du, H. Zhang, L.C. Fang, N. Zhang, Q. H. Zhang, F.Q. Ye, Design, synthesis, and activity of novel 2,6-disubstituted purine derivatives, potential small molecule inhibitors of signal transduce and activator of transcription 3, Eur. J. Med. Chem. 179 (2019) 218–232.

frontiers in Nutrition

ORIGINAL RESEARCH
published: 24 March 2021
doi: 10.3389/fnut.2021.647537

Flavor Characteristics of Ganpu Tea Formed During the Sun-Drying Processing and Its Antidepressant-Like Effects

Sui Xiao[1†], Jingyuan Huang[2†], Yahui Huang[3], Huiqing Lai[4], Yi Zheng[4], Dahua Liang[4], Hang Xiao[2‡] and Xu Zhang[1*‡]*

[1] Guangdong Key Laboratory for Innovative Development and Utilization of Forest Plant Germplasm, College of Forestry and Landscape Architecture, South China Agricultural University, Guangzhou, China, [2] Department of Food Science, University of Massachusetts, Amherst, MA, United States, [3] Department of Tea Science, College of Horticulture, South China Agricultural University, Guangzhou, China, [4] Yunding Ganpu Tea Industry Co., LTD, Guangzhou, China

Ganpu tea is a novel type of tea beverage with unique and pleasant flavor that encases Pu-erh tea leaves within an intact mandarin peel. However, to date, no holistic and detail studies on its chemical composition and biological activities have been reported yet. In the present study, by applying UPLC-Q-TOF and UPLC-MS technology, we systematically identified and analyzed 104 water-soluble compounds of Ganpu tea and their variation trend during the sun-drying processing. The results showed that the generation of pigments and gallic acid coincided with a dramatic decrease in catechin content, and a significant increase in alkaloid and flavonoid contents. The conversion of these compounds can contribute to the improvement of sensory attributes of Ganpu tea and maybe indispensable to its unique flavor. Moreover, the mice given orally with high dose of Ganpu tea (0.4 g/kg) showed a significantly reduced immobility duration as compared to that of the negative control group ($p < 0.01$) both in the forced swimming test and tail suspension test. Together, these results indicate that the sun-drying processing was indispensable to the formation of the unique flavor for Ganpu tea. Multiple types of compounds of Ganpu tea may collectively provide the synergistic attributes to its antidepressant-like properties.

Keywords: Ganpu tea, flavor, sun-drying processing, antidepressant-like properties, health functions

OPEN ACCESS

Edited by:
Fernando M. Nunes, University of Trás-os-Montes and Alto Douro, Portugal

Reviewed by:
Chi-Tang Ho, Rutgers, The State University of New Jersey, United States
Chuanyi Peng, Anhui Agricultural University, China

***Correspondence:**
Hang Xiao
hangxiao@foodsci.umass.edu
Xu Zhang
zhangxu919@hotmail.com

[†]These authors have contributed equally to this work and share first authorship

[‡]These authors share senior authorship

Specialty section:
This article was submitted to Food Chemistry, a section of the journal Frontiers in Nutrition

Received: *30 December 2020*
Accepted: *01 March 2021*
Published: *24 March 2021*

Citation:
Xiao S, Huang J, Huang Y, Lai H, Zheng Y, Liang D, Xiao H and Zhang X (2021) Flavor Characteristics of Ganpu Tea Formed During the Sun-Drying Processing and Its Antidepressant-Like Effects. Front. Nutr. 8:647537. doi: 10.3389/fnut.2021.647537

INTRODUCTION

Ganpu tea is a novel type of tea beverage and has gained considerable popularity in China since 2015 due to its potential health-promoting effects and unique flavor. The production value of Ganpu tea in 2016 was ∼1.6 billion RMB, almost a 3-fold increase as compared to that in 2015 (1). Due to the rapidly increasing consumption of Ganpu tea, over 2,000 new Ganpu tea enterprises have been registered in Xinhui city, Guangdong in 2017. The consumption of a combination of tea leaves and citrus peel as brewed tea can be dated back to the eighth century in Tang dynasty. It is also well-known that mandarin peel can be used as an ingredient in traditional Chinese medicine as well as functional foods (2, 3). Nowadays, the contemporary Ganpu tea product is made with both Pu-erh

tea and mandarin peel. The processing of Ganpu tea involves (a) the removal of pulp from the fruit peel while keeping the peel intact; (b) cleaning the peel and filling it with Pu-erh tea; and (c) finally sun-drying and packaging.

Pu-erh tea can be divided into Pu-erh raw tea and Pu-erh ripen tea, depending on the processing techniques and quality characteristics. For the production of Pu-erh ripen tea, the sun-dried green tea is generally used as a substrate for microbial fermentation under the high temperature and humidity conditions (4). Due to pretense of a large number of active microorganisms in this processing, such as *Aspergillus niger, Penicllium, Rhizopus,* and *Aspergillus gloucus* (5), production of Pu-erh ripen tea will face considerable risk to food safety if it is used as the ingredient for Ganpu tea. Conversely, Pu-erh raw tea is made directly from the sun-dried green tea and does not include a microbial fermentation step, and therefore, the chemical constituents and quality are more similar to those of the sun-dried green tea than to those of Pu-erh ripen tea (6). In the present study, Pu-erh raw tea was used as the ingredient for production of Ganpu tea, due to not only its relatively high food safety, but also its flavor profile being relatively well-matched with those of mandarin peel. The mandarin peel is a popular product with strong geographical indication, as the most authentic production areas are confined to the specific regions in Xinhui, Guangdong, China. Citrus peels are rich in various functional components and enzymes, which catalyze the conversion of major chemical compounds during the sun-drying processing, and provide a fruity flavor to Ganpu tea.

To date, numerous methods including hot-air drying, freeze drying, vacuum drying, and infrared drying, have been applied to dry agricultural products (7–9). Hot-air drying is the method most commonly used to dry Ganpu tea. This method has the advantages of higher efficiency, lower cost, and easier control over the external odor infiltration. However, the quality of Ganpu tea dried with this technique is questionable because the hot-air drying can impact the thermosensitive substances in the mandarin peel, causing them to crack over time. In contrast, the sun-drying method has a more suitable temperature and humidity for aging, with ample time for development and improvement of the potential flavor compounds in Ganpu tea.

In the present study, we processed Ganpu tea from both Pu-erh raw tea and mandarin peel using the sun-drying technique. Pu-erh raw tea and mandarin peel have been studied extensively in the functional drink and health product fields, respectively (4, 10–13). However, as a recently popularized commodity, to date, no holistic and detailed studies on its chemical characteristics and biological activities of Ganpu tea have been reported yet. We previously analyzed the aromatic substances of Ganpu tea and discovered a number of volatile compounds that were newly generated during the sun-drying processing (14). In this study, we systematically identified and analyzed the water-soluble compositions of Pu-erh raw tea, mandarin peel, and Ganpu tea by applying the UPLC-Q-TOF-MS and UPLC-MS technology, and investigated the conversions of potential flavor compounds of Ganpu tea during the sun-drying processing. We also conducted formal sensory evaluation to assess the final influence of these compositional changes on flavor quality criteria. Additionally, we also evaluated the preventive effects of Ganpu tea extract on depression pathology both in the FST and TST mice models. Collectively, our experiments aimed to reveal the possible chemical basis for the flavor formation of Ganpu tea and to demonstrate whether these compounds can exert antidepressant effects.

Abbreviations: GC, gallocatechin; EGC, (-)-epigallocatechin; C, catechin; EC, epicatechin; EGCG, epigallocatechin gallate; GCG, gallocatechin gallate; ECG, epicatechin gallate; CG, Catechin gallate; UPLC-Q-TOF, Ultra performance liquid chromatography coupled with Q-TOF mass spectrometry; UPLC-MS, Ultra-high performance liquid chromatography- mass spectrometry; Rt, retention time; DSA, descriptive sensory analysis; FST, forced swimming test; TST, tail suspension test.

MATERIALS AND METHODS

Plant Materials

The tea plant materials were collected from Yunding Ganpu tea industry co., LTD (Guangzhou, China). Information regarding the tea plant samples used in this study are described in **Table 1**. S1, S2, and S3 were prepared to compare the chemical compositions among Pu-erh raw tea, mandarin peel, and Ganpu tea. S4, S5, S6, and S7 were prepared for research on the variation trend of potential flavor compounds in Ganpu tea during the sun-drying processing. All samples were tested in time on the harvesting year.

Chemicals and Drugs

HPLC-grade acetonitrile, methanol, and formic acid were purchased from Fisher Scientific (Pittsburg, PA, USA). Water was purified using a Milli-Q water purification system (Millipore, Bedford, MA, USA). Clomipramine hydrochloride tablets were purchased from Beijing Novartis Pharmaceutical Co., Ltd (Beijing, China). All the other chemicals and reagents used were of the highest grade available.

Preparation of Samples

Tea plant samples were dried to constant weight using a vacuum freeze-drying machine, and the remaining weight was milled into a powder with ∼60 meshes. Approximately 2.0 g of the prepared powder sample was weighed and extracted with 100 mL of distilled water at 100°C for 45 min with shaking, and the extracts were further filtered through filter paper. The obtained supernatants were filtered through a 0.22 um membrane for subsequent UPLC-Q-TOF and UPLC-MS analysis, and then dried into powder by vacuum freeze-drying machine. The dried extract powder was subsequently used in antidepressant-like testing in mice described below (15).

UPLC-Q-TOF Analysis

An Agilent UPLC1290-6540-UHD Q-TOF system and an ACQUITY UPLC BEH C18 column (2.1 mm × 100 mm id, 1.7 μm, Waters) were used for the qualitative analysis. The mobile phase was composed of A (0.2% formic acid, v/v) and B (acetonitrile) with a gradient elution as follows: 0–15 min, 95%−95% A; 15–35 min, 95%−85% A; 35–50 min, 85%−50% A; 50–60 min, 50%−20% A; and 60–65 min, 20%−95% A. The

TABLE 1 | Sample information sheet.

Sample No.	Sample name	Description	Collection time
S1	Pu-erh raw tea	Harvested from Yunnan	2016.12
S2	Mandarin peel	Harvested from Xinhui, Guangdong	2016.12
S3	Ganpu tea	Made from S1 and S2	2016.12
S4	Ganpu tea 0 day	0 day of the full sun-drying processing	2018.09
S5	Ganpu tea 3 day	3 day of the full sun-drying processing	2018.09
S6	Ganpu tea 9 day	9 day of the full sun-drying processing	2018.09
S7	Ganpu tea 15 day	15 day of the full sun-drying processing	2018.09

column and auto-sampler temperatures were maintained at 40 and 20°C, respectively. The mobile phase was directly delivered into the electrospray ionization source at a flow rate of 0.3 mL/min. The injection volume was 5 μL. Mass spectroscopy (MS) analysis was performed in both positive and negative ion mode with the full scan mode from m/z 0 to 1,200. The capillary and cone voltages were 3.5 kV and 30 V, respectively. The collision energy was 40 eV. Nitrogen was used as desolvation gas at flow rate of 500 L/h. The temperatures of ion source and desolvation gas were set at 100 and 300°C, respectively.

UPLC-MS Analysis

An Waters ACQUITY™ QDA system coupled with PDA detector (Waters, Milford, MA, USA) were used for further research on the flavor characteristics of Ganpu tea. The chromatographic parameters, including column, mobile phase, gradient elution condition, flow rate, and injection volume, were the same as UPLC-Q-TOF-MS system described in 2.4. The UV chromatogram was monitored at 278 nm. MS analysis was performed both in positive and negative ion mode and using the full scan mode from m/z 50 to 1,200. The capillary and cone voltages were 3.5 kV and 25 V, respectively.

Analysis of Biochemical Compositions

The contents of moisture, water extract, total free amino acids and tea polyphenols were determined according to GB 5009.3-2016, GB/T 8305-2013, GB/T8314-2013, and GB/T 8313-2008, respectively. The content of tea pigment was determined using the method described in our previous work with proper modifications (15).

Descriptive Sensory Analysis (DSA)

The tea infusion was evaluated by a well-trained panel of 10 members (five males and five females, age: 20–45). Tea samples were assessed using the flavor profile method of ISO 6564 (ISO, 1985). The DSA was performed according to the procedures described previously by Kraujalyt et al. (16) and GB/T 14487-2017, with a slight modification. Briefly, 3.00 g of Ganpu tea was infused with 150 mL of freshly boiled water for 5 min in a specialized DSA tea pot, then 50 mL of tea infusion was poured into a 150 mL-cup covered with a porcelain cover, which was provided to panelists in an odor-free laboratory at 25°C. Three-digit numbers were used to code samples, and they were randomly offered to panelists after brewing for aroma and flavor assessment. Panelists agreed that the samples could be described using six attributes for aroma: stale, woody, floral, fruity, sweet, and off-flavor, as well as six attributes for flavor: bitter, silky, sweet, umami, mellow, and astringent. The intensities of the aroma and flavor attributes were scored using a scale from 0 to 10, where 0 = none or negligible perceptible intensity, and 10 = extremely high intensity. Each sample was evaluated three times by each panelist on different days. Data were expressed as a mean.

Animals

Both male and female Chinese Kun Ming (KM) mice (20 ± 2 g) were obtained from Laboratory Anima Center of Guangzhou University of Chinese Medicine (Guangzhou, Guangdong Province, China) and used in this study. The mice were housed individually in cages for 3 days to adapt to the environment under the following controlled conditions: 25 ± 2°C under a 12 h light/dark cycle and 60 ± 5% humidity with free access to water and food pellets. Each mouse was used only once. Behavioral testing was performed between 7:00 and 12:00 AM. All the procedures were conducted according to the National Institutes of Health Guide for the Care and Use of Laboratory Animals, and the animal handling and experimental procedures were approved by the Local Animal Use Committee (SCXK 2013-0020).

Measurement of Depressive-Like Behaviors

Behavior tests were performed in five groups with 12 mice in each group. The mice were given orally twice a day with the extract of Ganpu tea at 0.1 g /kg, 0.2 g /kg, and 0.4 g /kg for 15 consecutive days, respectively. Mice in positive control group were given with clomipramine hydrochloride tablets (0.02 g /kg) as the positive reference also for 15 consecutive days. The mice in negative control group were given only with the same volume of physiological saline solution for 15 consecutive days. The mice in both positive and negative control groups were tested in parallel with those receiving various doses of extract of Ganpu tea. Animal behaviors were assessed at 45 min after administration of the final dose.

Forced Swimming Test (FST)

The FST is one of the most common animal models used for examination of the depressive-like behaviors. The test was conducted as previously described (17) with slight modifications. Mice were individually inserted in an open cylinder container

(10 cm in diameter and 25 cm in height) containing 19 cm of water at 24 ± 2°C. Each mouse was judged to be immobile when it ceased struggling and remained floating motionless in the water, making only small movements necessary to keep its head above water. The duration of immobility was recorded during the last 5 min of the 7 min testing period.

Tail Suspension Test (TST)

The TST is another model commonly used for examination of depressive-like behaviors (18). The tails of mice were taped in a balance bracket at a distance of 2 cm from the tail tip, with tail straight and head being hung down 15 cm above the desktop after 45 min from the last administration. The mice were separated by cardboard just in the case when they were interfered with each other. Each mouse was treated for 7 min; the first 2 min was for adaptation. The duration of immobility (no other body movements except respiration) in the last 5 min was recorded.

Statistical Analysis

UPLC-Q-TOF-MS and UPLC-MS system were re-calibrated after analysis of every 5 samples to ensure and maintain data accuracy and stability. All the results were recorded and expressed as mean ± standard deviation (SD) of three replicates. The Heatmap analysis was carried out using the website https://software.broadinstitute.org/morpheus, and based on the relative abundances by untargeted metabolomics. The statistical analyses were performed using one-way analysis of variance (ANOVA), followed by least significant difference (LSD) test or Duncan's test. $p < 0.05$ was considered statistically significant.

RESULTS AND DISCUSSION

Comparisons of Chemical Compositions Among Pu-erh Raw Tea, Mandarin Peel and Ganpu Tea

After being extracted with boiling water, the extract was filtered and injected into the UPLC-Q-TOF system and the UPLC-MS system, respectively. Good separation was achieved after screening a series of mobile phases, UPLC columns, and gradient profiles. Meanwhile, MS conditions were optimized after testing a set of instrument parameters, as described in UPLC-Q-TOF Analysis and UPLC-MS Analysis. The total ion chromatograms (both positive and negative ion modes) and the representative UPLC chromatograms (278 nm) of Pu-erh raw tea (S1), mandarin peel (S2), and Ganpu tea (S3) were obtained by the UPLC-MS system (**Figure 1**). Peak identification of compounds in **Table 2** was performed based on the precise molecular weight and fragment ions by UPLC-Q-TOF analysis, and a comparison of them with data in the previously published literature (19–23).

The retention times (Rt), the ratio of deprotonated/protonated molecules ($[M+H]^+/[M-H]^-$), measured value, fragment ions and formula are listed in **Table 2**. Furthermore, some of the compounds in **Table 2** were identified by standard comparisons, such as gallocatechin (GC), (-)-epigallocatechin (EGC), catechin (C), epicatechin (EC), epigallocatechin gallate (EGCG), gallocatechin gallate (GCG), epicatechin gallate (ECG), catechin gallate (CG), caffeine, theobromine, theophylline, gallic acid, rutin, quercetin, and synephrine.

As shown in **Table 2**, Compounds 1–72 were detected in Pu-erh raw tea (S1) and Ganpu tea (S3, S4, S5, S6, S7) except those labeled with asterisk, which were newly generated compounds during the sun-drying processing. For example, isoleucine, threonine, arginine, and glutamine were detected only from S3 (finished product), S6 (sun-drying for 9 days), and S7 (sun-drying for 15 days), and catechin-4a-epicatechin-3-O-gallate, catechin-4a-epicatechin 3'-o-gallate, myricetin−3- locust glycoside, quercetin−3-o- rhamnoside galactoside, and vitexin were detected only from S3 (finished product), S5 (sun-drying for 3days), S6 (sun-drying for 9 days), and S7 (sun-drying for 15 days), which means these compounds were produced at different times during the sun-drying processing. Meanwhile, compounds 73-104 were detected in mandarin peel (S2) and Ganpu tea (S3, S4, S5, S6, S7) except 4H-1-Benzopyran-4-one,2,3-dihydro-5,6,7,8-tetramethoxy-2-[4-(phenylmethoxy)phenyl]- and 4H-1-Benzopyran-4-one,2-phenyl-,dihyroxy trimethoxy deriv, which were detected only from S3 (finished product), S6 (sun-drying for 9 days), and S7 (sun-drying for 15 days).

As shown in **Figure 1**, the water-soluble chemical compounds of Pu-erh raw tea (S1), mandarin peel (S2), and Ganpu tea (S3) exhibited noticeable differences and intrinsic connections in all the chromatograms. The intensities of ionization varied frequently between the positive (**Figure 1A**) and the negative ion modes (**Figure 1B**), and the mechanisms also varied between MS (**Figures 1A,B**) and UV detectors (**Figure 1C**). Still, we found similar results, i.e., water-soluble chemical compounds of Ganpu tea (S3) were more abundant and diversified as compared with those of Pu-erh raw tea (S1) and mandarin peel (S2). A total of 104 compounds were detected in Ganpu tea (S3), while only 63 and 30 compounds were detected in Pu-erh raw tea (S1) and mandarin peel (S2), respectively. Water-soluble compounds of Ganpu tea (S3) were consisted of six amino acids, 16 catechins, three alkaloids, seven pigments, 19 organic acids, and 12 flavonoids, which were also detected in the Pu-erh raw tea (S1), and 30 compounds, which were also detected in the mandarin peel (S2). Furthermore, 11 compounds labeled with asterisk and listed in **Table 2** were detected only in Ganpu tea (S3), which were newly generated during the sun-drying processing. The potential flavor compounds of Ganpu tea (S3) were shared with 59.6% compounds of Pu-erh raw tea (S1), and with 29.8% compounds of mandarin peel (S2). The remaining 10.6% potential flavor compounds in Ganpu tea were newly generated during the sun-drying processing.

Analysis of Flavor Substances From Ganpu Tea

A total of 104 potential flavor compounds were identified in Ganpu tea by UPLC-Q-TOF system. The characteristic peaks of these potential flavor compounds are classified in **Figure 2**, while other details are listed in **Table 2**. Our results showed that ten amino acids were identified in Ganpu tea. Theanine (1) is the most abundant compound, followed by pyroglutamic acid (6), threonine (8), and phenylalanine (3).

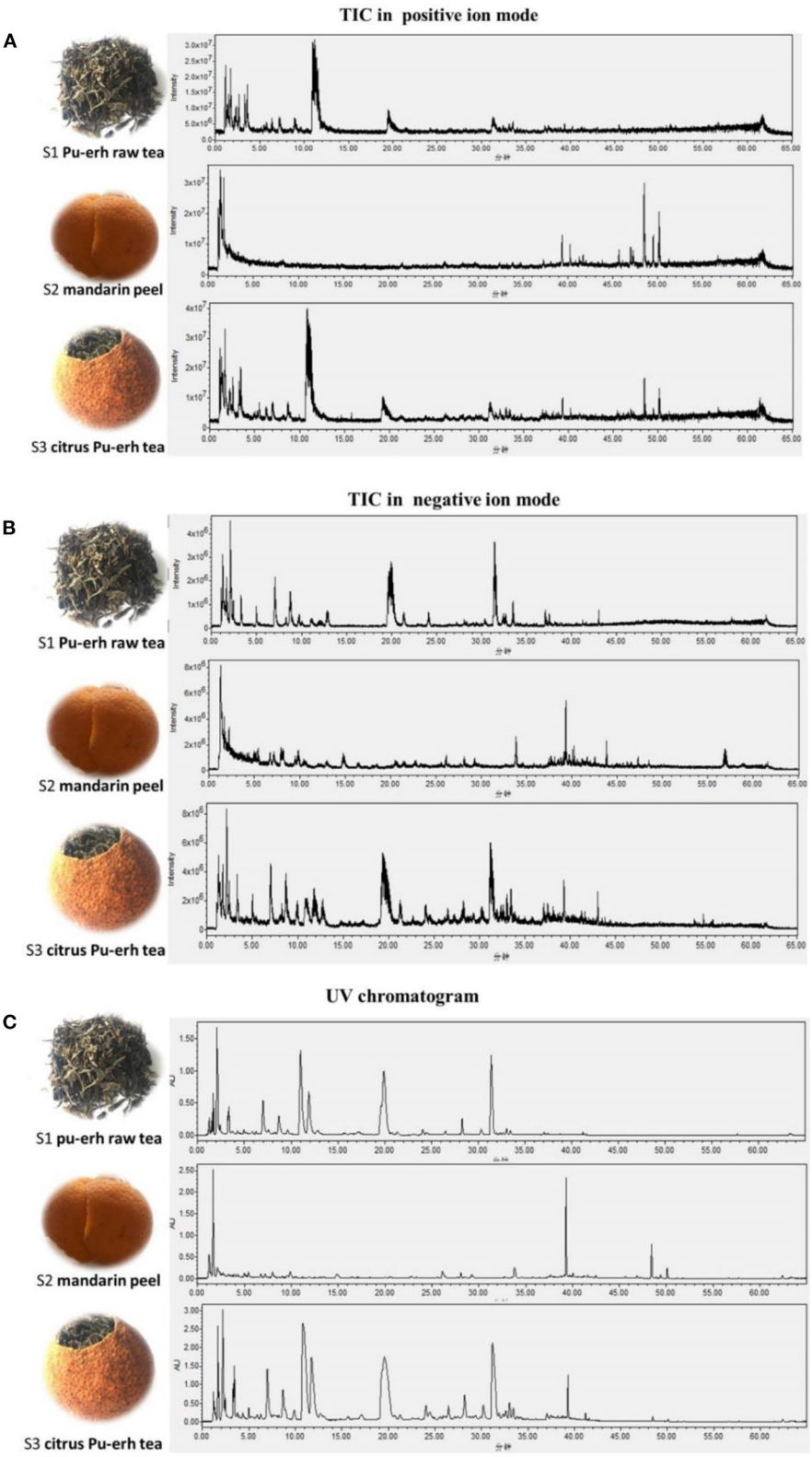


FIGURE 1 | Comparisons of the chemical compositions among Pu-erh raw tea, mandarin peel, and Ganpu tea by TIC in positive ion mode **(A)**, TIC in negative ion mode **(B)**, and UV chromatogram **(C)**, respectively. In our previous study, we investigated the source and conversion of aromatic substances of Ganpu tea. The fruity sweet aromas compounds of Ganpu tea were consisted of the main volatile components of Pu-erh raw tea and mandarin peel, in addition to the newly generated

(Continued)

FIGURE 1 | compounds during the sun-drying processing (14). Based on the data obtained from the present study, we could draw a similar conclusion that the water-soluble substances of Ganpu tea were not just a simple combination of the compounds of Pu-erh raw tea and mandarin peel. Rather, the water-soluble substances of Ganpu tea were mainly attributed to the development and transformation of the precursor ingredients that it contains and to several newly generated substances during the sun-drying processing. The final formation of the flavor of Ganpu tea may be closely related to the production and conversion of these water-soluble substances. Further researches are necessary to investigate the contribution of these compounds to the flavor characteristic of Ganpu tea.

Moreover, isoleucine (7), threonine (8), arginine (9), and glutamine (10), labeled with asterisks in **Figure 2A**, were newly generated amino acids during the full sun-drying processing, as they were identified exclusively in Ganpu tea, but not in Pu-erh raw tea or mandarin peel. In addition to the common tea catechins, such as GC (11), EGC (12), C (13), EC (14), EGCG (15), GCG (16), ECG (17), and CG (18), 10 other catechins and catechin metabolites were also identified in Ganpu tea. For example, epiafzelechin-3-O-gallate (21), gallocatechin-(4a-8)-catechin-3-O-gallate (22), and trigalloylglucose (24) all displayed a strong intensity of ionization. Notably, catechin-4a-epicatechin-3-O-gallate (25) and catechin-4a-epicatechin-3'-O-gallate (26) were newly generated during the sun-drying process, as they were discovered exclusively in Ganpu tea (**Figure 2B**). Caffeine (27) and theobromine (28) were the main alkaloids in Ganpu tea. The pigments were composed of theaflavin (29) and some anthocyanins (30–35) (**Figure 2C**). Flavonoids and their derivatives were identified in Ganpu tea and shown in **Figure 2D**. Rutin (36), kaempferol (37), myricetin-3-O-galactoside (47), quercetin (48), and their derivatives, which originated from Pu-erh raw tea were also identified in Ganpu tea. Three newly generated compounds, including myricetin−3-locust glycoside (46), quercetin−3-o- rhamnoside galactoside (49), and vitexin (53) were formed during the sun-drying processing. Meanwhile, flavonoids originating from mandarin peel are shown in **Figure 2F**. For example, naringenin (75), naringin (78), narirutin (81), hesperidin (84), poncirin (85), pentamethoxyflavanone (89), isosinensetin (91), sinensetin (92), limonin (94), nobiletin (95), and tangeretin (98) were the important chemical constituents for mandarin peel (24, 25). Nineteen organic acids and their derivatives (54–72) were identified and shown in **Figure 2E**.

As we known, catechins, pigments, amino acids, organic acids, alkaloids, and flavonoids were important for the flavor of tea drink and mandarin peel (24–26, 38). Therefore, we speculated that the unique flavor of Ganpu tea could co-attributed to these water-soluble compounds. Further researches are necessary to verify the 11 newly generated compounds whether also contribute to the flavor characteristic of Ganpu tea. The chemical compound identification of 104 metabolites of Ganpu tea was tentative in this paper. We need to positively identify major and effective compounds of Ganpu tea in our future research. Based on our previous study on the aroma of Ganpu tea (14), we predicted that potential flavor compounds would be changed considerably during the sun-drying processing due to *de novo* biosynthesis and/or enzymatic modification of the existing compounds, which were influenced by exogenous stimuli, including temperature, humidity, light, and microorganisms. To study the conversions of water-soluble compounds of Ganpu tea, we further analyzed the biochemical compositions in this study.

The Variation Trend of Potential Flavor Compounds in Ganpu Tea During the Sun-Drying Processing

Analysis of Biochemical Components

Moisture, water extract, total free amino acids, tea polyphenols, theaflavins, thearubigins, and theabrownine have respective influences on the sensory flavor and health-promoting function of Ganpu tea. These primary biochemical components and their contents were assessed within four samples with different durations of sun-drying treatment, and listed in **Table 3**. Data were expressed from three independent chemical replicates. Sun-drying treatment for 15 days could significantly decrease the moisture contents from 24.16 to 5.04% of Ganpu tea, and the 15-day-period of sunlight was necessary to reach the final moisture content. It was clear that S4 without sun-drying treatment, contained the higher moisture contents, mainly due to the fresh mandarin peel of Ganpu tea. The sun-drying processing not only reduced the moisture content but also imposed significant effect on tea polyphenols and pigments. The concentration of tea polyphenols in S7 was significantly lower than those in other samples, due to the fact that catechins had undergone a series of oxidative, condensing and degradative chemical processes to form gallic acid, theaflavins, thearubigins, and theabrownine under the sun-drying conditions (11).

As shown in **Table 3**, at the end of sun-drying processing, the contents of thearubigins and theabrownine were clearly increased. On the contrary, the content of theaflavins was clearly decreased, suggesting that theaflavins are oxidized and accumulated into thearubigins and theabrownine. The content of total free amino acids was only slightly changed during the sun-drying processing since the contents of several free amino acids, including theanine and leucine, were decreased, while other amino acids, including isoleucine, threonine, arginine, and glutamine were newly generated. The total content of water extract was increased during the sun-drying processing, suggesting that new substances are formed from oxidation, degradation, and condensation of various compounds, which collectively contribute to the unique color, taste, and aroma of the Ganpu tea.

The Variation Trend of Potential Flavor Compounds

A heatmap analysis was applied to visualize the dynamic changes of potential flavor compounds in Ganpu tea during the sun-drying processing (**Figure 3**). Each column represents a tea sample with different durations of sun-drying processing and each row represents a critical compound. A color-coded scale grading from blue to red corresponds to the content of these potential flavor compounds shifting from low to high. The sun-drying processing requires 15 days of high humidity and high

TABLE 2 | List of the identified components in tested samples.

Peak No.	Putative identification	Rt (min)	$[M+H]^+$/ $[M-H]^-$	Measured value	Fragment ions	Formula	Detection						
							S1	S2	S3	S4	S5	S6	S7
1	Theanine	1.7	[M+H]+	175.1082	158, 129	$C_7H_{14}N_2O_3$	✓	_	✓	✓	✓	✓	✓
2	Leucine	2.1	[M+H]+	132.1012	132, 86	$C_6H_{13}NO_2$	✓	_	✓	✓	✓	✓	✓
3	Phenylalanine	3.28	[M+H]+	166.0863	120	$C_9H_{11}NO_2$	✓	_	✓	✓	✓	✓	✓
4	Tryptophan	6.3	[M+H]+	205.0974	143, 118	$C_{11}H_{12}N_2O_2$	✓	_	✓	✓	✓	✓	✓
5	Tyrosine	3.05	[M+H]+	182.0808	165, 136	$C_9H_{11}NO_3$	✓	_	✓	✓	✓	✓	✓
6	Pyroglutamic acid	2.6	[M+H]+	130.0501	_	$C_5H_7NO_3$	✓	_	✓	✓	✓	✓	✓
7	* Isoleucine	2.3	[M+H]+	132.1013	86	$C_6H_{13}NO_2$	_	_	✓	_	_	✓	✓
8	* Threonine	3.2	[M+H]+	120.0650	_	$C_4H_9NO_3$	_	_	✓	_	_	✓	✓
9	* Arginine	1.45	[M+H]+	175.1120	158, 129	$C_6H_{14}N_4O_2$	_	_	✓	_	_	✓	✓
10	* Glutamine	8.25	[M+H]+	147.0758	119, 91	$C_5H_{10}N_2O_3$	_	_	✓	_	_	✓	✓
11	Gallocatechin (GC)	3.35	[M+H]+	307.0813	_	$C_{15}H_{14}O_7$	✓	_	✓	✓	✓	✓	✓
12	(-)-Epigallocatechin (EGC)	7.00	[M+H]+	307.0814	223, 163	$C_{15}H_{14}O_7$	✓	_	✓	✓	✓	✓	✓
13	Catechin (C)	8.7	[M+H]+	291.0869	_	$C_{15}H_{14}O_6$	✓	_	✓	✓	✓	✓	✓
14	Epicatechin (EC)	19.4	[M+H]+	291.0863	165, 139	$C_{15}H_{14}O_6$	✓	_	✓	✓	✓	✓	✓
15	Epigallocatechin gallate (EGCG)	19.8	[M+H]+	459.0922	289, 139	$C_{22}H_{18}O_{11}$	✓	_	✓	✓	✓	✓	✓
16	Gallocatechin gallate (GCG)	24.0	[M+H]+	459.0924	289, 139	$C_{22}H_{18}O_{11}$	✓	_	✓	✓	✓	✓	✓
17	Epicatechin gallate (ECG)	31.3	[M+H]+	443.0972	273, 139	$C_{22}H_{18}O_{10}$	✓	_	✓	✓	✓	✓	✓
18	Catechin gallate (CG)	32.6	[M+H]+	443.0973	_	$C_{22}H_{18}O_{10}$	✓	_	✓	✓	✓	✓	✓
19	(-)-EGCG-3″-O-ME	22.6	[M-H]-	471.0920	_	$C_{23}H_{20}O_{11}$	✓	_	✓	✓	✓	✓	✓
20	Epiafzelechin	3.00	[M+H]+	275.0919	_	$C_{15}H_{14}O_5$	✓	_	✓	✓	✓	✓	✓
21	Epiafzelechin-3-O-gallate	37.2	[M-H]-	424.0795	273	$C_{22}H_{17}O_9$	✓	_	✓	✓	✓	✓	✓
22	Gallocatechin-(4a-8)-catechin-3-O-gallate	20.7	[M-H]-	745.1399	457, 423	$C_{37}H_{30}O_{17}$	✓	_	✓	✓	✓	✓	✓
23	Digallocatechin-catechin	25.9	[M-H]-	897.1869	423	$C_{45}H_{38}O_{20}$	✓	_	✓	✓	✓	✓	✓
24	*Catechin-4a-epicatechin-3-O-gallate	24.5	[M+H]+	731.1608	427, 289	$C_{37}H_{30}O_{16}$	_	_	✓	_	✓	✓	✓
25	Trigalloylglucose	28.25	[M-H]-	635.0880	423, 169	$C_{27}H_{24}O_{18}$	✓	_	✓	✓	✓	✓	✓
26	*Catechin-4a-epicatechin 3'-o-gallate	26.5	[M+H]+	731.1608	427, 289	$C_{37}H_{30}O_{16}$	_	_	✓	_	✓	✓	✓
27	Theasinesnsins A	32.00	[M+H]+	611.1395	465,303	$C_{30}H_{26}O_{14}$	✓	_	✓	✓	✓	✓	✓
28	Theasinesnsins B	33.1	[M+H]+	611.1396	465, 303	$C_{30}H_{26}O_{14}$	✓	_	✓	✓	✓	✓	✓
29	Caffeine	11.0	[M+H]+	195.0877	157	$C_8H_{10}N_4O_2$	✓	_	✓	✓	✓	✓	✓
30	Theobromine	3.45	[M+H]+	181.0721	138, 108	$C_7H_8N_4O_2$	✓	_	✓	✓	✓	✓	✓
31	Theophylline	5.3	[M+H]+	181.0718	_	$C_7H_8N_4O_2$	✓	_	✓	✓	✓	✓	✓
32	Theaflavin	30.0	[M-H]-	563.1190	_	$C_{29}H_{24}O_{12}$	✓	_	✓	✓	✓	✓	✓
33	*Procyanidin B1	15.17	[M+H]+	579.1497	409, 289	$C_{30}H_{26}O_{12}$	✓	_	✓	✓	✓	✓	✓
34	*Procyanidin B2	15.26	[M+H]+	579.1497	409, 289	$C_{30}H_{26}O_{12}$	✓	_	✓	✓	✓	✓	✓
35	*Procyanidin B3	15.7	[M+H]+	579.1495	409, 127	$C_{30}H_{26}O_{12}$	✓	_	✓	✓	✓	✓	✓
36	*Procyanidin B4	15.76	[M+H]+	579.1497	409, 289	$C_{30}H_{26}O_{12}$	✓	_	✓	✓	✓	✓	✓
37	Procyanidin B1 3-O-gallate	24.5	[M+H]+	731.1608	427, 289	$C_{37}H_{30}O_{16}$	✓	_	✓	✓	✓	✓	✓
38	Procyanidin B2 3-O-gallate	26.5	[M+H]+	731.1608	427, 289	$C_{37}H_{30}O_{16}$	✓	_	✓	✓	✓	✓	✓
39	Rutin	41.0	[M+H]+	611.1606	465, 303	$C_{27}H_{30}O_{16}$	✓	_	✓	✓	✓	✓	✓
40	Kaempferol	37.5	[M+H]+	287.0552	_	$C_{15}H_{10}O_6$	✓	_	✓	✓	✓	✓	✓
41	*Kaempferol-3-O-glucoside	35.91	[M-H]-	447.0929	284, 255	$C_{21}H_{20}O_{11}$	✓	_	✓	✓	✓	✓	✓
42	*Kaempferol-3-O-galactoside	37.56	[M-H]-	447.0925	284, 255	$C_{21}H_{20}O_{11}$	✓	_	✓	✓	✓	✓	✓
43	*Kaempferol-3- O-rutinoside	37.1	[M-H]-	593.1509	_	$C_{27}H_{30}O_{15}$	✓	_	✓	✓	✓	✓	✓
44	*Kaempferol-3- O-glucosylrutinoside	35.6	[M-H]-	755.2031	_	$C_{33}H_{40}O_{20}$	✓	_	✓	✓	✓	✓	✓
45	*Myricetin-3-O-glucoside	27.2	[M-H]-	479.0824	_	$C_{21}H_{20}O_{13}$	✓	_	✓	✓	✓	✓	✓
46	** Myricetin—3- locust glycoside	28.1	[M+H]+	625.1036	_	$C_{26}H_{24}O_{18}$	_	_	✓	_	✓	✓	✓
47	**Myricetin-3-O-galactoside	28.05	[M-H]-	479.0827	_	$C_{21}H_{20}O_{13}$	✓	_	✓	✓	✓	✓	✓
48	Quercetin	30.3	[M+H]+	303.0500	287, 257	$C_{15}H_{10}O_7$	✓	_	✓	✓	✓	✓	✓

(Continued)

TABLE 2 | Continued

Peak No.	Putative identification	Rt (min)	$[M+H]^+/[M-H]^-$	Measured value	Fragment ions	Formula	Detection						
							S1	S2	S3	S4	S5	S6	S7
49	***** Quercetin−3-o- rhamnoside galactoside	39.35	[M+H]+	611.1250	303	$C_{26}H_{26}O_{17}$	_	_	✓	_	✓	✓	✓
50	*Quercetin-**3-O-glucoside**	32.4	[M-H]-	463.0877	300, 271	$C_{21}H_{20}O_{12}$	✓	_	✓	✓	✓	✓	✓
51	*Quercetin-**3-O-galactoside**	33.5	[M-H]-	463.0878	300, 271	$C_{21}H_{20}O_{12}$	✓	_	✓	✓	✓	✓	✓
52	*Quercetin−3- O-glucosylrutinoside	31.85	[M+H]+	773.2136	303, 465	$C_{33}H_{40}O_{21}$	✓	_	✓	✓	✓	✓	✓
53	* Vitexin	49.5	[M+H]+	433.1129	395	$C_{21}H_{20}O_{10}$	_	_	✓	_	✓	✓	✓
54	Gallic acid	2.25	[M-H]-	169.0142	125	$C_7H_6O_5$	✓	_	✓	✓	✓	✓	✓
55	Quinic acid	1.3	[M-H]-	191.0560	111, 87	$C_7H_{12}O_6$	✓	_	✓	✓	✓	✓	✓
56	Caffeic acid	2.21	[M+H]+	181.0500	157	$C_9H_8O_4$	✓	_	✓	✓	✓	✓	✓
57	Malic acid	1.4	[M-H]-	133.0137	75	$C_4H_6O_5$	✓	_	✓	✓	✓	✓	✓
58	Ascorbic acid	1.9	[M-H]-	175.0240	115, 85	$C_6H_8O_6$	✓	_	✓	✓	✓	✓	✓
59	Caffeoylmalic acid	3.3	[M-H]-	295.0442	191, 113	$C_{13}H_{12}O_8$	✓	_	✓	✓	✓	✓	✓
60	*3-O-galloylquinic acid	2.15	[M-H]-	343.0662	191, 169	$C_{14}H_{16}O_{10}$	✓	_	✓	✓	✓	✓	✓
61	*5-O-galloylquinic acid	2.48	[M-H]-	343.0664	191, 169	$C_{14}H_{16}O_{10}$	✓	_	✓	✓	✓	✓	✓
62	Chlorogenic acid	5.0	[M-H]-	353.0870	191	$C_{16}H_{18}O_9$	✓	_	✓	✓	✓	✓	✓
63	*1-Caffeoylquinic acid	10.00	[M-H]-	353.0871	191	$C_{16}H_{18}O_9$	✓	_	✓	✓	✓	✓	✓
64	*3-Caffeoylquinic acid	10.09	[M-H]-	353.0869	291, 191	$C_{16}H_{18}O_9$	✓	_	✓	✓	✓	✓	✓
65	*1-p-Coumaroylquinic acid	16.01	[M-H]-	337.0915	305, 163	$C_{16}H_{18}O_8$	✓	_	✓	✓	✓	✓	✓
66	*3-p-Coumaroylquinic acid	16.3	[M-H]-	337.0917	305, 163	$C_{16}H_{18}O_8$	✓	_	✓	✓	✓	✓	✓
67	*4-p-Coumaroylquinic acid	16.87	[M-H]-	337.0918	305, 163	$C_{16}H_{18}O_8$	✓	_	✓	✓	✓	✓	✓
68	*5-p-Coumaroylquinic acid	16.92	[M-H]-	337.0918	305, 163	$C_{16}H_{18}O_8$	✓	_	✓	✓	✓	✓	✓
69	Galloylglucose	45.5	[M-H]-	331.0662	169	$C_{13}H_{16}O_{10}$	✓	_	✓	✓	✓	✓	✓
70	1,2,6-Trigalloylglucose	28.2	[M-H]-	635.0882	465, 313	$C_{27}H_{24}O_{18}$	✓	_	✓	✓	✓	✓	✓
71	3,6-Digalloylglucose	9.9	[M-H]-	483.0773	169	$C_{20}H_{20}O_{14}$	✓	_	✓	✓	✓	✓	✓
72	Strictinin	11.8	[M-H]-	633.0725	301, 275	$C_{27}H_{22}O_{18}$	✓	_	✓	✓	✓	✓	✓
73	Synephrine	1.66	[M+H]+	168.1012	150, 135	$C_9H_{13}NO_2$	_	✓	✓	✓	✓	✓	✓
74	Lucenin-2	3.691	[M+H]+	611.1609	575, 473	$C_{27}H_{30}O_{16}$	_	✓	✓	✓	✓	✓	✓
75	Naringenin	23	[M+H]+	273.0757	274, 202	$C_{15}H_{12}O_5$	_	✓	✓	✓	✓	✓	✓
76	Vicenin-2	37	[M+H]+	595.1658	457, 409	$C_{27}H_{30}O_{15}$	_	✓	✓	✓	✓	✓	✓
77	Diosmetin-6, 8-di-C-glucoside	28.1	[M+H]+	625.1762	607, 589	$C_{28}H_{32}O_{16}$	_	✓	✓	✓	✓	✓	✓
78	Naringin	37.75	[M+H]+	581.1864	_	$C_{27}H_{32}O_{14}$	_	✓	✓	✓	✓	✓	✓
79	Chysoeriol-6, 8-di-C-glucoside	29.2	[M+H]+	625.1766	409, 355	$C_{28}H_{32}O_{16}$	_	✓	✓	✓	✓	✓	✓
80	Diosmetin-6-C-glucoside	35.8	[M+H]+	463.1236	367, 343	$C_{22}H_{22}O_{11}$	_	✓	✓	✓	✓	✓	✓
81	Narirutin	37.7	[M-H]-	579.1711	271	$C_{27}H_{32}O_{14}$	_	✓	✓	✓	✓	✓	✓
82	Rhoifolin	12.0	[M+H]+	579.1709	433, 271	$C_{27}H_{30}O_{14}$	_	✓	✓	✓	✓	✓	✓
83	Diosmin	39.2	[M+H]+	609.1816	463, 301	$C_{28}H_{32}O_{15}$	_	✓	✓	✓	✓	✓	✓
84	Hesperidin	39.35	[M-H]-	609.1818	343, 301	$C_{28}H_{34}O_{15}$	_	✓	✓	✓	✓	✓	✓
85	Poncirin	26.1	[M+H]+	595.2023	463, 379	$C_{28}H_{34}O_{14}$	_	✓	✓	✓	✓	✓	✓
86	Citrusin III	43.8	[M+H]+	728.3982	700, 587	$C_{36}H_{53}N_7O_9$	_	✓	✓	✓	✓	✓	✓
87	Melitidin	44.5	[M+H]+	725.2293	419, 404	$C_{33}H_{40}O_{18}$	_	✓	✓	✓	✓	✓	✓
88	Monohydroxy-tetramethoxyflavone	48.95	[M+H]+	359.1125	329, 301	$C_{19}H_{18}O_7$	_	✓	✓	✓	✓	✓	✓
89	Pentamethoxyflavanone	50.15	[M+H]+	375.1441	211, 196	$C_{20}H_{22}O_7$	_	✓	✓	✓	✓	✓	✓
90	Monohydroxy-pentamethoxyflavone	51.2	[M+H]+	389.1231	374, 359	$C_{20}H_{20}O_8$	_	✓	✓	✓	✓	✓	✓
91	Isosinensetin	45.6	[M+H]+	373.1284	343, 153	$C_{20}H_{20}O_7$	_	✓	✓	✓	✓	✓	✓
92	Sinensetin	47	[M+H]+	373.1283	343, 153	$C_{20}H_{20}O_7$	_	✓	✓	✓	✓	✓	✓
93	Tetramethyl-O-isoscutellarein	47.2	[M+H]+	343.1176	328, 313	$C_{19}H_{18}O_6$	_	✓	✓	✓	✓	✓	✓
94	Limonin	43	[M+H]+	471.2015	425, 397	$C_{26}H_{30}O_8$	_	✓	✓	✓	✓	✓	✓
95	Nobiletin	48.5	[M+H]+	403.1386	373, 211	$C_{21}H_{22}O_8$	_	✓	✓	✓	✓	✓	✓
96	Tetramethyl-O-scutellarein	48.6	[M+H]+	343.1175	327, 313	$C_{19}H_{18}O_6$	_	✓	✓	✓	✓	✓	✓

(Continued)

TABLE 2 | Continued

Peak No.	Putative identification	Rt (min)	$[M+H]^+/[M-H]^-$	Measured value	Fragment ions	Formula	Detection						
							S1	S2	S3	S4	S5	S6	S7
97	3, 5, 6, 7, 8, 3′, 4′-Heptamethoxyflavone	49.5	[M+H]+	433.1496	403, 388	$C_{22}H_{24}O_9$	_	✓	✓	✓	✓	✓	✓
98	Tangeretin	50.2	[M+H]+	373.1285	358, 343	$C_{20}H_{20}O_7$	_	✓	✓	✓	✓	✓	✓
99	5-Hydroxy-6, 7, 8, 3′, 4′-pentamethoxyflavone	46.1	[M+H]+	389.1231	_	$C_{20}H_{20}O_8$	_	✓	✓	✓	✓	✓	✓
100	5-Hydroxy-4′- methoxy flavone-7-o-glycoside	37.5	[M+H]+	449.1440	287	$C_{22}H_{24}O_{10}$	_	✓	✓	✓	✓	✓	✓
101	*4H-1-Benzopyran-4-one,2,3-dihydro-5,6,7,8-tetramethoxy-2-[4-(phenylmethoxy)phenyl]-	44.45	[M+H]+	725.1870	_	$C_{39}H_{32}O_{14}$	_	_	✓	_	_	✓	✓
102	4H-1-Benzopyran-4-one,6,8-di-b-Dglucopyranosyl-5,7-dihydroxy-2-(4-hydroxy-3-me-thoxyphenyl)-	28.1	[M+H]+	625.1765	_	$C_{28}H_{32}O_{16}$	_	✓	✓	✓	✓	✓	✓
103	4H-1-Benzopyran-4-one,6,8-di-b-Dglucopyranosyl-5,7-dihydroxy-2-(3-hydroxy-4-me-thoxyphenyl)-	29.3	[M+H]+	625.1764	_	$C_{28}H_{32}O_{16}$	_	✓	✓	✓	✓	✓	✓
104	*4H-1-Benzopyran-4-one, 2-phenyl-,dihyroxy trimethoxy deriv	38.79	[M+H]+	343.0662	191	$C_{14}H_{14}O_{10}$	_	_	✓	_	_	✓	✓

Compounds labeled with asterisk (*) were newly generated during the sun-drying processing. Compounds labeled with star (*) means putative identification. "✓" means detected in this sample, and "_" means not detected in this sample.

temperature conditions, causing potential flavor compounds of Ganpu tea, including catechins, pigments, alkaloids, and flavonoids, to be transformed considerably.

Firstly, the contents of most catechins, particularly EGC, EGCG, GCG, and CG, were decreased by 20.2–27.2%. Meanwhile, with the exception of theaflavin, the pigments, including procyanidins and their derivatives, were clearly increased throughout the sun-drying processing. The significant reduction in catechin content from initial levels throughout the entire course of the sun-drying processing may be resulted from a series of chemical transformations of these compounds into gallic acid, pigments, and alkaloids, during the processes catalyzed by polyphenol oxidase and peroxidase enzymes (39).

Secondly, alkaloids were profoundly affected by the humid and hot sun-drying conditions. For example, the contents of caffeine, theobromine, and theophylline were increased considerably, with caffeine showing the most significant increase (28.7%). It has been proposed that extracellular enzymes produced by microorganisms, such as tannase, play a large role in catalyzing chemical reactions and promoting the transformation of the key chemical components (40).

Thirdly, organic acids showed different variation trends depending on their chemical compositions. For example, the content of 3-caffeoylquinic acid was decreased, while those of gallic acid, quinic acid, and chlorogenic acid were significantly increased with prolonging sun-drying time. Gallic acid is one of the most prominent phenolic acids in tea. The increase of its content during the sun-drying processing is likely due to the degradation of catechin gallates under high-temperature and high moisture conditions, which has been observed in a previous study (27).

Finally, a majority of the essential flavonoids identified in Ganpu tea were originated from the mandarin peel, and showed significant changes during the sun-drying processing. For instance, naringenin, naringin, narirutin, hesperidin, pentamethoxyflavanone, isosinensetin, sinensetin, limonin, nobiletin, and tangeretin were the crucial group of bioactive compounds in the mandarin peel, and they were all increased significantly during the sun-drying processing. Similarly, the contents of most common glycosidic group attached to the flavonoids in Ganpu tea were substantially increased as well. With the exception of kaempferol and its derivatives, whose contents were decreased, the contents of other flavone glycosides, including myricetin-3-O-galactoside and quercetin-3-O-galactoside, were increased significantly. Furthermore, the newly generated flavonoids, including myricetin-3-locust glycoside, quercetin-3-O-rhamnoside galactoside, and vitexin were detected starting from the third day of sun-drying processing. Biosynthesis and/or modification of constitutive flavonoids may be induced by exogenous stimuli, such as changes in sun light and temperature under the natural environments, as well as innate enzymatic activity of mandarin peel cells (28, 41). The persistent activities of enzymes involved in the flavonoid biosynthesis (chalcone flavanone isomerase, phenylalanine ammonia lyase, and cinnamate 4-hydroxylase), O-methylation enzymes (chalcone synthase, flavanone 7-O-glucosyltransferase, and flavanone 7-O-glucoside-2'-O-rhamnotransferase), methyltransferase, and chalcone-flavanone isomerase may be the important pathways for the accumulation and conversion of flavonoid compounds in Ganpu tea (29, 30, 39).

DAS With a Trained Panel

To date, the sensory characteristics of Gan*p*u tea have not been reported yet. In this study, we evaluated the influences of sun-drying processing on the sensory properties of Ganpu tea. The aroma and flavor attributes of Ganpu tea processed with different durations of sun-drying processing are presented in **Figure 4**. Six aroma attributes, including stale, woody, floral, fruity, sweet, and off-flavor, were evaluated in S4, S5, S6, and S7 (**Figure 4A**). The results showed that S7 demonstrated significantly higher intensities of sweet ($p < 0.01$) and fruity ($p < 0.01$) attributes. The 4-terpineol, thymol, and 4-isopropyl−3-

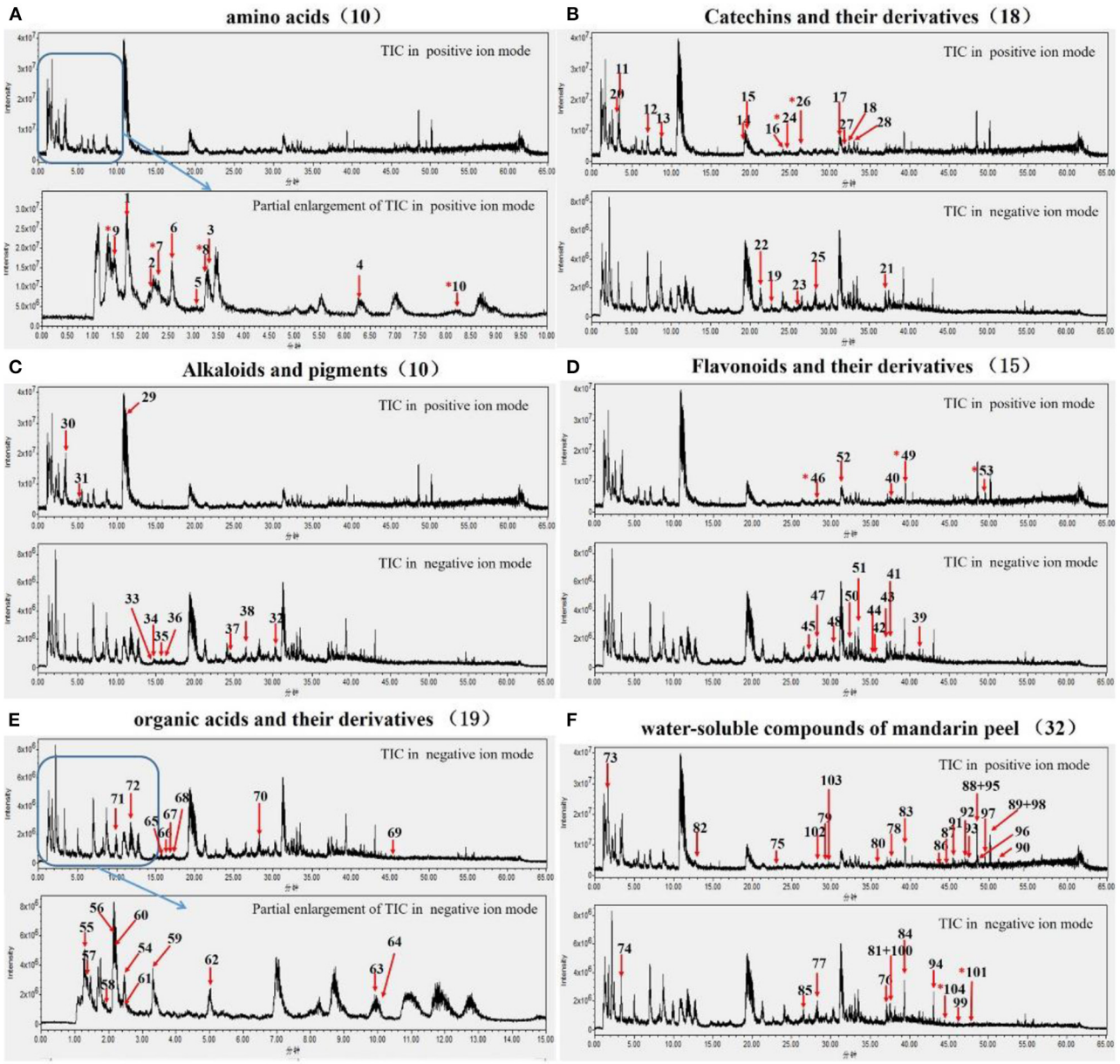


FIGURE 2 | Flavor substances of Ganpu tea were identified by UPLC-Q-TOF system in different categories, including ten amino acids **(A)**, 18 catechins and their derivatives **(B)**, three alkaloids and seven pigments **(C)**, 15 flavonoids and their derivatives **(D)**, 19 organic acids and their derivatives **(E)**, and 32 water-soluble compounds of mandarin peel **(F)**, respectively.

methyl phenol contribute to the sweet descriptor while α-ionone, β-ionone, terpinene, p-acetylanisole, and isoamyl alcohol leaf ester contribute to the fruity descriptor (16). These compounds were accumulated in significantly higher quantities in Ganpu tea with longer duration of sun-drying treatments. S7 also displayed significantly higher intensities of stale ($p < 0.05$) and floral ($p < 0.05$) descriptors. Alcohols and ketones often contribute to the floral descriptor (31), and significantly higher quantities of linalool, 4-terpineol, pinocarvone, piperitone, carvone, and carvenone were detected in S7 (14). The off-flavor was detected in S4 and S5, which may be due to a flavor resembling fermentation of Pu-erh raw tea. However, the detection of off-flavor went away with prolonging the duration of sun-drying treatment.

The flavor attributes of bitter, silky, sweet, umami, mellow, and astringent were evaluated across the four treatment groups (**Figure 4B**). Although no significant differences ($p > 0.05$) in the umami descriptor were observed, S7 did demonstrate significantly higher intensities of silky ($p < 0.01$), sweet ($p < 0.01$), and mellow ($p < 0.05$) attributes. Soluble saccharides and certain amino acids, including theanine, phenylalanine, and

TABLE 3 | Analysis of biochemical components of Ganpu tea samples with different durations of the full sun-drying processing.

Biochemical component (%)	S4 (0 day)	S5 (3 day)	S6 (9 day)	S7 (15 day)
Moisture	24.16 ± 1.38a	21.23 ± 1.04b	12.17 ± 0.76c	5.04 ± 0.98d
Water extract	30.04 ± 2.15d	31.72 ± 2.23cd	33.58 ± 2.02b	34.86 ± 1.93ab
Total free amino acids	2.37± 0.32a	2.03 ± 0.52b	2.33 ± 0.29a	2.43 ± 0.20a
Tea polyphenols	18.45 ± 1.02a	16.77±0.15b	14.10 ± 1.13c	12.12 ± 1.42d
Theaflavins	0.24 ± 0.13a	0.15 ± 0.46b	0.13 ± 0.65bc	0.10 ± 0.02c
Thearubigins	1.36 ± 0.10c	1.49 ± 0.13b	1.50 ± 0.11b	1.85 ± 0.12a
Theabrownine	1.25 ± 0.17c	1.26 ± 0.03c	1.34 ± 0.20b	1.77 ± 0.21a

Differences between samples were analyzed by Duncan's test. In each horizontal line, the mean ± SD values bearing different letters differ significantly ($p < 0.05$).

tryptophan, contribute to sweetness. Moreover, flavonoids could provide a unique taste, changing from bitter to sweet following consumption (32). Additionally, the conversions of catechins, gallic acid, and caffeine as described in the previous section may result in a softer and mellower flavor. Interestingly, S7 displayed a significantly lower intensity ($p < 0.05$) of bitter and astringent attributes, which could be attributed to the significant decrease in catechin content over the course of the sun-drying processing (33).

In general, Ganpu tea has distinctive characteristics, including bright orange liquor, silky mellow taste, and fruity sweet aroma. The sun-drying approach significantly affected the intensities of the sensory attributes of Ganpu tea. Constituents of Ganpu tea are mostly polyphenols, flavonoids, caffeine, and free amino acids, and all of them were changed continuously throughout the sun-drying processing, most probably contributing to the unique taste developed during the Ganpu tea production.

Effect of Ganpu Tea Consumption in the FST and TST

We hypothesized that tea polyphenols, flavonoids, pigments, theanine, caffeic acid, and vitexin detected in Ganpu tea in the present study would be collectively capable of conferring antidepressant-like effects through various mechanisms in animals, an effect that has been shown to take place following the regular consumption of most tea types (34). In order to test this hypothesis, we designed an *in vivo* experiment with mouse model, attempting to simulate the daily Ganpu tea consumption habits of humans. Both the FST and TST are the conventional experimental models of examining the depressive-like behaviors. The immobility times of these tests are shown in **Figure 5**. Results of the FST showed that no significant difference in immobility duration was seen between the NC group and the two oral dose groups (0.1 and 0.2 g/kg) of Ganpu tea extract ($p > 0.05$). The high oral dose group (0.4 g/kg) and PC group showed significantly reduced immobility duration as compared to that of the NC group ($p < 0.01$ and $p < 0.05$, respectively).

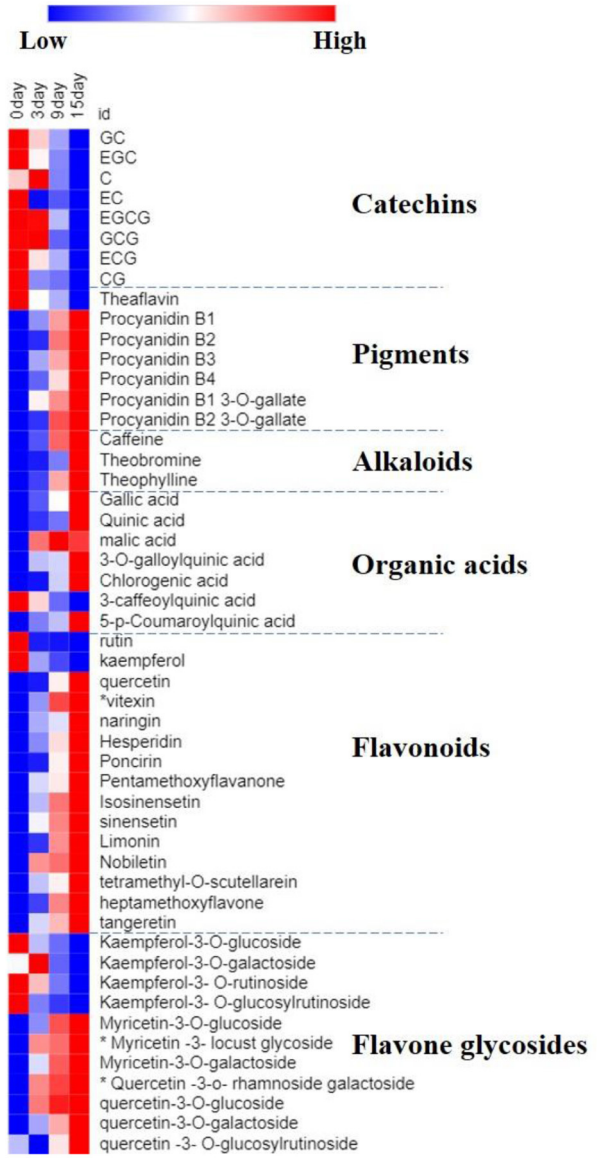


FIGURE 3 | Heatmap analysis of potential flavor compounds from Ganpu tea.

TST results showed a dose-dependent reduction in immobility duration following intake of Ganpu tea extract. The effects of oral doses at 0.1 and 0.2 g/kg of Ganpu tea extract were similar to that of the PC group, which were significantly shorter than that of the NC group ($p < 0.05$). Meanwhile, high oral dose group (0.4 g/kg) recorded an immobility time of only 26.6 s, which was significantly shorter than that of the NC group ($p < 0.01$).

The significantly reduced immobility duration of the high oral dose group (0.4 g/kg) as compared to that of the NC group ($p < 0.01$) in the FST and TST suggests that the Ganpu tea extract produced antidepressant-like effects or otherwise helps to alleviate the depressive symptoms in mice. The anti-depressive activity of Ganpu tea was likely the collective or

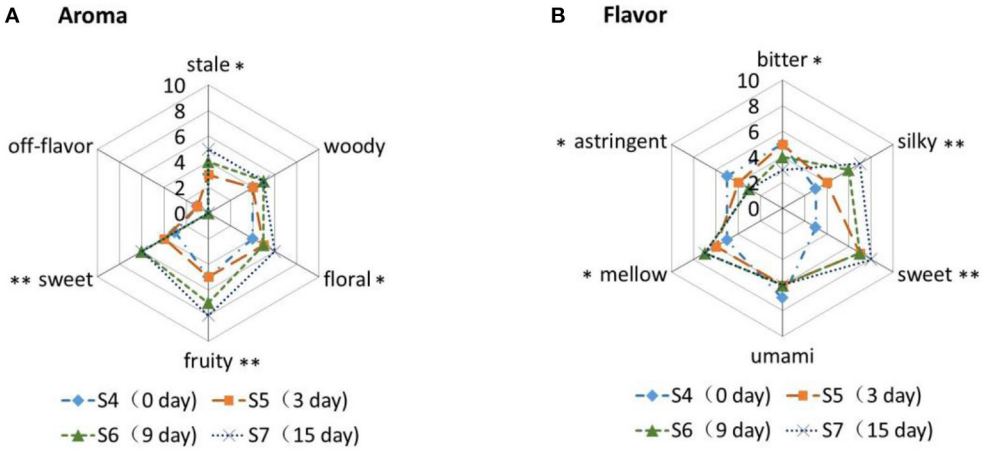


FIGURE 4 | Aroma and flavor profiles of Ganpu tea samples with different durations of sun-drying processing. The statistical analyses were performed using ANOVA, followed by LSD test (*$p < 0.05$, **$p < 0.01$).

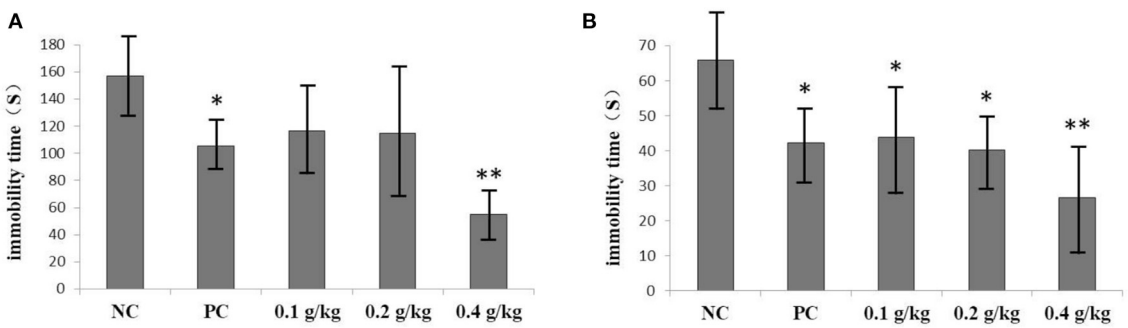


FIGURE 5 | Effects of Ganpu tea on the immobility duration of mice in the behavioral tests. **(A)** FST, and **(B)** TST. Data are expressed as mean ± SD ($n = 12$ mice per group). NC, normal control group; PC, clomipramine hydrochloride tablets group (0.02 g/kg). The statistical analyses were performed using ANOVA, followed by LSD test, *$p < 0.05$, **$p < 0.01$ as compared with that of the NC group.

synergistic result of numerous beneficial compounds present in the Ganpu tea extract. Tea polyphenols may be related to the amelioration of monoaminergic responses, antioxidant defenses, and the hypothalamic-pituitary-adrenal axis (35, 36). Flavonoids, such as quercetin, rutin, kaempferitrin, and hesperidin in Ganpu tea can attenuate the damaged monoamine neurotransmission, including that of serotonin, noradrenaline, dopamine, and 5-hydroxyindoleacetic acid, and regulate the expression levels of genes encoding neurotransmitter receptors (37). Anthocyanins were shown to regulate the activation of noradrenergic, serotonergic, and dopaminergic system (37). Caffeic acid was suggested to be active within the dopaminergic system (37). Theanine can also similarly mediate the interactions within monoaminergic systems (42). It is noteworthy that vitexin is a newly generated compound in the sun-drying processing, which was shown by Can et al. (43) to increase the catecholamine content in the synaptic cleft and to interact with serotonergic 1A, noradrenergic a2, and dopaminergic D1, D2, and D3 receptors. Further studies are necessary to determine whether other compounds in Ganpu tea are also responsible for conferring the antidepressant-like effects, and what are the underlying molecular mechanisms.

CONCLUSIONS

In the present study, we demonstrated that acquirement of the unique characteristics of high-quality Ganpu tea requires not only high-grade Pu-erh raw tea and mandarin peel, but also a full sun-drying processing for consecutive 15 days. The distinctive flavor of Ganpu tea was composed of a total of 104 water-soluble compounds, which were transformed considerably during sun-drying processing due to endogenous factors (biosynthesis or enzymatic modification of compounds within cells), as well as exogenous stimuli, including temperature, humidity, light, and microorganisms. The alterations in major chemical constituents contribute to the changes of aroma and taste of Ganpu tea. Meanwhile, tea polyphenols, flavonoids, pigments, theanine, caffeic acid, and vitexin may be also collectively responsible for the antidepressant-like effects of Ganpu tea

consumption. These findings provide a basis or understanding the chemical characteristics and health-promoting effects of Ganpu tea, and also for elucidating its value as a new flavorful beverage with potential benefit for humans suffering from the depressive symptoms.

DATA AVAILABILITY STATEMENT

The raw data supporting the conclusions of this article will be made available by the authors, without undue reservation.

ETHICS STATEMENT

All the procedures were conducted according to the National Institutes of Health Guide for the Care and Use of Laboratory Animals, and the animal handling and experimental procedures were approved by the Local Animal Use Committee (SCXK 2013-0020).

AUTHOR CONTRIBUTIONS

SX and XZ designed the concept of this study. SX, JH, HL, YZ, and DL drafted methodology and conducted formal analyses and investigation. HX and YH were project supervisors. Writing-Review and Editing were completed by HX, SX, JH, and YH. Funding Acquisition was by XZ. All authors contributed to the article and approved the submitted version.

FUNDING

This work was financially supported by the Guangdong Agricultural Science and Technology Innovation and Promotion Project (No. 2019LM1117), and Project of Strengthening Guangdong Province with Traditional Chinese Medicine (No. 20201248).

REFERENCES

1. Zhang L. The establishment of "industry standards" for the citrus Pu-erh tea has become a pressing task, China cooperation times (2017) 3:1–2.
2. Londono-Londono J, Lima VRD, Lara O, Gil A, Pasa TBC, Arango GJ, et al. Clean recovery of antioxidant flavonoids from citrus peel: optimizing an aqueous ultrasound-assisted extraction method. *Food Chem.* (2010) 119:81–7. doi: 10.1016/j.foodchem.2009.05.075
3. Zhang H, Cui J, Tian G, DiMarco-Crook C, Gao W, Zhao C, et al. Efficiency of four different dietary preparation methods in extracting functional compounds from dried tangerine peel. *Food Chem.* (2019) 289:340–50. doi: 10.1016/j.foodchem.2019.03.063
4. Lv HP, Zhang YJ, Lin Z, Liang YR. Processing and chemical constituents of Pu-erh tea: a review. *Food Res Int.* (2013) 53:608–18. doi: 10.1016/j.foodres.2013.02.043
5. Ahmed S, Unachukwu U, Stepp JR, Peters CM, Long C, Kennelly E. Pu-erh tea tasting in Yunnan, China: correlation of drinkers' perceptions to phytochemistry. *J Ethnopharmacol.* (2010) 132:176–85. doi: 10.1016/j.jep.2010.08.016
6. Wang T, Li X, Yang H, Wang F, Kong J, Qiu D, et al. Mass spectrometry-based metabolomics and chemometric analysis of Pu-erh teas of various origins. *Food Chem.* (2018) 268:271–8. doi: 10.1016/j.foodchem.2018.06.041
7. Musielak G, Kieca A. Influence of varying microwave power during microwave–vacuum drying on the drying time and quality of beetroot and carrot slices. *Dry Technol.* (2014) 32:1326–33. doi: 10.1080/07373937.2014.924135
8. Pei F, Yang WJ, Shi Y, Sun Y, Mariga AM, Zhao LY, et al. Comparison of freeze-drying with three different combinations of drying methods and their influence on colour, texture, microstructure and nutrient retention of button mushroom (*Agaricus bisporus*) slices. *Food Bioprocess Technol.* (2014) 7:702–10. doi: 10.1007/s11947-013-1058-z
9. Xu M, Tian G, Zhao C, Aftab A, Zhang H, Bi J, et al. Infrared drying as a quick preparation method for dried tangerine peel. *Int J Anal Chem.* (2017) 2017:1–11. doi: 10.1155/2017/6254793
10. Abdel-Aziz MM, Emam TM, Elsherbiny EA. Effects of mandarin (*Citrus reticulata*) peel essential oil as a natural antibiofilm agent against *Aspergillus niger* in onion bulbs. *Postharvest Biol Technol.* (2019) 156:110959. doi: 10.1016/j.postharvbio.2019.110959
11. Foo KY, Lee LK. Recent advances on the beneficial use and health implications of Pu-Erh tea. *Food Res Int.* (2013) 53:619–28. doi: 10.1016/j.foodres.2013.02.036
12. Hang X, Yang CS, Li S, Jin H, Patel T. Monodemethylated polymethoxyflavones from sweet orange (*Citrus sinensis*) peel inhibit growth of human lung cancer cells by apoptosis. *Mol Nutr Food Res.* (2009) 53:398–406. doi: 10.1002/mnfr.200800057
13. Randazzo W, Jiménez-Belenguer A, Settanni L, Perdones A, Moschetti M, Palazzolo E, et al. Antilisterial effect of citrus essential oils and their performance inedible film formulations. *Food Control.* (2016) 59:750–8. doi: 10.1016/j.foodcont.2015.06.057
14. Xiao S, Yu L-A, Lai H-Q, Cheng C, Liang D-H, Huang Y-H. Anslysis of specific aroma components in citrus Pu-erh tea by GC-MS. *Modern Food Sci Technol.* (2019) 35:1–12. doi: 10.13982/j.mfst.1673-9078.2019.11.034
15. Teng J, Zhou W, Zeng Z, Zhao W, Huang Y, Zhang X. Quality components and antidepressant-like effects of GABA green tea. *Food Funct.* (2017) 8:3311–8. doi: 10.1039/C7FO01045A
16. Kraujalyte V, Pelvan E, Alasalvar C. Volatile compounds and sensory characteristics of various instant teas produced from black tea. *Food Chem.* (2016) 194:864–72. doi: 10.1016/j.foodchem.2015.08.051
17. Lino-De-Oliveira C, Lima TCMD, Carobrez ADP. Structure of the rat behaviour in the forced swimming test. *Behav Brain Res.* (2005) 158:243–50. doi: 10.1016/j.bbr.2004.09.004
18. Steru L. The tail suspension test: a new method for screening antidepressants in mice. *Psychopharmacology.* (1985) 85:367. doi: 10.1007/BF00428203
19. Bosiljkov T, Karlović S, Brnčić M, JeŽek D, Dujmić F, Tripalo B. Extraction of bioactive compounds from tangerine peels, Eubis Cost Action, Citrus Waste Valorisation (2015) 8:23.
20. Monbaliu S, Wu A, Zhang D, Peteghem CV, Saeger SD. Multimycotoxin UPLC-MS/MS for tea, herbal infusions and the derived drinkable products. *J Agric Food Chem.* (2010) 58:12664–71. doi: 10.1021/jf1033043
21. Pongsuwan W, Bamba T, Harada K, Yonetani T, Kobayashi A, Fukusaki E. High-throughput technique for comprehensive analysis of Japanese green tea quality assessment using ultra-performance liquid chromatography with time-of-flight mass spectrometry (UPLC/TOF MS). *J Agric Food Chem.* (2008) 56:10705–8. doi: 10.1021/jf8018003
22. Yi LZ, Yuan DL, Liang YZ, Xie PS, Zhao Y. Fingerprinting alterations of secondary metabolites of tangerine peels during growth by HPLC–DAD and chemometric methods. *Anal Chim Acta.* (2009) 649:43–51. doi: 10.1016/j.aca.2009.07.009
23. Zhao Y, Chen P, Lin L, Harnly JM, Yu LL, Li Z. Tentative identification, quantitation, and principal component analysis of green pu-erh, green, and white teas using UPLC/DAD/MS. *Food Chem.* (2011) 126:1269–77. doi: 10.1016/j.foodchem.2010.11.055
24. Zhang H, Yang YF, Zhou ZQ. Phenolic and flavonoid contents of mandarin (*Citrus reticulata* Blanco) fruit tissues and their antioxidant capacity as

evaluated by DPPH and ABTS methods. *J Integr Agric.* (2018) 17:256–63. doi: 10.1016/S2095-3119(17)61664-2
25. Tumbas V, Cetkovic G, Djilas S, Canadanovic-Brunet J, Vulic J, Knez Z, et al. Antioxidant activity of mandarin (*Citrus reticulata*) peel. *J Integr Agric.* (2010) 41:256–63. doi: 10.2298/APT1041195T
26. Wang K, Ruan J. Analysis of chemical components in green tea in relation with perceived quality, a case study with Longjing teas. *Food Sci Technol.* (2009) 44:2476–84. doi: 10.1111/j.1365-2621.2009.02040.x
27. Ku KM, Kim J, Park HJ, Liu KH, Lee CH. Application of metabolomics in the analysis of manufacturing type of Pu-erh tea and composition changes with different postfermentation year. *J Agric Food Chem.* (2010) 58:345–52. doi: 10.1021/jf902818c
28. Manthey JA, Buslig BS. Flavonoids in the living system. *Q Rev Biol.* (1998) 439:1–7. doi: 10.1007/978-1-4615-5335-9_1
29. Xiao W, Li F, Zhang H, Geng Y, Yuan J, Jiang T. Preparative isolation and purification of polymethoxylated flavones from Tangerine peel using high-speed counter-current chromatography. *J Chromatogr A.* (2005) 1090:188–92. doi: 10.1016/j.chroma.2005.07.023
30. Yang Y, Zhao XJ, Pan Y, Zhou Z. Identification of the chemical compositions of Ponkan peel by ultra performance liquid chromatography coupled with quadrupole time-of-flight mass spectrometry. *Anal Methods.* (2016) 8:893–903. doi: 10.1039/C5AY02633D
31. Du L, Wang C, Zhang C, Ma L, Xu Y, Xiao D. Characterization of the volatile and sensory profile of instant Pu-erh tea using GC × GC-TOFMS and descriptive sensory analysis. *Microchem J.* (2019) 146:986–96. doi: 10.1016/j.microc.2019.02.036
32. Alasalvar C, Topal B, Serpen A, Bahar B, Pelvan E, Gökmen V. Flavor characteristics of seven grades of black tea produced in Turkey. *J Agric Food Chem.* (2012) 60:6323–32. doi: 10.1021/jf301498p
33. Wang ZH, Yue CN Tong HR. Analysis of taste characteristics and identification of key chemical components of fifteen Chinese yellow tea samples. *J Food Sci Technol.* (2020) 58:1378–88. doi: 10.1007/s13197-020-04649-2
34. Rothenberg DO, Zhang LY. Mechanisms underlying the anti-depressive effects of regular tea consumption. *Nutrients.* (2019) 11:1361. doi: 10.3390/nu11061361
35. Liu Y, Jia G, Gou L, Sun L, Yin X. Antidepressant-like effects of tea polyphenols on mouse model of chronic unpredictable mild stress. *Pharmacol Biochem Behav.* (2013) 104:27–32. doi: 10.1016/j.pbb.2012.12.024
36. Zhu WL, Shi HS, Wei YM, Wang SJ, Sun CY, Ding ZB, et al. Green tea polyphenols produce antidepressant-like effects in adult mice. *Pharmacol Res.* (2012) 65:74–80. doi: 10.1016/j.phrs.2011.09.007
37. Guan LP, Liu BY. Antidepressant-like effects and mechanisms of flavonoids and related analogues. *Eur J Med Chem.* (2016) 121:47–57. doi: 10.1016/j.ejmech.2016.05.026
38. Wang K, Liu F, Liu Z, Huang J, Xu Z, Li Y, et al. Analysis of chemical components in oolong tea in relation to perceived quality %. *J Int Food Sci Technol.* (2010) 45:913–20. doi: 10.1111/j.1365-2621.2010.02224.x
39. Zhang L, Li N, Ma Z-Z, Tu P-F. Comparison of the chemical constituents of aged pu-erh tea, ripened Pu-erh tea, and other teas using HPLC-DAD-ESI-MSn. *J Agric Food Chem.* (2011) 59:8754–60. doi: 10.1021/jf2015733
40. Zhao M, Ma Y, Wei Z-Z, Yuan W-X, Li Y-L, Zhang C-H, et al. Determination and comparison of γ-aminobutyric Acid (GABA) content in Pu-erh and other types of Chinese tea. *J Agric Food Chem.* (2011) 59:3641–8. doi: 10.1021/jf104601v
41. Min JK, John KMM, Choi JN, Lee S, Kim AJ, Kim YM, et al. Changes in secondary metabolites of green tea during fermentation by *Aspergillus oryzae* and its effect on antioxidant potential. *Food Res Int.* (2013) 53:670–7. doi: 10.1016/j.foodres.2012.12.053
42. Yin C, Gou L, Liu Y, Yin X, Zhang L, Jia G, et al. Antidepressant-like effects of L-theanine in the forced swim and tail suspension tests in mice. *Phytother Res.* (2011) 25:1636–9. doi: 10.1002/ptr.3456
43. Can ÖD, Demir Özkay Ü, Üçel UI. Anti-depressant-like effect of vitexin in BALB/c mice and evidence for the involvement of monoaminergic mechanisms. *Eur J Pharmacol.* (2013) 699:250–7. doi: 10.1016/j.ejphar.2012.10.017

Conflict of Interest: HL, YZ, and DL were employed by Yunding Ganpu Tea Company.

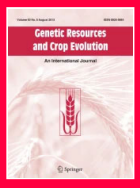
The remaining authors declare that the research was conducted in the absence of any conflict of interest.

Copyright © 2021 Xiao, Huang, Huang, Lai, Zheng, Liang, Xiao and Zhang. This is an open-access article distributed under the terms of the Creative Commons Attribution License (CC BY). The use, distribution or reproduction in other forums is permitted, provided the original author(s) and the copyright owner(s) are credited and that the original publication in this journal is cited, in accordance with accepted academic practice. No use, distribution or reproduction is permitted which does not comply with these terms.

SPRINGER LINK

Log in

Menu Search Cart

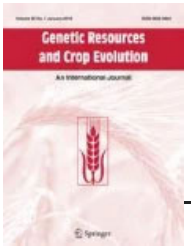


Genetic Resources and Crop Evolution

Publishing model: **Hybrid**

Back to Overview

Search all Genetic Resources and Crop Evolution articles →

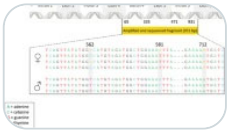


Volume 65, Issue 1

January 2018

26 articles in this issue

Gene-specific sex-linked genetic markers in date palm (*Phoenix dactylifera* L.)



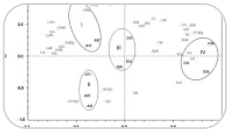
Short Communication | 05 October 2017 | Pages: 1 – 10

The echoes of the distant past of mustards (*Brassica* and *Sinapis*) among Slavic peoples



Short Communication | 10 October 2017 | Pages: 11 – 16

Morphological evaluation of cardoon (*Cynara cardunculus* L.): assessing biodiversity for applications based on tradition, innovation and sustainability

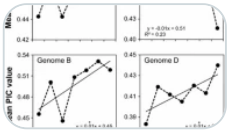


Short Communication | 10 November 2017 | Pages: 17 – 28

Maize (*Zea mays* L.) management in Yaxcaba, Yucatan, during the twentyfirst century's first decade is consistent with an overall loss of landrace diversity in southeast Mexico

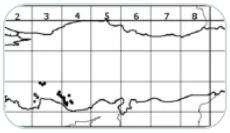
Research Article | 16 March 2017 | Pages: 29 – 54

The impact of modern plant breeding on dominant Chinese wheat cultivars (*Triticum aestivum* L.) revealed by SSR and functional markers



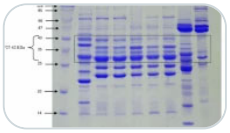
Research Article | 20 March 2017 | Pages: 55 – 65

Eco-geographic distribution of *Cicer isauricum* P.H. Davis and threats to the species



Research Article | 29 March 2017 | Pages: 67 – 77

Genetic resources for arcelin, a stored product insect antimetabolic protein from various accessions of pulses of Leguminosae



Research Article | 28 March 2017 | Pages: 79 – 90

Exploring an East Asian melon (*Cucumis melo* L.) collection for parthenocarpic ability



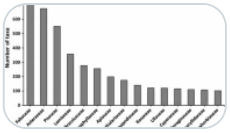
Research Article | 11 April 2017 | Pages: 91 – 101

A new subspecies of *Momordica cochinchinensis* (Cucurbitaceae) from Andaman Islands, India



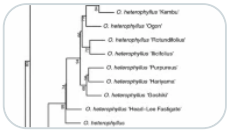
Research Article | 11 April 2017 | Pages: 103 – 112

Towards the conservation of crop wild relative diversity in North Africa: checklist, prioritisation and inventory



Research Article | Open access | 19 April 2017 | Pages: 113 – 124

Cross-transferability of SSR markers in *Osmanthus*

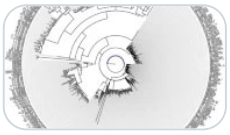


Research Article | 19 April 2017 | Pages: 125 – 136

Domestication, diversity and use of *Brassica oleracea* L., based on ancient Greek and Latin texts

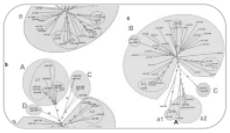
Research Article | Open access | 28 April 2017 | Pages: 137 – 159

Lophopyrum Á. Löve (1980), *Thinopyrum* Á. Löve (1980), *Trichopyrum* Á. Löve (1986): one, two or three genera? A study based on the nuclear 5S DNA



Research Article | 16 May 2017 | Pages: 161 – 186

Analysis of genetic diversity and evolutionary relationships among hexaploid wheats *Triticum* L. using LTR-retrotransposon-based molecular markers



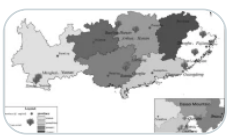
Research Article | 03 May 2017 | Pages: 187 – 198

Potential wild edible fruits of Nagaland, North-east India and its significance in the livelihood and nutritional security of rural, indigenous people



Research Article | 16 May 2017 | Pages: 199 – 215

A treasure reservoir of genetic resource of tea plant (*Camellia sinensis*) in Dayao Mountain



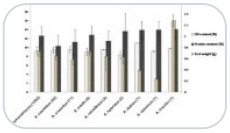
Research Article | Open access | 09 June 2017 | Pages: 217 – 227

Genetic structure of Lima bean (*Phaseolus lunatus* L.) landraces grown in the Mayan area



Research Article | 30 May 2017 | Pages: 229 – 241

Untapped amaranth (*Amaranthus* spp.) genetic diversity with potential for nutritional enhancement



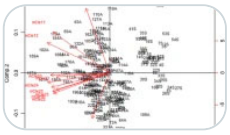
Research Article | 07 June 2017 | Pages: 243 – 253

Molecular and phenotypic diversity of ICARDA spring barley (*Hordeum vulgare* L.) collection



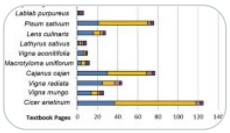
Research Article | 06 June 2017 | Pages: 255 – 269

Morphological patterns in a world collection of *Cleome gynandra*



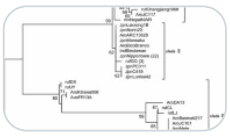
Original Paper | 13 June 2017 | Pages: 271 – 283

The origins and early dispersal of horsegram (*Macrotyloma uniflorum*), a major crop of ancient India



Research Article | Open access | 20 June 2017 | Pages: 285 – 305

Molecular evolution of the *TMS5* gene in rice (*Oryza sativa* L.)



Research Article | 16 June 2017 | Pages: 307 – 318

Wild edible fruits of Manipur, India: associated traditional knowledge and implications to sustainable livelihood



Research Article | 20 June 2017 | Pages: 319 – 332



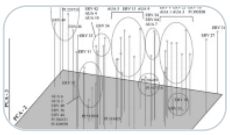
Opportunistic flowering and pollinating system as a survival strategy of the coconut (*Cocos nucifera* L.), a monotypic species of the Arecaceae family

Research Article | 05 July 2017 | Pages: 333 – 342



Potential areas for conservation of useful flora of the Tehuacán–Cuicatlán Valley, Mexico

Research Article | 26 June 2017 | Pages: 343 – 354



Assessment of phenotypic diversity in bitter vetch (*Vicia ervilia* (L.) Willd.) populations

Research Article | 04 July 2017 | Pages: 355 – 371

For authors

- Submission guidelines
- Language editing services
- Ethics and disclosures
- How to publish with us
- Open Access fees and funding
- Contact the journal



Language quality checker

Get your manuscript edited for free →

Use our pre-submission checklist →

Avoid common mistakes on your manuscript.

This journal's calls for papers →

Collections this journal is participating in.

Sign up for alerts →

Get notified when new articles are published.

Explore

Articles →

Volumes and issues

Collections

Genet Resour Crop Evol (2018) 65:217–227
https://doi.org/10.1007/s10722-017-0524-2

RESEARCH ARTICLE

A treasure reservoir of genetic resource of tea plant (*Camellia sinensis*) in Dayao Mountain

Chenkai Jiang · Wenfang Zhao · Zhen Zeng · Xingfei Lai · Chunlan Wu · Sisi Yuan · Yahui Huang · Xu Zhang

Received: 6 November 2016 / Accepted: 16 May 2017 / Published online: 9 June 2017
© The Author(s) 2017. This article is an open access publication

Abstract Components of 29 wild type tea single plants collected from Dayao Mountain, in Guangxi province, South China, were investigated. They included tea polyphenols, free amino acids, catechin, amino acid and alkaloid monomers etc. Genetic diversity and clustering analyses were conducted based on the main biochemical components. Meanwhile, genetic relationships among 6 wild type tea plants representing 3 tea populations of Daoyao Mountain with 15 tea varieties grown in Yunnan, Guangdong, Hunan, Fujian provinces were analyzed by random amplified polymorphic DNA. The results showed that wild type tea plants from Dayao Mountain were of rich genetic diversity. Furthermore, some tea germplasms with high quality, including high contents of amino acids, high epigallocatechin gallate, and high caffeine have been discovered. These wild type tea germplasms are of high values for further development values due to their geographical uniqueness.

Keywords Biochemical components · Dayao Mountain · Genetic diversity · Random amplified polymorphic DNA marker · Special tea resources · Wild tea plant (*Camellia sinensis*)

Introduction

Tea is the oldest and the most popular non-alcoholic beverage all over the world (Wambulwa et al. 2016). Tea plant is originated from China and has been grown

C. Jiang · W. Zhao · Z. Zeng · X. Lai · C. Wu · S. Yuan · Y. Huang (✉)
College of Horticulture, South China Agricultural University, Guangzhou 510642, Guangdong, People's Republic of China
e-mail: 13501513191@163.com

C. Jiang
e-mail: greenbreezekai@126.com

W. Zhao
e-mail: 921870317@qq.com

Z. Zeng
e-mail: zzhen2004@126.com

X. Lai
e-mail: 406651390@qq.com

C. Wu
e-mail: 623109678@qq.com

S. Yuan
e-mail: 390925022@qq.com

X. Zhang (✉)
College of Forestry and Lanscape Architecture, South China Agricultural University, Guangzhou 510642, Guangdong, People's Republic of China
e-mail: Zhangxu919@hotmail.com

in a geographical range from 18°N to 37°N in latitude and from 95°E to 122°E in longitude of this country (Chen et al. 2012; Long et al. 2012). A great number of tea plant germplasms, including the tea plant, allied species and cultivars in the section Theaceae genus *Camellia*, have been collected and conserved in China, Japan, India, Kenya as well as a number of other countries (Fang et al. 2012). Wild type tea plants are defined as the general name for wild woody evergreen plants belonging to *Camellia*, Theaceae, with significant value in science and application as they have been naturally selected and evolved during a long period of time. They possess some important characters such as the stubborn resistance to stressful conditions and unique quality etc. that the cultivars don't have. Consequently, they are the precious materials for development and cultivation of excellent tea varieties. Plants belonging to *Camellia* from each province in China were listed by Chang HT.A (Chang 1981): a total of 66, 55, and 50 varieties have been found in Guangxi, Yunnan and Guangdong provinces, respectively. The adjacent areas of Guangxi, Yunnan, and Guizhou were considered one of the secondary original centers of tea plants based on the geographic distribution of the wild type tea plants (Yao et al. 2005). The extraordinarily abundant wild tea plants have been growing in Guangxi owning to its unique and favorable geographical conditions.

Types and contents of biochemical components were the essential criteria for evaluation of tea plant quality, depending on the environmental conditions and related genes (Wei et al. 2011). Vital components of tea beneficial to human health are mainly the secondary metabolites of tea plants such as tea polyphenols, amino acids, caffeine etc., which are related to both resistance to stresses and tea quality (Anand et al. 2015; Kottur et al. 2010; Ma et al. 2014). Therefore, identification of the key biochemical components will pave the essential scientific basis for investigation, screening of high quality resources and application of wild type tea plants. To this end, molecular markers are the biomarkers at the DNA level. Random amplified polymorphic DNA (RAPD) is a highly effective tool to investigate the genetic diversity of living organisms and to differentiate tea germplasms at the inter-species level (Chen et al. 2005; Dhakshanamoorthy et al. 2015), represents dominant marker type known for easy handling, moderate cost of the technique, and the highly polymorphic nature (Bali et al. 2015).

There are rich resources of tea plants in China. However, previous researches on wild type tea plant germplasm resource were mainly focused on those growing in Yunnan and Guizhou provinces (Chen et al. 2005; Liu et al. 2010; Qi et al. 2013), scarce studies were done on those growing in Guangxi province (Huang et al. 2014; Zhu and Yahui 2015). However, there are plentiful wild type tea plant resources existing in the region of Daoyao Mountain, Guangxi, due to its unique geology, diverse climates and plentiful rainfall. The important ecological barrier of Dayao Mountain runing from northeast to southwest in the middle of Guangxi, formed in Permian of Paleozoic. Temple Mountain is its major peak with 1979 meters in height. Tea plant has to cross the Dayao Mountain from Yunnan-Guizhou Plateau, Southwest China, leading to the Southeast China.

In this study, we conducted a systemic analyses on the biochemical characteristic of 29 wild type tea plants collected from Liuxiang, Bainiu and Gonghe populations of Dayao Mountain. Liuxiang population mostly grows under the shade of primeval forest, Bainiu population partly grows under the tall trees; Gonghe population grows with scrubby shrubs. In addition, some special tea resources containing high contents of epigallocatechin gallate (EGCG), caffeine, and amino acid etc., have been discovered. This study may also contribute to development and utilization of wild type tea plants and scientific research on tea breeding and processing of high-quality tea.

Materials and methods

Samples and reagents

Sources of tea plants are described in Fig. 1. DYS1-13, DYS14-23 and DYS24-29 are selected from Liuxiang, Bainiu and Gonghe, respectively.

All of the following standard chemicals were purchased from Sigma-Aldrich (Co. LLC): Caffeine, theobromine, theophylline, catechins including (+)-gallocatechin (GC), catechin (C), (−)-epigallocatechin (EGC), (−)-epicatechin (EC), (+)-gallocatechin gallate (GCG), (−)-epicatechin gallate (ECG), catechin-3-gallate (CG), (−)-epigallocatechin gallate (EGCG), and amino acids (Siama, St. Luis, MO, USA). Methanol (HPLC), sodium carbonate (Analytical grade, AR), folin-ciocalteu (AR), galllic acid (AR), oxalic acid (AR), citric acid (AR), disodium hydrogen phosphate

(AR), potassium dihydrogen phosphate (AR), ninhydrin (AR), stannous chloride (AR), sodium bicarbonate (AR), trifluoroacetic acid (AR), and aluminium chloride (AR) were obtained from Tianjin, China.

Preparation of samples

Samples were prepared according to the method described in Descriptions and Data Standard for Tea (*Camellia* spp.) (Chen et al. 2005): one bud and two leaves were plucked in spring, fixed in microwave oven (Midea, Guangzhou, China), and dried in oven (DHG-101, Shanghai, China).

Methods for determination of biochemical components of tea

The contents of moisture, aqueous extract, tea polyphenols, and free amino acids were determined according to GB/T 8304-2013, GB/T 8305-2013, GB/T 8313-2008, and GB/T 8314-2013, respectively.

The contents of alkaloids and catechin monomers were determined by high performance liquid chromatography (HPLC) (Agilent 1200, Agilent Technologies, Santa Clara, CA, USA). C18 reverse phase column (HyPersil ODS2, 4.6 mm × 250 mm, 5 μm) (Thermo Fisher Scientific, USA) was used. The determination conditions were as set follows: solvent A was pure methanol and solvent B was 0.05% trifluoroacetic acid in water. Column temperature was set at 30 °C and the flow rate was 0.8 mL/min. UV spectra were measured at 278 nm. Sample size for injection was 20 μL. The gradient elution profile was 2% A at 0 to 2 min, to 8% A at 8 min, to 10% A at 30 min, to 20% A at 35 min, to 25% A at 45 min, to 30% A at 50 min. 30% A was maintained from 50 to 55 min, and then changed to 35% A for 60 min.

The contents of free amino acid monomers were determined with amino acid analyzer (L-8800, Japan). The determination conditions were set as follows: concentration of amino acid standard was 100 μmol/L, sample size for injection was 20 μL, column

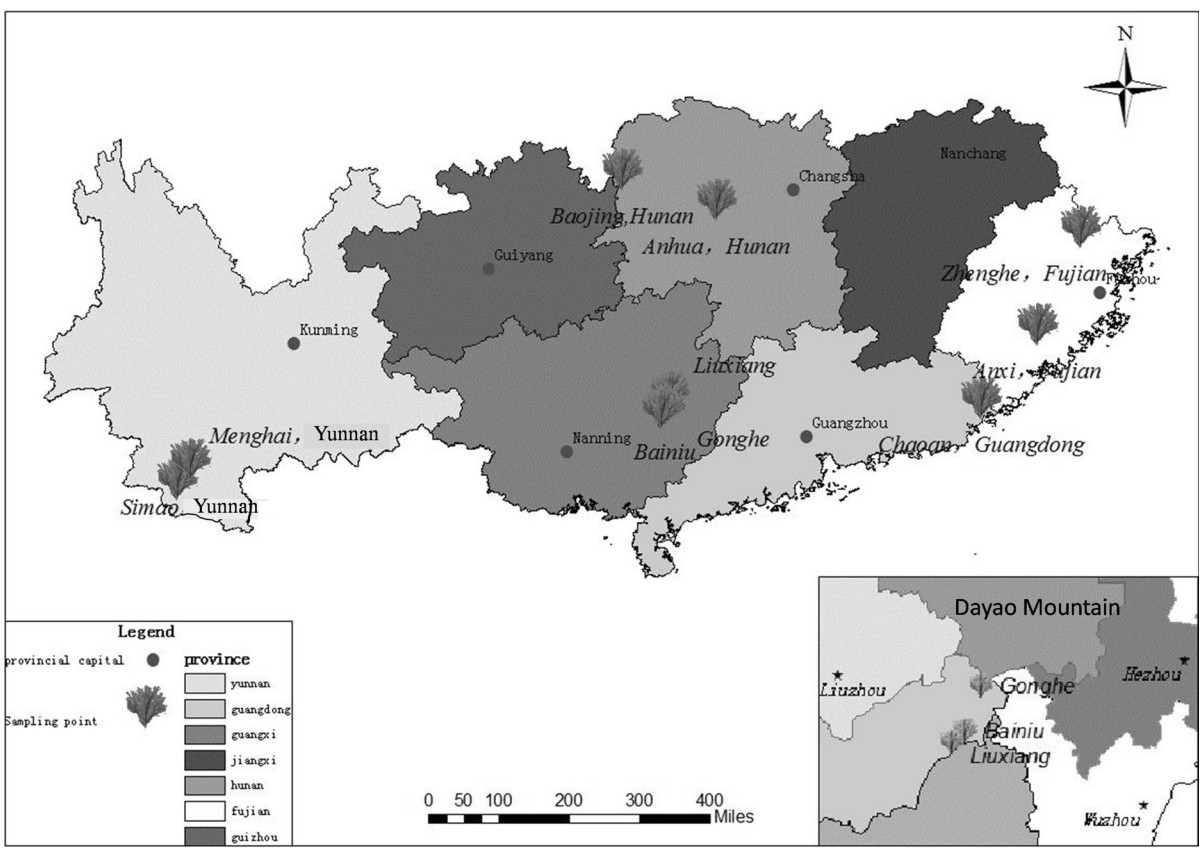


Fig. 1 Tea plant (*Camellia sinensis* (L.) Kuntze) sources in Dayao Mountain, South China

temperature was 134 °C, running time was 110 min, room temperature was 26 °C, and relative humidity was 76%.

DNA extraction

Two wild type tea plants collected from Liuxiang, Bainiu, and Gonghe population were randomly selected. Tea leaf DNA was extracted with the method described by Chen et al. (2002) with a modification. 1.0 g of fresh leaves was quickly ground into powder with liquid nitrogen and appropriate amount of polyvinylpolypyrrolidone (PVPP) in a mortar. The powder was mixed with 1 mL of cetyl trimethylammonium bromide extract (2% CTAB, 0.1 mmol/L Tris, 20 mmol EDTA, 1.4 mol NaCl, pH = 8.0) containing 1 μL of mercaptoethanol, and kept in water bath at 65 °C for 45 min, shaked every 8 min. Phenol–chloroform-isoamyl alcohol mixture (V_1:V_2:V_3 = 25:24:1) in the same volume was added, mixed well, and centrifuged at 12,000 r/min for 5 min. The supernatant was transferred to a fresh clean tube. The elution process was repeated three times. 1.5 mL of isopropanol was added to the centrifuge tube, kept at −20 °C for 1 h after shaking well, and centrifuged at 12,000 r/min for 5 min. White precipitation was transferred to a new clean tube, cleaned three times with 75% of ethanol, then dissolved in 100 μL of double distilled water with RNase after being dried in the air. DNA solution was kept in water bath at 37 °C for 30 min. A fraction was used for DNA quality test and the rest was reserved in the refrigerator at −20 °C for subsequent analysis.

DNA quality test

1 μL of DNA solution was diluted to 100 μL with double distilled water and its purity was analyzed with the ratio of A_{260}:A_{280} after detecting by nucleic acid protein detector (Biophotometer plus, Germany). Purified DNA solution was mixed with loading buffer in the ratio of 1:5. The DNA mixture was analyzed by 1.5% agarose gel electrophoresis apparatus (DYY-6C,Beijing, China) at 130 V for 20 min.

RAPD molecular marker

Polymerase chain reaction (PCR) assays were performed with Thermal Cycler (My Cycler Tm Thermal, USA) as described by Wang et al. (2008) with a modification. 18.5 μL of ddH_2O, 2.5 μL of 10 × Taq Buffer containing 20 mmol Mg^{2+}, 2 μL of dNTPs (2 mmol/L), 0.5 μL of primer (8 PM/μL), 0.5 μL of Taq DNA polymerase, and 1 μL of DNA template (40–100 ng) were in PCR reaction solution. PCR amplification was run under the following programmed procedures: pre-denaturation at 94 °C for 1 min, followed by 38 cycles of annealing at 33–37 °C for 50 s, and extension at 72 °C for 2 min and finally extended at 72 °C for 10 min. PCR products were separated by 1.5% agarose gel electrophoresis at 130 V for 80 min, stained with ethidium bromide and the stained bands were visualized with UV transilluminator.

Statistical analysis

Maximum, minimum, mean, and Shannon–Weaver index (H′) were calculated with Excel 2013. $H' = -\Sigma p_i \ln P_i$ ($P_i = N_i/N$, occurrence frequency of the ith character). Cluster analysis was done according to Ward method after data normalization by SPSS 18.0. RAPD data were analyzed by NTSYS-pc2.10e software, and PIC (polymorphism information content) = $1-\Sigma P_i^2$ (P_i: occurrence frequency of the ith polymorphic bands). Genetic similarity coefficient (GS) of germphlasm resources was calculated according to Jacard coefficient.

Results

Genetic diversity analysis

The higher the Shannon–Weaver index (H′) is, the more the information of community has. Species is abundant as $H' > 3.0$. H′ of aqueous extract, tea polyphenol, free amino acid, flavonoid, and alkaloid were higher than 3.0, showing that the genetic diversity of wild tea plants from Dayao Mountain is abundant (Table 1). H′ of total catechins, ester-catechins, and non-ester catechins were 3.08, 3.11, 3.01, respectively, which were also greater than 3.0, showing a wide range of evolution of wild type tea plants.

Cluster analysis of wild tea plant germplasms from Dayao Mountain

Tea plant population can be 90–96% correctly classified by the total contents of tea polyphenol, catechin

constitutions, the ratio of caffeine to total nitrogen, theanine (Liu and MJ 1991). The contents of C, EC, GC, EGC, CG, ECG, GCG, EGCG, caffine, theobromine and theophylline were analyzed by HPLC. And factor analysis was according to the dates of catechins and alkaloids after standardization. KMO was $0.609 > 0.500$ and the significance level of Bartlett's test of sphericity was $0.000 < 0.005$, showing that the result of factor analysis was credible. And the accumulative contribution rate of the first four public factors total variation accounted for $85.535\% > 85\%$, maintaining most of information of 11 characters.

Then cluster analysis was made according to the four major factors by Ward's method. The result was shown in Fig. 2A. 29 single plants were clustered into three groups. DYS4, DYS5, DYS6, DYS24, DYS25, DYS26, DYS27, DYS28 and DYS29 were in the first group, DYS8, DYS14, DYS15, DYS16, DYS17, DYS18, DYS19, DYS20, DYS21, DYS22 and DYS23 were in the second group, and DYS1, DYS2, DYS3, DYS7, DYS9, DYS10, DYS11, DYS12 and DYS13 were in the third group. On the one hand, all the Gonghe population was in the first group, all the Bainiu population was in the second group, and the third group was from Liuxiang. The result indicated that wild tea plants from Dayao Mountain were of significant geographical uniqueness. On the other hand, the Liuxiang population were distributed all over the three groups, which indicated the variation of Liuxiang population was the most abundant, and the genetic diversity was the most richest. Therefore, the Liuxiang population was the most primitive.

Diversity analysis of RAPD amplification production

A total of 17 primers with high polymorphism, clarity, and good repeatability were screened out from 120 common primers of tea plant. The polymorphism information was shown in Table 2. A total of 172 polymorphic bands were amplified by 17 primers ($PIC > 0.5$), of which, 136 were polymorphic and polymorphism proportion was 79.07%. The numbers of polymorphic bands of each primer ranged from 6 to 15 and the polymorphism of prime 11 reached to 93.33%.

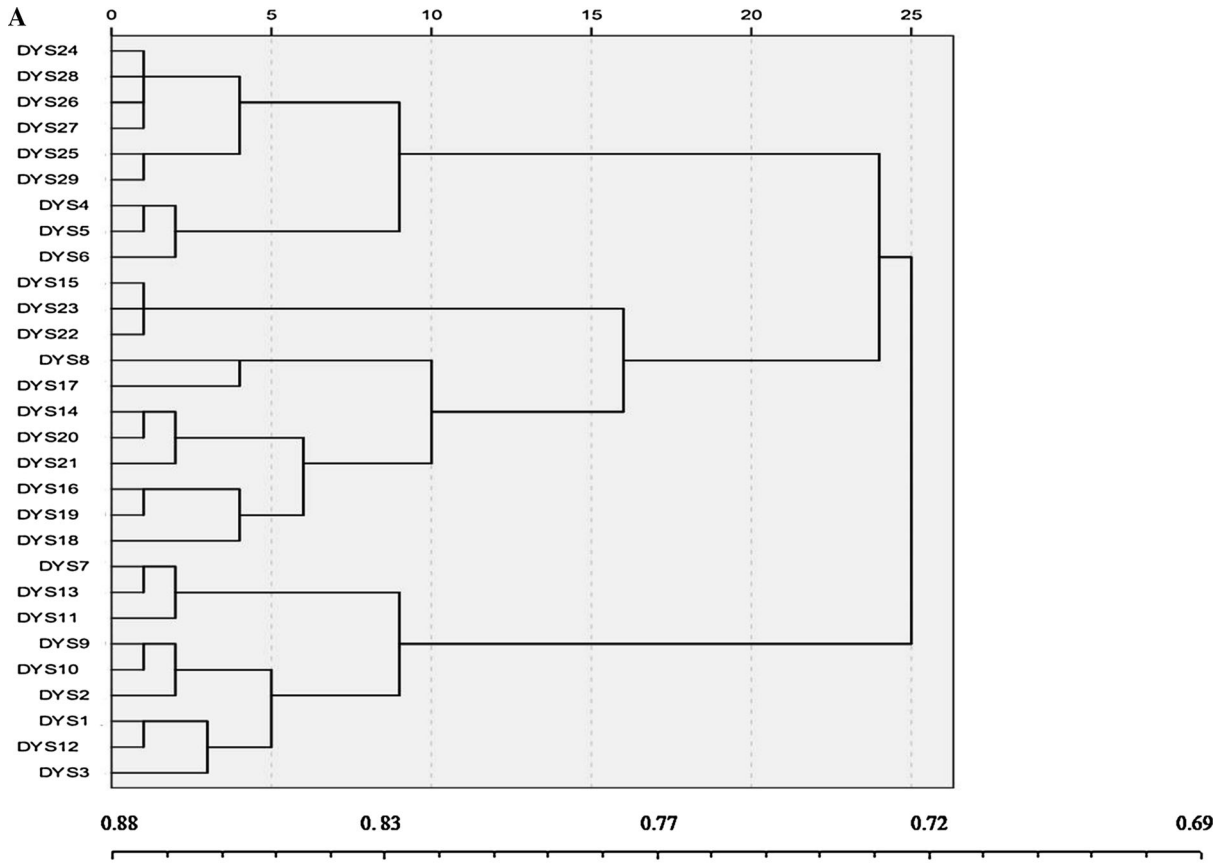
Cluster analysis of wild tea plants from Dayao Mountain based on GS

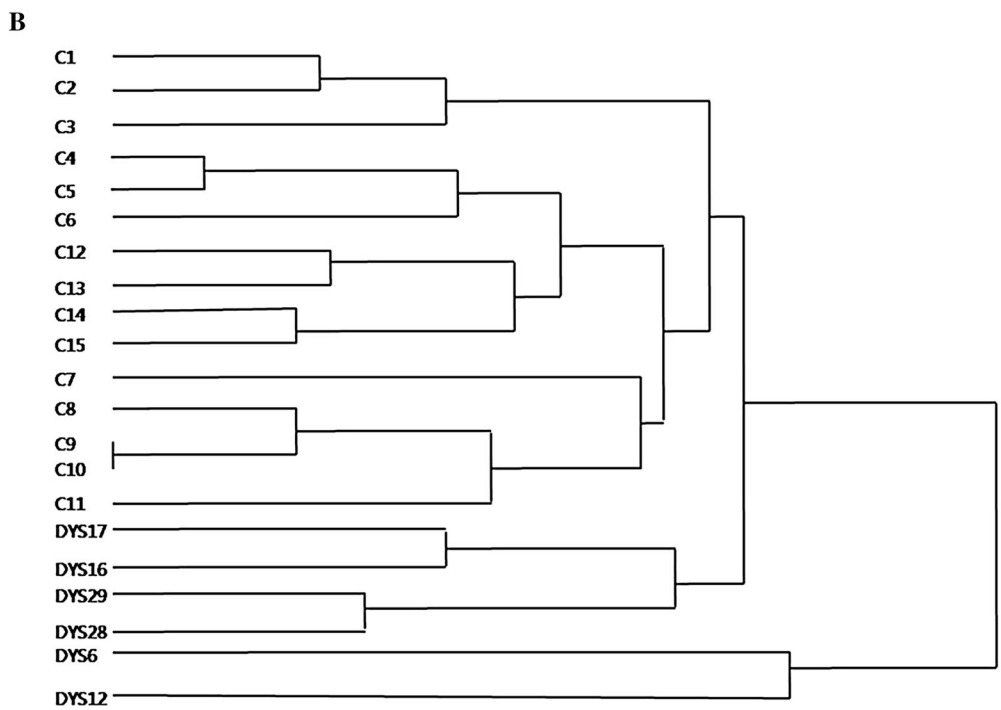
GS ranged from 0.65 to 0.88 among tea plant samples, and GS between DYS6 and Huangjingui, Changye Baihao was the minimum one (0.65), indicating that their genetic distance is far away. Genetic distances among tea plants from Liuxiang population and those in other areas were long according to their GS, which were 0.65–0.77. GS between DYS19 and Foxiang 3 was maximum one (0.83). Tieguanyin and Huangjincha were the most similar to DYS28 (0.80).

Cluster analyses of tea plants from five provinces based on GS were shown in Fig. 2B. 21 samples were

Table 1 Genetic diversity analysis according to main biochemical components

Biochemical component (%)	Average	Min	Max	SD	H′
Aqueous extract	47.69	43.44	56.55	2.62	3.04
Tea polyphenol	28.38	22.81	34.07	2.76	3.18
Free amino acid	3.60	1.96	4.76	0.75	3.08
Flavone	0.54	0.32	0.79	0.11	3.16
Total catechins	22.86	15.79	32.36	4.17	3.08
Ester-catechins	14.24	9.99	20.92	2.92	3.11
EGCG + GCG	3.66	7.18	15.21	5.43	3.03
ECG + CG	1.33	2.03	5.8	4.57	3.15
Non-ester catechins	8.62	3.35	15.09	3.23	3.01
EC + C	0.85	0.78	2.85	4.35	2.94
EGC + GC	3.52	2.23	13.6	3.04	2.85
Alkaloid	6.03	2.27	8.97	1.52	3.85
Caffeine	5.77	2.19	8.61	1.43	3.86


A
0
5
10
15
20
25
DYS24
DYS28
DYS26
DYS27
DYS25
DYS29
DYS4
DYS5
DYS6
DYS15
DYS23
DYS22
DYS8
DYS17
DYS14
DYS20
DYS21
DYS16
DYS19
DYS18
DYS7
DYS13
DYS11
DYS9
DYS10
DYS2
DYS1
DYS12
DYS3
0.88
0. 83
0.77
0.72
0.69


B
C1
C2
C3
C4
C5
C6
C12
C13
C14
C15
C7
C8
C9
C10
C11
DYS17
DYS16
DYS29
DYS28
DYS6
DYS12

◀**Fig. 2** Cluster analysis of wild tea plants from Dayao Mountain. **A** Was based on cataechins and alkaloids. **B** Was based on genetic similarity coefficient. *C1* Lintou Dancong, *C2* Hongbing Dancong, *C3* Huangzhixiang, *C4* Tieguanyin, *C5* Zhenghe large-leaved white tea, *C6* Huangjingui, *C7* Maoxie, *C8* Zijuan, *C9* Changye Baihao, *C10* Foxiang 3, *C11* Yungui, *C12* Xiang 1, *C13* Xiang 2, *C14* Xiang13, *C15* Huangjincha

classified into 2 groups based on their similarity coefficient, which was 0.74. DYS6 and DYS12 from Liuxiang population of Dayao Mountain were clustered into the same group; those from the rest regions of Dayao Mountain, Yunnan, Guangdong, Fujian, and Hunan were clustered in the other group. It suggested that tea resources from Liuxiang population of Dayao Mountain possessed extremely unique characters. 21 samples were classified into 4 groups based on their similarity coefficient, which was 0.76. Tea plants from Liuxiang population were clustered into two groups, those from Bainiu and Gonghe population were in one group, and those from Yunnan, Guangdong, and Hunan were clustered into the same group, further demonstrating that tea plants from Dayao Mountain are extremely diverse and unique.

Special germplasm resource of wild tea plant from Dayao Mountain

Some special germplasm resources of wild type tea plant from Dayao Mountain were discovered according to their biochemical components (Table 3). These special resources will be directly used for production or as breeding parents. Amino acid content in Tea plant of high free amino acid was more than 4% (Yu et al. 1992). Hereby, 9 tea plants were higher than, including 5 samples from Liuxiang population and 4 samples from Gonghe population. Germplasm with over 5% of caffeine is considered as high caffeine resource (Yang et al. 2013). Wild type tea plants from Dayao Mountain were expected to become a special resource with high caffeine content, as their average content of caffeine was 5.77%. Caffeine contents of 23 tea plants were high, including 13 samples from Liuxiang population, 6 samples from Gonghe population, and 4 samples from Bainiu population. Catechins, a majority components of tea polyphenols, account for 70–80% of tea polyphenols content, and tea with catechins higher than 30.40% is considered as

Table 2 Polymorphism information of PCR amplification products

Prime number	Prime sequence	Annealing temperature/°C	Number of bands	Number of polymorphic bands	Percentage of polymorphism/%	PIC
A4	AATCGGGCTG	35	7	5	71.43	0.70
A5	AGGGGTCTTG	33	9	6	66.67	0.82
B1	GTTTCGCTCC	35	11	9	81.82	0.87
B2	TGATCCCTGG	33	13	11	84.62	0.88
B4	GGACTGGAGT	33	10	7	70.00	0.80
B15	GGAGGGTGTT	34	11	7	63.64	0.80
C6	GAACGGACTC	35	10	7	70.00	0.78
C11	AAAGCTGCGG	36	15	14	93.33	0.90
D1	ACCGCGAAGG	37	11	8	72.73	0.73
D3	GTCGCCGTCA	37	12	11	91.67	0.85
D5	TGAGCGGACA	36	10	7	70.00	0.83
D13	GGGGTGACGA	36	8	5	62.50	0.66
E1	CCCAAGGTCC	35	9	8	88.89	0.83
E9	CTTCACCCGA	34	12	11	91.67	0.90
H7	CTGCATCGTG	33	9	8	88.89	0.80
H12	ACGCGCATGT	37	9	8	88.89	0.84
H18	GAATCGGCCA	35	6	4	66.67	0.91
Total			172	136	–	–
Average			10.12	8.00	79.07	0.82

resource of high catechins (Yu et al. 1992). DYS3 from Liuxiang population and DYS22 from Bainiu population were discovered, whose catechins contents were 32.10 ± 0.14% and 30.66 ± 0.08%, respectively. Tea plant with EGCG content over 10% is regarded as high EGCG resource (Zheng et al. 2007). EGCG content of samples were 4.18–12.13%, and DYS11 was the highest one (2.13 ± 0.06%). 3 samples from Liuxiang population were the high EGCG resources.

Discussion

Plants in *Camellia* are generally distributed in the southern and southwestern China, and the central parts in Yunnan, Guangxi, Guangdong and near the Tropical regions (Chang 1981). Consequently, Guangxi is of the vital geographical significance during the evolution of plants in *Camellia*. The most obvious character of original plants are their diverse transitional types ranging from primitive to evolutionary types (Fulian 1986). Previous studies have shown that evolutionary process of tea plant is successional, periodical and irreversible (Chen and Yajun 2013). Primitive type was large-sized leaves, arbor type with single terminal flowers while the evolutionary type has small leave, and is shrub type with fascicled flowers. Wild type tea plants from Liuxiang population had large leaves in the arbor or semi-arbor form, solitary or fascicled flowers, those from Bainiu population were middle leave, arbor form. Those from Gonghe population had small leaves and in shrub type with most fascicled flowers (Huang et al. 2014). Tea plants from Liuxiang population had large leaves, and were clustered in the same group with Yunnan large leaf species, Vienam large leaf species and Assam varieties based on their leaf area. Tea plants from Liuxiang and Bainiu populations had middle and small leaves, respectively (Fig. 3), whose palisade tissue were 1 layer while those from Gonghe population were 2 layers (Fig. 4). All above described features imply that Liuxiang and Bainiu tea population are relatively primitive, and Gonghe tea population is the most evolutionary one. These results are in accordance with cluster analysis based on RAPD markers, indicating that wild type tea plants from Dayao Mountain are consisted of various types from the primitive to more evolutionary one. These wild type tea germplasms are valuable for research on the origin, evolution and exploitation of tea.

The biochemical components of tea were mainly affected by variety, environment and cultivation conditions as well as plucking standard. Clouds and mist drift through Dayao Mountain, and soil there is rich in organic matters, which are favorable for cultivating abundant tea plants. The majority of catechins in primitive tea plant are non-galloylated catechins, while those of the evolved tea plant are ester-catechins. Ratios of ester catechins to non-ester catechins of 29 tea single plants varied hugely. Furthermore, genetic diversity of ester catechins was

Table 3 Special resources

Resource type	Resource name
High free amino acids (>4.00%)	DYS8 (4.72 ± 0.02%), DYS12 (4.59 ± 0.03%), DYS27 (4.59 ± 0.06%), DYS5 (4.53 ± 0.06%), DYS29 (4.52 ± 0.07%), DYS6 (4.32 ± 0.04%), DYS9 (4.26 ± 0.03%), DYS28 (4.22 ± 0.03%), DYS24 (4.15 ± 0.04%)
High caffeine (>5.00%)	DYS9 (8.39 ± 0.12%), DYS4 (8.10 ± 0.11%), DYS10 (8.02 ± 0.03%), DYS5 (7.88 ± 0.12%), DYS6 (7.85 ± 0.24%), DYS3 (7.23 ± 0.01%), DYS12 (6.50 ± 0.01%), DYS13 (6.30 ± 0.05%), DYS11 (6.29 ± 0.05%), DYS7 (6.21 ± 0.00%), DYS25 (5.98 ± 0.00%), DYS28 (5.95 ± 0.02%), DYS2 (5.89 ± 0.02%), DYS26 (5.84 ± 0.03%), DYS24 (5.83 ± 0.03%), DYS27 (5.57 ± 0.04%), DYS29 (5.56 ± 0.02%), DYS8 (5.49 ± 0.04%), DYS1 (5.45 ± 0.01%), DYS15 (5.25 ± 0.00%), DYS22 (5.15 ± 0.01%), DYS20 (5.04 ± 0.01%), DYS17 (5.03 ± 0.04%)
High catechins (>30%)	DYS3 (32.10 ± 0.14%), DYS22 (30.66 ± 0.08%)
High ester-catechin (>19%)	DYS11 (20.85 ± 0.04%)
High EGCG (>10%)	DYS11 (12.13 ± 0.06%), DYS12 (11.75 ± 0.64%), DYS3 (10.17 ± 0.06%)

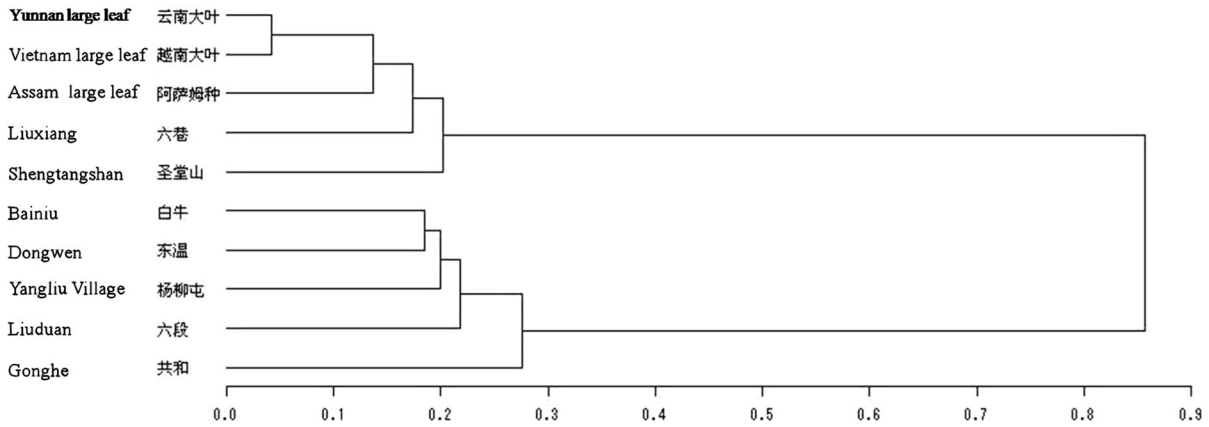


Fig. 3 Cluster analysis of Dayao Mountain based on leaf area (Huang et al. 2014)

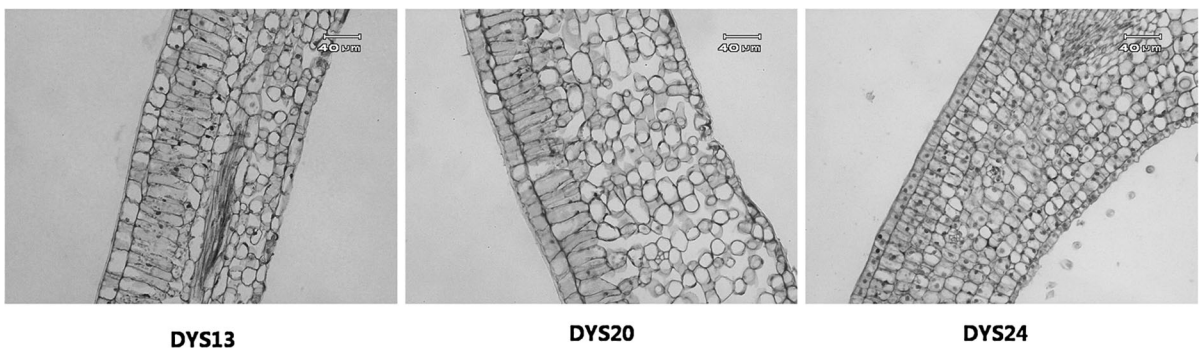


Fig. 4 Leaf transverse section of Dayao Mountain tea plants (Zhu and Yahui 2015)

greater. The contents of theophylline, theobromine of tea were decreased with the improvement of its evolution level (Shengxiang 2009). Theobromine content of single plants from Liuxiang ($\bar{x} = 0.34\%$) was greater than those from Bainiu $\bar{x} = 0.12\%$) and Gonghe ($\bar{x} = 0.03\%$), indicating that Liuxiang population is relatively primitive. However, catechin composition was just contrary, probably due to the reason that biochemical components of tea plant are affected by both environment and variety. Other studies have shown that variations of catechin contents were larger among locations than among cultivars (Wei et al. 2011). Since Liuxiang tea population grow under the shade of tall trees, this environmental condition contributes to the biosynthesis of non-ester catechin (Hong et al. 2014). In general, wild tea plants from Dayao Mountain are the mixture ranging from the primitive type to the evolutionary type, with abundant genetic diversity and geographical uniqueness according to the previous studies and molecular biology research in this study. Wild type tea plants from Liuxiang were the most primitive ones while those from Bainiu were in the middle-evolution stages, and those from Gonghe were the most evolutionary ones.

Changye Baihao was systematically bred among tea plant populations from Nannuoshan, Menghai county from 1973 to 1985 in Tea Research Institute, Yunnan Academy of Agricultural Sciences. Foxiang 3 was the hybrid from F1 with Fuding large-leaved white tea as male parent, Changye Baihao as female parent in Tea Research Institute, Yunnan Academy of Agricultural Sciences. Therefore, there is a genetic relationship between two varieties, which is consistent with result of genetic similarity coefficient, according to RAPD makers in this study. Besides, Zijuan and Changyebaihao were systematically bred from Yunnan dayezhong group, which is also consistent with result of RAPD makers. The above mentioned evidences suggest that genetic relationships among different varieties

analyzed according to genetic similarity coefficient based on RAPD maker are highly reliable. Result of cluster analysis showed that tea plants with similar genetic background are always classified in one group. Cluster analyses according to RAPD markers was accordant with that analyzed based on their biochemical components, which turned out that the diversity of biochemical components reflects DNA-based genetic diversity. It is further illustrated that tea plants from Dayao Mountain are of abundant genetic diversity and geographical uniqueness.

Special tea plant germplasm resource is the important source with higher added-value product, and wild tea plants possess a lot of the extraordinary characteristics due to the unique growth environment. Special tea plant resources with high catechin content are important for industrial production of tea polyphnols and catechins. DYS3 and DYS22 are the catechin at high levels in tea plants. DYS11 with high ester catechin tea plant is significant original material for ester catechin extraction and breed improvement. EGCG is a predominant ingredient of catechins (Vuong et al. 2010). There are broad application prospects for tea with high EGCG content due to its function in human health (Sur et al. 2016; Wei et al. 2016). However, EGCG can't be artificially synthesized at present, and it can only be extracted from tea. DYS11, DYS12, and DYS3 are the resources containing high EGCG (EGCG $\geq$ 10%), which is essential for high EGCG tea production. Caffeine has the functions of regulation of blood sugar level, antidepression, improvement of nerve excitability (Fang et al. 2015; Grosso et al. 2015). The average relative content of caffeine of wild type tea plants from Dayao Mountain is 5.77%, these tea plants are expected to become the resource with higher caffeine. Amino acids are one group of important biochemical components contributing to tea quality They have the intimate connection with taste and fragrance of tea. Besides, main amino acids in tea such as theanine have the physiological functions of tranquilization, depressurization, enhancement of the immunnity. Therefore, tea plant with high theanine content is of important values (Song et al. 2015; Zhao et al. 2013). A total of 26 types of amino acids have been identified in tea, accounting for about 1–4% of the dry weight (Xu et al. 2013). Wild tea plants from Dayao Mountain are rich in free amino acids with the average content of 3.60%, and DYS8 is up to 4.72 $\pm$ 0.02%. These special wild type tea germplasm resources can not only be used as the materials for extraction of some valuable natural products, but also can serve as breeding materials for commercial exploitation.

Acknowledgements The authors thank Fu Jian Province "2011 Collaborative Innovation Center" Chinese Oolong Tea Industry Innovation Center Special Project (J2015-75); The Research on the Innovation and Utilization of New Tea Germplasm for Cold Resistance in Guangdong (2013B020201003); Selection and Breeding of New Varieties of Specific Tea Resources in Guangdong (2015B020202007); Introduction, Domestication, Breeding Technology of High EGCGTea Plants (2016A020208012).

Compliance with ethical standards

Conflict of interest The authors declare that they have no conflict of interest.

Open Access This article is distributed under the terms of the Creative Commons Attribution 4.0 International License (http://creativecommons.org/licenses/by/4.0/), which permits unrestricted use, distribution, and reproduction in any medium, provided you give appropriate credit to the original author(s) and the source, provide a link to the Creative Commons license, and indicate if changes were made.

References

Anand J, Upadhyaya B, Rawat P, Rai N (2015) Biochemical characterization and pharmacognostic evaluation of purified catechins in green tea (*Camellia sinensis*) cultivars of India. 3. Biotech 5(3):285–294

Bali S, Mamgain A, Raina SN, Yadava SK, Bhat V, Das S, Pradhan AK, Goel S (2015) Construction of a genetic linkage map and mapping of drought tolerance trait in Indian beveragial tea. Mol Breed 35(5):1–20

Chang H (1981) A taxonomy of the genus *Camellia*. Guangzhou: The Editorial Staff of the Journal of Sun Yatsen University, pp 4–5

Chen Z, Yajun Y (2013) Dictionary of Chinese tea. Shanghai Culture Press, Shanghai, p 73

Chen L, Yu F, Tong Q (2002) Discussion on phylogenetic classification and evolution of Sect. Thea. J Tea Sci 20(2):89–94

Chen L, Yajun Y, Fulian Y (2005a) Description specification and data standard of tea plant germplasm. Chinese Agricultural Press, Beijing, p 10

Chen J, Wang P, Xia Y, Xu M, Pei S (2005b) Genetic diversity and differentiation of *Camellia sinensis* L. (cultivated tea) and its wild relatives in Yunnan province of China, revealed by morphology, biochemistry and allozyme studies. Genet Resour Crop Evol 52(1):41–52

Chen L, Apostolides Z, Zongmao C (2012) Global tea breeding: achievements, challenges and perspective. Zhejiang University Press, Hangzhou, p 1

Dhakshanamoorthy D, Selvaraj R, Chidambaram A (2015) Utility of RAPD marker for genetic diversity analysis in gamma rays and ethyl methane sulphonate (EMS)-treated *Jatropha curcas* plants. CR Biol 338(2):75–82

Fang W, Cheng H, Duan Y, Jiang X, Li X (2012) Genetic diversity and relationship of clonal tea (*Camellia sinensis*) cultivars in China as revealed by SSR markers. Plant Syst Evol 298(2):469–483

Fang C, Wang X, Huang Y, Hao S, Sheng J (2015) Caffeine is responsible for the bloodglucose-lowering effects of green tea and Puer tea extracts in BALB/c mice. Chin J Nat Med 13(8):595–601

Fulian Y (1986) Disscusion on source area and center of origin. pp 1–8

Grosso G, Micek A, Castellano S, Pajak A, Galvano F (2015) Coffee, tea, caffeine and risk of depression: a systematic review and dose– response meta-analysis of observational studies. Mol Nutr Food Res 60(1):223–234

Hong G, Jie W, Yong Z, Hochstetter D, Zhang S, Yue P, Shi Y, Ping X, Wang Y (2014) Biosynthesis of catechin components is differentially regulated indark-treated tea (*Camellia sinensis* L.). Plant Physiol Biochem 78(3):49–52

Huang Y, Lu Z, Wu C, Li Q, Lai X, Zhao W, Sisi Y (2014) Research on morphological of wide tea plants from Jinxiu, Guangxi. Tea Fujian 01:14–21

Kottur G, Venkatesan S, Murugesan S (2010) Diversity among various forms of catechins and its synthesizing enzyme (phenylalanine ammonia lyase) in relation to quality of black tea (*Camellia* spp.). J Sci Food Agric 90(9): 1533–1537

Liu WH, MJ L (1991) Discriminant analysis on population chemical classification of tea plant germplasm. Papers on Scientific Research. Shanghai Scientific and Technical Publication, Shanghai

Liu BY, You-Yong LI, Tang YC, Wang LY, Cheng H, Wang PS (2010) Assessment of genetic diversity and relationship of tea germplasm in Yunnan as revealed by ISSR markers. Acta Agron Sin 36(3):391–400

Long Z, Jiarong P, Zhu C (2012) Determination of the geographical origin of Chinese teas based on stable carbon and nitrogen isotope ratios. J Zhejiang Univ sci B 13(10):824–830

Ma JQ, Yao MZ, Ma CL, Wang XC, Jin JQ, Wang XM, Chen L (2014) Construction of a SSR-based genetic map and identification of QTLs for catechins content in tea plant (*Camellia sinensis*). PLoS ONE 9(3):1–11

Qi DH, Guo HJ, Sheng CY (2013) Assessment of plant species diversity of ancient tea garden communities in Yunnan, Southwest of China. Agrofor Syst 87(2):465–474

Shengxiang C (2009) Special tea plant germplasm screening and primary research on SSR maker with high caffeine content. Sichuan Agricultral University, Sichuan

Song HJ, Yong DK, Mi JJ, Ahn MS, Kim SW, Liu JR, Choi MS (2015) Rapid selection of theanine-rich green tea (*Camellia sinensis* L.) trees and metabolites profiling by Fourier transform near-infrared (FT-IR) spectroscopy. Plant Biotechnol Rep 9(2):55–65

Sur S, Pal D, Roy R, Barua A, Roy A, Saha P, Panda CK (2016) Tea polyphenols EGCG and TF restrict tongue and liver carcinogenesis simultaneously induced by N-nitrosodiethylamine in mice. Toxicol Appl Pharmacol 300:34–46

Vuong QV, Golding JB, Nguyen M, Roach PD (2010) Extraction and isolation of catechins from tea. J Sep Sci 33(21):3415–3428

Wambulwa MC, Meegahakumbura MK, Chalo R, Kamunya S, Muchugi A, Xu JC, Liu J, Li DZ, Gao LM (2016) Nuclear microsatellites reveal the genetic architecture and breeding history of tea germplasm of East Africa. Tree Genet Genomes 12(1):1–10

Wang H, Liang YR, Lu J (2008) Analysis of low caffeine tea lines by RAPD and cloning of special molecular markers. pp 29–33

Wei K, Wang L, Zhou J, He W, Zeng J, Jiang Y, Cheng H (2011) Catechin contents in tea (Camellia sinensis) as affected by cultivar and environment and their relation to chlorophyll contents. Food Chem 125(1):44–48

Wei Y, Chen P, Ling T, Wang Y, Dong R, Zhang C, Zhang L, Han M, Wang D, Wan X (2016) Certain (-)-epigallocatechin-3-gallate (EGCG) auto-oxidation products (EAOPs) retain the cytotoxic activities of EGCG. Food Chem 204:218–226

Xu YQ, Zhong XY, Chen SQ, Yin JF (2013) Hydrolysis of green tea residue protein using proteolytic enzyme derived from *Aspergillus oryzae*. J Food Sci Technol 50(1):171–175

Yang C, Luo JW, Chen TL, Gong X, Ping HE, Wang Q, Wang HC, Ran LQ (2013) Screening specific germplasm resources of tea plant with high caffeine content. Hunan Agric Sci 17:9–12

Yao M, Huang H, Yu J, Chen L (2005) Analysis on applicability of ISSR in molecular identification and relationship investigation of tea cultivars. pp 153–157

Yu F, Yu Y, Li M, Jilin S, Liu W, Lv W, Haisi W, Han Z, Weiji Z (1992) Systematic examination and comprehensive evaluation of high-quality tea plant germplasm. pp 95–125

Zhao M, Ma Y, Dai LL, Zhang DL, Li JH, Yuan WX, Li YL, Zhou HJ (2013) A high-performance liquid chromatographic method for simultaneous determination of 21 free amino acids in tea. Food Anal Methods 6(1):69–75

Zheng H, Huang Y, Huang H, Xiaoyang C (2007) Research on screening and suitable processing regions of tea germplasms with high EGCG content. pp 16–18

Zhu Y, Yahui H (2015) Research of the relationship between anatomical structure characteristics and traits of wide tea leaves of Jinxiu County, Guangxi. pp 16–21

ScienceDirect

LWT

Open access

9.6
CiteScore

6
Impact Factor

Submit your article ↗

Guide for authors

Menu

Search in this journal

Volume 98

Pages 1-662 (December 2018)

Download full issue

Previous vol/issue

Next vol/issue

Receive an update when the latest issues in this journal are published

Sign in to set up alerts

Full text access

IFC - Aims & Scope, Copyright, Publication information, Orders & Claims, Advertising information, Author inquiries, Permissions, Funding body, Permanence of paper and GFA link in double column

Page IFC

View PDF

Review articles

Research article ● Full text access

Oak barrel tannin and toasting temperature: Effects on red wine anthocyanin chemistry

Aude A. Watrelot, Andrew L. Waterhouse

Pages 444-450

View PDF Article preview

Research papers

Research article ● Full text access

Physicochemical and nutritional composition, volatile profile and antioxidant activity differences in Spanish jujube fruits

J. Reche, F. Hernández, M.S. Almansa, Á.A. Carbonell-Barrachina, ... A. Amorós
Pages 1-8

View PDF Article preview

Research article ● Full text access

Addition of buttermilk improves the flavor and volatile compound profiles of low-fat yogurt

Lili Zhao, Ran Feng, Fazheng Ren, Xueying Mao
Pages 9-17

View PDF Article preview

Research article ● Full text access

Characterization of sacha inchi protein hydrolysates produced by crude papain and Calotropis proteases

Saroat Rawdkuen, Nurdalila Rodzi, Suttiporn Pinijsuwan
Pages 18-24

View PDF Article preview

Research article ● Full text access

Effect of pre-treatment conditions and freeze-drying temperature on the process kinetics and physicochemical properties of pepper

Andrzej Krzykowski, Dariusz Dziki, Stanisław Rudy, Urszula Gawlik-Dziki, ... Beata Biernacka
Pages 25-30

View PDF Article preview

Research article ● Full text access

Use of talc in oil mills: Influence on the quality and content of minor compounds in olive oils

Alfonso M. Vidal, Sonia Alcalá, Antonia de Torres, Manuel Moya, Francisco Espínola
Pages 31-38

View PDF Article preview

Research article ● Full text access

Comparison of dextran molecular weight on wheat bread quality and their performance in dough rheology and starch retrogradation

Yao Zhang, Dandan Li, Na Yang, Zhengyu Jin, Xueming Xu
Pages 39-45

View PDF Article preview

Research article ● Full text access

Gelling properties of hake muscle with addition of freeze-thawed and freeze-dried soy phosphatidylcholine liposomes protected with trehalose

D. Marín-Peñalver, A. Alemán, P. Montero, M.C. Gómez-Guillén
Pages 46-53

View PDF Article preview

Research article ● Full text access

Proximal composition, sensorial properties and effect of ascorbic acid and α - tocopherol on oxidative stability of bread made with whole flours and vegetable oils

Mariana B. Osuna, Cecilia A. Romero, Ana M. Romero, María A. Judis, Nora C. Bertola
Pages 54-61

View PDF Article preview

Research article ● Full text access

Starch edible films loaded with donut-shaped starch microparticles

Yousof Farrag, Sara Malmir, Belén Montero, Maite Rico, ... Rebeca Bouza
Pages 62-68

View PDF Article preview

Research article ● Full text access

Guava, orange and passion fruit by-products: Characterization and its impacts on kinetics of acidification and properties of probiotic fermented products

Sabrina N. Casarotti, Tais F. Borgonovi, Carolina L.F.M. Batista, Ana Lúcia B. Penna
Pages 69-76

View PDF Article preview

Research article ● Full text access

Effect of chia seed on glycemic response, texture, and sensory properties of Chinese steamed bread

Fan Zhu, Coline Chan
Pages 77-84

View PDF Article preview

Research article ● Full text access

Novel autochthonous lactobacilli with probiotic aptitudes as a main starter culture for probiotic fermented milk

Yousef Nami, Babak Haghshenas, Reza Vaseghi Bakhshayesh, Hossein Mohammadzadeh Jalaly, ... Mohammad Amin Hejazi
Pages 85-93

View PDF Article preview

Research article ● Full text access

Intercalation technique can turn pomegranate industrial waste into a valuable by-product

Mohammadreza Balooch, Hossein Sabahi, Heshmatolah Aminian, Morteza Hosseini
Pages 99-105

View PDF Article preview

Research article ● Full text access

Characterization of functional properties of proteins from *Ganxet* beans (*Phaseolus vulgaris* L. var. *Ganxet*) isolated using an ultrasound-assisted methodology

Tomás Lafarga, Carlos Álvarez, Gloria Bobo, Ingrid Aguiló-Aguayo
Pages 106-112

View PDF Article preview

Research article ● Full text access

Multivariate analysis of essential elements in raw cocoa and processed chocolate mass materials from three different manufacturers

Bartosz Kruszewski, Mieczysław Wiesław Obiedziński
Pages 113-123

View PDF Article preview

Research article ● Full text access

Potentiality of the use of starter culture in PDO Strachitunt production on chemical-physical and microbiological features: A pilot study

E. Tirloni, M. Vasconi, P. Cattaneo, A. Ravasio, ... C. Bernardi
Pages 124-133

View PDF Article preview

Research article ● Full text access

Effect of heat treatment on physicochemical and emulsifying properties of polymerized whey protein concentrate and polymerized whey protein isolate

Shanshan Jiang, Muhammad Altaf hussain, Jianjun Cheng, Zhanmei Jiang, ... Juncai Hou
Pages 134-140

View PDF Article preview

Research article ● Full text access

The effect of organic acid and sodium chloride dips on the shelf-life of refrigerated Irish brown crab (*Cancer pagurus*) meat

A. McDermott, P. Whyte, N. Brunton, J. Lyng, ... D.J. Bolton
Pages 141-147

View PDF Article preview

Research article ● Full text access

Formula optimization approach for an alternative Ready-to-Use Therapeutic Food

Vincenzo Armini, Nicoletta A. Miele, Matteo Albero, Raffaele Sacchi, Silvana Cavella
Pages 148-153

View PDF Article preview

Research article ● *Open access*

Production, physicochemical stability of quercetin-loaded nanoemulsions and evaluation of antioxidant activity in spreadable chicken pâtés

Cynthia de Carli, Marília Moraes-Lovison, Samantha C. Pinho
Pages 154-161

View PDF Article preview

Research article ● Full text access

Effect of electrospun thymol-loaded nanofiber coating on vitamin B profile of gilthead sea bream fillets (*Sparus aurata*)

Zafer Ceylan, Mustafa Yaman, Osman Sağdıç, Ercan Karabulut, Mustafa Tahsin Yilmaz
Pages 162-169

View PDF Article preview

Research article ● Full text access

Effect of ozone or carbon dioxide pre-treatment during long-term storage of organic table grapes with modified atmosphere packaging

Naouel Admane, Francesco Genovese, Giuseppe Altieri, Antonella Tauriello, ... Giovanni Carlo Di Renzo
Pages 170-178

View PDF Article preview

Research article ● Full text access

Osmotic dehydration of mango: Effect of vacuum impregnation, high pressure, pectin methylesterase and ripeness on quality

Ita Sulistyawati, Matthijs Dekker, Vincenzo Fogliano, Ruud Verkerk
Pages 179-186

View PDF Article preview

Research article ● Full text access

Variability of free and glycosylated volatiles from strawberries destined for the fresh market and for processing, assessed using direct enzymatic hydrolysis

Stéphane Gaborieau, Aurélie Cendrès, David Page, Christian Ginies, Catherine M.G.C. Renard
Pages 187-196

View PDF Article preview

Research article ● Full text access

Comparison of rheological properties of wet gluten: Creep-recovery and biaxial compression

Pavalee Chompoorat, Zorba Josué Hernández-Estrada, Steven J. Mulvaney, Mark E. Payton, ... Patricia Rayas-Duarte
Pages 197-203

View PDF Article preview

Research article ● Full text access

Chemical compositions of Pu'er tea fermented by Eurotium Cristatum and their lipid-lowering activity

Chenkai Jiang, Zhen Zeng, Yahui Huang, Xu Zhang

Pages 204-211

View PDF Article preview

Research article ● Full text access

Camel whey protein hydrolysates displayed enhanced cholesteryl esterase and lipase inhibitory, anti-hypertensive and anti-haemolytic properties

Sabika Jafar, Hina Kamal, Priti Mudgil, Hassan Mohamed Hassan, Sajid Maqsood

Pages 212-218

View PDF Article preview

Research article ● Full text access

Interactions between mushroom powder, sodium chloride, and bovine proteins and their effects on lipid oxidation products and consumer acceptability

Natalie Tom, Hatouf Ahmed Alnoumani, Lilian Were

Pages 219-224

View PDF Article preview

Research article ● Full text access

Preservative effects of allicin microcapsules on daily foods

Yufeng Wang, Jinxia Jia, Jiangjuan Shao, Xu Shu, ... Zhiyong Yan

Pages 225-230

View PDF Article preview

Research article ● Full text access

The effect of glazing based on saponin-free quinoa (*Chenopodium quinoa*) extract on the lipid quality of frozen fatty fish

Marcos Trigo, Alicia Rodríguez, Gretel Dovale, Alexis Pastén, ... Santiago P. Aubourg

Pages 231-236

View PDF Article preview

Research article ● Full text access

Extraction of anthocyanins from haskap berry pulp using supercritical carbon dioxide: Influence of co-solvent composition and pretreatment

Guangling Jiao, Azadeh Kermanshahi pour

Pages 237-244

View PDF Article preview

Research article ● Full text access

Effect of addition of fermented bean seed flour on the content of bioactive components and nutraceutical potential of wheat wafers

Anna Jakubczyk
Pages 245-251

View PDF Article preview

Research article ● Full text access

Investigation of the mechanisms and strategies for reducing shell cracks of hazelnut (*Corylus avellana* L.) in hot-air drying

Wenjie Wang, Jooyeoun Jung, Robert J. McGorrin, Yanyun Zhao
Pages 252-259

View PDF Article preview

Research article ● Full text access

Antioxidant and antifungal effects of eugenol incorporated in bionanocomposites of poly(3-hydroxybutyrate)-thermoplastic starch

Karla A. Garrido-Miranda, Bernabé L. Rivas, Mónica A. Pérez -Rivera, Eugenio A. Sanfuentes, Carlos Peña-Farfal
Pages 260-267

View PDF Article preview

Research article ● Full text access

Oxidative stability of sunflower oil flavored by essential oil from *Coriandrum sativum* L. during accelerated storage

Dongying Wang, Wenchang Fan, Yifu Guan, Huina Huang, ... Junmin Ji
Pages 268-275

View PDF Article preview

Research article ● Full text access

Physicochemical and rheological properties of rice-based gluten-free blends containing differently treated chickpea flours

Gokcen Kahraman, Sebnem Harsa, Mara Lucisano, Carola Cappa
Pages 276-282

View PDF Article preview

Research article ● Full text access

Development of microwave-assisted dynamic extraction by combination with centrifugal force for polyphenols extraction from lettuce

Alice Angoy, Marc Valat, Pascal Ginisty, Alain Sommier, ... Farid Chemat
Pages 283-290

View PDF Article preview

Research article ● Full text access

Structural basis of the impact of microwave drying on survival and shelf life of *Lactobacillus paracasei*

S. Ambros, A.H. Vollmer, N.N. Youssef, U. Kulozik
Pages 291-298

View PDF Article preview

Research article ● Full text access

Effect of carrier agents on the physical properties and morphology of spray-dried *Monascus* pigment powder

Duoxia Xu, Yang Xu, Guorong Liu, Zhanqun Hou, ... Baoguo Sun
Pages 299-305

View PDF Article preview

Research article ● Full text access

Semi-solid state fermentation and enzymatic hydrolysis impeded the destroy of wheat bran on gluten polymerization

Huijuan Zhang, Xiaoshuang Zhang, Xin Ran Cao, Maryam Iftikhar, Jing Wang
Pages 306-313

View PDF Article preview

Research article ● Full text access

Thermal and water sorption properties of *Bifidobacterium* BB-12 microcapsules obtained from goat's milk and prebiotics

Silvani Verruck, Fabiani Santana, Carmen de Olivera Müller, Elane Schwinden Prudencio
Pages 314-321

View PDF Article preview

Research article ● Full text access

Biogenic amine and fermentation metabolite production assessments of *Lactobacillus plantarum* isolates for naturally fermented pickles

Yusuf Alan, Zeynal Topalcengiz, Metin Dığrak
Pages 322-328

View PDF Article preview

Research article ● Full text access

Synbiotic combination of *Lactobacillus rhamnosus* NCDC 298 and short chain fructooligosaccharides prevents enterotoxigenic *Escherichia coli* infection

Santosh Anand, Surajit Mandal, Kumar Siddharth Singh, Prasad Patil, Sudhir Kumar Tomar
Pages 329-334

View PDF Article preview

Research article ● Full text access

Biocompounds and physical properties of açaí pulp dried by different methods

Bárbara Franco Lucas, Rui Carlos Zambiazi, Jorge Alberto Vieira Costa
Pages 335-340

View PDF Article preview

Research article ● Full text access

Application of ion-exchange resin as solid acid for buffer-free production of γ-aminobutyric acid using *Enterococcus faecium* cells

Hui Zhu, Faizan A. Sadiq, Yun Li, ShengYuan Yang, Fei Zhou
Pages 341-348

View PDF Article preview

Research article ● Full text access

Kinetics, physicochemical properties, and antioxidant activities of *Angelica keiskei* processed under four drying conditions

Chengcheng Zhang, Daqun Liu, Haiyan Gao
Pages 349-357

View PDF Article preview

Research article ● Full text access

Optimization of ACE inhibitory peptides from black soybean by microwave-assisted enzymatic method and study on its stability

Meiqing Li, Shanwei Xia, Yijun Zhang, Xueling Li
Pages 358-365

View PDF Article preview

Research article ● Full text access

Effect of pasteurization on *in vitro* α-glucosidase inhibitory activity of apple juice

Marilisa Alongi, Giancarlo Verardo, Andrea Gorassini, Monica Anese
Pages 366-371

View PDF Article preview

Research article ● Full text access

Effects of sumac extract dipping and chitosan coating enriched with *Zataria multiflora* Boiss oil on the shelf-life of meat in modified atmosphere packaging

Ali Mojaddar Langroodi, Hossein Tajik, Tooraj Mehdizadeh, Mehran Moradi, ... Alireza Mahmoudian
Pages 372-380

View PDF Article preview

Research article ● Full text access

Effect of hydrocolloid and processing potentiality on water migration in apple jellies of *Yinduqing* cultivar

Tariq Kamal, Yukun Song, Tan Zhang, Bei-Wei Zhu, Mingqian Tan
Pages 381-389

View PDF Article preview

Research article ● Full text access

Developing functional yogurt rich in bioactive peptides and gamma-aminobutyric acid related to cardiovascular health

Alaa Abd El-Fattah, Sally Sakr, Samia El-Dieb, Hany Elkashef
Pages 390-397

View PDF Article preview

Research article ● Full text access

Effect of barrel temperature and moisture content on the composition and oxidative stability of extruded palm oil in an oil-starch model system

Liting Wan, Lin Li, Wenjuan Jiao, Linlu Mao, ... Xia Zhang
Pages 398-405

View PDF Article preview

Research article ● Full text access

Reliable determination of the induction period and critical reverse micelle concentration of lipid hydroperoxides exploiting a model composed of pseudo-first and -second order reaction kinetics

Reza Farhoosh
Pages 406-410

View PDF Article preview

Research article ● Full text access

Improvement of functional properties of sunflower protein isolates near isoelectric point: Application of heat treatment

Mudasir Ahmad Malik, Charanjiv Singh Saini
Pages 411-417

View PDF Article preview

Research article ● Full text access

Effect of mixed culture inoculation on chemical and sensory properties of aronia (*Aronia melanocarpa*)

Min-Seung Kang, Yu-Ra Kang, Youngseung Lee, Yoon Hyuk Chang
Pages 418-423

View PDF Article preview

Short communication ● Full text access

Fatty acid profiles of seeds from different *Ribes* species

Saša Piskernik, Rajko Vidrih, Lea Demšar, Darinka Koron, ... Tanja Pajk Žontar
Pages 424-427

View PDF Article preview

Research article ● Full text access

Tailoring egg white proteins by a GRAS redox pair for production of cold-set gel

Farhad Alavi, Shima Momen, Zahra Emam-Djomeh, Maryam Salami, Ali Akbar Moosavi-Movahedi
Pages 428-437

View PDF Article preview

Research article ● Full text access

Use of gamma radiation to inactivate stressed *Salmonella* spp., *Escherichia coli* O157:H7 and *Listeria monocytogenes* in tahini halva

Tareq M. Osaili, Anas A. Al-Nabulsi, Taqwa F. Aljaafreh, Amin N. Olaimat
Pages 438-443

View PDF Article preview

Research article ● Full text access

Effect of chestnut flour supplementation on physico-chemical properties and oxidative stability of gluten-free biscuits during storage

Maria Paciulli, Massimiliano Rinaldi, Antonella Cavazza, Tommaso Ganino, ... Emma Chiavaro
Pages 451-457

View PDF Article preview

Research article ● Full text access

Bioprotection as a tool to free additives winemaking: Effect on sensorial, anthocyanic and aromatic profile of young red wines

Pilar Rubio-Bretón, Ana Gonzalo-Diago, Miquel Iribarren, Teresa Garde-Cerdán, Eva P. Pérez-Álvarez
Pages 458-464

View PDF Article preview

Research article ● Full text access

Hercynine content in widely consumed commercial beverages

Salvatore Sotgia, Angelo Zinellu, Mauro Forteschi, Panagiotis Paliogiannis, ... Ciriaco Carru
Pages 465-469

View PDF Article preview

Research article ● Full text access

Reduction of biogenic amine contents in fermented soybean paste using food additives

Jun-Young Lee, Yong-gun Kim, Jae-Young Her, Mina K. Kim, Kwang-Geun Lee
Pages 470-476

View PDF Article preview

Research article ● Full text access

Improving physicochemical, antioxidative and sensory quality of raw chicken meat by using acorn extracts

Orhan Özünlü, Haluk Ergezer, Ramazan Gökçe
Pages 477-484

View PDF Article preview

Research article ● Full text access

Peptidase from *Aspergillus niger* NRRL 3: Optimization of its production by solid-state fermentation, purification and characterization

Débora N. López, Micaela Galante, Germán Ruggieri, Julia Piaruchi, ... Darío Spelzini
Pages 485-491

View PDF Article preview

Research article ● Full text access

Control of apple surface microflora for fresh-cut produce by post-harvest hot-water treatment

Tina Kabelitz, Karin Hassenberg
Pages 492-499

View PDF Article preview

Research article ● Full text access

A GICA strip for *Campylobacter jejuni* real-time monitoring at meat production site

Xiaoqi Zang, Ke Kong, Haiyan Tang, Yuanyue Tang, ... Jinlin Huang
Pages 500-505

View PDF Article preview

Research article ● Full text access

Evaluation of individual lactic acid bacteria for the fermentation of goat milk: Quality parameters

R. Muelas, A. Martí de Olives, G. Romero, J.R. Díaz, ... E. Sendra
Pages 506-514

View PDF Article preview

Research article ● Full text access

Effect of phenolics on amandin immunoreactivity

Ying Zhang, Changqi Liu, Mengna Su, Kenneth H. Roux, Shridhar K. Sathe
Pages 515-523

View PDF Article preview

Research article ● Full text access

Physicochemical and antibacterial effects of sodium bicarbonate and brine water on the electrolysed water generated by a portable sanitising unit

Jufang Zhang, Shaojuan Lai, Hongshun Yang
Pages 524-532

View PDF Article preview

Research article ● Full text access

Effect of milling, fermentation or roasting on water activity, fungal growth, and aflatoxin contamination of Bambara groundnut (*Vigna subterranea* (L.) Verdc)

Omotola Olagunju, Nokuthula Mchunu, Noel Durand, Pascaline Alter, ... Oluwatosin Ijabadeniyi
Pages 533-539

View PDF Article preview

Research article ● Full text access

Potential for enhanced soy storage protein breakdown and allergen reduction in soy-based foods produced with optimized sprouted soybeans

Ajibola B. Oyedeji, John J. Mellem, Oluwatosin A. Ijabadeniyi
Pages 540-545

View PDF Article preview

Research article ● Full text access

Investigation of betacyanins stability from peel and flesh of red-purple pitaya with food additives supplementation and pH treatments

Hui Yi Leong, Chien Wei Ooi, Chung Lim Law, Advina Lizah Julkifle, ... Pau Loke Show
Pages 546-558

View PDF Article preview

Research article ● Full text access

Thermal processing influences the digestibility and immunoreactivity of muscle proteins of *Scylla paramamosain*

Meng Liu, Guang-Yu Liu, Yang Yang, Xue-Jiao Mei, ... Guang-Ming Liu
Pages 559-567

View PDF Article preview

Research article ● Full text access

Gluten-free baked muffins developed with *Prosopis alba* flour

L.P. Sciammaro, C. Ferrero, M.C. Puppo
Pages 568-576

View PDF Article preview

Research article ● Full text access

Development of *Lactobacillus acidophilus*-fermented milk fortified with date extract

Seyedeh Maryam Abdollahzadeh, Maryam Ranjbar Zahedani, Samane Rahmdel, Fatemeh Hemmati, Seyed Mohammad Mazloomi
Pages 577-582

View PDF Article preview

Research article ● *Open access*

Effect of ripening time on proteolysis, free amino acids, bioactive amines and texture profile of Gorgonzola-type cheese

Gisela M.M. Moreira, Renata G.B. Costa, Vanessa A.M. Teodoro, Junio C.J. Paula, ... Maria Beatriz A. Gloria
Pages 583-590

View PDF Article preview

Research article ● Full text access

Efficacy of UV-A, UV-B, and UV-C irradiation on inactivation of foodborne pathogens in different neutralizing buffer solutions

Min-Jin Jeon, Jae-Won Ha
Pages 591-597

View PDF Article preview

Research article ● Full text access

Influence of calcium and sodium chloride on caseinomacropeptide self-assembly and flow behaviour at neutral pH

Karina G. Loria, Ana M.R. Pilosof, María E. Farías
Pages 598-605

View PDF Article preview

Research article ● Full text access

Arsenic species in herbal tea leaves and infusions determination by HPLC-ICP-MS

Raquel Fernanda Milani, Esther Lima de Paiva, Leandro Iagê Peron, Marcelo Antonio Morgano, Solange Cadore
Pages 606-612

View PDF Article preview

Research article ● Full text access

A comprehensive analysis of aroma compounds and microstructure changes in brown rice during roasting process

Yi Shi, Lingling Wang, Yong Fang, Hongpan Wang, ... Qiuhui Hu
Pages 613-621

View PDF Article preview

Research article ● Full text access

Quantification of rice and black gram *dal* proportions in *idli* batters by estimation of starch, daidzein and trypsin inhibitor activity

Dhanashree Amane, Laxmi Ananthanarayan
Pages 622-628

View PDF Article preview

Research article ● Full text access

Effect of thermal processing and reducing agents on trypsin inhibitor activity and functional properties of soybean and chickpea protein concentrates

Sara Avilés-Gaxiola, Cristina Chuck-Hernández, María del Refugio Rocha-Pizaña, Silverio García-Lara, ... Sergio O. Serna-Saldívar
Pages 629-634

View PDF Article preview

Research article ● Full text access

Survival kinetics of heat-stressed *Escherichia coli* O157:H7 and *Listeria monocytogenes* cells as post-fermentation contaminants in kefir during refrigerated storage

Serap Coşansu
Pages 635-641

View PDF Article preview

Research article ● Full text access

Rheological, micro-structural and sensorial properties of camel milk yogurt as influenced by gelatin

Priti Mudgil, Balsam Jumah, Mudasir Ahmad, Fathalla Hamed, Sajid Maqsood
Pages 646-653

View PDF Article preview

Research article ● Full text access

Fermenting liquid vinegar with higher taste, flavor and healthy value by using discarded *Cordyceps militaris* solid culture medium

Lu Liu, Yang Chen, Qing Luo, Ning Xu, ... Yong Shi
Pages 654-660

View PDF Article preview

Short communications

Short communication ● Full text access

Sensory evaluation of a novel prebiotic sheep milk strawberry beverage

Celso F. Balthazar, Antonella Santillo, Lucia Figliola, Hugo L.A. Silva, ... Marzia Albenzio
Pages 94-98

View PDF Article preview

Short communication ● Full text access

Fusarium culmorum multi-toxin screening in malting and brewing by-products

Kristina Mastanjević, Bojan Šarkanj, Benedikt Warth, Rudolf Krska, ... Vinko Krstanović

Pages 642-645

View PDF Article preview

Erratum ● Full text access

Corrigendum to "Anti quorum sensing and anti biofilm efficacy of cinnamaldehyde encapsulated chitosan nanoparticles against Pseudomonas aeruginosa PAO1" [LWT 97 (2018) pp. 752-759]

Pattnaik Subhaswaraj, Subhashree Barik, Chandrasekhar Macha, Potu Venkata Chiranjeevi, Busi Siddhardha

Page 661

View PDF

Previous vol/issue

Next vol/issue

ISSN: 0023-6438

Copyright © 2024 Elsevier Ltd. All rights reserved

ELSEVIER

All content on this site: Copyright © 2024 Elsevier B.V., its licensors, and contributors. All rights are reserved, including those for text and data mining, AI training, and similar technologies. For all open access content, the Creative Commons licensing terms apply.

RELX™

LWT - Food Science and Technology 98 (2018) 204–211

Contents lists available at ScienceDirect

LWT - Food Science and Technology

journal homepage: www.elsevier.com/locate/lwt

Chemical compositions of Pu'er tea fermented by Eurotium Cristatum and their lipid-lowering activity

Chenkai Jiang[a,b], Zhen Zeng[a], Yahui Huang[a,*], Xu Zhang[c,**]

[a] College of Horticulture, South China Agricultural University, Guangzhou, Guangdong, 510642, China
[b] Tea Research Institute, Chinese Academy of Agricultural Sciences, Hangzhou, Zhejiang, 310000, China
[c] College of Forestry and Lanscape Architecture, South China Agricultural University, Guangzhou, Guangdong, 510642, China

ARTICLE INFO

Keywords:
Pu'er raw tea
Flowering fermentation
Chemical compositions
Polar extracts
Lipid-lowering

ABSTRACT

In order to reveal the effect of microorganisms on the chemical composition of tea and their lipid-lowering function, Pu'er raw tea (PR) made from sun-dried leaves of Yunnan large-leaf tea cultivars was processed through a period of flowering fermentation mainly facilitated by *Eurotium cristatum,* and thus converted into flowering Pu'er tea (FP) in the present study. Tea aqueous extracts were successively extracted by chloroform, ethyl acetate and n-butyl alcohol. Afterwards, non-volatile and volatile compounds of PR and FP were identified and compared through high performance liquid chromatography (HPLC) and gas chromatography-mass spectrometer (GC-MS), respectively. Furthermore, high lipid HepG2 cells induced by OA were treated by those extracts of different polar to explore their impact on lipid-lowering. It can be observed that the contents of tea polyphenols (TPs) and amino acids of FP significantly decreased whereas the total amount of flavonoids significantly increased, compared to those of PR. Besides, the ethyl acetate fraction of FP (EAF-FP) was of the most prominent effect on lipid-lowering, and its optium effective concentration was 80 μg/mL.

1. Introduction

Obesity caused by excess lipid accumulation is one of the worldwide major health problems, as it is a risk factor for a number of chronic diseases, particularly the cardiovascular diseases, metabolic diseases, tumor and skeletal muscle diseases. Furthermore, expected life of obesity patients whose body mass index is greater than 40 kg/m^2 will be reduced by 10 years (Huxley, Mendis, Zheleznyakov, Reddy, & Chan, 2010; Whitlock et al., 2009). Hyperlipidemia is the high-occurrence chronic diseases in the 21st century, which severely threatens human's health as it triggers a series of complications, involving coronary diseases, high blood pressure, diabetes, hepatic adipose infiltration, atherosclerosis and even death (Comar & Sterling, 2006; Ma, Zhang, Su, & Bai, 2018; Rajagopalan et al., 2007; Ripatti et al., 2017; Rämö et al., 2017). To date, approximately one billion of people in the world are hyperpimelic (Adabag et al., 2015). Therefore, it is an increasing intense research to find out medicines effective for prevention and treatment of obesity from natural products.

Tea is one of drinks the most widely consumed only second to water and has been spread in more than 160 countries and regions in the world (Chen & Lin, 2015). The functions of tea are closely related to its active chemical components, such as tea polyphenols, amino acids, and alkaloids etc. One of its essential functions is lipid-lowering and anti-hypolipidemic effects on reduction of body fat and hepatic lipid, lean tissues increasement, prevention of hepatic steatosis and fatty liver verified in numerous preceding investigations (Braud et al., 2017; Ding, Pu, & Kan, 2017; He, 2017; Nam et al., 2018; Neyrinck et al., 2017; Yi et al., 2017). Apparently, different ratio of various compounds of tea, mainly determined by materials and manufacturing methods, gives rise to diverse lipid inhibitory activity. Fungal flowering fermentation shortly and commonly called “flowering” is the most indispensable stage for good qualities of some dark teas. During this time, *Eurotium spp.*, as predominant bacteria, grows dynamically within the tea leaves at the controlled temperature and moisture conditions (Li et al., 2017; Luo et al., 2013). Accordingly, various trials have been performed to explore the relationship between microbial activity and metabolic changes of tea, particularly in concentrating on Fu-brick tea, Liu Pao Tea and some other dark teas (Fu, Lv, & Chen, 2016; Mao, Wei, Teng, Huang, & Xia, 2017; Li et al., 2017). Nevertheless, few studies published providing insights into the influence of microorganisms on

* Corresponding author.
** Corresponding author.
E-mail addresses: greenbreezekai@126.com (C. Jiang), zzhen2004@126.com (Z. Zeng), 13501513191@163.com (Y. Huang), Zhangxu919@hotmail.com (X. Zhang).

https://doi.org/10.1016/j.lwt.2018.08.007
Received 8 March 2018; Received in revised form 28 July 2018; Accepted 2 August 2018
Available online 03 August 2018
0023-6438/ © 2018 Published by Elsevier Ltd.

multifarious compounds of Pu'er raw tea (PR) made from sun-dried leaves of Yunnan large-leaf tea or the possible explanation for its lipid inhibitory activity. Therefore, PR was treated with “flowering” (covered by “golden flora”) after being cultivated with *Eurotium cristatum* to reveal the diverse tea compositions with the functions of prevention and curative effect of hyperlipemia, which systematically explore the influence of flowering processing on the chemical composition of PR in the current study. In addition, it also discussed the polar part with the most remarkable effect on lipid reduction of high lipid HepG2 cells and its optimum dose through high throughput screening, which will pave a preliminary basis for further research on relationship between components of PR facilitated by *Eurotium cristatum* and their lipid-lowering activity.

2. Materials and methods

2.1. Materials and reagents

PR was obtained from Menghai Huanong Tea Co., Ltd.; *Eurotium cristatum* was purchased from BNCC); HepG2 cells were obtained from American Type Culture Collection (ATCC) (Manassas, VA, USA); Caffeine (Caf), theobromine (Tb), theophylline (Tp), catechins including (+)-gallocatechin (GC), catechin (C), (−)-epigallocatechin (EGC), (−)-epicatechin (EC), (+)-gallocatechin gallate (GCG), (−)-epicatechin gallate (ECG), catechin gallate (CG), (−)-epigallocatechin gallate (EGCG), amino acids, and imethyl Sulphoxide (DMSO) were purchased from Sigma (St. Luis, MO, USA); Methanol (HPLC grade); Other chemical reagents involving 3-(4,5-dimethyl-2-thiazolyl)-2,5-diphenyl-2-H-tetrazolium bromide (MTT), oleinic acid (OA), and so on were purchased from Guangzhou Haoma Biotechnology Co., Ltd. (Guangzhou, Guangdong, China).

2.2. Processing of FP

FP was processed as follows: PR→Humidification→Steaming (vapor pressure = 4 kg/cm2, temperature = 110 °C ± 5 °C, time = 15 s) → Cooling →Incubation with *Eurotium cristatum* →Hyther (temperature = 25 °C, humidity = 80%) for one week → Drying (temperature = 70 °C) for 4 h.

2.3. Separation of polar parts

Tea samples were ground to powders and extracted with water in a ratio of tea to water of 1:100 (g/mL) at 100 °C for 2 h. Then they were successively separated by chloroform, ethyl acetate and n-butyl alcohol and concentrated with vacuum freeze – dried afterwards aqueous extract was concentrated at 60 °C.

2.4. Determination of chemical components of tea

The contents of moisture, aqueous extract, tea polyphenols, and free amino acids were determined according to GB/T 8304–2013, GB/T 8305–2013, GB/T 8313–2008, and GB/T 8314–2013, respectively. Flavonoids were determined refered to $AlCl_3$ colorimetry method (Gressel, 1991).

The contents of alkaloid and catechin monomers were determined through high performance liquid chromatography (HPLC) (Agilent 1200, Agilent Technologies, Santa Clara, CA, USA). C18 reverse phase column (HyPersil ODS2, 4.6 mm × 250 mm, 5 μm) (Thermo Fisher Scientific, Waltham, MA, USA) was applied. The determination conditions were set as follows: solvent A, pure methanol; and solvent B, 0.05% trifluoroacetic acid in water. Column temperature was set at 30 °C and the flow rate was 0.8 mL/min. UV spectra was measured at 278 nm. Sample size for injection was 20 μL. The gradient elution profile was programmed as follows: 2% A at 0–2 min, to 8% A at 8 min, to 10% A at 30 min, to 20% A at 35 min, to 25% A at 45 min, and to 30% A at 50 min. 30% A was maintained from 50 to 55 min, and then changed to 35% A for 60 min.

The contents of volatile aroma compounds were determined as follows: DB-5MS column was 60 m × 0.25 μm × 0.32 mm; the carrier gas was helium (with 99.999% purity) at a constant flow rate of 1 mL/min; held at 50 °C for 5 min, then increased to 180 °C at a rate of 3 °C/min, held for 5 min; and lastly changed to 240 °C at a rate of 10 °C/min; EI electron energy was 70 eV; Voltage of photomultiplier was 350 V; mass scan range was 35–335 u. The relative contents of volatile aroma compounds were calculated against that of ethyl caprate as the internal standard reference.

2.5. Lipid-lowering activity of different polar parts and SV

Toxicity test of tea extracts: HepG2 cells were seeded in 96 well plates at a density of 6000 cells per well in high DMEM supplemented with 10% FBS and incubated at 37 °C and 5% CO_2 for 24 h. Then the supernatant was replaced by 100 μL of culture medium containing tea extracts at different concentrations. Cells were incubated with 20 μL of MTT (5 mg/mL) per well for 4 h followed by incubation for 24 h. The culture medium was withdrawn with a disposable aspiration needle and 100 μL of DMSO was added. The solution was read at 570 nm (OD_{570}) to obtain its absorbancy using an automatic microplate reader (Spectra Max 190, USA) after shaken well.

Test of Lipid-lowering Effects: HepG2 cells were seeded to 96 well plate at a density of 4000 cells per well and incubated for 12 h. Then the supernatant was replaced with 100 μL of culture medium containing 150 μg/mL of OA. 24 h later, the supernatant of the experimental groups was replaced with 100 μL of culture medium containing tea extracts. The supernatant of the positive control groups was replaced by 100 μL of culture medium containing simvastatin (SV). The cells of control group were cultured with culture medium without OA. 24 h later, the culture medium was withdrawn by a disposable aspiration needle and washed with 100 μL of PBS per well twice. Then 100 μL of 1 μg/mL of Nile red was added to stain the cells and kept from the light for 5 min at 37 °C。 The fluorescence intensity was detected by chemiluminescence apparatus (Thermo Scientific Fluoroskan Ascent FL, USA) under the excitation wavelength at 580 nm and the emission wavelength at 612 nm. The relative lipid content was calculated as follows:

The relative lipid content = Fluorescence intensity of the experimental group/Fluorescence intensity of the control group.

2.6. Observation of cell morphology

The slides (Φ = 25 mm, δ = 0.17 mm) coated by L-poly lysine after being sterilized were put in the 6 wall plate with a small amount of culture medium. HepG2 cells were de-attached from culture well with the trypsin, and transferred to the 6 wall plate at a density of 2×10^5/mL, 100 μL per well. 2 mL of culture medium was added after cell adherence. 24 h later, culture medium was discarded and the plate was cleaned with PBS twice. Then the cells were fixed with 1 mL of 4% paraformaldehyde for 30 min. Paraformaldehyde was discarded prior to washing plate with PBS 3 times. The cells were stained with NR and kept from the light at 37 °C for 5 min, then their morphologies were observed under the fluorescence microscope (SZH, USA) under the excitation wavelength at 542 ± 12 nm and the emission wavelength at 575–640 nm.

3. Results

3.1. The relative contents of volatile aroma compounds

A total of 46 kinds of volatile aroma compounds had been determined (Table 1). The relative contents of esters were highest, which were 17.53% for PR and 22.75% for FP, respectively, and rose by 29.78% after flowering. And relative contents of alcohols were 42.32%

Table 1
Composition and relative contents of volatile fragrant compounds in three tea samples.

Names	PR%	FP%	Names	PR%	FP%
Alcohols	17.53	22.75	ι-calamenene	1.27	0.52
Aldehydes	42.32	51.14	Nonanoic acid	1.2	0.72
Acids	9.65	5.74	cis-Geraniol	1.19	0.48
Hydrocarbons	14.02	10.3	Linalool Oxide I (fr.1)	1.15	1.11
Ketones	13.44	8.38	β-Cedrene	1.07	0.8
Heterocyclic compounds	1.2	0.72	1-Oxaspiro [4.5]dec-6-ene, 2,6,10,10-tetramethyl-	0.93	0.59
Esters	1.55	0.85	Acetophenone	0.91	0.72
β-Linalool	14.56	12.42	cis-β-Ocimene	0.8	0.42
Salicylic acid, methyl ester	14.14	20.53	cis-Jasmone	0.78	0.44
trans-Geraniol	12.16	4.68	Trans-2-trans-4-Heptadienal	0.7	0.37
β-Ionone	5.32	3.37	2,2,6-Trimethylcyclohexanone	0.64	0.21
β-Cyclocitral	3.72	2.63	2-Decanone	0.64	0.41
α-Terpineol	3.38	14.03	2-Pentylfuran	0.62	0.26
α-Cedrol	3.23	13.88	Trans,trans-3,5-Octadien-2-one	0.6	0.42
Benzaldehyde	3	1.42	Nonanal	0.6	0.31
dihydro actinidiolide	2.95	1.82	Dehydro-ar-ionene	0.58	0.2
Olivetol	2.6	1.48	Oct-1-en-3-ol	0.58	0.21
α-Calacorene	2.44	1.35	Trans-β-Ocimene	0.49	0.26
Cedrene	2.11	2.83	β-Damascenone	0.47	0.3
5,6-Epoxy-β-ionone	2.04	1.33	cis-Hexanoic Acid, 3-hexenyl ester	0.44	0.4
Linalool Oxide II (fr.2)	1.95	2.23	τ-Terpinene	0.39	0.25
α-Ionone	1.71	1.05	6-Methyl-5-heptene-2-one	0.33	0.13
Limonene	1.68	1.63	Trans-2-Octenal	0.26	0.13
Safranal	1.63	1.01	α-Terpinene	0.25	0.17
Nerolidol	1.52	0.62	β-Phellandrene	0.2	0.13
δ-Cadinene	1.3	0.7	α-Pinene	0.15	0.33
β-Myrcene	1.29	0.71			

for PR and 51.14% for FP, respectively, which increased by 20.84% after flowering fermentation. Therefore, it could be inferred that the increases in esters and alcohols possibly attributed to the decomposing activity of microorganisms by making use of some saccharides and proteins in tea leaves. Compared to PR, the relative contents of salicylic acid methyl ester, α-terpineol and α-cedrol of RF increased significantly, while the contents of trans-geraniol, β-ionone, β-cyclocitral, benzaldehyde, dihydro actinidiolide, olivetol and α-calacorene of FP fallen significantly.

3.2. The contents of aqueous extraction, tea polyphenols, flavones and aminol acids

As described in Fig. 1, compared to tea polyphenol content of PR, those of FP extremely decreased by 22.31% ($P < 0.01$), while flavonoid content of FP notably increased by 19.15% ($P < 0.05$). And the content of amino acids of FP significantly declined by 24.34% ($P < 0.01$). By contrast, the aqueous extraction remained steady with the striking change of above mentioned compounds, demonstrating some compounds generated during the flowering fermentation.

3.3. The contents of catechins and alkaloids

Catechins and alkaloids were mainly in the ethyl acetate layer (Table 2). The contents of total catechins of EAF-PR and EAF-FP were 69.72 ± 0.09% and 70.35 ± 0.10%, respectively. And the contents of total alkaloids of EAF-PR and EAF-FP were 9.47 ± 0.03% and 12.47 ± 0.04%, respectively. According to significance analysis, after flowering, the content of total catechins of FP reached up to 21.24%. More precisely, the ester catechin content of FP reduced by 33.63%, while non-ester catechin content of FP increased by 52.85%, which will benefit the improvement of tea flavour especially the reduction of bitter taste. Stimutaneously, alkaloid content of FP significantly grew ($P < 0.05$). The content of total alkaloids of EAF-FP was drastically higher than that of EAF-PR ($P < 0.01$). Furthermore, the contents of ECG, CG, EGCG, GCG, EGC, EC, GC and C of EAF-FP successively decreased. It is reported that the alternation of ester catechins into non-ester catechins makes contributions to decrease in bitterness and astringence of tea soup (Xu et al., 2018).

3.4. Toxicity test of OA and different polar parts of tea extraction

As shown in Fig. 2, the survival rate of HepG2 cells increased with growing OA concentration when its concentration was lower than 100 μg/mL, indicating that it was essential for HepG2 cells to maintain fatty acids at certain concentration. It was evident that the toxicity of OA initially appeared at 150 μg/mL. Subsequently, the survival rate of HepG2 cells was significantly decreased by OA at 180 μg/mL. And HepG2 cells could not survive at OA concentration over 300 μg/mL. Thus, it was reasonable to induce high lipid HepG2 cells with 150 μg/mL of OA. Similarly, the lipid-lowering effect of tea extraction should be determined under concentrations of CE-PR, CE-FP, CF-PR and CF-FP lower than 200 μg/mL, concentrations of EAF-PR and EAF-FP lower than100 μg/mL, concentrations of NAF-PR and NAF-FP lower than 60 μg/mL, and the concentrations of WF-PR and WF-FP lower than 500 μg/mL.

3.5. The lipid-lowering effects

As described in Fig. 3, the lipid formation of HepG2 cells was strongly restricted by 50–200 μg/mL of CE-PR, 100–200 μg/mL of CE-FP, CF-PR and CF-FP, 60–100 μg/mL of EAF-PR and EAF-FP, while it were not influenced by NAF-PR, NAF-FP, WF-PR or WF-FP, suggesting that EAF-FP possessed the most outstanding lipid-lowering activity. In addition, the lipid inhibition rates were 24.06%, 31.03% and 67.99% at 60, 80 and 100 μg/mL of EAF-FP, respectively. The lipid accumulation of HepG2 cells was strikingly reduced by SV varying from 200 to 500 μg/mL. Moreover, the inhibition ratio of SV against lipid was 10.04% at 500 μg/mL.

3.6. The observation of cells morphology

The cells of control group arranged in fusiform polygon exhibited stained intracellular lipid droplets and clear edges in accordance with Fig. 4. While intracellular lipid droplets of model group distributed around the nucleus of round cells, inside the clear edge of the plasma membrane. And lipid droplets of cells cultured in the medium containing 100 μg/mL of SV, were of no obvious dissimilarity, with the clear edges. The cells cultured in medium with 80 μg/mL of EAF-FP, however, appeared clear edges and shrunken lipid droplets. Although the lipid droplets of the cells were shrunken in the medium containing 100 μg/mL of EAF-FP, the cells became smaller in size and their edges were fuzzy. In terms of 500 μg/mL of SV, the cells presented clear edges and partly shrunken lipid droplets. As a consequence, these results indicated that 80 μg/mL of EAF-FP was the optimum condition for lipid-lowering of high lipid HepG2 cells.

4. Discussions

Processed tea consists of a considerable number of chemical components, which can be divided into two categories: non-volatile compounds and volatile aroma compounds. It is evident that the synthesis of some substances is accompanied by the decomposition of others, as the result of constant of aqueous extract level of FP. Catechins, representing more than 50% of total amount of tea polyphenols, were transferred to theaflavins, thearubigins and theabrownins (He-yuan Jianga et al., 2011). And it was also illustrated in the previous study that tea polyphenols may combine with proteins to form insoluble

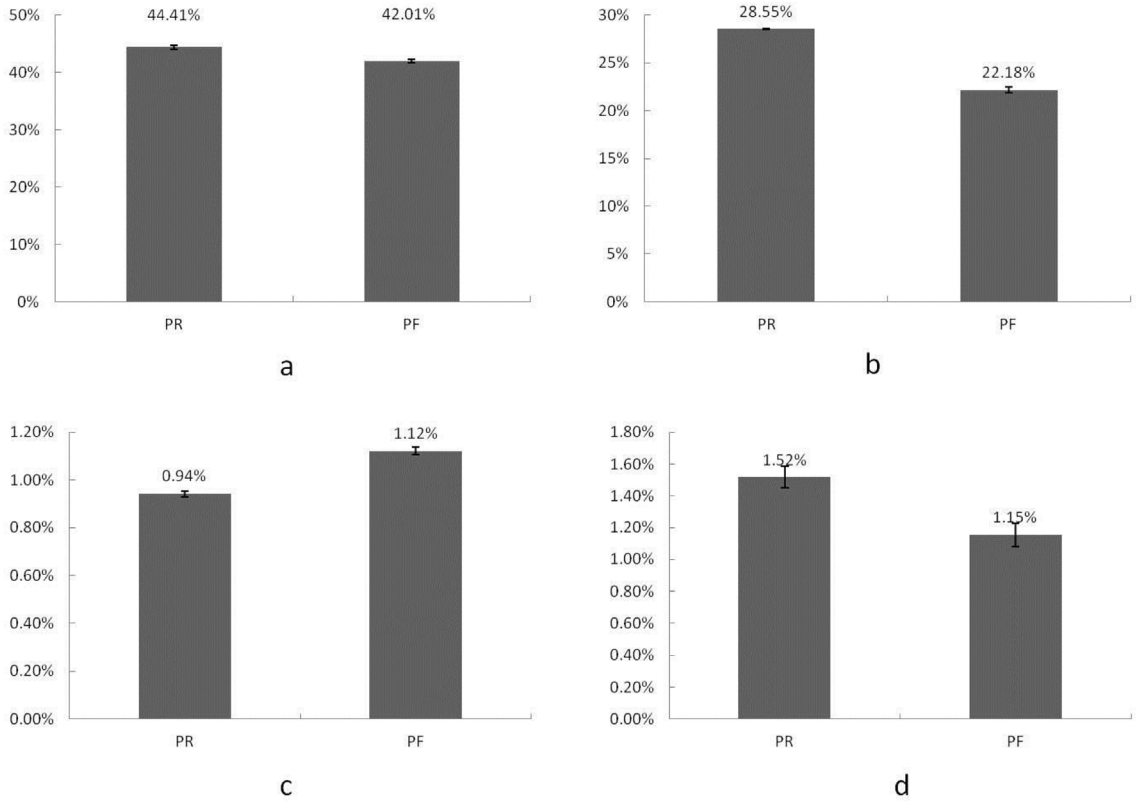


Fig. 1. Main chemical components of three samples. Variations of aqueous extract (a); Variations of tea polyphenols(b); Variations of flavones (c) and Variations of amino acid (d).

compounds and decomposition of catechins in the process of polymerization and oxidative cracking of benzene ring, due to the humic acids produced by microbial fermentation (He-yuan Jianga et al., 2011). Likewise, the total contents of amino acids of PR also decreased at the end of flowering period, possibly owing to the complex chemical changes caused by the microorganism metabolism in the Maillard reaction and enzymatic reaction. The alternations in amino acids are highly correlated with that of acylamide, which is formed in the Maillard reaction between free amino acid and saccharide at the temperature higher than 120 °C, as well as in the reaction between acrolein and amine at the room temperature (Mottram, Wedzicha, & Dodson, 2002).

Numerous investigations have concluded that the chemical components of tea not only play an important role on its quality, but also contribute to its pharmaceutical functions, including anti-senile, anti-carcinogenic, and anti-adipogenic effect etc. (Masaki Funamoto et al., 2016; Su, Zhang, Wang, & Li, 2012; Xu et al., 2011a, 2011b). It is found that polyphenols are the vital compounds of tea possessing lipid-lowering activity, as well as some other components, such as alkaloids and polysaccharides (Okuda et al., 2014; Gong, Peng, Chen, Gao, & Zhou, 2010; Way et al., 2009; Xu et al., 2015; Zhu et al., 2017). It can be seen that EAF-FP is highly effective at inhibiting lipogenesis in high lipid HepG2 cells, which potentially links with the highest content of catechins and alkaloids in EAF-FP compared with other polar fractions of FP through HPLC analysis. Those preceding observations coupled to experimental results obtained in this study, as a consequence, suggest that catechins and alkaloids are the prominent constituents of tea that contain inhibitory activity on lipid of high lipid HepG2 cells.

Volatile fragrance compounds also play critical roles in determining the quality of tea, some of which exist in the tea fresh leaves, whereas most are formed during the manufacturing processes. 1,2,3-trimethoxybenzene, 1,2-dimethoxybenzene and 1,2,4- trimethoxybenzene with

Table 2
Constitutes of catechins and alkaloids in different polar extracts.

Content%	PR	FP	CF-PR	CF-FP	EAF-PR	EAF-FP	NAF-PR	NAF-FP	WF-PR	WF-FP
GA	0.27 ± 0.00	1.64 ± 0.01	0.80 ± 0.00	0.91 ± 0.00	0.37 ± 0.00	0.07 ± 0.00	1.18 ± 0.01	1.65 ± 0.01	2.01 ± 0.01	2.30 ± 0.01
GC	9.45 ± 0.05	18.26 ± 0.11	9.10 ± 0.03	8.77 ± 0.03	4.37 ± 0.02	3.49 ± 0.02	13.20 ± 0.03	14.03 ± 0.04	1.00 ± 0.01	0.89 ± 0.00
C	0.28 ± 0.00	0.48 ± 0.00	0.42 ± 0.00	0.97 ± 0.00	1.29 ± 0.01	1.84 ± 0.01	1.76 ± 0.01	3.34 ± 0.01	0.00 ± 0.00	0.00 ± 0.00
EGC	2.43 ± 0.03	0.78 ± 0.00	2.44 ± 0.01	1.25 ± 0.01	13.04 ± 0.04	4.89 ± 0.03	2.14 ± 0.01	2.67 ± 0.01	0.22 ± 0.01	0.19 ± 0.00
EGCG	3.93 ± 0.03	3.05 ± 0.03	3.39 ± 0.02	4.61 ± 0.02	6.43 ± 0.02	9.15 ± 0.03	3.62 ± 0.02	5.33 ± 0.02	2.87 ± 0.02	3.87 ± 0.02
EC	2.06 ± 0.01	2.23 ± 0.02	1.18 ± 0.01	1.66 ± 0.01	2.85 ± 0.01	3.69 ± 0.02	1.49 ± 0.01	2.08 ± 0.01	1.01 ± 0.01	1.02 ± 0.00
GCG	2.62 ± 0.02	0.91 ± 0.00	1.19 ± 0.01	1.50 ± 0.01	6.29 ± 0.02	6.84 ± 0.02	1.23 ± 0.01	1.21 ± 0.01	0.17 ± 0.00	0.20 ± 0.00
ECG	1.01 ± 0.00	0.72 ± 0.00	5.43 ± 0.02	7.62 ± 0.02	20.03 ± 0.07	25.52 ± 0.06	3.39 ± 0.01	3.71 ± 0.03	2.47 ± 0.01	3.42 ± 0.01
CG	0.41 ± 0.00	0.61 ± 0.00	3.07 ± 0.02	3.15 ± 0.01	15.42 ± 0.04	14.94 ± 0.04	1.86 ± 0.01	0.80 ± 0.00	0.16 ± 0.00	0.28 ± 0.00
Caf	5.64 ± 0.01	5.97 ± 0.01	1.36 ± 0.01	2.11 ± 0.01	7.61 ± 0.02	10.21 ± 0.03	1.00 ± 0.01	1.05 ± 0.01	0.00 ± 0.00	0.00 ± 0.00
Tb	0.07 ± 0.01	0.05 ± 0.00	0.03 ± 0.00	0.00 ± 0.00	0.20 ± 0.00	0.26 ± 0.00	0.12 ± 0.00	0.12 ± 0.00	0.02 ± 0.00	0.00 ± 0.00
Tp	0 ± 0.00	0 ± 0.00	0.44 ± 0.00	0.48 ± 0.00	1.65 ± 0.01	2.00 ± 0.01	0.22 ± 0.00	0.26 ± 0.00	0.01 ± 0.00	0.02 ± 0.00
Catechins	21.80 ± 0.04	26.43 ± 0.06	26.23 ± 0.05	29.53 ± 0.04	69.72 ± 0.09	70.35 ± 0.10	28.69 ± 0.05	33.18 ± 0.06	7.91 ± 0.02	9.87 ± 0.03
Alkaloids	5.71 ± 0.02	6.02 ± 0.02	1.83 ± 0.01	2.59 ± 0.01	9.47 ± 0.03	12.47 ± 0.04	1.34 ± 0.01	1.43 ± 0.01	0.04 ± 0.00	0.02 ± 0.00

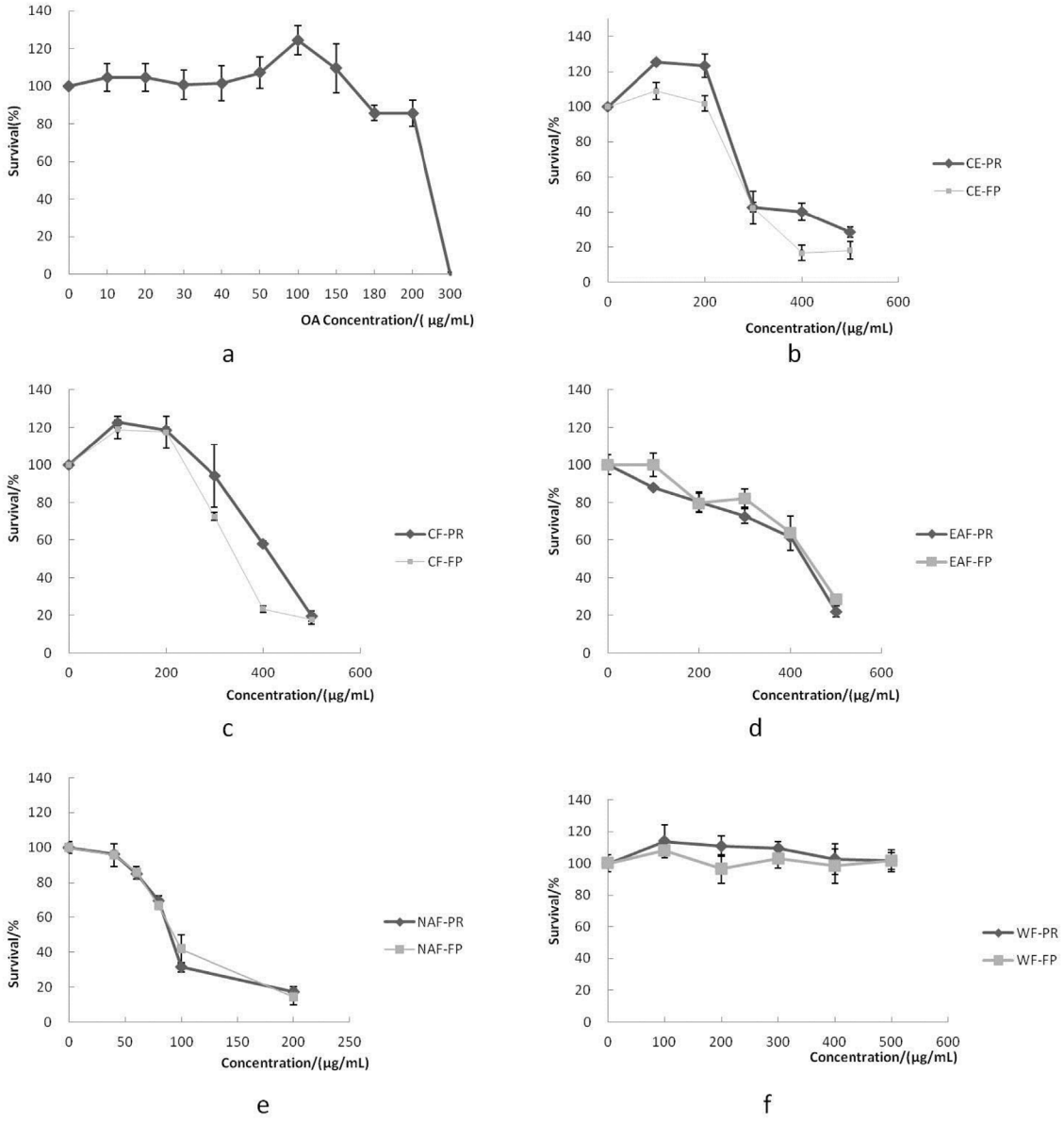


Fig. 2. Effects of OA and different polar parts of tea samples on survival of HepG2. OA(a); Crude extract(b); Chloroform fraction (c); Ethyl acetate fraction(d); N-butyl alcohol fraction(e) and Water fraction(f).

stale flavour are characteristic aroma compounds in Pu'er ripe tea made from sun-dried tea after pile fermentation (Zhu et al., 2016). Simultaneously, the relative content of β-linalool significantly declined from 21.01% to 2.97%, compared to that of sun-dried tea (Lv et al., 2012). Furthermore, *Aspergilli*, including *Aspergillus niger* and *Aspergillus fumigates*, was the dominant fungi during the pile fermentation of tea (Zhang et al., 2016). In the present study, no 1,2,3-trimethoxybenzene, 1,2-dimethoxybenzene or 1,2,4- trimethoxybenzene were detected in FP while the relative content of β-linalool was 12.42%.

Sun-dried tea is also a kind of raw material of Pu'er ripe tea fermented by dominant fungi including *Aspergillus niger* and *Saccharomyces cerevisiae* (Schuster, Dunn-Coleman, Frisvad, & van Dijck, 2002). Yet raw dark green tea is the raw material of Fu brick-tea fermented by *Eurotium cristatum* and other fungi such as *Saccharomyces spp., Debaryomyces* and *Aspergillus spp.*(Xu et al., 2011a, 2011b; Zheng, Wan, & Bao, 2015). It indicates that the microbiologic populations are influenced by manufacturing technology, based on the similarity of fungal colony in Fu brick-tea from Zhejiang and Hu'nan (Fu et al., 2016). In addition, the aroma compounds of FP was significantly diverse from those of Pu'er ripe tea and Fu brick-tea, further proving that the various aroma compounds influenced by both the raw material and manufacturing technology, and the latter makes more contributions.

Besides some chemical compounds originated from tea leaves, some metabolites produced by microorganisms during the flowering fermentation also have an effect on restricting lipogenesis and propelling lipoclasis. 3-hydroxy-3-methyl glutaryl coenzyme A reductase (HMGR) is the rate - limiting enzyme at the first step of biosynthesis of cholesterols. Statins, with the structure of lactone and hydroxyl acid, are the inhibitors of HMGR and thus, they can prevent angiocardiopathy and reduce the cardiovascular disease risk of the populations without angiocardiopathy (Houslay, Sarma, & Uren, 2007). The statins increased during the fermentation of dark tea (Hou, Jeng, & Chen, 2010). Lovastatin detected in the liquid fermented by *Eurotium cristatum,* as revealed by thin-layer chromatography and HPLC analyses (Mao et al., 2017). The exopolysaccharides produced by *Eurotium cristatum* were capable of activating PPARγ and reducing weight (Fu et al., 2011). The aqueous extract from dark tea fermented by *Eurotium cristatum* reduced the body weight of SD rats fed with high-fat diet and the triglyceride

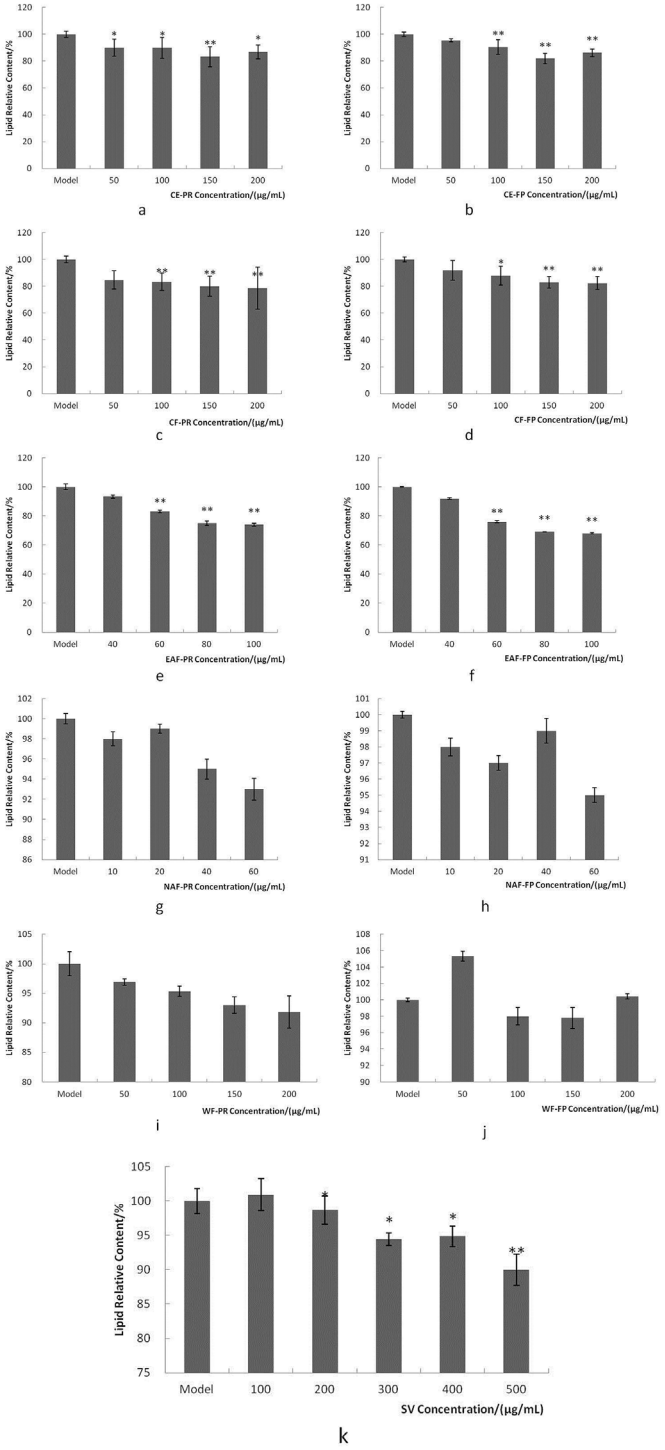


Fig. 3. Lipid-lowering effect of different polar parts of two samples. CE-PR (a); CE-FP (b); CFR (c); CF-FP (d); EAF-PR (e); EAF-FP (f); NAF-PR (g); NAF-FP (h); WF-PR (i); WF-FP (j) and SV(k).

level in serum noted in other experiments (Liu, 2016). Although it has been known that flavonoids could lower serum total cholesterol, glycerin trilaurate and low-density fatty acid (Hirata et al., 2017; Jin et al., 2013), the contents of catechins and flavonoids decreased after flowering. Moreover, it is likely that the ester catechins could have hydrolyzed into non-ester catechins and gallic acid by the end of flowering process, depending on the rising of non-ester catechins level and falling of eater catechins level. The lipid-lowering activity of ester catechins is relatively higher than that of non-ester catechins (Zhao, Yang, Huang,

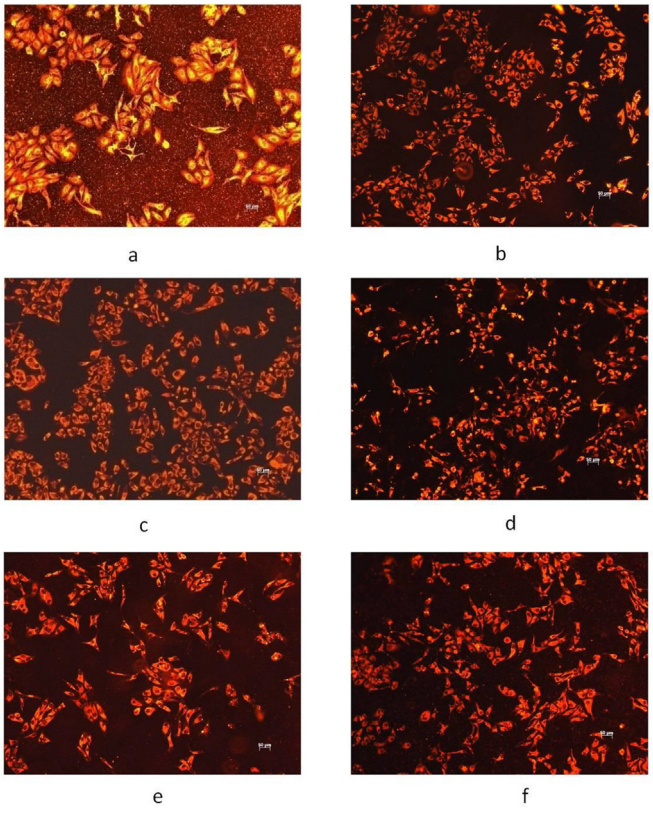


Fig. 4. Morphology of HepG2 cells under different conditions. Crontrol group (a); OA = 150 μg/mL(b); EAF-FP = 80 μg/mL(c); EAF-FP = 100 μg/mL(d); SV = 100 μg/mL(e) and SV = 500 μg/mL(f).

Lin, & Zheng, 2017). Additionally, quite a few explorations presented that non-ester catechins also have weak lipid-lowering effects (Matsuzaki et al., 2017; Zhao et al., 2017). However, there is no great variation between the influence of lipid-lowering activity of PR and FP. Even some polar substances of FP involving EAF-FP are of greater lipid prevention than that of PR, suggesting that the metabolites of microorganisms possibly make contributions to lipid-lowering effect. Consequently, this experiment provides insights into the primary chemical conversion of PR during the flowering fermentation mainly promoted by *Eurotium cristatum* and it deserves further research on the metabolites of microorganisms in particular statins and their functions of lipid inhibition.

5. Conclusions

It can be concluded that the process of flowering fermentation confers great effects on the main chemical components of tea, including tea polyphenols, amino acids, alkaloids and volatile aroma compounds. Furthermore, it revealed that those diverse chemical constitutes contribute to diverse lipid inhibitory activity of various polar constituents of PR and FP on high lipid HepG2 cells induced by OA. In addition, 80 μg/mL of EAF-FP is of the most potent lipid-lowering effect. And further investigations should be concentrated on the mechanism of PR fermented mainly facilitated by *Eurotium Cristatum* of lipid-lowering activity.

Acknowledgements

The authors thank Fu Jian Province “2011 Collaborative Innovation Center” Chinese Oolong Tea Industry Innovation Center Special Project (J2015-75); The Research on the Innovation and Utilization of New Tea Germplasm for Cold Resistance in Guangdong (2013B020201003);

Selection and Breeding of New Varieties of Specific Tea Resources in Guangdong (2015B020202007); Introduction, Domestication, Breeding Technology of High EGCGTea Plants(2016A020208012).

Appendix A. Supplementary data

Supplementary data related to this article can be found at https://doi.org/10.1016/j.lwt.2018.08.007.

Abbreviations

PR	Pu'er raw tea
FP	Flowering Pu'er tea
GA	Gallic acid
C	Catechin
EC	Epicatechin
EGC	Epigallocatechin
GC	Gallocatechin
CG	Catechin gallate
ECG	Epicatechin gallate
GCG	Gallocatechin gallate
EGCG	Epigallocatechin gallate
Caf	Caffeine
Tb	Theobromine
Tp	theophylline
OA	Oileinic acid
FBS	Fetal bovine serum
PBS	Phosphate buffer
MTT	3-(4,5-dimethyl-2-thiazolyl)-2,5-diphenyl-2-H-tetrazolium bromide
DMSO	Dimethyl Sulphoxide
CE-PR	Crude extraction of Pu'er raw tea
CE-FP	Crude extraction of Flowering Pu'er tea
CF-PR	Chloroform fraction of Pu'er raw tea
CF-FP	Chloroform fraction of Flowering Pu'er tea
EAF-PR	Ethyl acetate fraction of Pu'er raw tea
EAF-FP	Ethyl acetate fraction of Flowering Pu'er tea
NAF-PR	N-butyl alcohol fraction of Pu'er raw tea
NAF-FP	N-butyl alcohol fraction of Flowering Pu'er tea
WF-PR	Water fraction of Pu'er raw tea
WF-FP	Water fraction of Flowering Pu'er tea
SV	Simvastatin
HPLC	high performance liquid chromatography
GC-MS	gas chromatography-mass spectrometer

References

Adabag, S., Huxley, R. R., Lopez, F. L., Chen, L. Y., Sotoodehnia, N., Siscovick, D., et al. (2015). Obesity related risk of sudden cardiac death in the atherosclerosis risk in communities study. *Heart,* 215–221.

Braud, L., Battault, S., Meyer, G., Nascimento, A., Gaillard, S., de Sousa, G., et al. (2017). Antioxidant properties of tea blunt ROS-dependent lipogenesis: Beneficial effect on hepatic steatosis in a high fat-high sucrose diet NAFLD obese rat model. *The Journal of Nutritional Biochemistry,* 95–104.

Chen, Z. M., & Lin, Z. (2015). Tea and human health: Biomedical functions of tea active components and current issues. *Journal of Zhejiang University - Science B,* 87–102.

Comar, K. M., & Sterling, R. K. (2006). Review article: Drug therapy for non-alcoholic fatty liver disease. *Alimentary Pharmacology and Therapeutics,* 207–215.

Ding, Y., Pu, L., & Kan, J. (2017). Hypolipidemic effects of lipid-lowering granulated tea preparation from Monascus-fermented grains (adlay and barley bran) mixed with lotus leaves on Sprague–Dawley rats fed a high-fat diet. *Journal of Functional Foods,* 80–89.

Fu, J., Lv, H., & Chen, F. (2016). Diversity and variation of bacterial community revealed by MiSeq Sequencing in Chinese dark teas. *PLoS One,* 1–12.

Fu, D., Ryan, E. P., Huang, J., Liu, Z., Weir, T. L., Snook, R. L., et al. (2011). Fermented Camellia sinensis, Fu Zhuan Tea, regulates hyperlipidemia and transcription factors involved in lipid catabolism. *Food Research International,* 2999–3005.

Gong, J. G. C., Peng, C., Chen, T., Gao, B., & Zhou, H. (2010). Effects of theabrownin from Pu-erh tea on the metabolism of serum lipids in rats: Mechanism of action. *Journal of Food Science,* H182–H189.

Gressel, A. S. A. J. (1991). Elicitation of a flavonoid phytoalexin accumulation in Cassia obtusifolia by a mycoherbicide: Estimation by AlCl3-spectrofluorimetry. *Pesticide Biochemistry and Physiology,* 142–149.

He, H. (2017). Research progress on theaflavins: Efficacy, formation, and preparation. *Food & Nutrition Research*1344521 1–9.

He-Yuan Jianga, B., Shiia, T., Matsuoa, Y., Tanakaa, T., Jiangc, Z., & Kounoa, I. (2011). A new catechin oxidation product and polymeric polyphenols of post-fermented tea. *Food Chemistry,* 830–836.

Hirata, H., Uto-Kondo, H., Ogura, M., Ayaori, M., Shiotani, K., Ota, A., et al. (2017). Xanthohumol, a hop-derived prenylated flavonoid, promotes macrophage reverse cholesterol transport. *The Journal of Nutritional Biochemistry,* 29–34.

Hou, C. W., Jeng, K. C., & Chen, Y. S. (2010). Enhancement of fermentation process in Pu-erh tea by tea-leaf extract. *Journal of Food Science* H44-H48.

Houslay, E. S., Sarma, J., & Uren, N. G. (2007). The effect of intensive lipid lowering on coronary atheroma and clinical outcome. *Education in Heart,* 149–151.

Huxley, R. R. G. O., Mendis, S., Zheleznyakov, E., Reddy, S., & Chan, J. (2010). Body mass index, waist circumference and waist:hip ratio as predictors of cardiovascular risk–a review of the literature. *European Journal of Clinical Nutrition,* 16–22.

Jin, D., Xu, Y., Mei, X., Meng, Q., Gao, Y., Li, B., et al. (2013). Antiobesity and lipid lowering effects of theaflavins on high-fat diet induced obese rats. *Journal of Functional Foods,* 1142–1150.

Li, Q., Huang, J., Li, Y., Zhang, Y., Luo, Y., Chen, Y., et al. (2017). Fungal community succession and major components change during manufacturing process of Fu brick tea. *Scientific Reports,* 6947.

Liu, T. (2016). Effect of Eurotium Cristatum fermented dark tea extract on body weight and blood lipid in rats. *Journal of the Academy of Nutrition and Dietetics,* A77.

Luo, Z., Du, H., Li, L., An, M., Zhang, Z., Wan, X., et al. (2013). Fuzhuanins a and B: The B-ring fission lactones of flavan-3-ols from Fuzhuan brick-tea. *Journal of Agricultural and Food Chemistry,* 6982–6990.

Lv, H., Zhong, Q., Lin, Z., Wang, L., Tan, J., & Guo, L. (2012). Aroma characterisation of Pu-erh tea using headspace-solid phase microextraction combined with GC/MS and GC–olfactometry. *Food Chemistry,* 1074–1081.

Mao, Y., Wei, B., Teng, J., Huang, L., & Xia, N. (2017). Analyses of fungal community by Illumina MiSeq platforms and characterization of Eurotium species on Liupao tea, a distinctive post-fermented tea from China. *Food Research International,* 641–649.

Masaki Funamoto, M., Hidetoshi Masumoto, M. P., Koji Takaori, M., Tomofumi Taki, M., Shuji Setozaki, M., Kazuhiro Yamazaki, M. P., et al. (2016). Green tea polyphenol prevents diabetic rats from acute kidney injury after cardiopulmonary bypass. *The Annals of Thoracic Surgery,* 1507–1513.

Matsuzaki, T., Ito, H., Chevyreva, V., Makky, A., Kaufmann, S., Okano, K., et al. (2017). Adsorption of galloyl catechin aggregates significantly modulates membrane mechanics in the absence of biochemical cues. *PCCP: Physical Chemistry Chemical Physics,* 19937–19947.

Ma, C., Zhang, W., Su, Z., & Bai, Y. (2018). Resonance Rayleigh scattering method for the determination of chitosan using erythrosine B as a probe and PVA as sensitization. *Food Chemistry,* 126–131.

Mottram, D. S., Wedzicha, B. L., & Dodson, A. T. (2002). Acrylamide is formed in the Maillard reaction. *ON Nature,* 448–449.

Nam, M., Choi, M., Choi, J., Kim, N., Kim, M., Jung, S., et al. (2018). Effect of green tea on hepatic lipid metabolism in mice fed a high-fat diet. *The Journal of Nutritional Biochemistry,* 1–7.

Neyrinck, A. M., Bindels, L. B., Geurts, L., Van Hul, M., Cani, P. D., & Delzenne, N. M. (2017). A polyphenolic extract from green tea leaves activates fat browning in high-fat-diet-induced obese mice. *The Journal of Nutritional Biochemistry,* 15–21.

Okuda, M. H. M. O., Zemdegs, J. C. S., de Santana, A. A., Santamarina, A. B., Moreno, M. F., Hachul, A. C. L., et al. (2014). Green tea extract improves high fat diet-induced hypothalamic inflammation, without affecting the serotoninergic system. *The Journal of Nutritional Biochemistry,* 1084–1089.

Rajagopalan, S. S. R. O., Zannad, F., Radauceanu, A., Glazer, R., Jia, Y., Prescott, M. F., et al. (2007). Effects of valsartan alone versus valsartan/simvastatin combination on ambulatory blood pressure, C-reactive protein, lipoproteins, and monocyte chemoattractant protein-1 in patients with hyperlipidemia and hypertension. *The American Journal of Cardiology,* 222–226.

Rämö, J., Ripatti, P., Tabassum, R., Söderlund, S., Matikainen, N., Gerl, M., et al. (2017). Mass spectrometry of circulating lipid species highlights similarity of familial hyperlipidemias and hyperlipidemias in the general population. *Atherosclerosis,* e61.

Ripatti, P., Rämö, J., Söderlund, S., Surakka, I., Matikainen, N., Salomaa, V., et al. (2017). Polygenic hyperlipidemia and coronary artery disease risk. *Atherosclerosis, e4*.

Schuster, E., Dunn-Coleman, N., Frisvad, J., & van Dijck, P. (2002). On the safety of *Aspergillus Niger*–a review. *Applied Microbiology and Biotechnology,* 426–435.

Su, Y., Zhang, C., Wang, Y., & Li, P. (2012). Antibacterial property and mechanism of a novel Pu-erh tea nanofibrous membrane. *Applied Microbiology and Biotechnology,* 1663–1671.

Way, T., Lin, H., Kuo, D., Tsai, S., Shieh, J., Wu, J., et al. (2009). Pu-erh tea attenuates hyperlipogenesis and induces hepatoma cells growth arrest through activating AMP-activated protein kinase (AMPK) in human HepG2 cells. *Journal of Agricultural and Food Chemistry,* 5257–5264.

Whitlock, G., Lewington, S., Sherliker, P., Clarke, R., Emberson, J., Halsey, J., et al. (2009). Body-mass index and cause-specific mortality in 900 000 adults: Collaborative analyses of 57 prospective studies. *Lancet,* 1083–1096.

Xu, A., Wang, Y., Wen, J., Liu, P., Liu, Z., & Li, Z. L. Y. C. (2011a). Fungal community associated with fermentation and storage of Fuzhuan brick-tea. *International Journal of Food Microbiology,* 14–22.

Xu, Y. Q., Zhang, Y. N., Chen, J. X., Wang, F., Du, Q. Z., & Yin, J. F. (2018). Quantitative analyses of the bitterness and astringency of catechins from green tea. *Food Chemistry,* 16–24.

Xu, Y., Zhang, M., Wu, T., Dai, S., Xu, J., & Zhou, Z. (2015). The anti-obesity effect of

green tea polysaccharides, polyphenols and caffeine in rats fed with a high-fat diet. *Food and Function,* 296–303.
Xu, Y., Zhao, H., Zhang, M., Li, C., Lin, X., Sheng, J., et al. (2011b). Variations of antioxidant properties and NO scavenging abilities during fermentation of tea. *International Journal of Molecular Sciences,* 4574–4590.
Yi, W., Xie, X., Du, M., Bu, Y., Wu, N., Yang, H., et al. (2017). Green tea polyphenols ameliorate the early renal damage induced by a high-fat diet via ketogenesis/SIRT3 Pathway. *Oxidative Medicine and Cellular Longevity,* 1–14.
Zhang, W., Yang, R., Fang, W., Yan, L., Lu, J., Sheng, J. S. Y. E., et al. (2016). Characterization of thermophilic fungal community associated with pile fermentation of Pu-erh tea. *International Journal of Food Microbiology,* 29–33.
Zhao, Y., Yang, L., Huang, Z., Lin, L., & Zheng, G. (2017). Synergistic effects of caffeine and catechins on lipid metabolism in chronically fed mice via the AMP-activated protein kinase signaling pathway. *European Journal of Nutrition,* 2309–2318.
Zheng, W., Wan, X., & Bao, G. (2015). Brick dark tea: A review of the manufacture, chemical constituents and bioconversion of the major chemical components during fermentation. *Phytochemistry Reviews,* 499–523.
Zhu, Z., Lin, Z., Jiang, H., Jiang, Y., Zhao, M., & Liu, X. (2017). Hypolipidemic effect of Youcha in hyperlipidemia rats induced by high-fat diet. *Food Funct,* 1680–1687.
Zhu, Y., Luo, Y., Wang, P., Zhao, M., Li, L., Hu, X., et al. (2016). Simultaneous determination of free amino acids in Pu-erh tea and their changes during fermentation. *Food Chemistry,* 643–649.

Volume 8 | Number 9 | September 2017 | Pages 2985–3396

Food & Function

Linking the chemistry and physics of food with health and nutrition

rsc.li/food-function



ISSN 2042-650X

ROYAL SOCIETY OF CHEMISTRY

REVIEW ARTICLE

Seishi Shimizu, Steven Abbott and Nobuyuki Matubayasi

Quantifying non-specific interactions between flavour and food biomolecules

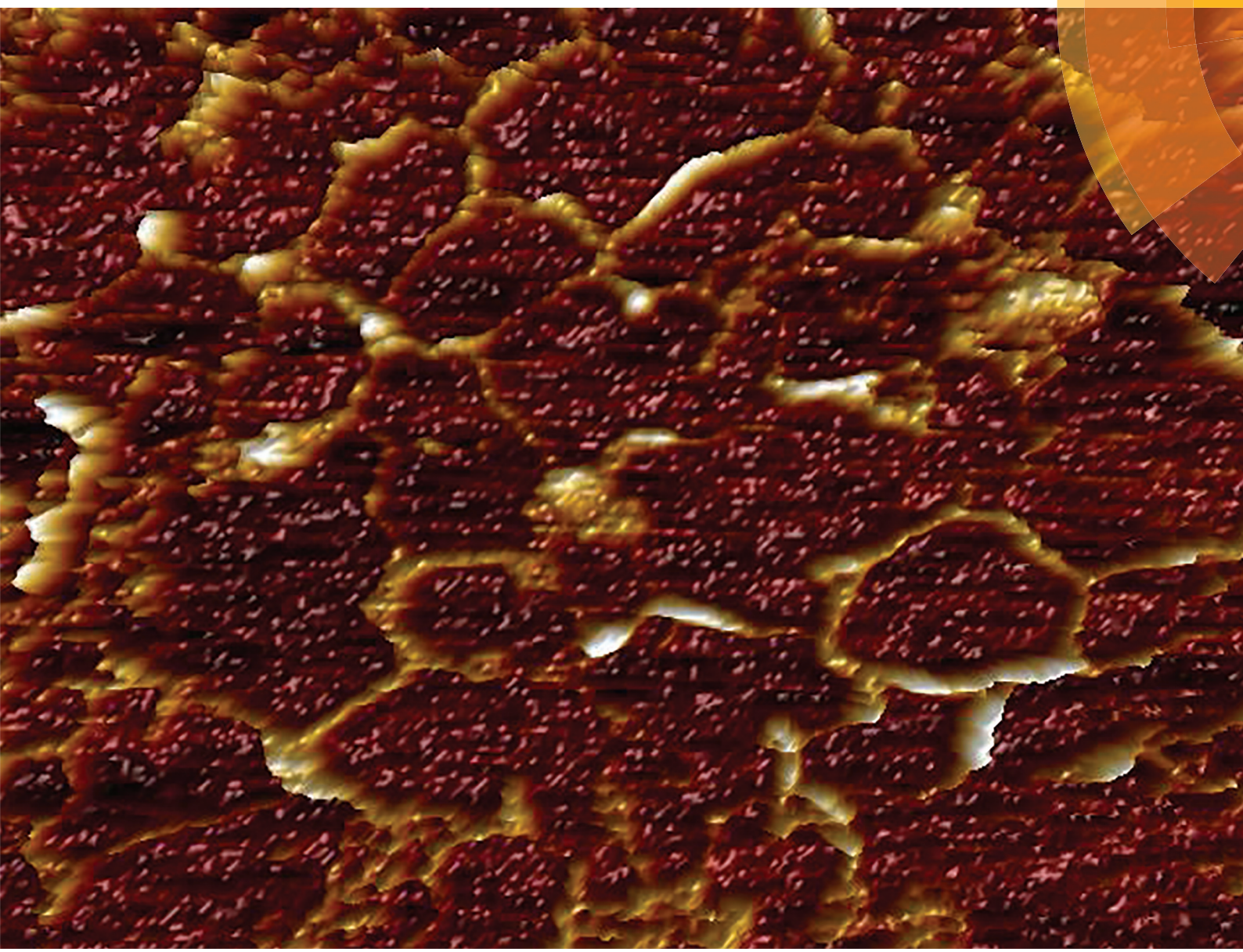
第344页，共417页

Volume 8 | Number 9 | September 2017 | Pages 2985–3396

Food & Function

Linking the chemistry and physics of food with health and nutrition

rsc.li/food-function



ISSN 2042-650X

ROYAL SOCIETY OF CHEMISTRY

PAPER

Mouming Zhao *et al.*

A comparison study on polysaccharides extracted from *Laminaria japonica* using different methods: structural characterization and bile acid-binding capacity

Published on 20 September 2017. Downloaded on 3/5/2024 12:24:02 AM.

Food & Function

rsc.li/food-function

The Royal Society of Chemistry is the world's leading chemistry community. Through our high impact journals and publications we connect the world with the chemical sciences and invest the profits back into the chemistry community.

IN THIS ISSUE

ISSN 2042-650X CODEN FFOUAI 8(9) 2985–3396 (2017)



Cover
See Seishi Shimizu, Steven Abbott and Nobuyuki Matubayasi, pp. 2999–3009.

Image produced with the help of Tom Nicol and reproduced by permission of Seishi Shimizu from *Food Funct.*, 2017, **8**, 2999.



Inside cover
See Mouming Zhao *et al.*, pp. 3043–3052.

Image reproduced by permission of Mouming Zhao from *Food Funct.*, 2017, **8**, 3043.

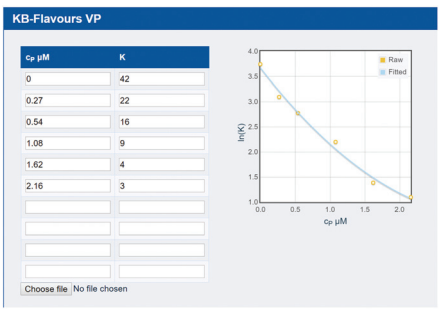
REVIEWS

2999

Quantifying non-specific interactions between flavour and food biomolecules

Seishi Shimizu,* Steven Abbott and Nobuyuki Matubayasi

Non-specific protein–flavour interactions can be captured by assumption-free statistical thermodynamics.

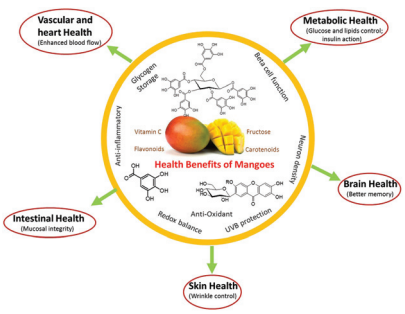


3010

Mangos and their bioactive components: adding variety to the fruit plate for health

Britt M. Burton-Freeman,* Amandeep K. Sandhu and Indika Edirisinghe

The diet is an essential factor affecting the risk for development and progression of modern day chronic diseases, particularly those with pathophysiological roots in inflammation and oxidative stress-induced damage.



Published on 20 September 2017. Downloaded on 3/5/2024 12:24:02 AM.

Editorial Staff

Executive Editor
Philippa Hughes

Deputy Editor
Rebecca Brodie

Editorial Production Manager
Sarah Kenwright

Development Editor
Hannah Aitchison

Publishing Editors
Jeremy Allen, Susan Askey, Harriet Brewerton, Ziva Whitelock

Publishing Assistant
Andrea Whiteside

Editorial Assistant
Keir Hollingsworth

Publisher
Jamie Humphrey

For queries about submitted articles please contact Sarah Kenwright, Editorial production manager, in the first instance. E-mail **food@rsc.org**

For pre-submission queries please contact Philippa Hughes, Executive Editor. E-mail **food-rsc@rsc.org**

Food & Function (electronic: ISSN 2042-650X) is published 12 times a year by the Royal Society of Chemistry, Thomas Graham House, Science Park, Milton Road, Cambridge, CB4 0WF, UK.

All orders, with cheques made payable to the Royal Society of Chemistry, should be sent to the Royal Society of Chemistry Order Department, Royal Society of Chemistry, Thomas Graham House, Science Park, Milton Road, Cambridge, CB4 0WF, UK Tel +44 (0)1223 432398; E-mail **orders@rsc.org**

2017 Annual (electronic) subscription price: £1750; US$3015. Customers in Canada will be subject to a surcharge to cover GST. Customers in the EU subscribing to the electronic version only will be charged VAT.

If you take an institutional subscription to any Royal Society of Chemistry journal you are entitled to free, site-wide web access to that journal. You can arrange access via Internet Protocol (IP) address at **www.rsc.org/ip**

Customers should make payments by cheque in sterling payable on a UK clearing bank or in US dollars payable on a US clearing bank.

Whilst this material has been produced with all due care, the Royal Society of Chemistry cannot be held responsible or liable for its accuracy and completeness, nor for any consequences arising from any errors or the use of the information contained in this publication. The publication of advertisements does not constitute any endorsement by the Royal Society of Chemistry or Authors of any products advertised. The views and opinions advanced by contributors do not necessarily reflect those of the Royal Society of Chemistry which shall not be liable for any resulting loss or damage arising as a result of reliance upon this material. The Royal Society of Chemistry is a charity, registered in England and Wales, Number 207890, and a company incorporated in England by Royal Charter (Registered No. RC000524), registered office: Burlington House, Piccadilly, London W1J 0BA, UK, Telephone: +44 (0) 207 4378 6556.

Advertisement sales:
Tel +44 (0) 1223 432246; Fax +44 (0) 1223 426017;
E-mail **advertising@rsc.org**

For marketing opportunities relating to this journal, contact **marketing@rsc.org**

Food & Function

Linking the chemistry and physics of food with health and nutrition

rsc.li/food-function

Editorial Board

Editor-in-Chief
Kevin Croft, University of Western Australia, Australia

Associate Editors
Laura Bravo-Clemente, Institute of Food Science, Technology and Nutrition, Spain
Isabel C.F.R Ferreira, Polytechnic Institute of Bragança, Portugal
Mario Ferruzzi, North Carolina State University, USA
Tim Foster, University of Nottingham, UK
Cesar Fraga, University of Buenos Aires, Argentina & University of California, Davis, USA
Duo Li, Zhejiang University, China
Hang Xiao, University of Massachusetts Amherst, USA

Members
Hitoshi Ashida, Kobe University, Japan
H. Douglas Goff, University of Guelph, Canada

Advisory Board

Aedin Cassidy, University of East Anglia, UK
Junshi Chen, China National Center of Food Safety Risk Assessment, China
Steven Feng Chen, Peking University, China
Zhen-yu Chen, Chinese University of Hong Kong, Hong Kong
Peter Clifton, Baker IDI Heart & Diabetes Institute
Eric Decker, University of Massachusetts, USA
E. Allen Foegeding, North Carolina State University, USA
Nissim Garti, Hebrew University of Jerusalem, Israel
Mike Gidley, University of Queensland, Australia
Chi-Tang Ho, Rutgers University, USA
Richard Hurrell, ETH Zurich, Switzerland
Rui Hai Liu, Cornell University, USA
Alejandro Marangoni, University of Guelph, Canada
Julian McClements, University of Massachusetts, USA
Paul Moughan, Riddet Institute, Massey University, New Zealand
Patricia Oteiza, University of California, Davis, USA
Augustin Scalbert, International Agency for Research on Cancer (IARC), France
Helmet Sies, University of Dusseldorf, Germany
Leif Skibsted, University of Copenhagen, Denmark
David Stuart, Food & Nutrition Impact, LLC, USA
Young-Joon Surh, Seoul National University, South Korea
Arthur Tatham, University of Wales Institue, Cardiff, UK
Junji Terao, University of Tokushima, Japan
George van Aken, NIZO Food Research, The Netherlands
Rob van Dam, National University of Singapore, Singapore
Erik van der Linden, TI Food & Nutrition, The Netherlands
Jose Vina, University of Valencia, Spain
Gary Williamson, University of Leeds, UK
Xingbin Yang, Shaanxi Normal University, China
Gow-Chin Yen, National Chung Hsing University, Chinese Taipei

Information for Authors

Full details on how to submit material for publication in Food & Function are given in the Instructions for Authors (available from **http://www.rsc.org/authors**). Submissions should be made via the journal's homepage: **rsc.li/food-function**

Authors may reproduce/republish portions of their published contribution without seeking permission from the Royal Society of Chemistry, provided that any such republication is accompanied by an acknowledgement in the form: (Original Citation)–Reproduced by permission of the Royal Society of Chemistry.

This journal is © The Royal Society of Chemistry 2017. Apart from fair dealing for the purposes of research or private study for non-commercial purposes, or criticism or review, as permitted under the Copyright, Designs and Patents Act 1988 and the Copyright and Related Rights Regulation 2003, this publication may only be reproduced, stored or transmitted, in any form or by any means, with the prior permission in writing of the Publishers or in the case of reprographic reproduction in accordance with the terms of licences issued by the Copyright Licensing Agency in the UK. US copyright law is applicable to users in the USA.

Registered charity number: 207890

Published on 20 September 2017. Downloaded on 3/5/2024 12:24:02 AM.

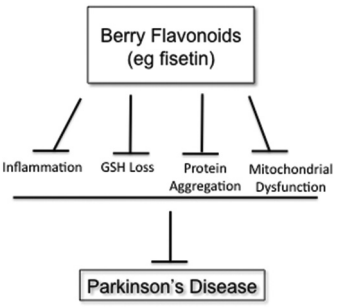
REVIEWS

3033

Protective effects of fisetin and other berry flavonoids in Parkinson's disease

Pamela Maher

Parkinson's disease (PD) is an age-associated degenerative disease of the midbrain that results from the loss of dopaminergic neurons in the substantia nigra.



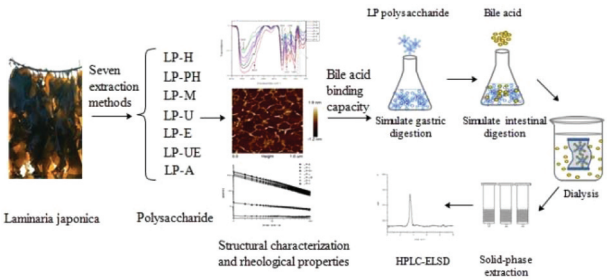
PAPERS

3043

A comparison study on polysaccharides extracted from *Laminaria japonica* using different methods: structural characterization and bile acid-binding capacity

Jie Gao, Lianzhu Lin, Baoguo Sun and Mouming Zhao*

The structural characterization, rheological properties and bile acid-binding capacity of LP obtained by seven different extraction methods were investigated.



3053

***In vitro* modulation of gut microbiota by whey protein to preserve intestinal health**

T. Sánchez-Moya,* R. López-Nicolás, D. Planes, C. A. González-Bermúdez, G. Ros-Berruezo and C. Frontela-Saseta

The effect of several types of whey milk was assessed in the human microbiota.

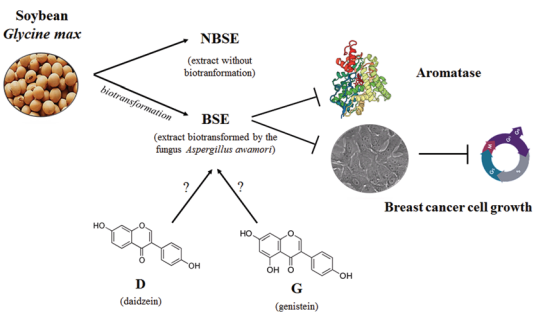


3064

The role of soybean extracts and isoflavones in hormone-dependent breast cancer: aromatase activity and biological effects

Cristina Amaral, Maria Regina T. Toloi, Luis Daniel Vasconcelos, Maria José V. Fonseca, Georgina Correia-da-Silva and Natércia Teixeira*

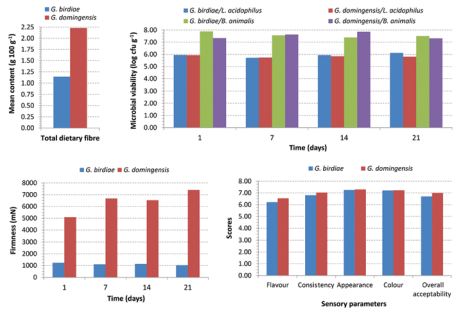
Biotransformed soybean extract has anti-aromatase and anti-tumoral properties in Estrogen receptor-positive (ER^+) breast cancer.



Published on 20 September 2017. Downloaded on 3/5/2024 12:24:02 AM.

PAPERS

3075

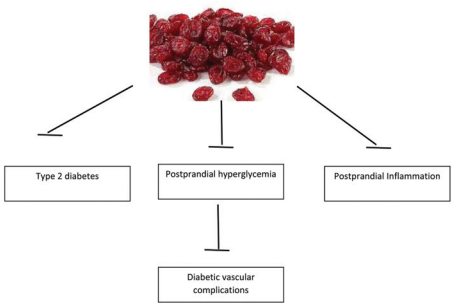


Comparison of dairy desserts produced with a potentially probiotic mixed culture and dispersions obtained from *Gracilaria birdiae* and *Gracilaria domingensis* seaweeds used as thickening agents

Adriana Carneiro Tavares Estevam, Michele Correia de Almeida, Tiago Almeida de Oliveira, Eliane Rolim Florentino, Flávia Carolina Alonso Buriti and Ana Lúcia Figueiredo Porto*

Best results were achieved for *G. domingensis* seaweed.

3083

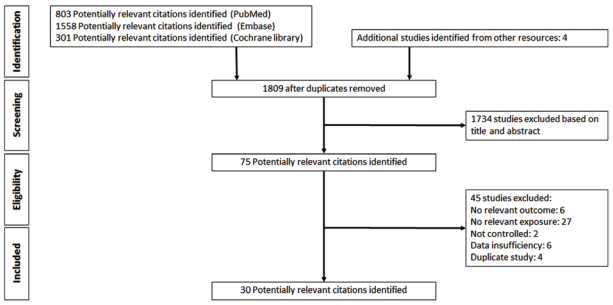


Cranberries improve postprandial glucose excursions in type 2 diabetes

Jace Schell, Nancy M. Betts, Megan Foster, R. Hal Scofield and Arpita Basu*

An overview of the role of dried cranberries in reducing postprandial hyperglycemia and inflammation in type 2 diabetes and the subsequent risks of vascular complications.

3091

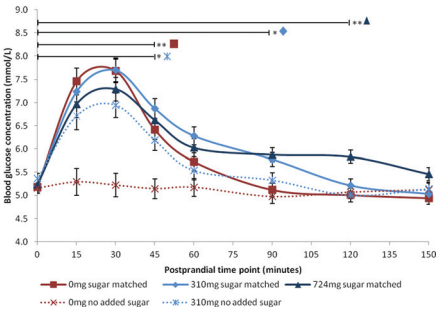


Dietary linoleic acid intake and blood inflammatory markers: a systematic review and meta-analysis of randomized controlled trials

Hang Su, Ruijie Liu, Ming Chang, Jianhua Huang and Xingguo Wang*

This meta-analysis aims at investigating the effect of linoleic acid intake on inflammatory cytokines, acute phase reactants and adhesion molecules.

3104



A study of glycaemic effects following acute anthocyanin-rich blueberry supplementation in healthy young adults

L. Bell, D. J. Lamport, L. T. Butler and C. M. Williams*

The postprandial response to ingested carbohydrate is recognised as a marker of metabolic health, and is altered favourably by the consumption of anthocyanin-rich wild blueberry.

This journal is © The Royal Society of Chemistry 2017

Published on 20 September 2017. Downloaded on 3/5/2024 12:24:02 AM.

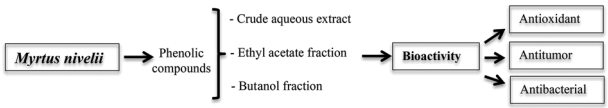
PAPERS

3111

Detailed phytochemical characterization and bioactive properties of *Myrtus nivelii* Batt & Trab

W. Rached, M. Bennaceur, L. Barros,* R. C. Calhelha, S. Heleno, M. J. Alves, A. M. Carvalho, A. Marouf and I. C. F. R. Ferreira*

Myrtus nivelii Batt & Trab is a rich source of flavonols and ellagitannin derivatives. The tested extract and purified fractions revealed excellent bioactivity and ethyl acetate fraction resulted to be the most potential source in bioactives.

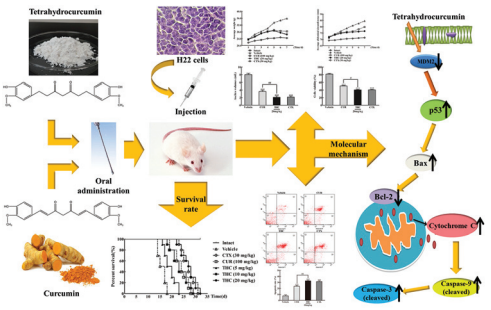


3120

Tetrahydrocurcumin is more effective than curcumin in inducing the apoptosis of H22 cells *via* regulation of a mitochondrial apoptosis pathway in ascites tumor-bearing mice

Weihai Liu, Zhenbiao Zhang, Guosheng Lin, Dandan Luo, Hanbin Chen, Hongmei Yang, Jiali Liang, Yuhong Liu, Jianhui Xie, Ziren Su* and Hongying Cao*

Curcumin (CUR), a widely used food additive, is derived mainly from *Curcuma* species that has been applied traditionally for treating hepatocellular carcinoma (HCC).

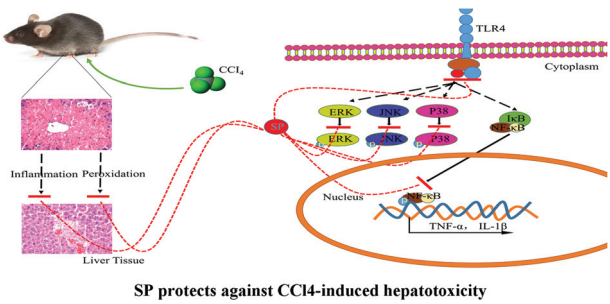


3130

Seabuckthorn berry polysaccharide protects against carbon tetrachloride-induced hepatotoxicity in mice *via* anti-oxidative and anti-inflammatory activities

Wei Zhang, Xiaohui Zhang, Kai Zou, Jiming Xie, Shimin Zhao, Jingran Liu, Huan Liu, Jinling Wang and Yuzhen Wang*

The berries of Seabuckthorn (*Hippophae rhamnoides* L.) are traditional medicinal foods that have been used by Tibetans and Mongolians for thousands of years.



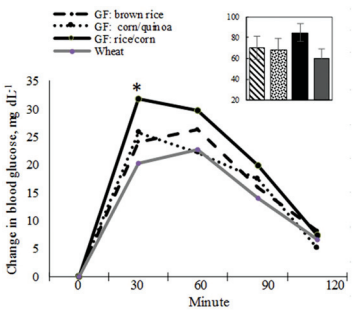
SP protects against CCl4-induced hepatotoxicity

3139

Commercially available gluten-free pastas elevate postprandial glycemia in comparison to conventional wheat pasta in healthy adults: a double-blind randomized crossover trial

C. S. Johnston,* D. Snyder and C. Smith

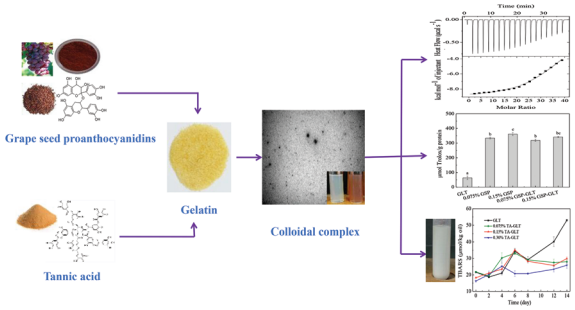
Given the popularity of gluten-free diets, research regarding the health implications of gluten-free (GF) products is necessary.



Published on 20 September 2017. Downloaded on 3/5/2024 12:24:02 AM.

PAPERS

3145

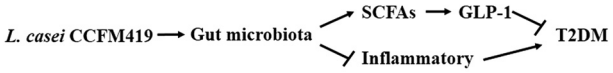


Self-assembled colloidal complexes of polyphenol–gelatin and their stabilizing effects on emulsions

Yu Huang, Aijun Li, Chaoying Qiu,* YingLai Teng and Yong Wang*

We studied the in-depth characteristics including the binding interactions and morphological structure of tannic acid (TA)/grape seed proanthocyanidins (GSP) and gelatin (GLT) colloidal complexes, and evaluated the lipid oxidation of emulsions formed by the colloidal complexes.

3155

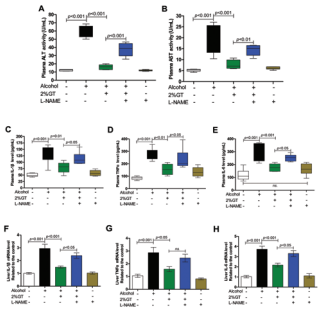


***Lactobacillus casei* CCFM419 attenuates type 2 diabetes *via* a gut microbiota dependent mechanism**

Gang Wang,* Xiangfei Li, Jianxin Zhao,* Hao Zhang and Wei Chen

Probiotics, as dietary supplements, transmit their major effects through the regulation of gut microbiota.

3165

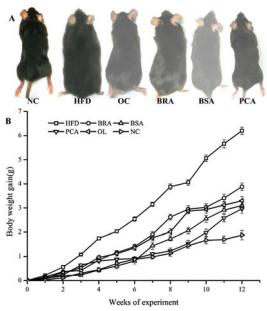


Green tea infusion protects against alcoholic liver injury by attenuating inflammation and regulating the PI3K/Akt/eNOS pathway in C57BL/6 mice

Dongxu Wang, Qiang Gao, Taotao Wang, Guangshan Zhao, Frank Qian, Jinbao Huang, Haisong Wang, Xin Zhang and Yijun Wang*

Alcohol intake is a major risk factor for the pathogenesis of alcoholic liver diseases.

3178



Anthocyanins in black rice, soybean and purple corn increase fecal butyric acid and prevent liver inflammation in high fat diet-induced obese mice

Tao Wu, Xueqi Guo, Min Zhang,* Lu Yang, Rui Liu and Jinjin Yin

Epidemiological evidence indicates that anthocyanin consumption reduces the incidence of chronic and degenerative diseases.

This journal is © The Royal Society of Chemistry 2017

Published on 20 September 2017. Downloaded on 3/5/2024 12:24:02 AM.

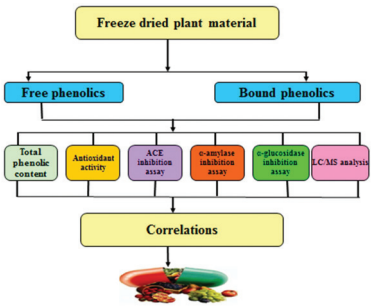
PAPERS

3187

Profiles of free and bound phenolics extracted from *Citrus* fruits and their roles in biological systems: content, and antioxidant, anti-diabetic and anti-hypertensive properties

M. H. Alu'datt,* T. Rababah, M. N. Alhamad, M. A. Al-Mahasneh, K. Ereifej, G. Al-Karaki, M. Al-Duais, J. E. Andrade, C. C. Tranchant, S. Kubow and K. A. Ghozlan

Rutaceae plant extracts were investigated for their potential to inhibit hyperglycemia and hypertension related enzymes.

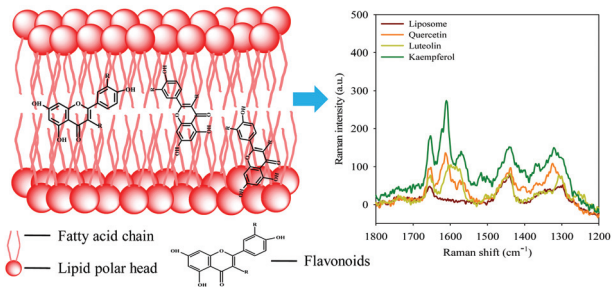


3198

Encapsulation of flavonoids in liposomal delivery systems: the case of quercetin, kaempferol and luteolin

Meigui Huang, Erzheng Su, Fuping Zheng* and Chen Tan*

The instability of dietary flavonoids is currently a challenge for their incorporation in functional foods.

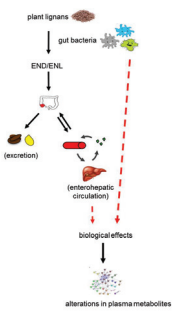


3209

Plasma metabolite abundances are associated with urinary enterolactone excretion in healthy participants on controlled diets

Fayth L. Miles, Sandi L. Navarro, Yvonne Schwarz, Haiwei Gu, Danijel Djukovic, Timothy W. Randolph, Ali Shojaie, Mario Kratz, Meredith A. J. Hullar, Paul D. Lampe, Marian L. Neuhouser, Daniel Raftery and Johanna W. Lampe*

Enterolignans, gut bacterial metabolites of plant lignans, affect biologic pathways relevant to chronic disease.

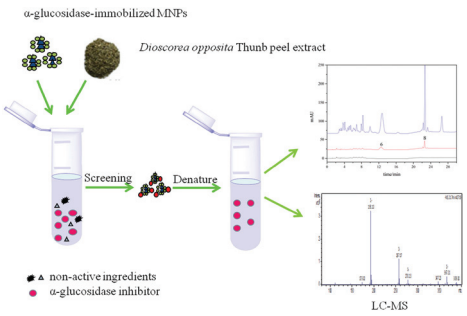


3219

Rapid identification of α-glucosidase inhibitors from *Dioscorea opposita* Thunb peel extract by enzyme functionalized Fe_3O_4 magnetic nanoparticles coupled with HPLC-MS/MS

Songsong Zhang, Dandan Wu, Huan Li, Jinhua Zhu,* Weiping Hu, Minghua Lu and Xiuhua Liu*

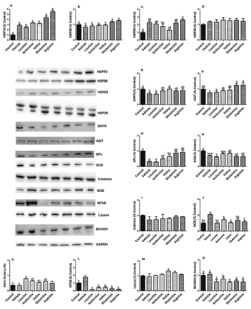
Two α-glucosidase inhibitors identified as 2,4-dimethoxy-6,7-dihydroxyphenanthrene and batatasin I were conveniently extracted from *Dioscorea opposita* Thunb peel extract using αG-MNPs.



Published on 20 September 2017. Downloaded on 3/5/2024 12:24:02 AM.

PAPERS

3228

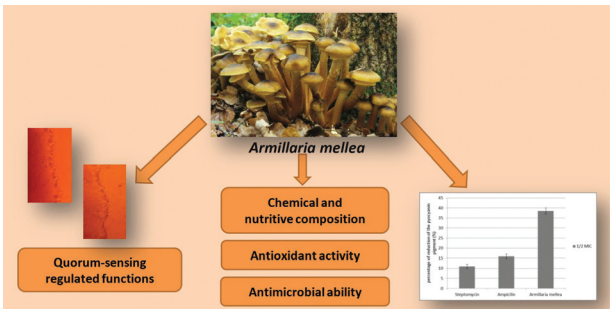


Modulatory effects of arginine, glutamine and branched-chain amino acids on heat shock proteins, immunity and antioxidant response in exercised rats

Carolina Soares Moura,* Pablo Christiano Barboza Lollo, Priscila Neder Morato, Eder Muller Risso and Jaime Amaya-Farfan

Heat shock proteins (HSPs) are endogenous proteins whose function is to maintain the cell's tolerance to insult, including intense exercise.

3239

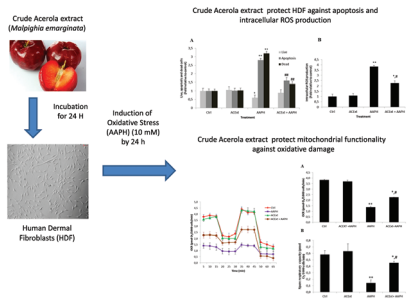


Chemical, nutritive composition and a wide range of bioactive properties of honey mushroom *Armillaria mellea* (Vahl: Fr.) Kummer

Marina Kostić, Marija Smiljković, Jovana Petrović, Jasmina Glamočlija, Lillian Barros, Isabel C. F. R. Ferreira, Ana Ćirić* and Marina Soković*

A methanolic extract prepared from these samples was tested for antioxidant, quorum sensing and antimicrobial assays, as well as for its cytotoxicity effects.

3250

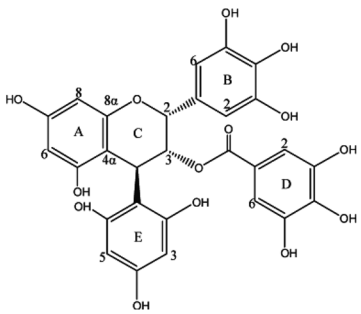


The protective effect of acerola (*M. emarginata*) against oxidative damage in human dermal fibroblasts through the improvement of antioxidant enzyme activity and mitochondrial functionality

J. M. Alvarez-Suarez, F. Giampieri,* M. Gasparrini, L. Mazzoni, C. Santos-Buelga, A. M. González-Paramás, T. Y. Forbes-Hernández, S. Afrin, T. Páez-Watson, J. L. Quiles and M. Battino*

Acerola fruits are shown as an important natural source of bioactive compounds with beneficial properties for health.

3259



The anti-obesity properties of the proanthocyanidin extract from the leaves of Chinese bayberry (*Myrica rubra* Sieb.et Zucc.)

Xiaozhou Zhou, Shiguo Chen and Xingqian Ye*

The anti-obesity effects of different proanthocyanidin extracts (PE) from Chinese bayberry (*Myrica rubra* Sieb.et Zucc.) leaves were evaluated in a high-fat (HF) diet-induced obese rat model.

This journal is © The Royal Society of Chemistry 2017

Published on 20 September 2017. Downloaded on 3/5/2024 12:24:02 AM.

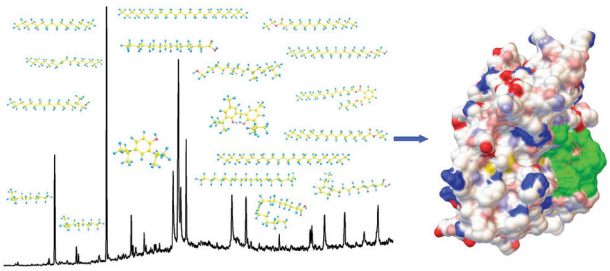
PAPERS

3271

Characterization of active compounds from *Gracilaria lemaneiformis* inhibiting the protein tyrosine phosphatase 1B activity

Xinfeng Guo, Dongyu Gu,* Miao Wang, Yu Huang, Haoquan Li, Yue Dong, Jing Tian, Yi Wang and Yi Yang*

Gracilaria lemaneiformis, an edible alga, with various bioactivities is a traditional dish and a favorite food.

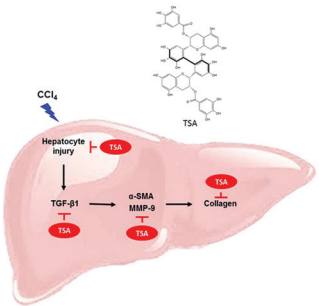


3276

Protective effects of theasinensin A against carbon tetrachloride-induced liver injury in mice

Wei-Lun Hung, Guliang Yang, Yu-Chuan Wang, Yi-Shiou Chiou, Yen-Chen Tung, Meei-Ju Yang, Bi-Ni Wang, Chi-Tang Ho, Yu Wang* and Min-Hsiung Pan*

TSA markedly reduced the CCl_4-induced liver injury in mice.

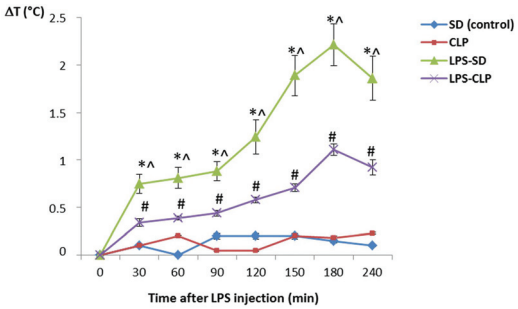


3288

Antioxidant and anti-inflammatory effects of cauliflower leaf powder-enriched diet against LPS induced toxicity in rabbits

Marilena Larocca, Anna Maria Perna, Amalia Simonetti, Emilio Gambacorta, Alessandra Iannuzzi, Angela Perucatti and Rocco Rossano*

Brassica phytochemicals exert a broad spectrum of health-promoting activities.

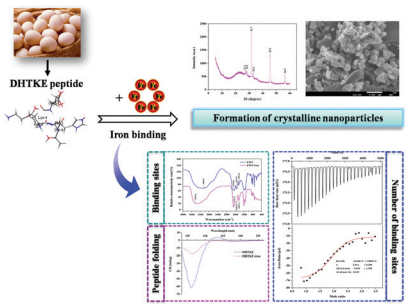


3297

Formation of crystalline nanoparticles by iron binding to pentapeptide (Asp-His-Thr-Lys-Glu) from egg white hydrolysates

Na Sun, Pengbo Cui, Dongmei Li, Ziqi Jin, Shuyu Zhang and Songyi Lin*

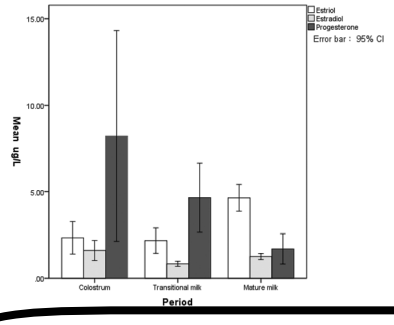
A novel peptide (DHTKE) from egg white hydrolysates could bind iron ions in a 1 : 2 ratio *via* its amide and carboxyl groups, forming the DHTKE-iron complex which belongs to crystalline nanoparticles.



Published on 20 September 2017. Downloaded on 3/5/2024 12:24:02 AM.

PAPERS

3306

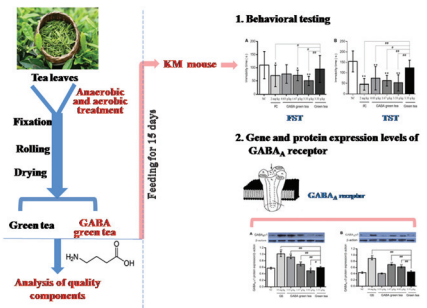


Concentrations of estrogen and progesterone in breast milk and their relationship with the mother's diet

Mengqing Lu, Hailong Xiao, Kelei Li, Jiajing Jiang, Kejian Wu and Duo Li*

The aim of the present study was to determine the concentrations of estradiol (E2), estriol (E3) and progesterone in breast milk over different lactation periods, and to assess their relationship with the mother's diet.

3311

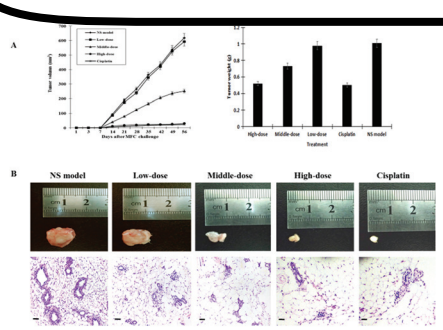


Quality components and antidepressant-like effects of GABA green tea

Jie Teng, Wen Zhou, Zhen Zeng, Wenfang Zhao, Yahui Huang* and Xu Zhang*

After vacuum anaerobic and aerobic treatment, the GABA content in green tea is significantly increased, reaching the standard of GABA tea. And daily oral GABA green tea extract can prevent depression or improve the depressive state of animals.

3319

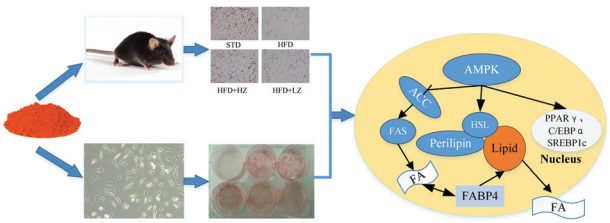


Anti-tumor bioactivities of curcumin on mice loaded with gastric carcinoma

Xiao-Ping Wang,* Qiao-Xia Wang, Huan-Ping Lin and Na Chang

Curcumin, a derivative from the dried rhizome of *curcuma longa*, has been proven to possess anti-tumor effects.

3327



Anti-obesity effects of zeaxanthin on 3T3-L1 preadipocyte and high fat induced obese mice

Meihong Liu, Huimin Liu, Jiahan Xie, Qian Xu, Cong Pan, Jiaojiao Wang, Xi Wu, Sanabil, Mingzhu Zheng and Jingsheng Liu*

Zeaxanthin inhibited lipogenesis in adipocytes and attenuated progression of obesity in mice by inducing AMPK activation and suppressing adipocyte-specific factors.

This journal is © The Royal Society of Chemistry 2017

Published on 20 September 2017. Downloaded on 3/5/2024 12:24:02 AM.

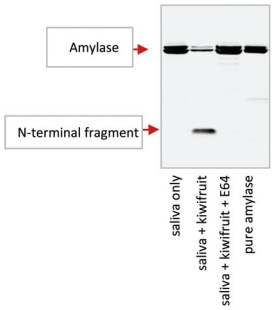
PAPERS

3339

Kiwifruit actinidin digests salivary amylase but not gastric lipase

Harry Martin,* Sarah B. Cordiner and Tony K. McGhie

Kiwifruit actinidin rapidly digests human salivary amylase: will this lower the glycaemic index when starch and kiwifruit are consumed together?

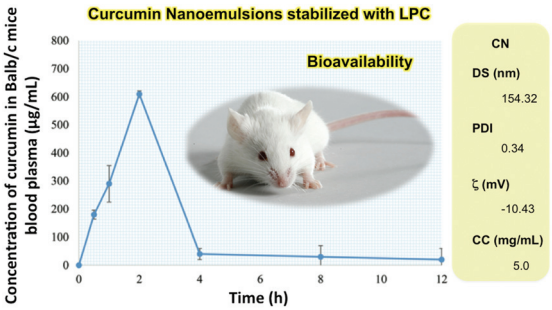


3346

Preparation, characterization and bioavailability by oral administration of O/W curcumin nanoemulsions stabilized with lysophosphatidylcholine

Rubi Chávez-Zamudio, Angélica A. Ochoa-Flores, Ida Soto-Rodríguez, Rebeca Garcia-Varela and Hugo Sergio García*

Curcumin has low solubility in aqueous media. In our study, O/W nanoemulsions of curcumin were prepared using lysophosphatidylcholine, to increase its bioavailability when administered orally.

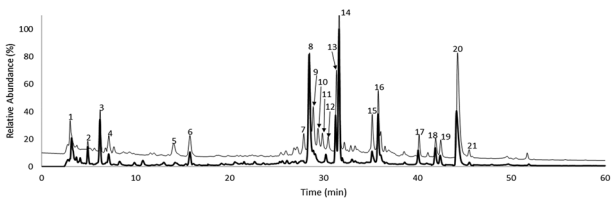


3355

Antioxidant and anti-inflammatory activities of *Geranium robertianum* L. decoctions

Marcelo D. Catarino, Artur M. S. Silva, Maria Teresa Cruz and Susana M. Cardoso*

The phenolic profile of *Geranium robertianum* L. decoctions as well as their antioxidant and anti-inflammatory activities were investigated.

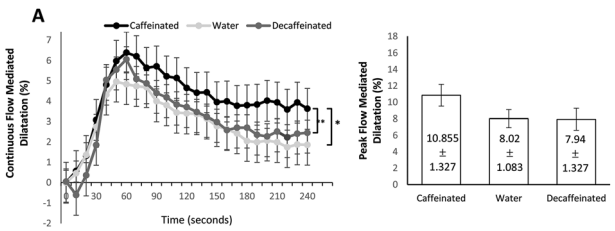


3366

The acute effect of coffee on endothelial function and glucose metabolism following a glucose load in healthy human volunteers

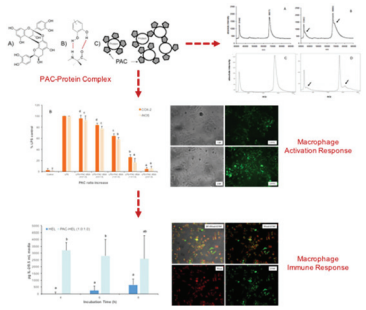
Evan A. J. Boon, Kevin D. Croft, Sujata Shinde, Jonathan M. Hodgson and Natalie C. Ward*

The consumption of coffee, as a whole beverage, may improve vascular function, although this may be due to the caffeine.



PAPERS

3374

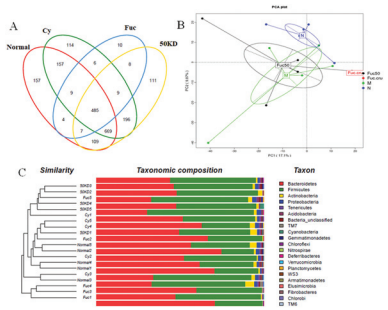


Cranberry Proanthocyanidins – Protein complexes for macrophage activation

Sergio M. Carballo, Linda Haas, Christian G. Krueger and Jess D. Reed*

In this work we characterize the interaction of cranberry (*Vaccinium macrocarpon*) proanthocyanidins (PAC) with bovine serum albumin (BSA) and hen egg-white lysozyme (HEL) and determine the effects of these complexes on macrophage activation and antigen presentation.

3383



Dietary fucoidan of *Acaudina molpadioides* alters gut microbiota and mitigates intestinal mucosal injury induced by cyclophosphamide

Hongjie Shi, Yaoguang Chang, Yuan Gao, Xiong Wang, Xin Chen, Yuming Wang, Changhu Xue and Qingjuan Tang*

Cyclophosphamide (cy) is a widely used cancer drug.

Published on 20 September 2017. Downloaded on 3/5/2024 12:24:02 AM.

This journal is © The Royal Society of Chemistry 2017

Food & Function

PAPER

Check for updates

Cite this: *Food Funct.*, 2017, **8**, 3311

Quality components and antidepressant-like effects of GABA green tea

Jie Teng,†[a] Wen Zhou,†[b] Zhen Zeng,[a] Wenfang Zhao,[a] Yahui Huang *‡[a] and Xu Zhang*‡[c]

Received 14th July 2017,
Accepted 10th August 2017

DOI: 10.1039/c7fo01045a

rsc.li/food-function

Gamma (γ)-aminobutyric acid (GABA) green tea, with high GABA content, is a kind of special green tea. The goals of this study are to analyze the changes in quality components of green tea during anaerobic treatment, and to investigate whether or not the extract of GABA present in green tea can prevent depression or improve the depressive state of animals. Results showed that GABA content in green tea had increased significantly after anaerobic treatment. The contents of tea polysaccharides, total free amino acids, and water extracts were also increased whereas tea polyphenols were reduced. More importantly, the extract of GABA green tea could alleviate mouse depression and stress from desperate environments through the forced swim test (FST), tail suspension test (TST), mRNA and protein expression levels of $GABA_A$ receptors. Therefore, these results indicate that GABA green tea may have a health effect on prevention and alleviation of depression, and it works on the GABAergic neurotransmission of mouse cerebral cortex *via* up-regulating expression of the $GABA_A$ receptor α1 subunit, thus ameliorating depression.

1 Introduction

As the pace of life becomes faster and work pressure gets heavier, the problem of depressive disorders has shown an upward trend year by year, until it has become one of the main diseases that threaten people's health and influences the quality of people's lives. There is no doubt that depression is a common and frequently occurring psychiatric disorder worldwide and threatens human health. A study has shown that more than 17% of worldwide population suffers from depression in their lives.[1] Depressive disorders are characterized by psychological and behavioral alterations, including insomnia, suicidal behavior, feelings of hopelessness and guilt, and cognitive changes.[2] However, the exact mechanisms underlying depression development are still elusive.[3] Numerous anti-depressant compounds are available and they presumably act *via* different mechanisms, including through serotonergic, noradrenergic, and/or dopaminergic systems.[4,5] Although antidepressants have been clinically available for several decades, most of them are not completely effective; only 33% of depressed patients are sensitive to the first antidepressant medication, and many are associated with serious adverse effects.[6] Currently, increased attention is being paid to research on plant-derived natural products in China and other countries.[7] It is of great significance to search for new natural products for the prevention and/or treatment of depression.

The compound γ-aminobutyric acid (GABA), a non-proteinous amino acid, is the predominant inhibitory neurotransmitter in the central nervous system (CNS)[8–10] and it is widely distributed among organisms from bacteria to plants and vertebrates.[11–13] GABA mediates the function of nerve conduction in about 30%–40% of the central neurons, and exerts crucial influence on physiological activities such as analgesia, sedation, hypnosis, and anti-convulsion,[14,15] mainly *via* its interactions with the $GABA_A$ receptor, $GABA_B$ receptor, and $GABA_C$ receptor.[16] However, the γ-aminobutyric acid class A ($GABA_A$) receptor is the most important among these three subtypes, because it acts as the target of neurologically active drugs such as sedatives lorazepam, barbiturates, and picrotoxinism. $GABA_A$ receptor dysfunction is closely related to neurological and psychiatric disorders such as depression, insomnia, anxiety, epilepsy, *etc.*[17,18] $GABA_A$ receptor is a macromolecule glycoprotein consisting of GABA recognition sites, benzodiazepine (BDZ) recognition sites, and Cl^- channels. These three components are able to produce allosteric interactions.[16,19]

As a natural and safe drink, tea is one of the most popular beverages consumed around the world, and has been widely

[a]*Department of Tea Sciences, College of Horticulture, South China Agricultural University, Guangzhou, People's Republic of China. E-mail: 13501513191@163.com; Fax: +86(020)85280228; Tel: +86(020)38297601*
[b]*School of Chinese Meterla Medica, Guangzhou University of Chinese Medicine, Guangzhou, People's Republic of China*
[c]*Guangdong Key laboratory for innovative Development and Utilization of Forest Plant Germplasm, College of Forestry and Landscape Architecture, South China Agricultural University, Guangzhou, People's Republic of China. E-mail: zhangxu919@hotmail.com*
† Both authors contributed equally to the work.
‡ These two authors share senior authorship.

studied in the functional drink and health product fields.[20] Tea, especially green tea, contains many bioactive components, such as polyphenols, amino acids, polysaccharides, purine alkaloids, *etc*. They exhibit physiological and pharmacological properties responsible for neuroprotective, anti-inflammatory, anti-radiation, antioxidant, antihypertensive, and hypoglycemic activities.[21–23] In tea, the amount of GABA can be increased by vacuum anaerobic and aerobic treatment,[10,24] and GABA content has been significantly increased, reaching the standard of GABA tea which is higher than 1.50 mg g^{-1}.[25] In our previous studies, we focused on researching GABA tea, including GABA Maoyecha tea, GABA black tea, and GABA green tea. We conducted a number of system-related researches on its processing and making, sleep-promoting effect, and quality components, and have gained remarkable achievements.[10,24,26] Among them, there are some identical action principles between anti-depression and promoting sleep, which have the effect of calming and nerve protection. With the discoveries of many of its beneficial physiological functions in GABA, a number of antidepressant studies have been conducted on GABA-containing foods.[3,7,27] However, there have been no holistic studies on the prevention of depression and biochemical components. Thus, in this study, we compared biochemical characteristics and qualities between two different green teas after repeated anaerobic treatment to investigate whether or not the extract of GABA green tea has any antidepressant-like effect. We also evaluated preventive effects of GABA green tea in anti-depression or improvement of the depressive state through conducting behavioral tests in mice, including the forced swimming test (FST), tail suspension test (TST), and by examining the expression levels of anti-depression-related genes and proteins of the ionotropic $GABA_A$ receptor.

2 Materials and methods

2.1 Plant materials

Fresh leaves of Mingfeng tea (*C. sinensis*), consisting mainly of two leaves and a bud, were harvested in Changsha, China in April 2015. These tea leaves were randomly divided into two parts, one for green tea and another for GABA green tea. The green tea was manufactured with a microwave technology; after being harvested, fresh leaves were fixed, rolled and dried at 110 °C until they were adequately dried. For GABA green tea, all the young leaves were packed into a bag, placed under vacuum for 3 h, and then removed under aerobic conditions for 2 h. These two steps were repeated three times, respectively, followed by microwave fixation, rolled and dried at 110 °C until they were adequately dried.[10]

2.2 Chemicals and drugs

GABA, caffeine, and theanine (purity > 99%) were purchased from Sigma-Aldrich Chemical (St Louise, MO, USA). Methanol and acetonitrile (HPLC grade) obtained from Tianjin Kemiou Chemical Reagent Co., Ltd (Tianjin, China) were used as solvents. Clomipramine hydrochloride tablets and GABA drugs (GD) were purchased from Beijing Novartis Pharmaceutical Co., Ltd (Beijing, China). RNase-free DNase I and PrimeScript™ RT reagent Kits were purchased from TaKaRa Bio., Co., Ltd (Dalian, China). All the other chemicals and reagents used were of the highest grade available.

2.3 Tea extract and analysis of quality components

Accurately weighed 3.0 g of tea powder was extracted with 500 mL of distilled water at 100 °C for 45 min with shaking and the extracts were filtered through filter paper. The residues were re-extracted once as described above. Supernatants of the extracted solutions were combined and used for the analysis of compounds. Contents of tea polyphenols were measured with a ferrous tartrate method at 540 nm with a spectrophotometer as described previously.[28] The water extracts were determined with an oven drying method.[10] Anthocyanin content was measured as described previously.[29] For measurements of total free amino acids, a ninhydrin colorimetric method was used; absorption values of the solutions at 570 nm were determined using a spectrophotometer.[28] Free amino acids were determined by an amino acid analyzer according to the general principles of the amino acid analysis method.[30] Contents of tea polysaccharides were measured with the anthrone method at 620 nm with a spectrophotometer as described previously.[28] All the assay methods mentioned above were based on the National Standard of the People's Republic of China. The obtained supernatants were filtered through a 0.22 μm membrane before HPLC analysis.

Contents of GABA, theanine, and caffeine were determined by high performance liquid chromatography (HPLC) with slight modifications, respectively.[31–33] GABA was derivatized by *ortho*-phthalaldehyde (OPA), and used for detection of GABA with HPLC. The derivative was detected with a fluorometric detector (RF-530, Ex 348 nm, Em 450 nm). Mobile phase was 0.2 mol L^{-1} sodium citrate buffer, pH 3.2–10.0, and gradient elute at a flow rate of 0.3 mL min^{-1}, 55 °C column temperature, and injection volume was 5 μL. GABA identification was performed *via* elution time of the obtained derivative and compared to a standard substance submitted to derivation in identical test conditions. Theanine content was analyzed on an Agilent Eclipse XDB-C18 column (4.6 × 150 mm, 5 μm) using an Agilent LC-1200; the wavelength was monitored at 199 nm with a 25 °C column temperature. The mobile phase consisted of 0.05% (v/v) trifluoroacetic acid (A) in water, 100% acetonitrile (B), and the gradient elution was as follows: B 33% from 0 to 14 min, to 5% at 20 min. The solvent flow rate was 1.0 mL min^{-1}, and injection volume was 10 μL. Caffeine content was analyzed on an Agilent Eclipse XDB-C18 column (4.6 × 150 mm, 5 μm) using the Agilent LC-1200. The wavelength was monitored at 230 nm with a 37 °C column temperature and mobile phase A (water) and mobile phase B (methanol). The constant gradient of mobile phase B was kept 10% for 60 min. The solvent flow rate was 1.0 mL min^{-1}, and injection volume was 10 μL. All samples were analyzed in triplicate.

 This journal is © The Royal Society of Chemistry 2017

2.4 Animals

Both male and female KM mice (20 ± 2 g; Laboratory Animal Center of Guangzhou University of Chinese Medicine, Guangdong Province, China) were used. The mice were housed individually in cages for 3 days to adapt to the environment under the following controlled conditions: 25 ± 2 °C under a 12 h light/dark cycle and 60 ± 5% humidity with free access to water and food pellets. Each mouse was used only once. Behavioral testing was performed between 7:00 and 12:00 AM. All the procedures were conducted according to the National Institutes of Health Guide for the Care and Use of Laboratory Animals, and the animal handling and experimental procedures were approved by the Local Animal Use Committee (SCXK 2013-0020).

2.5 Measurement of depressive-like behaviors

The test was performed in six groups of fifteen mice each. The mice received orally once daily various doses of the extract of GABA green tea at 0.83 g kg^{-1}, 1.67 g kg^{-1}, and 3.33 g kg^{-1} or positive reference clomipramine hydrochloride tablets (2 mg kg^{-1}) for 15 consecutive days. Control mice were tested in parallel with the animals receiving saline only; the mice in last group were given green tea extract (3.33 g kg^{-1}). Animal behavior was assessed 45 min after administration of the final dose.

2.5.1 Forced swimming test (FST). The FST is one of the most common animal models used for examination of depressive-like behaviors. The test was conducted as previously described[34] with slight modifications. Mice were individually inserted in an open cylinder container (10 cm diameter and 25 cm height) containing 19 cm of water at 24 ± 2 °C. Each mouse was judged to be immobile when it ceased struggling and remained floating motionless in the water, making only small movements necessary to keep its head above water. The duration of immobility was recorded during the last 5 min of the 7 min testing period.

2.5.2 Tail suspension test (TST). The TST is another common model used for examination of depressive-like behaviors.[35] The tails of mice were taped in a balance bracket at a distance of 2 cm from the tail tip, with tail straight and head hung down 15 cm above the desktop after 45 min from the last administration. The mice were separated by cardboard just in the case they interfered with each other. Each mouse was treated for 7 min; the first 2 min was for adaptation. The immobility time (no body movement except respiration) in the last 5 min was recorded.

2.6 Collection of brain tissue and quantitative analysis of GABA in mouse brain

At the end of the experimental period the animals were fasted overnight before sacrifice and the cerebral cortex was taken out in an ice bath. Cerebral cortex was homogenized in 80% ice-cold acidic ethanol after being weighed within one minute. The ratio of cortex to acidic ethanol was 1 : 15 and 5 mL of homogenate was stored at 4 °C for 1 h and then centrifuged at 3000*g* at 4 °C for 20 min. After that, $CHCl_3$ was added into the collected supernatant and centrifuged for 20 min under the same conditions. The upper water phase was derivatized by *ortho*-phthalaldehyde (OPA), and used for detection of GABA with HPLC. The derivative was detected with a fluorometric detector (RF-530, Ex 348 nm, Em 450 nm). Mobile phase was 0.2 mol L^{-1} sodium citrate buffer, pH 3.2–10.0, and gradient elute at a flow rate of 0.3 mL min^{-1}, 55 °C column temperature, and injection volume was 5 μL. GABA identification was performed *via* elution time of the obtained derivative and compared to a standard substance submitted to derivation in identical test conditions.

2.7 Gene and protein expression levels of $GABA_A$ receptor

Mice in six groups were first treated as described in section 2.5. GABA solution (GS, 10 mg kg^{-1}) was used as a positive control. At the end of the experimental period, the mice were decapitated and their cerebral cortex tissues were taken in an ice bath.

2.7.1 Preparation of tissue homogenate. The whole brain tissue of each animal was homogenized in 10 volumes (% w/v) of phosphate buffer saline (PBS) (100 mM, pH 7.4) containing 1 mM ethylenediaminetetraacetic acid (EDTA) and centrifuged at 12 000*g*, at 4 °C for 30 min. The supernatant was collected and used for molecular analysis.

2.7.2 Total RNA extraction. Total RNA was extracted using TRIzol reagent (Invitrogen, Carlsbad, CA, USA) according to the manufacturer's instructions. Cortex tissue was thoroughly homogenized with a homogenizer in polypropylene tubes. The RNA precipitate was washed twice by gentle vortexing with 70% ethanol, collected by centrifugation at 12 000*g* for 5 min, dried under vacuum for 8 min, dissolved in 50 μL of diethylpyrocarbonate (DECP)-treated water, and incubated for 15 min at 60 °C. The RNA was quantified and checked for purity and condition by a ND-1000 K2800 UV-vis spectrophotometer (Beijing Kaiao Technology Ltd, China) at a wavelength of 260 nm. The extract integrity was assessed by 1.2% agarose gel electrophoresis and the gel was stained with ethidium bromide, visualized under UV light, and recorded by photography.

2.7.3 Reverse transcription and real-time quantitative PCR. A total of 1.5 μg RNA was reverse transcribed using RNase-free DNase I (TaKaRa, Dalian, China). First-strand cDNA was synthesized using a PrimeScript™ RT reagent Kit with gDNA Eraser (TaKaRa, Dalian, China) according to the manufacturer's instructions. Oligonucleotide primers targeting the *Mus musculus* gene sequence (http://www.ncbi.nlm.nih.gov/pubmed/) were designed for the β-actin, $GABA_A$ αl, and $GABA_A$ α5 genes using Primer 5 software (Premier Co., Canada). Primers were as follows: rat β-actin forward primer: GGCTGTCTTCCCCTCCATCG, reverse primer: CAGGATGCCTCTCTTGCTCTGG; rat $GABA_A$ αl forward primer: CATGAGGGAT CTCCACTTTTAGC, reverse primer: AGGGCAGCAGTGAAGTTATGAG; rat $GABA_A$ α5 forward primer: GGT TCATTGCTGTCTGCTATGC, and reverse primer: TTTGGGATGTTTGGAGGATGGG. The protocol used was a 95 °C for 10 min holding time that was followed by 45 cycles of 95 °C for 30 s and 60 °C for 34 s for amplification and quantification. For determi-

nation of the melting curve, the temperature was increased from 60 °C to 95 °C at a rate of 1 °C within each 60 s. At the end of real-time PCR, the threshold cycle (CT) value of each reaction was determined. The relative expression fold was calculated by the following formula: Relative mRNA level of target gene (fold of control) = 2 − (ΔΔCT), where ΔΔCT = (CT Target − CT β-actin) treatment − (CT Target − CT β-actin) control. All qRT-PCR analyses were performed with three biological and three technical replications.

2.7.4 Western blotting. Cerebral cortex was homogenized in ice-cold lysis buffer and proteins were extracted. Protein concentration of tissue extracts was determined by the Bradford method (Bio-Rad, USA). Samples were incubated in boiling water for 8 min and centrifuged at 10 000*g* for 8 min. Then 15 μg of protein samples was separated by reducing 10% sodium dodecyl sulfate-polyacrylamide gel electrophoresis (SDS-PAGE) electrophoresis at 70 V for 30 min and then at 120 V for 60 min. After electrophoresis, proteins were transferred to a 0.45 μm polyvinylidene fluoride membrane (PVDF) with a transfer apparatus (Bio-Rad, USA). After the transfer, membranes were blocked with 5% non-fat milk in Tris-Tween buffered saline (20 mM Tris, pH 7.5, 150 mM NaCl, and 0.1% Tween-20, TBST) for 2 h. Membranes were incubated overnight at 4 °C with antibodies diluted in TBST as follows: $GABA_A$ α1 (1 : 1000), $GABA_A$ α5 (1 : 1000) and β-actin (1 : 2000). Horseradish peroxidase (Sigma-Aldrich, USA) conjugated secondary antibodies were subsequently incubated for 1 hour at room temperature. The membranes were washed 5 times in TBST buffer. Finally, the PVDF membrane was immersed in solution with mixed ECL fluorescent substrate solution for 30 min. Liquids in the PVDF surface were removed with a filter paper, and the membrane was covered with medical X-ray film and placed in a dark room. After being exposed for 1 min it was developed, fixed, scanned into images, and normalized to β-actin as an internal control for total protein loading.

2.8 Statistical analysis

All data were subjected to analysis of variance using SPSS (19.0, SPSS Inc., Chicago, IL, USA). Data were expressed as mean ± standard deviation (SD) per group. The statistical analyses were performed using one-way analysis of variance (ANOVA), followed by least significant difference (LSD) test and Duncan's test. $P < 0.05$ was considered statistically significant.

3 Results

3.1 Biochemical compositions of green tea and GABA green tea

Variations in the quality components of green tea processed with or without repeated anaerobic and aerobic treatment are presented in Table 1. In untreated tea (green tea), the contents of water extracts, tea polyphenols, tea polysaccharides, total free amino acids, anthocyanins, and caffeine were 35.75%, 26.99%, 2.58%, 2.57%, 0.42%, and 2.48%, respectively. After anaerobic and aerobic treatment (GABA green tea), the contents of water extracts, tea polysaccharides, and total free amino acids were significantly increased ($P < 0.05$), but content of tea polyphenols was reduced from oxidation and mutual transformation of catechins.[10,24] The average contents of anthocyanins and caffeine were not changed. Under anaerobic conditions, non-proteinous amino acids in GABA green tea were significantly increased ($P < 0.01$), and the contents of GABA and theanine reached 2.33 mg g^{-1} and 2.76 mg g^{-1}, respectively. After anaerobic treatment, GABA content in green tea was higher than the standard of GABA tea at 1.50 mg g^{-1},[36] and higher than that of green tea (0.13 mg g^{-1}). We also found a similar correlation between the content of amino acids and GABA, which is an increasing trend in GABA green tea. For amino acid monomers, the amounts of Pro, His, Val, Gly, Ser, Lys, Ile, Tyr, Phe, Ala, and Thr were significantly increased ($P < 0.01$) whereas those of Asp and Glu were reduced, the amounts of Arg and Met were unchanged.

Table 1 Variations in the contents of quality components in green tea and GABA green tea

	Green tea	GABA green tea
Routine bioactive components (%)		
Water extracts	35.75 ± 1.26[b]	37.21 ± 1.72[a]
Tea polyphenols	26.99 ± 1.73[a]	25.04 ± 1.89[b]
Tea polysaccharides	2.58 ± 0.25[b]	3.25 ± 0.26[a]
Total free amino acids	2.57 ± 0.15[b]	3.41 ± 0.17[a]
Anthocyanins	0.42 ± 0.01[a]	0.41 ± 0.01[a]
Caffeine	2.48 ± 0.24[a]	2.50 ± 0.23[a]
Non-proteinous amino acids (mg g^{-1})		
GABA	0.13 ± 0.02[b]	2.33 ± 0.05[a]
Theanine	2.22 ± 0.13[b]	2.76 ± 0.14[a]
Proteinous amino acids (mg g^{-1})		
Glu	1.49 ± 0.07[a]	0.73 ± 0.04[b]
Asp	0.65 ± 0.04[a]	0.37 ± 0.03[b]
Pro	2.04 ± 0.05[b]	6.23 ± 0.08[a]
Arg	0.23 ± 0.01[a]	0.24 ± 0.01[a]
His	0.10 ± 0.01[a]	0.13 ± 0.02[a]
Met	0.02 ± 0.00[a]	0.02 ± 0.00[a]
Val	0.63 ± 0.42[b]	0.81 ± 0.03[a]
Gly	0.04 ± 0.00[b]	0.20 ± 0.01[a]
Ser	0.01 ± 0.00[b]	0.17 ± 0.02[a]
Lys	0.05 ± 0.01[b]	0.20 ± 0.02[a]
Ile	0.05 ± 0.01[b]	0.28 ± 0.01[a]
Tyr	0.07 ± 0.01[b]	0.33 ± 0.03[a]
Phe	0.04 ± 0.00[b]	0.10 ± 0.00[a]
Ala	0.16 ± 0.01[b]	0.24 ± 0.02[a]
Thr	0.19 ± 0.02[b]	0.23 ± 0.02[a]

[a,b]The means in each row followed by the same letter are not significantly different at the 5% level. Each value is expressed as mean ± standard deviation (n = 3), and all values on dry weight basis. Abbreviations: Asp, aspartate; GABA, gramma-aminobutyric acid; Glu, glutamic acid; Gly, glycine; His, histidine; Ile, isoleucine; Lys, lysine; Met, methionine; Phe, phenyalanine; Pro, proline; Ser, serine; Thr, threonine; Tyr, tyrosine; Val, valine.

3.2 Effect of GABA green tea in the forced swimming test

FST is an important model of depressive-like behavior, registered for the immobility periods of the test (Fig. 1A) show statistically significant differences ($P < 0.05$) between NC and PC, confirming that this behavioral test is useful for studying antidepression. Compared with the NC and green tea group, all doses of the extract of GABA green tea (0.83 g kg^{-1}, 1.67 g kg^{-1},

 This journal is © The Royal Society of Chemistry 2017

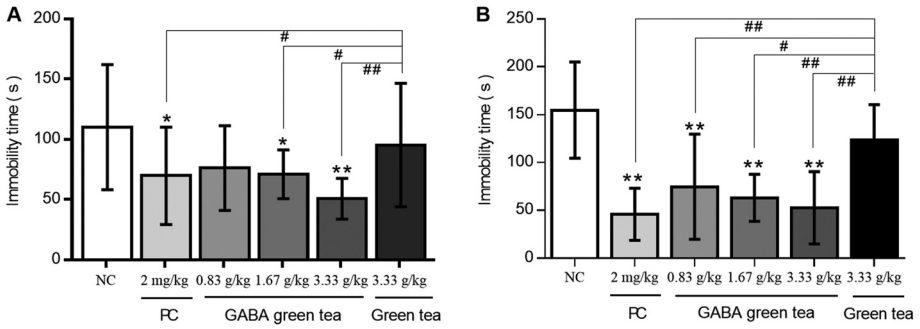


Fig. 1 Effects of GABA green tea on the immobility duration of mice in the behavioral test. (A) The forced swimming test, and (B) the tail suspension test. Data are expressed as mean ± SD (n = 15 mice per group). NC, normal control group; PC, clomipramine hydrochloride tablets group. *P < 0.05, **P < 0.01 as compared with the NC. $^{\#}P$ < 0.05, $^{\#\#}P$ < 0.01 as compared with the green tea.

and 3.33 g kg^{-1}) significantly reduced immobility duration (P < 0.05, P < 0.01). Immobility duration was significantly prolonged in the higher dose of GABA green tea extract-treated groups (3.33 g kg^{-1}) as compared with that in the NC and was close to that of the PC.

3.3 Effect of GABA green tea in the tail suspension test

As shown in Fig. 1B, no significant difference in immobility duration was detected between the NC and green tea group (P > 0.05). However, oral administration of mice with GABA green tea extract at doses of 1.67 g kg^{-1} and 3.33 g kg^{-1} significantly reduced immobility duration as compared to those of the green tea group and NC group (P < 0.05, P < 0.01). The immobility times of mice receiving the extract of GABA green tea at doses of 0.83 g kg^{-1}, 1.67 g kg^{-1}and 3.33 g kg^{-1} were 76.17 s, 70.92 s, and 50.58 s, respectively. It is worth noting that the doses of GABA green tea may be commensurate with the effect of anti-depression.

3.4 GABA content of mouse brain tissue

The results reported in Fig. 2 showed that there are no remarkable differences in GABA content in brain tissues between NC, PC, and green tea groups, and GABA content stayed at a relatively low level (352.12–364.46 μg g^{-1}). Although behavioral testing (Fig. 1) of PC showed that the anti-depressant effects were significant (P < 0.05, P < 0.01), the effect of PC was irrelevant with GABA content in mouse brain tissue. The GABA content in mouse brain was highly increased after being treated with GABA green tea extract. The effects were highly significant (P < 0.01) in the high dose group and significant (P < 0.05) in the medium dose group. They showed that GABA content in mouse brain tissue and GABA intake were positively correlated and were also positively correlated with behavioral testing. These findings suggested that anti-depressant effects of GABA green tea might be associated with the increase in GABA concentration in mouse brain tissue.

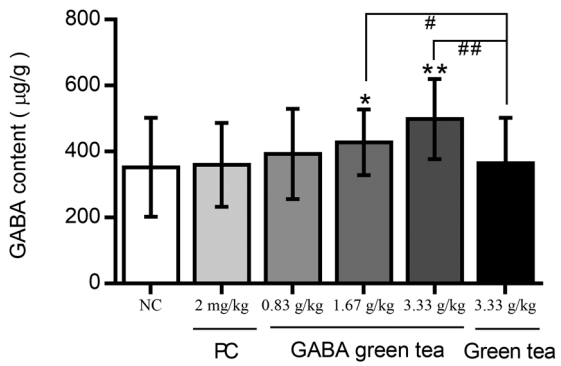


Fig. 2 GABA content of mouse brain tissue. Data are expressed as mean ± SD (n = 15 mice per group). NC, normal control group; PC, clomipramine hydrochloride tablets group. *P < 0.05, **P < 0.01 as compared with the NC. $^{\#}P$ < 0.05, $^{\#\#}P$ < 0.01 as compared with the green tea.

3.5 Effect of GABA green tea on mRNA expression of $GABA_A$ receptor αl and α5 subunits

Since antidepressant effects from the positive drug (clomipramine hydrochloride tablets) did not cause an increase of GABA content in brain tissue of experimental rats, we used GABA drugs (GD) as a positive control group to observe the genes and protein expression of the $GABA_A$ receptor, in order to explore in depth the relationship between the depression assays and GABA contents. The mRNA expression levels of $GABA_A$ receptor αl and α5 subunits of in cerebral cortex tissues of mice treated with different doses of GABA green tea extract were examined. Levels of target gene mRNA had been normalized with β-actin (Table 2). Compared with those of NC or green tea groups, the GABA drug group (10 mg kg^{-1}), a drug that works as a positive control for anti-depression, the mRNA expression levels of $GABA_A$ receptor αl and α5 subunits were significantly increased (P < 0.01). The GABA green tea extracts at 0.83 g kg^{-1}, 1.67 g kg^{-1}, and 3.33 g kg^{-1} enhanced the mRNA expression of $GABA_A$ receptor αl and α5 subunits in mice in a dose-dependent manner. Effects of the extract at 3.33 g kg^{-1} on mRNA expression level of $GABA_A$ receptor αl and α5 subunits were increased significantly (P < 0.01) by 64.19% and 52.47%, respectively, which were comparable with those in mice treated with GABA drug (GD). The extract of GABA green tea extract at 1.67 g kg^{-1} also significantly

Table 2 Effect of GABA green tea on mRNA expression levels of $GABA_A$ receptor αl and α5 subunits

	$GABA_A$ αl	$GABA_A$ α5
NC	1.63 ± 0.47^{Bc}	0.73 ± 0.20^{Cc}
GS (10 mg kg^{-1})	24.52 ± 2.76^{Aa}	25.92 ± 3.44^{Aa}
GGT (0.83 g kg^{-1})	4.43 ± 1.86^{Bbc}	1.39 ± 0.34^{Cc}
GGT (1.67 g kg^{-1})	8.97 ± 1.26^{Bb}	5.56 ± 0.91^{Cc}
GGT (3.33 g kg^{-1})	15.74 ± 2.35^{Bb}	13.60 ± 1.63^{Bb}
GT (3.33 g kg^{-1})	1.85 ± 0.72^{Bc}	0.91 ± 0.39^{Cc}

Each value is expressed as mean ± standard deviation, (n = 15 mice per group). GABA, gamma-aminobutyric acid; NC, normal control; GS, GABA solution; GGT, GABA green tea extract; GT, green tea extract. Different capital letters in same column data have highly significant differences ($P < 0.01$), different small letters mean significant differences ($P < 0.05$).

increased mRNA expression levels of $GABA_A$ receptor αl and α5 subunits ($P < 0.05$). The mRNA expression levels of $GABA_A$ receptor αl and α5 subunits of mice treated with 0.83 g kg^{-1} GABA green tea also up-regulated relatively, but did not reach a statistical significance ($P > 0.05$). By contrast, at the same concentration, the mRNA expression levels of $GABA_A$ receptor αl subunits exceed those of the α5 subunits.

3.6 Effect of GABA tea on protein expression levels of $GABA_A$ receptor α1 and α5 subunits

Effects of oral treatment of mice with extracts of GABA green tea on the protein expression levels of $GABA_A$ receptor α1 and α5 in cerebral cortex tissues of their brain are presented in Fig. 3. It can be seen that protein levels varied between $GABA_A$ receptor αl and α5 subunits treated at the same concentration of GABA solution (GS). With extracts of GABA green tea in the 1.67 g kg^{-1} and 3.33 g kg^{-1} groups, the protein expression levels of $GABA_A$ receptor α1 were higher than those of $GABA_A$ receptor α5 subunit. Their protein levels are displayed by a grayscale ratio of targeted band to β-actin. Fig. 3A shows that protein levels of $GABA_A$ receptor α1 in all groups are significantly higher than those in the NC and green tea group ($P < 0.01$) except for the low dose GABA green tea group (0.83 g kg^{-1}), suggesting that the effect of GABA tea extract is positively correlated with the doses of GABA. The protein expression levels of $GABA_A$ receptor α5 in all groups were increased extremely significantly as compared with those of the NC and green tea group ($P < 0.01$) except for the high dose GABA tea group (Fig. 3B). In the extract of GABA green tea at 3.33 g kg^{-1}, the protein expression levels were significantly lower, and the ratio was 45.68%, which was comparable with that in mice treated with GABA drugs. It is noteworthy that the doses of GABA green tea may not be commensurate with the effect of promoting protein expression of $GABA_A$ receptor α5. Protein expression levels of $GABA_A$ receptor α1 and α5 subunits in GS group were the highest. Yet low dose GABA green tea extract (0.83 g kg^{-1}) protein expression in α1 subunits minimum value, relative to expression of α5 subunit minimum value were in the high dose GABA green tea extract (3.33 g kg^{-1}). In conclusion, protein expression levels of $GABA_A$ receptor α1 and α5 subunits in the cerebral cortex were changed after treatments of GS and GABA green tea extract, but GABA green tea extract exerted a prompting effect on the expression of $GABA_A$ receptor α1 subunit.

4 Discussion

During processing of green tea, the anaerobic and aerobic treatment of tea fresh leaves were repeated, and both green tea and GABA green tea were found to have quite different qualitative and quantitative compositions. Strikingly, after alternative sequences of anaerobic and aerobic treatment, the GABA content in GABA green tea was increased up to 2.33 mg g^{-1}, which was higher than the standard of GABA tea (1.50 mg g^{-1}) and also higher than that of green tea (0.13 mg g^{-1}) and that of a previously reported GABA tea.[27,37] In general, when the

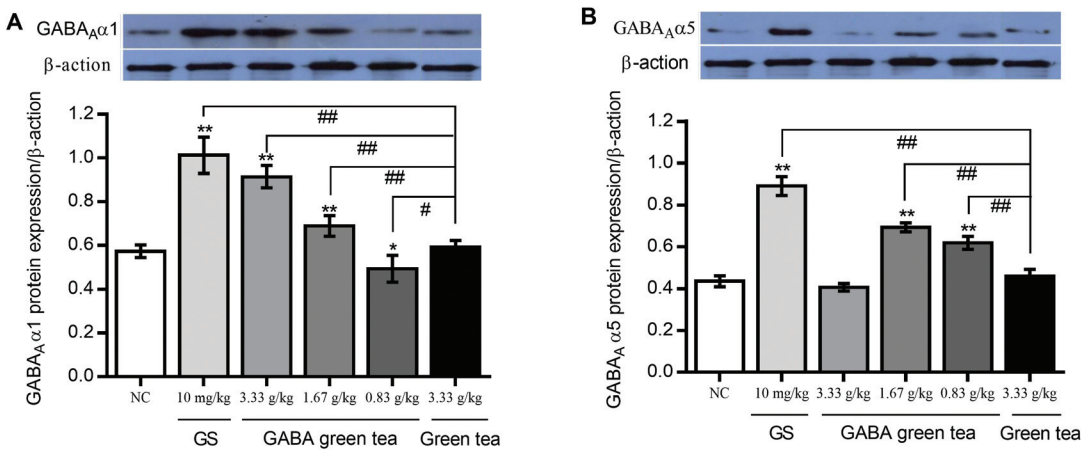


Fig. 3 Effect of GABA green tea on protein expression level of $GABA_A$ receptor (A) α1 subunit and (B) α5 subunit. Data are expressed as mean ± SD. (n = 15 mice per group). NC, normal control group; GS, GABA solution group. $^{*}P < 0.05$, $^{**}P < 0.01$ as compared with the NC. $^{\#}P < 0.05$, $^{\#\#}P < 0.01$ as compared with the green tea.

 This journal is © The Royal Society of Chemistry 2017

plants are suffering stress from hypoxia, strong acid, low temperature, high temperature, drought, and/or pest infestation, glutamate (Glu) in plants is irreversibly transformed by glutamate decarboxylase (GAD) to form GABA, and the decarboxylation of Glu in the cytoplasm and exchange of the reaction product GABA with extracellular Glu take place.[38] The amounts of water extracts, tea polysaccharide, total free amino acids, and theanine were increased significantly whereas the amount of tea polyphenols was reduced. We speculated that under the condition of repeated anaerobic and aerobic treatment, fresh tea leaves were adversity stressed, catechins in tea polyphenols were oxidized, and polymerization reactions occurred, resulting in a decrease of tea polyphenols content. The increase in tea polysaccharide content may be related to the reason that excised tea leaves try to maintain their respiration and polysaccharide substances are degraded, leading to the formation of monosaccharide or other soluble saccharides. Under adverse conditions, the degradation reaction is more violent. Moreover, due to the replacement of the Krebs cycle with glycolysis reactions, the energy process needed for protein biosynthesis of excised fresh tea leaves conflicts with the dramatic decline of ATP production rate. As a result, the total amount of free amino acids produced by protein degradation was increased.

$GABA_A$ receptor is a macromolecule glycoprotein consisting of γ-aminobutyric acid recognition sites, benzodiazepine (BDZ) recognition sites, and chloride ion channels. These three components are able to produce allosteric interactions. At present, pharmacological researches on $GABA_A$ receptor have been focused on the BDZ receptor recognition sites. During the process of $GABA_A$ receptor complexes synthesis and functioning, $GABA_A$ receptor subunits transform at any time, and the α type subunit determines its affinity and efficacy. Pharmacological studies on recombinant receptors have shown that α subunits had the greatest impact on the affinity of recombinant BDZ receptor ligands, which was also the basis of classification of BDZ receptors.[16] The molecular mechanism of BDZ recognizing sites is generally considered to conjugate specific recognition sites on the $GABA_A$ receptor and enhance effects of the inhibitory neurotransmitter GABA.[39] Sedation is a primary feature of many binding sites of BDZ ligands, which are thought to be mediated by the α1 receptor. $GABA_A$ receptors containing α5 subunits are the most important receptors outside synapses, and participate in regulation of tension conductance of central neurons, and also in regulation of neuronal excitability and information processing.[40] Therefore, $GABA_A$ α1 and α5 subunits were chosen as the research objects based on a mechanism mediated by a GABAergic nervous system.

However, oral administration of mice with GABA green tea has an effect of degrading biologically active ingredients of tea and can generate their low oral bioavailability, which is different from an intraperitoneal injection. In fact, the primary route of absorption is into the mesenteric vessels, which drain into the portal vein and pass through the liver where they undergo hepatic metabolism before reaching systemic circulation.[41] In this study, we gave mice oral green tea and GABA green tea extract in order to simulate people's daily drinking tea behavior, aiming to demonstrate the effect of GABA tea on preventing depression. The extract of GABA green tea showed a strong depression prevention effect while green tea didn't show that effect. Simultaneously, it was found that extracts of GABA green tea and GABA solution (GS, 10 mg kg^{-1}) significantly enhanced the GABA concentration in brain tissue of rats, indicating that GABA has an antagonist effect on the stimulatory action of caffeine and is suggestive of a sedative action and antidepressant-like effect of the extract.[10] Previous studies have shown that GABA, which is difficult to be transported across the blood brain barrier, a selective barrier mainly formed by the brain capillary endothelial cells, could play an important role in preventing paracellular transport of small and large water-soluble compounds from blood to the brain.[42] Using oral GABA tea, the GABA content in rat brain tissue increased, but in the groups of NC, PC, and green tea, the contents were not increased. A high concentration of GABA in the blood can lead to an increase of GABA concentration in the brain. Further studies are still needed to determine how effective GABA is to be absorbed after oral administration, and how it passes through the blood–brain barrier and reaches CNS with various beneficial effects. Conclusive answers to these questions require additional molecular biology and pharmacological metabolism investigations.

5 Conclusions

This study has indicated that after repeated anaerobic and aerobic treatments, GABA content in green tea is significantly increased, reaching the standard of GABA tea, and that the contents of water extract, tea polysaccharides, and free amino acids also are significantly increased whereas the content of tea polyphenols is reduced. Behavioral tests in mice suggest that long-term diets of GABA green tea extract could ameliorate the desperate depression of mice under stressful conditions. These neuropharmacological properties of GABA green tea possibly work on the GABAergic neurotransmission of the mouse cerebral cortex *via* up-regulating the expression of $GABA_A$ receptor α1 subunits. These results indicate that GABA green tea may have a health effect on the prevention and alleviation of depression. This study has provided novel experimental evidence for antidepressant-like effects of GABA green tea.

Abbreviations

GABA	Gamma (γ)-aminobutyric acid
CT	Clomipramine hydrochloride tables group
GS	GABA solution
NC	Normal control
PC	Positive drug control
GGT	GABA green tea extract
TST	Tail suspension test
FST	Forced swim test
HPLC	High pressure liquid chromatography.

Conflicts of interest

The authors declare they have no actual or potential competing financial interests.

Acknowledgements

This study was supported by the financial support from Natural Science Foundation of Guangdong Province (2015B020202007, 2016A020208012), "2011 Collaborative Innovation Center" Chinese Oolong Tea Industry Innovation Center Special Project (Fujian 2015-75), Guangdong Tea Research System (2016LM1117), Natural Science Foundation of Guangxi Province (AB16380063), and Science and Technology Development Special Funds (Public Interest Research and Capacity Building Direction) Project of Guangdong Province (2017A020208048).

References

1 J. Peng, H. L. Yu, T. Lan, Z. Feng and Z. S. Quan, *Pharmacol., Biochem. Behav.*, 2015, **133**, 146–154.
2 B. C. Detanico, Â. L. Piato, J. J. Freitas, F. L. Lhullier, M. P. Hidalgo, W. Caumo and E. Elisabetsky, *Eur. J. Pharmacol.*, 2009, **607**, 121–125.
3 L. Yi, G. Jia, L. Gou, L. Sun, X. Fu, N. Lan, S. Li and X. Yin, *Pharmacol., Biochem. Behav.*, 2013, **104**, 27–32.
4 A. J. Granger, N. Mulder, A. Saunders, B. L. Sabatini and S. Aglawe, *Neuropharmacology*, 2016, 40–46.
5 N. Eshel, M. Bukwich, V. Rao, V. Hemmelder, J. Tian and N. Uchida, *Nature*, 2015, **525**, 243–246.
6 W. L. Zhu, H. S. Shi, Y. M. Wei, S. J. Wang, C. Y. Sun, Z. B. Ding and L. Lu, *Pharmacol. Res.*, 2012, **65**, 74–80.
7 X. Chen, L. Lan and X. T. Ren, *J. Ethnopharmacol.*, 2004, **91**, 345–349.
8 P. Brambilla, J. Perez, F. Barale, G. Schettini and J. C. Soares, *Mol. Psychiatry*, 2003, **8**, 721–737.
9 I. Mody, Y. D. Koninck, T. S. Otis and I. Soltesz, *Trends Neurosci.*, 1994, **17**, 517–525.
10 C. Wu, Y. Huang, X. Lai, R. Lai, W. Zhao, M. Zhang and W. Zhao, *J. Funct. Foods*, 2014, **7**, 180–190.
11 N. Bouché and H. Fromm, *Trends Plant Sci.*, 2004, **9**, 110–115.
12 M. Diana, J. Quílez and M. Rafecas, *J. Funct. Foods*, 2014, **10**, 407–420.
13 W. C. Liao, C. Y. Wang, Y. T. Shyu, R. C. Yu and K. C. Ho, *J. Funct. Foods*, 2013, **5**, 1108–1115.
14 A. J. Granger, N. Mulder, A. Saunders and B. L. Sabatini, *Neuropharmacology*, 2016, **100**, 40.
15 C. L. Faingold, G. Gehlbach and D. M. Caspary, *Brain Res.*, 1989, **500**, 302–312.
16 J. Bormann, *Trends Pharmacol. Sci.*, 2000, **21**, 16–19.
17 X. K. Wang and M. Nielsen, *Foreign Med. Sci., Sect. Pharm.*, 2001, **28**, 29–34.
18 K. A. Wafford, *Curr. Opin. Pharmacol.*, 2005, **5**, 47–52.
19 S. Pappata, A. Varrone, G. Milan, V. Sansone, A. Iavarone, M. R. Panico, M. Quarantelli, C. Mollica, C. D. Falco and E. Loré, *NeuroImage*, 2006, **31**, T169.
20 C. Y. Huang, W. W. Kuo, H. F. Wang, C. J. Lin, Y. M. Lin, J. L. Chen, C. H. Kuo, P. K. Chen and J. Y. Lin, *J. Funct. Foods*, 2014, **6**, 534–544.
21 C. S. Yang, G. Y. Yang, J. Y. Chung, M. J. Lee and C. Li, *J. Nutr.*, 2000, **130**, 39–53.
22 M. Serafini, A. Ghiselli and A. Ferroluzzi, *Eur. J. Clin. Nutr.*, 1996, **50**, 28–32.
23 M. Zu, Y. Fan, W. Zhou, A. Liu, G. Du and L. Zheng, *Antiviral Res.*, 2012, **94**, 217–224.
24 W. Zhao, Y. Li, W. Ma, Y. Ge and H. Yahui, *Food Funct.*, 2015, **09**, 40–45.
25 T. Tsushida, T. Murai, M. Omori and J. Okamoto, *J. Agric. Chem. Soc. Japan*, 1987, **7**, 817–822.
26 Z. Zeng, C. Wu, Y. Huang and J. Wu, *Afr. J. Biotechnol.*, 2012, **51**, 11333–11341.
27 A. Di Lorenzo, S. F. Nabavi, A. Sureda, A. H. Moghaddam, S. Khanjani, P. Arcidiaco, S. M. Nabavi and M. Daglia, *Mol. Nutr. Food Res.*, 2015, **60**, 566–579.
28 L. M. He, L. Peng, C. R. Li, *et al.*, *Guangdong Agric. Sci.*, 2011, **18**, 10–13.
29 Y. Tai, C. L. Wei, H. Yang, L. Zhang, Q. Chen, W. Deng, S. Wei, J. Zhang, C. Fang, C. Ho and X. Wan, *BMC Plant Biol.*, 2015, **15**, 1–13.
30 Y. H. Huang and J. H. Chen, *Chin. Agric. Sci. Bull.*, 2010, **26**, 236–240.
31 Y. Tai, C. Wei, Y. Hua, Z. Liang, C. Qi, W. Deng, W. Shu, Z. Jing, C. Fang, C. Ho and X. Wan, *BMC Plant Biol.*, 2015, **15**, 1–13.
32 L. Peng, X. Song, X. Shi, J. Li and C. Ye, *J. Food Compos. Anal.*, 2008, **21**, 559–563.
33 H. Horie and K. Kohata, *J. Chromatogr. A*, 2000, **881**, 425–438.
34 C. Lino-De-Oliveira, T. C. M. De Lima and A. D. P. Carobrez, *Behav. Brain Res.*, 2005, **158**, 243–250.
35 L. Steru, R. Chermat, B. Thierry and P. Simon, *Psychopharmacology*, 1985, **85**, 367–370.
36 T. Tsushida, T. Murai, M. Omori and J. Okamoto, *J. Agric. Chem. Soc. Japan*, 1987, **61**, 817–822.
37 M. Zhao, Y. Ma, Z. Z. Wei, W. X. Yuan, Y. L. Li, C. H. Zhang, X. T. Xue and H. J. Zhou, *J. Agric. Food Chem.*, 2011, **59**, 3641–3648.
38 D. Ma, P. Lu, C. Yan, C. Fan, P. Yin, J. Wang and Y. Shi, *Nature*, 2012, **483**, 632.
39 K. C. Chou, *Biochem. Biophys. Res. Commun.*, 2004, **316**, 636–642.
40 U. Rudolph, F. Crestani and H. Möhler, *Trends Pharmacol. Sci.*, 2001, **22**, 188–194.
41 S. Leong and E. Ling, *J. Neurosci. Methods*, 1990, **32**, 15–23.
42 W. M. Pardridge, *Pharm. Res.-DORDR*, 2007, **24**, 1733–1744.

 This journal is © The Royal Society of Chemistry 2017

Back

Advertise

Find high-quality, validated conte
supports your organization's cha
R&D needs

Journal of
Food Biochemistry

Volume 41, Issue 1

February 2017

Previous Issue | Next Issue

GO TO SECTION

Export Citation(s) Download PDF(s)

ISSUE INFORMATION

Free Access

Issue Information

First Published: 11 February 2017

PDF | Request permissions

FULL ARTICLES

Angiotensin-I Converting Enzyme Inhibitory Activities of Common Edible Cephalopods and their Antioxidative Effects using different *in vitro* Models

Kajal Chakraborty, Minju Joy, Vamshi Krishna Raola, Fasina Makkar

First Published: 16 March 2016

Back

The Inhibitory Effects of Yixing Black Tea Extracts on A-Glucosidase

Wenxing Hao, Miao Wang, Mengxian Lv

First Published: 23 March 2016

Abstract | **Full text** | **PDF** | **References** | **Request permissions**

Bacillus Subtilis-Fermented Red Bean (Red Bean Natto) Reduces Hyperlipidemia Levels in Hamsters Fed an Atherogenic Diet

Nai-Nu Lin, Yen-Feng Lee, Yi-Jen Chi, Ming-Fu Wang, Yin-Ching Chan, Kung-Chi Chan, Ying-Ju Chen, Yung-Tsung Chiu

First Published: 15 April 2016

Abstract | **Full text** | **PDF** | **References** | **Request permissions**

Blends of Cold Pressed Black Cumin Oil and Sunflower Oil with Improved Stability: A Study Based on Changes in the Levels of Volatiles, Tocopherols and Thymoquinone during Accelerated Oxidation Conditions

Mustafa Kiralan, Merve Ulaş, Ayşegül Özaydin, Necla Özdemır, Gülcan Özkan, Alı Bayrak, Mohamed Fawzy Ramadan

First Published: 17 April 2016

Abstract | **Full text** | **PDF** | **References** | **Request permissions**

Optimization Study in Extracting Anti-Oxidative and A-Amylase Inhibitor Peptides from Cumin Seeds (*Cuminum Cyminum*)

Hwee-Leng Siow, Chee-Yuen Gan

First Published: 15 April 2016

Abstract | **Full text** | **PDF** | **References** | **Request permissions**

Phytochemical Profile, Antioxidant Properties and Hypoglycemic Effect of Chaya (*Cnidoscolus Chayamansa*) in STZ-Induced Diabetic Rats

Minerva Ramos-Gomez, Marely G. Figueroa-Pérez, Horacio Guzman-Maldonado, Guadalupe Loarca-Piña, Sandra Mendoza, Teódulo Quezada-Tristán, Rosalia Reynoso-Camacho

First Published: 27 April 2016

Back

Protective Effect of Astaxanthin on Primary Retinal Cells of the Gerbil *Psammomys Obesus* Cultured in Diabetic *Milieu*

Basma Baccouche, Sihem Mbarek, Ahmed Dellaa, Imane Hammoum, Concetta M. Messina, Andrea Santulli, Rafika Ben Chaouacha-Chekir

First Published: 27 April 2016

Abstract | **Full text** | **PDF** | **References** | **Request permissions**

Apium Graveolens Extract Attenuates Adjuvant Induced Arthritis by Reducing Oxidative Stress

Nutjanat Choosri, Supita Tanasawet, Pennapa Chonpathompikunlert, Wanida Sukketsiri

First Published: 20 April 2016

Abstract | **Full text** | **PDF** | **References** | **Request permissions**

Antioxidant and Antibacterial Properties of Essential Oil Extracted from an Edible Seaweed *Undaria Pinnatifida*

Jayanta Kumar Patra, Se-Weon Lee, Jae Gyu Park, Kwang-Hyun Baek

First Published: 29 April 2016

Abstract | **Full text** | **PDF** | **References** | **Request permissions**

Antioxidant Activity and α-Amylase Inhibitory Effect of Polyphenolic-Rich Extract from *Origanum Glandulosum* Desf

Afef Béjaoui, Abdennacer Boulila, Adnen Sanaa, Mohamed Boussaid, Xavier Fernandez

First Published: 03 May 2016

Abstract | **Full text** | **PDF** | **References** | **Request permissions**

Induction of Apoptosis in MCF-7 Breast Cancer Cells by Sri Lankan Endemic Mango (*Mangifera zeylanica*) Fruit Peel through Oxidative Stress and Analysis of its Phytochemical Constituents

Meran Keshawa Ediriweera, Kamani Hemamala Tennekoon, Sameera Ranganath Samarakoon, Ira Thabrew, E. Dilip De Silva

First Published: 28 May 2016

Back

HPLC Analysis of Twelve Compounds from *Artemisia sacrorum* Ledeb and their Structural Elucidation

Wugedunqiqige Bao, Qinghu Wang, Jingjing Han, Narenchaoketu Han

First Published: 18 May 2016

Abstract | **Full text** | **PDF** | **References** | **Request permissions**

Antimicrobial Impact for *Lactococcus lactis* subsp. *lactis* A15 and *Enterococcus faecium* A15 Isolated from Some Traditional Egyptian Dairy Products on Some Pathogenic Bacteria

Shady El-Ghaish, Mohamed Khalifa, Ahmed Elmahdy

First Published: 18 May 2016

Abstract | **Full text** | **PDF** | **References** | **Request permissions**

Effect of High Intensity Ultrasound on the Gel and Structural Properties of *Ctenopharyngodon idellus* Myofibrillar Protein

Qing-Hui Wen, Zong-Cai Tu, Lu Zhang, Hui Wang, Hai-Xia Chang

First Published: 28 May 2016

Abstract | **Full text** | **PDF** | **References** | **Request permissions**

Biological Activity and Characterization of Volatile Compounds of *Teucrium orientale* Var. *glabrescens* by SPME and GC-FID/MS

Sermet Yildirmiş, Rezzan Aliyazicioglu, Ozan Emre Eyupoglu, Ufuk Ozgen, Sengul Alpay Karaoglu

First Published: 13 June 2016

Abstract | **Full text** | **PDF** | **References** | **Request permissions**

Characterization and Antibacterial Mode of Action of Lactic Acid Bacterium *Leuconostoc mesenteroides* HJ69 from Kimchi

Vivek K. Bajpai, Irfan Ahmad Rather, Rajib Majumder, Fanar Hamad Alshammari, Gyeong-Jun Nam, Yong-Ha Park

First Published: 13 June 2016

Abstract | **Full text** | **PDF** | **References** | **Request permissions**

Back

and Horseradish (*Moringa oleifera*) Seeds Extracts: A Comparative Study

Stephen A. Adefegha, Ganiyu Oboh, Sunday I. Oyeleye, Felix A. Dada, Isaac Ejakpovi, Aline A. Boligon

First Published: 02 June 2016

Abstract | **Full text** | **PDF** | **References** | **Request permissions**

Enzymatic Water Extraction of Polysaccharides from *Epimedium brevicornu* and Their Antioxidant Activity and Protective Effect Against DNA Damage

Juan Yang, Hua-Feng Zhang, Xiao-Yan Cao, Xiao-Hua Yang, Feng-Zhong Wang, Qiang Guo, Chen-Qian Sun

First Published: 14 June 2016

Abstract | **Full text** | **PDF** | **References** | **Request permissions**

Studies on the Antioxidant and Antiproliferative Potentials of *Cirsium arvense* subsp. *vestitum*

Ibrahim Demirtas, Ali Riza Tufekci, Ayse Sahin Yaglioglu, Mahfuz Elmastas

First Published: 10 June 2016

Abstract | **Full text** | **PDF** | **References** | **Request permissions**

Supplementation of Mango (*Mangifera indica* L.) Peel in Diet Ameliorates Cataract in Streptozotocin-Induced Diabetic Rats

Mahendranath Gondi, Shaik Akbar Basha, Paramahans V. Salimath, Ummiti J.S. Prasada Rao

First Published: 05 July 2016

Abstract | **Full text** | **PDF** | **References** | **Request permissions**

Structural Properties of Phycoerythrin from Dulse *Palmaria palmata*

Yoshikatsu Miyabe, Tomoe Furuta, Tomoyuki Takeda, Gaku Kanno, Takeshi Shimizu, Yoshikazu Tanaka, Zuoqi Gai, Hajime Yasui, Hideki Kishimura

First Published: 05 July 2016

Abstract | **Full text** | **PDF** | **References** | **Request permissions**

Back

Ali Sen, Meral Yuksel, Gizem Bulut, Leyla Bitis, Feriha Ercan, Nagehan Ozyilmaz-Yay, Ozben Akbulut, Hamit Cobanoğlu, Sevil Ozkan, Goksel Sener

First Published: 05 July 2016

Abstract | **Full text** | **PDF** | **References** | **Request permissions**

Study on the Anti-Tumor Ability of Niaowangzhong Green Tea

Dan Li, Yingyu Chen, Yahui Huang, Lijuan Zhang, Jiagan Yang, Xingguo Xu, Qing Liu, Xu Zhang

First Published: 26 July 2016

Abstract | **Full text** | **PDF** | **References** | **Request permissions**

Lipid Oxidation and Biochemical Quality of Indian Mackerel during Frozen Storage: Effect of Previous Treatment with Plant Extracts

Pankyamma Viji, Puthanpurackal Kizhakkethil Binsi, Sivam Visnuvinayagam, Chitradurga Obaiah Mohan, Gudipati Venkateshwarlu, Teralandur Krishnaswamy Srinivasa Gopal

First Published: 08 August 2016

Abstract | **Full text** | **PDF** | **References** | **Request permissions**

The Protective Effect of Antioxidant Enriched Fractions from Colored Potatoes Against Hepatotoxic Oxidative Stress in Cultured Hepatocytes and Mice

Da Hye Kim, Myungsuk Kim, Sang-Bin Oh, Kyung Mi Lee, Sang Min Kim, Chu Won Nho, Won Byong Yoon, Kyungsu Kang, Cheol-Ho Pan

First Published: 08 August 2016

Abstract | **Full text** | **PDF** | **References** | **Request permissions**

Characterization of Endogenous Protease and the Changes in Proteolytic Activity of *Acetes vulgaris* and *Macrobrachium lanchesteri* During *Kapi* Production

Jaksuma Pongsetkul, Soottawat Benjakul, Punnanee Sumpavapol, Kazufumi Osako, Nandhsha Faithong

First Published: 05 September 2016

Abstract | **Full text** | **PDF** | **References** | **Request permissions**

Back

Hanan M. F. Abd El-Wahab, Mona A. Mohamed, Hanaa H. El Sayed, Alshimaa E. Bauomy

First Published: 18 August 2016

Abstract | **Full text** | **PDF** | **References** | **Request permissions**

The biochemical composition of the leaves and seeds meals of *moringa* species as non-conventional sources of nutrients

Fahad Al Juhaimi, Kashif Ghafoor, Elfadıl E. Babiker, Bertrand Matthäus, Mehmet Musa Özcan

First Published: 12 September 2016

Abstract | **Full text** | **PDF** | **References** | **Request permissions**

In vitro studies on the effect of watercress juice on digestive enzymes relevant to type 2 diabetes and obesity and antioxidant activity

Vítor Spínola, Joana Pinto, Paula C. Castilho

First Published: 29 September 2016

Abstract | **Full text** | **PDF** | **References** | **Request permissions**

β-Glucan, but not *Lactobacillus plantarum* P-8, inhibits lipid accumulation through selected lipid metabolic enzymes in obese rats

Hsiu-Chuan Lee, Wei-Ting Yu, Yu-Ru Guo, Shih-Yi Huang

First Published: 07 October 2016

Abstract | **Full text** | **PDF** | **References** | **Request permissions**

Antioxidant activity and the potential for cholesterol-lowering of phenolic extract of *Morus alba*, *Morus multicaulis*, and *Morus laevigata* leaves from Yunnan (China)

Yanxin Zhang, Wei Du, Xuewen Zhang, Hongmu Zhao, Yanhui Wang

First Published: 10 October 2016

Abstract | **Full text** | **PDF** | **References** | **Request permissions**

Back

Preservation effect of high pressure processing on ascorbic acid of fruits and vegetables: A review

Somya Tewari, Rachna Sehrawat, Prabhat K. Nema, Barjinder Pal Kaur

First Published: 25 September 2016

Abstract | Full text | PDF | References | Request permissions

Sign up for email alerts

Enter your email to receive alerts when new articles and issues are published.

Email address*

Enter email

Continue

Submit an article

Journal Metrics

Special Issue: Call for Papers

More from this journal

- Wiley Job Network

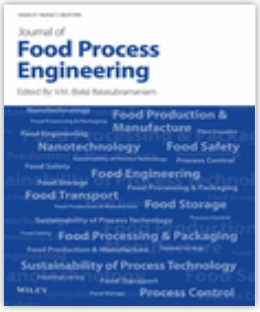
Tweets by @wileyfoodsci

Related Titles

Back

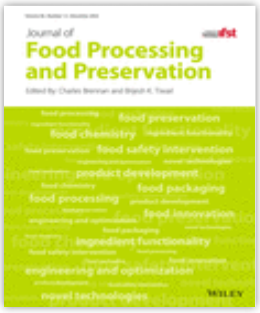


Pages: 1, 639-1363
February 2024



ISSUE

Volume 47, Issue 3
March 2024



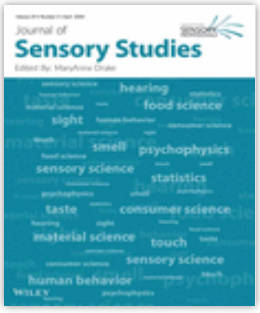
ISSUE

Volume 46, Issue 12
December 2022



ISSUE

Volume 44, Issue 2
April 2024



ISSUE

Volume 39, Issue 2
April 2024

Back



February 2024



ISSUE

Volume 6, Issue 1
March 2024

DIVERSITY
in Research Jobs

Please contact us to see your job listed here

Manager, Food Science and Standards
North Bethesda, MD

Who is USP? The U.S. Pharmacopeial Convention (USP) USP is an independent scientific organization that collaborates with the world's top experts in...

Employer: United States Pharmacopeia Apply for this job

R&D Formulist senior - Nutraceutico - San Marino
Rimini | Negotiable

Hai esperienza nella formulazione in aziende produttrici di integratori alimentari e vuoi entrare a far parte di un gruppo in continua espansione?Sei

NonStop CONSULTING

ABOUT WILEY ONLINE LIBRARY

Privacy Policy
Terms of Use
About Cookies
Manage Cookies
Accessibility
Wiley Research DE&I Statement and Publishing Policies
Developing World Access

HELP & SUPPORT

Contact Us
Training and Support

Back

Subscription Agents
Advertisers & Corporate Partners

CONNECT WITH WILEY

The Wiley Network
Wiley Press Room

Copyright © 1999-2024 John Wiley & Sons, Inc or related companies. All rights reserved, including rights for text and data mining and training of artificial technologies or similar technologies.

WILEY

Journal of Food Biochemistry

Journal of Food Biochemistry ISSN 1745–4514

STUDY ON THE ANTI-TUMOR ABILITY OF NIAOWANGZHONG GREEN TEA

DAN LI[1], YINGYU CHEN[1], YAHUI HUANG[1,6], LIJUAN ZHANG[2], JIAGAN YANG[1], XINGGUO XU[2], QING LIU[2] and XU ZHANG[3,4,5,6]

[1]College of Horticulture, South China Agricultural University, Guangzhou, Guangdong 510642, People's Republic of China
[2]Tea Development Management Office of Qiannan, Duyun, Guizhou 558000, People's Republic of China
[3]College of Forestry and Landscape Architecture, South China Agricultural University, Guangzhou, Guangdong 510642, People's Republic of China
[4]Guangdong Key Laboratory for Innovative Development and Utilization of Forest Plant Germplasm, Guangzhou 510642, People's Republic of China
[5]State Key Laboratory for Conservation and Utilization of Subtropical Agro-bioresources (South China Agricultural University), Guangzhou 510642, People's Republic of China

[6]Corresponding author.
TEL: +86(020)38297601;
FAX: +86(020)85280228;
EMAIL: 13922206070@163.com

TEL/FAX: 186(020)85280256;
EMAIL: zhangxu919@hotmail.com

Dan Li and Yingyu Chen contributed equally to the work.

Received for Publication April 4, 2016
Accepted for Publication May 21, 2016

doi: 10.1111/jfbc.12305

ABSTRACT

It has been known that green tea not only possesses certain chemo-preventive effects on cancer, but also can kill directly some types of tumor cells. Niaowangzhong tea (*C. sinensis*), a special tea resource growing in Qiannan Buyi, a Miao Minority Autonomous Prefecture in Guizhou province, China, is one of the most popular medicinal beverages for local people there. The aims of this study were to analyze the quality components and their relative contents present in Niaowangzhong green tea and to investigate whether or not the water extract of this green tea has the antitumor capability *in vitro* and *in vivo*. Biochemical analysis indicated that this green tea extract contained relatively higher levels of tea polyphenols, alkaloids, flavonoids compounds and polysaccharides. In the MTT (3-(4,5-dimethyl-2-thiazolyl)−2,5-diphenyl-2-*H*-tetrazolium bromide) assay, this green tea extract showed inhibitory activity against several types of tumor cells, including breast, prostate, colorectal and gastric cancer cell lines, with higher selectivity toward human gastric cancer cell line MGC-803. Its 50% inhibition concentration (IC50) of MGC-803 was 32.5 μM as compared to that (367.9 μM) of normal vascular endothelial cells. Cell cycle and apoptosis analyses showed that the proportion of cells arrested at the G0/G1 phase was increased with the increase in concentration, and the proportion of apoptotic cells was also increased. Niaowangzhong green tea extract could significantly inhibit tumor-sphere formation in the *in vivo* antitumor experiment and the growth of MGC-803-derived tumor in nude mice. At the concentration of 500 mg/kg/day, inhibition rate was 31.0% without causing obvious toxic side effects. This study revealed a potent anti-cancer activity of this special green tea and its promising potential as chemo-preventive agent and proper dietary practice for prevention and control of cancers.

PRACTICAL APPLICATION

This study has indicated that Niaowangzhong green tea extract caused stronger cytotoxic effects on two kinds of digestive tract tumor cells HCT-15 and MGC-803, suggesting that as one of the most popular medicinal beverages, this green tea extract may be more suitable for treating digestive tract cancers since it can be more accessible to the locations of digestive and intestinal tracts. Therefore, this specific green tea merits further depth study on underlying mechanisms at the

cellular and molecular levels and further development for potential medical application and dietary practices for prevention of cancers, especially for digestive and intestinal tracts. Co-administration of the anti-cancer drugs and Niaowangzhong green tea may reduce the toxic side effects and drug resistance while achieving desired effect because of the reason that Niaowangzhong green tea extract are mediated through the synergic effects of a variety of anti-cancer compounds present it and had no obvious toxic side effects.

INTRODUCTION

Cancer is an important and serious disease characterized by the rapid growth and spread of the abnormal cells free from control (Reya *et al.* 2001). Cancer cells often invade the normal tissues/organs around the body and can metastasize to other organs of the body (Bateman *et al.* 2010; Bomken *et al.* 2010). Since the 21st century, cancer has been one of the important diseases seriously affecting human health and its mortality rate has been in a rising trend (Ferlay *et al.* 2010; Chen *et al.* 2011, 2013). The latest statistics reported by World Health Organization have shown that there were more than 14 million new cancer cases in 2012 world-wide, resulting in the death of ~8.2 million people. Furthermore, it is estimated that in the next 20 years, cancer cases will be rising to 22 million per year. According to "Reports of Third National Cause of Death in China" Issued by Ministry of Health of China, the malignant tumors have been ranked the top cause of death among urban residents in China. At the same time, the increase in the cancer mortality rate was significantly higher among rural residents than among urban residents. Thus the harm caused by malignant tumors to the health of people has become an increasingly serious public health problem in China (The Third National Cause of Death in China 2008), calling for the urgent needs of developing effective anti-cancer medicines and the proper dietary practices of control and prevention of cancers.

Traditionally, green tea has been one of the most popular beverages in China since ancient time. It has been shown by current studies that green tea not only possesses certain chemo-preventive effects on cancer, but also can kill directly some types of tumor cells (Forester and Lambert 2011; Zhao *et al.* 2013). While the main effective anti-cancer components of green tea are tea polyphenols, other substances, including vitamins, trace elements and polysaccharose present in green tea, also have certain anti-cancer effects (Friedman *et al.* 2007; Senanayake 2013). Niaowangzhong tea (*Camellia sinensis*) is a special tea resource growing in Qiannan Buyi, a Miao Minority Autonomous Prefecture in Guizhou province, China (Zhang 2015). Because the people of Miao minority nationality in Buyi live in the mountainous areas, it is very difficult for them to see a medical doctor and/or to obtain the medicines. The only therapeutic method for them is to find the natural materials. Niaowangzhong green tea is one of the most popular medicinal beverages for them. There are many folk stories about the magical curative effects, especially to tumor, of the Niaowangzhong green tea (Yang 1988). However, the exact anti-cancer effects of this green tea extract remain mystery. It is of interest, importance and significance to investigate its anti-tumor effects and the underlying cellular and molecular mechanisms.

Therefore, this study aimed to analyze the contents of quality components present in Niaowangzhong green tea and to investigate its anti-tumor efficacy for paving the theoretical foundation for the further study on its health effects and the cellular and molecular mechanisms of its action and for its potential application in anti-cancer therapy as well as for proper dietary practices for cancer prevention.

MATERIALS AND METHODS

Materials and Equipment

Plant Materials. Fresh leaves of Niaowangzhong green tea (*C. sinensis*) consisting mainly of two leaves and one bud were harvested from Niaowangzhong green tea plants growing in Buyi, Guizhou Province in China in April 2015 and used in this study. The Niaowangzhong green tea was manufactured with fixing machines. After being picked up, the fresh leaves were fixed, rolled and dried at 100C until they were adequately dried. The dried powders were used as the green tea extract.

Sources of Human Cancer Cell Lines and Normal Vascular Endothelial Cells. Human breast cancer cells MCF-7, human prostate cancer cells DU145, human colorectal cancer cells HCT-15, human gastric cancer cells MGC-803 and normal human vascular endothelial cells (VEC) were used in this study. They were all purchased from Cell Resource Center, Shanghai Institute of Life Science, Chinese Academy of Sciences (Shanghai, China).

Animals. Male nude mice (20.0 ± 2.0 g, 4–6 weeks old) were purchased from Shanghai Silaike Experimental Animal

Co., Ltd. (Shanghai, China). All the animals were housed in cages at a constant temperature (21C ± 2C), humidity (50% ± 10%) and maintained on a 12 h light–12 h dark cycle with free access to food and water. The animal experiments were performed in Shanghai Jiaotong University (Shanghai, China). All the procedures were approved and conducted according to the Guidelines formulated by The Ethical Committee of Laboratory Animals of Shanghai Jiaotong University.

Chemicals and Drugs. Caffeine (Caff), theobromine (TB), theophylline (TP), gallocatechin (GC), catechin (C), epigallocatechin (EGC), epigallocatechingallate (EGCG), epicatechin (EC), gallocatechingallate (GCG), epicatechingallate(ECG) and catechingallate (CG) were purchased from Sigma-Aldrich Chemical (St. Louise, MO). High performance liquid chromatography (HPLC) grade methanol was obtained from Tianjin Kemiou Chemical Reagent Co., Ltd. (Tianjin, China) and used as the solvent. All the other chemicals and reagents used were of the highest grade available. 3-(4,5-Dimethyl-2-thiazolyl)−2,5-diphenyl-2-*H*-tetrazolium bromide (MTT) was purchased from Sigma-Aldrich Chemicals. Dimethyl sulfoxide (DMSO) was obtained from Amresco LLC (Solon, OH). 5-Fluorouracil (5-Fu) was purchased from Shanghai Aladdin Reagent co., Ltd (Shanghai, China). Fetal bovine serum (FBS), trypsin, penicillin/streptomycin, phosphate buffer (PBS) and RPMI 1640 medium were purchased from Hyclone LLC (Logan, UT). Sodium chloride (analytic purity) was obtained from Shanghai State Pharmaceutical Group (Shanghai, China). One time filter (0.22 m) was purchased from Millipore Corporation (Billerica, MA). Hoechst, propidium iodide (PI), cell cycle and apoptosis detection kits and V-FITC Annexin apoptosis detection kit were obtained from Bi Yuntian Biological Technology Co., Ltd. (Shanghai, China).

Methods

Analyses of Biochemical Compositions Present in Niaowangzhong Green Tea. About 3 grams (g) of tea powder was extracted with 500 mL of distilled water at 100C for 45 min with shaking. The extracted solutions were filtered through a 0.22-mm filter paper. The residue was used to determine water extracts and the supernatants were collected for subsequent analysis of other components. Contents of tea polyphenols were measured with ferrous tartrate method at 540 nm with the spectrophotometer as described previously (He *et al.* 2011). The contents of total free amino acids (TFAAs) were determined by the ninhydrin colorimetry at 570 nm using a spectrophotometer according to the method by He *et al.* (2011). All the assay methods mentioned above were based on the National Standard of People's Republic of China. The contents of catechins and alkaloids were determined by high performance liquid chromatography (HPLC) according to the method developed by Dalluge *et al.* (1998) and Lu *et al.* (2009) with slight modifications, respectively.

Preparation of Niaowangzhong Green Tea Extract. About 100 g of dried tea powder was extracted with 450 mL of distilled water at 100C for 45 min with shaking. Immediately after extraction, the extract was passed through a vacuum filter to a 500-mL volumetric flask. The extract was concentrated with a rotating enrichment device stress to the appropriate concentration, and dried with a vacuum freezing dryer for 24 h. The dried tea powder was collected.

Cell Culture and Subculture. Cells were cultured in RPMI 1640 culture medium containing 10% FBS as follows: the frozen cells stored in liquid nitrogen tank were removed and quickly placed in 37C water bath for thawing, and abandoned the frozen liquid after 1,000 rpm centrifugation for 5 min. With the appropriate complete medium, the cells are packed in the culture dish and placed in cell culture incubator in 37C, under 5% CO_2. When the cells grew to 70–80% confluence, they were detached by trypsin digestion and then sub-cultured.

Measurement of the *In Vitro* Anti-tumor Effects With MTT Method. The cells growing at the logarithmic growth phase were detached by trypsin digestion for 10 min and the detached cells were centrifuged at 1,000 × g for 5 min. After being centrifuged, the precipitated cells were suspended with complete medium. Cell suspension was adjusted with complete medium to the appropriate concentration. About 100 μL of cell suspension solutions were added into the 96-microwell plates per well and statically cultured for 48 h. After the cells adhered to the well, 100 μL of complete medium dilution compounds was added into each well with 3 wells in each group. For each 96-microwell plate, the zero well, in which only compound and medium were added but without adding cells, and a blank control well, in which only cells and medium were added without adding compound, were set. According to different experimental needs, the cells were cultured in the incubator for different periods of time. About 20 μL of MTT solution (5 mg/mL) was added into each well and cultured for 4 h at dark and then the culture was terminated. The culture medium was withdrawn. About 100 μL of DMSO was added to each well and the culture plate was oscillated at low speed on shaking table for 10 min. The absorbance (OD) value of each well was read at the wavelength of 570 nm after the blue crystal was completely dissolved in the wells.

The inhibition rate on cell growth was calculated according to the following formula: the growth inhibition rate

TABLE 1. PI STAINING SOLUTION WAS PREPARED

	One sample	Six samples	Twelve samples
Buffer	0.5 mL	3 mL	6 mL
PI staining solution (20×)	25 μL	150 μL	300 μL
RNase A (50×)	10 μL	60 μL	120 μL
Final volume	0.535 mL	3.21 mL	6.42 mL

(%) = (1 – the medicine group OD value/the control group OD value) × 100%.

For IC_{50} calculation, numerical of dose was used as abscissa and the inhibition rate was taken as ordinate, the curve was an S-shaped one, the curve between steep and flat at both ends. For regression analysis, it usually need to be introduced to suppress the concept of rate of probability unit (probit), the curve was converted into a straight line (Zhao *et al.* 2007). In this article, the analysis of regression probit program was used to fit a straight line, and the IC_{50} value was calculated.

Experiment of *In Vitro* Tumor-sphere Formation. The cells growing to logarithmic growth phase were subcultured with RPMI 1640 complete medium containing 10% FBS. Single cell suspension was prepared by the digestion of adherent cells with trypsin. The cells density was adjusted to 1,000 cells/mL and inoculated with super lowadsorption6 orifice plate, the cell suspension was cultured with culture medium consisting of DMEM/F12, B27, epidermal growth factor (EGF) and basic fibroblast growth factor (BFGF) without adding FBS. The cells were treated with Niaowangzhong green tea extract at different concentrations in six orifice plates and the growth of tumor-spheres was monitored by photo counting after 7 days. The sizes of the tumor spheres were in the range of 50–250 μm.

Assay of the Cell Cycle With Flow Cytometry. The cell samples were prepared as follows: The cells were detached with trypsin digestion and the culture medium was added at the end of digestion. All the adherent cells were collected to a centrifuge tube and centrifuged at 1,000 × g for 5 min. The supernatant was discarded and the precipitated cells were suspended with precooling phosphate buffered saline (PBS). The remaining medium was rinsed into centrifugal tube and centrifuged at 1,000 × g for 5 min. The supernatant was discarded. The precipitated cells were suspended with PBS and the cell number was counted. The concentration of cell suspension was adjusted to 1–2 × 10^6 cells/mL and the cells were transferred to a 1.5-mL microcentrifuge tube, and centrifuged to sediment cells again. The supernatant was suctioned carefully.

The cells were fixed by adding 1 mL of precooling 70% ethanol (EtOH), cell pellet was gently beat, settled at 4C and fixed for 12 h. Thereafter, the cells were centrifuged at 1,000 × g for 5 min at 4C. The supernatant was carefully aspirated and the precipitated cells were re-suspended by adding the precooling PBS, and then centrifuged to pellet the cells again. The supernatant was carefully aspirated. PI staining solution was prepared as shown in Table 1.

A 0.5 mL of the prepared PI staining solution was added to each sample tube. The precipitated cells were slowly and fully re-suspended, incubated at 37C for 30 min at dark and then placed on ice away from light for subsequent assay. The red fluorescence was detected at the excitation wavelength of 488 nm by flow cytometry, and the light scattering was detected at the same time as well. After being stained, assay of the sample should be completed within 24 h.

The Qualitative Detection of Cell Apoptosis by Hoechst-PI Double Staining. Double staining solution was prepared as follows: to 50 mL of Hoechst 33342 stock solution (1 mg/mL), 950 μL of 1× binding buffer was added to obtain the final concentration of 50 μg/mL of Hoechst 33342 working solution. To 50 μL of PI stock solution (1mg/mL), 950μL of 1× binding buffer was added to obtain the final concentration of PI solution of 50 g/mL. The staining solutions were stored at 4C away from light.

Detection of apoptotic cells with fluorescence microscope: HCT-15 cells at logarithmic growth phase were seeded in six-well plates and cultured overnight. After overnight cultivation, the culture medium was discarded. The complete media containing different concentrations of DNAKO-20 were added. After the cells were cultured for 24 h, the culture medium was aspirated and the cells were washed with PBS twice. Both Hoechst33342 and PI staining solutions were added and incubated at 37C for 15 min away from light. The cells were visualized under fluorescent microscope.

Quantitative Detection of Apoptotic Cells by Flow Cytometry. The cell culture solution was transferred to a centrifuge tube and washed with PBS, trypsin was added to digest cells. When the digestion was completed, cell culture medium was collected on the last step and used to terminate the digestion. The detected cells were transferred to centrifuge tubes, centrifuged at 1,000 × g for 5 min. The supernatant was discarded. The cells were suspended with PBS and counted.

Approximately 5–10 × 10^4 cells were taken and centrifuged at 1,000 × g for 5 min. The supernatant was discarded and 195 μL of Annexin V-FITC solution was added to re-suspend cells. About 5 μL of Annexin V-FITC solution was added and gently mixed. Then 10 μL of PI staining solution was added and gently mixed. The mixed double staining solution was incubated at room temperature for 10–20 min and placed on the ice away from light. The cell samples were detected with flow cytometry

TABLE 2. THE BIOCHEMICAL COMPOSITIONS AND THEIR CONTENTS OF NIAOWANGZHONG GREEN TEA*

Parameters	TPs†	TFAA	WEs	Caff	TB	TP	TFS
Niaowangzhong green tea	28.18 ± 0.18	28.18 ± 0.18	36.26 ± 0.17	3.18 ± 0.01	0.12 ± 0.00	0.02 ± 0.00	0.83 ± 0.01
Guiding Fuding Dabai cha	28.01 ± 0.02	2.27 ± 0.01	2.27 ± 0.01	3.01 ± 0.02	3.01 ± 0.02	0.04 ± 0.00	0.88 ± 0.02
Duyun Fuding Dabai cha	27.71 ± 0.01	1.83 ± 0.01	1.83 ± 0.01	2.52 ± 0.02	2.52 ± 0.02	trace	0.94 ± 0.01

Note: Data shown are the average value of three trials in triplicate and expressed as the mean with standard deviation (SD).

*g/100 g on dry weight basis.

†TPs, tea polyphenols; TFAA, total free amino acids; WEs, water extracts; Caff, caffeine; TB, theobromine; TP, theophylline; and TFS, total flavonoids.

through dual-channel (FITC channel and PI channel, or FL1-H channel and FL2-H channel) and all the samples were detected within 1 h.

Animal Experiments for Antitumor Activity *In Vivo*. When the cells were normally cultivated to the required number, the cell concentration was adjusted to 1×10^7cells/mL with PBS. The cells were inoculated into the right axillary subcutaneous of mice (0.2 mL/mouse). At 24 h after inoculation, the mice were randomly divided into the drug group, the positive group and the control group with five mice per group. The body weight of each mouse was recorded. Each of the prepared Niaowangzhong green tea extract solution (0.2 mL/mouse) was infused into the stomach of mice. The injection of Niaowangzhong green tea extract solution was continued consecutively for 10 days. At 24 h after the last administration, mice were weighted and then killed via cervical dislocation. The transplanted tumors were removed, weighted and photographed.

The tumor inhibition rate was calculated using the following formula:

$$\text{Tumor inhibition rate (\%)} = (\text{the tumor weight of the control group} - \text{the tumor weight of the drug group}) / \text{the tumor weight of negative control group} \times 100\%$$

Statistical Analysis. Microsoft excel was used to analyze the collected data. The significance of the difference in each parameter between the treatment group and the control group was examined by student *t*-test. The difference between groups with $P < 0.05$ was considered statistically significant, in the generated graphs marked "*"; the difference between groups with $P < 0.01$ was considered highly significant, in the generated graphs labeled as "* *"; The difference between groups with $P < 0.001$ was considered highly significant, in the generated graphs labeled as "* * *."

RESULTS AND ANALYSIS

Biochemical Compositions of Niaowangzhong Green Tea

Analysis of Biochemical Components. The biochemical components of both Niaowangzhong green tea, Guiding Fuding Dabai cha and Duyun Fuding Dabai cha were analyzed. The major biochemical components and their relative contents based on 100 g dry weight are presented in Table 2. Compared to the contents of these biochemical compositions in different varieties of green tea growing in the same location, the contents of tea polyphenols (TPs), water extracts (Wes), caffeine (Caff) and theobromine (TB) of Niaowangzhong green tea were higher than those of Guiding Fuding Dabai cha, which were increased by 0.6, 0.8, 5.65 and 9.09%, respectively. Compared to the contents of these biochemical compositions in different varieties of green tea growing in other location, the contents of tea polyphenols (TPs), total free amino acids (TFAA), water extracts (Wes), caffeine (Caff) and theobromine (TB) of Niaowangzhong green tea were higher than those of Duyun Fuding Dabai

TABLE 3. CONTENTS OF CATECHINS IN NIAOWANGZHONG GREEN TEA*

Parameters	EGCG†	GCG	ECG	CG	C	EC	GC	EGC
Niaowangzhong green tea	5.00 ± 0.07	0.80 ± 0.01	0.98 ± 0.03	0.27 ± 0.00	0.19 ± 0.00	0.57 ± 0.00	1.27 ± 0.02	2.66 ± 0.03
Guiding Fuding Dabai cha	4.96 ± 0.01	1.17 ± 0.02	1.15 ± 0.11	0.39 ± 0.01	0.19 ± 0.00	0.62 ± 0.01	1.13 ± 0.11	2.45 ± 0.01
Duyun Fuding Dabai cha	4.88 ± 0.01	0.47 ± 0.01	1.12 ± 0.02	0.24 ± 0.00	0.04 ± 0.00	0.70 ± 0.01	0.52 ± 0.01	2.46 ± 0.10

Note: Data are the average values of three trials in triplicate and expressed as mean with standard deviation (SD) less than 0.05%.

*g/100 g on dry weight basis.

†EGCG, epigallocatechingallate; GCG, gallocatechingallate; ECG, epicatechingallate; CG, catechingallate; C, catechin; EC, epicatechin; GC, gallocatechin; and EGC, epigallocatechin.

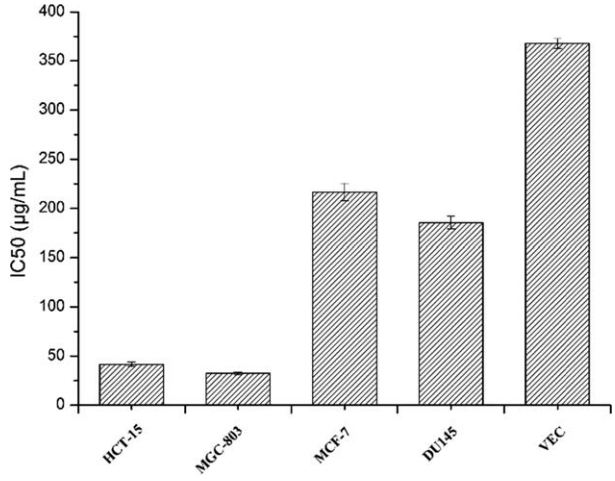


FIG. 1. CYTOTOXIC EFFECT OF DMAKO-05 ON CANCER AND NORMAL CELL LINES

cha, which were increased by 1.70, 23.50, 2.34, 26.19 and 50.00%, respectively. These results showed that Niaowangzhong green tea contained abundant bioactive substances.

Analysis of Contents of Catechins

Niaowangzhong green tea contained a number of catechins, including epigallocatechingallate (EGCG), gallocatechingallate (GCG), epicatechingallate (ECG), catechingallate (CG), catechin (C), epicatechin (EC), gallocatechin (GC) and epigallocatechin (EGC). Their total content was 11.73 ± 0.01/100 g dry weight. The contents of these catechins in Niaowangzhong green tea, Guiding Fuding Dabai cha and Duyun Fuding Dabai cha are given in Table 3. Contents of individual catechins in Niaowangzhong green tea were in order from high to low of EGCG>EGC>GC>ECG>GCG>EC>CG>C (Table 3). Compared to the contents of catechins, the contents of EGCG, GC and EGC were higher in Niaowangzhong green tea than in Guiding Fuding Dabaicha, which were increased by 0.80%, 12.39% and 8.57%, respectively. Compared to the contents of catechins, the contents of EGCG, GCG, CG, C, GC and EGC were higher in Niaowangzhong green tea than in Duyun Fuding Dabaicha, which were increased by 2.46, 70.21, 12.50, 375, 144.23 and 20.00%, respectively.

Screening of Antitumor Effects of Niaowangzhong Green Tea in Different Cancer Cell Lines *In Vitro*

Four kinds of tumor cell lines, including human breast cancer cells MCF-7, prostate cancer cells DU145, human colon cancer cells HCT-15 and human gastric cancer cell line MGC-803, as well as one strain of normal cell lines, human VEC, were chosen in this experiment to evaluate the antitumor activity of Niaowangzhong tea extraction *in vitro*. Experimental results are shown in Fig. 1. The cytotoxic effects of Niaowangzhong green tea extraction were stronger on four kinds of tumor cell lines than on normal cell lines. The IC_{50} of normal VECc was 367.9 μM whereas those for MCF-7, DU145, HCT-15 and MGC-803 were 226.7, 184.0, 41.7 and 32.5 μM, respectively. Niaowangzhong green tea extract caused more potent cytotoxic effects on two kinds of digestive tract tumor cells, HCT-15 and MGC-803, than on MCF-2 and DU145 cells. The selective coefficient for HCT-15 and MGC-803 cells reached 8.8 and 11.3, respectively, indicating that the Niaowangzhong green tea extraction is more selective for the digestive tract tumor cells. Therefore, Niaowangzhong green tea extraction possesses quite good selectivity for these types of tumor cells.

Inhibitory Effects on MGC-803 Cells

Since Niaowangzhong green tea extraction displayed the highest selectivity for MGC-803 cells, we conducted more detailed study on the dose- and time-dependent inhibitory

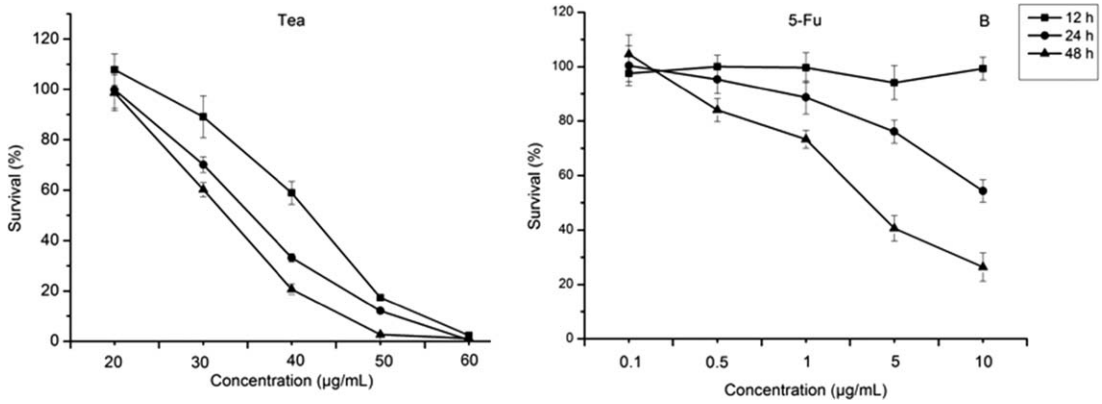


FIG. 2. DOSE- AND TIME-DEPENDENT INHIBITORY EFFECTS OF NIAOWANGZHONG GREEN TEA (A) AND 5-FU (B) ON THE GROWTH OF MGC-803 CELLS DETECD BY USING A MTT ASSAY

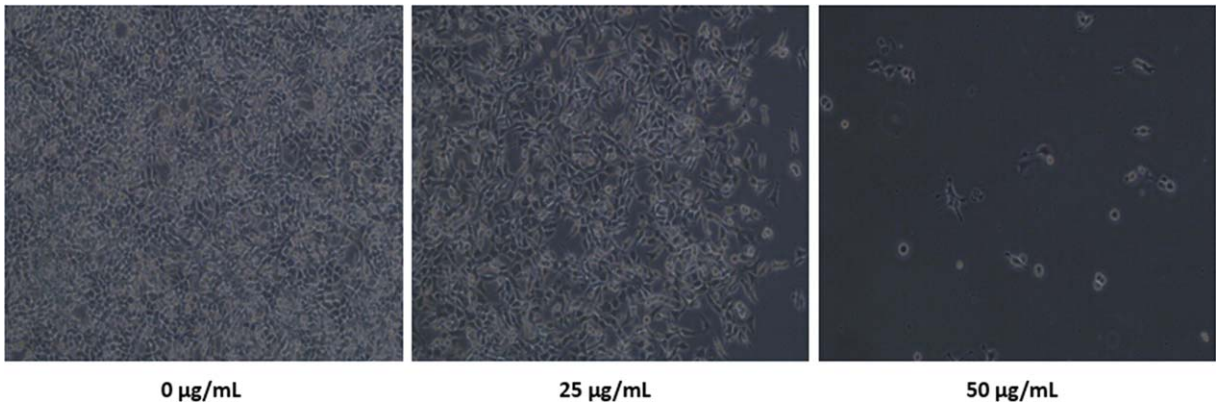


FIG. 3. THE CHANGES IN MORPHOLOGY AND CELL NUMBER OF MGC-803 CELLS CAUSED BY NIAOWANGZHONG GREEN TEA EXTRACT IN 48 H

effects of this tea extract on the growth of MGC-803 cells and compared its effects with that caused by the typical anti-cancer drug, 5-FU. Concentrations of Niaowangzhong green tea extract were set at 0, 20, 30, 40, 50 and 60 μg/mL while those of 5-FU were set at 0.1, 0.5, 1, 5 and 10 μg/mL, respectively. The reaction times were set for 0, 12, 24 and 48 h, respectively for both agents. Figure 2 shows that similar to those of 5-FU in general, the inhibitory effects of Niaowangzhong green tea extract on MGC-803 cells were in a dose- and time-dependent manner. However, there was difference in the time-cause inhibitory effects on cancer cells between 5-Fu and this green tea extract. When MGC-803 cells were exposed in the culture medium containing 5-Fu for the first 12 h, 5-Fu caused no inhibitory effect on MGC-803 cells at the concentrations tested; starting from 24 h, the inhibitory effects of 5-FU on MGC-803 cells were seen in a dose- and time-dependent manner in that the inhibitory effect was increasingly obvious with the increase in its concentration; comparing the inhibitory effects at different treatment time points, inhibitory effect were gradually enhanced at the same concentration of compound with prolonging the action time. Starting from the 12 h, the

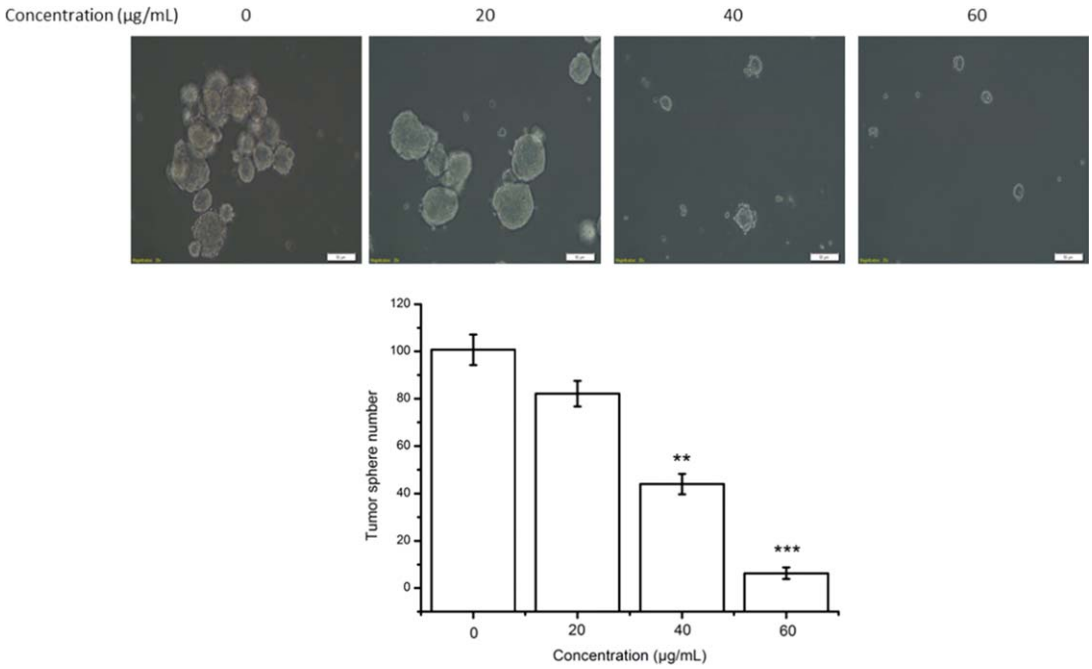


FIG. 4. DOSE-DEPENDENT INHIBITORY EFFECTS OF NIAOWANGZHONG GREEN TEA EXTRACT ON TUMOR SPHERE-FORMATION OF MGC-803 CELLS

Data shown are the mean ±SEM of three independent experiments. $*P<0.05$, $**P<0.01$, $***P<0.001$ vs. control.

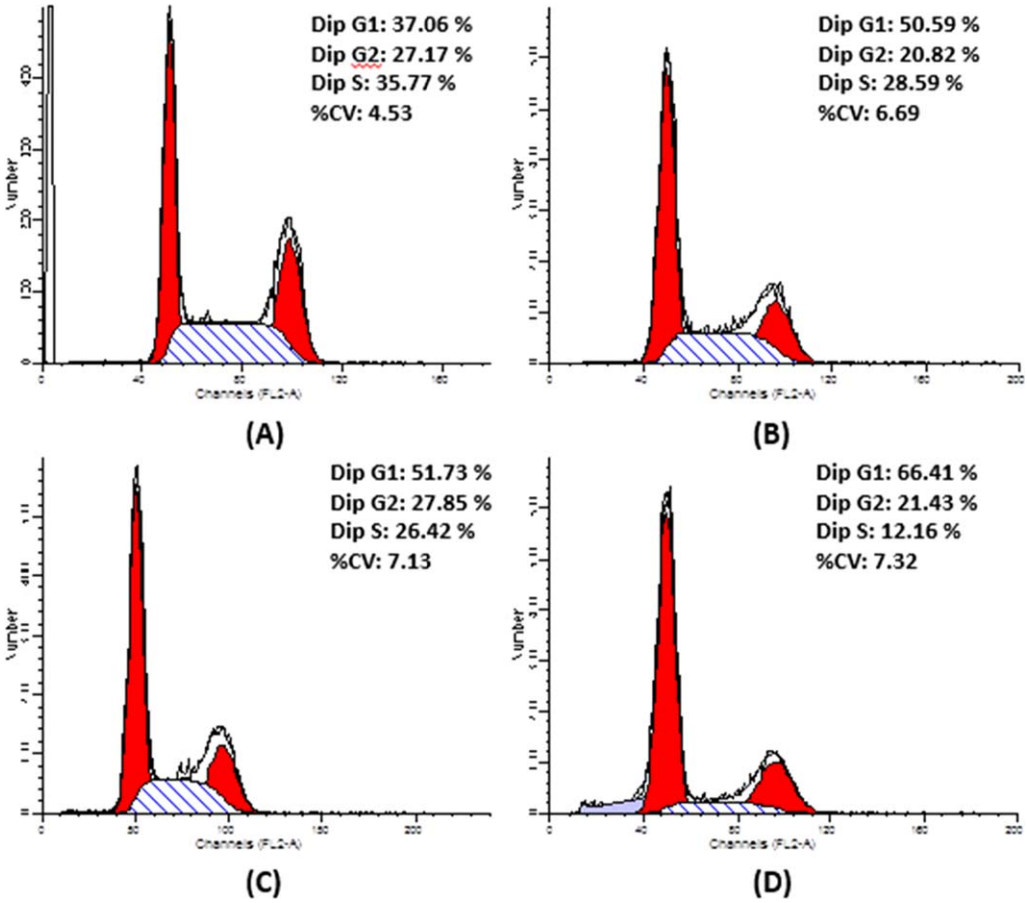


FIG. 5. EFFECTS OF DIFFERENT CONCENTRATIONS (A, 0 μG/ML; B, 20 μG/ML; C, 40 μG/ML; AND D, 60 μG/ML) OF NIAOWANGZHONG GREEN TEA EXTRACT ON CELL CYCLE ARREST IN MGC-803 CELLS.

inhibitory effect of Niaowangzhong green tea extraction was detected in a dose- and time-dependent manner, which almost fully suppressed the proliferation of MGC-803 cells at the concentration of 60 μg/mL. The inhibitory effects were still closely corresponded to the concentration as the extension of treatment time. The results showed that inhibition effect was most significant when the duration of treatment with Niaowangzhong green tea extraction was 48 h. Comparing the inhibitory effects of two agents on MGC-803 cells, inhibitory effect of 5-FU on MGC-803 cells was stronger than that of Niaowangzhong green tea extraction ($IC_{50} = 2.6$ μg/mL), whereas the onset time of inhibitory effect caused by Niaowangzhong green tea extract was earlier than 5-Fu was.

Effects of Niaowangzhong Green Tea Extraction on Cell Growth and Morphology of MGC-803 Cells

As shown in Fig. 3, when the cells were treated without Niaowangzhong green tea extraction (i.e., at 0 μg/mL), their adherent state was in good condition (panel 1), and cells were of tight junction with a clear outline, monolayer and polygon; when treatment concentration was increased to 25 μg/mL, intercellular contact became loose, a part of the cells began to shrivel and to be round or oval. The adherent cells became gradually shedding (panel 2). When treatment concentration was increased to 50 μg/mL, a large number of cells were detached and suspended in medium. Almost all the remaining adherent cells were shrunken and became round. The number of cells was decreased obviously as the concentration of Niaowangzhong green tea extract was increased (panel 3).

Effects of Niaowangzhong Green Tea Extract on Formation of Tumor Spheres of MGC-803 Cells

To further evaluate the antitumor activity *in vitro* of the Niaowangzhong green tea extract on gastric cancer cells MGC-803, we choose the phase of tumor-spheres formation

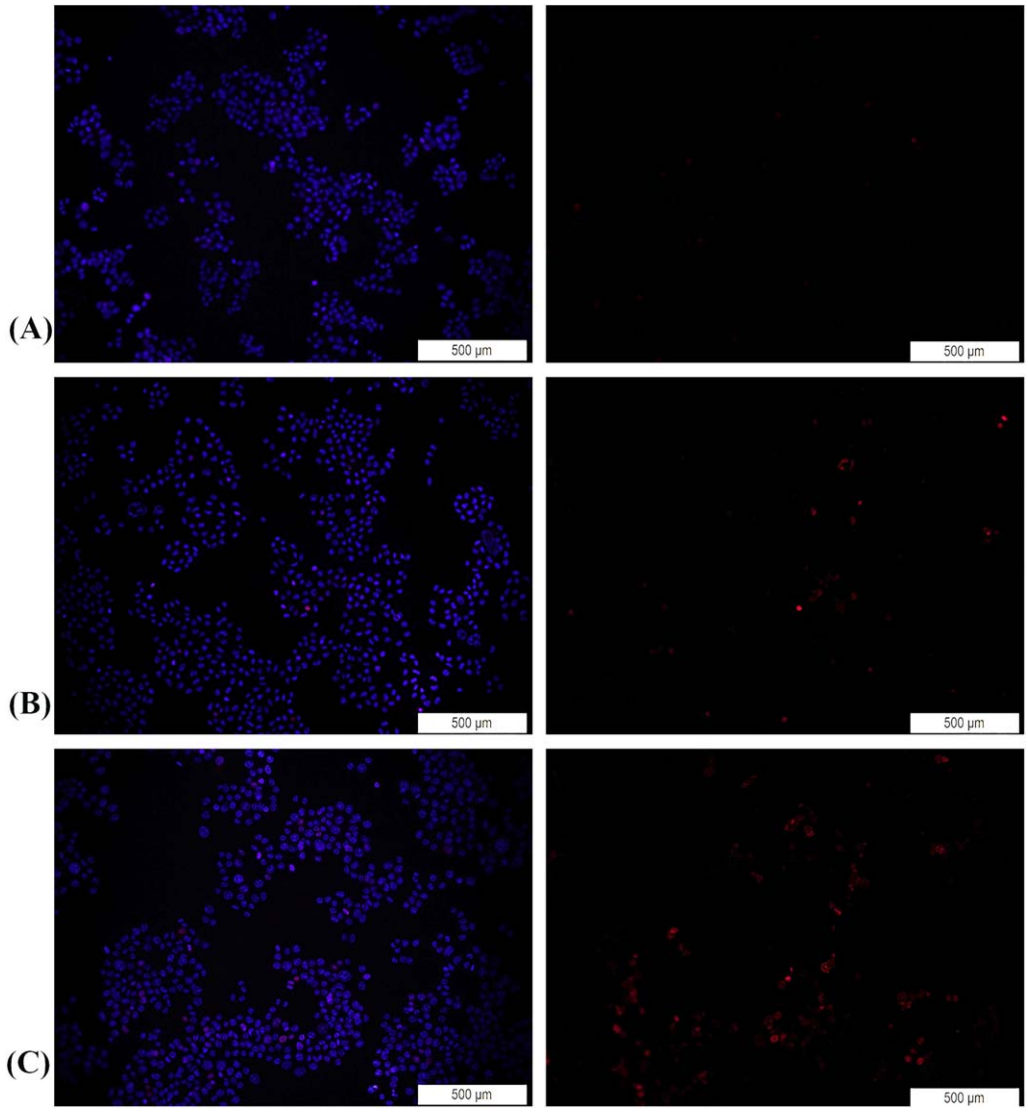


FIG. 6. CELL APOPTOSIS OF MGC-803 TREATED WITH DIFFERENT CONCENTRATION OF TEA (A, 0 μG/ML; B, 30 μG/ML; C, 60 μG/ML) FOR 24 H.

to study the inhibition of tumor stem cells. Tumor stem cells are able to maintain their vitality through self-renewal and unlimited proliferation. While most of bulky tumor cells were eliminated after the conventional treatment, a few cancer stem cells remain unaffected and still keep live. Thus, after a while, tumor cells will recur. As shown in Fig. 4, the inhibitory effect of Niaowangzhong green tea extract on tumor-sphere formation was concentration-dependent. The inhibitory effect was remarkable when treatment concentrations were at 40 and 60 μg/mL, respectively, with 43.9% and 91.1% of inhibition, respectively. These results showed that Niaowangzhong green tea extract have strong inhibitory effect on cancer stem cells and can possibly prevent tumor recurrence after chemotherapy.

Effects of Niaowangzhong Green Tea Extract on Cell Cycle Progression

Fluorescent dye propidium iodide pyridine can emit fluorescence in embedded double stranded DNA. According to the different DNA contents in different stages of cell cycle, the cells can be directly divided into three categories in the histogram shown in Fig. 5. DNA replication in cells at G0 and G1 phases are not initiated and they contain the same ploidy DNA, as a peak shown in the figure; the cells at G2 and M phases have completed DNA replication but are not or are split into two daughter cells, displaying a peak due to tetraploid DNA; the cells at G2 and M phases are distributed between the two peaks and DNA replication in G2 and M phases are distributed between the two peaks and DNA

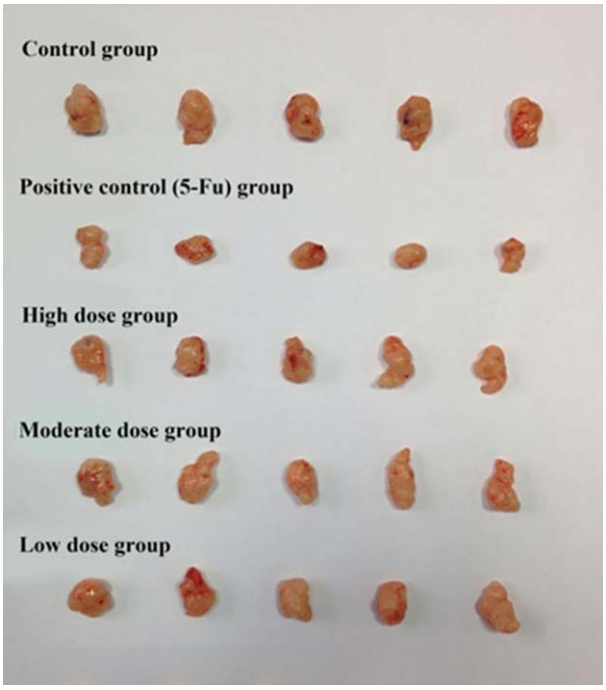


FIG. 7. THE ANTI-TUMOR EFFECT OF NIAOWANGZHONG GREEN TEA EXTRACT TEA ON MGC-803-DERIVED XENOGRAFT TUMOR
Note: Each of five tumors shown was taken out from each of five mice in the each group.

replication is going on in the cells at S phases. From the above we found the percentage of cells in S phase was decreased significantly from 35.77% in the control group to 12.16%, whereas the percentage of cells in G0/G1 phases was increased from 37.06% to 66.41%. The cells in G2/M phase in each group displayed no significant difference, when the concentration reached 1 μM. Figure 5 suggests that the cellular DNA might be damaged and the cell cycle cannot pass through G1 DNA damage checkpoint and the cells were arrested at the S phase. These cells may initiate apoptosis program after an attempt to repair the damaged DNA unsuccessfully.

Effects of Niaowangzhong Green Tea Extract on Induction of Cell Apoptosis

Little Hoechst dye can internalize into normal cells through their intact membrane, when normal cells were stained with Hoechst dye, a pale blue circle appeared after combining with nuclear DNAs, with darker blue granules. When the permeability of apoptotic cell membrane increased, more Hoechst dye entered into apoptotic cells than into normal cells, the fluorescence intensity was higher in apoptotic cells than in normal cells. At the same time, the function of P-glycoprotein pump of the apoptotic cell membrane was destroyed and the dye cannot be expelled out of the cell, leading to dye accumulation and enhancement of blue fluorescence. PI was the DNA-binding dye unable to pass through the intact membrane, so live cells refused to PI dye. At the late apoptotic cells, because the cell membrane was damaged, the nucleus can be stained red by PI. When Fig. 6 was contrasted, differences between the different treatment groups can be found in that the negative control group without adding tea extraction, only darker blue fluorescence was seen after cultured for 24 h and the cell morphology was not changed, almost without red fluorescence. With the increase in tea concentration, more cells showed blue fluorescence and red fluorescence. In Hoechst staining images, it can be seen obviously that the cells were contracted and the number of bright blue cells was increased whereas the control normal cells showed low blue and low red or the red cells did not appear. In contrast, high blue and low red cells were seen in early apoptotic cells; and low blue and high red was the characteristic color of the late apoptotic cells. The specific apoptosis data obtained by flow cytometry are shown in Table 4. When the staining and flow cytometric analysis results were combined, it can be clearly seen that in the MGC-803 cells treated with different concentrations of tea extraction, early apoptosis and late apoptotic cells showed rising trend.

Antitumor Activity *In Vivo* of Niaowangzhong Green Tea Extract

After an *in vivo* xenograft model with gastric cancer MGC-803 cells was established in nude mice, the anti-tumor efficacy of this green tea extract was evaluated at the dosages of 0, 100, 250 and 500 mg/kg/day, respectively, in three groups. The dosage for positive anticancer compound 5-FU was 25 mg/kg/day. The drugs were intragastrically administrated. It can be clearly seen from Fig. 7 and Table 5 that with the increase in dosage, the volume of MGC-803-derived tumor was decreased gradually, indicating that the inhibitory effects of the compound on the proliferation of MGC-803 gastric cancer xenografts *in vivo* are increased gradually. The inhibition rate of tumor of the high dose treatment group was 31.0%, which was significantly different from that of the control group.

While inhibitory effect of 5-Fu on tumor was stronger than that of green tea extract (inhibition rate reached 71.5%), the body weight of nude mice of the 5-Fu group was

TABLE 4. THE EFFECTS OF DIFFERENT CONCENTRATIONS OF TEA ON APOPTOSIS OF MGC-803 CELLS

	Apoptosis rate (%)	
Concentration (μg/mL)	Early apoptosis rate	Late apoptosis rate
0	4.83 ± 0.53	5.54 ± 0.80
30	9.72 ± 0.68	6.38 ± 0.47
60	20.64 ± 1.21	17.18 ± 2.02

TABLE 5. THE INHIBITORY EFFECT OF TEA EXTRACT ON THE GROWTH OF MGC-803-DERIVED XENOGRAFT TUMOR

		Weight (g)			
Group	Dose (mg/kg day)	Pre-dose	Post-dose	Volume of tumor (mm^3)	Inhibition ratio (%)
Control group	0	19.3 ± 1.1	25.9 ± 1.0	853.4 ± 92.6	–
Positive group	25	19.6 ± 0.9	14.0 ± 1.0***	242.8 ± 37.1**	71.5
High-dose group	500	18.8 ± 0.6	25.4 ± 0.4	589.1 ± 45.6*	31.0
Moderate-dose group	250	19.7 ± 0.3	24.5 ± 0.5	721.4 ± 58.8	15.5
Low-dose group	100	20.0 ± 0.8	25.3 ± 1.0	742.4 ± 65.2	13.0

Note: The data presented in Table 5 are expressed as mean ± standard deviation (Mean ± SD). Significant difference was tested by *t*-test (Student's *t*-test), significant difference with the negative control group was indicated by $*P < 0.05$, $**P < 0.01$, $***P < 0.001$, respectively.

lighter than that of the blank control, and the symptoms of diarrhea occurred in the nude mice during the period of the experiment. Furthermore, the amounts of food and water consumed were also lower than those of the other groups, and the physical condition and activities of these mice were very poor. Meanwhile, there was no significant difference in body weight between the tea extract treatment group and the control group with the same condition of nude mice. Therefore, the tea extraction can significantly inhibit the growth of MGC-803 xenograft tumor without causing obvious toxic side effect.

DISCUSSIONS

In the present study, we investigated both the *in vitro* and *in vivo* anti-tumor effects of Niaowangzhong green tea extract on four different kinds of human tumor cell lines and compared them with to those on one normal cell line. We found that this tea extract caused strong inhibitory effect on tumor cells without significant inhibitory effects on normal cells. Our results showed that same as that of human cells, the IC_{50} value of tumor cell lines MGC-803, the most sensitive to this green tea extract, was 32.5 μM, while the IC_{50} value of normal VECs was 367.9 μM, and the selection coefficient for tumor cells was 11.3, showing a quite good selectivity for tumor cells, and the selection coefficient between the tumor cell MGC-803 and the breast tumor cells MCF-7 ($IC_{50} = 226.7$ μM) reached 8.2, reflecting that the compound is more selective for digestive track tumor cells. The inhibitory effects of this tea extract on MGC-803 cells were dose- and time-dependent, and the onset of inhibitory effect caused by this tea extract occurred earlier than that caused by the anti-cancer drug, 5-Fu.

The analytic results on cell cycle progression of MGC-803 cells treated with different concentrations of Niaowangzhong green tea extract with a flow cytometry showed that with increase in its concentration, a large number of cells were arrested at G0/G1 phases, indicating that cellular DNA of cancer cells may be damaged by this tea extract before the S phase. The p21 protein can be activated through p53-dependent and p53-independent pathways and the activated p21 binds to cyclin-dependent kinase (CDK)-Cyclin and inhibits its function, then arrests the cell cycle at G1 phase so that the damaged cells will have sufficient time to be repaired. In this study, we did not examine whether this tea extract affects the activities of p21, p53 and CDK-cyclins, more studies are needed to determine whether the inhibition of Niaowangzhong green tea extract on cell cycle progression are mediated via p21-p53-CDK-Cyclins cascade or by other pathways. Furthermore, we also qualitatively and quantitatively analyzed the apoptotic cells double stained by Hoechst 33342 and PI with fluorescence microscopy and flow cytometry, respectively. We found that the proportions of the early and late apoptotic cells were increased with the increase in the concentration of this tea extract. Therefore, we judged that MGC-803 cells were induced by the Niaowangzhong green tea extract to initiate apoptosis program, leading to cell death. The detailed cellular and molecular mechanisms underlying the induction of apoptosis by this green tea extract need to be further investigated.

We examined the anti-tumor effects of Niaowangzhong green tea extract with *in vitro* experiment by testing its inhibitory effects on proliferation of four types of tumor cell lines. The results showed that this green tea extract caused inhibitory effect on the proliferation of all four types of tumor cells to different extents with a better selectivity toward human colon cancer cells HCT-15 and human gastric cancer cell line MGC-803 cells. MGC-803 cells were the most sensitive cells to the tea extract. This green tea extract could significantly inhibit the tumor-sphere formation of the cell line in the tumor-sphere forming experiment, and showed strong inhibition on the proliferation *in vitro* experiments. We transplanted the MGC-803 cells into nude mice to form a tumor and tested the inhibitory effects of this green tea extract on the xenograf tumors. This tea extract still showed a quite strong inhibition on tumor cell proliferation with the inhibition rate being increased with the increase of the dosage. The significant inhibition was found in the dosage of 500 mg/kg/day. More importantly, unlike the mice in 5-Fu group, which appeared diarrhea, ate less and displayed notable weight loss and other symptoms, the nude mice treated with DMAKO-20 at each of these dose

groups did not show any abnormal symptoms and their body weights were similar to that of the control group, indicating that this green tea extract did not cause obvious toxic side effects at the dosages tested. This can be the favorable attribute for this green tea extract in potentially treating patients with cancers.

While the precise reasons for the potent anti-cancer effects of this green tea extract are not clear in the present study, its potent anti-cancer effects may be related to the presence of relatively higher levels of polyphenols, alkaloids and other effective components with anti-cancer activity in this tea extract. Our analysis indicated that this green tea extract contained as high as 28.18 ± 0.18 polyphenols/100 g dry weight, this level of polyphenols is higher than that of Guiding Fuding Dabai cha which grew in the same location and Duyun Fuding Dabai cha, and is comparable with those in other types of green tea plants growing in other places (Liu *et al.* 2012; Dong 2014; Zhao 2014). It has been known that tea polyphenols can selectively inhibit tumor cell growth, induce the apoptosis and cell cycle arrest by inhibiting specific receptor tyrosine kinase activity of tumor cell and downstream signaling pathways (Shimizu *et al.* 2011), blockage of the NF-B signaling pathway (Khan and Mukhtar 2008), decrease of proteasome activity (Dou 2009), inhibition of matrix metalloproteinase activity and DNA methylation of multiple targets (Chen and Zhen 2013). In addition, alkaloids can inhibit tumor cell division and proliferation in general by the direct destruction of tumor cells or interfere with the mitotic phase of the cell cycle. The antitumor effects of flavonoids are mainly expressed in the aspects of cell proliferation, cell apoptosis and the enhancement of tumor suppressor gene activity and the inhibition of expression of tumor genes. Polysaccharides achieve their antitumor effects mainly through their regulation of the immune system in a number of ways (Xu *et al.* 2008). The tea contains rich tea polyphenols, alkaloids, flavonoids compounds and polysaccharides (Miketova *et al.* 1996 ; Wu and Wei 2002; Wu *et al.* 2014). Our analysis of the biochemical components of Niaowangzhong green tea extract indicated that this green tea extract contained relatively higher levels of tea polyphenols, alkaloids, flavonoids compounds and polysaccharides. Therefore, the strong *in vitro and in vivo* inhibition on tumor cells by Niaowangzhong green tea extract are likely mediated through the synergic effects of a variety of anti-cancer compounds present it, which may resolve drug resistance caused easily by the single compound in cancer prevention and thus, can be superior to the individual chemo-preventive agent.

More importantly, in the present study, we found that this green tea extract had potent inhibitory effects on the formation of tumor-spheres derived from MGC-803 gastric cancer cells. Tumor-sphere is initiated, formed and developed from the proliferation of a single cancer stem/progenitor cell. Cancer stem cells have been regarded as the root of tumor formation and recurrence. The inhibitory effects caused by this green tea extract on the tumor sphere-formation of MGC-803 gastric cancer cells suggest that it may have the potential capability of inhibiting cancer stem cells. Currently, most of the anti-cancer drugs kill the bulk of the tumor but have no effective inhibition on cancer stem cells, leaving cancer stem cells behind. Therefore, the agents capable of specifically targeting this cancer initiating cell population may have potential of clinical implications. If Niaowangzhong green tea extract possesses the inhibitory effects on cancer stem cells, it may have a potential role in future anticancer therapy by eliminating the cancer stem cells.

Moreover, this study has indicated that green tea extract caused stronger cytotoxic effects on two kinds of digestive tract tumor cells HCT-15 and MGC-803, suggesting that as one of the most popular medicinal beverages, this green tea extract may be more suitable for treating digestive tract cancers since it can be more accessible to the locations of digestive and intestinal tracts. Therefore, this specific green tea merits further depth study on underlying mechanisms at the cellular and molecular levels and further development for potential medical application and dietary practices for prevention of cancers, especially for digestive and intestinal tracts.

CONCLUSIONS

1. Niaowangzhong green tea extract can selectively and potently inhibit the proliferation of human gastric cancer cell line MGC-803 *in vitro* in a dose -and time-dependent manner, with IC_{50} values of 32.5 μM and the selection coefficient of 11.3, as compared with those of normal cells;
2. Niaowangzhong green tea extract can induce both MGC-803 cell cycle arrest in G0/G1 phase, leading to cell apoptosis;
3. Niaowangzhong green tea extract is capable of inhibiting the formation of tumor-spheres derived from MGC-803 cells, suggesting its potential capability of eliminating cancer stem cells;
4. When being administered in a dose of 500 mg/kg/day, Niaowangzhong green tea extract could significantly inhibit the growth of transplanted xenograft tumor derived from MGC-803-cells without obvious toxic side effects.

Therefore, it is worth to conduct further in-depth study on cellular and molecular mechanisms underlying the anti-cancer effects of this green tea extract and on further developing its anti-cancer and other medical applications.

ACKNOWLEDGMENTS

This study was financially supported by Fu Jian Province "2011 Collaborative Innovation Center" Chinese Oolong Tea

Industry Innovation Center Special Project (J2015-75); The Research on the Innovation and Utilization of New Tea Germplasm for Cold Resistance in Guangdong (2013B020201003); Selection and Breeding of New Varieties of Specific Tea Resources in Guangdong (2015B020202007).

REFERENCES

BATEMAN, N.W., SUN, M.B., HOOD, L., FLINT, M.S. and CONRADS, T.P. 2010. Defining central themes in breast cancer biology by differential proteomics: Conserved regulation of cell spreading and focal adhesion kinase. J. Proteome Res. *9*, 5311–5324.

BOMKEN, S., FISER, K., HEIDENREICH, O. and VORMOOR, J. 2010. Understanding the cancer stem cell. Br. J. Cancer. *103*, 439–445.

CHEN, S.Z. and ZHEN, Y.S. 2013. Molecular targets for tea polyphenols and its role in the treatment of anti-tumor drug experiments. J. Med. *48*, 1–7.

CHEN, J.G., ZHU, J., ZHANG, Y.H. and LU, J.H. 2011. Cancer survival in Qidong, China, 1992–2000. IARC Sci. Publ. *162*, 43–53.

CHEN, J.G., EGNER, P.A., NG, D., JACOBSON, L.J., MUNOZ, A., ZHU, Y.R., QIAN, G.S., WU, F., YUAN, J.M., GROOPMAN, J.D., ET AL. 2013. Reduced aflatoxin exposure presages decline in liver cancer mortality in an endemic region of China Cancer Prev. Res. *6*, 1038–1045.

DALLUGE, J.J., NELSON, B.C. and BROWN, T.J. 1998. Selection of column and gradient elution system for the separation of catechins in green tea using high-performance liquid chromatography. J. Chromatogr. *2*, 265–274.

DONG, Y.L. 2014. Study on the main taste and aroma compounds of Mending Ganlu tea. Food Sci. *35*, 158–163.

DOU, Q.P. 2009. Molecular mechanisms of green tea polyphenols. Nutr. Cancer. *61*, 827–835.

FERLAY, J., SHIN, H.R., BRAY, F., FORMAN, D., MATHERS, C. and PARKIN, D.M. 2010. Estimates of worldwide burden of cancer in 2008: GLOBOCAN 2008. Int. J. Cancer. *127*, 2893–2917.

FORESTER, S.C. and LAMBERT, J.D. 2011.The role of antioxidant versus pro-oxidant effects of green tea polyphenols in cancer prevention. Mol. Nutr. Food Res. *55*, 844–854.

FRIEDMAN, M., MACKEY, B.E., KIM, H.J., LEE, I.S., LEE, K.R., LEE, S.U., KOZUKUE, E. and KOZUKUE, N. 2007. Structure–activity relationships of tea compounds against human cancer cells. J. Agric. Food Chem. *55*, 243–253.

HE, Y.M., PENG, L., LI, C.R., LI, J.X., HUANG, H.L., QIAO, X.Y., YAN, C.Y., WU, H.L., YE, C.X. and SONG, X. H. 2011. Research on the biochemical ingredients of cultivated varieties of cocoa tea. Guangdong Agric. Sci. *6*, 10–13.

KHAN, N. and MUKHTAR, H. 2008. Multitargeted therapy of cancer by green tea polyphenols. Cancer Lett. *269*, 269–280.

LIU, C., ZHANG, L., LIU, J., LIU, J.L. and LI, B.Y. 2012. Simultaneous differmination of four kinds of catechins and caffeines of Biluochun tea by RP-HPLC. J. Anhui Agric. Sci. *40*, 7425–7427.

LU, Y.G., ZHANG, H., MENG, X.Y., WANG, L., GUO, X.N., and TAO, G.J. 2009. Determination of glutamate decarboxylase activity in plant by pre-column 30 derivatization with 2, 4-dinitrophenylhydrazine. Chin. J. Anal. Chem. *37*, 347–350.

MIKETOVA, P., SCHRAM, K.H., WHITNEY, J. L., KERNS, E.H., VALCIC, S., PAN, H.M., ZHENG, S. and WU, J.M. 1996. The preventive effect of tea and tea polyphenols on tumor. Cancer *16*, 46–49.

REYA, T., MORRISON, S.J., CLARKE, M.F. and WEISSMAN, I.L. 2001. Stem cells, cancer, and cancer stem cells. Nature *414*, 105–111.

SENANAYAKE, S.P.J.N. 2013. Green tea extract: Chemistry, antioxidant properties and food applications—a review. J. Funct. Foods. *5*, 1529–1541.

SHIMIZU, M., ADACHI, S., MASUDA, M., KOZAWA, O. and MORIWAKI, H. 2011. Cancer chemoprevention with green tea catechins by targeting receptor tyrosine kinases. Mol. Nutr. Food Res. *55*, 832–843.

The Third National Cause of Death in China. 2008. China Cancer *5*, 344–345.

WU, C.D. and WEI, G. 2002. Tea as a functional food for oral health. Nutrition *18*, 443–444.

WU, C.L., HUANG, Y.H., LAI, X.F., LAI, R.H., ZHAO, W.X., ZHANG, M., and ZHAO, W.F. 2014. Study on quality components and sleep-promoting effect of GABA Maoyecha tea. J. Funct. Foods. *7*, 180–190.

XU, X.D., HU, X.R., and YANG, J.S. 2008. Antitumor activein gredients of medicinal plants research. J. Chin. Tradit. Med. *33*, 2073–2081.

YANG, C.X. 1988. Study of the history of Guizhou Miao "Yuwu Tea". Agric. Archaeol. *1*, 180–190.

ZHANG, Q.Q., ZHOU, F.Y., YANG, C., ZHANG, Z.Q. and HU, J.Q. 2015. Diversity analysis of economical character and quality traits of Guiding Niaowangzhong. Mol. Plant Breed. *2*, 415–423.

ZHAO, X.T. 2014. Study on the differences and similarities of aroma and taste of Longjing tea in three producing areas. Inst. China Meas. 47–49.

ZHAO, B., GE, J.F., ZHU, J.J., HUANG, X.H., and LI, J. 2007. The discussion in the inhibition rate measured by MTT method to calculate IC_{50} proliferation. J. Anhui Med. Pharm. *9*, 834–836.

ZHAO, X., WANG, Q., LI, G.J., CHEN, F., QIAN, Y., and WANG, R. 2013. *In* vitro antioxidant, anti-mutagenic, anti-cancer and anti-angiogenic effects of Chinese Bowl tea. J. Funct. Foods. *7*, 590–598.


现代食品科技
07
MODERN FOOD SCIENCE AND TECHNOLOGY
2020 JUL
·中文核心期刊·中国科技核心期刊·RCCSE中国核心学术期刊·SCOPUS/CSA/FSTA/IC收录期刊
第36卷 月刊
现代食品科技
第三十六卷 第七期
二〇二〇年七月
华南理工大学主办

1985 年创刊
国内外公开发行
2020 年第 36 卷第 7 期(总 251 期)
Monthly (Start Publication in 1985)
Vol.36, No.7, 2020

主　编　李琳
副主编　李晓玺(常务)　张学武
　　孙东晓　　唐传核
　　孙为正
编辑部主任　古志平
编辑部常务副主任　赖富饶
主　办　华南理工大学
承　办　华南理工大学食品科学与工程学院
编辑出版　《现代食品科技》编辑部
发　行　本刊编辑部
地　址　广州五山华南理工大学麟鸿楼 508 房
邮政编码　5106410
电　话　(020)87112532　87112373
　　87113352
投稿系统　http://xdspkj.ijournals.cn
责任编辑　闵　甜　王　婷
英文编辑　李晓凤　尹寿伟
网络编辑　文　羽　孙　旭
印　刷　广州市东盛彩印有限公司
出版日期　2020 年 7 月 20 日
邮发代号　46-349
国内统一刊号　CN 44-1620/TS
国际标准刊号　ISSN 1673-9078
定　价　40 元/期　480 元/全年

声明

本刊已许可中国学术期刊(光盘版)电子杂志社在中国知网及其系列数据库产品中,以数字化方式复制、汇编、发行、信息网络传播本刊全文。该社著作权使用费与本刊稿酬一并支付。本刊所刊发的文章,其专有出版权和网络传播权等所有版权即授予本刊,但作者仍享有非专有使用权。作者向本刊提交文章发表的行为即视为同意上述声明。如有异议,烦请来稿时予以申明。

现代食

目　次

食品营养

发酵糙米乙醇提取物改善 3T3-L1 脂肪细胞糖脂代谢
……宋家乐,曾榛,钱波,桂中玉,朴建荣,谭兴勇(1)
人参皂苷 F2 干预 Caspase 级联反应抑制 H_2O_2 诱导的细胞凋亡
……刘迪,张浩,张寒雪,孙宏宇,郑美玉,冯宪敏(11)
亚麻籽油对多囊卵巢综合征大鼠胰岛素抵抗和氧化应激的保护作用
……汪婷,张晓霞,李一唯,岳江东,田红艳,翁欣,刘萍,董幼平,王浩(17)
刺梨果酒通过胰岛素介导的 PI3K 途径改善 1-型糖尿病大鼠机体糖代谢紊乱
……安玉红,陆敏涛,卢秀,黎代余,黄燕,彭永贤(25)
诸葛菜种子水提物激活 AMPK/AKT/GSK-3β 通路保护对乙酰氨基酚诱导的小鼠急性肝损伤
……庞航,单宇,王菲菲,杨淑贤,李文勇,曹丽(34)
柑普提取物对 HepG2 和 SGC-7901 肿瘤细胞系的抗增殖作用
……俞乐安,肖遂,黄亚辉,李小晓,赖惠清,郑意,梁大华,张旭(42)
锦南复方对 2 型糖尿病大鼠血糖的辅助调节作用
……尹志强,汤海莲,姜泽昆,焦宇知(50)
甜菜红素对厌食症大鼠胃肠道功能的改善作用
……周国(57)

生物工程

GPD1 过表达调控葡萄酒酵母酒精和风味物质的生成量
……高莹莹,李凭,李彤,林良才,张翠英(63)
比较传统老面中戊糖片球菌的代谢活性与亲缘关系
……龚云霞,齐小保(70)
北部湾茅尾海副溶血性弧菌的分离鉴定与致病性分析
……唐金利,李晓丽,陈星,赵华显,李楠(75)

食品生化

铁皮石斛低温干燥抑制其水溶性多糖的聚合反应
……邢丽,马厚雨,江凌,缪冶炼(88)
不同品种紫薯的质构特征比较
……牛丽影,万玉炜,李大婧,刘春泉,宋江峰,谢一芝(96)

品 科 技

核桃粕乙醇提取物降脂活性的谱效关系
.....王祖坤,马雅鸽,杨婧娟,张希,赵声兰(105)
水生蔬菜提取物的抗氧化活性分析及其对菜籽油的抗氧化作用
.....徐筱莹,胡晓潇,单恬恬,易阳,王宏勋,王丽梅(113)
胡萝卜干燥加工过程中维生素含量的变化规律
.....王秋玉(120)

贮藏保鲜

生湿面的气调包装-辐照协同保鲜
.....欧阳梦云,王燕,孙子钦,吴卫国,赵传文,曹胜(125)
二氧化硫对葡萄采后有机酸含量及苹果酸代谢途径的调控作用
.....闫波雯,袁宇尧,魏佳,张政,张健,吴斌(133)
抗菌肽壳聚糖复合膜对水果黄瓜的保鲜作用
.....罗雪云,吴晓彤,谢颖思,弓佳卉,梁嘉妍,段星星,陈军丽,等(142)
山苍子精油结合 1-MCP 处理对杨桃的保鲜效果
.....林媛,林莹,蔡婷(150)
不同品种龙眼采后品质及贮藏特性的比较
.....武泽爽,陈晓东,罗森,吴振先,韩冬梅(157)

食品加工

不同酚酸对三华李清汁贮藏期间色泽稳定性的比较分析
.....李依娜,邹颖,余元善,肖更生,徐玉娟,邹波(165)
酶解发酵酸肉制备抗氧化肽的工艺优化
.....吴慧琳,李苗云,朱瑶迪,赵改名,郝云鹏,任宏荣,马阳阳,等(173)
藜麦-小麦粉的流变学特性及其面条研制
.....梁霞,孟婷婷,周柏玲,田志芳,任元(184)
连翘苷的提取工艺优化及其抑菌活性
.....张俊顺,骆嘉原,姜喆卉,包怡红,包洪涛(193)
大豆蛋白酶解产物的微胶囊化及理化性质表征
.....黄晓梅,韦翠兰,侯俊杰,王忠合,骆兆娇,王金梅(202)
甜玉米馒头的加工工艺优化
.....张康逸,王慧洁,张国治,康志敏,宋江峰(209)
干酪乳杆菌发酵番茄酸汤的工艺优化
.....郑莎莎,胡萍,王晓宇,田亚,徐俐,丁筑红,杨晓玲,李娟,等(218)



- 中文核心期刊
- 中国科技核心期刊
- RCCSE 中国核心学术期刊
- 荷兰《SCOPUS》数据库收录期刊
- 英国《食品科学技术文摘》(FSTA)收录期刊
- 美国《化学文摘》(CA)收录期刊
- 美国《剑桥科学文摘》(CSA)收录期刊
- 美国《乌利希期刊指南》收录期刊
- 哥白尼索引(IC)收录期刊
- 英国《国际农业与生物科学研究中心》(CABI)来源期刊
- 《中国核心期刊(遴选)数据库》收录期刊
- 中文期刊全文数据库收录期刊
- 万方《数字化期刊全文数据库》收录期刊
- 中文科技期刊数据库收录期刊

编委会顾问(按笔画顺序排序)

丘泰球 杨大行 杨连生 陈绮绮
姚汝华 郭祀远 曾庆孝 温其标

编委会委员(按笔画顺序排序)

于淑娟 方贵权 王三永 王小宁
王双飞 王锡昌 贝惠玲 艾连中
白卫东 古志平 石彦国 江 波
江连洲 刘安军 刘淑华 刘洁生
孙远明 李 华 李 斌 李 琳
李洪军 李来好 励建荣 吴克刚
吴 晖 吴清平 何国庆 杨晓泉
陆兆新 张 瀚 张兰威 张名位
陈绍军 陈 峰 陈嘉东 宗敏华
林 洪 孟江洪 欧仕益 欧阳瑞文
罗云波 金征宇 周朝晖 姜 松
姜绍通 胡卓炎 赵谋明 殷涌光
章超桦 黄雪松 蒋文真 蒋爱民
谢明勇 廖森泰 薛长湖

刺梨果渣水不溶性膳食纤维提取工艺优化
……夏洁,薛浩岩,贾祥泽,高晴,李超,黄强(227)
海藻糖对水饺皮保水性及质构特性的改良
……高文倩,邢雪羽,胡炎华,陈翠玲(235)

食品风味

酶解前后牡蛎风味变化的对比分析
……苏国万,黄可欣,何伟炜,赵谋明(242)
采用 HS-SPME-GC/MS 和电子鼻技术解析生咖啡豆加速贮藏期挥发性组分的变化规律
……丛莎,董文江,赵建平,迟晓星,陈治华,蒋快乐,山云辉(250)
酸浆豆腐冷藏期间的品质变化分析
……黄宝玲,王洁,廖振林,王丽,钟青萍,方祥(263)
不同产地香椿抗氧化活性及挥发性成分的差异分析
…王晓敏,史冠莹,王赵改,张乐,程菁菁,蒋鹏飞,赵丽丽,王旭增(271)

安全控制

河北酿造高粱籽粒中 7 种常用农药的残留与安全评价
……王金萍,杜瑞恒,籍贵苏,邢国胜,吕芃(282)
食物慢性砷暴露对小鼠脑组织中砷形态的影响
……王琛绯,石明,王佳婷,张贵伟,邱嘉怡,李银菲,窦昕皓,等(289)
潮州市市售豆制品的转基因成分检测
……王茂先,肖亮媛,吴丹霞,邓钰婷,王新彦(298)
胶粘剂中丙烯酸正丁酯向干性模拟物 Tenax 的迁移行为
……陈燕芬,马宁宁,曾莹,李丹,钟怀宁,郑建国(306)
胶体金免疫层析法定量检测鱼和虾中苯巴比妥残留
……黄佳佳,李燕杰,梁志理,杨慧晴,雷洪涛,徐振林(313)
高效液相色谱-串联质谱法测定厚朴中的厚朴酚与和异构厚朴酚
……吕思雨,陈驰,闫徐,王唯秀,何星瑶,焦禄,王志兵(321)
不同产地西瓜农药残留分析与膳食风险评估
……韦凯丽,华震宇,曹叶青,陶永霞,王成(331)
番茄红素原料及保健食品中番茄红素、β-胡萝卜素含量测定通用方法的建立
……李彬,于佳,侯俐南,刘慧锦,何欢,张伟清,王海燕(338)

专题综述

虾蟹壳中甲壳素绿色提取技术研究进展
……杨锡洪,辛荣玉,宋琳,董泽群,李钰金,解万翠(344)

Modern Food Science and Technology
(2020, Vol.36, No.7)

Food Nutrition

Ethanolic Extract of Fermented Brown Rice Improves the Metabolism of Glucose and Lipids in 3T3-L1 Adipocytes.....SONG Jia-le, ZENG Zhen et al. (1)
Ginsenoside F2 Interferes with the Cascade Reactions of Caspase to Inhibit H_2O_2-induced Apoptosis.....LIU Di, ZHANG Hao, et al. (11)
Protective Effects of α-linolenic acid Riched Flaxseed Oil on Suppressing Insulin Resistance and Oxidative Stress in Rats with Polycystic Ovary Syndrome.....WANG Ting, ZHANG Xiao-xia, et al. (17)
Rosa roxburghii Tratt Wine can Improve Glucose Metabolism Disorder in Type 1 Diabetic Rats through Insulin- PI3K Pathway.....AN Yu-hong, LU Min-tao, et al. (25)
Protective Effect of Water Extracts of *Orychophragmus violaceus* Seeds on Acetaminophen-induced Acute Liver Injury in Mice: Roles of Activating Hepatic AMPK/AKT/GSK-3β Signaling.....PANG Min, SHAN Yu, et al. (34)
The Antiproliferative Activities in Ganpu Tea on HepG2 and SGC-7901 Tumor Cell Lines.....YU Le-an, XIAO Sui, et al. (42)
Auxiliary Effect of Jinnan Compound on the Regulation of Blood Glucose in Type 2 Diabetic Rats.....YIN Min-qiang, TANG Hai-lian, et al. (50)
Betaine Improves Gastrointestinal Function in Anorexic Rats.....ZHOU Wei, et al. (57)

Bioengineering

Regulating the Production of Ethanol and Flavor by Overexpression of *GPD1* in Wine Yeast.....GAO Ying-ying, LI Ping, et al. (63)
Comparison of Metabolic Activity and Relationship of *Pediococcus pentosaceus* in Traditional Chinese Sourdough.....GONG Yun-xia, QI Xiao-bao. (70)
Isolation, Identification and Pathogenicity Analysis of *Vibrio parahaemolyticus* Strains from Maowei Sea, Beibu Gulf.....TANG Jin-li, LI Xiao-li, et al. (75)

Food Biochemistry

Low-temperature Drying of *Dendrobium officinale* Inhibit Polymerization of Water-soluble Polysaccharides.....XING Li, MA Hou-yu, et al. (88)
Texture Comparison of Different Purple Sweetpotato Cultivars.....NIU Li-ying, WAN Yu-wei, et al. (96)
Spectrum-Activity Relationship of Lipid-Lowering Ethanolic Extracts from Defatted Walnut Meal.....WANG Zu-kun, MA Ya-ge, et al. (105)
Analysis of Antioxidant Activity of Aquatic Vegetable Extracts and Its Role in Antioxidation of Rapeseed Oil.....XU Xiao-ying, HU Xiao-xiao, et al. (113)
Changing Trend of the Vitamin Content in Carrot during Drying.....WANG Qiu-yu. (120)

Food Storage and Preservation

Synergistic Effects of Modified Atmosphere Packaging and Irradiation for Preserving Fresh Noodles.....OUYANG Meng-yun, WANG Yan, et al. (125)
Regulation of Sulfur Dioxide on Organic Acids Content and Malate Metabolism Pathway of Grapes in Postharvest.....YAN Bo-wen, YUAN Yu-yao, et al. (133)
Preservation of Fruit Cucumber Treated by Antibacterial Peptide and Chitosan Composite Film.....LUO Xue-yun, WU Xiao-tong, et al. (142)
Preservation Effects of *Litsea cubeba* Essential Oil Combined with 1-MCP Treatment on *Averrhoa carambola* Fruits.....LIN Yuan, LIN Ying, et al. (150)
Comparison of Postharvest Quality and Storability of Different Longan Varieties.....WU Ze-yi, CHEN Xiao-dong, et al. (157)

Food Processing

Comparative Analysis of Color Stability of Sanhua Plum Juice during Storage with Different Phenolic Acids.....LI Yi-na, ZOU Ying, et al. (165)
Optimization of Enzymatic Hydrolysis of Fermented Acid Meat to Produce Antioxidant Peptides.....WU Hui-lin, LI Mio-yun, et al. (173)
Rheological Properties of Quinoa-wheat Flour and Development of its Noodles.....LIANG Xia, MENG Ting-ting, et al. (184)
Optimization of Extraction Process of Phillyrin and Its Antibacterial Activity.....ZHANG Jun-shun, LUO Jia-yuan, et al. (193)
Microencapsulation and Characterization of Soybean Protein Hydrolysates.....HUANG Xiao-mei, WEI Cui-lan, et al. (202)
Optimization of Processing Technology of Sweet Corn Buns.....ZHANG Kang-yi, WANG Hui-jie, et al. (209)
Optimization of Tomato Sour Soup Fermented by *Lactobacillus casei*.....ZHENG Sha-sha, HU Ping, et al. (218)
Extraction Optimization of Water-insoluble Dietary Fiber from *Rosa roxburghii* Tratt Fruit Pomace.....XIA Jie, XUE Hao-yan, et al. (227)
Improvement of Trehalose on Water Retention and Texture Properties of Dumpling Wrapper.....GAO Wen-qian, XING Xue-yu, et al. (235)

Food Flavor

Comparative Analysis on Flavor Changes of Oyster before and after Enzymatic Hydrolysis.....SU Guo-wan, HUANG Ke-xin, et al. (242)
Changing Trend of the Volatile Compounds in Robusta Green Coffee Beans During an Accelerated Storage Analyzed by HS-SPME-GC/MS and Electronic Nose Technology.....CONG Sha, DONG Wen-jiang, et al. (250)
Changes in the Quality of Acid Whey Tofu during Refrigerated Storage.....HUANG Bao-ling, WANG Jie, et al. (263)
Differences in the Antioxidant Activities and Volatile Components of *Toona sinensis* from Different Regions.....WANG Xiao-min, SHI Guan-ying, et al. (271)

Food Safety and Control

Analysis and Risk Assessment of Seven Conventional Pesticides Residue in Brewing Sorghum Grains Grown in Hebei Province.....WANG Jin-ping, DU Rui-heng, et al. (282)
Arsenic Species Analyses of Mice Brain under Chronic Arsenic Exposure through Food.....WANG Chen-fei, SHI Ming, et al. (289)
Transgenic Analysis of Soybean Products Sold in Chaozhou City.....WANG Mao-xian, XIAO Liang-yuan, et al. (298)
Migration Behavior of Butyl Acrylate from Adhesive to Dry Simulant Tenax.....CHEN Yan-fen, MA Ning-ning, et al. (306)
Development of a Colloidal Gold Immunochromatographic Assay for the Quantitative Determination of Phenobarbital Residues in Fish and Shrimp.....HUANG Jia-jia, LI Yan-jie, et al. (313)
Determination of Magnolol and Honokiol from *Magnolia officinalis Rehd. et Wils* by HPLC-MS.....LYU Si-yu, CHEN Chi, et al. (321)
Pesticide Residue Analysis and Dietary Risk Assessment of Watermelon in Different Habitats.....WEI Kai-li, HUA Zhen-yu, et al. (331)
Establishment of a General Method for the Determination of Lycopene and β-Carotene in Raw Materials of Lycopene and Health Food.....LI Bin, YU Jia, et al. (338)

Reviews

Green Extraction Technology of Chitin from Shrimp Shells and Crab Shells: a Review.....YANG Xi-hong, XIN Rong-yu, et al. (344)

Sponsor: South China University of Technology
Editorship, Publisher and Distributor: Editorial Board of Modern Food Science and Technology; Tel: 020-87112373
Address: Linhong Building, South China University of Technology, Wushan Road, Guangzhou, China 510640
Editor-in-chief: LI Lin, Vice editor-in-chief: LI Xiao-xi

现代食品科技

MODERN FOOD SCIENCE AND TECHNOLOGY

ISSN 1673-9078
CN 44-1620/TS
邮发代号 46-349
定价：40元

ISSN 1673-9078

柑普提取物对 HepG2 和 SGC-7901 肿瘤细胞系的抗增殖作用

俞乐安[1]，肖遂[2]，黄亚辉[1]，李小晓[1]，赖惠清[3]，郑意[3]，梁大华[3]，张旭[2]
（1.华南农业大学园艺学院，广东广州 510642）（2.华南农业大学林学与风景学院，广东广州 510642）
（3.广州市云鼎柑普茶业有限公司，广东广州 510642）

摘要：本实验研究了柑普茶加工后的成分变化以及对 HepG2 与胃癌细胞 SGC-7901 细胞的抗增殖作用。采用高效液相色谱法对柑普茶品质成分进行了鉴定；以肿瘤细胞 HepG2 与 SGC-7901 为模型，测定了柑普茶及其原料茶抗增殖活性（IC_{50}），对效果较明显的 HepG2 细胞系进行了进一步的细胞周期与凋亡分析。结果表明，柑普茶加工后，多酚类物质含量为 17.22%，较原料茶显著降低，其中，酯型儿茶素与非酯型儿茶素含量降低显著，而以茶黄素、茶红素为代表的茶色素含量则有所提高。柑普茶在抑制 SGC-7901 与 HepG2 细胞体外增值方面的作用明显强于普洱茶和柑橘皮，其 IC_{50} 分别为 176.61 μg/mL 与 143.60 μg/mL。通过对 HepG2 细胞周期与凋亡分析，表明柑普茶对肝癌细胞系的抑制作用主要通过阻滞细胞周期在 G0/G1 期后进而诱导细胞凋亡引起。柑普茶特殊加工工艺有利于其风味改善，也有利于活性物质积累，使得其在抑制 HepG2 与 SGC-7901 肿瘤细胞增殖方面表现出更好的活性。

关键词：柑普茶；品质成分；抗增殖；肿瘤；细胞系
文章篇号：1673-9078(2020)07-42-49 DOI: 10.13982/j.mfst.1673-9078.2020.7.1222

The Antiproliferative Activities in Ganpu Tea on HepG2 and SGC-7901 Tumor Cell Lines

YU Le-an[1], XIAO Sui[2], HUANG Ya-hui[1], LI Xiao-xiao[1], LAI Hui-qing[3], ZHENG Yi[3], LIANG Da-hua[3], ZHANG Xu[2]
(1.College of Horticulture, South China Agricultural University, Guangzhou 510642, China)
(2.College of Forestry and Landscape Architecture, South China Agricultural University, Guangzhou 510642, China)
(3.Yundingganpu Tea Company, Guangzhou 510642, China)

Abstract: In this study, the changes of components in the processed ganpu tea and their antiproliferative effects on HepG2 and SGC-7901 cells were investigated. The change of quality components in ganpu tea was determined by high performance liquid chromatography, and the activity of ganpu tea extracts against HepG2 and SGC-7901 colonies was determined by the MTT method. Then, the cell cycle and apoptosis of HepG2 cell line with obvious effect were further analyzed. The results showed that after the processing, the content of polyphenols was 17.22% which was lower than the material tea. Among them, the ester catechins and non-ester catechins were remarkably reduced. Moreover, the increase of tea pigments (theaflavins and thearubigins) was prominent. Ganpu tea had a higher tumor inhibition rate on SGC-7901 and HepG2 cell lines than puer tea and citrus peel, and the IC50 values were up to 176.61 μg/mL and 143.60 μg/mL, respectively. The analysis of cell cycle and apoptosis indicated that ganpu tea induced cell apoptosis through retarding the G0/G1 in HepG2 cells. As a result, the special processing of ganpu tea not only prompted the amelioration of flavor but also improved the accumulation of active substances so that ganpu tea showed better

引文格式：
俞乐安,肖遂,黄亚辉,等.柑普提取物对 HepG2 和 SGC-7901 肿瘤细胞系的抗增殖作用[J].现代食品科技,2020,36(7):42-49
YU Le-an, XIAO Sui, HUANG Ya-hui, et al. The antiproliferative activities in ganpu tea on HepG2 and SGC-7901 tumor cell lines [J]. Modern Food Science and Technology, 2020, 36(7): 42-49

收稿日期：2019-12-12
基金项目：广东省茶叶产业体系(2019LM1117)

作者简介：俞乐安（1995-），女，硕士研究生，研究方向：茶叶内含物质与活性
通讯作者：张旭（1984-），男，博士，讲师，研究方向：药用植物的开发和利用

(C)1994-2023 China Academic Journal Electronic Publishing House. All rights reserved. http://www.cnki.net

antiproliferative activities in HepG2 and SGC-7901 tumor cell lines.

Key words: ganpu tea; quality components; antiproliferation; tumor; cell lines

柑普茶是一种将柑橘果肉掏空，内部填塞普洱茶，后经日晒风干的复合茶类[1]。柑普茶的干燥工艺有别于其他茶类的快速高温干燥方式，以日光下的缓慢氧化为主，也带动了其内含物质，主要是酚类的缓慢热降解。柑普茶的原料为新会柑橘皮与云南普洱茶。柑橘种类繁多，以新会地区的柑橘皮制品为品质最佳，由新会柑橘制得的新会陈皮也是中国地理标志产品[2]。柑橘皮经日晒风干、陈化一系列工艺后，即成为陈皮。中医将陈皮入药，具有促消化，抗心脑血管疾病的功能[3,4]。普洱茶的主要产区是云南，以大叶种晒青绿茶为原料，主要活性成分为多酚类物质，以儿茶素、没食子酸与茶色素为主[5]。柑普茶结合原料的特点与功能，口感醇厚带柑橘香，迅速在市场上流行。

柑普茶的主要活性物质是儿茶素、咖啡碱、橙皮苷、川陈皮素、橘皮素等[6,7]，兼具普洱茶与柑橘皮的香气成分，其挥发性成分主要有烯烃类、酯类、醇类等[8]。作为饮料，无论是茶、柑橘皮，还是柑普茶，水溶性物质均可直接作用于人消化道细胞。其中，世界范围内，中国胃癌调整死亡率居于首位，90 年代，胃癌调整死亡率男性增长 11.0%，女性增长 6.3%[9]。同时，也有报道指出柑橘中提取的黄酮类化合物（主要物质为柚皮苷，含量为 2.99%；橙皮苷，含量为 2.10%）通过抑制 p-Akt 途径诱导 HepG2 细胞系的细胞凋亡，进而抑制其增殖[10]，该抑制活性可能与其 *α*-环甲氧基化的结构有关[11]。尽管，柑普茶兼具普洱茶的酚类物质与柑橘皮的黄酮类物质，但迄今为止，除了对柑普茶的橙皮苷、儿茶素与挥发性成分的研究外[6-8]，还没有对其加工前后的成分变化与活性的相关研究。因此，有必要对柑普茶加工工艺对其内含物质变化，与其对肿瘤细胞抑制活性进行研究。本实验以简单高效的高效液相色谱法为主要研究手段，采用新会柑皮和云南生普为原料加工而成并经两年存放的柑普茶及其原材料为研究材料。将柑普茶成品的柑橘皮部分与普洱茶分开，分别测量其内含物质，对比分析柑普茶原料与成品之间差异。选取陈皮与普洱茶活性较好的肿瘤细胞 HepG2 与 SGC-7901，探究柑普茶及其原料对两种肿瘤细胞的抑制活性差异，选取其中抑制活性较好的 HepG2 细胞系进行细胞周期与凋亡的分析，旨在阐明柑普茶加工工艺对其主要活性物质的影响及其对肿瘤细胞抑制作用，为科学饮用、加工柑普茶提供理论依据。

1 材料与方法

1.1 材料与试剂

经历两年存放的柑橘皮、普洱茶、柑普茶中剥出茶（以下简称剥出茶）、柑普茶中剥出柑橘皮（剥出皮）和柑普茶，均购于云鼎柑普有限公司；儿茶素单体（CG，EGC，C，EGCG，EC，GCG，ECG，CG）标准品、橙皮苷标准品、川陈皮素标准品、7-甲氧基黄酮标准品、橘皮素标准品、辛弗林标准品，均购于美国 Sigma 公司；异丙醇，十二烷基苯磺酸钠，磷酸，三氟乙酸（AR 级）均购于天津科密欧化学试剂有限公司；甲醇（HPLC 级），购于美国 ThermoFisher 公司。实验室自制：1640 高糖培养基，胎牛血清，0.25% 胰蛋白酶，50 μg/mL 青霉素和 50 μg/mL 链霉素，均购于美国 Glibco 公司；二甲基亚砜（DMSO）国产分析纯，购于上海沪试公司；四甲基偶氮唑盐（MTT）购于美国 Sigma 公司，配制成 5 mg/mL 的原药贮存液，-20 ℃保存；SGC-7901 人胃癌细胞株和 HepG2 肝癌细胞株，均购于 American type culture collection；临使用时以 1640，购于美国 Glibco 公司（完全培养基稀释）；Annexin V-FITC/PI 双染细胞凋亡检测试剂盒，凯基生物。

1.2 仪器与设备

酶标仪，美国 Thermo 公司产品；超净工作台，上海瑞净智化设备有限公司产品；倒置相差显微镜购自日本 Olympus 公司；真空冷冻干燥机，上海源起有限公司；旋转蒸发仪，上海亚荣化学仪器厂；高压蒸汽灭菌锅，上海申安医疗设备厂；离心机，-80 ℃低温冰箱，美国赛默飞世尔科技公司；96 孔板，美国 Corning 公司；高效液相色谱仪，美国 Aglient 公司；分光光度计，流式细胞仪（Guava easy Cyte TM）Merck。

1.3 柑普茶及其原料体外抑制肿瘤细胞活性测定

1.3.1 柑普茶生晒与存放过程

生晒：样品均摊在竹制篾子，置于室外，阳光直射区域，15 d，时间从 2016 年 10 月 16 日至同月 10

(C)1994-2023 China Academic Journal Electronic Publishing House. All rights reserved. http://www.cnki.net

月 31 日。温度维持在 18~27 ℃，湿度维持在 75%~85%。

存放：样品均摊在竹制篾子，置于室内干燥区域，2 a，时间从 2016 年 11 月 1 日至 2018 年 11 月 1 日。温度维持在 10~30 ℃，湿度维持在 75%~85%。

1.3.2 生化成分指标测定

茶多酚含量参照 GB/T 8313-2013 的方法进行测定；茶色素含量（茶黄素，茶红素，茶褐素），采用比色系统分析法测定；儿茶素，四种黄酮含量采用高效液相色谱法（HPLC）测定。将不同样品经 100 ℃水浴浸提 45 min，趁热抽滤，滤液转入 100 ml 容量瓶，定容后，上样测定。色谱柱：Aglient Eclipse XDB-C18（5 μm，150 mm×4.6 mm）分析柱；柱温 38 ℃；进样量 10 μL；流动相流速 0.8 mL/min。

儿茶素测定条件：运行时间 45 min；检测波长 278 nm。流动相 A：0.1%三氟乙酸水溶液，流动相 B：甲醇。流动相洗脱梯度（以 A 相的变化为准）：0~30 min，70%；30~40 min，20%；40~40.1 min，90%；40.1~45 min，保持 90%。

四种黄酮测定条件：运行时间 50 min；检测波长 330 nm。流动相 A：0.1%三氟乙酸水溶液，流动相 B：甲醇。流动相洗脱梯度（以 A 相的变化为准）：0~15 min，80%；15~25 min，60%；25~30 min，40%；30~38 min，40%；38~43 min，10%；43~50 min，保持 80%。

1.3.3 茶样感官品质审评

根据 GB/T 23776-2018 茶叶感官审评方法进行审评[12]。分别称取各样品 3.0 g，用容积为 200 mL 的白瓷审评碗，以 150 mL 80℃的沸水冲泡 5 min；由 8 名具有高级评茶员资质的自愿者组成审评小组，采用密码审评方法，对供试茶样的外形、汤色、香气和滋味 4 项因子进行评分，将所得分数去掉 1 个最高分和 1 个最低分后的 6 个分数进行平均，最后计算总分。因为柑普茶有苷皮包裹，外形，叶底审评较普洱茶较为不一致，故而不对外形与叶底进行评分。感官审评总分按照公式进行计算：

$$C = 30\% * C_{\alpha} + 30\% * C_{\beta} + 40\% * C_{\gamma}$$

其中：C 表示感官总分，C_{α} 表示汤色评分，C_{β} 表示香气评分，C_{γ} 代表滋味评分。

1.3.4 供试样品提取

经历两年存放的柑橘皮、普洱茶与柑普茶，柑普茶内的剥出皮与剥出茶，共计五个样品研磨成粉末，过五十目筛，与水以 1:20 的比例，100 ℃水浴提取 60 min，反复浸提三次，过滤后，合并滤液。于旋转蒸发仪进行浓缩，置于真空冷冻干燥机，72 h，制得水溶性冻干粉。

1.3.5 细胞培养

采用含有 10%灭活胎牛血清（FBS）和 1%双抗（50 μg/mL 青霉素和 50 μg/mL 链霉素）的 1640 高糖培养基培养（5% CO_2，37 ℃）对细胞进行培养。待细胞生长至视野 80%时采用胰蛋白酶，进行消化、传代。

1.3.6 MTT 法测量半致死率

将 SGC-7901 和 HepG2 细胞株经胰酶消化后，以每孔 3000 个，100 μL 接种到 96 孔板，设置 3 个平行对照和一个不加药完全培养基作为空白对照。次日，每孔加入 100 μL 含有不同浓度柑普茶、柑橘皮与普洱茶水溶性物质的培养液，每个浓度设三个平行，培养 48 h 后，每孔中加入 20 μL MTT 溶液，于 37 ℃细胞培养箱中孵育 4 h，小心吸去上清液体，每孔加入 100 μL DMSO 溶液，避光条件下在缓慢摇动的摇床上反应 10 min，在酶联免疫检测仪上读数，波长为 570 nm 处测量各孔吸光度值（OD 值），将空白对照组的 OD 值设为 100%，计算不同处理组中的细胞存活率。

其中细胞存活率计算公式：

$$A(\%) = \frac{A_i}{A_o} \times 100\%$$

其中，A 表示细胞存活率，Ai 表示不同处理组的 OD 值；Ao 表示空白对照组的 OD 值。

1.3.7 流式细胞术检测细胞周期

将细胞密度为 2×10^4 细胞/孔接种于六孔板中，培养 24 h 后，行加药操作。其中对照组不加药，处理组加入不同浓度（80、160、240 μg/mL）柑普茶水浸出物溶液，培养箱培养 48 h 后，用冷 PBS 洗涤两次，加入 1 mL 75%的冰乙醇固定，置于 4 ℃冰箱过夜。次日离心，加入 400 μL PI 工作液，置于 4 ℃冰箱避光孵育 30 min 后流式细胞仪检测。

1.3.8 流式细胞术检测细胞凋亡

细胞密度为 2×10^4 细胞/孔接种于六孔板中，培养 24 h 后，行加药操作。其中对照组不加药，处理组加入不同浓度（120、240 μg/mL）柑普茶水浸出物溶液，培养箱培养 48 h 后，用不含 EDTA 的胰酶消化收集、用磷酸缓冲盐溶液洗涤细胞 2 次，于 1000 r/min 离心 5 min，弃上清，PBS 洗 2 次，加入 500 μL 1X Annexin V buffer 轻轻重悬细胞，再加入 5 μL Annexin V-FITC 和 5 μL 碘化丙啶染色液，轻轻混匀，室温（20~25 ℃）避光孵育 15 min，随即进行流式细胞仪检测。

1.4 统计分析

所有指标均进行 3 次重复测定，取平均值。采用 Excel 制图，用 SPSS 22.0 进行分析，计量资料以 x±s 表示，采用单样本均数的方差检验（ANOVA）分析

(C)1994-2023 China Academic Journal Electronic Publishing House. All rights reserved. http://www.cnki.net

数据间的差异，显著性检验水平 α=0.05，p<0.05 视为有统计学差异。

2 结果与讨论

2.1 柑普茶及其原料内含物质变化

样品内含物成分由表 1 所示。与普洱茶原料相比，剥出茶茶色素含量显著增加（p<0.05），达到 0.42%，其中茶黄素与茶褐素含量极显著增加（p<0.01）。茶色素中，茶黄素对茶汤的感官品质起着重要作用，主要影响茶汤亮度、滋味鲜爽度和强度。茶红素是茶汤汤色中的主体物质，对茶汤滋味与汤色浓度起极重要作用。茶褐素是由茶黄素与茶红素进一步氧化形成的，主要反映为茶汤汤色中的褐色，只有在茶黄素与茶红素含量都较高且比例适当时才能形成普洱茶优良的品质。Obanda 等人的研究证实，提高温度会加速儿茶素降解，茶黄素水平的变化方向与温度和时间有关，发酵温度不同，茶黄素单体变化速率不同。因此，提高温度与延长时间（超过 60 min）可加速茶黄素降解，而该降解加速可能与前体物质 EGCG 与 ECG 存在有关[13]。

柑普茶中，儿茶素的主要成分为 EGCG，ECG，EGC 与 EC。剥出茶中，总儿茶素含量降低极为显著（p<0.01），为 6.34%，是普洱茶原料相应含量的 28.69%。其中以 EGCG 为代表的酯型儿茶素含量降低极为显著（p<0.01），为 3.17%，是原料相应含量的 22.64%。以 EC 和 C 为代表的非酯型儿茶素含量降低程度极显著(p<0.01)，达到 3.17%。在柑普茶长时间的生晒与存放加工中，这些消耗的酯型儿茶素 EGCG 与 ECG 作为前体物质，在缓慢的热降解过程中，促进了茶黄素的降解。

表 1 样品总酚、儿茶素、茶色素与部分黄酮含量

Table 1 The content of total polyphenols, catechins, tea pigments and flavonoids in samples

含量/%	普洱茶	剥出茶	柑橘皮	剥出皮	柑普茶
橙皮苷	-	-	3.20±0.24	4.20±0.23**	0.85±0.11
川陈皮素	-	-	0.67±0.07	0.69±0.07	0.18±0.01
7-甲氧基黄酮	-	-	0.28±0.03	0.34±0.03*	0.07±0.01
橘皮素	-	-	0.31±0.03	0.53±0.05**	0.11±0.01
总黄酮	-	-	4.49±0.22	6.11±0.32*	1.18±0.17
GA	1.47±0.21	1.27±0.15*	-	-	1.19±0.14
GC	0.45±0.07	0.33±0.06*	-	-	0.23±0.06
EGC	1.26±0.00	1.24±0.02	-	-	0.69±0.01
C	1.70± 0.07	0.88±0.08**	-	-	0.60±0.10
EC	3.22±0.20	1.21±0.18**	-	-	0.83±0.02
非酯型儿茶素总量	8.10±0.31	4.93±0.17**	-	-	2.31±0.01
EGCG	4.10±0.21	3.14±0.11**	-	-	0.68±0.04
GCG	1.31±0.01	0.77±0.02**	-	-	0.06±0.01
ECG	3.72±0.10	2.94±0.10**	-	-	0.49±0.01
CG	4.87±0.15	3.98±0.22*	-	-	0.06±0.00
酯型儿茶素总量	14.00±0.41	10.83±0.28**	-	-	1.30±0.11
儿茶素总量	22.10±1.45	15.76±1.43**	-	-	4.79±0.26
茶黄素	0.12±0.02	0.21±0.02**	-	-	0.13±0.01
茶红素	1.80±0.12	2.03±0.10*	-	-	1.79±0.12
茶褐素	1.35±0.41	1.63±0.08**	-	-	1.35±0.12
茶色素	3.25±0.60	3.67±0.42*	-	-	3.24±0.43
多酚总量	25.31±2.11	17.22±2.09**	2.36±0.12	2.43±0.13	7.73±1.35

注：剥出茶和剥出皮的*分别表示与普洱茶和柑橘皮组比较具有显著性差异（p<0.05）；**表示与普洱茶和柑橘皮组比较具有极显著性差异（p<0.01）；“-”表示未检出。

(C)1994-2023 China Academic Journal Electronic Publishing House. All rights reserved. http://www.cnki.net

表 2 样品感官审评结果

Table 2 The results for the sensory evaluation of samples

	汤色	香气	滋味	总评分	名次
普洱茶	红浓尚明亮 23.51±2.11	香气纯正 24.55±1.78	较醇厚，略带涩味 36.32±1.84	84.38±3.12	3
剥出茶	红浓明亮 22.71±1.98	香气纯正，带柑橘香 26.33±1.96	醇厚，有回味 37.65±2.32	86.69±2.98	2
柑普茶	橙红明亮 27.56±2.08**	香高爽，柑橘香明显 28.51±2.45**	醇厚，回味甘爽 39.66±2.71*	95.72±3.44*	1

注：柑普茶的*表示与普洱茶组比较具有显著性差异（p<0.05）；**表示与普洱茶组比较具有极显著性差异（p<0.01）。

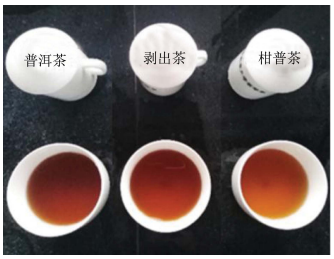


图 1 样品茶感官审评汤色结果

Fig.1 The sensory result of liquor color in samples

茶多酚含量极显著下降（p<0.01），同时茶色素含量则显著增加（p<0.05），这些内含物质的变化进一步形成柑普茶口感与茶汤色泽。与此同时，相较原料茶，剥出茶的茶多酚总量为 17.22%，其降低程度极为显著（p<0.01），表明柑普茶的加工工艺有助于多酚类物质热降解与茶色素物质的合成，进一步促进柑普茶品质形成。有研究证实，茶色素抑制肿瘤繁殖活性突出，Chakrabarty 等的研究指出 50 μg/mL 茶黄素和 20 μg/mL EGCG 的组合可以有效抑制 Hela 细胞通过 G(2)/M 期，进而诱导细胞凋亡发生[14]。

与原料柑橘皮对比，剥出皮的黄酮含量更高，达到 6.11%，远高于 Wang 等人之前对大红袍茶枝柑橘皮的黄酮含量[15]。剥出皮中，以橙皮苷含量增加最为显著（p<0.01），增加了 1.00%，是柑橘皮原料的 31.25%。

结合感官审评评价，柑普茶的加工工艺，有利于水分挥发，茶色素增加，主要体现在茶黄素与茶红素含量增加带来的汤色明亮度与色泽的改变。在香气上，与剥出皮相比较柑橘皮历经两年储存，黄酮类内含物质，橙皮苷、多甲氧基黄酮与橘皮素含量增加显著（p<0.05），也进一步促进柑普茶的高爽、柑橘香等香气品质形成。Xu 等人发现，绿茶茶汤中苦味主要由儿茶素（EGCG、ECG）决定，涩味主要由儿茶素（EGCG、ECG）决定[16]。而在柑普茶生晒加工过程中，柑普茶的多酚类物质中的酯型儿茶素发生了热降解，同时也促进了非酯型儿茶素的缓慢积累，使得剥出茶口感上的苦涩味较普洱茶原料降低，形成了柑普茶醇厚、回味甘爽的品质。

总体来说，由于柑普茶特殊的加工工艺，在缓慢的热降解过程中，内部柑普茶中的多酚类物质发生缓慢降解，促进了色素类物质与黄酮类物质的积累，同时其风味改变也更为充分、协调。

2.2 柑普茶水溶性物质对肿瘤细胞增殖的体外抑制作用

2.2.1 柑普茶水溶性物质对 SGC-7901 与 HepG2 细胞系增殖的体外抑制作用

用 MTT 法评价了不同浓度普洱生茶、柑橘皮与柑普茶对 HepG2 和 SGC-7901 细胞系的体外生长抑制作用，其中普洱茶、柑橘皮与柑普茶对 SGC-7901 和 HepG2 细胞系存活率的影响如图 2 所示。

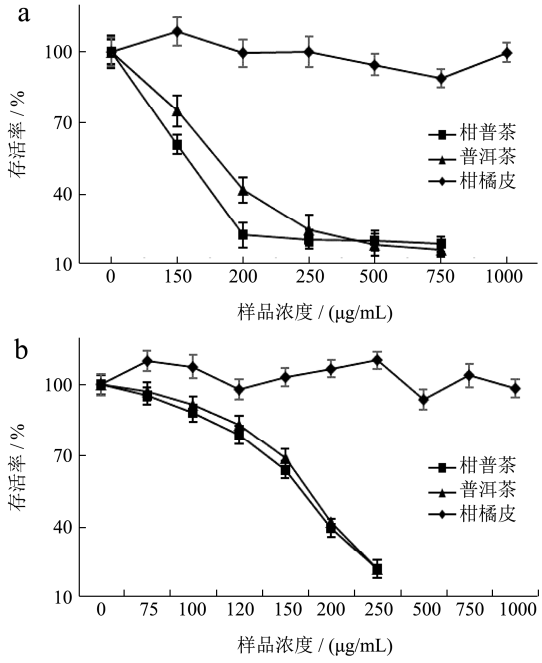


图 2 不同浓度柑普茶、普洱茶和柑橘皮对 HepG2 和 SGC-7901 细胞系存活率影响

Fig.2 The survival rate in SGC-7901 and HepG2 of different concentration of Ganpu tea, Puer tea and citrus peel

(C)1994-2023 China Academic Journal Electronic Publishing House. All rights reserved. http://www.cnki.net

注：a: 为不同浓度柑普茶、普洱茶与柑橘皮对 HepG2 细胞存活率影响，b: 为不同浓度样品对 SGC-7901 存活率影响。

由图 2 可知，柑普茶水浸出物的浓度与 SGC-7901 和 HepG2 细胞系的存活率呈剂量依赖关系，随着柑普茶水浸出物的浓度的增大，细胞存活率逐渐降低。

将柑普茶、柑橘皮与普洱茶冻干粉作用于 SGC-7901 细胞系，与对照相比，当柑普茶提取物浓度高于 100 μg/mL 时，细胞存活率有显著性降低（p<0.05），说明高剂量柑普茶提取物对 SGC-7901 细胞繁殖有一定抑制作用；柑普茶提取物浓度在 0~75 μg/mL 范围，对细胞存活率没有显著性影响（p<0.05）。经计算普洱茶，柑普茶对 SGC-7901 细胞作用 48 h 的半数生长抑制浓度（IC_{50}）分别为 176.61 μg/mL，145.00 μg/mL，柑普茶对 SGC-7901 的抑制活性显著强于普洱生茶（p<0.05），柑橘皮水溶性物质对 SGC-7901 无抑制活性。

表 3 普洱茶与柑普茶作用于 HepG2 与 SGC-7901 细胞系的 IC_{50}

Table 3 The IC_{50} of puer tea and ganpu tea in HepG2 and SGC-7901

IC_{50}/(μg/mL)	HepG2	SGC-7901
普洱茶	143.60±5.98	176.61±6.03
柑普茶	83.65±4.56**	145.00±6.34**

注：柑普茶的*表示与普洱茶组比较具有显著性差异（p<0.05）；**表示与普洱茶组比较具有极显著性差异（p<0.01）。

Zhang 等人的研究表明 EGCG 可降低 SGC-7901 细胞迁移速度[17]，而柑普茶的 EGCG，可能导致柑普茶的抑制 SGC-7901 细胞增殖活性。曹等人研究发现，川陈皮素对人胃癌细胞 SGC-7901 有较强的增殖抑制作用，含量在 2.5~80 mg/L 时，对 SGC-7901 细胞的抑制率为 19%~90%，抑制作用呈明显时效和量效关系[18]。而柑普茶中川陈皮素含量在 0.18%，柑橘皮的含量在 0.67%，均没有达到此前报导的有效浓度。闫等人研究结果证实，茶色素通过使胃粘膜腺体的萎缩及肠化不典型增生等病理情况发生逆转，从而对胃癌早期病变存在一定治疗效果[19]。因此，柑普茶水溶性物质的较强抑制 SGC-7901 细胞系生长活性，可能源于柑橘皮中的黄酮类物质与普洱茶的多酚类物质与茶色素的协同作用。这表明柑普茶的独特加工工艺有助于其抑制肝癌肿瘤细胞增殖活性进一步增强。

将柑普茶、柑橘皮与普洱茶冻干粉作用于 HepG2 细胞系。与对照相比，当柑普茶提取物浓度高于 100 μg/mL 时，细胞存活率有极显著性降低（p<0.01），说明高剂量柑普茶提取物对 HepG2 细胞繁殖有一定抑制作用；柑普茶提取物浓度在 0~100 μg/mL 范围，对细胞存活率没有显著性影响（p>0.05）。经计算普洱生茶，柑普茶对 HepG2 细胞作用 48 h 的半数生长抑制浓度（IC_{50}）分别为 83.65 μg/mL，143.60 μg/mL，柑普茶对 HepG2 的抑制活性显著强于普洱生茶（p<0.05），柑橘皮水溶性物质对 HepG2 细胞系无抑制活性。有研究表明，EGCG 和 EC 通过增加 HepG2 细胞的凋亡和引起细胞周期阻滞来降低癌细胞活力[20]。同时，茶多酚与茶色素可以通过抑制 Bcl-2 表达，诱导 Bax 蛋白表达，从而进一步诱导 HepG2 细胞凋亡的发生[21]。对柑橘皮黄酮类物质活性的研究主要集中在肝细胞脂质积累上，有报道指出柑橘皮中的川陈皮素可通过激活 Amp 激活的蛋白激酶依赖性信号，来减弱高糖诱导的肝细胞脂质积累[22]，Shi 等人的研究发现川陈皮素（2.5 μM）显著抑制 HepG2 细胞的侵袭和迁移，以及抑制抗肝细胞生长因子引起的细胞结构改变，而橘皮素没有显著的抑制相关性[23]。有实验证明，柑橘内的多甲氧基黄酮可通过促进细胞凋亡，抑制人肝癌细胞株 HepG2 的生长[24]。因此，柑普茶水溶性物质的较强抑制 HepG2 细胞系增殖活性，可能源于柑橘皮水溶性物质中多甲氧基黄酮与普洱茶内的酚类物质的协同作用。

柑普茶独特的加工工艺，使得内含物质主要是酚类物质发生了热降解，同时促进茶色素积累。这些内含物质的变化，在促进柑普茶风味转化的同时，也使得其在抑制 SGC-7901 和 HepG2 细胞系活性较普洱生茶强。

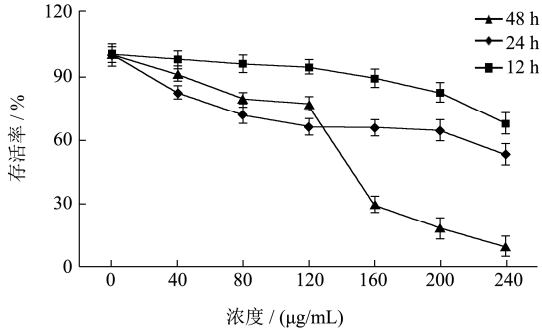


图 3 不同浓度的柑普茶处理 HepG2 细胞不同时间对其细胞存活率的影响

Fig.3 Effects of ganpu tea with different concentrations and different periods oftime on cell viability of HepG2 cells

其次，采取 MTT 法评价柑普茶水溶性物质对 HepG2 细胞系存活率的影响，从而进一步筛选出对 HepG2 细胞存活率影响最大的柑普茶水溶性物质浓度和作用时间。实验结果如图 3 所示。由图 3 可知，当柑普茶水溶性物质处理 HepG2 细胞 12 h 后，随着柑普茶水溶性物质浓度（40~240 μg/mL）的升高，细胞存活率从 98.01%降低到 68.01%。当处理时间从 12 h 增加到 48 h 时，随着柑普茶水溶性物质浓度（40~240

(C)1994-2023 China Academic Journal Electronic Publishing House. All rights reserved. http://www.cnki.net

μg/mL）的升高，细胞存活率从 91.51%降低到 10.33%。实验结果表明，HepG2 细胞存活率均随柑普茶水溶性物质浓度的升高和处理时间的增加呈下降趋势。当柑普茶水溶性物质为 240 μg/mL 处理 HepG2 细胞 48 h 后，其细胞存活率达到最低为 10.33%。

2.2.2 柑普茶水溶性物质对 HepG2 细胞系周期与细胞凋亡的影响

由表 4 可知，S 期细胞比例由对照组的 18.36%明显下降至 9.55%（p<0.01），而 G0/G1 期细胞比例由 52.36%显著上升至 66.26%（p<0.01），提示细胞 DNA 可能受损，细胞周期无法通过 G1 DNA 损伤检查点，被阻滞在 G0/G1 期。这些细胞可能在修复受损 DNA 失败后启动凋亡程序。

表 4 柑普茶对 HepG2 细胞系的细胞周期影响

Table 4 The influence of ganpu tea in the cell cycle of HepG2 cell lines

样品浓度	G0/G1 期/%	S 期/%	G2/M 期/%
240 μg/mL	66.26±3.21**	9.55±1.54**	21.01±2.87**
160 μg/mL	62.07±3.09**	7.06±1.89**	26.71±3.08*
80 μg/mL	61.98±2.98**	11.26±2.43**	24.16±2.56*
0 μg/mL	52.36±2.77	18.36±2.75	26.92±3.43

注：*表示与 0 μg/mL 组比较具有显著性差异（p<0.05）；**表示与 0 μg/mL 组比较具有极显著性差异（p<0.01）。

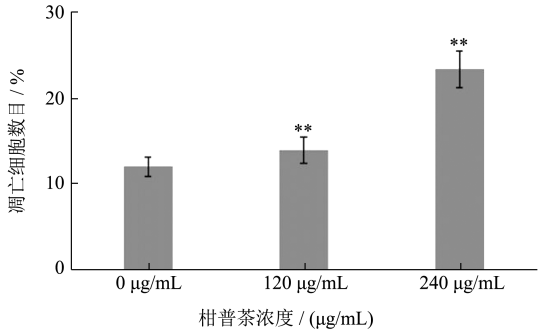


图 4 不同浓度的柑普茶对 HepG2 细胞凋亡数目的影响

Fig.4 Effects of different concentration of ganpu tea inclusion complex on population of apoptotic HepG2 cells

注：*表示与 BC 组比较具有显著性差异（p<0.05）；**表示与 BC 组比较具有极显著性差异（p<0.01）。

在肿瘤细胞中，抑制肿瘤细胞增殖常常是通过诱导细胞凋亡和诱导细胞周期阻滞实现的。为了进一步阐明柑普茶抑制 HepG2 肿瘤细胞增殖的机理，采用流式细胞仪考察不同浓度柑普茶对 HepG2 细胞周期分布的影响。细胞凋亡比率的测定可进一步验证柑普茶对 HepG2 细胞存活率的影响。柑普茶对 HepG2 细胞凋亡比率的影响如图 4 所示。细胞凋亡的数目随着柑普茶浓度的增加呈现增加的趋势，空白对照组细胞凋亡比率仅为 8.92%，当 120 μg/mL 柑普茶处理 HepG2 细胞 12 h 后，细胞凋亡数量为 13.86%，极显著高于对照（p<0.01）。当柑普茶的浓度提高到 240 μg/mL 时，其细胞凋亡总数提高到 23.34%，极显著高于对照组（p<0.01）。上述结果表明，柑普茶通过诱导细胞凋亡来抑制 HepG2 细胞系增殖。

3 结论

本研究通过对柑普茶酚类物质成分测定，测得柑普茶及其原料中儿茶素、茶色素、黄酮类物质含量，探明柑普茶加工工艺使得其内含物质发生转化并带动风味优化，主要体现在多酚类物质缓慢的热降解。其中，以EGCG为代表的酯型儿茶素含量降低最为显著，同时茶色素与黄酮类物质进一步积累。将柑普茶、柑橘皮与普洱茶分别作用于 HepG2 与 SGC-7901 细胞系。结果表明，柑普茶水溶性物质能通过阻滞细胞周期在 G0/G1 期进而显著抑制细胞增殖。总之，柑普茶的加工工艺带动风味优化，促进活性物质积累的同时，也使得其抑制肿瘤细胞增殖活性较原料进一步增强。因此，在日常生活中适当饮用柑普茶，会对肝癌与胃癌有一定防治作用。

参考文献

[1] DBS 44/010-2018,新会柑皮含茶制品[S]
DBS 44/010-2018, The Tea Product with Xinhui Citrus Peel [S]

[2] 罗政,郭媛媛,陈飞平,等.广陈皮原料茶枝柑与其他典型柑橘成分差异分析[J].热带作物学报,2019,40(1):174-179
LUO Zhen, GUO Yuan-yuan, CHEN Fei-ping, et al. Difference between ingredients of *Citrus chachiensis* tanaka and other typical citrus [J]. Chinese Journal of Tropical Crops, 2019, 40(1): 174-179

[3] 傅曼琴,肖更生,吴继军,等.广陈皮促消化功能物质基础的研究[J].中国食品学报,2018,18(1):56-64
FU Man-qin, XIAO Geng-sheng, WU Ji-jun, et al. Studies on chemical basis of digestion promoting function of pericarpium citri reticulatae (citrus reticulate 'Chachi') [J]. Journal of Chinese Institute of Food Science and Technology, 2018, 18(1): 56-64

[4] 俞静静,苏洁,吕圭源.陈皮抗心脑血管疾病相关药理研究进展[J].中草药,2016,47(17):3127-3132
YU Jing-jing, SU Jie, LYU Gui-yuan. Research progress in anti-cardiovascular and cerebrovascular disease activity of *Citri reticulatae* pericarpium [J]. Chinese Traditional and Herbal Drugs, 2016, 47(17): 3127-3132

[5] Shao W, Powell C, Clifford MN. The analysis by HPLC of

(C)1994-2023 China Academic Journal Electronic Publishing House. All rights reserved. http://www.cnki.net

green, black and Pu'er teas produced in Yunnan [J]. Journal of the Science of Food and Agriculture, 1995, 69(4): 535-540

[6] 朱国军,区棋铭,李振球,等.高效液相色谱法同时测定柑普茶中橙皮苷和 6 种儿茶素[J].化学分析计量,2018,27(6):51-55
ZHU Guo-jun, QU Qi-ming, LI Zhen-qiu, et al. Determination of hesperidin and six catechins in ganpu tea by high performance liquid chromatography [J]. Chemical Analysis and Meterage, 2018, 27(6): 51-55

[7] 郑玉莹,郭芳,彭维,等.新会柑普茶高效液相色谱指纹图谱研究[J].中南药学,2018,16(6):721-725
ZHENG Yu-ying, GUO Fang, PENG Wei, et al. HPLC fingerprints of ganpu tea from Xinhui [J]. Central South Pharmacy, 2018, 16(6): 721-725

[8] 郑敏,黄晓兵,彭政,等.柑普茶挥发性成分分析[J].热带作物学报,2017,38(4):758-762
ZHENG Ming, HUANG Xiao-bing, PENG Zhen, et al. Analysis of volatile components in gan-pu tea [J]. Chinese Journal of Tropical Crops, 2017, 38(4): 758-762

[9] 孙秀娣,牧人,周有尚,等.中国胃癌死亡率 20 年变化情况分析及其发展趋势预测[J].中华肿瘤杂志,2004,1:6-11
SUN Xiu-di, MU Ren, ZHOU You-shang, et al. Analysis of mortality rate of stomach cancer and its trend in twenty years in China [J]. Chinese Journal of Oncology, 2004, 1: 6-11

[10] Lee SH, Yumnam S, Hong GE, et al. Flavonoids of Korean *Citrus aurantium* L. induce apoptosis via intrinsic pathway in human hepatoblastoma HepG2 cells [J]. Phytotherapy Research, 2015, 29(12): 1940-1949

[11] Lin Y, Vermeer MA, Bos W, et al. Molecular structures of citrus flavonoids determine their effects on lipid metabolism in HepG2 cells by primarily suppressing apob secretion [J]. Journal of Agricultural and Food Chemistry, 2011, 59(9): 4496-4503

[12] GB/T 23776-2018, 茶叶感官审评方法[S]
GB/T 23776-2018, The Sensory Evaluation Method of Tea [S]

[13] Obanda M, Owuor PO, Mang'Oka R. Changes in the chemical and sensory quality parameters of black tea due to variations of fermentation time and temperature [J]. Food Chemistry, 2001, 75(4): 395-404

[14] Chakrabarty S, Nag D, Ganguli A, et al. Theaflavin and epigallocatechin-3-gallate synergistically induce apoptosis through inhibition of PI3K/Akt signaling upon depolymerizing microtubules in HeLa cells [J]. Journal of Cellular Biochemistry, 2019, 120(4): 5987-6003

[15] Wang F, Chen L, Chen H, et al. Analysis of flavonoid metabolites in citrus peels (*Citrus reticulata* "Dahongpao") using UPLC-ESI-MS/MS [J]. Molecules, 2019, 24(15): 2680

[16] Xu Y, Zhang Y, Chen J, et al. Quantitative analyses of the bitterness and astringency of catechins from green tea [J]. Food Chemistry, 2018, 258(16-24)

[17] Zhang J, Zhou Y, Chen H, et al. Effect of EGCG on SGC-7901 cells migration and metastasis [C]. Faseb Journal, Boston, MA: Federation American Social Experimental Biology, 2008: 22

[18] 曹弟勇,曾云,唐建平.川陈皮素对人胃癌细胞 SGC-7901 抑制作用的实验研究[J].临床合理用药杂志,2009,2(21):18-19
CAO Di-yong, ZENG Yun, TANG Jian-ping. The experimental research of inhibitory effect of nobiletin on human gastric carcinoma cell lineSGC-7901 [J]. Chinese Journal of Clinical Rational Drug Use, 2009, 2(21): 18-19

[19] 闫小雪,袁红霞,雒名池.茶色素治疗胃癌前期病变临床观察[J].天津医科大学学报,2001,2:268-270
YAN Xiao-xue, YUAN Hong-xia, LUO Ming-chi. Clinical observation on the treatment of precancerous lesion with tea pigment [J]. Journal of Tianjin Medical University, 2001, 2: 268-270

[20] Khiewkamrop P, Phunsomboon P, Richert L, et al. Epistructured catechins, EGCG and EC facilitate apoptosis induction through targeting de novo lipogenesis pathway in HepG2 cells [J]. Cancer Cell International, 2018, 18(1): 46

[21] 贾旭东,韩驰,陈君石.茶多酚和茶色素对人肝癌细胞株 HepG2 细胞凋亡的影响[J].卫生研究,2005,1:73-75
JIA Xu-dong, HAN Chi, CHEN Jun-shi. Effects of tea polyphenols and tea pigments on apoptosis in HepG2 cell line [J]. Journal of Hygiene Research, 2005, 1: 73-75

[22] Park Y, Yuk T, Lee J. Nobiletin attenuates high glucose-induced lipid accumulation in HepG2 hepatocytes through activation of AMP-activated protein kinase-dependent signaling [C]. Faseb Journal, Boston, MA: Federation American Social Experimental Biology, 2015: 29

[23] Shi M, Liao Y, Shih Y, et al. Nobiletin attenuates metastasis via both ERK and PI3K/Akt pathways in HGF-treated liver cancer HepG2 cells [J]. Phytomedicine, 2013, 20(8-9): 743-752

[24] Vermeer MA, Lin Y, Bos W, et al. Molecular structures of citrus polymethoxylated flavonoids (PMFs) determine their inhibitory effect on apoB secretion in HepG2 cells [C]. Faseb Journal, Boston, MA: Federation American Social Experimental Biology, 2010: 24

(C)1994-2023 China Academic Journal Electronic Publishing House. All rights reserved. http://www.cnki.net

证书号第6371559号

发明专利证书

发 明 名 称：一种发酵陈皮的制备方法、产品及应用

发　明　人：黄亚辉;张旭;曾小羊;林木勤;胡海娥

专　利　号：ZL 2021 1 0911757.6

专利申请日：2021年08月10日

专 利 权 人：华南农业大学;东鹏饮料（集团）股份有限公司

地　　址：510642 广东省广州市天河区五山

授权公告日：2023年09月29日　　授权公告号：CN 113598255 B

国家知识产权局依照中华人民共和国专利法进行审查，决定授予专利权，颁发发明专利证书并在专利登记簿上予以登记。专利权自授权公告之日起生效。专利权期限为二十年，自申请日起算。

专利证书记载专利权登记时的法律状况。专利权的转移、质押、无效、终止、恢复和专利权人的姓名或名称、国籍、地址变更等事项记载在专利登记簿上。

局长
申长雨

国家知识产权局
2023年09月29日

其他事项参见续页

证书号第3914567号

发明专利证书

发明名称：一种微生物发酵制作GABA茶的方法

发 明 人：黄亚辉;陈莹玉;张旭;曾贞

专 利 号：ZL 2017 1 0352191.1

专利申请日：2017年05月18日

专利权人：华南农业大学

地 址：510642 广东省广州市天河区五山路483号

授权公告日：2020年07月31日　　授权公告号：CN 107197966 B

国家知识产权局依照中华人民共和国专利法进行审查，决定授予专利权，颁发发明专利证书并在专利登记簿上予以登记。专利权自授权公告之日起生效。专利权期限为二十年，自申请日起算。

专利证书记载专利权登记时的法律状况。专利权的转移、质押、无效、终止、恢复和专利权人的姓名或名称、国籍、地址变更等事项记载在专利登记簿上。

局长
申长雨

2020年07月31日

其他事项见续页

ICS 67.140.10
CCS B 05

DB44

广 东 省 地 方 标 准

DB44/T 2419—2023

全生晒柑普茶生产技术规程

Technical regulations for Sun-Drying Ganpu_Tea

地方标准信息服务平台

2023－03－28 发布　　2023－06－28 实施

广东省市场监督管理局　　发 布

地方标准信息服务平台

前　言

本文件按照GB/T 1.1—2020《标准化工作导则 第1部分：标准化文件的结构和起草规则》给出的规则起草。

请注意本文件的某些内容可能涉及专利。本文件的发布机构不承担识别专利的责任。

本文件由广东省农业农村厅提出并组织实施。

本文件由广东省种植业标准化技术委员会归口。

本文件起草单位：广东省云鼎柑普茶业有限公司、华南农业大学园艺学院。

本文件主要起草人：黄亚辉、赖惠清、黄健美、张旭、肖遂、梁大华、彭艳、田秋燕、宋鹏。

地方标准信息服务平台

地方标准信息服务平台

全生晒柑普茶生产技术规程

1 范围

本文件规定了全生晒柑普茶的术语与定义、原料要求、加工、品质要求、运输和贮存等要求。

本文件适用于以广东省茶枝柑柑皮和云南省普洱茶为原料再加工的柑普茶的生产。

2 规范性引用文件

下列文件中的内容通过文中的规范性引用而构成本文件必不可少的条款。其中，注日期的引用文件，仅该日期对应的版本适用于本文件。不注日期的引用文件，其最新版本（包括所有的修改单）适用于本文件。

GB 2763 食品安全国家标准 食品中农药最大残留限量
GB/T 22111—2008 地理标志产品 普洱茶
GB/T 23776 茶叶感官审评方法
GB/T 30375 茶叶贮存
GH/T 1070 茶叶包装通则

3 术语和定义

下列术语和定义适用于本文件。

3.1

全生晒柑普茶 Sun-Drying Ganpu_Tea

将茶枝柑柑果肉掏空，内部填塞普洱茶，后经高温汽蒸处理和日晒风干的再加工复合茶类产品。按内部填塞普洱茶的不同，全生晒柑普茶分为全生晒柑普生茶和全生晒柑普熟茶两种类型。

3.2

茶枝柑 *Citrus reticulata* cv. 'Chachigan'

芸香科、柑橘属柑橘的栽培品种。

3.3

普洱茶 puer tea

以地理标志保护范围内的云南大叶种晒青茶为原料，并在地理标志保护范围内采用特定的加工工艺制成，具有独特品质特征的茶叶，按其加工工艺及品质特征，分为普洱茶（生茶）和普洱茶（熟茶）两种类型。

[来源：GB/T 22111—2008，4.1，有修改]

4 原料要求

4.1 茶枝柑

选择外形周正、色泽油亮、匀齐、符合GB 2763规定的茶枝柑，茶枝柑的定档分类按表1执行。

地方标准信息服务平台

表1　新会柑的定档分类

类别	采摘颜色	采摘时间	大小要求
小青柑	青色	约农历立秋至寒露	果实直径：38 mm±3 mm
二黄柑（二红柑）	微黄色	约农历寒露至小雪	果实直径：55 mm±3 mm
大红柑	橙红或橙黄色	约农历小雪至小寒	果实直径：63 mm±3 mm

4.2　普洱茶

选择符合GB/T 22111的规定的普洱茶。

5　加工

5.1　加工工艺

全生晒柑普茶加工工艺流程包括采果——选果——清洗鲜果表面和二次选果——开盖挖孔和去果肉——清洗果壳和晾干——第三次选果——普洱茶汽蒸——装填普洱茶——杀青——日晒风干等。

5.2　工艺要求

5.2.1　采果

5.2.1.1　采摘方法

采摘茶枝柑柑果时，需特定工具，一果两剪，且平剪。首剪是在果蒂适当部位剪下，留叶的第二剪在靠果柄两片叶处剪掉，不留叶的第二剪沿果蒂平齐剪下。

5.2.1.2　采摘要求

采摘前10 d～15 d内，果园不进行漫灌，极其干旱情况下建议进行适量淋水，宜在晴天、雾水干后采摘，下雨天不采，虫果坏果不采。特定工具判定合适尺寸大小后采摘，采摘后要轻、稳放置，避免碰撞损伤。

5.2.1.3　茶枝柑盛装

采用透气、卫生、无污染、无异味的容器盛装，用果框盛装，不得使用不透气的布袋、塑料袋等盛装，不得挤压。

5.2.1.4　茶枝柑运输

运输工具必须清洁卫生、干燥、无异味，运输过程中避免日晒、雨淋。不得与有异味、有毒、有害的物品混装。

5.2.2　选果

整个柑普茶加工过程进行3次新会柑/柑果壳的筛选。采摘后进行第一次（人工）筛选，去掉部分不符合采摘要求的柑果；清洗鲜果表面过程中进行第二次筛选，去掉偏大或偏小的柑果；果壳清洗后进行第三次筛选，去掉开口破裂等不符合要求的果壳。

5.2.3　清洗鲜果表面

地方标准信息服务平台

将采摘的新鲜新会柑，上机清洗除去柑果表面灰尘等不洁物质。

5.2.4 开盖挖孔和去果肉

用特定工具在柑果顶部切开圆形小口，开口圆整，取果盖；并在柑果底部打孔。用特定工具取出果肉，掏空，不能破坏整个柑果的形状，避免碰撞损伤。

5.2.5 清洗果壳和晾干

清洗果壳，去除果肉碎渣。并于自然通风处阴干至表皮无水渍，约1 h。

5.2.6 普洱茶汽蒸

将普洱茶进行100 ℃汽蒸处理5 s～10 s。

5.2.7 装填

向处理好的果壳里装填普洱茶，盖上前面步骤去掉的柑果盖。小青柑填充7 g～12 g普洱茶，二黄柑填充19 g～25 g普洱茶，大红柑填充26 g～32 g普洱茶。

5.2.8 杀青

将装填好普洱茶的柑普茶进行100 ℃汽蒸处理1 min～3 min。

5.2.9 日晒风干

将蒸汽处理过的柑普茶均匀平铺于晾晒架上，于室外阳光直射处自然晒干，开口朝上，中间翻转多次。日晒15 d～30 d，晒至柑普茶整体含水量≤10%即可。日晒时间以太阳升起为开始，日落为结束，日晒过程中根据含水量调整日晒时长。遇连续阴雨天气，则以（热）风机风干和抽湿方式弥补。

6 品质要求

6.1 品质要求

淘汰品相不佳的柑普茶，品质正常，无异味，无劣变，洁净，除柑皮和普洱茶外，无其他物质和任何添加剂。

6.2 理化指标

应符合表2的要求。

表2 全生晒柑普茶理化指标

项目		指标
水分%	≤	10.0
总灰分%	≤	7.5

6.3 农药残留限量

应符合GB 2763对茶叶的规定。

6.4 感官要求

柑普茶产品各等级的感官品质应符合表3和表4的要求，感官审评方法按GB/T 23776的规则执行。

地方标准信息服务平台

表3　全生晒柑普生茶感官要求

项目	要求			
	特级	一级	二级	三级
外形	茶叶黄绿、匀整、肥嫩紧结，芽毫显；柑皮色泽油润，金星密布	茶叶绿黄、匀整、肥壮紧结，芽毫较显；柑皮色泽较润，有金星	茶叶绿黄、匀整、肥壮紧结，显毫；柑皮色泽尚润	茶叶黄褐、较匀整、紧结，较显毫；柑皮色泽欠润
香气	茶香果香协调、高锐、持久	茶香果香协调、持久	果香显露，持久	果香明显
滋味	浓醇甘爽	较浓醇甘爽	浓厚回甘	较浓厚回甘
汤色	橙黄明亮	黄亮	黄亮	浅黄，尚亮
叶底	柔嫩显芽，匀齐	柔嫩有芽，较匀齐	肥嫩匀齐	肥嫩较匀齐

表4　全生晒柑普熟茶感官要求

项目	要求			
	特级	一级	二级	三级
外形	茶叶红褐润、紧细、匀整、显毫；柑皮色泽油润，金星密布	茶叶红褐润、紧结、匀整、较显毫；柑皮色泽较润，有金星	茶叶红褐润、较紧结、匀整、尚显毫；柑皮色泽尚润	茶叶红褐、尚紧结、较匀整、稍显毫；柑皮色泽欠润
香气	柑香和茶香浓郁丰富，持久	柑香和茶香较丰富，较持久	柑香和茶香纯正，尚持久	柑香和茶香纯正
滋味	浓醇回甘	较浓醇回甘	浓厚回甘	较浓厚回甘
汤色	红艳明亮	深红明亮	红浓尚亮	褐红尚亮
叶底	红褐柔嫩、匀齐	红褐较柔嫩、较匀齐	红褐尚柔嫩、尚匀齐	红褐欠柔嫩、较匀

6.5　包装

应符合GH/T 1070的规定。包装材料应干燥、清洁、密封性能好、无异味、不影响茶叶品质。包装要牢固、防潮、整洁、能保护茶叶品质、便于装卸、运输和仓储。

7　运输和贮存

7.1 运输

运输工具必须清洁、干燥、无异味、无污染；运输时应防潮、防晒；装卸时轻拿轻卸，严禁与有毒、有异味等损害茶叶品质的物品混装混运。

7.2 贮存

应符合GB/T 30375的规定。在符合贮存条件的情况下，产品可长期保存。

地方标准信息服务平台

证 书

为表彰“第八届全国医药院校药学/中药学专业大学生实验技能竞赛”中成绩优异者，特颁发此证书。

获奖等级：二等奖

获奖姓名：刘玉洁

指导教师：张旭　李雁群　屈畅

高等学校国家级实验教学示范中心联席会

全国药学类院校大学生专业技术与实验技能竞赛组委会

教育部药学课程虚拟教研室

“101计划”中药新药研究课程虚拟教研室

中国药科大学

2024年12月15日

证书编号：NDC24A110003534

奖 状

唐珂、盛翀、廖映红、吴纳兰、胡绩宇、左世雄、梁艳珊、王婉娜、
周慧盈、赖宇翔、黄子米、叶美玲、张中良、张轩瑞、赵安琪：

你们的作品《可茶——高GABA低咖啡因茶产品开拓者》，在2024年华南农业大学“创客杯”大学生创新大赛中荣获

铜奖

指导老师：张旭、黄亚辉、肖遂、吴玉红

特发此证，以资鼓励。

党委学生工作部（党委研究生工作部）

2024年5月24日